

FINAL REPORT

ENVIRONMENTAL SURVEYS OF POTENTIAL BORROW AREAS OFFSHORE NORTHERN NEW JERSEY AND SOUTHERN NEW YORK AND THE ENVIRONMENTAL IMPLICATIONS OF SAND REMOVAL FOR COASTAL AND BEACH RESTORATION

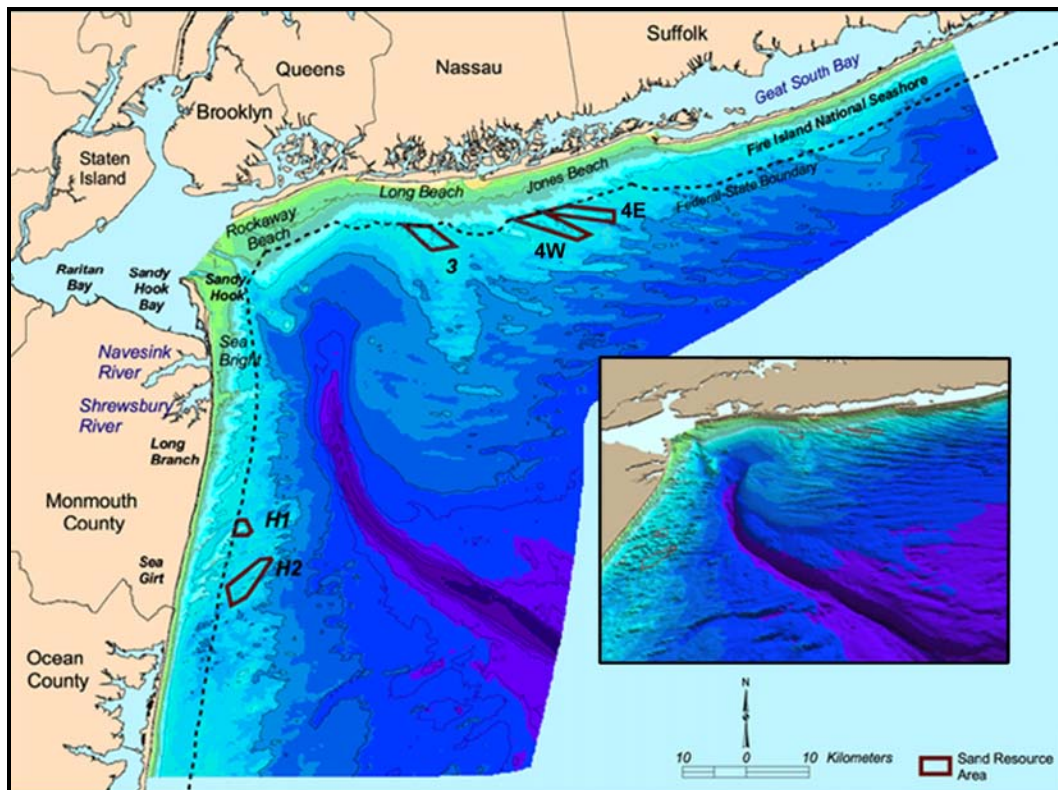
Volume I: Main Text

Prepared by:

Applied Coastal Research and Engineering, Inc.
766 Falmouth Road, Suite A-1
Mashpee, MA 02649

In Cooperation With:

Continental Shelf Associates, Inc.
Barry A. Vittor & Associates, Inc.
Germano & Associates, Inc.



Prepared for:

U.S. Department of the Interior
Minerals Management Service
Leasing Division
Marine Minerals Branch

MMS

Funded Under Contract Number 1435-01-01-CT-31118

DISCLAIMER

This manuscript has been reviewed by the Minerals Management Service and approved for publication. The opinions, findings, conclusions, and recommendations expressed in this report are those of the authors, and do not necessarily reflect the views or policies of the MMS. Mention of trade names or commercial products does not constitute endorsement or recommendation for use. This report has been technically reviewed according to contractual specifications; however, it is exempt from further review by the MMS Technical Publication Unit.

SUGGESTED CITATION

Byrnes, M.R., R.M. Hammer, S.W. Kelley, J.L. Baker, D.B. Snyder, T.D. Thibaut, S.A. Zichichi, L.M. Lagera, S.T. Viada, B.A. Vittor, J.S. Ramsey, and J.D. Germano, 2004. Environmental Surveys of Potential Borrow Areas Offshore Northern New Jersey and Southern New York and the Environmental Implications of Sand Removal for Coastal and Beach Restoration. U.S. Department of the Interior, Minerals Management Service, Leasing Division, Marine Minerals Branch, Herndon, VA. OCS Report MMS 2004-044, Volume I: Main Text 264 pp. + Volume II: Appendices 194 pp.

FINAL REPORT

ENVIRONMENTAL SURVEYS OF POTENTIAL BORROW AREAS OFFSHORE NORTHERN NEW JERSEY AND SOUTHERN NEW YORK AND THE ENVIRONMENTAL IMPLICATIONS OF SAND REMOVAL FOR COASTAL AND BEACH RESTORATION

November 2004

Mark R. Byrnes

Physical Processes Project Manager, Co-Editor
(Applied Coastal Research and Engineering, Inc.)

Richard M. Hammer

Biological Component Project Manager, Co-Editor
(Continental Shelf Associates, Inc.)

With Contributions from:

Sean W. Kelley

Applied Coastal Research and Engineering, Inc.

Jessica L. Baker

Applied Coastal Research and Engineering, Inc.

David B. Snyder

Continental Shelf Associates, Inc.

Tim D. Thibaut

Barry A. Vittor & Associates, Inc.

Salvatore A. Zichichi

Applied Coastal Research and Engineering, Inc.

Luis M. Lagera, Jr.

Continental Shelf Associates, Inc.

Stephen T. Viada

Continental Shelf Associates, Inc.

Barry A. Vittor

Barry A. Vittor & Associates, Inc.

John S. Ramsey

Applied Coastal Research and Engineering, Inc.

Joseph D. Germano

Germano & Associates, Inc.

Prepared by:

Applied Coastal Research and Engineering, Inc.
766 Falmouth Road, Suite A-1
Mashpee, MA 02649

Prepared for:

U.S. Department of the Interior
Minerals Management Service
Leasing Division
Marine Minerals Branch
381 Elden Street, MS 4010
Herndon, VA 22070

In Cooperation with:

Continental Shelf Associates, Inc.
Barry A. Vittor & Associates, Inc.
Germano & Associates, Inc.

Contract Number 1435-01-01-CT-31118

ACKNOWLEDGMENTS

Numerous people contributed to the project titled *Environmental Surveys of Potential Borrow Areas Offshore Northern New Jersey and Southern New York and the Environmental Implications of Sand Removal for Coastal and Beach Restoration*, which was funded by the U.S. Department of the Interior, Minerals Management Service (MMS), Leasing Division, Marine Minerals Branch. Mr. Barry S. Drucker provided assistance and direction during the project as the MMS Contracting Officer's Technical Representative. Ms. Jane Carlson served as the MMS Contracting Officer.

Dr. Mark R. Byrnes of Applied Coastal Research and Engineering, Inc. (Applied Coastal) served as Project Manager; Physical Processes Component Manager; co-authored Sections 1.0 (Introduction), 2.1 (Offshore Sedimentary Environment), 2.2 (General Circulation), 3.0 (Regional Geomorphic Change), 5.1 (Currents and Circulation), 7.1 (Offshore Sand Resource Areas), 7.3 (Currents and Circulation), 7.4.1 (Historical Sediment Transport Patterns), 7.7 (Potential Cumulative Effects), and 8.0 (Conclusions); and was Co-Editor of the report. Dr. Richard M. Hammer of Continental Shelf Associates, Inc. (CSA) served as Biological Component Manager; authored Sections 7.5.1 (Effects of Offshore Dredging on Benthic Biota) and 7.5.2 (Recolonization Periods and Success); co-authored Sections 1.0 (Introduction) and 8.0 (Conclusions); and was Co-Editor of the report.

Other Applied Coastal personnel who participated in the project included Ms. Jessica L. Baker who was responsible for shoreline and bathymetric change data compilation and surface modeling and co-authored Sections 2.1 (Offshore Sedimentary Environment), 3.0 (Regional Geomorphic Change), and 7.4.1 (Historical Sediment Transport Patterns). Mr. Sean W. Kelley and Mr. John S. Ramsey co-authored Sections 4.0 (Assessment of Wave Climate Impact by Offshore Borrow Sites), 5.2 (Offshore Sediment Transport), 7.2 (Wave Transformation Modeling), 7.4.2 (Sediment Transport Modeling at Potential Borrow Sites), and 7.4.3 (Nearshore Sediment Transport Potential). Mr. Salvatore A. Zichichi co-authored Sections 2.2 (General Circulation), 5.1 (Currents and Circulation), and 7.3 (Currents and Circulation). Ms. Elizabeth Hunt was responsible for report compilation and editorial assistance during production of the report.

Other CSA personnel who contributed to the project included Mr. David B. Snyder, who served as Chief Scientist for the biological field surveys; authored the sections concerning fishes and squids throughout the document; and incorporated sections from other authors concerning infauna, epifauna, and discussion into the remainder of Section 6.0 (Biological Field Surveys) that he authored. Dr. Luis M. Lagera, Jr. was responsible for the spatial data files and exclusionary mapping. Dr. Alan D. Hart led the sampling design and statistical analyses for the biological data. Mr. Stephen T. Viada wrote the sections on sea turtles and marine mammals. Mr. Frank R. Johnson served as Operations Manager for the field surveys. Mr. Frederick B. Ayer, III and Mr. Lynwood R. Powell, Jr. directed operations for the field surveys. Ms. Karen Stokesbury assisted in literature and data collection. Ms. Melody B. Powell provided editorial assistance. Ms. Deborah Raffel supervised CSA support staff during production of the report.

Personnel from Barry A. Vittor & Associates, Inc. (BVA) contributing to the project included Dr. Barry A. Vittor, who served as Manager of BVA's responsibilities for the field surveys and report. Mr. Tim D. Thibaut authored the sections regarding infauna and epifauna throughout the document. He also wrote Section 6.4 (Discussion) concerning the biological field surveys. Mr. Marco Cianciola served as Scientist during the first field survey. Mr. J. Dobbs Lee served as Scientist during the second biological field survey. Ms. Linda W. Sierke supervised personnel associated with taxonomic identifications. Ms. Robbin R. Alley served as BVA's Data Manager.

Dr. Joseph D. Germano from Germano & Associates, Inc. was responsible for the sediment profile image aspects of the project. Mr. Dave Browning of Browning Environmental collected sediment profile images in the field.

Mr. James Nickels of Aqua Survey, Inc. provided the survey vessel, logistical support, and assistance at sea for the biological field surveys. Dr. Wayne C. Isphording from the University of South Alabama conducted the laboratory grain size analyses.

TABLE OF CONTENTS VOLUME I: MAIN TEXT

1.0 INTRODUCTION	1
1.1 BACKGROUND.....	2
1.2 STUDY AREA	3
1.3 STUDY PURPOSE AND OBJECTIVES.....	3
1.4 STUDY APPROACH.....	4
1.4.1 Borrow Site Locations and Characteristics	4
1.4.2 Wave Modifications.....	7
1.4.3 Sediment Transport Patterns.....	7
1.4.4 Benthic Ecological Conditions	10
1.4.5 Benthic Infaunal Evaluation	10
1.4.6 Project Scheduling Considerations.....	10
1.5 DOCUMENT ORGANIZATION	10
2.0 ENVIRONMENTAL SETTING	11
2.1 OFFSHORE SEDIMENTARY ENVIRONMENT	18
2.1.1 Seabed Morphology.....	20
2.1.2 Surface Sediment	23
2.1.3 Subsurface Deposits.....	27
2.1.4 Offshore Sand Resources	31
2.2 GENERAL CIRCULATION	38
2.2.1 Tidal Currents	39
2.2.2 Density Gradients	39
2.2.3 Wind Driven Currents	39
2.2.4 Low-Frequency Current.....	40
2.2.5 Nearshore Sediment Transport.....	40
2.3 BIOLOGY	41
2.3.1 Benthic Environment.....	41
2.3.1.1 Infauna	41
2.3.1.2 Epifauna	45
2.3.1.3 Demersal Fishes	46
2.3.2 Pelagic Environment.....	47
2.3.2.1 Squids	47
2.3.2.2 Fishes.....	48
2.3.2.3 Marine Turtles	50
2.3.2.4 Marine Mammals.....	52
3.0 REGIONAL GEOMORPHIC CHANGE	55
3.1 SHORELINE POSITION CHANGE	55
3.1.1 Physical Setting and Previous Studies	56
3.1.1.1 Physical Characteristics of Southwestern Long Island	57
3.1.1.2 Physical Characteristics of Northeastern New Jersey	57
3.1.1.3 Physical Characteristics of the New York Bight	58
3.1.1.4 Storms.....	60
3.1.1.5 Beach Nourishment and Structure Development.....	60
3.1.2 Shoreline Position Data Base	65
3.1.3 Historical Shoreline Change Trends	68

TABLE OF CONTENTS (Continued)

3.1.3.1 Southwestern Long Island.....	69
3.1.3.2 Northern New Jersey Shoreline Change.....	80
3.2 NEARSHORE BATHYMETRY CHANGE.....	90
3.2.1 Bathymetry Data Base and Potential Errors.....	90
3.2.2 Digital Surface Models.....	96
3.2.2.1 1927/37 Bathymetric Surface.....	96
3.2.2.2 1927/97 Bathymetric Surface.....	99
3.2.3 Shelf Sediment Transport Dynamics.....	99
3.2.4 Magnitude and Direction of Change.....	103
3.2.5 Net Longshore Sand Transport Rates.....	103
3.3 SUMMARY.....	104
4.0 ASSESSMENT OF WAVE CLIMATE IMPACT BY OFFSHORE BORROW SITES.....	106
4.1 ANALYSIS APPROACH.....	109
4.1.1 Wave Modeling.....	109
4.1.1.1 Input Spectra Development.....	110
4.1.1.2 Grid Development.....	115
4.1.2 Sediment Transport Potential.....	117
4.2 MODEL RESULTS.....	118
4.2.1 Wave Modeling.....	119
4.2.1.1 Offshore Southwestern Long Island.....	123
4.2.1.2 Offshore Northeastern New Jersey.....	125
4.2.2 Sediment Transport Potential.....	128
4.2.2.1 Model Comparison with Historical Shoreline Change.....	133
4.2.2.2 Significance of proposed dredging.....	135
4.3 SUMMARY.....	138
5.0 CIRCULATION AND SEDIMENT TRANSPORT DYNAMICS.....	140
5.1 CURRENTS AND CIRCULATION.....	140
5.1.1 Historical Data.....	140
5.1.1.1 Description and Analysis of Observed Currents.....	146
5.1.1.2 Tidal Currents.....	154
5.1.1.3 Summary of Flow Regimes at Offshore Borrow Sites.....	155
5.2 OFFSHORE SEDIMENT TRANSPORT.....	155
5.2.1 Determining Bottom Transport and Infilling Rates.....	156
5.2.2 Model Input Data.....	158
5.2.3 Infilling Model Results.....	160
6.0 BIOLOGICAL FIELD SURVEYS.....	162
6.1 BACKGROUND.....	162
6.2 METHODS.....	162
6.2.1 Survey Design.....	162
6.2.1.1 Spatial Data Files and Exclusionary Mapping.....	166
6.2.1.2 Water Column.....	166
6.2.1.3 Sediment and Infauna.....	166
6.2.1.4 Sediment Profile Imaging.....	167
6.2.1.5 Epifauna and Demersal Fishes.....	167
6.2.2 Field Methods.....	167

TABLE OF CONTENTS (Continued)

6.2.2.1 Vessel	167
6.2.2.2 Navigation	167
6.2.2.3 Water Column	167
6.2.2.4 Sediment and Infauna	168
6.2.2.5 Sediment Profile Imaging	168
6.2.2.6 Epifauna and Demersal Fishes	168
6.2.3 Laboratory Methods	168
6.2.3.1 Sediment	168
6.2.3.2 Sediment Profile Imaging	169
6.2.3.3 Infauna	173
6.2.4 Data Analysis	174
6.2.4.1 Water Column	174
6.2.4.2 Sediment	174
6.2.4.3 Infauna	174
6.2.4.4 Epifauna and Demersal Fishes	175
6.3 RESULTS	175
6.3.1 Water Column	175
6.3.2 Sediment	176
6.3.3 Sediment Profile Imaging	178
6.3.3.1 Site H1	179
6.3.3.2 Site H2	182
6.3.3.3 Site 3	182
6.3.3.4 Site 4	182
6.3.4 Infauna	182
6.3.4.1 Juvenile Surfclam	188
6.3.4.2 Cluster Analysis	191
6.3.4.3 Canonical Discriminant Analysis	192
6.3.5 Epifauna	192
6.3.6 Demersal Fishes	197
6.4 DISCUSSION	198
7.0 POTENTIAL EFFECTS	203
7.1 OFFSHORE SAND BORROW SITES	204
7.2 WAVE TRANSFORMATION MODELING	205
7.2.1 Offshore Southwestern Long Island	205
7.2.2 Offshore Northeastern New Jersey	206
7.3 CURRENTS AND CIRCULATION	206
7.4 SEDIMENT TRANSPORT	207
7.4.1 Historical Sediment Transport Patterns	208
7.4.2 Sediment Transport Modeling at Potential Borrow Sites	209
7.4.3 Nearshore Sediment Transport Potential	209
7.5 BENTHIC ENVIRONMENT	210
7.5.1 Effects of Offshore Dredging on Benthic Biota	211
7.5.1.1 Sediment Removal	211
7.5.1.2 Sediment Suspension/Dispersion	212
7.5.1.3 Sediment Deposition	214
7.5.2 Recolonization Periods and Success	215
7.5.2.1 Adaptations for Recolonization and Succession	215
7.5.2.2 Successional Stages	215

TABLE OF CONTENTS (Continued)

7.5.2.3	Recolonization Periods	217
7.5.2.4	Recolonization Success and Recovery	219
7.5.3	Predictions Relative to the Borrow Sites	220
7.5.3.1	Potential Benthic Effects	220
7.5.3.2	Potential Recolonization Periods and Success	222
7.6	PELAGIC ENVIRONMENT	224
7.6.1	Squids	224
7.6.1.1	Physical Injury	224
7.6.1.2	Attraction	225
7.6.1.3	Project Scheduling	225
7.6.2	Fishes	225
7.6.2.1	Physical Injury	225
7.6.2.2	Attraction	225
7.6.2.3	Turbidity	225
7.6.2.4	Noise	226
7.6.2.5	Project Scheduling	226
7.6.3	Marine Turtles	227
7.6.3.1	Physical Injury	227
7.6.3.2	Habitat Modification	228
7.6.3.3	Turbidity	228
7.6.3.4	Noise	228
7.6.3.5	Project Scheduling	229
7.6.4	Marine Mammals	229
7.6.4.1	Physical Injury	229
7.6.4.2	Turbidity	229
7.6.4.3	Noise	230
7.6.4.4	Project Scheduling	230
7.7	ESSENTIAL FISH HABITAT	230
7.8	POTENTIAL CUMULATIVE EFFECTS	237
8.0	CONCLUSIONS	238
8.1	WAVE TRANSFORMATION MODELING	238
8.2	CIRCULATION AND SEDIMENT TRANSPORT DYNAMICS	240
8.2.1	Historical Sediment Transport Patterns	241
8.2.2	Sediment Transport Modeling at Potential Borrow Sites	242
8.2.3	Nearshore Sediment Transport Potential	242
8.3	BENTHIC ENVIRONMENT	243
8.4	PELAGIC ENVIRONMENT	244
8.5	SYNTHESIS	245
9.0	LITERATURE CITED	246

TABLE OF CONTENTS

VOLUME II: APPENDICES

APPENDIX A. HIGH-WATER SHORELINE POSITION CHANGE FOR NEW YORK.....	A-1
APPENDIX B. HIGH-WATER SHORELINE POSITION CHANGE FOR NEW JERSEY.....	B-1
APPENDIX C. WAVE TRANSFORMATIONAL NUMERICAL MODELING	C-1
C1. EXISTING CONDITIONS WAVE TRANSFORMATION RESULTS.....	C-1
C2. WAVE HEIGHT DIFFERENCE PLOTS: POST-DREDGING VERSUS EXISTING CONDITIONS	C-24
APPENDIX D. BIOLOGICAL FIELD SURVEY DATA	D-1
APPENDIX E. SPATIAL DATA FILES, EXCLUSIONARY MAPPING, AND SAMPLING DESIGN FOR BIOLOGICAL FIELD SURVEYS	E-1
E1. INTRODUCTION	E-2
E2. SPATIAL DATA FILES.....	E-2
E3. EXCLUSIONARY MAPPING	E-3
E4. FIELD SURVEY DESIGN	E-4

LIST OF FIGURES

Figure	Page
Figure 1-1. Physical setting for the northeastern New Jersey and southwestern Long Island study area and key geographic features.....	3
Figure 1-2. Identified sand borrow sites within the project study area relative to the Federal-State boundary.....	6
Figure 1-3. Grab samples collected during September 2001 (top) and June 2002 (bottom) within and adjacent to Borrow Sites H1 and H2.....	8
Figure 1-4. Grab samples collected during September 2001 (top) and June 2002 (bottom) adjacent to Borrow Sites 3, 4W, and 4E.	9
Figure 2-1. Physical setting of the New York and New Jersey coastlines.	12
Figure 2-2. Coastal geomorphic components of New York and New Jersey. (Adapted from Uptegrove et. al., 1995 and Taney, 1961).....	13
Figure 2-3. Geologic Units and average sediment grain size along the northern New Jersey coast (Geologic data from NJDEP GIS Data CD and sediment sample data from USACE, 1995).	14
Figure 2-4. Narrow barrier spit seaward of the north-directed outflow channel for the Navesink and Shrewsbury Rivers (USGS TerraServer image, 13 March 1995).	15
Figure 2-5. Net longshore transport rates estimated along Long Island and New Jersey coasts. Littoral transport rates obtained from Taney (1961) and Caldwell (1966).	17
Figure 2-6. Middle Atlantic continental shelf illustrating dominant surface sedimentary facies as >75% sand sized material (adapted from Duane and Stubblefield, 1988; data from Emery and Uchupi, 1965; Uchupi, 1968; Swift, 1976).	19
Figure 2-7. Middle Atlantic Province showing historical strandlines and sand ridge orientations on the continental shelf (adapted from Duane and Stubblefield, 1988).	20
Figure 2-8. Prominent geomorphic features of the New York Bight continental shelf.....	21
Figure 2-9. Continental Shelf sediment distribution in the New York Bight (adapted from Poppe et al., 1994).....	24
Figure 2-10. Surface sediment distribution within the inner New York Bight (adapted from Williams and Duane, 1974).	26
Figure 2-11. Inner New York Bight continental shelf sediment classification based on backscatter imagery (adapted from Schwab et al., 2002).	27
Figure 2-12. Locations of previous geologic investigations within the New York Bight region.	28

LIST OF FIGURES (Continued)

Figure	Page
Figure 2-13. Stratigraphic characterization interpreted from seismic reflection profiles (from Williams, 1976).	30
Figure 2-14. Seismic-reflection profile showing Upper Cretaceous coastal-plain strata and overlying Quaternary sediments (from Schwab et al., 2002).....	31
Figure 2-15. Locations of borrow areas, vibracores, and seismic reflection profile lines collected as part of the Alpine Ocean Seismic Survey (1988).....	33
Figure 2-16. Borrow Areas M and N defined by Williams (1976) with vibracores used to delineate suitable sediment thicknesses for the areas. Borrow Area M was assigned a minimum potential thickness of 5.5 m and Borrow Area N was assigned a range of 1.8 to 3.2 m of suitable sediment. Interpretations of vibracores are shown in Figure 2-17.	34
Figure 2-17. Lithologic interpretation of cores collected as part of the sewer outfall study. Core locations are shown in Figure 2-16. Depths are shown in feet below MSL (from Williams, 1976).....	35
Figure 2-18. Isopach map of modern shelf sediment, southern Long Island (from Foster et al., 1999).	36
Figure 2-19. Thickness of the Quaternary (Pleistocene and Holocene) sedimentary deposits near Borrow Site 3 (after Schwab et al., 2002).	37
Figure 3-1. Geographic locations within the New York Bight.....	56
Figure 3-2. Net littoral transport rates along beaches in the study area (Taney, 1961; Caldwell, 1966).....	58
Figure 3-3. Prominent features on the New York Bight continental shelf.	59
Figure 3-4. Documented beach nourishment activity from Rockaway Point to Moriches Inlet, NY and Sandy Hook to Barnegat Inlet, NJ.....	61
Figure 3-5. Southwestern Long Island reaches between Rockaway Point and Moriches Inlet, NY.	69
Figure 3-6. Westward island migration along south shore beaches of Long Island, 1873/88 to 1933/34.	70
Figure 3-7. Shoreline change along south shore beaches of Long Island, 1873/88 to 1933/34.	72
Figure 3-8. Shoreline change along south shore beaches of Long Island, 1933/34 to 1983.	74
Figure 3-9. Incremental changes in shoreline position adjacent to the jetty at the western end of Rockaway Beach, 1933/34 to 1983.	75
Figure 3-10. Incremental changes in shoreline position adjacent to the jetty at the western end of Long Beach, 1933/34 to 1983.....	75
Figure 3-11. Shoreline change along south shore beaches of Long Island, 1983 to 1991/97.	78

LIST OF FIGURES (Continued)

Figure	Page
Figure 3-12. Cumulative shoreline change for southern Long Island beaches between Rockaway and Moriches Inlets, 1873/88 to 1991/97.....	80
Figure 3-13. Northern New Jersey shoreline reaches, Sandy Hook to Barnegat Inlet, NJ.....	82
Figure 3-14. Shoreline change along northern beaches of New Jersey, 1836/39 to 1855/75.	83
Figure 3-15. Shoreline change along northern beaches of New Jersey, 1855/75 to 1932/33.	84
Figure 3-16. Shoreline change along northern beaches of New Jersey, 1932/33 to 1977.	87
Figure 3-17. Shoreline change along northern New Jersey beaches, 1836/39 to 1977.....	89
Figure 3-18. Locations of 1927/37 bathymetric data used to fill gaps in the most recent surface.....	92
Figure 3-19. Sandy Hook, NJ tidal benchmark elevation information.....	93
Figure 3-20. Sandy Hook, NJ sea level change, 1932 to 2002.....	93
Figure 3-21. Beach profile location for coastal New York and New Jersey.	94
Figure 3-22. Line pairs used to estimate potential uncertainty for the 1927/37 surface.	95
Figure 3-23. Depths extracted along Line Pair 1 for determining potential surface uncertainty.....	95
Figure 3-24. 1927/37 bathymetric surface within the New York Bight.	97
Figure 3-25. Three-dimensional view of the 1927/37 bathymetric surface in the New York Bight region.....	98
Figure 3-26. 1927/97 bathymetric surface.	100
Figure 3-27. Three-dimensional representation of the 1927/97 bathymetric surface.	101
Figure 3-28. Bathymetric change in the New York Bight between 1927/37and 1927/97.....	102
Figure 4-1. Example of spatial/temporal variability method for determining significance of borrow site dredging impacts (Kelley et al., 2004). The difference plot illustrates modeled change in net transport potential (solid black and dotted lines) resulting from two different dredging scenarios at the proposed borrow site. The plot also illustrates the dredging significance envelope ($\pm 0.5\sigma$) determined for this shoreline (gray-shaded area). The 4.5 m excavation (dotted line, $24 \times 10^6 \text{ m}^3$) exceeds the significance envelope boundary and would be rejected. However, the 2.3 m excavation (solid line, $12 \times 10^6 \text{ m}^3$) does not exceed the natural variability envelope, and would be acceptable.	108
Figure 4-2. Wave and current vectors used in STWAVE. Subscript <i>a</i> denotes values in the <i>absolute</i> frame of reference, and subscript <i>r</i> denotes values in the <i>relative</i> frame of reference (with currents).....	110

LIST OF FIGURES (Continued)

Figure	Page
Figure 4-3. Shoreline of northeastern New Jersey and southwestern Long Island with coarse grid limits and OCTI wave input data station locations.....	112
Figure 4-4. Wave height and period roses for OCTI hindcast data offshore southwestern Long Island (Station OCTI-NY) for the 20-year period January 1980 to December 1999. Direction indicates from where waves were traveling relative to true north. Length of gray tone segments indicates percent occurrence for each wave height and period range. Combined length of segments in each sector indicates percent occurrence of waves from that direction.....	112
Figure 4-5. Wave height and period roses for OCTI hindcast data offshore northeastern New Jersey (OCTI-NJ) for the 20-year period between January 1980 and December 1999. Direction indicates from where waves were traveling relative to true north. Length of gray tone segments indicates percent occurrence for each wave height and period range. Combined length of segments in each sector indicates percent occurrence of waves from that direction.....	113
Figure 4-6. STWAVE input spectrum developed using 20-year OCTI hindcast spectral data. Plots show a) frequency distribution of energy at peak direction, b) directional distribution of energy at peak frequency, and c) surface plot of two-dimensional energy spectrum ($H_{mo} = 0.9$ m, $\theta_{mean} = 130^\circ$ grid relative).	113
Figure 4-7. Coarse model grid (200 x 200 m spacing) used for STWAVE simulations offshore southwestern Long Island. Depths are relative to NAVD. Borrow site locations are indicated by solid black lines, and fine grid limits are indicated by a dashed line.....	115
Figure 4-8. Color contour plot of coarse model grid (200 m x 200 m grid spacing) used for STWAVE model simulations of waves offshore Shark River Inlet, New Jersey. Depths are relative to NAVD. Borrow site locations are indicated by solid black lines, and fine grid limits are indicated by a dashed line.....	116
Figure 4-9. STWAVE output for the coarse grid (200 x 200 m grid cells) offshore Shark River Inlet in northeastern New Jersey (model case 13B; $H_{mo} = 1.1$ m, $T_p = 7.7$ sec, $\theta_{peak} = 113^\circ$). Color contours indicate H_{mo} wave height. Vectors indicate mean wave direction. Seafloor contours are shown as black lines at a 10 m interval.....	119
Figure 4-10. STWAVE output for the fine grid (20 x 20 m grid cells) offshore Shark River Inlet in northeastern New Jersey (model case 13B; $H_{mo} = 1.1$ m, $T_p = 7.7$ sec, $\theta_{peak} = 113^\circ$). Color contours indicate H_{mo} wave height. Vectors indicate mean wave direction. Seafloor contours are shown as black lines at a 10-m interval.....	120
Figure 4-11. Wave height difference plot ($H_{difference} = H_{post} - H_{existing}$) for coarse grid model of offshore Shark River Inlet. Seafloor contours are shown at a 10-m interval.....	121

LIST OF FIGURES (Continued)

Figure	Page
Figure 4-12. Wave height difference plot for fine grid model simulations offshore Shark River Inlet. Seafloor contours are shown at a 10-m interval.....	122
Figure 4-13. STWAVE model output for offshore southwestern Long Island, wave Case 11A ($H_s = 1.3$ m, $T_{peak} = 9.1$ sec, $\theta_{peak} = 112^\circ$). Color contours indicate wave height, and vectors show mean direction of wave propagation. Seafloor contours are shown at 10-m intervals.	123
Figure 4-14. STWAVE model output for offshore southwestern Long Island, wave Case 14A ($H_s = 1.6$ m, $T_{peak} = 9.1$ sec, $\theta_{peak} = 137^\circ$). Color contours indicate wave height, and vectors show mean direction of wave propagation. Seafloor contours are shown at 10-m intervals.	124
Figure 4-15. Wave height change between existing and post-dredging conditions for offshore southwestern Long Island, wave Case 11A ($H_s = 1.3$ m, $T_{peak} = 9.1$ sec, $\theta_{peak} = 112^\circ$). Seafloor contours are shown at 10-m intervals.	124
Figure 4-16. Wave height change between existing and post-dredging conditions for offshore southwestern Long Island, wave Case 14A ($H_s = 1.6$ m, $T_{peak} = 9.1$ sec, $\theta_{peak} = 137^\circ$). Seafloor contours are shown at 10-m intervals.	125
Figure 4-17. STWAVE output for offshore northeastern New Jersey, wave Case 11B ($H_s = 1.3$ m, $T_{peak} = 9.1$ sec, $\theta_{peak} = 88^\circ$). Color contours indicate wave height, and vectors show mean direction of wave propagation. Bottom contours are also shown at 10-m intervals.	126
Figure 4-18. STWAVE output for offshore northeastern New Jersey, wave Case 16B ($H_s = 1.3$ m, $T_{peak} = 7.7$ sec, $\theta_{peak} = 158^\circ$). Color contours indicate wave height, and vectors show mean direction of wave propagation. Bottom contours are also shown at 10-m intervals.	127
Figure 4-19. Wave height change between existing and post-dredging conditions for offshore northeastern New Jersey, wave Case 11B ($H_s = 1.3$ m, $T_{peak} = 9.1$ sec, $\theta_{peak} = 88^\circ$). Seafloor contours are shown at 10-m intervals.	128
Figure 4-20. Wave height change between existing and post-dredging conditions for offshore northeastern New Jersey, wave Case 16B ($H_s = 1.3$ m, $T_{peak} = 7.7$ sec, $\theta_{peak} = 158^\circ$). Seafloor contours are shown at 10-m intervals.	129
Figure 4-21. Average annual sediment transport potential (solid black line) computed for the shoreline landward of Borrow Sites 3, 4W, and 4E. Net transport potential curves determined for 20 individual years of wave hindcast data are indicated by the gray shaded area. The $\pm 0.5\sigma$ significance envelope (black dot-dash lines) about the mean net transport was determined using the 20 net potential curves.	130
Figure 4-22. Average net transport potential (black line) with gross westerly- and easterly-directed transport potential (red and blue lines, respectively) for the shoreline landward of Borrow Sites 3, 4W, and 4E.	131

LIST OF FIGURES (Continued)

Figure	Page
Figure 4-23. Average annual sediment transport potential (solid black line) computed for the shoreline landward of Borrow Sites H1 and H2. Net transport potential curves determined for 20 individual years of wave hindcast data are indicated by the gray shaded area. The $\pm 0.5\sigma$ significance envelope (black dot-dash lines) about the mean net transport was determined using the 20 net potential curves.	132
Figure 4-24. Average net transport potential (black line) with gross southerly- and northerly-directed transport potential (red and blue lines, respectively) for the shoreline landward of Borrow Sites H1 and H2.....	133
Figure 4-25. Historical shoreline change and gradient of modeled transport potential (dQ/dy) for the modeled shoreline landward of Sites 3, 4W, and 4E offshore southwestern Long Island. The middle plot illustrates measured shoreline change for the period 1878 to 1997. The gradient in transport potential was determined using the total net transport computed using 20 years of wave hindcast data.....	135
Figure 4-26. Historical shoreline change and gradient of modeled transport potential (dQ/dy) for the modeled shoreline landward of Sites H1 and H2 offshore northeastern New Jersey. The middle plot illustrates measured shoreline change for the period 1855/75 to 1933. The gradient in transport potential was determined using the total net transport computed using 20 years of wave hindcast data.....	136
Figure 4-27. Transport potential difference between existing and post-dredging conditions, with transport significance envelope for the shoreline landward of Borrow Sites 3, 4W, and 4E. Negative change indicates that the post-dredging transport potential is more southerly than the computed existing transport potential.....	137
Figure 4-28. Transport potential difference between existing and post-dredging conditions, with transport significance envelope for the shoreline landward of Borrow Sites H1 and H2. Negative change indicates that the post-dredging transport potential is more southerly than the computed existing transport potential.....	138
Figure 5-1. Current meter and borrow site locations in the New York Bight.	141
Figure 5-2. Location of current meter mooring Station D on the Long Island shelf to the east of the Hudson Shelf Valley (~26 m water depth; see Figure 5-1) showing the location of the tripod mooring, bottom photographs, and sediment grab samples. The photograph below the map illustrates bottom topography and sediment texture representative of the area surrounding the mooring tripod (from Butman et al., 2003).....	142

LIST OF FIGURES (Continued)

Figure	Page	
Figure 5-3.	Location of current meter mooring Station E on the northern New Jersey shelf to the west of the Hudson Shelf Valley (~25 m water depth; see Figure 5-1) showing the location of the tripod mooring, bottom photographs, and sediment grab samples. The photographs below the map illustrate bottom topography and sediment texture representative of the low backscatter intensity area west of the tripod (blue) and the high backscatter intensity area east of the tripod (green to red) (from Butman et al., 2003).	144
Figure 5-4.	Hourly averaged bottom current speed and variability at Station D (December 5, 1999 to April 15, 2000 at 25 meters below the surface [mbs]) and Station E (December 4, 1999 to April 15, 2000 at 24.6 mbs). Low-passed plots exclude tidal currents (from Butman et al., 2003).....	145
Figure 5-5.	Speed and direction for surface currents at Station D, December 5, 1999 to April 15, 2000. The percentage of reliable data points is provided in the lower left corner of each plot. Current speeds are represented by percent occurrence and shading in the inter-cardinal bars. The length of each bar represents total percent occurrence by direction (data from Butman et al., 2003).	145
Figure 5-6.	Summer current flows in the New York Bight. Left panel: modeled currents with no wind and no river inflow. Right panel: modeled current flows with southwesterly wind of 28 dynes/cm ² (~3.9 m/s) and Hudson River summer inflow rates (from Scheffner et al., 1994).	146
Figure 5-7.	Surface current speed and direction east of the Hudson Shelf Valley for Station D, December 5, 1999 to April 15, 2000. Current speeds are represented by percent occurrence and shading in the inter-cardinal bars. The length of each bar represents total percent occurrence by direction (data from Butman et al., 2003).....	147
Figure 5-8.	Surface current speed and direction west of the Hudson Shelf Valley for Station E, December 4, 1999 to April 15, 2000. Current speeds are represented by percent occurrence and shading in the inter-cardinal bars. The length of each bar represents total percent occurrence by direction (data from Butman et al., 2003).....	148
Figure 5-9.	Bottom current speed (25 mbs) and direction east of the Hudson Shelf Valley for Station D, December 5, 1999 to April 15, 2000. Current speeds are represented by percent occurrence and shading in the inter-cardinal bars. The length of each bar represents total percent occurrence by direction (data from Butman et al., 2003).	149
Figure 5-10.	Bottom current speed (24.6 mbs) and direction west of the Hudson Shelf Valley for Station E, December 4, 1999 to April 15, 2000. Current speeds are represented by percent occurrence and shading in the inter-cardinal bars. The length of each bar represents total percent occurrence by direction (data from Butman et al., 2003).	150

LIST OF FIGURES (Continued)

Figure	Page
Figure 5-11. Wind speed and direction from NDBC Buoy #40255; December 1, 1999 to April 30, 2000. Wind speeds are represented by percent occurrence and shading in the inter-cardinal bars. The length of each bar represents total percent occurrence by direction (data from Butman et al., 2003).....	151
Figure 5-12. Monthly observed mean current flow and the variability (shown as an ellipse centered around the tip of the mean flow arrow) for near-bottom current for Station D. Up is to the north and right is to the east. The current ellipse calculated from hour-averaged data is typically dominated by tidal currents, whereas low-pass filtered mean flow has tidal currents removed (from Butman et al., 2003).....	152
Figure 5-13. Monthly observed mean current flow and the variability (shown as an ellipse centered around the tip of the mean flow arrow) for near-bottom current for Station E. Up is to the north and right is to the east. The current ellipse calculated from hour-averaged data is typically dominated by tidal currents, whereas low-pass filtered mean flow has tidal currents removed (from Butman et al., 2003).....	152
Figure 5-14. Wind speed and direction versus surface and bottom currents, March 19 to 31, 2000 (data from Butman et al., 2003).....	153
Figure 5-15. Tidal ellipses for major tidal constituents at 15 m below the surface (adapted from Butman et al., 2003).....	154
Figure 6-1. Sand Borrow Sites H1, H2, 3, and 4 offshore New Jersey and New York.	163
Figure 6-2. Environmental features, area excluded, and sampling stations relative to Sand Borrow Site H1 offshore New Jersey.	164
Figure 6-3. Environmental features and sampling stations relative to Sand Borrow Site H2 offshore New Jersey.	164
Figure 6-4. Environmental features, area excluded, and sampling stations relative to Sand Borrow Site 3 offshore New York.	165
Figure 6-5. Environmental features, area excluded, and sampling stations relative to Sand Borrow Site 4 offshore New York.	165
Figure 6-6. The successional change in benthic community following a disturbance over time (top) or over distance from a source of pollution (bottom) is illustrated (from Rhoads and Germano, 1982, 1986).	173
Figure 6-7. Temperature and salinity profiles recorded during the September 2001 Survey 1 in Sand Borrow Sites H1, H2, 3, and 4 offshore New Jersey and New York.	176
Figure 6-8. Temperature and dissolved oxygen (DO) profiles recorded during the September 2001 Survey 1 in Sand Borrow Sites H1, H2, 3, and 4 offshore New Jersey and New York.	177
Figure 6-9. Temperature and salinity profiles recorded during the June 2002 Survey 2 in Sand Borrow Sites H1, H2, 3, and 4 offshore New Jersey and New York.	177

LIST OF FIGURES (Continued)

Figure	Page
Figure 6-10. Temperature and dissolved oxygen (DO) profiles recorded during the June 2002 Survey 2 in Sand Borrow Sites H1, H2, 3, and 4 offshore New Jersey and New York.	178
Figure 6-11. Sediment profile image from Site 3, Station 1 showing the pebble to granule-sized layer of gravel on top of poorly sorted medium to coarse sands. Scale: width of image = 16.8 cm.	180
Figure 6-12. Sediment profile image from Site H1, Station 1 showing small-scale ripples on the sediment surface. Scale: width of image = 16.7 cm.	181
Figure 6-13. Sediment profile image from Site H1, Station 2 showing a clear gradation from fine sand to finer silt/clay particles at the bottom of the image (arrow). Scale: width of image = 16.8 cm.	181
Figure 6-14. Sediment profile image from Site H1, Station 1 showing one of the numerically dominant polychaetes (<i>Polygordius</i>) found in grab samples from this location. Scale: width of image = 16.7 cm.	184
Figure 6-15. Replicate sediment profile images from site H1, Station 4 showing buried sand dollars (<i>Echinarachnius parma</i>) (arrows). Note the hermit crab (circle) on the sediment surface in the image on the left. Scale: width of image = 16.7 cm.	184
Figure 6-16. Both replicate sediment profile images from Site H2, Station 3 showed a layer of fine detritus (arrow) on the sediment surface. Note the bisected edge of a partially buried sand dollar (<i>Echinarachnius parma</i>) on the right side of image (circle). Scale: width of image = 16.7 cm.	185
Figure 6-17. Sediment profile image from Site H2, Station 3 showing a prominent tube of the polychaete <i>Diopatra</i> projecting above the sediment-water interface. Scale: width of image = 16.7 cm.	185
Figure 6-18. Sediment profile image from Site 3, Station 3 showing well-sorted, rippled, granitic fine sands. Scale: width of image = 16.7 cm.	186
Figure 6-19. Sediment profile image from Site 3, Station 3 showing two gammarid amphipods in the upper right corner swimming above the rippled fine sandy bottom. Scale: width of image = 16.7 cm.	186
Figure 6-20. Sediment profile image from Site 4, Station 7 showing a sharply defined arcuate bedform with an active mobile surface layer (arrow). Scale: width of image = 16.7 cm.	187
Figure 6-21. Sediment profile image from Site 4, Station 6 showing partially buried sand dollars (<i>Echinarachnius parma</i>) found at many station in this site. Scale: width of image = 16.7 cm.	187
Figure 6-22. Normal cluster analysis of infaunal samples collected during the September 2001 Survey 1 and June 2002 Survey 2 in Sand Borrow Sites H1, H2, 3, and 4 offshore New Jersey and New York.	193

LIST OF FIGURES (Continued)

Figure	Page
Figure 6-23. Station Groups A through C formed by normal cluster analysis of infaunal samples collected during the September 2001 Survey 1 and June 2002 Survey 2 in Sand Borrow Sites H1, H2, 3, and 4 offshore New Jersey and New York. Two outlying samples are represented by an X.....	194
Figure 6-24. Inverse cluster analysis of infaunal samples collected during the September 2001 Survey 1 and June 2002 Survey 2 in Sand Borrow Sites H1, H2, 3, and 4 offshore New Jersey and New York.....	195

LIST OF TABLES

Table	Page
Table 1-1. Sand resource characteristics at potential borrow sites offshore northeastern New Jersey and southwestern Long Island, NY.....	6
Table 2-1. Calculated versus published excavation depths determined for sand borrow sites offshore southwestern Long Island and northeastern New Jersey.....	37
Table 3-1. Notable storm events recorded for the New York Bight region.	60
Table 3-2. Documented beach nourishment events, Rockaway Inlet to Moriches Inlet, NY (data are in thousands of cubic meters from Kana, 1999).....	62
Table 3-3. Documented beach nourishment events, Sandy Hook to Barnegat Inlet, NJ (data are in thousands of cubic meters from Valverde et al. (1999) and USACE, NY District).....	62
Table 3-4. Inlet management activities from Rockaway to Moriches Inlet, NY and Sandy Hook to Manasquan Inlet, NJ.....	65
Table 3-5. Long Island, NY shoreline source data characteristics.....	66
Table 3-6. Northeastern New Jersey shoreline source data characteristics.....	67
Table 3-7. Estimates of potential error associated with Long Island, NY and northeastern New Jersey shoreline position surveys.	68
Table 3-8. Bathymetry source data characteristics.....	91
Table 4-1. Input wave spectra parameters used for existing and post-dredging STWAVE runs for modeled borrow sites offshore Jones Inlet, New York.	114
Table 4-2. Input wave spectra parameters used for existing and post-dredging STWAVE runs for modeled borrow sites offshore Shark River Inlet, New Jersey.....	114
Table 4-3. Numerical grid dimensions for offshore (coarse) and nearshore (fine) grids. Dimensions are given as cross-shore x along-shore.....	117
Table 4-4. Sand resource characteristics at potential borrow sites offshore northeastern New Jersey and southwestern Long Island, NY.....	117
Table 5-1. Wave model input conditions used to compute offshore sediment transport potential for borrow sites offshore northeastern New Jersey. STWAVE model output from each modeled condition, and at each borrow site perimeter grid node, was used as input to the wave-current interaction model used to determine bottom sediment transport potential.	158
Table 5-2. Wave model input conditions used to compute offshore sediment transport potential for borrow sites offshore southwestern Long Island. STWAVE model output from each modeled condition, and at each borrow site perimeter grid node, was used as input to the wave-current interaction model used to determine bottom sediment transport potential.	159

LIST OF TABLES (Continued)

Table	Page
Table 5-3.	Surface currents used to compute offshore sediment transport potential for sites offshore northeastern New Jersey based on the analysis in Section 5.1. Currents were binned by four compass sectors (N, E, S and W) and magnitude (<10, 10 to 20, 20 to 30, and >30 cm/sec). 159
Table 5-4.	Surface currents used to compute offshore sediment transport potential for sites offshore southwestern Long Island based on the analysis in Section 5.1. Currents were binned by four compass sectors (N, E, S and W) and magnitude (<10, 10 to 20, 20 to 30, and >30 cm/sec). 160
Table 5-5.	Sand resource and bottom characteristics at potential borrow sites offshore northeastern New Jersey and southwestern Long Island, NY..... 160
Table 5-6.	Sand resource characteristics and transport rates at potential borrow sites offshore northeastern New Jersey and southwestern Long Island, NY..... 161
Table 6-1.	Sampling plan summary for the September 2001 Survey 1 and June 2002 Survey 2 offshore New Jersey and New York. 163
Table 6-2.	Sediment type summary from grab samples for the September 2001 Survey 1 and June 2002 Survey 2 in the sand borrow sites and adjacent stations offshore New Jersey and New York. 179
Table 6-3.	Ten most abundant taxa in grab samples from Sand Borrow Sites H1, H2, 3, and 4 and Adjacent Areas NJA and NYA for the September 2001 Survey 1 offshore New Jersey and New York. 183
Table 6-4.	Ten most abundant taxa in grab samples from Sand Borrow Sites H1, H2, 3, and 4 and Adjacent Areas NJA and NYA for the June 2002 Survey 2 offshore New Jersey and New York. 189
Table 6-5.	Summary of infaunal statistics for the September 2001 Survey 1 and June 2002 Survey 2 in Sand Borrow Sites H1, H2, 3, and 4 and Adjacent Areas NJA and NYA offshore New Jersey and New York. 190
Table 6-6.	Occurrence and density of juvenile surfclam, <i>Spisula solidissima</i> , in grab samples taken in Sand Borrow Sites H1, H2, 3, and 4 and Adjacent Areas NJA and NYA during the September 2001 Survey 1 and June 2002 Survey 2 offshore New Jersey and New York. 191
Table 6-7.	Infaunal species groups resolved from inverse cluster analysis of all samples collected during the September 2001 Survey 1 and June 2002 Survey 2 in the four sand borrow sites and adjacent stations offshore New Jersey and New York. 196
Table 6-8.	Epifauna and demersal fishes collected by mongoose trawl during the September 2001 Survey 1 of the four sand borrow sites offshore New Jersey and New York. 197
Table 6-9.	Epifauna and demersal fishes collected by mongoose trawl during the June 2002 Survey 2 of the four sand borrow sites offshore New Jersey and New York. 199

LIST OF TABLES (Continued)

Table	Page
Table 7-1. Invertebrate species and life stages with Essential Fish Habitat identified in the project area (source Mid-Atlantic Fishery Management Council, 1998a ¹ , b ²).....	232
Table 7-2. Coastal shark species and life stages with Essential Fish Habitat identified in the project area (source Mid-Atlantic Fishery Management Council, 1999 ¹ ; National Marine Fisheries Service, 1999 ²).....	233
Table 7-3. Coastal pelagic fish species and life stages with Essential Fish Habitat identified in the project area (source Reid et al., 1999 ¹ ; Fahay et al., 1999 ² ; Mid-Atlantic Fishery Management Council, 1999 ³).....	234
Table 7-4. Demersal fish species and life stages with Essential Fish Habitat identified in the project area (source Steimle et al., 1999 ¹ ; New England Fishery Management Council, 2004 ² ; Mid-Atlantic Fishery Management Council, 1998c ³ ; Chang et al., 1999 ⁴).....	235
Table 7-5. Highly migratory fish species and life stages with Essential Fish Habitat identified in the project area (source National Marine Fisheries Service, 1999).....	236
Table 7-6. Summary matrix of impact producing factors and potential effects on members of managed species groups and their Essential Fish Habitat expected from dredging the sand borrow sites offshore of northern New Jersey and southern New York.....	237

LIST OF ABBREVIATIONS

μ	micron
ADCP	Acoustic Doppler Current Profiler
ASTM	American Society for Testing and Materials
BASS	Benthic Acoustic Stress Sensor
BVA	Barry A. Vittor & Associates, Inc.
CEQ	Council on Environmental Quality
CERC	Coastal Engineering Research Center
CETAP	Cetacean and Turtle Assessment Program
cm	centimeter
CO-OPS	Center for Operational Oceanographic Products and Services
CSA	Continental Shelf Associates, Inc.
CTD	Conductivity-Temperature-Depth Sensor
deg	degrees
DGPS	Differential Global Positioning System
EA	Environmental Assessment
EFH	Essential Fish Habitat
EIS	Environmental Impact Statement
FMP	Fishery Management Plan
FR	Federal Register
ft	feet
GIS	Geographic Information System
ICONS	Inner Continental Shelf Sediment and Structure (USACE program)
kg	kilogram
km	kilometers
LEO-15	Long-term Ecosystem Observatory at 15 m water depth
LPIL	Lowest Practical Identification Level
m	meter
MAFMC	Mid-Atlantic Fisheries Management Council
MAVS	Modular Acoustic Velocity Sensor
mbs	meters below surface
mcm	million cubic meters
mg/l	milligrams per liter
mm	millimeter
MMS	Minerals Management Service
MSL	Mean Sea Level
mt	metric tons
NAD83	North American Datum of 1983
NAVD	North American Vertical Datum of 1988
NDBC	National Data Buoy Center
NEFMC	New England Fisheries Management Council
NEFSC	Northeast Fisheries Science Center
NEPA	National Environmental Policy Act
NGDC	National Geophysical Data Center
NJBPN	New Jersey Beach Profile Network
NJDEP	New Jersey Department of Environmental Protection
NMFS	National Marine Fisheries Service
NOAA	National Oceanic and Atmospheric Administration
NOS	National Ocean Service
OCS	Outer Continental Shelf
OCSLA	Outer Continental Shelf Lands Act
OCTI	Offshore & Coastal Technologies, Inc.
ppt	parts per thousand

LIST OF ABBREVIATIONS (Continued)

REF/DIF S	Refraction/Diffraction Model for Spectral Wave Conditions
RPD	Redox Potential Discontinuity
sec	seconds
SOD	Sediment Oxygen Demand
SPI	Sediment Profile Imaging
STWAVE	Steady-State Spectral Wave Model
SWAN	Simulation of Waves Nearshore
USACE	U.S. Army Corps of Engineers
USC&GS	U.S. Coast and Geodetic Survey
USDOI	U.S. Department of the Interior
USFWS	U.S. Fish and Wildlife Service
USGS	U.S. Geological Survey
UTM	Universal Transverse Mercator
WES	Waterways Experiment Station
WIS	Wave Information Study
yr	year

1.0 INTRODUCTION

The U.S. Department of the Interior (USDOI), Minerals Management Service (MMS), has responsibility for managing all mineral resources on the Federal Outer Continental Shelf (OCS), a zone that extends from three miles seaward of State coastline boundaries to 200 miles offshore. Although most interest in this zone relates to oil and gas resources, the potential for exploitation of sand resources as a source for beach and barrier island restoration has grown rapidly in the last several years as similar resources in State waters are being depleted or contaminated. Existing regulations governing offshore sand and gravel mining provide a framework for comprehensive environmental protection during operations. Specific requirements exist for evaluations and lease stipulations that include appropriate mitigation measures (Hammer et al., 1993; Woodworth-Lynas and Davis, 1996). Guidelines for protecting the environment stem from a wide variety of laws, including the OCS Lands Act (OCSLA), National Environmental Policy Act (NEPA), Endangered Species Act, Marine Mammal Protection Act, and others. Regulations require activities to be conducted in a manner that prevents or minimizes the likelihood of any occurrences that may cause damage to the environment. The MMS takes a case-by-case approach in conducting environmental analyses, as required by NEPA and Council on Environmental Quality (CEQ) regulations.

Houston (1995, 2002) discussed the value of beaches and their maintenance through beach nourishment to America's economy. Not only are beaches the dominant component of most coastal economies, but they also provide protection against high winds and waves associated with storms. This is particularly true in northern New Jersey and along the south shore of Long Island (New York) where coastal development has flourished since the early 1900s. In fact, some of the earliest beach erosion control structures along the coast of New Jersey were built in the 1890s, and beach nourishment became an important component of coastal engineering and management for southern Long Island in the 1920s (Kana, 1999; Dornhelm, 2004) and along New Jersey beaches in the 1960s (Wiegel and Saville, 1996). Miller (1993) stresses the importance of coastal and marine tourism as the world's largest industry and its continual rise over the past 50 years. As such, beaches are key elements of coastal tourism because they represent the leading tourist destination.

Coastal community master plans are being developed and revised to address concerns associated with population growth, storm protection, recreation, waste disposal and facilities management, and zoning (e.g., New Jersey Department of Environmental Protection Shore Protection Master Plan and U.S. Army Corps of Engineers [USACE] New Jersey Shore Protection Study; see Williams, 1992). Often, problems stemming from these issues are in direct conflict with natural coastal processes. Some of the more direct problems are related to coastal erosion and storm protection. The practice of replenishing beaches with sand from upland and nearshore sources as protection for community infrastructure has increased in direct relation to population growth. Extraction of sand resources in Federal waters may be preferred relative to State waters due to concerns over changes in physical and biological oceanographic

conditions resulting from large quantities of sediment dredged from resource areas impacted by waves and currents. This has generated a need for technical information to ensure that offshore minerals are developed with due concern for potential environmental considerations.

1.1 BACKGROUND

Development of beaches for urban and recreational purposes along the coasts of New York and New Jersey has been occurring since the late-1800s. The quality of barrier island beaches, with the warm summer climate and ocean water, in addition to their proximity to metropolitan areas of New York City, created an environment that was initially attractive to many summer visitors (Quinn, 1977). As beaches became increasingly accessible by boat, wagon, and later rail, city sprawl began to reach some of the beaches as coastal communities began developing. Rockaway Beach was one of the first urbanized beaches with commuters driving or taking the train to downtown New York City (Kana, 1999). Most coastal communities that started developing in this area were initially faced with erosion problems. To accommodate increasing numbers of visitors and mitigate shoreline recession that dominated parts of the coast, extensive beach nourishment projects began taking place very early in this area (Kana, 1999; Dornhelm, 2004). Along parts of the southern Long Island coast, the first nourishment projects were completed in the early 1920s, and sections of the New Jersey coast were first nourished in the 1950s (Kana, 1999). The 1923 beach nourishment project at Coney Island was the first completed in the United States (Kana, 1999; Dornhelm, 2004). Rockaway and Jones Beaches were not far behind, with projects beginning along these two beaches in the mid-1920s.

Uptegrove et al. (1997) documented the importance of offshore sand ridges as potential borrow sites offshore New Jersey for beach-quality sediment. These deposits exist in State and Federal waters, but potential physical environmental impacts for a specific project of set size and extraction requirements are expected to be minimized as distance from shore increases. Studies of surface and subsurface sediments found on the New York Bight continental shelf have concluded that large volumes of material considered suitable for beach fill activities exist within these areas (Williams, 1976; Williams and Meisburger, 1987; USACE 1990, 1995; Foster et al., 1999). The abundance of sand ridges and suitable sedimentary characteristics on the New York Bight continental shelf provides potential borrow sites to meet sand resource requirements for beach nourishment within the confines of State and Federal environmental regulations.

The degree of development within the study area varies greatly, but the maintenance of beaches is of vital social and economic importance to communities. The need for sand to replenish eroding beaches continues to be an area of concern for local, State, and Federal resource agencies, prompting the exploration and environmental evaluation of offshore resource sites for future use. Beach nourishment has been combined with structural development within the study area to further prevent erosion problems and stabilize Federal entrances. Piers and boardwalks were built, along with shoreline protection structures to combat the forces of ocean waves at the coastline. Between 1930 and 1960, each of the six major entrances in the study area along the south shore of Long Island had been reinforced with at least one jetty, and by 1940, the three major inlets in the study area in New Jersey were all armored with jetties on both of their banks. Estimated volumes and locations of beach nourishment activities as well as the history of structural development are summarized in Section 3.1.1.5.

1.2 STUDY AREA

The study area for this offshore sand resources environmental project encompassed OCS waters seaward of the Federal-State boundary offshore northeastern New Jersey and southwestern Long Island, New York (Figure 1-1).

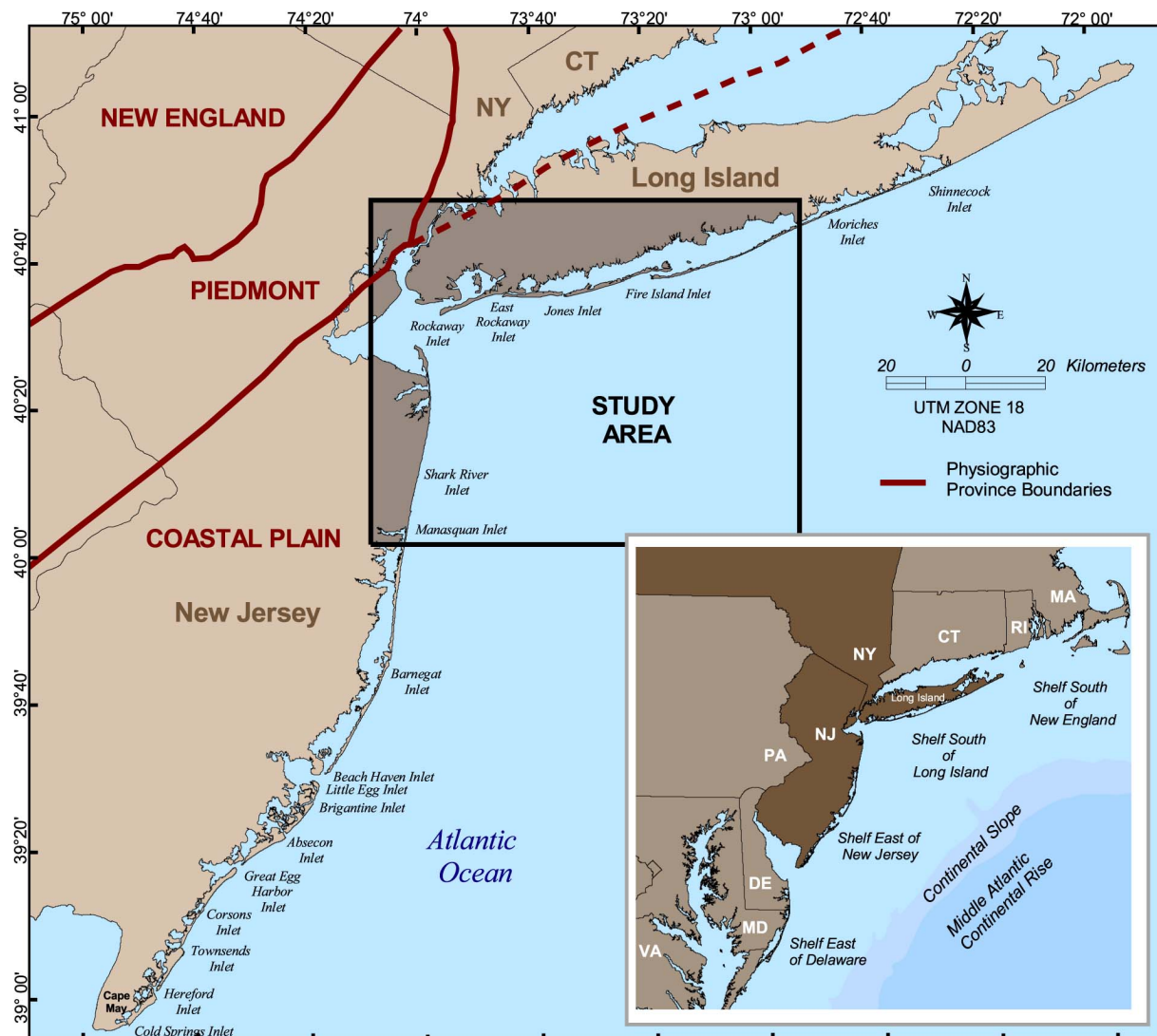


Figure 1-1. Physical setting for the northeastern New Jersey and southwestern Long Island study area and key geographic features.

1.3 STUDY PURPOSE AND OBJECTIVES

As specified by the MMS, the primary purpose of the study was to address environmental concerns raised by the potential for dredging OCS sand offshore northeastern New Jersey and southwestern Long Island, and to document the findings in a technical report. Environmental information was collected and compiled to assist the MMS in making future decisions relative to negotiated agreements (non-competitive leases), NEPA documents (Environmental Assessments and Environmental Impact Statements), and other regulatory requirements concerning Federal sand deposits offshore New Jersey and Long Island.

Primary environmental concerns focused on physical and biological components of the OCS environment. To this end, the MMS identified five study objectives at the beginning of the project:

Physical Objectives

- *Wave Modifications*: Evaluate potential modifications to waves and currents in the study region due to offshore dredging within potential sand resource areas.
- *Sediment Transport Patterns*: Evaluate impacts of dredging in Federal waters and beach nourishment in terms of potential alterations in sediment transport patterns and sedimentary environments, and impacts to local shoreline processes.

Biological Objectives

- *Benthic Ecological Conditions*: Characterize benthic ecological conditions in and around potential sand resource areas identified by the MMS, NJGS, and USACE-NY District.
- *Benthic Infaunal Evaluation*: Evaluate benthic infauna resident in potential sand resource areas and assess potential effects of offshore dredging activity on these organisms, including an analysis of recolonization periods and success following cessation of dredging activities.
- *Project Scheduling Considerations*: Evaluate times for dredging in the sand resource areas relative to transitory pelagic species.

1.4 STUDY APPROACH

1.4.1 Borrow Site Locations and Characteristics

Five potential sand borrow sites were defined for this study based on practical water depth extraction, environmental impact minimization, and suitable geologic characteristics. All potential sand borrow sites exist on either shoreface-attached or offshore linear sand shoals immediately seaward of the Federal-State boundary, which have been described by Duane et al. (1972), Swift et al. (1972), Williams and Duane (1974), Williams (1976), Stubblefield et al. (1984), Duane and Stubblefield (1988), McBride and Moslow (1991), and USACE (1995) as providing a primary source of sand-sized sediment for potential beach nourishment activities. Three primary criteria were used to isolate potential borrow sites. First, water depths greater than 20 m were excluded as a practical limitation for sand extraction. This eliminated any potential site east of Fire Island Inlet because the 20 m depth contour exists at or landward of the Federal-State boundary. Second, sand ridges were of most interest as potential borrow sites to minimize the extent of excavation below the ambient continental shelf surface adjacent to these sites. This procedure was expected to limit potential physical environmental impacts to waves and currents resulting from dredging. Third, the geologic characteristics of offshore sand deposits, as described by U.S. Geological Survey (USGS) and New Jersey Department of Environmental Protection (NJDEP) studies, had to be compatible with beach environments where fill is to be placed.

The amount of dredging that occurs at any site is a function of Federal, State, and local requirements for beach replenishment. It is nearly impossible to predict the exact sand quantities needed in the foreseeable future, so a representative value for any given project was estimated based on discussions with MMS, USACE, and State personnel. Preliminary analysis of short-term impacts (storm and normal conditions) at specific locations along the coast

landward of sand borrow sites indicates that at least $1 \times 10^6 \text{ m}^3$ of sand would be needed for a given beach replenishment event. Long-term shoreline change data sets indicate that a replenishment interval of about 5 to 10 years would be expected to maintain beaches. This interval does not consider the potential for multiple storm events impacting the coast over a short time interval, nor does it consider longer time intervals without destructive storm events. Instead, the estimate represents average change over decades that is a reasonable measure for coastal management applications.

Given the quantity of at least $1 \times 10^6 \text{ m}^3$ of sand per beach replenishment event, the surface area covered for evaluating potential environmental impacts is a function of average dredging depth. Two factors should be considered when establishing dredging practice and depth limits for proposed extraction scenarios. First, regional shelf sediment transport patterns should be evaluated to determine net transport directions and rates. It is good sand resource management practice to dredge the leading edge of a migrating shoal because infilling of dredged sites occurs more rapidly at these locations (Byrnes and Groat, 1991; Van Dolah et al., 1998). Second, shoal relief above the ambient shelf surface should be a determining factor controlling depth of dredging. Geologically, shoals form and migrate on top of the ambient shelf surface, indicating a link between fluid dynamics, sedimentology, and environmental evolution (Swift, 1976). As such, average shoal relief is a reasonable threshold for maintaining environmentally-sound sand extraction procedures.

Two sand borrow sites (H1 and H2) in northeastern New Jersey were identified within NJDEP designated Resource Area H seaward of the Federal-State boundary and between Manasquan and Shark River Inlets (Figure 1-2). Water depth over the ridges ranged from about 14 to 20 m, and maximum relief above the surrounding sea floor was about 5 m. Sand borrow sites south of Long Island were characterized as Holocene sand and gravel ridges by the USGS (Foster et al., 1999). Borrow Site 3 exists south of Long Beach Island, encompassing a relatively broad northwest-southeast trending shoal defined by the -19 m contour. Water depth over the shoal ranges from about 17 to 19 m, and maximum relief above the surrounding sea floor was about 2 m. Borrow Sites 4W and 4E exist as two shoreface-attached shoals seaward of the Federal-State boundary and south of Jones Beach (Figure 1-2). Shoals in these two areas show increased relief and thus provide greater potential for available excavation material than at Site 3, with shoal depths ranging from 16 to 20 m. Maximum relief above the surrounding sea floor was about 4 m.

Potential sand excavation quantities were determined for each of the borrow sites using bathymetric surface data. Excavation depths were determined based on average depth of the ambient shelf surface adjacent to each of the shoals comprising the borrow sites. Using lower-bounding contour elevations of -19 and -20 m, shoal volumes were calculated to determine the availability of potential excavation material. Borrow Sites H1 and H2 provided a total volume of about 4.8 and $9.5 \times 10^6 \text{ m}^3$ of sand, respectively (Table 1-1). Surface areas associated with the excavation volumes were 3.3 and $13.1 \times 10^6 \text{ m}^2$, respectively. Depths associated with shoal features ranged from 14 to 20 m (relative to the North American Vertical Datum of 1988 [NAVD]) at Borrow Site H1 and 15 to 20 m (NAVD) at Borrow Site H2, with shoal depths at Borrow Site H1 generally shallower than those at Borrow Site H2. The majority of the H1 shoal crests were above the -18 m contour, whereas the shoal comprising Borrow Site H2 maintains only small peaks along the -18 m contour, with the majority of the shoal ranging from -18 to -20 m (NAVD). The average thickness of sediment comprising the total excavation volume in H1 is about 1.5 m, and the average sand thickness associated with the volume calculated for H2 is 0.7 m.

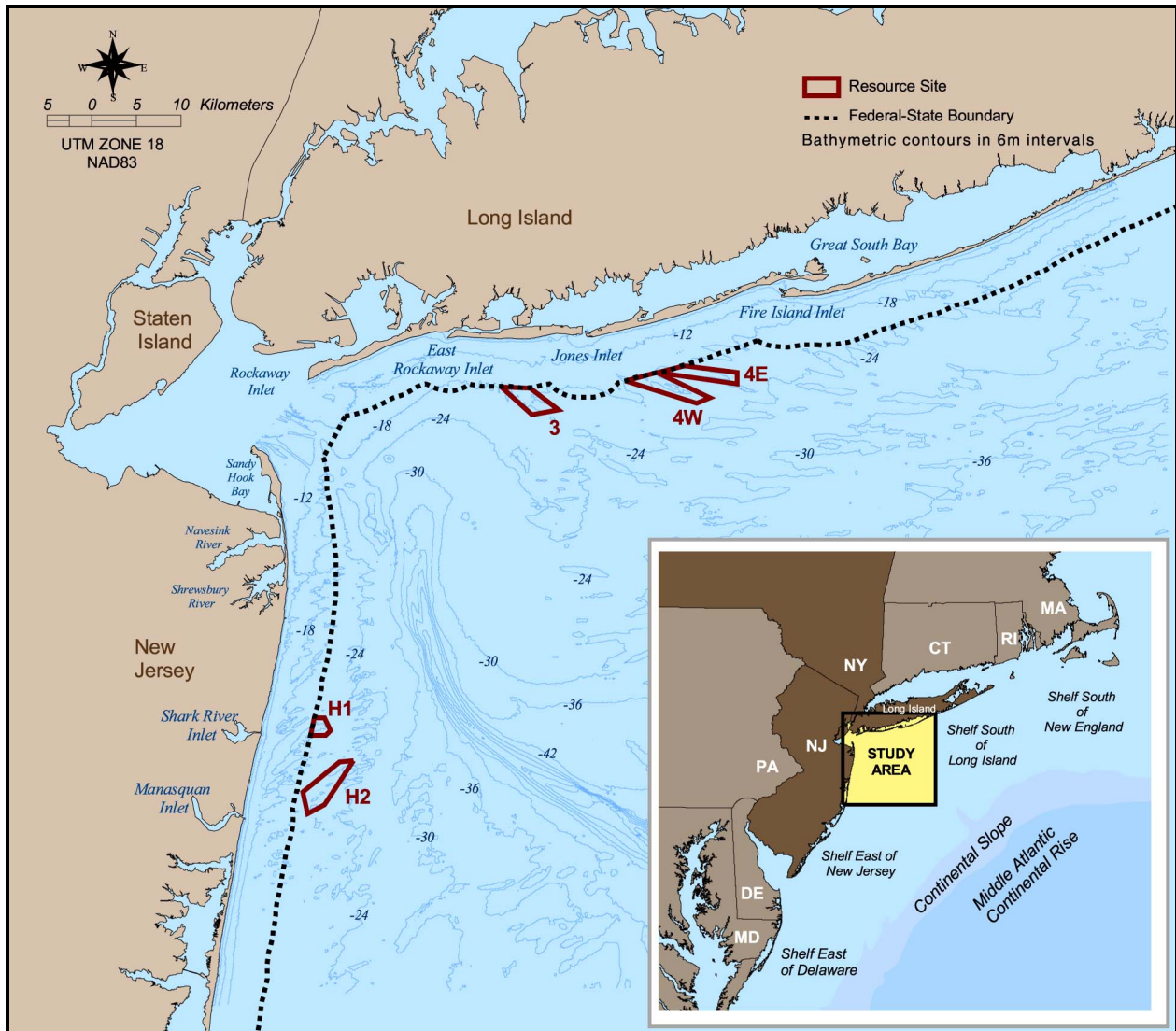


Figure 1-2. Identified sand borrow sites within the project study area relative to the Federal-State boundary.

Table 1-1. Sand resource characteristics at potential borrow sites offshore northeastern New Jersey and southwestern Long Island, NY.

Borrow Site	Borrow Site Surface Area (x 10 ⁶ m ²)	Maximum Excavation Depth (m)	Borrow Site Sand Volume (x 10 ⁶ m ³)	Shoal Relief (m)	D10 (mm)	D50 (mm)	D90 (mm)
H1	3.28	20	4.8	5	0.95	0.52	0.26
H2	13.13	20	9.5	5	0.67	0.35	0.19
3	9.40	19	11.2	2	1.92	1.13	0.36
4W	12.23	20	19.8	4	0.65	0.36	0.22
4E	9.39	20	16.6	4	1.05	0.45	0.27

D10 = grain diameter above which 10% of the distribution is retained; D50 = median grain diameter; D90 = grain diameter above which 90% of the distribution is retained

For Borrow Sites 3, 4W, and 4E south of Long Island, potential sand volumes were calculated at 11.2 , 19.8 , and $16.7 \times 10^6 \text{ m}^3$, respectively. Surface areas associated with these volumes were 9.4 , 12.2 , and $9.4 \times 10^6 \text{ m}^2$, which corresponds to average thicknesses 1.2 , 1.6 , and 1.8 m , respectively. Borrow Site 3 is located along the shallowest features in the study area, with the majority of the borrow site located in depths shallower than 18 m (NAVD). As discussed previously, it also is located in a different geologic unit than 4W and 4E, and as such, has the coarsest sediment composition. Shoals comprising Borrow Sites 4W and 4E have very similar depths. Based on geologic information presented by Foster et al. (1999), thicknesses of suitable sediment along shoals south of Fire Island tend to increase from west to east. As such, it is not surprising that Borrow Site 4E maintains the greatest excavation thickness.

Grab samples were collected at and adjacent to each of the borrow sites during surveys completed in September 2001 and June 2002 (see Section 6.1; Figures 1-3, 1-4). Median grain sizes were averaged for samples collected within each borrow site to determine average median grain size of surficial sediments at each site (Table 1-1). Overall, average median grain size for all sites ranged from medium to very coarse sand. Three of the five sites (H2, 4W, and 4E) consisted primarily of medium-grained sand. Borrow Site 3 had the highest average median grain size, which was expected due to its location immediately north of Cholera Banks, a very coarse-grained outcrop of Cretaceous strata. Borrow Sites 4W and 4E, located to the east of Borrow Site 3, were comprised generally of medium-grained sand. Offshore northeastern New Jersey, Borrow Site H1 was classified as medium- to coarse-grained sand and Borrow Site H2 contained medium sand. This change in distribution is consistent with trends reported for sediment grain size variations along northern New Jersey beaches (grain size generally decreases with distance from the coastal bluffs). Overall, median grain size averages among the borrow sites were consistent with beach sediments sampled along adjacent shorelines.

1.4.2 Wave Modifications

The goal of this study element was to perform wave transformation numerical modeling to predict the potential for adverse modification of waves resulting from sand dredging operations. Changes in bathymetry in sand borrow sites can cause wave energy focusing, resulting in substantial alterations in sediment transport at the site of dredging operations as well as along the shoreline landward of borrow sites. Because the purpose of dredging offshore sand from a specific site will be driven by the need for beach replenishment, it is critical to understand the impact of changing wave transformation patterns on shoreline response before potentially exacerbating a problem. Numerical comparisons of existing conditions and post-dredging impacts provided a means of documenting modifications to waves as they crossed the sand resource areas.

1.4.3 Sediment Transport Patterns

The goal of this study element was to predict changes in sediment transport patterns resulting from sand dredging operations using numerical information generated from wave transformation modeling, combined with offshore current data. Existing current measurements were analyzed to document temporal variations in flow throughout the study area (detailed in Section 5.0). Sediment transport rates were quantified for sand borrow sites using an analytical approach, and transport rates at the shoreline were determined numerically using output from wave transformation numerical modeling.

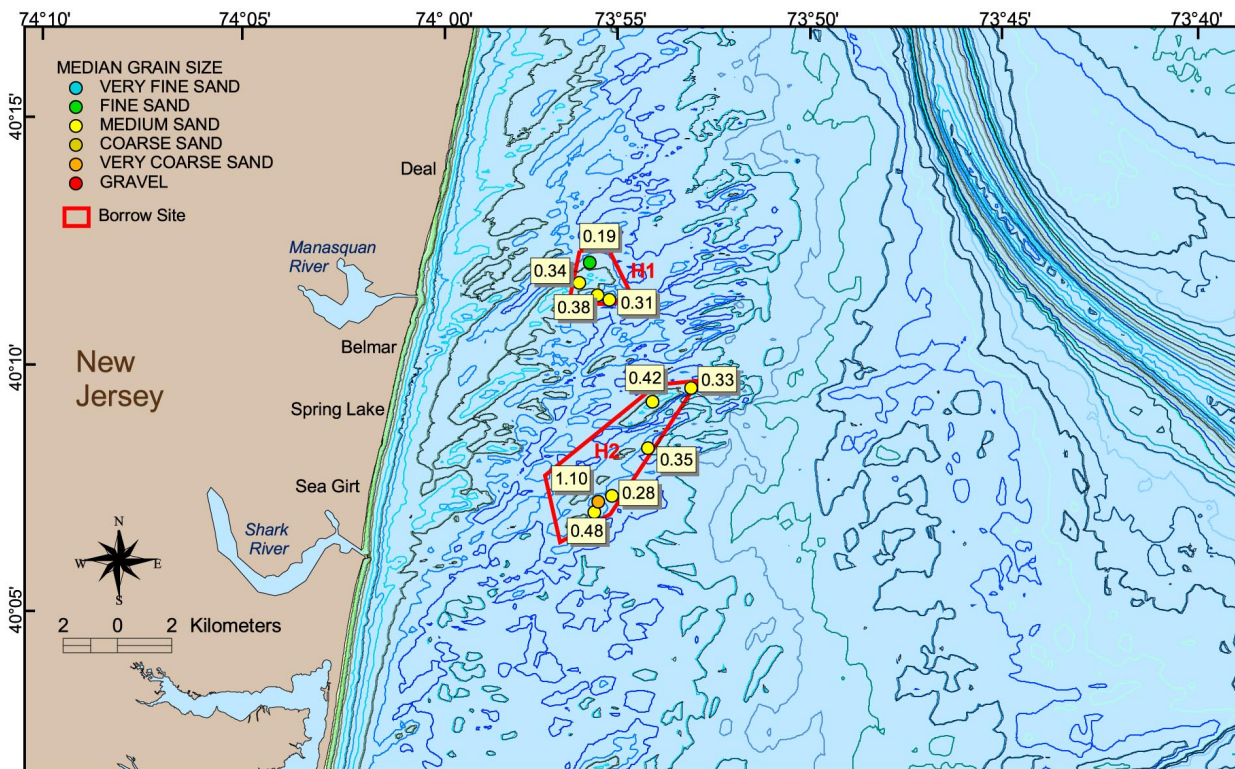
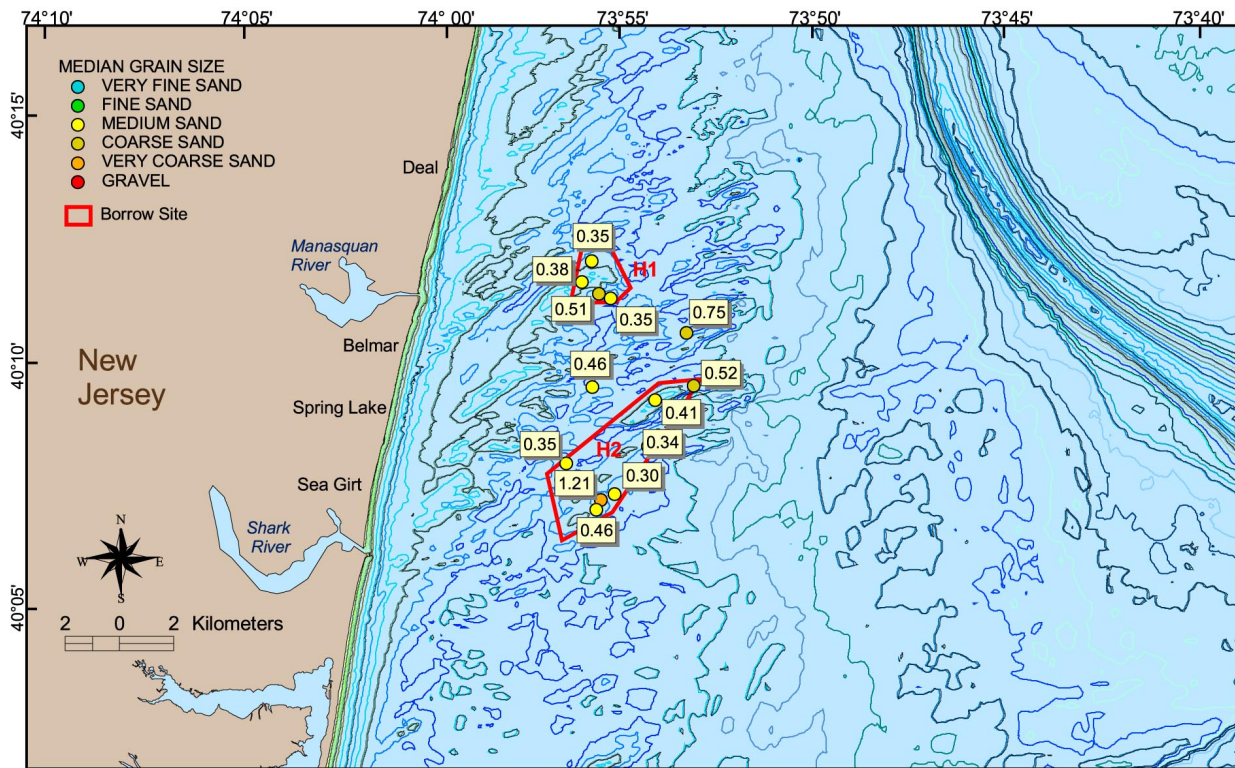


Figure 1-3. Grab samples collected during September 2001 (top) and June 2002 (bottom) within and adjacent to Borrow Sites H1 and H2.

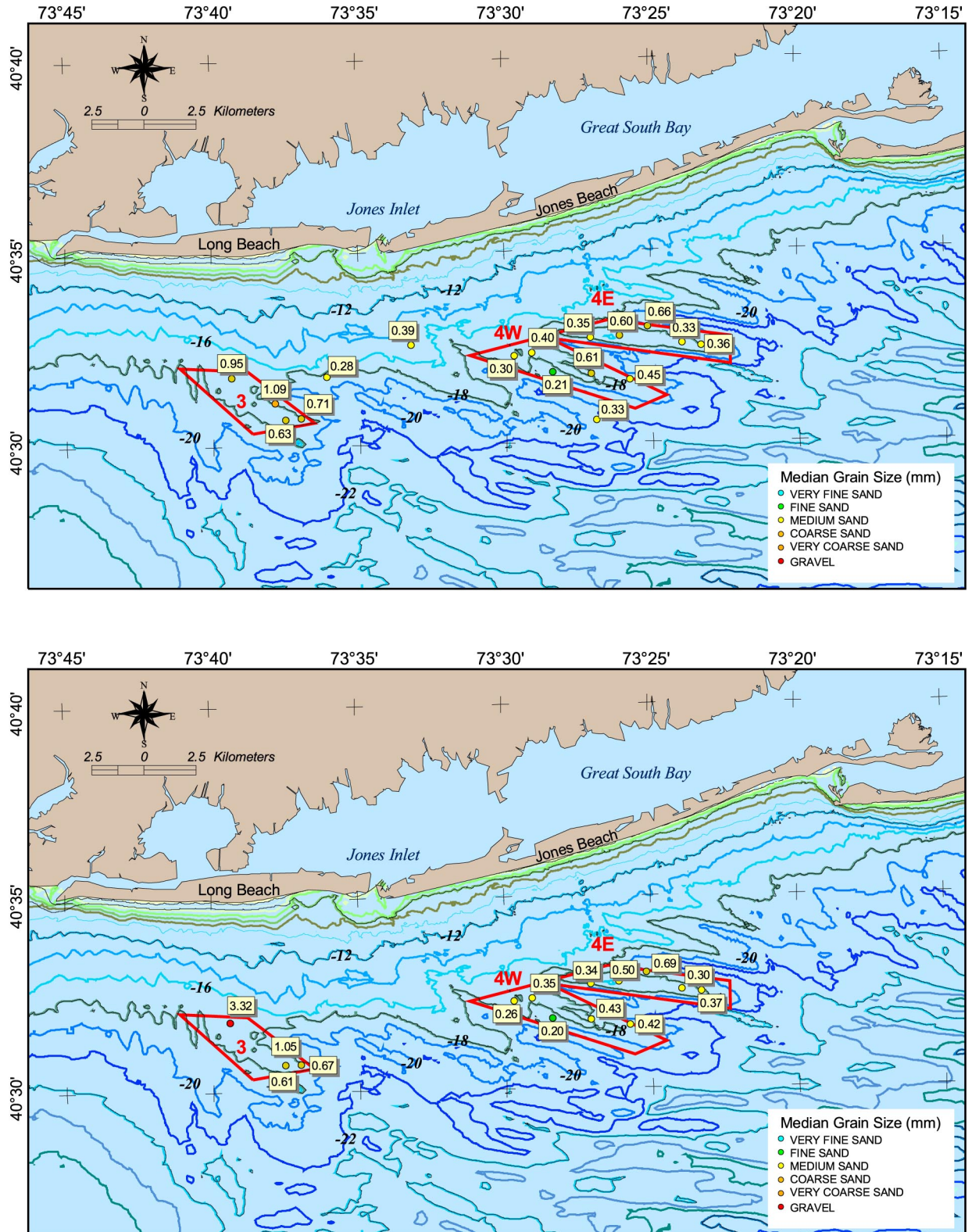


Figure 1-4. Grab samples collected during September 2001 (top) and June 2002 (bottom) adjacent to Borrow Sites 3, 4W, and 4E.

Historical shoreline and bathymetric data were compiled to document regional sediment transport patterns over a 60- to 70-yr time period. Net changes in sediment erosion and deposition on the shelf surface provided a direct method for identifying patterns of sediment transport and quantifying net rates of change throughout the sand resource areas. These data also were used to verify numerical results for direction and magnitude of sediment transport.

1.4.4 Benthic Ecological Conditions

The goal of this study element was to characterize benthic ecological conditions in and around the sand resource areas. Existing literature and data were searched, collected, analyzed, and summarized to characterize the ecological environment and to form the foundation for biological field survey design. Biological field surveys were conducted to characterize infauna, soft bottom epifauna and demersal fishes, sediment, and water column parameters.

1.4.5 Benthic Infaunal Evaluation

The goal of this study element was to assess potential effects of offshore dredging on benthic infauna and analyze recolonization periods and success following cessation of dredging activities. Existing literature and data on dredging effects were used in conjunction with biological field survey results to examine potential benthic effects and recolonization in the sand resource areas.

1.4.6 Project Scheduling Considerations

The goal of this study element was to evaluate times for offshore dredging relative to pelagic species. Environmental windows are temporal constraints placed on dredging activities to protect biological resources from potentially detrimental effects (Dickerson et al., 1998). Existing information concerning seasonal occurrence of pelagic species and potential impacts from dredging was used to evaluate project scheduling considerations for pelagic fishes, sea turtles, and marine mammals.

1.5 DOCUMENT ORGANIZATION

This document was organized into nine major sections as follows:

- Introduction
- Environmental Setting
- Regional Geomorphic Change
- Assessment of Wave Climate Impact by Offshore Borrow Sites
- Circulation and Sediment Transport Dynamics
- Biological Field Surveys
- Potential Effects
- Conclusions
- Literature Cited

In addition to the main document, appendices were prepared in support of many analyses presented in the report. Furthermore, an Executive Summary, a Technical Summary, and a Non-Technical Summary will be prepared as separate documents to provide brief study descriptions for audiences including managers, researchers, and the general public.

2.0 ENVIRONMENTAL SETTING

The New Jersey-New York offshore sand resource study area is situated along the north Atlantic coast of New Jersey and the southwest Atlantic coast of Long Island and represents part of the passive, slowly subsiding eastern North American continental margin (Klitgord et al., 1988; Smith, 1996). It includes the northernmost component of the Coastal Plain Physiographic Province that extends along the Atlantic and Gulf coasts of North America from Long Island to Mexico and is underlain at shallow depths by Upper Cretaceous, Tertiary, and Quaternary semi-consolidated, clastic sedimentary rocks (Williams and Duane, 1974). The southern coast of Long Island is approximately 190 km long and marks the southern terminus of late Pleistocene glacial advance in eastern North America. The outer coast of New Jersey is approximately 210 km long and lies south of the extent of the most recent glacial advance. The two coasts are oriented almost perpendicular to one another, forming a wedge-shaped region within the northern Middle Atlantic Bight in an area known as the New York Bight. Coastal features include bluffs, headlands, and barrier spits and islands that are punctuated by inlets, allowing for the exchange of sediment and water between estuaries and the continental shelf, primarily as a function of tide (Figure 2-1).

The project site forms a rectangular area along the two outer coastlines and adjacent continental shelf. It encompasses about 50 km of the northernmost New Jersey coastline from Manasquan Inlet to Sandy Hook (74°01'03", 40°28'37" to 74°05'48", 39°45'43") and about 110 km of coastline in southwestern Long Island from Rockaway Point to Moriches Inlet (73°56'27", 40°32'33" to 72°45'19", 40°45'52"; Figure 2-1). The site encompasses seven major federal entrances, with two of these located in northern New Jersey (Shark River and Manasquan Inlets) and five located in southwest Long Island (Rockaway, East Rockaway, Jones, Fire Island, and Moriches Inlets). Entrances along both shorelines have been armored with rock jetties to provide channel protection and inlet stability (outlined in Section 3). The project area extends offshore from the shoreline across the continental shelf to about the 30-m depth contour (NAVD), a distance of about 10 to 30 km. Although the offshore Federal-State jurisdictional boundary marks the landward limit of the study area, the ultimate use of sand extracted from the OCS is for beach replenishment along the New Jersey and Long Island outer coasts. Consequently, a description of the environmental setting from the coast to the OCS is pertinent for addressing the overall study purpose.

Topographic characteristics along southwestern Long Island and northeastern New Jersey differ due to the influence of the most recent Pleistocene glacial advance. Long Island marks the southern boundary of the Wisconsin-Laurentide continental ice sheet, which is recognized as two terminal moraines that comprise the backbone of the northern half of Long Island and the glaciofluvial outwash plain that forms its southern flank (Taney, 1961). Termination of the ice sheet at Long Island has created regional topographic features that characterize the Long Island landscape but not the topography of northern New Jersey. As a result, the New York Bight is a relatively complex geologic setting as it has been influenced by differential subaerial erosion of near surface Coastal Plain strata and by several episodes of Pleistocene glaciation (Williams and Duane, 1974). Despite the contrast in geologic processes,



Figure 2-1. Physical setting of the New York and New Jersey coastlines.

general geomorphic characteristics of the outer coastline exhibit similar coastal compartments and patterns of shoreline evolution. In both regions, eroding headland bluffs supply sediment that is transported through littoral currents to downdrift beaches. This process has contributed to the development and evolution of extensive chains of barrier spits and islands along both coasts, which have historically migrated rapidly in the direction of net longshore transport (Fisher, 1968). Much of this natural barrier island migration has been halted in recent years through extensive structural development, including construction of numerous groins and seawalls in addition to large rock jetties that have been placed at each entrance within the study area. The combination of these factors has altered the natural physiography of the outer coastline, influencing shoreline change patterns and affecting sediment supply to downdrift beaches. Beach sediment size along both coasts tends to decrease with distance from headland bluffs. Specific properties of shoreline composition and orientation, barrier island migration, and the magnitude and direction of net littoral transport vary between the southern Long Island and northern New Jersey coasts. As such, the physical landscape of the outer coast within each state is discussed separately below.

The outer coast of northern New Jersey is a relatively straight and regular north-south orientation from Sandy Hook to Barnegat Inlet, south of which it trends increasingly northeast-southwest and is more frequently interrupted by inlets. The outer coast has been classified into four major geomorphic compartments, including the Northern Spit Complex at Sandy Hook, the Headlands Section from Monmouth Beach to Mantoloking, the Southern Spit Complex from Mantoloking to Beach Haven/Little Egg Inlet, and the Barrier Island Complex from Beach Haven/Little Egg Inlet south to Cape May (Figure 2-2; USACE, 1995). Coastal bluffs of the Headlands Section serve as a significant source of sediment for coastal compartments to the north and south, where wave-generated longshore currents distribute eroding sediment into spit deposits and barrier islands (Caldwell, 1966; USFWS, 1997). The extent of the present study area in northern New Jersey includes the entire Northern Spit Complex and Headlands Section (Figure 2-2).

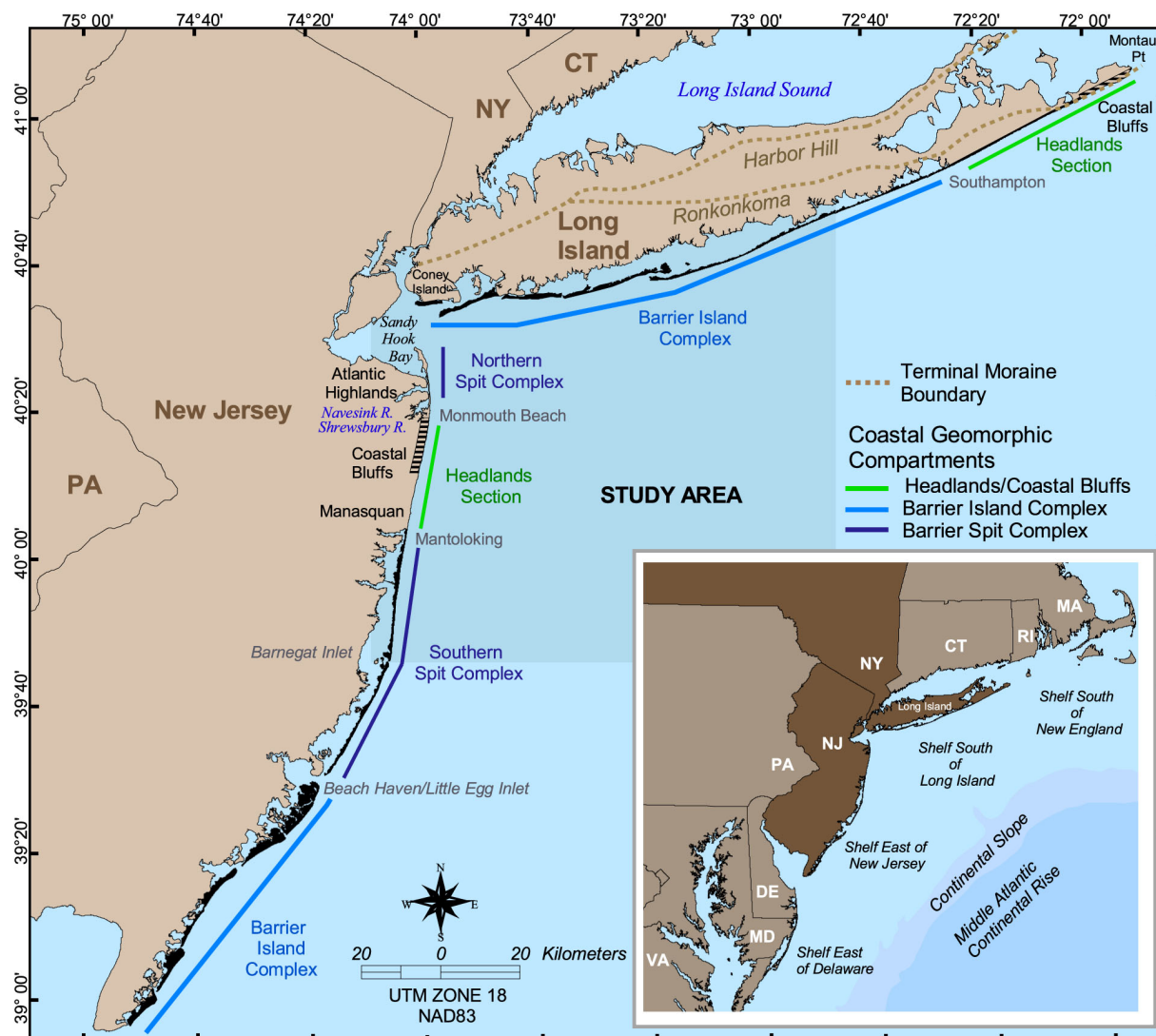


Figure 2-2. Coastal geomorphic components of New York and New Jersey. (Adapted from Uptegrove et. al., 1995 and Taney, 1961).

Sediments along northern New Jersey beaches are comprised mainly of medium- to coarse-grained sand, composed principally of unconsolidated quartz from underlying and nearby formations (USACE, 1990). The outer coastline of the Northern Spit Complex is composed primarily of beach and estuarine deposits, while the Headlands Section contains primarily Tertiary sands, marls, and clays (Figure 2-3). Beaches along the northern coast of New Jersey consist mainly of fine- to medium-grained sands, with grain sizes from samples collected between Sandy Hook and Manasquan ranging from 0.17 to 0.41 mm (USACE, 1990, 1995). Mean grain size for samples collected on beaches between Sandy Hook and Asbury Park averages 0.29 mm, and median grain size on beaches between Asbury Park and Manasquan averages 0.23 mm (USACE, 1990, 1995). Throughout this area, median grain size on beaches generally decreases with distance from eroding coastal bluffs of the Headlands Section (Uptegrove et al., 1995).

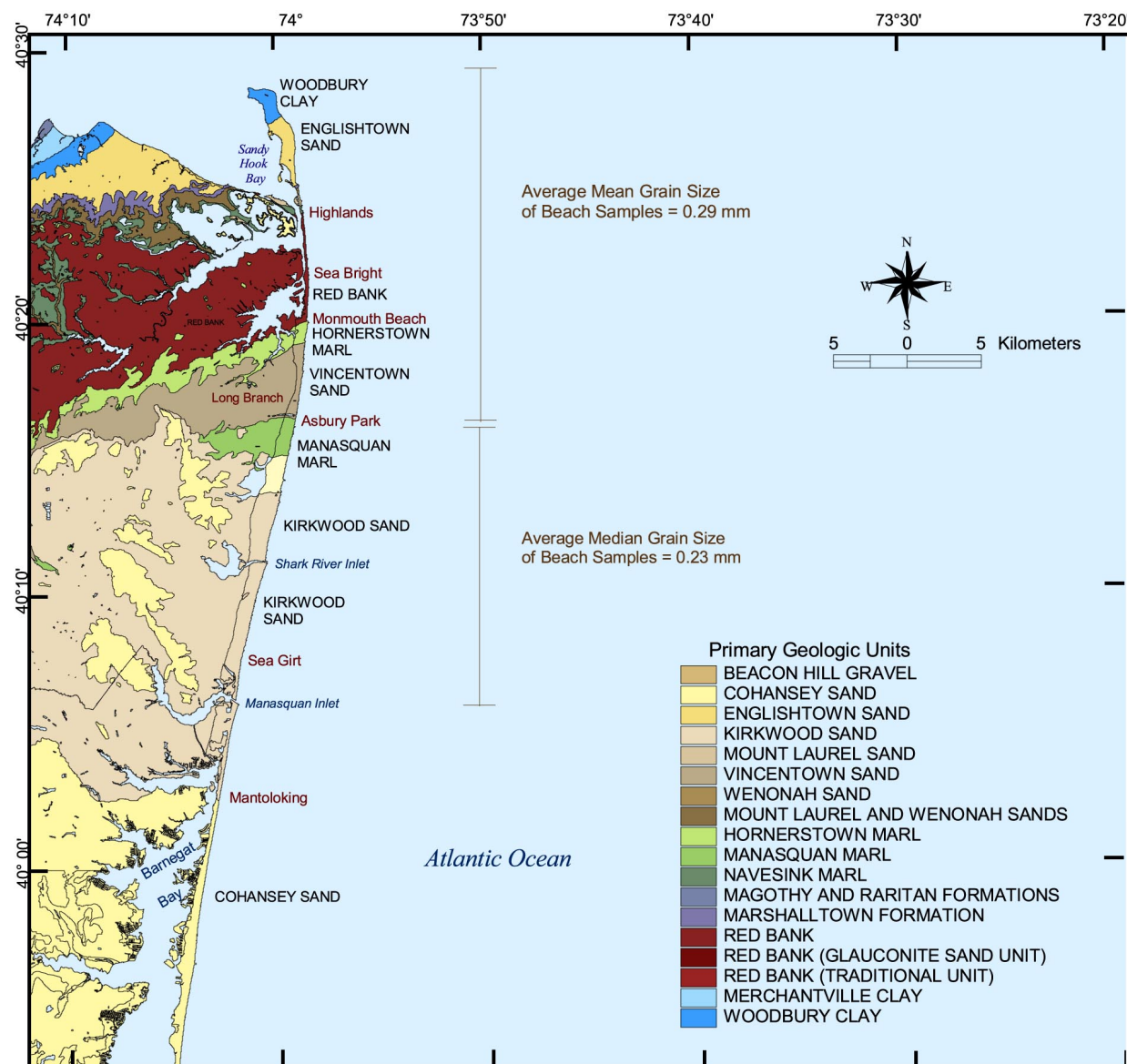


Figure 2-3. Geologic Units and average sediment grain size along the northern New Jersey coast (Geologic data from NJDEP GIS Data CD and sediment sample data from USACE, 1995).

The Northern Spit Complex is backed by Navesink and Shrewsbury Rivers and protrudes north into New York Harbor where it is backed by Sandy Hook Bay and protected somewhat by the presence of Long Island to the north. Sandy Hook is a classic example of a recurved spit that has prograded north toward New York Harbor from north-directed longshore drift (USACE, 1995). The rate of sediment transport associated with this growth has been estimated at about 382,000 m³/yr (Caldwell, 1966). The Navesink River separates Sandy Hook from the Atlantic Highlands region of northern New Jersey. Atlantic Highlands are the highest headlands along the Atlantic Coast south of Maine and are composed of a resistant Tertiary-aged ironstone conglomerate caprock that overlies gently seaward-dipping Cretaceous marine mudrocks (Stoffer, 1996). Paralleling the Navesink River to the south is the Shrewsbury River. These two water bodies trend in an east-northeast direction and discharge to the north into Sandy Hook Bay. In historic times, both rivers had direct access to the Atlantic Ocean; however the north-directed growth of Sandy Hook Spit has resulted in a diversion of their courses to the north such that they now empty into Sandy Hook Bay (Williams and Duane, 1974). The portion of the spit seaward of the area where the rivers divert north is very narrow and has experienced on-going erosion problems in the recent past (Figure 2-4). This area, located in the vicinity of the town of Sea Bright, has undergone significant beach nourishment activity since the 1950s, with nourishment planned for this section of coastline over the next 30 years (USACE, 2003). The spit terminus to the north historically has experienced significant deposition as the continuous supply of sediment from longshore currents and other marine currents on the continental shelf have caused the shoreline to prograde down-current and seaward (Stoffer, 1996). Beach sediment is composed principally of unconsolidated quartz from underlying and nearby formations. Grain size ranges from clay to small pebbles, but the sand is mainly medium to coarse (USACE, 1990).



Figure 2-4. Narrow barrier spit seaward of the north-directed outflow channel for the Navesink and Shrewsbury Rivers (USGS TerraServer image, 13 March 1995).

The area south of Sandy Hook from the town of Monmouth to the vicinity of Mantoloking has been called the headlands region by Fisher (1967) and Nordstrom et. al. (1977). The headlands region encompasses about 30 km of coastline and is composed of Cretaceous, Tertiary, and Quaternary Coastal Plain strata that are directly exposed to wave action. The beach in this area lies directly seaward of the bluff which rises as much as 8 m above the beach (Uptegrove et al., 1995). The fronting shoreline within this stretch of coastline is oriented primarily north-south at an angle of about 10 degrees, and is interrupted by two relatively small inlets located at the mouths of the Shark and Manasquan Rivers. These rivers intersect the project shoreline in a northeast-southwest orientation and are currently maintained as federal entrances with rock jetties armoring their northern and southern banks. Coastal plain sediments in this region are comprised of sand, marl, gravel, and clay and serve as the primary source of sediment for adjacent beaches (Figure 2-3; USACE, 1995).

Eroded materials enter the littoral system and are transported northward to form Sandy Hook and southward toward the barrier islands (USFWS, 1997). Net littoral drift to the north and south of this region is centered about a nodal point located near Manasquan. North of Manasquan, net littoral drift is estimated at about 382,000 m³/yr (Caldwell, 1966); south of Manasquan, net drift is southerly at about 38,000 m³/yr (Figure 2-5, Caldwell, 1966).

The location of Long Island as the southern terminus of the last glacial advance has resulted in a topographic composition that is uncharacteristic for the Atlantic Coastal Plain Province (Taney, 1961). The effects of glaciation are apparent in the topography of the island; as it is marked by two terminal moraines, the younger more northerly Harbor Hill Moraine and the older more southerly Ronkonkoma Moraine (Figure 2-2). The southern portion of Long Island is characterized by gently sloping outwash plains fronted by shallow lagoons and a low-relief barrier island system consisting of reworked glacial sediment deposited during the last glacial advance (Schwab et. al., 2000a). Similar to the New Jersey coastline, the outer coast of Long Island is divided into two major coastal geomorphic compartments, including an eastern Headlands Section making up about 25 percent of the outer coast, and a western Barrier Island Complex comprising the remaining 75 percent (Figure 2-2, Taney, 1961). The Barrier Island Complex portion of the outer coast is comprised of four barrier islands, two peninsulas, and Coney Island, which has been joined to the mainland through fill operations (Taney, 1961). These are backed by shallow back-barrier bays and marshes, and are presently separated from each other by tidal entrances. To the east of the Barrier Island Complex are the eroding coastal bluffs adjacent to Montauk Point that encompass the Headlands Section.

The ocean beaches along southern Long Island vary in width from zero at the coastal bluffs to the east to over 150 m in localized areas; the average width is between 30 and 60 m (Taney, 1961). Landward of the beachface are sand dunes that crest between 1 and 3 m above mean sea level for most of the Barrier Island Complex between Jones Inlet and Southampton, becoming taller to the east of Southampton (Taney, 1961). Beaches in this area consist primarily of reworked fluvioglacial outwash characterized by sandy (medium- to coarse-grained sand) sediment, with coarser morainal deposits along the eastern quarter of the shoreline (Kana, 1999). Similar to grain size trends observed along New Jersey beaches, the median diameter of beach sand generally decreased with increasing distance from the Headlands Section (from east to west in this case) (Taney, 1961).

The Headlands Section of the south coast of Long Island stretches from the vicinity of Southampton east to Montauk Point. The shoreline within this area is characterized by coastal bluffs along the easternmost 6 km of coast, followed by dunes and sandy beaches west of the



Figure 2-5. Net longshore transport rates estimated along Long Island and New Jersey coasts. Littoral transport rates obtained from Taney (1961) and Caldwell (1966).

bluffs. The bluffs at Montauk Point rise abruptly to about 20 m above sea level and are fronted by narrow beaches of coarse sand and gravel composed of morainal deposits from the Ronkonkoma Moraine (Taney, 1961). The western portion of the headlands region is characterized by long continuous sand dunes that are fronted by beaches composed of morainal deposits and increasingly sandy littoral material that has been transported west (Taney, 1961). The erosion of glacial moraine and till deposits at Montauk Point serves as the headland source for beach sands that comprise the Barrier Island Complex to the east.

Because prevailing winds in this area are from the east-southeast, long fetches from the Atlantic produce net longshore transport from east to west, with rates showing considerable variation (Figure 2-5). Eroded glacial sediments from headlands are carried west in the littoral current and are deposited by wave action on barrier beaches and offshore bars (USFWS, 1997). Net littoral transport for parts of the south shore of Long Island has been estimated by Taney (1961) and the US Army Corps of Engineers [USACE] (1971) to be between 344,000 and 460,000 m³/yr (Figure 2-5; Williams and Duane, 1974).

The Barrier Island Complex of the south coast of Long Island stretches west from Southampton to Coney Island and is comprised primarily of barrier islands, including (from west to east) Long Beach, Jones Beach, Fire Island, and Westhampton Beach. The barrier beaches in this region are separated from the mainland by numerous interconnected tidal bays, inlets, marshes, and lagoons; some of the more prominent water bodies include Great South Bay and Moriches Bay. Each of the barriers is relatively narrow and long, with widths generally ranging from about 0.5 to 1 km and lengths ranging from a maximum of about 50 km at Fire Island to a minimum of about 7 km at Coney Island. There are six permanent tidal inlets that separate the barrier islands in southern Long Island, including (from west to east) Rockaway Inlet, East Rockaway, Jones, Fire Island, Moriches, and Shinnecock. The number of inlets has varied in the recent past, with Moriches Inlet closing intermittently throughout the past two centuries (see Section 3). As barrier beaches migrate westward due to west-directed littoral transport, rapid movement of large volumes of littoral sediment from east to west has resulted in a shift in inlet orientation at three entrances (Taney, 1961). Rockaway, East Rockaway, and Fire Island Inlets have experienced rapid westward migration such that their eastern banks now overlap their western banks (Figure 2-5). The remaining two tidal entrances (Moriches and Jones) are oriented north-south, indicating that these features are young relative to offset inlets. Each of the entrances was armored with at least one jetty on its eastern side by 1960 to control rapid west-directed island migration.

The beaches fronting southern Long Island have been formed by wave and littoral forces. Presently, the only confirmed source of sediment to beaches along southern Long Island is the Headlands Section to the west, which has been estimated by Taney (1961) to supply approximately 76,000 cubic meters of material to the littoral current system annually. Onshore movement of sediment has been proposed by Wolff (1982) and Schwab et al. (1999) as another possible source to the littoral system but volumes are presently unverified. As such, the only confirmed source of material contributing to the littoral drift system has been determined to be from the Headlands Section.

2.1 OFFSHORE SEDIMENTARY ENVIRONMENT

The submerged extension of the Atlantic Coastal Plain forms the continental shelf of the New York Bight. It is characterized by a gentle slope that dips slightly to the southeast and is deeply incised by the submarine Hudson River channel which bisects the area as it connects with the Hudson Canyon at the Continental Shelf edge (Williams and Duane, 1974). The New York Bight is located in a unique geologic setting at the intersection of two major geomorphic provinces. Unlike other areas to the north and south, it has been influenced by several episodes of Pleistocene glaciation and differential subaerial erosion (Williams and Duane, 1974). The last glacial advance of the Pleistocene and the following recent transgression of the sea have contributed greatly to the evolution of the modern landscape in the New York Bight. Seafloor topography and Holocene sediment distribution reflect this combination of processes, including shelf modification through ancient fluvial incision during Pleistocene regression followed by active reworking of the exposed shelf surface from coastal processes during subsequent Holocene rise in sea level (Duane and Stubblefield, 1988). Redistribution of sediment by waves and currents during transgression formed modern shelf deposits as subaerial coastal features became submerged and reworked during relative rising sea level. As such, much of the shelf in the New York Bight is classified as sand (Figure 2-6; Knebel, 1981).

Sea level rise across the New York Bight continental shelf was probably interrupted by a series of near stillstands followed by rapid rises during the Holocene (Duane and Stubblefield, 1988). This process resulted in a series of shore-parallel features that have been interpreted as

old shorelines composed of sand (Figure 2-7; Uchupi, 1968; Swift, 1976; Knebel and Spiker, 1977). Large sections of the continental shelf surface within the Middle Atlantic Province contain isolated and shoreface sand ridges oriented obliquely to the modern shoreline (Figure 2-7; Swift et al., 1972; Stubblefield et al. 1984; McBride and Moslow, 1991). These demonstrate opposing ridge and swale orientations on either side of the Hudson River Channel (Figure 2-7). South of Long Island, prominent ridge and swale morphology with a northwest-southeast orientation dominates, a distinct contrast to the northeast-southwest orientation of ridges dominating the shelf west of the Hudson Channel. There are many interpretations of the origin of these features ranging from modern hydraulic processes to relict Pleistocene subaerial exposure. Ridges within the study area are generally spaced about 1 to 6 km apart and their lengths vary from about 2 to 7 km, with the exception of localized features interpreted as outcroppings of coastal plain strata, which are much larger and do not form oblique angles with the shoreline. The following sections describe these shoreface deposits and their relationship to presently defined sand resource areas.

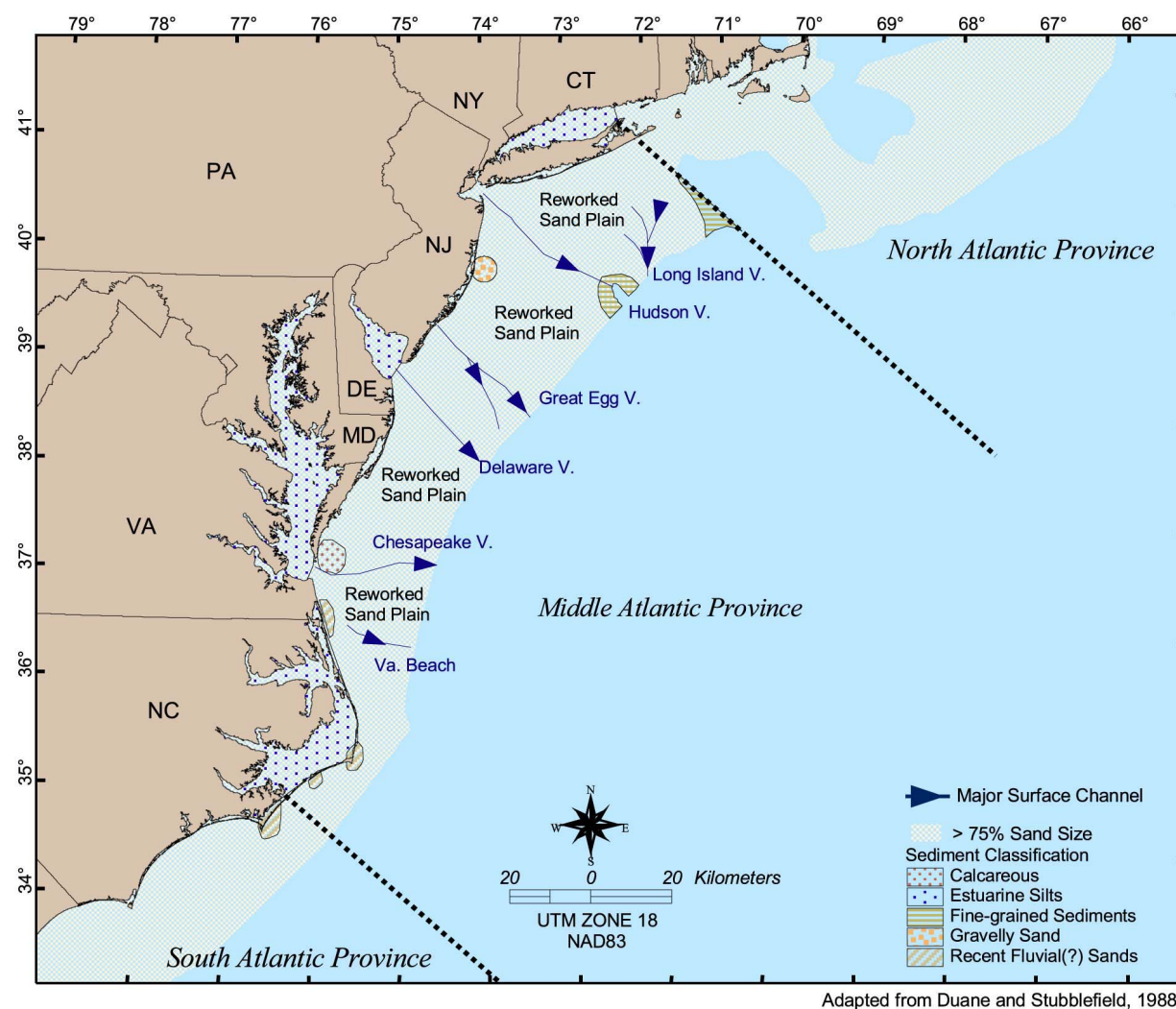


Figure 2-6. Middle Atlantic continental shelf illustrating dominant surface sedimentary facies as >75% sand sized material (adapted from Duane and Stubblefield, 1988; data from Emery and Uchupi, 1965; Uchupi, 1968; Swift, 1976).

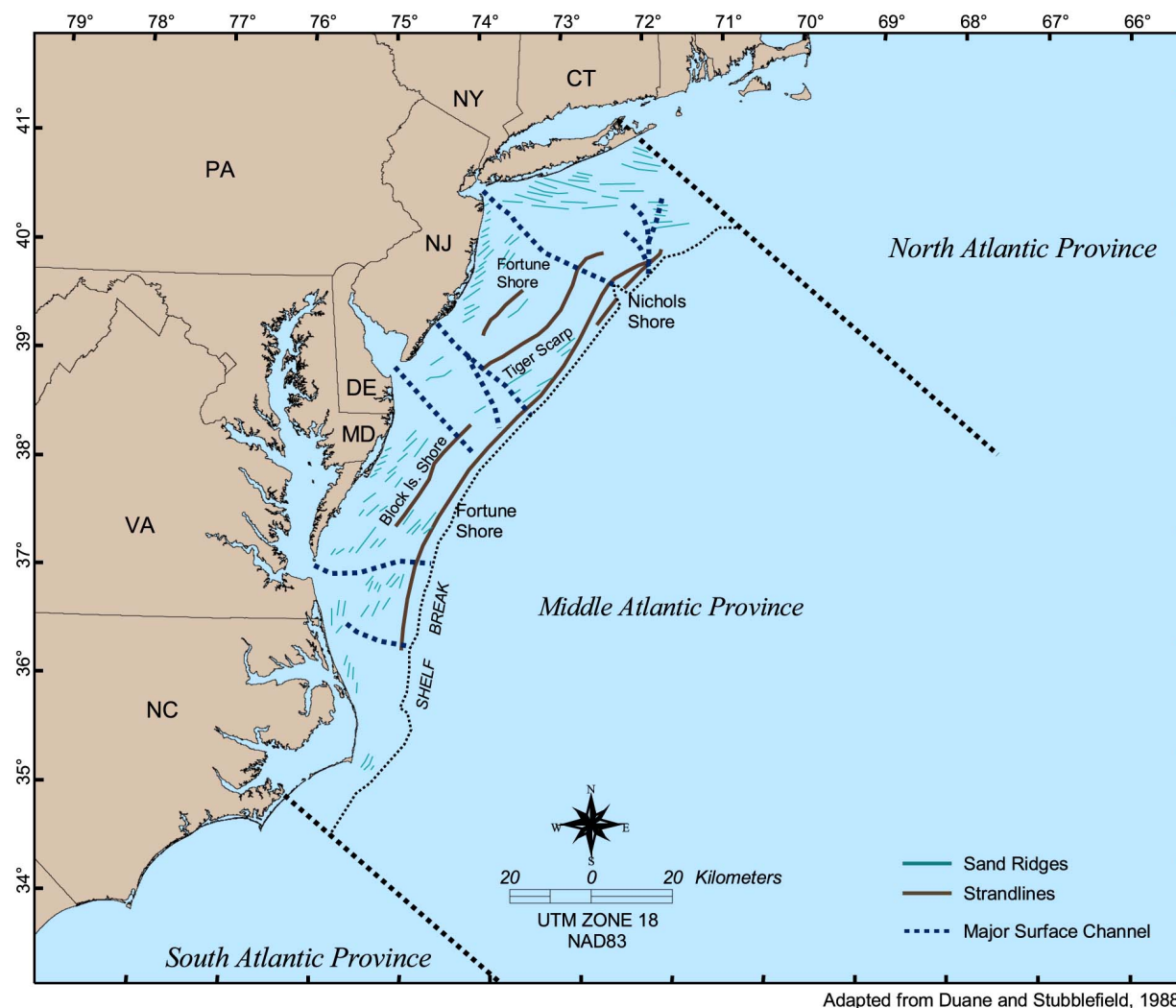


Figure 2-7. Middle Atlantic Province showing historical strandlines and sand ridge orientations on the continental shelf (adapted from Duane and Stubblefield, 1988).

2.1.1 Seabed Morphology

The continental shelf within the New York Bight region is characterized primarily by ridge and swale topography, isolated and shore-attached linear sand shoals and ridges, and localized artificial topographic highs (Figure 2-8). The most prominent sea floor feature in this area is the 170-km-long submarine Hudson River Channel, which extends southeasterly across the continental shelf offshore New York City toward the shelf break until it connects with the Hudson Canyon (Butman et. al, 1998; Figure 2-8). The Hudson River Valley is the drowned valley of the Hudson River that was formed at lower stands of sea level. It is the principal topographic feature of the Middle Atlantic Bight and is the best developed of any submarine channel-canyon system on the Atlantic shelf (Butman, 1998). The Hudson Shelf Valley is very deeply incised, and it was suggested by Veatch and Smith (1939) that during part of the late Wisconsin ice retreat, the Hudson Shelf Valley received the entire Great Lakes drainage, which may account for this strikingly deep incision.

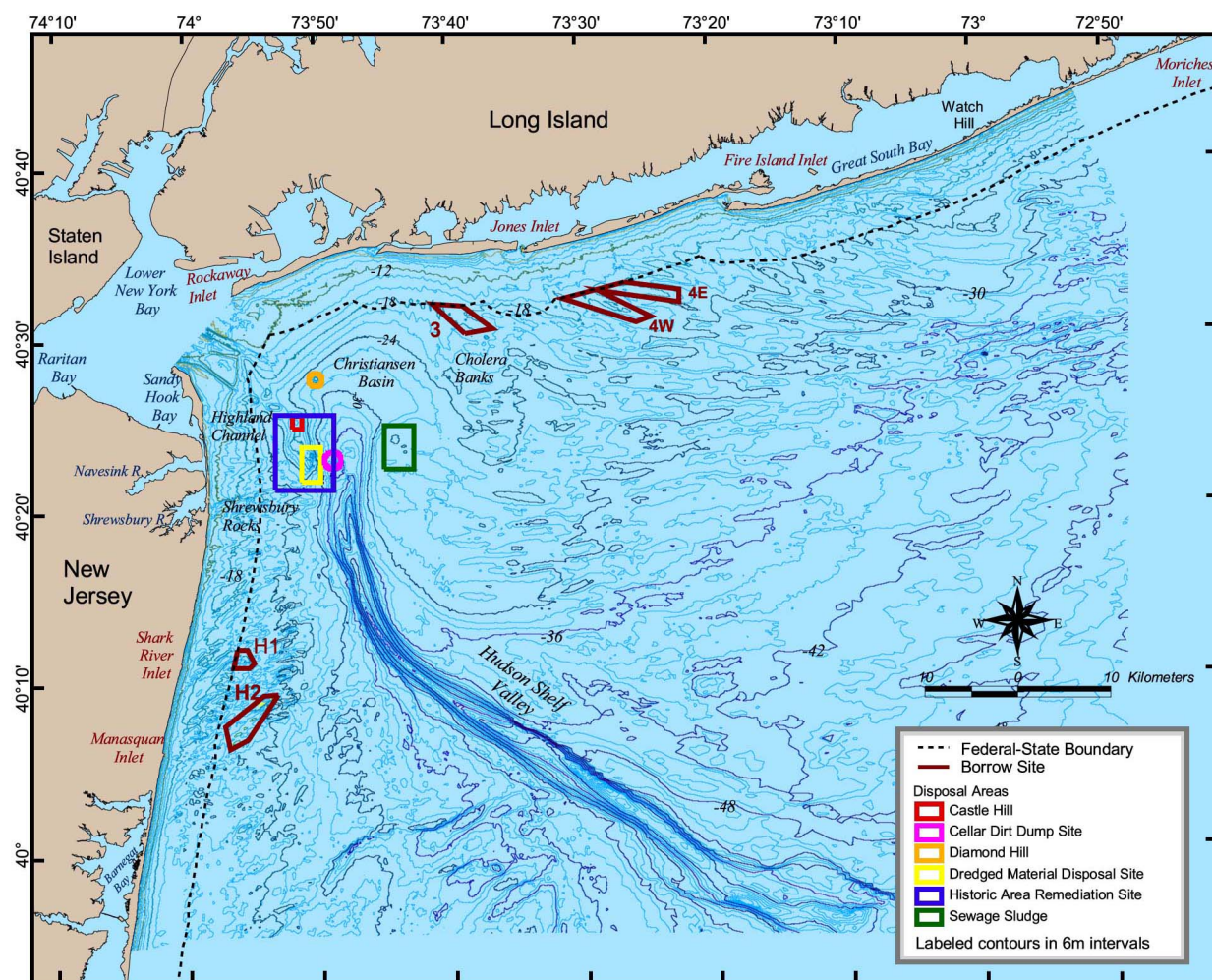


Figure 2-8. Prominent geomorphic features of the New York Bight continental shelf.

The shelf in this region is dominated by ridge and swale topography, with numerous linear shoals that trend oblique to regional contours and form a small acute angle with the coastline (Duane et al., 1972). Local topographic highs and lows include Shrewsbury Rocks, Cholera Banks, Diamond Hill, Castle Hill, Highland Channel, and the Christiansen Basin, with multiple additional anthropogenic disposal mounds (Figure 2-7). Anthropogenic disposal of various materials has been occurring within the New York Bight since the early 1800s, evidence of which is apparent in the bathymetric contours of the shelf. Dumping is visible as multiple topographically positive mounds in the vicinity of Christiansen Basin. Sources and quantities of material have been well documented in recent reports by the USGS (Butman, 1998; Schwab et al., 2000b) and in earlier reports by the USACE (Williams and Duane, 1974). Figure 2-7 illustrates major disposal site designations.

On either side of the Hudson Channel, continental shelf features illustrate opposing orientations of ridge and swale morphology. Numerous hypotheses exist for the genesis of ridge and swale features found along the shelf in this region. Based on bathymetric analysis and grain size characteristics, McKinney and Friedman (1970) concluded that present shelf topography was relict from Pleistocene subaerial exposure during lowered sea level, and that the ridges and swales were the remainder of an intricate fluvial drainage system modified by modern coastal processes. Garrison and McMaster (1966) also interpreted the ridge and swale

morphology east of Long Island as primarily fluvial in origin. Emery et al. (1967), Uchupi (1970), McClennen and McMaster (1971), and Sanders and Kumar (1975) describe sand ridges of the U.S. Middle Atlantic Bight as indicative of overstepped coastlines. Swift et al. (1972), Duane et al. (1972), and McClennen (1973) attributed this morphology to interaction of relict shelf sediment with modern hydraulic forces on the sea floor, suggesting a modern origin for these features in that they are presently being modified by sea floor currents (Williams, 1976). Knebel and Spiker (1977) and Stubblefield et al. (1984) argued that shelf sand ridges reflect a combination of degraded barrier deposits reworked by shelf currents and post-transgressive deposits. McBride and Moslow (1991) evaluated the geomorphology of hundreds of shoreface sand ridges and determined a genetic link between tidal inlet shoal deposits and sand ridges. They also stated that not all ridges could be explained by one ridge evolution model. Snedden et al. (1994) concluded that the ridge-evolution model of McBride and Moslow (1991) best explained the development of Peahala Ridge (New Jersey), where a combination of long-term transgressive and short-term hydrodynamic factors determined the morphology and internal structure of the ridge. Knott and Hoskins (1968) inferred that this shelf was shaped by fluvial and glacial processes.

On the shelf south of Long Island, the area offshore Rockaway Beach exhibits a gentle seaward slope with relatively even contour spacing and minor irregularities from the shoreface seaward to the head of Christiansen Basin (Figure 2-8). East of this area, the bathymetry surface begins to follow the northwest-southeast trend of alternating sand ridges that is predominant on the shelf south of Long Island (Figure 2-8). Backscatter imagery compiled by Schwab et al. (2002) in this area illustrates a number of north-south trending lineations which are interpreted as rippled scour depressions. Analysis of these depressions depicts them as floored with straight-crested, rippled, sandy gravel and gravelly sand with intervening areas of fine sand. The sandy gravel and gravelly sand is interpreted as Pleistocene glaciofluvial sediment exposed and reworked at the sea floor (Schwab et al., 2002). It was suggested that the rippled scour depressions formed due to ongoing erosion of the inner-continental shelf were a result of the active formation and modification of a ravinement surface (Schwab et al., 2002). Immediately east of these features is a prominent northeast-southwest trending shoal identified by the -18 m contour. This shoal encompasses the majority of Borrow Site 3, and it is situated immediately north of one of three prominent outcrops of Cretaceous strata within the study area. This outcrop has been identified by numerous studies of the inner shelf (Williams and Duane, 1974; Foster et al., 1999; Schwab et al., 2002) and is visible within the -24 m contour interval. It is referred to as Cholera Banks (Figure 2-6), and is characterized as an eastward extension of one or more Coastal Plain strata (Williams and Duane, 1974). It has been suggested that this area was an emergent headland cored by coastal plain strata during the early Holocene (Schwab et al., 2000b). Additional ridges along the -18 to -24 m contours located to the east of Cholera Banks display an increasing northwest southeast orientation along their crests (Figure 2-7).

East of Long Beach, in the vicinity of Borrow Sites 4W and 4E, seafloor morphology is dominated by linear shoreface-attached sand ridges. The features are visible along the -18 m contour and are oriented more obliquely to the shoreline than those found offshore Long Beach. Sites 4W and 4E are located on two of these sand shoals seaward of the Federal-State Boundary off Jones Beach. The sand ridges form angles of 30° to 40° with the shoreline and thicken to the east, from about 1 m thick south of Fire Island Inlet to about 5 m thick immediately west of an outcrop of Cretaceous strata offshore Watch Hill (Foster et al., 1999; Figure 2-8). Southward asymmetry exhibited by these shoals is attributed to the action of coast-parallel, southeasterly, storm-generated currents (Duane et al., 1972). Schwab et al. (1999) attribute the formation of these shoals to erosion during the early Holocene of the outcrop of Cretaceous

strata offshore Watch Hill. Sediment transported downdrift (to the west) during marine transgression was reworked by oceanographic processes into a series of shoreface-attached ridges (Schwab et al., 1999). This shoal pattern is especially evident shoreward of the -36 m contour. It has been suggested that ridges present in this area are a significant source of sediment to the western part of Fire Island (Schwab et al., 1999). This hypothesis follows on work completed by Taney (1961) and Rosati et al. (1999) that suggested that additional sources may be contributing to total littoral drift estimates supplying sediment to Fire Island Inlet.

The continental shelf east of New Jersey is characterized by a steeper and narrower shoreface than that observed for southern Long Island, and it is marked by numerous northeast-southwest trending linear shoals. Typically, the Federal-State boundary lies seaward of the -18 m contour in this region, while it coincides with the -18 m contour for a majority of the shelf south of Long Island. Bathymetric contours north of Barnegat Inlet are primarily straight and parallel to -18 m, seaward of which isolated shoals reside. The sea floor in the northern section of coast adjacent to Sandy Hook is relatively irregular and random, unlike the more regular northeast-southwest trending ridge and swale topography found to the south (Figure 2-8). The prominent topographic high separating these two regions is a coastal plain strata outcropping known as Shrewsbury Rocks (Williams and Duane, 1974). Shrewsbury Rocks is a shore-attached linear shoal located east of Monmouth, NJ that extends offshore in a northeast direction where it is truncated by the head of the Hudson River Channel (Figure 2-8). It is the only shoreface-attached shoal located offshore the northern New Jersey coastline, and it varies from the isolated shoals found to the south in that it is wider, longer, and oriented on a more easterly direction (Duane et al., 1972). According to Williams and Duane (1974), Shrewsbury Rocks persisted as a barrier during the Pleistocene and had a definite influence on diverting the course of drainage of the Raritan River and possibly the Hudson River.

To the south, isolated linear shoals are abundant in the nearshore area between Long Branch and Manasquan. Characteristics of linear shoals within this portion of the continental shelf have been well characterized by Duane et al. (1972). Shoals in this area typically are separated from the coast by about 4 km, vary in length from 2 to 6 km, and have a mean width of about 300 m (Duane et al., 1972). All shoals have their long axis oriented east-northeast and have an average angle of about 30° to 85° with the shoreline. Borrow Sites H1 and H2 are located on two of these shoals. Investigation of northern New Jersey surface and subsurface shoal sediments from cores indicated that the shoals were composed of medium-grained, polished, well-sorted quartzose sand (Duane et al., 1972). Further offshore, the shelf becomes increasingly flat as it slopes toward the Hudson Valley.

2.1.2 Surface Sediment

Surface sediment on the New York Bight continental shelf has been analyzed in numerous studies to produce a very detailed characterization of the project area. A regional characterization of shelf surface sediments shows the overall predominance of sand-sized material for a majority of the Atlantic continental shelf (Figure 2-9; Poppe et al., 1994). Additional characterizations of the shelf surface for areas specific to the New York Bight have added considerable detail to this regional view, including characterizations by Williams and Duane (1974), Williams (1976), and numerous reports by the USGS (Foster et al., 1999; Schwab et al., 2002). These depictions have been combined with recent grab sample data collected at and adjacent to each of the borrow sites for the present study to characterize surficial sediment variations.

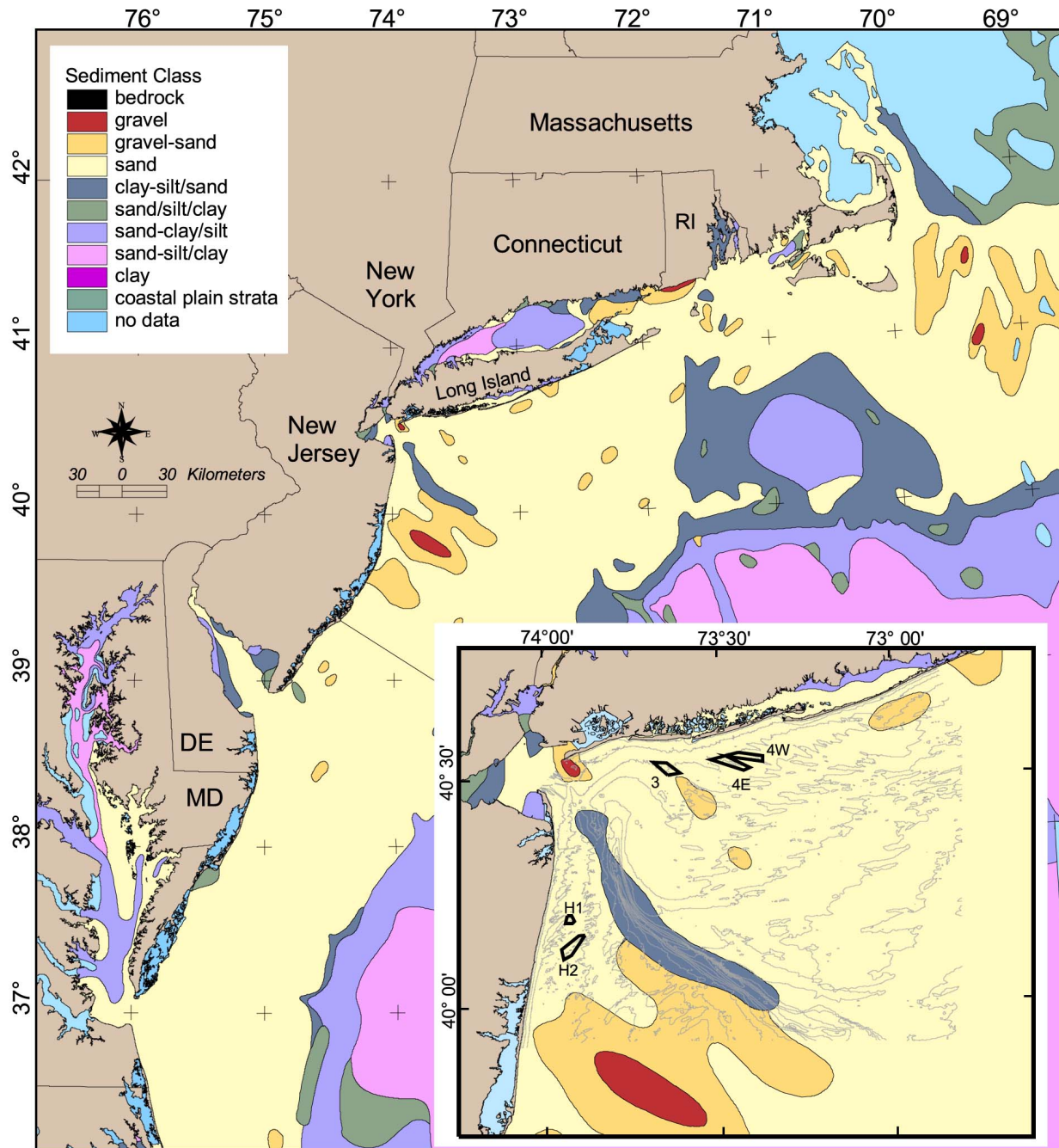


Figure 2-9. Continental Shelf sediment distribution in the New York Bight (adapted from Poppe et al., 1994)

The predominant sediment type on the inner shelf within the New York Bight is fine-to medium-grained sand, with intervening patches of coarse sand and rounded pea gravel (Williams and Duane, 1974; Williams, 1976). Areas of coarse sand and gravel generally corresponded with regions of outcropping coastal plain strata, including Shrewsbury Rocks on the northern New Jersey coast, Cholera Banks south of Long Island in the vicinity of Long Beach, and an unnamed outcrop south of Watch Hill, Long Island (Figure 2-8). Additionally, a zone of silt and mud is present along parts of the Hudson River Channel and within the sewer

sludge and dredged-material disposal areas (Figure 2-9). Modern deposits are typically well sorted, originating from glacial processes and reworking of coastal plain strata (Williams and Duane, 1974). Major sources of modern shelf deposits are the terminal moraines of Long Island to the north and Coastal Plain strata underlying the shelf and comprising the New Jersey landscape to the west (Williams and Duane, 1974).

Regional classification of the Atlantic continental shelf (Poppe et al., 1994; Figure 2-9) provided a good overall view of its surficial sediment composition. Within the study area, this characterization illustrates the predominance of sand-sized material, with smaller areas of gravelly sands, gravels, and silts mixed throughout. A patch of coarse sand visible offshore Long Beach coincides with the location of Cholera Banks (Figure 2-8). This feature was characterized by Williams and Duane (1974) as an eastward extension of one or more Coastal Plain strata, and recent interpretive maps completed by Schwab et al. (2002) have identified this area as consisting of Tertiary/late Cretaceous outcrops.

North of Cholera Banks, in the vicinity of Borrow Site 3, grab samples collected by the USGS indicated that a majority of the sand in this region is medium- to coarse-grained, with some fines intermixed. Grab samples collected by the USGS immediately north of Borrow Site 3 exhibit a large range in sediment size, from 0.14 to 1.28 mm, with an average median grain size of 0.45 mm (Polloni et al., 2000). This large size variation is consistent with later studies that have identified gravelly Pleistocene lag deposits intermixed with modern Holocene fill along the ridges in this region (Schwab et al., 2002). West of this area, a large zone of residual Coastal Plain strata is located offshore Fire Island in the vicinity of Watch Hill. The area has been identified as a potential sediment source for down-current sand ridges during marine transgression. On the shelf east of New Jersey, near Sites H1 and H2, Duane et al. (1972) documented surface and subsurface sediments along isolated linear shoals between Long Branch and Manasquan composed of medium-grained, polished, well-sorted quartzose sand. The unconsolidated sediment cover of these ridges has been shown to be a combination of Pleistocene outwash sediment from the north and material derived from land erosion to the west (Duane et al., 1972). South of this area, large regions of coarse sand and gravel deposits have been attributed to fluvial processes associated with the drowned Hudson River Valley (Schlee, 1964; Amato, 1993; Poppe et al., 1994).

Williams and Duane (1974) produced a more detailed characterization of the inner portion of the New York Bight west of Long Beach, NY and north of Long Branch, NJ (Figure 2-10). The study identified additional coarse sand and gravel patches, along with coastal plain strata outcropping offshore Sea Bright, NJ that were associated with Shrewsbury Rocks. A large area of coarse sediment located northeast of Sandy Hook has been attributed to removal of overlying material by channel dredging and tidal currents that scour the area and leave a lag of coarser sediment. Williams and Duane (1974) also produced general boundaries delineating the different origins of shelf sediment, including a northern glacially derived component and a southern reworked Coastal Plain component (Figure 2-10).

Vibracores and seismic reflection profiles, along with relative mineral abundance, were used to delineate offshore sedimentary facies. Because the boundaries illustrate relative abundance of source materials in the region, glacially derived materials may exist further south than the demarcation but are insignificant compared with the volume derived from Coastal Plain sources (Williams and Duane, 1974). It has been proposed that the Hudson River channel may influence this separation between sedimentary compositions by acting as a barrier to sediment transport while also funneling glacial detritus farther out on the continental shelf, accounting for the large areal extent of outwash across the shelf south of New England (Williams and Duane,

1974). Overall, this characterization was consistent with the regional characterization, showing a predominance of fine- to medium-grained sands along the inner shelf. Williams (1976) characterized shelf sediment between Atlantic Beach and Montauk Point as consisting primarily of fine to medium quartz sand, with secondary occurrences of coarse sand and pea gravel.

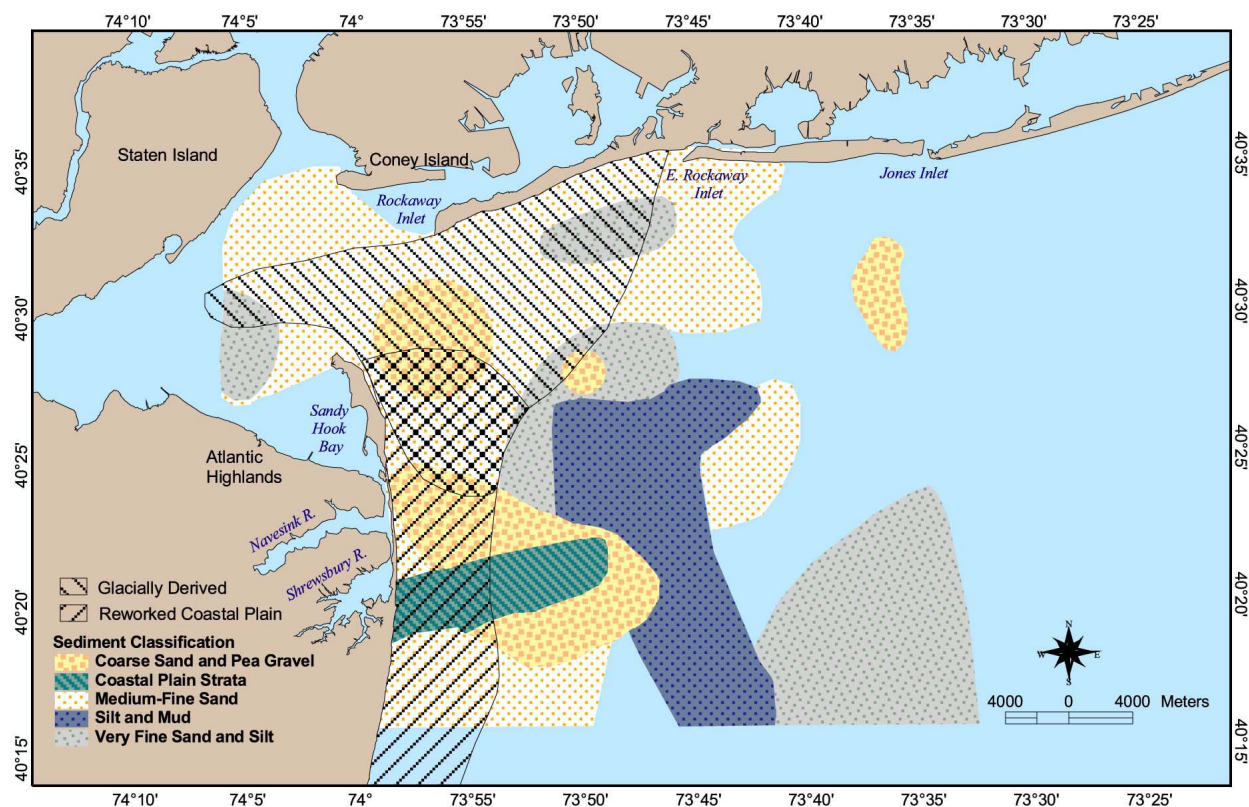


Figure 2-10. Surface sediment distribution within the inner New York Bight (adapted from Williams and Duane, 1974).

The most recent characterization of shelf sedimentary facies, completed by Schwab et al. (2002), includes the inner New York Bight from Raritan Bay to the west side of Jones Island and from Sandy Hook south to Shark River Inlet (Figure 2-11). This area includes Borrow Site 3 and intersects a portion of Site 4W (Figure 2-11). Schwab et al. (2002) identified eight (8) distinct geologic units and provided information on the geometry and structure of Cretaceous and Quaternary deposits in the region. South of Long Beach, the northern half of Site 3 is located in an area classified as Pleistocene fluvio-glacial gravelly sands reworked into a series of low-amplitude, fine-sand, transverse bedforms. The southern half of Borrow Site 3 was defined as Early Tertiary/Late Cretaceous strata with associated reworked gravelly lag deposits. Borrow Site 4W lies within a zone characterized as Holocene sand ripples. Surficial sediment comprising the ripples were characterized as fine sand along ridge crests, with reworked Pleistocene gravelly sand exposed within the troughs (Schwab et al., 2002).

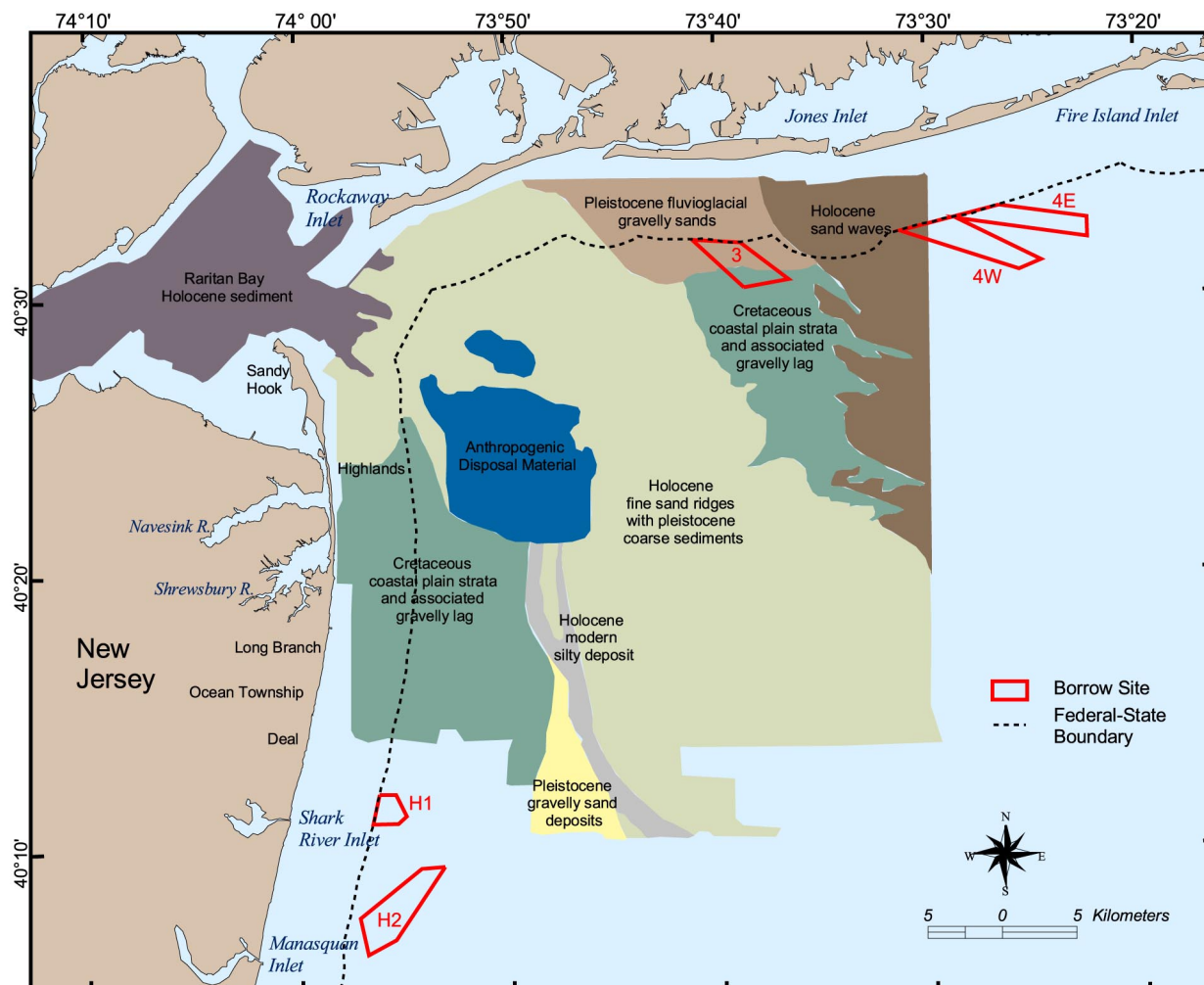


Figure 2-11. Inner New York Bight continental shelf sediment classification based on backscatter imagery (adapted from Schwab et al., 2002).

2.1.3 Subsurface Deposits

Numerous geologic investigations have been conducted within the study area to document continental shelf sedimentation processes and describe the regional character of shelf stratigraphy and sedimentology. Early investigations completed under the USACE Inner Continental Shelf Sediment and Structure (ICONS) program developed regional characterizations of the continental shelf within the Inner New York Bight, south of Long Island and east of northern New Jersey. Recent studies completed by the USGS have built upon this early work and provide detailed depictions of surficial and subsurface geology within the inner portion of the New York Bight and along the shelf south of Long Island. A number of additional studies documenting shelf characteristics adjacent to northern New Jersey were summarized by Uptegrove et al. (1995), four (4) of which fall within present study limits. An additional study completed by Duane et al. (1972) documents the shallow geology of nearshore and offshore sand ridges for determining the genesis of shoreface sand ridge deposits. General boundaries of previous investigations intersecting the current study area are shown in Figure 2-12.

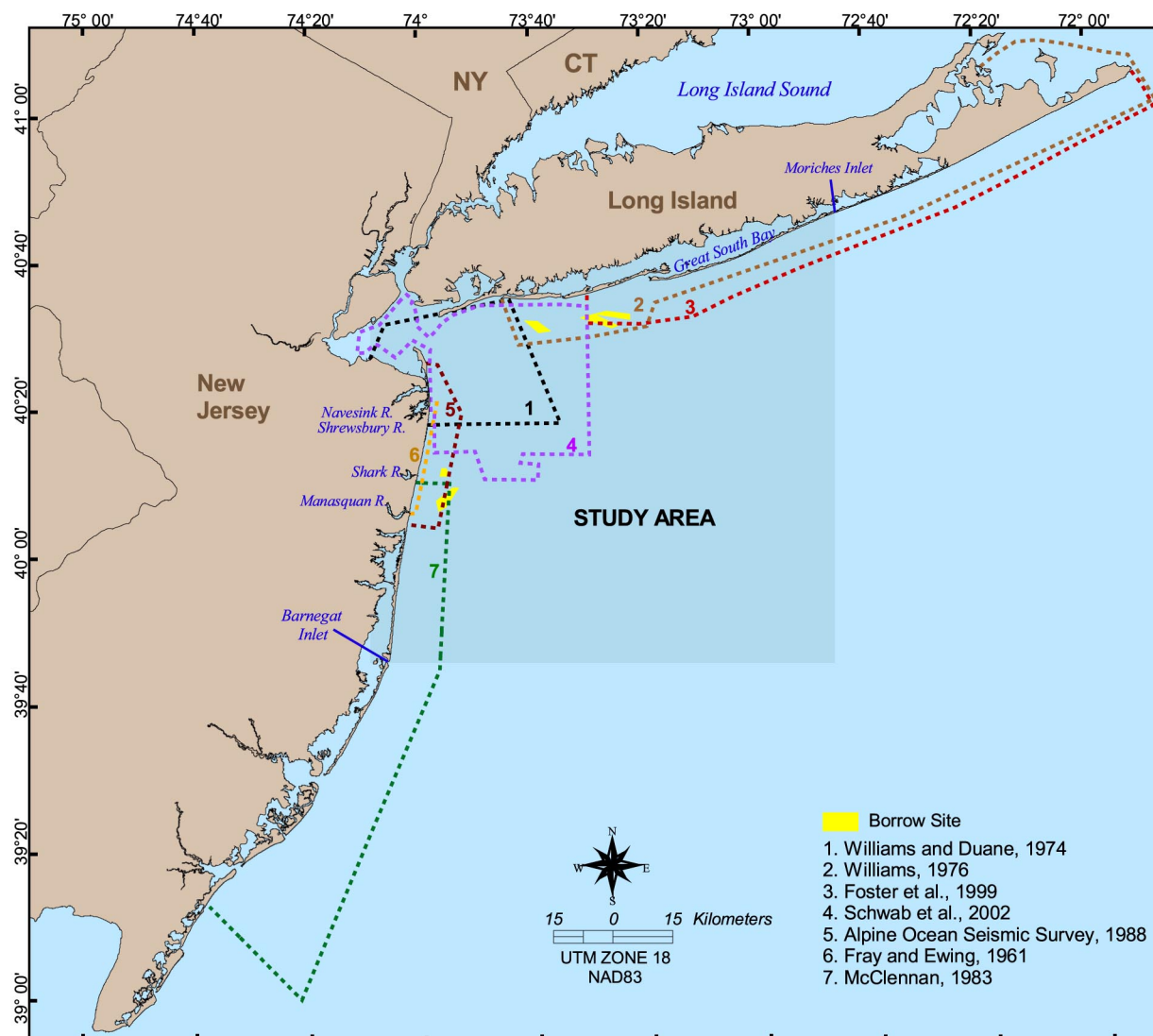


Figure 2-12. Locations of previous geologic investigations within the New York Bight region.

The geology and geomorphology of shelf deposits offshore northern New Jersey were described by Fray and Ewing (1961), Duane et al. (1972), Williams and Duane (1974), McClennan (1983), and Alpine Ocean Seismic Survey (1988). The area of coverage includes Sand Borrow Sites H1 and H2 offshore northern New Jersey (Figure 2-12). Fray and Ewing (1961) collected subsurface data offshore northern New Jersey between the Shrewsbury River and Manasquan Inlet. As part of this study, sparker survey and echo sounder data were collected along two transects parallel to the New Jersey shoreline, and twenty piston cores were drilled to a depth of about 2 m. Offshore components of the Navesink, Red Bank, Manasquan, and Kirkwood formations tentatively were identified on the inner continental shelf within the study area. Duane et al. (1972) characterized linear sand shoals along the entire New Jersey continental shelf, describing shoal composition and surficial sediment texture. Williams and Duane (1974) obtained seismic reflection profiles and 61 vibracores within the Inner New York Bight to characterize the geomorphology and sediments comprising the region. Two distinct geomorphic provinces were identified, separated by the submarine outcrop of resistant coastal plain sediments known as Shrewsbury Rocks. McClennan (1983) conducted a sidescan sonar

and seismic reflection survey seaward of the central New Jersey coast to investigate the shallow subsurface character of shelf deposits. Numerous active megaripples were documented across the shelf surface. Shallow seismic data recorded sub-bottom reflectors as deep as 42 m that outlined sediment-filled valleys and buried channels. Alpine Ocean Seismic Survey (1988) collected seismic and vibracore data to characterize offshore areas potentially suitable for sand borrow material. Approximately 55 million cubic yards of sand was identified on sand shoals immediately west of Borrow Sites H1 and H2 (described in Section 2.1.4).

The geology and geomorphology of shelf deposits south of Long Island have been well characterized by Williams (1976), Butman et al. (1998), Foster et al. (1999), and Schwab et al. (1997; 1999; 2000a, b, c; and 2002). The area covered includes Sand Borrow Sites 3, 4W, and 4E. Williams (1976) initially documented the geomorphology, shallow bottom structure, and sediments of the continental shelf offshore southern Long Island by collecting about 1,200 line-km of seismic profile data and 70 vibratory cores. A number additional cores and seismic records were available for this study from other sources as well. The study extent included the offshore region south of Long Island from Atlantic Beach east to Montauk Point and seaward about 16 km to the -32 m contour (Figure 2-12). Williams (1976) concluded that much of the surficial sand on the inner shelf is suitable as fill for beach restoration activities, with linear sand shoals representing the areas considered best suited for recovery. Sand resource areas were delineated along the shelf with potential volumes and thicknesses assigned within each zone. Total potential sand reserves within the study limits were estimated at more than 6 billion cu m. A thickness of about 3.5 m of suitable fill material was generally assigned to the study area.

Data collected within the study area by Butman et al. (1998), Foster et al. (1999), and Schwab et al. (1997, 1999, 2000a, 2000b, and 2002) include multibeam bathymetric and backscatter imagery, high-resolution sidescan-sonar imagery, seismic-reflection profiles, and bottom sediment samples. These studies were intended to produce detailed descriptions of shelf surface and subsurface characteristics to determine regional-scale sand-resource availability for planned beach-nourishment programs, in addition to developing an understanding of the role inner-shelf morphology and geologic framework play in shelf evolution.

Williams (1976) characterized the subsurface structure of the New York Bight based on four primary acoustic horizons. The horizons were identified using seismic reflection profiles and were established by correlation with cores, land borings, and surface exposures of the reflectors. The oldest and deepest surface identified was granitic bedrock, but the recognition of this horizon was limited to Gardiners Bay due to sub-bottom penetration problems. The surface slopes southeast and shows considerable relief where glacial ice has enlarged pre-Pleistocene drainage channels. Upper Cretaceous and Tertiary semi-consolidated clastic sediments overlie the bedrock and dip and thicken to the southeast. A truncated cuesta of coastal plain strata was identified extending northeast from Long Branch, NJ to Fire Island and continued under the Long Island mainland. The Pleistocene erosion surface comprises the third surface, which consists of blanket-like deposits of outwash sand and gravel. The fourth unit contains Holocene age deposits that were not well defined in seismic profiles collected by Williams (1976), probably due to limited vertical resolution. However, core samples delineated offshore Holocene deposits as modern marine sands deposited over organic-rich mud, interpreted by Williams (1976) as typical back-barrier-beach deposits. Numerous buried ancestral drainage channels were identified on the shelf surface that generally trend from north to south from southern Long Island. Figure 2-13 shows an interpretation of offshore stratigraphy developed from seismic reflection profiles collected between Long Beach and Jones Beach.

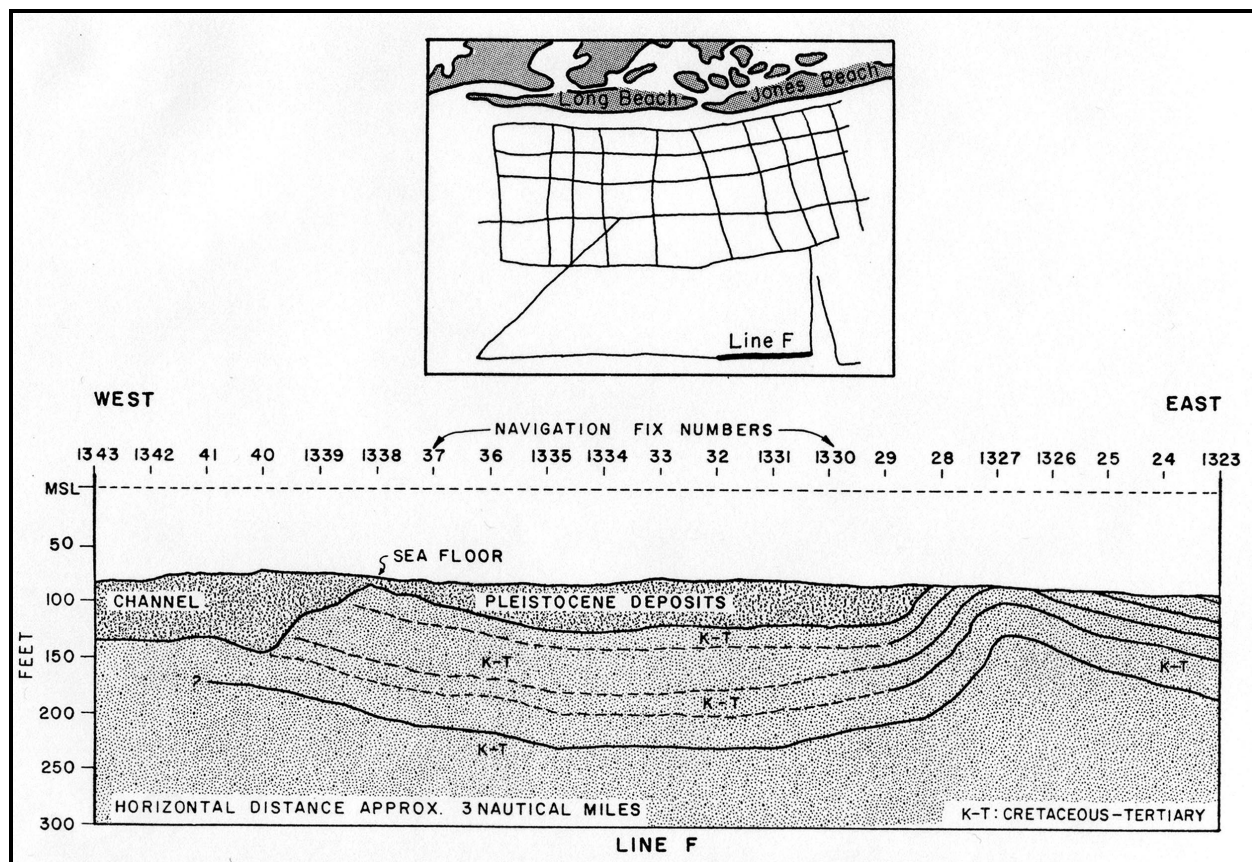


Figure 2-13. Stratigraphic characterization interpreted from seismic reflection profiles (from Williams, 1976).

Subsequent studies by the USGS (Foster et al., 1999; Schwab et al. 2002) are consistent with Williams (1976) original stratigraphic interpretations and have provided significantly more detail. Schwab et al. (2002) provided delineations of stratal thicknesses and identified two regional subsurface unconformities separating the top three units. The deeper of these two unconformities separates Upper Cretaceous to lower Tertiary coastal-plain strata from the overlying Quaternary sedimentary deposit and was informally designated as the coastal-plain unconformity (Schwab et al., 2002). The geometry of the coastal-plain unconformity limited the accommodation space available for subsequent deposition of Quaternary sediment. Outcrops of coastal-plain strata formed resistant bathymetric highs that outcrop on the sea floor and continue to be sites of sea bed erosion (Schwab et al., 2002). The second regional unconformity separates the Pleistocene sedimentary deposit from overlying Holocene sediments and was informally designated as the Holocene Ravinement surface. (Schwab et al. 2002). Paleochannels previously identified by Williams (1976) also were better characterized by recent USGS studies, with sedimentary composition within the channels better developed. Schwab et al. (2002) illustrates a subsurface paleochannel filled with quaternary sediment and the depth to the top of the Coastal Plain Unconformity (Figure 2-14). The outcrop of coastal plain strata associated with Cholera Banks is visible within this depiction as well. Results from USGS investigations, including characterization of the composition, depths and thicknesses of regional stratal units in addition to the delineation of Pleistocene drainage channels and modern reworked sedimentary deposits are used for this study to help quantify potential sedimentary thicknesses for defined borrow sites.

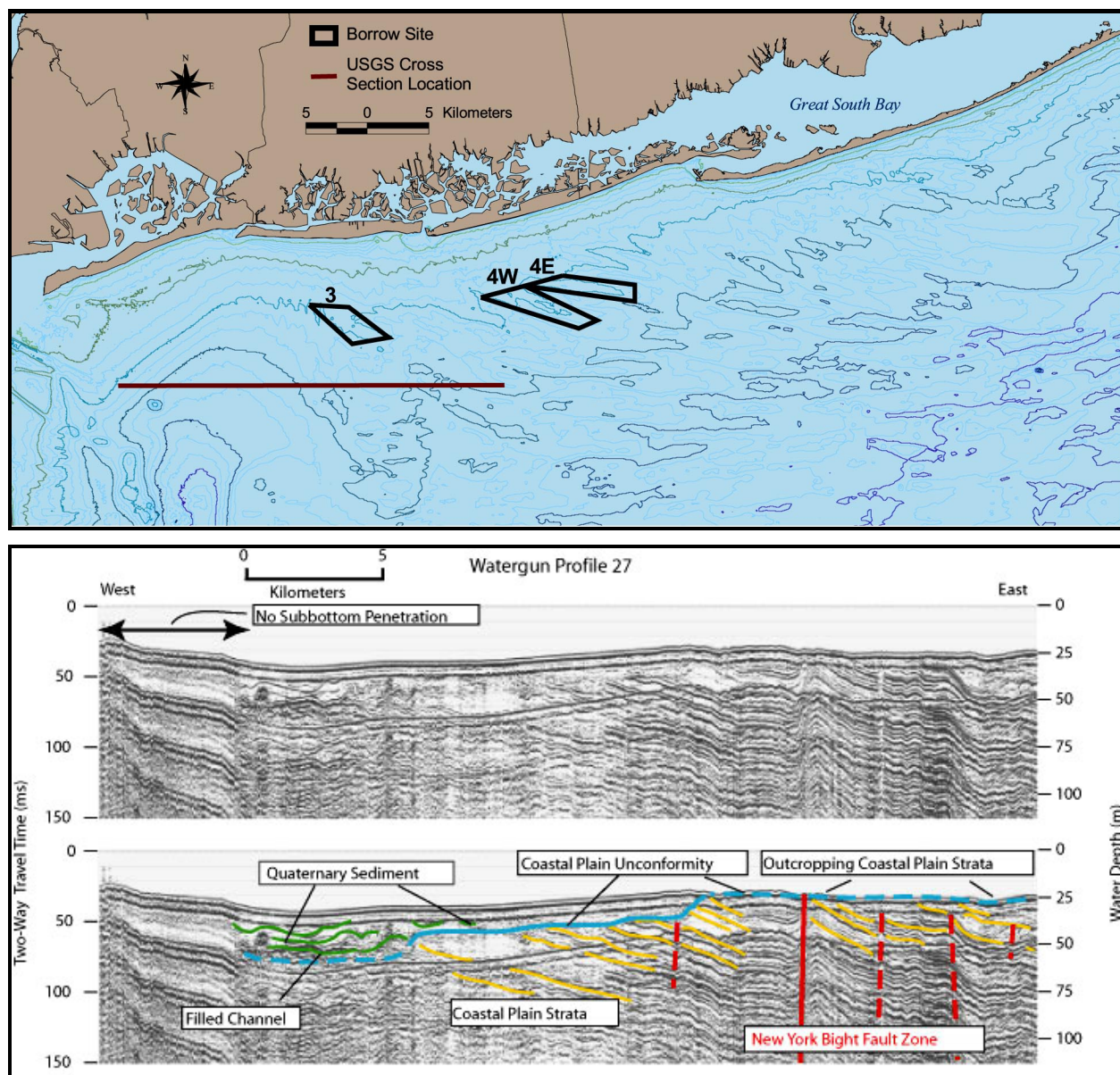


Figure 2-14. Seismic-reflection profile showing Upper Cretaceous coastal-plain strata and overlying Quaternary sediments (from Schwab et al., 2002).

2.1.4 Offshore Sand Resources

The resource potential of offshore sand deposits within the study area was estimated using a combination of geologic and bathymetric data. Volume calculations were generated using bathymetry data within each borrow site, and potential volumes were compared with geologic information in Duane et al. (1972), Field and Duane (1976), Williams (1976), Alpine Ocean Seismic Survey (1988), Foster et al. (1999), and Schwab et al. (2002). Shoal characteristics and sand volume estimates for Borrow Sites H1 and H2 were developed using geologic information on shoal characteristics from Duane et al. (1972), in addition to vibracore data and seismic reflection profiles collected by the Alpine Ocean Seismic Survey (1988). Shoal characteristics and sand volume estimates for Borrow Sites 3, 4W, and 4E were developed using geologic information on shoal characteristics from Duane et al. (1972) and

sediment thickness and subsurface stratigraphic information from Williams (1976) and USGS (Foster et al., 1999; Schwab et al. 2002). Geologic data were correlated with sediment grab samples and potential excavation volumes calculated using bathymetric data to estimate sand resource quantities.

Duane et al. (1972) evaluated surface and subsurface sediments along the isolated linear shoals between Long Branch and Manasquan and indicated that they were composed of medium-grained, polished, well-sorted quartzose sand. These shoals are superimposed on a thin veneer of coarse, poorly sorted, iron-stained and pitted quartz and glauconite, overlying a substrate of fine-grained sands, silts, and clays. The change in substrate occurs at the uppermost acoustic reflector. The unconsolidated sediment cover of these ridges is a combination of Pleistocene outwash sediment from the north and sediment derived from land erosion to the west (Duane et al., 1972). This characterization of shoals offshore New Jersey is consistent with results from grab samples obtained for Borrow Sites H1 and H2. The average median grain size of grab samples collected within these two sites characterizes them as medium to coarse grained sand, with averages of 0.52 and 0.35 mm, respectively.

Alpine Ocean Seismic Survey (1988) identified seven potential sand borrow areas within State and Federal waters offshore New Jersey between Shark River and Manasquan Inlets (Figure 2-15). While the majority of vibracore samples and seismic reflection profiles collected as part of this study are landward of the Federal-State Boundary, general characteristics of the shoals comprising Borrow Sites H1 and H2 can be obtained through extrapolation of these data, assuming shoal characteristics within the region are consistent. Borrow Sites H1 and H2 exist on shoals that were partially characterized by Alpine Ocean Seismic Survey (1988). As such, shoal characteristics were used as proxies for determining characteristics of the seaward portion of each shoal. Borrow Site H1 for this study is adjacent to Alpine's Borrow Area BA-7. Three vibracores (87-17, 87-18, and 87-19) were collected within this borrow area near the -16 and -18 m contours. The majority of the shoal encompassed by Borrow Site H1 is within this depth range. Core 87-17 is located on the westernmost portion of the shoal and furthest from Site H1. The top 4 m of the core consisted of fine to medium sand. Core 87-18, to the east of 87-17, was characterized as fine to medium sand with traces of shell fragments in the top 3.4 m of the shoal. Core 87-19, located closest to Borrow Site H1 was characterized as fine to medium sand for the top 2.7 m of core. Of these three cores, the Alpine Ocean Seismic Survey study concluded that 87-17 and 87-18 were suitable as beachfill material for New Jersey beaches, but that 87-19 was not. Borrow Site H2 is located on a shoal south and west of the remaining borrow areas defined by the Alpine Ocean Seismic Survey. These six borrow areas are located along shoals with similar depths as those associated with Borrow Site H2. Of the six remaining sites, five were considered compatible with beach sediments (BA-2 through BA-6), with thicknesses in these sites ranging from 2 to 5 m (Figure 2-15).

Subsurface sediment characteristics within borrow sites south of Long Island were initially described by Williams (1976). Fourteen (14) potential borrow areas were identified by Williams (1976), of which two (2) intersect the borrow sites defined for the present study (Figure 2-16). These two borrow areas, designated as M and N, were analyzed using vibracore and seismic reflection profile data and were determined to contain potential sand thicknesses of about 5.5 m (Area M) and 3.2 m (Area N). Williams' (1976) Borrow Areas M and N intersect portions of Borrow Sites 3, 4W, and 4E (Figure 2-16). Borrow Area M was well-characterized by a large number of cores, the majority of which were collected along three shore-normal transects offshore Jones Beach. These transects were established by Suffolk and Nassau counties as part of a sewer outfall pipe study but were used by Williams (1976) to characterize the shelf in

this region and assign thicknesses to Borrow Area M (Figure 2-16). Graphical representations of lithologic units comprising these cores are shown in Figure 2-17.

All cores collected along transect C showed that the upper 3.6 to 9.2 m of shelf sediment in this region was composed of fine-to-medium sand with lesser amounts of coarse detritus. All cores located seaward of 15 m water depth contained 3 to 7 m of sand overlying a flat, featureless silt-clay horizon at about -22.3 m MSL. The horizon is continuous under the shoal, which is analogous with data reported by Duane et al. (1972) for similar shoal studies along the Atlantic inner shelf. The remaining cores used to characterize this portion of the shelf were collected by Williams (1976) and had minimum thickness values ranging from 0 to 4.7 m, with an average of about 2 m.

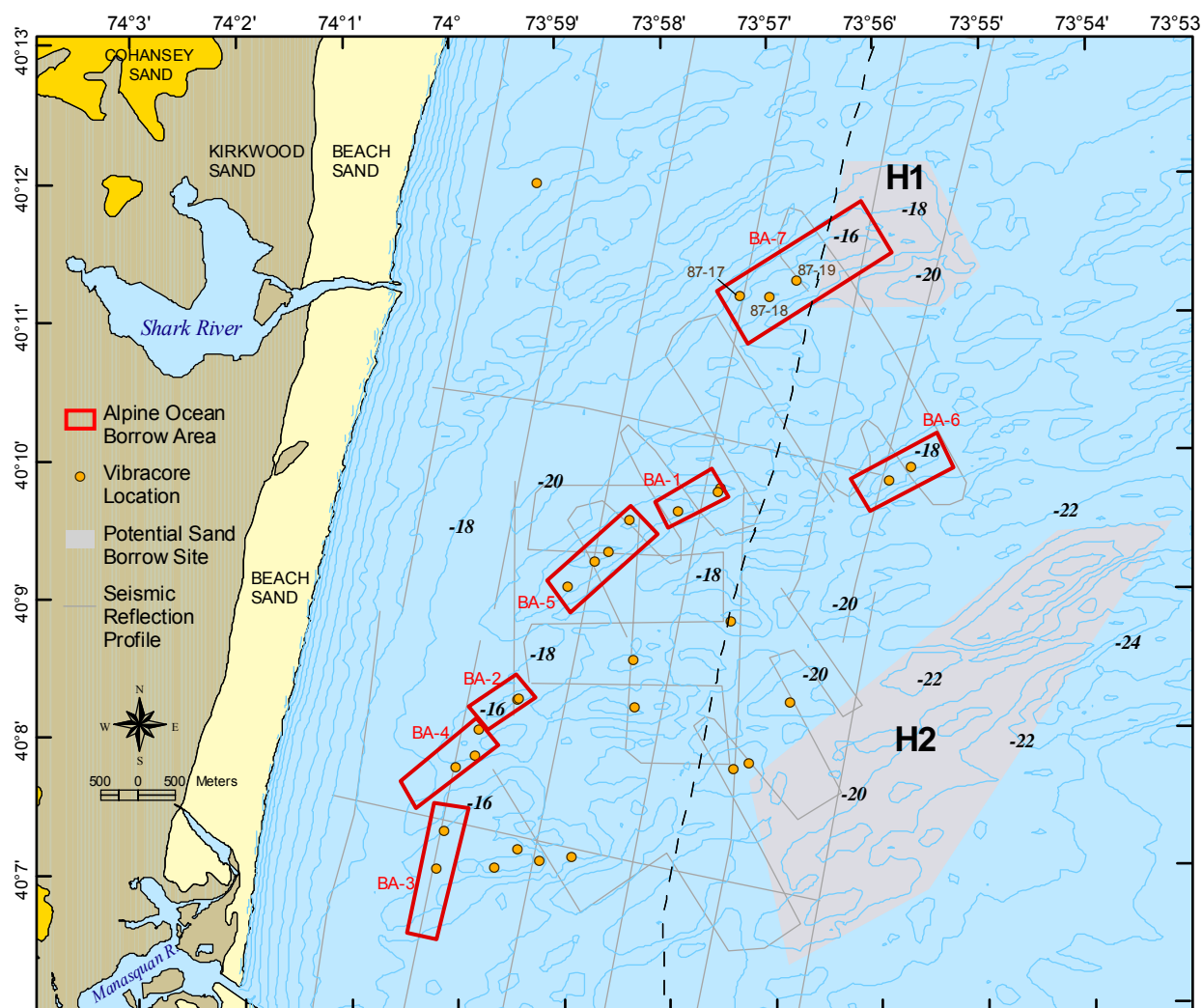


Figure 2-15. Locations of borrow areas, vibracores, and seismic reflection profile lines collected as part of the Alpine Ocean Seismic Survey (1988).

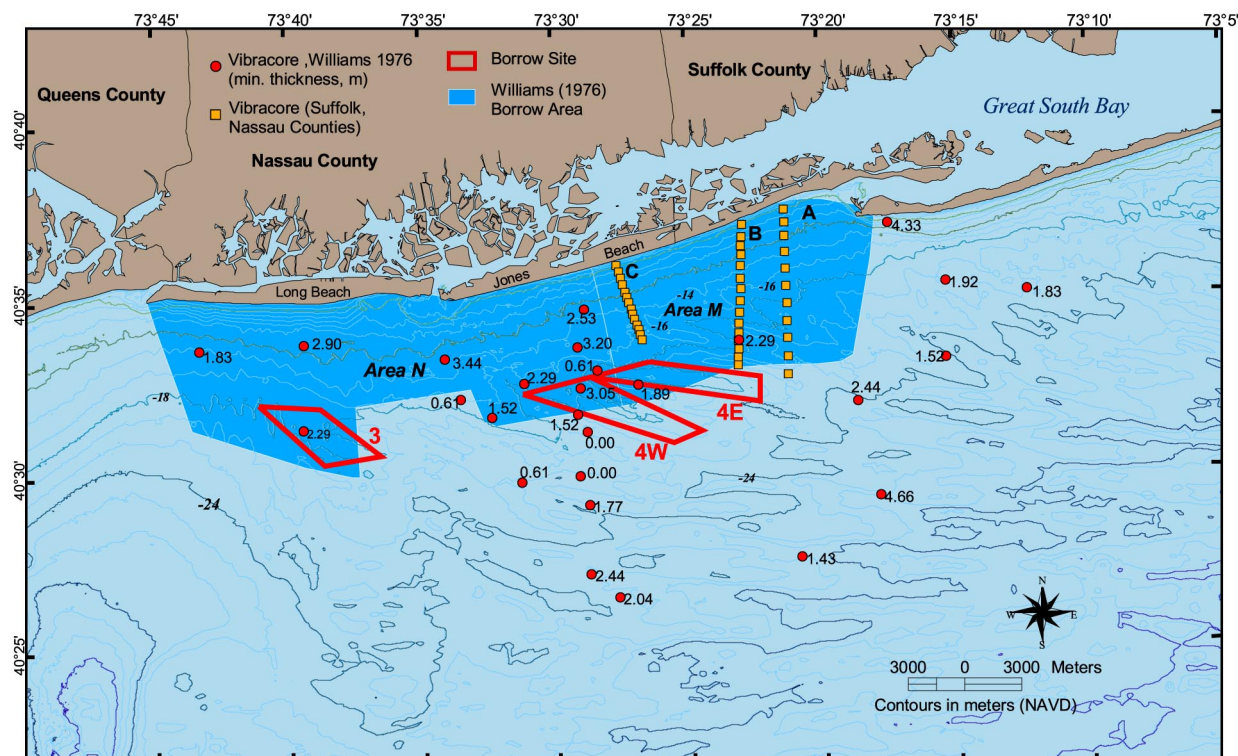


Figure 2-16. Borrow Areas M and N defined by Williams (1976) with vibracores used to delineate suitable sediment thicknesses for the areas. Borrow Area M was assigned a minimum potential thickness of 5.5 m and Borrow Area N was assigned a range of 1.8 to 3.2 m of suitable sediment. Interpretations of vibracores are shown in Figure 2-17.

Borrow Site 4E is intersected by Borrow Area M. The four cores closest to Borrow Site 4E along transects A and B (cores V-23, V-24, V-11, and V-12) show minimum thicknesses ranging from 2.4 to 4.6 m. These four cores are located along the flank of the shoal, generally in water depths greater than the majority of the shoal comprising the borrow site (vibracores are located in depths greater than 20 m, whereas shoal depths range from 16 to 20 m, NAVD). As such, it is possible that thicknesses of suitable material greater than 4.6 m may be present within the majority of the Borrow Site 4E. A vibracore collected along the boundary of Site 4E shows a minimum thickness of 1.9 m at a depth of 20 m (NAVD). Subsurface interpretations developed from these cores indicated that a thickness range of 1.9 to 4.6 m is a suitable estimate for Borrow Site 4E. Foster et al. (1999) also mapped a portion of the shelf within Borrow Site 4E, delineating thicknesses of modern sediments and paleochannel fill areas. According to Foster et al. (1999), the areas between the paleochannels are Pleistocene glacial deposits and probably consist of coarse sediment that may be suitable for beach nourishment. These coarser-grained glacial deposits are the source for modern sand deposits. Modern sands have been reworked primarily from glacial deposits and a Cretaceous outcrop off Watch Hill. Reworked deposits provided well-sorted clean sand that naturally nourished southern Long Island beaches (Foster et al, 1999). Thicknesses of modern sand deposits within Borrow Sites 4W and 4E range from about 0.5 to 3.5 m (Figure 2-18).

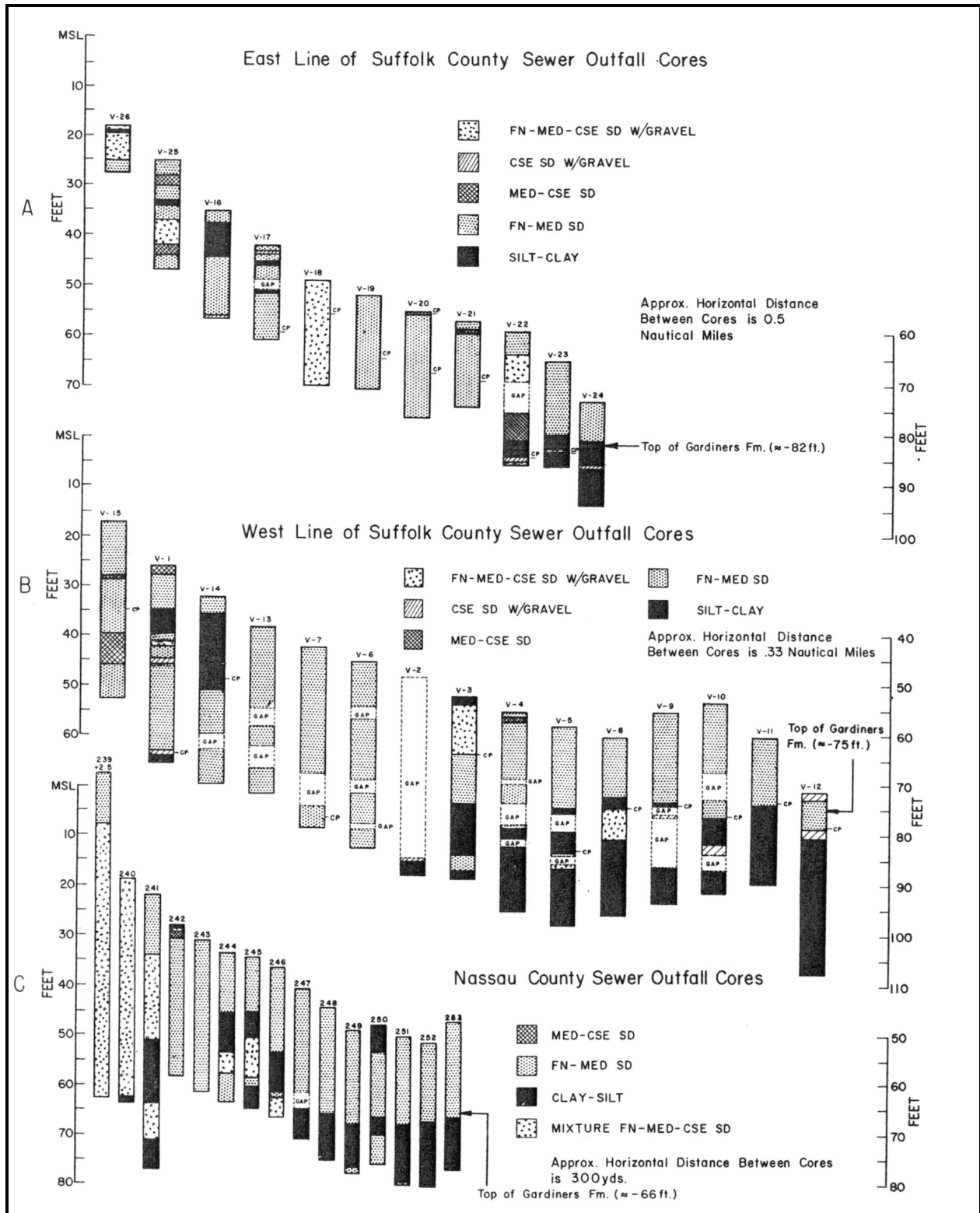


Figure 2-17. Lithologic interpretation of cores collected as part of the sewer outfall study. Core locations are shown in Figure 2-16. Depths are shown in feet below MSL (from Williams, 1976).

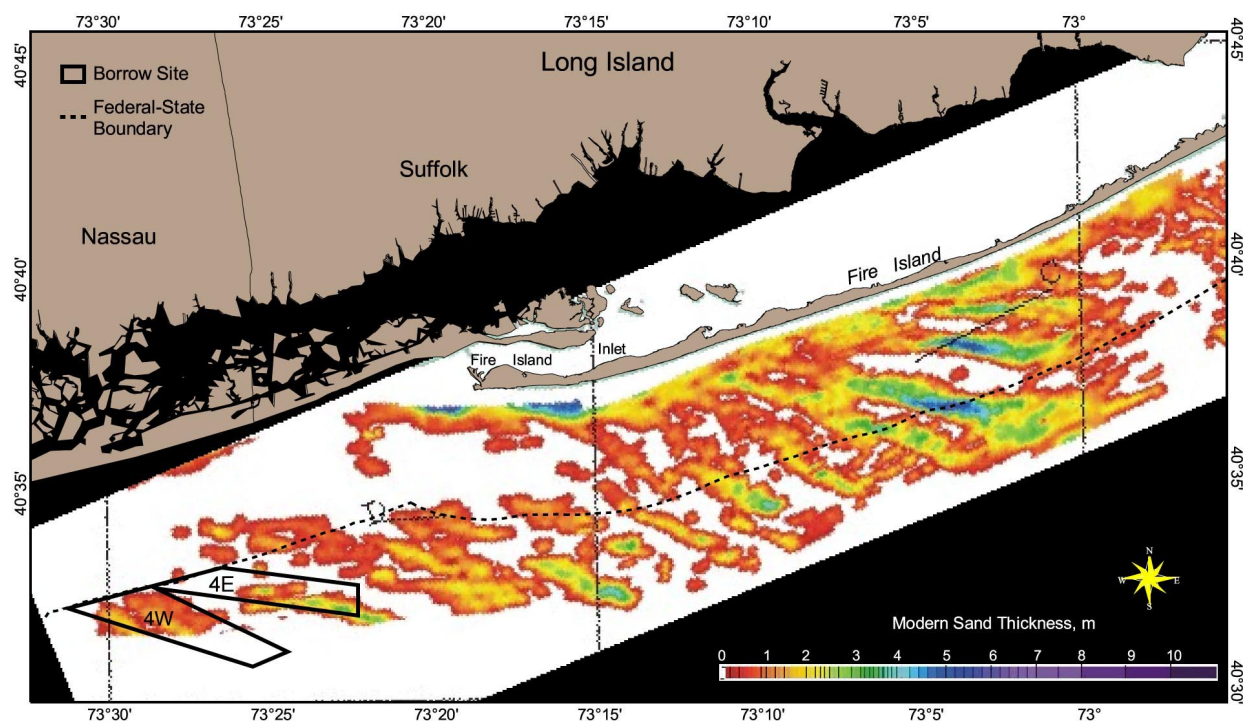


Figure 2-18. Isopach map of modern shelf sediment, southern Long Island (from Foster et al., 1999).

Borrow Site 4W is located along a shoal adjacent to Site 4E. Characteristics of this shoal (shoal orientation, depth, distance offshore, surface sediment grain size) are very similar to those observed at 4E. As such, it is reasonable to believe that subsurface characteristics for the two shoals may be similar, and that a thickness range similar to Site 4E would likely apply. Borrow Site 4W straddles Borrow Areas M and N, though it is primarily located in Area N. Area N was characterized by significantly less vibracore data, and shows greater stratigraphic variation than that observed at Area M. As a result, potential thicknesses determined for this area are less than that for Area M, with a minimum of 1.8 m and a potential of 3.2 m (Williams, 1976). One vibracore was located within the boundary of Site 4W, and it indicated a minimum sediment thickness of 3.1 m along the crest of the shoal (Williams, 1976). Other cores located in the vicinity of Borrow Site 4W range from 0.6 to 2.3 m minimum thickness.

Borrow Site 3 is located in the shallowest portion of all borrow sites developed for this study. Depths along this shoal range from 17 to 19 m (NAVD) and the proposed excavation depth determined for this site was 19 m. One vibracore along the crest of the shoal indicates a minimum thickness of 2.3 m, which is in the middle of the range designated for Borrow Area N. As such, a minimum of 1.8 to 3.2 m of suitable sediment should be available within Borrow Site 3. Schwab et al. (2002) also characterized the subsurface of the continental shelf within Borrow Site 3. Contours showing the thickness of Quaternary sediments illustrate a local thickening of shelf sediment within Borrow Site 3. Thickness ranges within the borrow site from about 20 to 70 m (Figure 2-19).

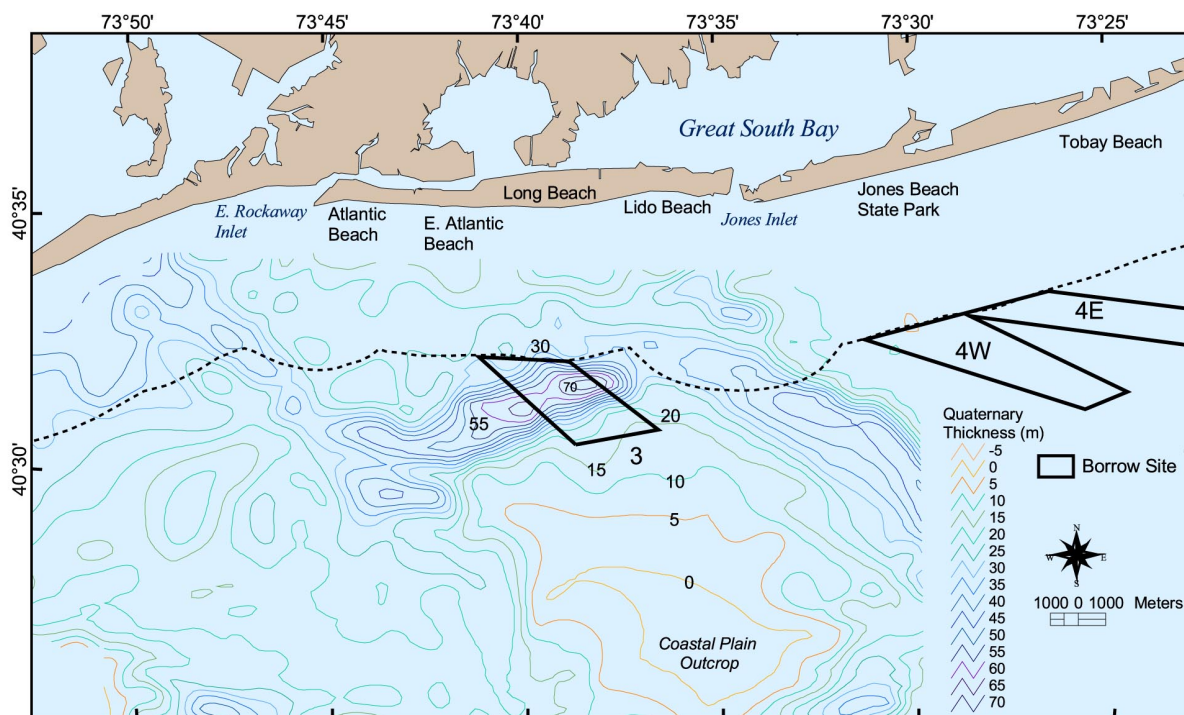


Figure 2-19. Thickness of the Quaternary (Pleistocene and Holocene) sedimentary deposits near Borrow Site 3 (after Schwab et al., 2002).

Total available sediment volume within borrow sites, calculated using bathymetric data, was about 62 million cubic meters (mcm). Average excavation depths ranged from about 0.7 to 1.8 m across the study area. Excavation depths used for calculating sediment volumes were compared with previous reports describing suitable sediment thicknesses within or adjacent to each borrow site (Table 2-1). In general, proposed extraction depths for the present study are within ranges indicated by previous investigations as suitable for beach nourishment. Borrow Site 4W is the only site where minimum thickness values are less than the average value calculated for the site. However, vibracore data used to define this minimum thickness was collected outside the boundary of the borrow site and may not reflect available sediment within the limits of the site.

Table 2-1. Calculated versus published excavation depths determined for sand borrow sites offshore southwestern Long Island and northeastern New Jersey.				
Site	Calculated Average Thickness (m)	Published Thickness Range (m)	Source	Data Used
H1	1.5	2.7 to 4.0	Alpine Ocean Seismic Survey (1988)	Cores 87-17 through 87-19
H2	0.7	2.0 to 5.0	Alpine Ocean Seismic Survey (1988)	Adjacent borrow site volumes
3	1.2	1.8 to 3.2	Williams (1976)	Vibracores collected in and adjacent to the borrow site
4W	1.6	0.6 to 2.3	Williams (1976)	Vibracores collected in and adjacent to the borrow site
4E	1.8	1.9 to 4.6	Williams (1976)	Vibracores collected adjacent to the borrow site

2.2 GENERAL CIRCULATION

General circulation in the New York Bight and adjacent shelf waters is directly related to regional atmospheric surface pressure, wind stress distributions, and the regional density field along and across the shelf. Regional wind climate in the northeast US is influenced by two dominant pressure systems, the Bermuda High and the Icelandic Low. In summer, the Bermuda High is located over more northerly latitudes, creating generally weak southwesterly winds. In winter, the Bermuda High pressure zone weakens and is depressed to the south, allowing the Icelandic Low to generate strong northerly and northwesterly winds out of Canada (Louis Berger Group, 1999). Seasonal changes in atmospheric surface pressure and winds significantly affect currents over the entire shelf, and they are particularly effective in winter when energetic low pressure storm systems create strong northeast winds on the backside of low pressure centers. These strong winds and pressure gradients accelerate southwest flows over the shelf throughout the water column (Noble et al., 1983).

Three major regional currents found within coastal waters offshore the eastern United States influence processes in the New York Bight. They include the northerly flowing Gulf Stream located in waters off the eastern US, southerly flowing coastal or shelf water located offshore northeastern states, and slope water associated with the confluence of these two systems at the continental slope. The Gulf Stream flows northerly, paralleling the east coast of the US until it heads offshore at the approximate location of Cape Hatteras (varies seasonally). Waters carried northward as part of the Gulf Stream are derived from the Gulf of Mexico and Caribbean regions and contribute a relatively warm source of water to the North Atlantic Ocean. The southerly flowing coastal or shelf water originates in Canada with a comparatively cold, dense, and less saline composition. The shelf water current flows southerly along the continental shelf, paralleling northeastern states and incorporating properties of the watershed from coastal rivers that intercept its flow until it converges with the Gulf Stream between Nantucket Shoals and Cape Hatteras. This flow convergence creates an elongated cyclonic gyre offshore New Jersey, encompassing most of the Middle Atlantic Bight (Louis Berger Group, 1999). The inshore edge of this gyre flows towards the south and may also contribute average southwesterly flow detected in this region. Williams and Godshall (1977) measured a 5 cm/sec mean flow along the New Jersey coast. The position of this gyre varies with the northern edge of the Gulf Stream, and it may contribute to low frequency current variability on the New Jersey inner shelf.

Currents within the Middle Atlantic Bight, extending from Cape Hatteras to Montauk Point, were first studied by Bumpus (1973). This study encompassed a ten-year period using sea surface drift bottles and seabed drifters, as well as historical data (vessel logbooks, etc.) to determine flow rates of surface and sub-surface currents. Flow rates along the coast were documented at 5 cm/sec to the west-southwest and south along the coast in this region (e.g., Miller, 1952; Bumpus, 1973; Bishop, 1975) with a slight offshore movement along the coast of Long Island in winter months (Bumpus, 1973; Bishop, 1975).

A summary of the general circulation and other currents in the Middle Atlantic Bight was provided by Beardsley and Boicourt (1981). Based on long-term measurements (>1 year) of currents at many locations in this region, they showed that the annual mean along-shelf flow was toward the southwest near the surface and above the seabed. In about 12-m water depth offshore New Jersey, Beardsley and Boicourt (1981) found that the annual mean currents were toward the southwest at about 4 and 1 cm/s at 4.5- and 10-m water depths, respectively. In water depths <60 m, mean velocity vectors showed onshore veering with increasing depth, a tendency also found by Bumpus (1973). The slow mean across-shelf flow may be related to the

long-term wind-driven circulation (due to seasonal upwelling and downwelling conditions). More detailed discussion of the variability and dynamics in along-shelf flow on the continental shelf in this region was provided by Noble et al. (1983). This study relied on numerous long-term current meter moorings on the shelf to relate long-term current dynamics to wind and density forcing.

2.2.1 Tidal Currents

A semi-diurnal rotary current dominates tidal currents within the Middle Atlantic Bight. The principal lunar semidiurnal tide (M2) accounts for a tidal period of 12.42 hours and a maximum amplitude of about 10 to 15 cm/sec oriented in the cross-shelf direction (Mayer, 1982; Moody et al., 1983). As the M2 rotates counter-clockwise in the northern Atlantic, it generates a high tide along northern shorelines and works its way south along the coast. This progressive wave may travel inshore paralleling the Hudson Shelf Valley before heading south along the coast (Griscom, 1968). Also included in tidal variations are the S2 (solar semidiurnal) and O1 (diurnal) tides, which contribute less energy to the overall tide signature in the region (Louis Berger Group, 1999). Variations in this tidal current occur during spring and neap tides. Within the New York Bight region, spring tides were found to be 45 to 50% greater than neap tides (Griscom 1968).

2.2.2 Density Gradients

Water density over the continental shelf in the New York Bight varies seasonally. In summer months, the water column is highly stratified due to increased surface temperature and higher evaporation rates. In winter months, the water column is largely homogeneous with little temperature and salinity differences (Bishop, 1975). According to Bishop (1975), currents in New York Bight area are dominated by density gradients in the summer and by wind strength and direction in the winter.

2.2.3 Wind Driven Currents

Two major pressure systems affect wind direction in the Middle Atlantic Bight; the Bermuda High and the Icelandic Low. The interaction of these two pressure systems causes annual variations in wind velocity and direction within the region. During summer, anti-cyclonic rotation of winds around the Bermuda High generates southwesterly winds along the east coast of the United States. This pressure cell loses intensity in winter, when the Icelandic Low transports cold air into the region from the west and northwest. Local wind patterns are influenced by the interplay of these two systems over a time period on the order of two to five days (Louis Berger Group, 1999). Winds in the New York Bight region are predominantly from the northwest, except in July and August when winds shift to the south (Williams and Duane, 1974).

Along-shelf currents have a predominant southwest component throughout the water column (Beardsley and Boicourt, 1981). This southwest flow of coastal shelf water may vary with seasonal changes. Strong southerly winds associated with summer weather patterns, coupled with a reduction in river flow rates, causes a reversal in coastal currents, resulting in a net northerly current flow (Bumpus, 1973; Louis Berger Group, 1999). Studies have shown that along-shelf currents generally lag behind along-shelf surface wind stresses by about 5 to 10 hours (Flagg, 1977; Chuang et al., 1979; Mayer et al., 1979; Beardsley and Boicourt, 1981). The same correlation has not been shown to be true with cross-shelf wind stress and along-shelf currents (Csanady, 1982).

2.2.4 Low-Frequency Current

Atmospheric forcing has been shown to be related to low frequency currents in the synoptic-scale time domain (2 to 10 days). Considerable information and analysis of currents in this time domain is available for the Middle Atlantic Bight. Results illustrate that long-term current fluctuations have a strong along-shelf component accounting for 70 to 90% of sub-tidal current variance in the Middle Atlantic Bight (Beardsley and Boicourt, 1981). Previous studies of current fluctuations in this frequency band have shown that along-shelf currents and cross-shelf pressure gradients are coherent and in phase, essentially in geotropic balance.

In comparison, cross-shelf currents are incoherent over very short distances (<70 km) (Mayer, 1982), with the exception of the Hudson Shelf Valley in the New York Bight. This region has shown significant across-shelf flow that is coherent along the entire thalweg, (Mayer et al., 1979) flowing at about 10 to 25 cm/s.

2.2.5 Nearshore Sediment Transport

Nearshore sediment transport is the process by which sediment is moved along a beach through parallel (along-shore) and perpendicular (cross-shore) transport mechanisms. Net transport associated with these processes accounts for shoreline erosion and accretion patterns. The processes that govern these rates are a complex combination of the interaction of winds, waves, tides, and currents. Time scales of sediment movement vary drastically, from extratropical cyclones (northeasters) and hurricanes that can change a beachfront within hours and days, to geological processes forming barrier islands and shorelines over thousands of years.

Sediment characteristics also affect transport rates at the shoreline. These characteristics include grain size, mass, shape, and durability. In general, an inverse relationship exists between sediment grain size and transport rates. Larger sized sediments require a greater amount of energy to move and thus contribute to a lower overall transport rate, whereas smaller sediments require less energy for movement, and therefore allow for greater rates of transport. Simply put, more mass requires greater transport energy, more surface area requires less transport energy, and the less durable the sediment, the easier it breaks apart and the easier it is to suspend and transport sediment in the water column.

When waves break at an angle to the beach, along-shore currents are generated, capable of lifting and moving sediment along the coast. For example, waves approaching most of the New Jersey and Long Island shoreline from the east tend to move sand along-shore from north-to-south and east-to-west, respectively. Superimposed on this regional pattern are the smaller scale reversals in longshore transport direction associated with tidal inlets. Toward the northern portion of New Jersey, the shoreline becomes oriented nearly north-south. In this region, the net sediment transport direction is controlled by mean wave conditions that tend to drive sediment from south-to-north (Caldwell, 1966). Eroded materials enter the littoral system and are transported northward to feed Sandy Hook and southward toward the barrier islands (USFWS, 1997). Net littoral drift to the north and south of this region is centered about a nodal point located near Manasquan Inlet. North of Manasquan, net littoral drift is estimated at about 382,000 m³/yr (Caldwell, 1966); south of Manasquan, net drift is southerly at about 38,000 m³/yr. While prevailing winds along the Long Island coast are southwesterly, long fetches from the east produce net longshore transport from east to west, with rates showing considerable variation. Eroded glacial sediments from headlands are carried west in the littoral current and are deposited by wave action on barrier beaches and offshore bars (USFWS, 1997). Net littoral

transport for parts of the south shore of Long Island has been estimated by Taney (1961) and the USACE (1971) to be between 344,000 and 460,000 m³/yr (Williams and Duane, 1974).

2.3 BIOLOGY

2.3.1 Benthic Environment

2.3.1.1 Infauna

Infaunal assemblages inhabiting shelf waters offshore New Jersey and New York resemble assemblages common within much of the Middle Atlantic shelf (Wigley and Theroux, 1981). Organisms collected during previous investigations of the New York Bight included members of the major invertebrate groups commonly found in sand bottom marine ecosystems, primarily crustaceans, echinoderms, mollusks, and polychaetous annelids. Generally, inner shelf infaunal assemblages are numerically dominated by polychaetes in terms of abundance (Wigley and Theroux, 1981) and taxa (Reid et al., 1991). Other conspicuous members of the coastal infaunal community include amphipod crustaceans and bivalves. Infaunal taxa that inhabit soft sediments of the Bight comprise assemblages that exhibit spatial and seasonal variability (Steimle and Stone, 1973; Pearce et al., 1981; Wigley and Theroux, 1981; USDOJ, MMS, 1989; Reid et al., 1991; Chang et al., 1992).

Large-scale investigations of the Bight identified the most common infaunal taxa inhabiting inner shelf waters. The USACE, New York District, sponsored a 1995 benthic invertebrate survey of the Bight Apex (Barry A. Vittor & Associates, Inc., 2002). Thirty-six stations in the Apex survey area included inshore stations parallel to the Long Island and New Jersey coastlines as well as offshore stations at depths of 40 to 50 m, within an area of approximately 3,703 km². The archiannelid *Polygordius* sp. was numerically dominant in grab samples, comprising 40.5% of all individuals collected. The remaining annelids (polychaetes and oligochaetes) were the next most dominant group at 24.9%. Bivalves and amphipods contributed 18.9% and 11.4% of the individual abundance, respectively. Annelids also accounted for the highest proportion of taxa present (127 taxa, or 52%), followed by amphipods (41 taxa, or 16.7%), other crustaceans (38 taxa, or 15.4%), and bivalves (22 taxa, or 8.9%). Twenty-one taxa accounted for 86.2% of the total assemblage abundance, and the 47 most abundant taxa comprised over 94.5% of the total individuals collected.

Chang et al. (1992) identified infaunal assemblages based on 1980 to 1982 benthic data and found a widespread group of infaunal taxa determined to be a basic, natural assemblage for the Bight. Common taxa in this widespread assemblage are predominantly polychaetes, including *Aricidea catherinae*, *Goniadella gracilis*, *Mediomastus ambiseta*, *Monticellina dorsobranchialis*, *Parougia caeca*, *Scoletoma acicularum*, *S. hebes*, and *Tharyx acutus*. Other taxa include the amphipods *Ampelisca agassizi*, *Byblis serrata*, *Corophium crassicorne*, *Erichthonius fasciatus*, *Leptocheirus pinguis*, and *Unciola* spp., the bivalve *Nucula proxima*, and the echinoid *Echinarachnius parma*. Pearce et al. (1981) summarized and synthesized results from several benthic investigations (1973 to 1976) of the Bight inner shelf. Common infaunal taxa censused during those investigations include the amphipods *Protohastorius wigleyi* and *Unciola irrorata*, the bivalves *N. proxima*, surfclam *Spisula solidissima*, and *Tellina agilis*, the echinoid *E. parma*, and the polychaetes *Glycera dibranchiata*, *G. gracilis*, *Nephtys buccera*, *N. picta*, *Pherusa affinis*, *Spiophanes bombyx*, and *T. acutus*. Steimle and Stone (1973) reported on inner shelf benthic fauna collected during 1966 and 1967 offshore southwestern Long Island. Their survey found infaunal assemblages numerically dominated by the amphipod

Protohaustorius deichmannae, bivalve *N. proxima*, echinoderm *E. parma*, and polychaete *Nephtys incisa*.

The Asbury Park to Manasquan Inlet Beach Erosion Control Project included monitoring of sand borrow and reference areas located 2 to 8 km offshore Manasquan and Belmar, New Jersey (Burlas et al., 2001). Overall abundance was numerically dominated by *Polygordius* (lowest practical identification level [LPIL]), which accounted for 35.5% of all animals collected. The amphipod *Pseudunciola obliquua* and tanaid *Tanaissus psammophilus* comprised 9.6% and 6.0% of the total abundance, respectively. Other taxa contributing 1% or more to total abundance included the polychaetes *Caulleriella* cf. *killariensis*, *Magelona papillicornis*, and *S. bombyx*, the mollusks *N. proxima*, *S. solidissima*, and *T. agilis*, the amphipods *Acanthohaustorius millsi*, *P. wigleyi*, and *Rhepoxynius hudsoni*, the sand dollar *E. parma*, and non-identified oligochaetes and rhynchocoels.

These populations that comprise open shelf benthic communities are affected by abiotic environmental parameters, resulting in both seasonal and spatial variability in their distribution and abundance. Shallow coastal waters are characterized by a variety of environments having great diurnal, seasonal, and annual fluctuations in their chemical, hydrographic, and physical properties. Distributions and abundances of benthic invertebrates are regulated at a basic level by these physical environmental forces.

Temporal variation in population abundance may be a result of response to proximal environmental variability or due ultimately to the life history patterns of individual species. Seasonality of macrobenthic assemblages inhabiting open shelf sediments has been noted in numerous investigations (e.g., Frankenberg and Leiper, 1977; Flint and Holland, 1980; Schaffner and Boesch, 1982; Weston, 1988; Byrnes et al., 2000). Patterns of seasonal reproductive periodicity in marine systems apparently are related to ambient climatic conditions, primarily temperature, for most marine invertebrates (Sastry, 1978). Reproduction is more or less continuous at deeper shelf depths (Warwick, 1980), where greater environmental stability promotes seasonal persistence of outer shelf infauna (Schaffner and Boesch, 1982).

An absence of temporal patterns of abundance for some macrobenthic species in many cases is related to reproductive strategies. Transitional infaunal species that do not emerge necessarily on a seasonal basis often colonize an area because of intermittent conditions that are favorable for reproduction. Opportunistic species generally are tolerant to fluxes within their environment, but more importantly they are early and successful primary colonists due to their reproductive capacity and dispersal ability (Grassle and Grassle, 1974). These species often undergo eruptive population peaks, depending on their adaptive ability to withstand varying environmental conditions, and can exploit an open niche while avoiding competitive interaction (Boesch, 1977). Because habitat availability often is the result of random perturbations of the environment, such as significant riverine outflow due to flooding, the appearance of these opportunistic taxa often occurs in tandem with such episodes. For non-opportunistic species inhabiting marine soft sediments, a lack of temporal patterns of abundance may indicate simply that seasonal patterns of variability do not exist for these species (Pearce et al., 1976).

Despite yearly fluctuations in infaunal community composition, open shelf systems can exhibit remarkable consistency over temporal scales consisting of multiple years. Reid et al. (1991) found that, although absolute numbers of species decreased in many portions of the area between 1980 and 1985 and then increased in certain areas between 1986 and 1989, there was little change in species composition and numerically dominant species over a decade or more in the New York Bight.

In addition to temporal differences in benthic assemblage composition, conspicuous spatial variability often is evident in the distributions of populations inhabiting open shelf sediments. Spatially variable environmental parameters such as hydrography, water depth, and sediment type influence benthic assemblage composition and the extent of numerical dominance of those assemblages by various infaunal populations.

Changes in infaunal assemblage composition along broad depth gradients have been noted in several studies of shelf ecosystems. Day et al. (1971) determined the distribution of infauna along a depth gradient from the beach zone to the edge of the continental shelf off Cape Lookout, North Carolina and found four subtidal zones delineated at increasing depth intervals. The turbulent zone included the inner shelf between 3- and 20-m depths, and corresponds with the location of the present study. The most common taxa of the turbulent zone were best represented at the 20-m depth station (Day et al., 1971). Tenore (1985) and Harper (1991) both reported a transition between inner shelf and continental slope fauna of the South Atlantic Bight and northern Gulf of Mexico, respectively.

Wigley and Theroux (1981) reported that highest infaunal densities in the New York Bight occurred at relatively shallow depths. With increasing water depth, abundance of each of the major taxonomic groups (e.g., bivalves) generally decreases, although not uniformly across taxonomic groups. At depths less than 24 m, polychaetous annelids are numerically dominant (1,120 individuals/m²), followed by bivalves (590/m²) and amphipod crustaceans (487/m²). At depths from 25 to 49 m in Bight waters, amphipods (459/m²) are the most common group, followed by polychaetes (137/m²) and bivalves (51/m²) (Wigley and Theroux, 1981). Reid et al. (1991) and Chang et al. (1992) studied the same infaunal data for the New York Bight, and both found a depth-related trend where the number of species increased from inshore to offshore stations.

Certain infaunal populations are distributed in approximately equal numbers from shallow waters to the edge of the shelf (e.g., the polychaete *S. bombyx*), whereas others occur mostly on the inner shelf (e.g., the bivalve *S. solidissima*) or middle to outer shelf (e.g., the polychaete *Scalibregma inflatum*) (Pearce et al., 1981). Although there is a negative correlation between infaunal abundance and water depth, it is unclear whether such faunal distributions are affected mostly by absolute water depth, or whether depth-related factors such as hydrology, sedimentary regime, and seasonality override any effects of sediment particle size and type on infaunal assemblages. The effect of water depth on benthic assemblages may in some cases be defined more precisely as an effect of depth-related environmental factors, including physical parameters that vary with increasing depth, such as current regime, dissolved oxygen, sedimentary regime, and temperature. Surficial sediments tend to be well sorted at shallow depths, due primarily to the mixing of shelf waters by storms. Moreover, inner shelf waters generally are less depositional in nature than outer shelf or slope waters due to a dynamic current regime near the bottom, although shallow areas affected by estuarine outflow may experience episodic deposition of fine materials, which can influence benthic community structure.

Although some descriptions of depth-related differences in benthic assemblages have encompassed geographically broad areas (Day et al., 1971; Flint and Holland, 1980; Wigley and Theroux, 1981; Tenore, 1985), local variability in bathymetric relief can result in habitat heterogeneity within an area of relatively minor differences of absolute depth. Trough features, especially those that are bathymetrically abrupt, can dissipate current flow along the substratum surface, resulting in deposition of fine materials, including organic material. Presence of fine sediments and organics in bathymetric depressions can support benthic assemblages that are

distinct from nearby areas without depressions (Boesch, 1972; Lyons, 1989; Barry A. Vittor & Associates, Inc., 1999a; Byrnes et al., 2000).

Previous sampling efforts in open shelf waters have demonstrated the importance of sediment type in determining infaunal population densities. Coarse-grained sediments generally support greatest numbers of infauna, while fine-grained sediments support the fewest (USDOI, MMS, 1989). In a report based on over 1,000 quantitative samples of benthic fauna collected from Maine to northern New Jersey between 1956 and 1965, Theroux and Wigley (1998) summarized the relationship between sediment type and infaunal abundance. Coarse-grained sediments generally support the greatest numbers of infauna, while fine-grained sediments support the least. Amphipods are found in all sedimentary habitats, although densities are greatest in sand-gravel and sand habitats. Generally, bivalve densities are greatest in sand-shell sediments and decrease with increasing sediment particle size, although shell fragment habitats can support moderately high bivalve numbers. In general, gravel bottoms support the lowest densities of bivalves. Polychaetes occur in all sediment types, although abundances are greater in sand and gravel bottoms than in silt-clay habitats (Theroux and Wigley, 1998).

Not only do sediment particle size and type influence faunal densities, they have a strong effect on the species composition of benthic assemblages (Sanders, 1958; Young and Rhoads, 1971; Pearce et al., 1981; Weston, 1988; Chang et al., 1992; Byrnes et al., 2000). Although many infaunal species occur across a range of sediment types, most infaunal taxa tend to predominate in specific sedimentary habitats.

Studies in and near the New York Bight have affirmed findings of numerous other studies that found sediment type a reliable predictor of the distribution of infaunal taxa (Steimle and Stone, 1973; Pearce et al., 1981; Chang et al., 1992). Distinct assemblages offshore southwest Long Island (Steimle and Stone, 1973) were delineated according to sedimentary habitat, where medium- to coarse-grained sands supported infaunal assemblages numerically dominated by the amphipods *A. millsi*, *P. deichmannae*, and *U. irrorata*, the bivalves *S. solidissima* and *T. agilis*, the echinoderm *E. parma*, and the polychaetes *Sthenelais limicola* and *S. bombyx*. Silty sand assemblages supported the bivalve *N. proxima* and polychaetes *N. incisa* and *Pherusa affinis*. Aggregations of the blue mussel *Mytilus edulis* provided habitat for certain motile fauna, including the scale-worm polychaetes *Harmothoe extenuata*, *H. imbricata*, and *Lepidonotus squamatus* (Steimle and Stone, 1973). In another survey of the study area, Pearce et al. (1981) found that the medium- to coarse-grained sand community is represented by *E. parma*, *N. buccera*, *Protohaustorius* spp., *S. bombyx*, *S. solidissima*, *T. agilis*, and *U. irrorata*. Sedimentary habitats with finer materials support relatively high densities of taxa such as the amphipods *A. agassizi* and *U. irrorata*, the bivalve *N. proxima*, and the polychaetes *Mediomastus* and *T. acutus* (Pearce et al., 1981; Chang et al., 1992).

Infaunal assemblages are composed of taxa that are adapted to particular sedimentary habitats through differences in behavioral, morphological, physiological, and reproductive characteristics. Feeding is one of the behavioral aspects most closely related to sedimentary habitat (Sanders, 1958; Rhoads, 1974). Fine-textured sediments are generally characteristic of depositional environments, where occluded interstitial space and accumulated organic material supports surface and subsurface deposit-feeding burrowers. All marine sediments are anoxic at some depth below the sediment-water interface, and the depth of oxygen penetration generally varies with sediment type. In very fine sediments, occlusion of interstitial space limits the depth of oxygen diffusion to a few millimeters into the sediment (Revsbech et al., 1980). Environments with more shallow penetration of dissolved oxygen tend to support deposit-

feeding taxa that are able to maintain some form of hydrologic contact with the sediment-water interface, via manufacture of tubes or through construction of irrigating burrows. Coarse sediments in high water current habitats, where organic particles are maintained in suspension in the water column, favor the occurrence of suspension-feeding taxa that strain food particles from the water column and facilitate feeding by carnivorous taxa that consume organisms occupying interstitial spaces (Fauchald and Jumars, 1979). In between these habitat extremes are a variety of habitat types that differ with respect to various combinations of sedimentary regime, depth, bathymetry, and hydrological factors. Different sedimentary habitats support particular infaunal assemblages that tend to vary with time. Because multiple interacting processes influence complex ecosystems, controlling mechanisms sometimes cannot confidently be inferred from resultant community patterns. Among the factors that most affect diversity in benthic communities are the heterogeneity of the physical environment, the vagaries of larval recruitment, and biological interaction (Johnson, 1970).

2.3.1.2 Epifauna

Investigations of epifaunal communities inhabiting New York Bight waters reveal seasonal and spatial variations in the distribution and abundance of taxa. Many numerically dominant epifauna that inhabit the inner shelf may be described more precisely as epibenthic, especially gastropods and decapods, as these taxa routinely are collected along with infauna using grab samplers. Certain epifaunal taxa, such as lady crab (*Ovalipes ocellatus*), commonly burrow deeply into sediments, and adaptive behaviors of this type can complicate efforts to categorize such taxa into a specific, lifestyle-based, invertebrate group. In addition, many bivalves are effectively sampled using either a trawl or grab method. Given this dilemma of ecological classification, the taxa discussed below commonly are collected in trawl samplers and, for the sake of comparison and consistency, herein are considered epifauna.

Abundant epifauna of the New York Bight and adjacent waters include crustaceans such as *Pagurus* spp., Atlantic rock crab (*Cancer irroratus*), and sevenspine bay shrimp (*Crangon septemspinosa*), echinoderms such as the sea star *Asterias forbesi* and sand dollar *E. parma*, and moon snails (*Euspira heros* and *Nevirita duplicata*) (Pearce et al., 1981; Hales et al., 1995; Viscido et al., 1997).

Epifaunal taxa were collected and described during 18 cruises from October 1991 to November 1992 on the inner continental shelf (water depth 8 to 16 m), offshore Great Egg Inlet, New Jersey (Hales et al., 1995; Viscido et al., 1997). Monthly samples were taken with a 2-m beam trawl at and adjacent to the Beach Haven Ridge, an offshore sand shoal. Crustaceans, echinoderms, and mollusks were the most abundant epifauna in trawl collections. Commonly sampled epifauna included the bivalve *S. solidissima*, echinoderms, such as the asteroid *A. forbesi* and echinoids *E. parma* and *Arbacia punctulata* (sea urchin), and the gastropods *Busycon* spp., *E. heros*, and *N. duplicata* (Hales et al., 1995). Viscido et al. (1997) reported on epibenthic decapods sampled during the Beach Haven Ridge investigation. The sevenspine bay shrimp was the most abundant decapod found in the study, followed by Atlantic rock crab, lady crab, and spider crab (*Libinia emarginata*). Together with sevenspine bay shrimp, these taxa comprised over 98% of all decapods collected.

Seasonal patterns in abundance were similar for nearly all taxa in the Beach Haven Ridge studies. Abundance of most epifaunal taxa was low in winter, then increased to peak densities in summer and declined in fall (Hales et al., 1995). Exceptions to this seasonal pattern included members of the Gastropoda (including the moon snails *E. heros* and *N. duplicata*), which were most abundant in winter or spring. Temporal variation of the numerically dominant epibenthic

decapods also was evident in the Viscido et al. (1997) study. Abundance of sevenspine bay shrimp showed two clear peaks, in spring and fall, as did spider crab. Atlantic rock crab and lady crab each showed a single peak in individual density of very small individuals in summer and appeared to use the site for settlement. The most common pattern of distribution found by the Beach Haven sand ridge studies was that epifauna were abundant around the shoal (landward and seaward) but not on the shoal (Hales et al., 1995; Viscido et al., 1997). The observed distribution patterns of epifauna may be attributable to a number of factors, including but not limited to sediment type and local hydrology. As with infaunal invertebrates, epifaunal populations have distributions limited by depth-related variability of temperature and sedimentary habitat (Cerame-Vivas and Gray, 1966; Wenner and Read, 1982).

Certain epifauna tend to be associated with particular sedimentary habitats (Wigley and Theroux, 1981). Gastropod densities generally are greatest in areas of coarse sand and gravel. Lyons (1989) found that some mollusk species were most abundant in an offshore trough feature with poorly sorted sediments, whereas other mollusks were abundant on an offshore shoal that had well-sorted, coarse sediments. Decapods generally are found in areas of gravel and shell, although species such as sevenspine bay shrimp tend to occur in areas of sand and Atlantic rock crab inhabits a variety of sediment types. Wenner and Read (1982) suggested that the combination of extremely variable sediments and temperatures may be sufficient to cause marked zonation between decapod assemblages on the outer shelf. Sand dollars such as *Mellita quinquesperforata* most commonly are associated with sand habitats. Brittle stars are most common in silty sand, probably due to greater efficiency of burrowing in finer sediments. Sea stars tend to be distributed across a range of sediments, from shelly sand to silt habitats (Wigley and Theroux, 1981).

2.3.1.3 Demersal Fishes

The ichthyofauna of the New York Bight is composed of about 180 species from 82 families. The demersal component of this fauna consists of about 85 species represented mostly by skates (Rajidae), dogfishes (Squalidae), searobins (Triglidae), hakes (Gadidae), sculpins (Cottidae), scup (Sparidae), wrasses (Labridae), and flounders (Paralichthyidae). The demersal ichthyofauna is transitory, and movements are closely related to large-scale temperature fluctuations. When water temperatures rise in spring, there is an influx of warm temperate fishes from the south, and several cold water species migrate back to the north in response. Following fall and winter cooling of the shelf waters, warm temperate species return south and offshore whereas some of the cold temperate forms move into the area (Grosslein and Azarovitz, 1982). Typical warm temperate forms found in the New York Bight during spring and summer include black sea bass (*Centropristis striata*), butterfish (*Peprilus triacanthus*), northern searobin (*Prionotus carolinus*), scup (*Stenotomus chrysops*), spotted hake (*Urophycis regia*), and summer flounder (*Paralichthys dentatus*) (Grosslein and Azarovitz, 1982; Colvocoresses and Musick, 1984; Mahon et al., 1998). In addition to the warm temperate species found during summer months, there are several expatriated tropical forms such as butterflyfishes that settle in nearshore waters of the area (McBride and Able, 1998). Northern or boreal species found in New York Bight waters during winter and spring include goosfish (*Lophius americanus*), red hake (*Urophycis chuss*), silver hake (*Merluccius albidus*), and spiny dogfish (*Squalus acanthias*) (Colvocoresses and Musick, 1984). Although there is considerable variation in the abundance and distribution of demersal fishes between both seasons and years, numerical dominants at any one time generally are represented by a relatively small group of fishes. Winter is a time of low abundance and diversity, as most species leave the area for warmer waters offshore and to the south. Species that remain in the area year-round include blackbelly rosefish (*Helicolenus dactylopterus*), blueback herring (*Alosa aestivalis*), dusky shark

(*Carcharhinus obscurus*), lined seahorse (*Hippocampus erectus*), scup, snake eel (*Ophichthus sp.*), striped bass (*Morone saxatilis*), tilefish (*Lopholatilus chamaeleonticeps*), summer flounder, and windowpane (*Scophthalmus aquosus*).

Within the temporal framework described above, species are distributed across the shelf in broad depth-related groups most simply characterized as inner, middle, and outer shelf (Sullivan et al., 2000). The spatial distribution changes with ontogeny of individual species (Steves et al., 1999). Many demersal fishes also use estuarine areas along the coast. During spring, increasing numbers of fishes are attracted to the New York Bight coast because of the proximity of estuaries that fishes use for adult spawning and early life stage nurseries. Some demersal fishes that use estuaries during their ontogeny include red hake, spot (*Leiostomus xanthurus*), weakfish (*Cynoscion regalis*), windowpane, and winter flounder (*Pseudopleuronectes americanus*) (Able and Fahay, 1998). While the aforementioned species utilize estuaries as nurseries, several species of demersal fishes use the open shelf as a nursery area. There are depth-related settlement patterns for several of the common species.

Feeding habits of demersal fishes of the region can be summarized by recognizing that several dietary guilds exist (Garrison and Link, 2000). Dietary guilds are composed of species exploiting similar food resources on the open shelf. These guilds include crab eaters, planktivores, amphipod/shrimp eaters, shrimp/small fish eaters, benthivores, and piscivores. Feeding guild composition depends on morphological characteristics that change with growth of the fish, thus many species will change guild membership as they grow.

The affinity of certain demersal fishes for particular sediment types often is related to the types of prey items supported by those sediments. Species such as butterfish, skates, and winter flounder predominantly are bottom feeders that consume infaunal and epibenthic crustaceans and polychaetes. Amphipods are known to be important in the diets of some demersal fishes, including Atlantic cod (*Gadus morhua*), haddock (*Melanogrammus aeglefinus*), and winter flounder. Certain demersal foragers may therefore be attracted to areas of medium to coarse sands, where crustaceans and polychaetes are most abundant (Theroux and Wigley, 1998).

Demersal fishes of the region associate with benthic habitats on a variety of spatial scales. At large scales (kilometers), ridges and swales provide relief and habitat complexity, but for juvenile fishes, structure at smaller scales (meters to centimeters) is more important (Diaz et al., 2003). Small-scale structure used by juvenile fishes as refuge from predation can be either physical (sand waves or bedforms) or biogenic (shell fragments, worm tubes, and pits) in nature. Diaz et al. (2003) reported high fish densities associated with higher sand wave heights and concentrated worm tube aggregations on the inner continental shelf.

2.3.2 Pelagic Environment

2.3.2.1 Squids

Squids (cephalopods) display patchy distributions and periodic vertical and horizontal migrations. Water quality, currents, and temperature principally control the occurrence of squids, while food and population density affect movements within suitable water masses.

Two squid species are common in New York Bight waters: the longfin squid, *Loligo pealei*, and the shortfin squid, *Illex illecebrosus* (Lange and Sissenwine, 1980). These are the squids most likely to occur in or near the four sand borrow sites. The longfin squid, a member of the

family Loliginidae, occurs primarily in shelf and shelf edge waters from Newfoundland to the Gulf of Venezuela. Its distribution, determined by fishery independent sampling, is influenced by water temperature, depth, and time of day (Brodziak and Hendrickson, 1999). A general seasonal migratory pattern has been observed for the Middle Atlantic Bight population. Adults move offshore in fall and remain there until April, when adults and young migrate back into shelf waters for summer (Lange and Sissenwine, 1980). Spawning reportedly occurs year-round with major peaks in spring (April and May) and fall (August and September). The longfin squid grows rapidly and lives about 1 year (Lange and Sissenwine, 1980; Brodziak and Macy, 1996). This species represents an important fishery in the Middle Atlantic Bight with annual landings averaging 18,200 metric tons (mt) (Cadrin, 1998). Commercial fishing for longfin squid takes place from Cape Hatteras to Georges Bank. It is caught with small-mesh trawls, pound nets, and traps (Cadrin, 1998). Fishing effort tracks the seasonal distribution, with offshore (i.e., shelf edge) fishing taking place from October to March and inshore (i.e., middle and inner shelf) fishing taking place from April to September.

The shortfin squid belongs to the family Ommastrephidae, a family consisting entirely of oceanic species. This species is distributed accordingly in oceanic and shelf edge waters from Greenland to Cape Hatteras (Lange and Sissenwine, 1980). It migrates into shallower waters (10 to 50 m) during summer months; in late fall it moves south and offshore in the area from Georges Bank to Cape Hatteras (Lange and Sissenwine, 1980). Spawning occurs from December to June in offshore waters. Most individuals die following spawning. The species lives up to 1 year (Hendrickson, 1998). In Middle Atlantic Bight waters, commercial trawl fisheries are concentrated in outer shelf waters from June to September, when abundance peaks. The 1986 to 1996 annual catch of shortfin squid averaged 12,800 mt (Hendrickson, 1998). Most commercial fishing is conducted in shelf edge waters with small-mesh trawls.

2.3.2.2 Fishes

Common pelagic fishes inhabiting New York Bight shelf waters include herrings such as alewife (*Alosa pseudoharengus*), American shad (*Alosa sapidissima*), Atlantic menhaden (*Brevoortia tyrannus*), and Atlantic herring (*Clupea harengus*), as well as Atlantic mackerel (*Scomber scombrus*), bluefish (*Pomatomus saltatrix*), and butterfish. Other pelagic species occurring offshore New Jersey and New York but not mentioned further include anchovies (*Anchoa hepsetus* and *A. mitchilli*), jack crevalle (*Caranx hippos*), and mullets (*Mugil cephalus* and *M. curema*).

All of these pelagic species form schools and migrate seasonally with peaks during various portions of the year. Most of these species are important to recreational and commercial fisheries. As with demersal fishes, most pelagic species in the New York Bight are transitory, originating in waters either to the north (Gulf of Maine or Georges Bank) or to the south (south of Cape Hatteras). Their occurrence in the New York Bight is generally a response to seasonal changes in water temperature, which trigger southerly or northerly movements by species of southern or northern origin, respectively.

The herring species exhibit two basic spawning patterns: the alewife and American shad are anadromous, migrating from the sea into freshwater rivers to spawn, whereas Atlantic menhaden and Atlantic herring spawn in continental shelf waters. The alewife is found along the coast of eastern North America from the Gulf of St. Lawrence to South Carolina (Kocik, 1998a). During autumn, most of the population overwinters in waters near the edge of the continental shelf. In spring, the population moves into shelf waters throughout the region. Adults enter coastal rivers and migrate to freshwater to spawn during spring. The American

shad is another anadromous species found in shelf waters during summer and fall (Kocik, 1998b). It moves up rivers to spawn during spring. Water temperature is the key environmental determinant of spawning in this species. Temperature may vary within a season, thus timing of the upstream migration may vary slightly from year to year. Alewife and American shad are important to commercial and recreational fisheries in the region. Commercial catches of alewife averaged about 500 mt for the Middle Atlantic Bight since 1994 (Kocik, 1998a). American shad catches, mostly by gill net, averaged 1,100 mt since 1980 (Kocik, 1998b).

Atlantic menhaden occurs in shelf waters, where it forms large schools. Atlantic menhaden schools in the Middle Atlantic Bight migrate northward in summer and southward in fall to overwinter in warmer waters. Some spawning may occur offshore New Jersey and New York during fall, while the fishes are migrating south. This species is not fished north of Virginia. Atlantic herring is most abundant in northern waters of the Gulf of Maine and Georges Bank. The Georges Bank stock overwinters in the New York Bight from December to April. Spawning occurs year-round with peaks in spring and fall. Adult females lay demersal eggs. Spawning probably does not occur offshore of New Jersey and New York (Able and Fahay, 1998). The primary fisheries for this species occur north of New Jersey and New York on Georges Bank and in the Gulf of Maine.

Atlantic mackerel occurs in two spawning populations in the northwest Atlantic: a northern population in the Gulf of St. Lawrence that spawns in June and July, and a southern population that spawns in the Middle Atlantic Bight during July and August (Overholtz, 1998a). In the Middle Atlantic Bight, it spends winter months in offshore waters near the shelf edge; in spring it migrates inshore and to the north. Spawning occurs during this migration in shelf waters. This species is sought by commercial and recreational fishers. Commercial fishing occurs primarily from January through May; recreational fishing occurs mostly from April to October (Overholtz, 1998a). Landings in the Middle Atlantic Bight averaged 14,840 mt from 1987 to 1996.

Bluefish is a migratory species occurring in inshore, coastal, and shelf waters. It migrates into the Middle Atlantic Bight during spring, and south or offshore during fall. The bluefish is an important fishery species. Early investigations held that the bluefish spawned during two discrete events, one in the South Atlantic Bight and the other in the Middle Atlantic Bight. New evidence indicates that spawning is a continuous event beginning during spring and ending during late summer in South Atlantic Bight waters (Cowan et al., 1993; Smith et al., 1994). The bluefish spawns during midsummer months in waters south of Cape Hatteras; however, young fish immigrate to inshore waters of the Middle Atlantic Bight coast including Long Island Sound (Nyman and Conover, 1988). This species is important to commercial and recreational fisheries of the region. The 1994 to 1996 average commercial landings were 11,400 mt for the eastern U.S.; recreational landings for the Middle Atlantic Bight were 7,400 mt (Terceiro, 1998). Primary commercial gear for bluefish are otter trawl and gill net.

The Middle Atlantic Bight butterfish population migrates northward and inshore in summer. In winter months, the population moves southward and offshore. The butterfish spawns continuously from late January to at least July in the Middle Atlantic Bight (Rotunno and Cowen, 1997). This species exhibits high natural mortality and serves as prey for many predatory species. It grows rapidly and reaches a maximum age of about 3 years (Rotunno and Cowen, 1997; Overholtz, 1998b). The current Middle Atlantic Bight fishery lands an average of 3,000 mt annually. Otter trawl is the principal gear used in the fishery.

2.3.2.3 Marine Turtles

The four marine turtle species likely to occur within inner shelf waters off New Jersey and New York, in frequency of occurrence, are loggerhead (*Caretta caretta*), leatherback (*Dermochelys coriacea*), Kemp's ridley (*Lepidochelys kempii*), and green (*Chelonia mydas*) (Shoop and Kenney, 1992). The hawksbill (*Eretmochelys imbricata*), also found in waters off North America, inhabits coral reefs and other hard bottom habitats in tropical and subtropical latitudes, and thus is considered to be extremely rare in the study area. The seasonal window for presence of marine turtles in New Jersey and New York waters extends from June through November (National Marine Fisheries Service [NMFS], 1996).

All marine turtles are protected under the Endangered Species Act of 1973. Currently, the leatherback and Kemp's ridley are Federally listed as endangered species and the loggerhead as a threatened species. The green turtle also is Federally listed as threatened, except for the Florida breeding population, which is listed as endangered in the State of Florida. However, due to the inability to distinguish which breeding population an individual green turtle belongs to when away from the nesting beach, all green turtles are considered endangered wherever they occur in U.S. waters (NMFS, 1996).

Loggerhead Turtle

The loggerhead turtle occurs throughout temperate and tropical waters of the Atlantic, Pacific, and Indian Oceans (Dodd, 1988). In the western Atlantic, it is found in estuarine, coastal, and shelf waters from South America to Newfoundland. Because it is the most temperate of the marine turtles in terms of nesting habits, it is the species most likely to be present along the Middle Atlantic coast. The loggerhead was the most abundant turtle species seen during Cetacean and Turtle Assessment Program (CETAP) aerial surveys off the Middle Atlantic and New England coasts (Winn, 1982) and during recent aerial surveys within the study area (T. Cole, 2003, personal communication, NMFS Northeast Fisheries Science Center [NEFSC]).

Most loggerhead sightings, strandings, and incidental captures in coastal and estuarine New Jersey waters are immature individuals (i.e., juveniles or subadults) that use shallow, coastal and inner shelf waters as developmental foraging habitat (NMFS, 1996). These animals are most common during spring and summer months. Immature loggerheads migrate northward from south of Cape Hatteras during spring, moving south again during fall (Marine Turtle Expert Working Group, 1996a). Loggerhead turtles may be present in New Jersey and New York waters from June through November (NMFS, 1996).

Four nesting subpopulations of loggerhead turtles have been identified (Marine Turtle Expert Working Group, 1996a). These are 1) the northern subpopulation, extending from North Carolina to northeastern Florida; 2) the south Florida subpopulation; 3) the Florida Panhandle subpopulation; and 4) the Yucatan subpopulation. Ninety percent of loggerhead nesting in the U.S. occurs in south Florida. Only minor loggerhead nesting occurs along the Atlantic coast as far north as New Jersey, where reported nesting activity occurs only during July (Dodd, 1988; Frazier, 1995).

After hatching, loggerheads swim offshore and begin a pelagic existence within *Sargassum* rafts, drifting in current gyres for several years (Marine Turtle Expert Working Group, 1996a). At approximately 40 to 60 cm carapace length, juveniles move into nearshore and estuarine areas, where they become benthic feeders for a decade or more prior to maturing

and making reproductive migrations (Carr, 1987). Loggerheads captured incidentally in New Jersey coastal waters are typically in this size range (NMFS, 1996).

Loggerhead adults and subadults are generalist carnivores feeding primarily on nearshore benthic crustaceans (particularly crabs) and mollusks (Dodd, 1988). Studies in New York waters have shown that these turtles generally feed in water depths of approximately 15 m or less (NMFS, 1996). All potential sand borrow sites within the study area include depths near 15 m.

Leatherback Turtle

The leatherback turtle is a circumglobal species that inhabits waters of the western Atlantic Ocean from Newfoundland to northern Argentina. The leatherback is the largest living turtle (Eckert, 1995). It is considered the most pelagic of the marine turtles (Marquez, 1990) because of its unique deep-diving abilities (Eckert et al., 1986) and wide-ranging migrations. This species was the second most abundant turtle seen off the Middle Atlantic coast during CETAP surveys (Winn, 1982) and during recent surveys within the study area (T. Cole, 2003, personal communication, NMFS NEFSC). Most sightings within this area occurred during summer months.

Leatherbacks nest on coarse-grained, high-energy beaches in tropical latitudes (Eckert, 1995). Florida is the only location in the continental U.S. where significant leatherback nesting occurs. Very little is known of the pelagic distribution of hatchling and/or juvenile leatherback turtles.

Adult leatherbacks feed in the water column, primarily on cnidarians (medusae [jellyfish], siphonophores) and ascideans (salps, pyrosomas) (Eckert, 1995). The turtles are sometimes observed in association with jellyfish, but actual feeding behavior has only occasionally been documented. Foraging has been observed at the surface, but also is likely to occur at depth (Eckert, 1995).

Kemp's Ridley Turtle

The Kemp's ridley is the smallest and most endangered marine turtle. Its distribution extends from the Gulf of Mexico to Nova Scotia and Newfoundland (Marine Turtle Expert Working Group, 1996b). Adult Kemp's ridleys are found almost exclusively in the Gulf of Mexico, primarily in shallow coastal waters less than 50 m deep (Byles, 1988).

Kemp's ridleys found along the New Jersey and New York coasts are mostly juveniles that use shallow, Middle Atlantic coastal waters as developmental habitat (Morreale et al., 1992). They move northward along the coast in spring with the Gulf Stream to feed in productive, coastal waters between Georgia and New England (NMFS and U.S. Fish and Wildlife Service [USFWS], 1992). These migrants then move southward with the onset of cool temperatures in late fall and winter (Morreale et al., 1992).

Nesting of Kemp's ridleys occurs almost entirely at Rancho Nuevo beach, Tamaulipas, Mexico, where 95% of the nests are laid along 60 km of beach (NMFS and USFWS, 1992; Weber, 1995). In the U.S., nesting occurs infrequently on Padre and Mustang Islands in south Texas and in a few other locations (Marine Turtle Expert Working Group, 1996b).

After emerging, Kemp's ridley hatchlings swim offshore to inhabit *Sargassum* mats and drift lines associated with convergences, eddies, and rings. Hatchlings feed at the surface and

are dispersed widely by Gulf and Atlantic surface currents. After reaching a size of about 20 to 60 cm carapace length, juveniles enter shallow coastal waters and become benthic carnivores (Marine Turtle Expert Working Group, 1996b). This is the life stage that could be present in the study area. Kemp's ridleys prefer crabs but also occasionally eat mollusks, shrimps, dead fishes, and marine vegetation (Mortimer, 1982; Lutcavage and Musick, 1985; Shaver, 1991; Burke et al., 1993; Werner and Landry, 1994).

Green Turtle

The green turtle has a circumglobal distribution in tropical and subtropical waters. In the U.S., it occurs in Caribbean waters around the U.S. Virgin Islands and Puerto Rico, and along the mainland coast from Texas to Massachusetts. Adult green turtles typically are found in shallow tropical and subtropical waters, particularly in association with seagrass beds (NMFS and USFWS, 1991).

Green turtles along the New Jersey and New York coasts are juveniles and subadults, because adults do not migrate from their preferred habitat (tropical/subtropical seagrass beds) except to nest. As with other turtles found in the area, juvenile and subadult green turtles may use shallow, coastal waters along the Middle Atlantic coast as developmental habitat.

Primary nesting sites in U.S. Atlantic waters are high-energy beaches along the east coast of Florida, with additional sites in the U.S. Virgin Islands and Puerto Rico (NMFS and USFWS, 1991). Hatchlings swim out to sea and enter a pelagic stage in *Sargassum* mats associated with convergence zones. Juveniles go through an omnivorous stage of 1 to 3 years (NMFS and USFWS, 1991).

Adult green turtles commonly feed on seagrasses, algae, and associated organisms, and frequent reefs and rocky outcrops near seagrass beds for resting areas. Major feeding grounds in U.S. waters are located in Florida. In coastal New York waters, green turtles feed mainly on algae and the seagrass *Zostera marina* (Burke et al., 1992).

2.3.2.4 Marine Mammals

Numerous marine mammal species may occur off the New Jersey and New York coasts (Winn, 1982). These include members of the taxonomic orders Cetacea (whales, dolphins, and porpoises) and Pinnipedia (walrus, sea lions, and true seals) (National Audubon Society, 2002). This discussion focuses on marine mammal species that may occur within shelf waters in and near the sand borrow sites. All marine mammals are protected under the Marine Mammal Protection Act of 1972. Several species also are Federally listed as endangered or threatened species under the Endangered Species Act of 1973. The following subsections cover listed and non-listed species.

Listed Species

Three species of endangered cetaceans that may occur offshore of New Jersey and New York are associated primarily with shelf waters (Winn, 1982; NMFS, 1996). They are the fin whale (*Balaenoptera physalus*), humpback whale (*Megaptera novaeangliae*), and North Atlantic right whale (*Eubalaena glacialis*). There are no "resident" populations of any of these whales in the study area. Fin and humpback whales may be present during any season, although most likely during winter and spring. North Atlantic right whales would be present only as transients during spring and fall migrations. The harbor porpoise (*Phocoena phocoena*) occurs seasonally in coastal waters of the study area and has been proposed for listing as a threatened species

(62 Federal Register [FR] 37562). No critical habitat for listed marine mammals is located in or near the project area.

Fin Whale. Fin whales range from the Arctic to the Greater Antilles. They are among the largest and fastest baleen whales and commonly are found inshore of the continental shelf break (Winn, 1982). This species occurs widely in the Middle Atlantic throughout the year, with concentrations from Cape Cod north in summer and from Cape Cod south in winter. Fin whales are frequently found along the New England coast from spring to fall in areas of fish concentration (Blaylock et al., 1995). It is thought that fin whales migrate north in nearshore waters along the coast during spring, and south in offshore waters during winter. This species feeds on krill, planktonic crustaceans, and schooling fishes such as herring and capelin.

Humpback Whale. Humpback whales range from the Arctic to the West Indies. During summer, there are at least five geographically distinct feeding aggregations in the northern Atlantic (Blaylock et al., 1995). During fall, humpbacks migrate south to the Caribbean where calving and breeding occur from January to March (Blaylock et al., 1995). Aerial surveys during CETAP detected only a few humpback whale sightings from New Jersey southward during any season (Winn, 1982). However, subsequently there have been numerous sightings and strandings off the Middle Atlantic coast, particularly during winter and spring (Swingle et al., 1993; Wiley et al., 1995). Most stranded animals were juveniles, suggesting that the area may be an important developmental habitat (Wiley et al., 1995). Humpbacks feed largely on euphausiids and small fishes such as capelin, herring, and sand lance, and their distribution has been largely correlated to prey species and abundance (Blaylock et al., 1995). They have not historically used New Jersey and New York waters as a major feeding ground (NMFS, 1996). Critical habitats have been identified in the western Gulf of Maine and the Great South Channel (Massachusetts).

North Atlantic Right Whale. North Atlantic right whales range from Iceland to eastern Florida, primarily in coastal waters. This is the rarest of the world's baleen whales, with a population of between 325 and 350 individuals (New England Aquarium, 2004). Coastal waters of the southeastern U.S. (off Georgia and northeast Florida) are important wintering and calving grounds for North Atlantic right whales, while waters around Cape Cod and Great South Channel are used for feeding, nursery, and mating during summer (Kraus et al., 1988; Schaeff et al., 1993). From June to September, most animals are found feeding north of Cape Cod. Southward migration occurs offshore from mid-October to early January (Kraus et al., 1993). Migration northward along the Middle Atlantic coast takes place during late winter and early spring (NMFS, 1996). Designated critical habitat for the North Atlantic right whale includes portions of Cape Cod Bay and Stellwagen Bank and the Great South Channel (off Massachusetts) and waters adjacent to the coasts of Georgia and northeast Florida (59 FR 28793).

Harbor Porpoise. Harbor porpoises are found in cool temperate and subpolar waters of the Northern Hemisphere (Blaylock et al., 1995). Harbor porpoises were the most common odontocete species sighted on the continental shelf during CETAP (Winn, 1982). However, they were primarily concentrated in New England waters, well to the northeast of the study area (Winn, 1982). As the name implies, harbor porpoises are typically found in shallow water, most often in bays and harbors, although they occasionally travel over deeper offshore waters (Jefferson et al., 1993). The Gulf of Maine population, which would include harbor porpoises occurring off New Jersey and New York, has been proposed for listing as a threatened species (62 FR 37562). During summer, these animals are concentrated in Canada and the northern Gulf of Maine. During fall (October to December) and spring (April to June), they are widely

distributed from Maine to North Carolina (Blaylock et al., 1995). Little is known of their distribution during winter (December through March), although it is assumed that they could reside in the study area during this season (T. Cole, 2003, personal communication, NMFS NEFSC). It is thought that harbor porpoises feed on pelagic schooling fishes such as herring and mackerel (Gaskin, 1992).

Other Listed Species. Three other endangered marine mammals occurring offshore the Middle Atlantic are rarely seen in near-coastal waters. These are the blue whale (*B. musculus*), sei whale (*B. borealis*), and sperm whale (*Physeter macrocephalus*). Because these large whales prefer deep water well offshore of the continental shelf (Winn, 1982; Roden, 1998), they are unlikely to occur in the study area and are not discussed here.

Non-Listed Species

Numerous non-listed cetacean species may occur in waters off New Jersey and New York. These include one mysticete (the minke whale, *Balaenoptera acutorostrata*) and a variety of odontocetes (toothed whales and dolphins). The most common odontocetes in Middle Atlantic shelf waters are bottlenose dolphin (*Tursiops truncatus*) and common dolphin (*Delphinus delphis*), both of which may be present year-round (Winn, 1982; Kenney, 1990). Recent aerial survey data show that the bottlenose dolphin is the predominant marine mammal species within inner shelf waters of the study area (T. Cole, 2003, personal communication, NMFS NEFSC). Other shelf species potentially occurring in the area but generally found in more northern waters include Atlantic white-sided dolphin (*Lagenorhynchus acutus*), white-beaked dolphin (*L. albirostris*), and the previously discussed harbor porpoise. Odontocete species that occur off the Middle Atlantic coast but typically in deeper waters (along the shelf edge and beyond) include long-finned pilot whale (*Globicephala melas*), Risso's dolphin (*Grampus griseus*), northern bottlenose whale (*Hyperoodon ampullatus*), dwarf and pygmy sperm whales (*Kogia simus* and *K. breviceps*), Atlantic spotted dolphin (*Stenella frontalis*), clymene dolphin (*S. clymene*), striped dolphin (*S. coeruleoalba*), spinner dolphin (*S. longirostris*), and rough-toothed dolphin (*Steno bredanensis*) (Winn, 1982; Blaylock et al., 1995; Roden, 1998). Beaked whales (*Mesoplodon* spp. and *Ziphius cavirostris*) also occur off the Middle Atlantic but are believed to be principally deepwater (continental slope and beyond) species. The killer whale (*Orcinus orca*) may occur on both the shelf and slope (Winn, 1982) but is considered uncommon or rare in Middle Atlantic waters (Blaylock et al., 1995).

Five non-listed pinniped species may occur off the New Jersey and New York coasts (Reeves et al., 1992; National Audubon Society, 2002). The harbor seal (*Phoca vitulina*) and gray seal (*Halichoerus grypus*) are most common. Harbor seals normally occur year-round in coastal waters of Canada and New England, moving south to winter (Blaylock et al., 1995). Occurrences off New Jersey and New York would be most likely from November through May. Gray seals (*Halichoerus grypus*) normally range from Labrador to New England (Blaylock et al., 1995), with wintering individuals likely to occur in the New York Bight during November through May. Three "ice seals" of the northwest Atlantic, the harp seal (*Phoca groenlandica*), hooded seal (*Cystophora cristata*), and ringed seal (*Phoca hispida*), are uncommonly found in U.S. waters (Reeves et al., 1992; National Audubon Society, 2002).

3.0 REGIONAL GEOMORPHIC CHANGE

Nearshore sediment transport processes influence the evolution of shelf sedimentary environments to varying degrees depending on temporal and spatial response scales. Although micro-scale processes, such as turbulence and individual wave orbital velocities, determine the magnitude and direction of individual grain motion, variations in micro-scale processes are considered noise at regional-scale and only contribute to coastal response in an average sense. By definition, regional-scale geomorphic change refers to the evolution of depositional environments for large coastal reaches (10 km or greater) over extended time periods (decades or greater) (Larson and Kraus, 1995). An underlying premise for modeling long-term morphologic change is that a state of dynamic equilibrium is reached as a final stage of coastal evolution. However, the interaction between the scale of response and forces causing change may result in a net sediment deficit or surplus within a system, creating disequilibrium. This process defines the evolution of coastal depositional systems.

Topographic and hydrographic surveys of coastal and nearshore morphology provide a direct source of data for quantifying regional geomorphology and change. Historically, hydrographic data have been collected in conjunction with regional shoreline position surveys by the U.S. Coast and Geodetic Survey (USC&GS); currently Office of Coast Survey of the National Ocean Service (NOS), National Oceanic and Atmospheric Administration (NOAA). Comparison of digital bathymetric data for the same region but different time periods provides a method for calculating net sediment movements into (accretion) and out of (erosion) an area of study. Coastal scientists, engineers, and planners often use this information for estimating the magnitude and direction of sediment transport, monitoring engineering modifications to a beach, examining geomorphic variations in the coastal zone, establishing coastal erosion setback lines, and verifying shoreline change numerical models. The purpose of this portion of the study is to document patterns of geomorphic change to quantify the magnitude and direction of net sediment transport over the past 110 to 140 years. These data, in combination with wave and current measurements and model output, provide a temporally integrated technique for evaluating the potential physical impacts of offshore sand mining on sediment transport dynamics.

3.1 SHORELINE POSITION CHANGE

Creation of an accurate map is always a complex surveying and cartography task, but the influence of coastal processes, relative sea level, sediment source, climate, and human activities make shoreline mapping especially difficult. In this study, shoreline surveys are used to define landward boundaries for bathymetric surfaces and to document net shoreline movements between specified time periods. Consequently, net change results can be compared with wave model output and nearshore sediment transport simulations to evaluate cause and effect. Results integration provides a direct method of documenting potential environmental impacts related to sand mining on the OCS.

3.1.1 Physical Setting and Previous Studies

The present study area is located along the north Atlantic coast of New Jersey and the southwest Atlantic coast of Long Island. The region is situated within the northern portion of the Middle Atlantic Bight in an area known as the New York Bight (Figure 3-1). The area of interest includes about 80 km of exposed coastline in northeastern New Jersey from Sandy Hook to Barnegat Inlet (74°01'03", 40°28'37" to 74°05'48", 39°45'43") and about 110 km of coastline in southwestern Long Island from Rockaway Point to Moriches Inlet (73°56'27", 40°32'33" to 72°45'19", 40°45'52"), encompassing an area of about 8,800 square km. The outer coast includes seven major federal entrances, with two of these located in northeastern New Jersey (Shark River and Manasquan) and five located in southwestern Long Island (Rockaway, East Rockaway, Jones, Fire Island, and Moriches). These entrances have been armored with rock jetties to provide channel protection and inlet stability (Section 3.1.1.6).

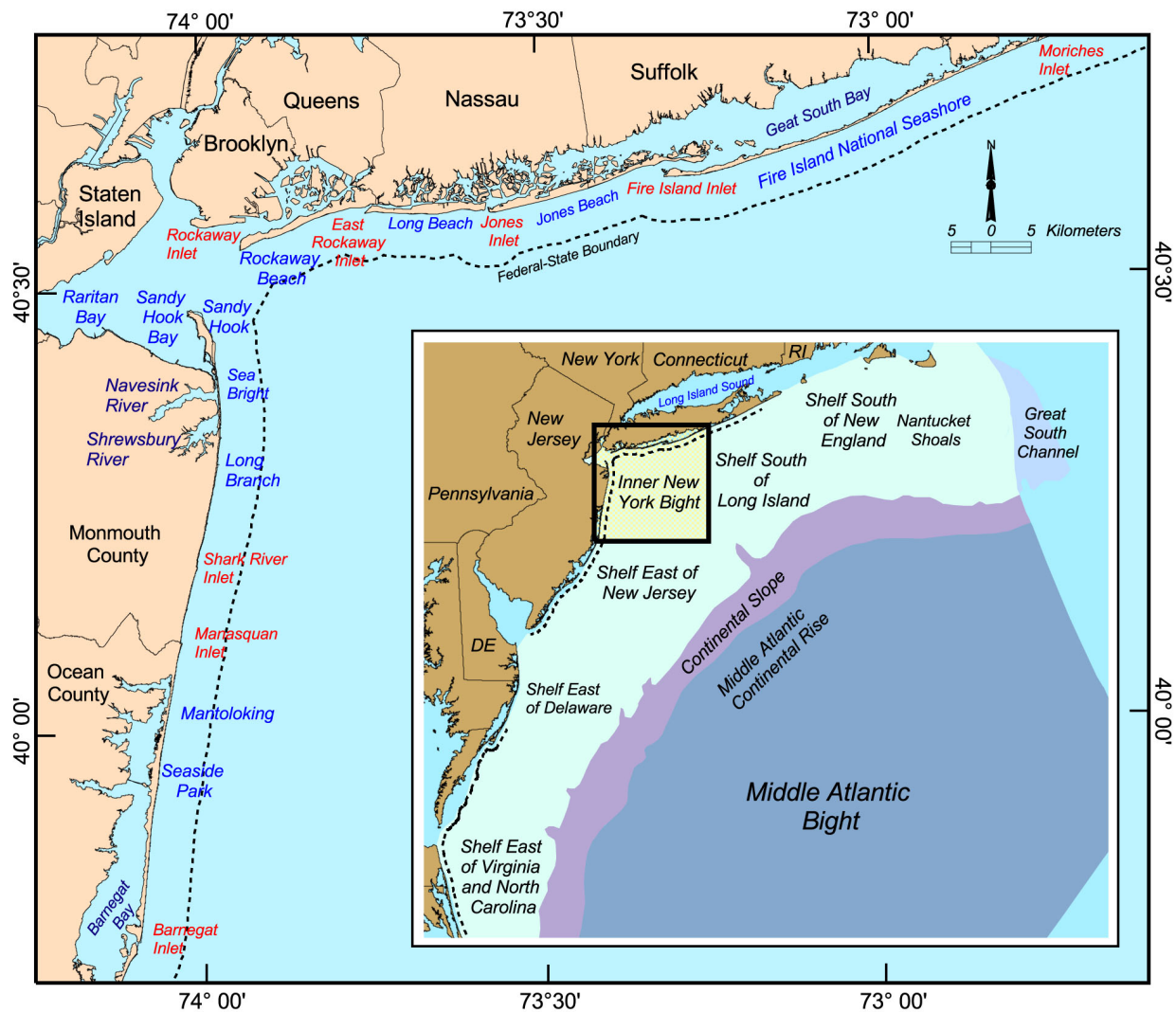


Figure 3-1. Geographic locations within the New York Bight.

The New York Bight lies within the Coastal Plain Physiographic Province, which is underlain at shallow depths by Upper Cretaceous, Tertiary, and Quaternary semiconsolidated,

clastic sedimentary rocks (Williams and Duane, 1974). The origin of present-day coastal features and topography of southwestern Long Island varies from that of northeastern New Jersey due to the influence of the most recent Pleistocene glacial advance. Long Island marks the southern terminus of the Wisconsinan-Laurentide continental ice sheet, which greatly impacted its topography. As such, visible topographic effects in the Long Island landscape from the most recent glacial advance are not present in the topography of northeastern New Jersey. Furthermore, the continental shelf within the New York Bight is a relatively complex geologic site as it has been influenced by differential subaerial erosion of near surface Coastal Plain strata and by several episodes of Pleistocene glaciation (Williams and Duane, 1974).

3.1.1.1 Physical Characteristics of Southwestern Long Island

The location of Long Island along the southern terminus of the last glacial advance has resulted in a topographic composition that is uncharacteristic for much of the Atlantic Coastal Plain Province. The southern portion of Long Island is characterized by gently sloping outwash plains fronted by shallow lagoons and a low-relief barrier island system consisting of reworked glacial sediment deposited during the last glacial advance (Figure 3-2; Schwab et al., 2000a). The shoreline is composed of barrier island and beach complexes including Rockaway Beach, Long Beach, Jones Island, and Fire Island (Figure 3-1). These features are backed by shallow back-barrier bays and marshes. Beaches consist of reworked fluvio-glacial outwash characterized primarily by fine- to medium-grained sand (Schwab et al., 1999). Erosion of glacial morainal and till deposits at Montauk Point serves as the headland source for beach sands that comprise the barrier island system. Eroded glacial sediments are carried westward from Montauk Point as littoral drift and deposited by wave action on barrier beaches and offshore bars (USFWS, 1997). Net littoral transport for parts of the south shore of Long Island has been estimated by Taney (1961) and the USACE (1971) to be about 344,000 to 460,000 m³/yr from east to west (Figure 3-2). According to Taney (1961), this rate exhibits considerable variation from one place to another along the coast, showing a larger range of about 122,000 to 460,000 m³/yr between Montauk Point and Rockaway Inlet (see Figure 2-5 for explicit variations). The southern shoreline of Long Island has been extensively developed and contains numerous groins, jetties, and seawalls to protect beaches and inlets. Between 1930 and 1960, each major entrance along the south shore of Long Island was reinforced with jetties. Structure placement has been combined with extensive beach nourishment and restoration projects since the 1920s. Volumes and locations of beach nourishment projects in the study area are summarized in Section 3.1.1.6.

3.1.1.2 Physical Characteristics of Northeastern New Jersey

The northeastern New Jersey coastline also is located along the emerged portion of the Atlantic Coastal Plain, but it is south of the maximum advance of the most recent Pleistocene glaciation that heavily influenced the geology of Long Island. The shoreline is comprised of three major coastal geomorphic compartments, including the northern spit complex at Sandy Hook, the headland region from Monmouth Beach to Mantoloking, and the southern spit complex from Mantoloking to Barnegat Inlet (USACE, 1995; Figure 3-2). Northern and southern spit complexes are backed by Sandy Hook and Barnegat Bays, respectively. Sandy Hook, at the northern extent of the New Jersey shoreline, is a classic recurved spit which has prograded north toward New York Harbor from north-directed longshore drift (USACE, 1995). Net northward-directed littoral drift associated with this growth has been estimated at 382,000 m³/yr (Caldwell, 1966). Observations indicate that a nodal point for net littoral drift exists near Manasquan Inlet. South of Manasquan, the direction of net drift is southerly with an estimated volume of 38,000 m³/yr passing Barnegat Inlet (Caldwell, 1966). Beaches along the northern New Jersey coastline are comprised primarily of medium- to coarse-grained sands, composed

principally of unconsolidated quartz from underlying and nearby formations (USACE, 1990). Coastal plain deposits of the Atlantic Highlands serve as the primary headland source of sand for beaches along the Atlantic coast of New Jersey. Eroded sediments from the Highlands enter the littoral current and are transported northward to form Sandy Hook and southward toward Barnegat Inlet (USFWS, 1997). Similar to the south shore of Long Island, the northern New Jersey shoreline has been extensively developed and altered by engineered structures and beach nourishment projects over the past century. By 1940, Barnegat, Manasquan, and Shark River Inlets were armored with stone jetties. Additionally, beach nourishment activities began taking place in the 1950s. Estimated volumes and locations of beach nourishment activities and structures are summarized in Section 3.1.1.6.

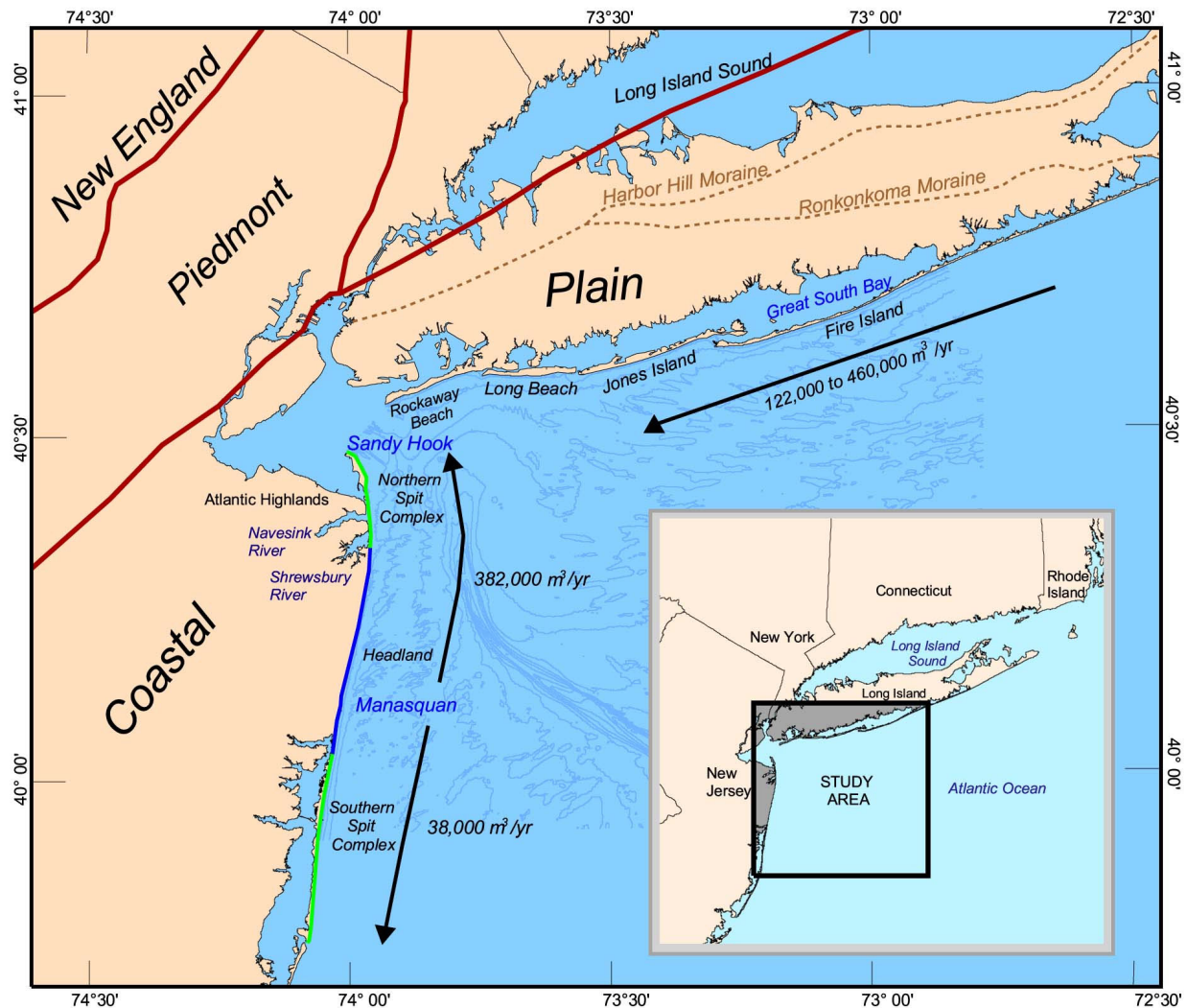


Figure 3-2. Net littoral transport rates along beaches in the study area (Taney, 1961; Caldwell, 1966).

3.1.1.3 Physical Characteristics of the New York Bight

The submerged extension of the Atlantic Coastal Plain forms the continental shelf of the New York Bight. It is characterized by a gentle slope that dips slightly to the southeast. The offshore region extends from the shoreline across the continental shelf to about the 30-m depth contour, a total distance of approximately 10 to 40 km. The most prominent seafloor feature is

the submarine Hudson River Channel, which is the submerged seaward extension of the ancestral Hudson River drainage system connecting the sub-aerial Hudson River Valley with the Hudson Canyon at the Continental Shelf edge (Williams and Duane, 1974). The continental shelf is dominated by ridge and swale topography, with numerous linear shoals that trend oblique to regional contours and form a small acute angle with the coastline (Duane et al., 1972) (Figure 3-3). Local topographic highs and lows include Shrewsbury Rocks, Cholera Banks, Diamond Hill, Castle Hill, Highland Channel, and the Christiansen Basin with multiple additional anthropogenic disposal mounds (Figure 3-3). Solid waste disposal of various materials has been occurring in the New York Bight since the 1800s. Waste disposal areas are visible as topographically positive mounds in the modern bathymetric contours. Sources and quantities of material have been well documented in recent reports by the USGS (Butman et al., 1998; Schwab et al., 2000b) and in earlier reports by the USACE (Williams and Duane, 1974). The predominant sediment type found on the inner shelf is fine-to medium-grained sand, with discrete patches of coarse sand and rounded pea gravels (Williams and Duane, 1974; Williams 1976). Modern surficial sediments documented along the shelf are glacially derived and reworked coastal plain strata (Williams and Duane, 1974).

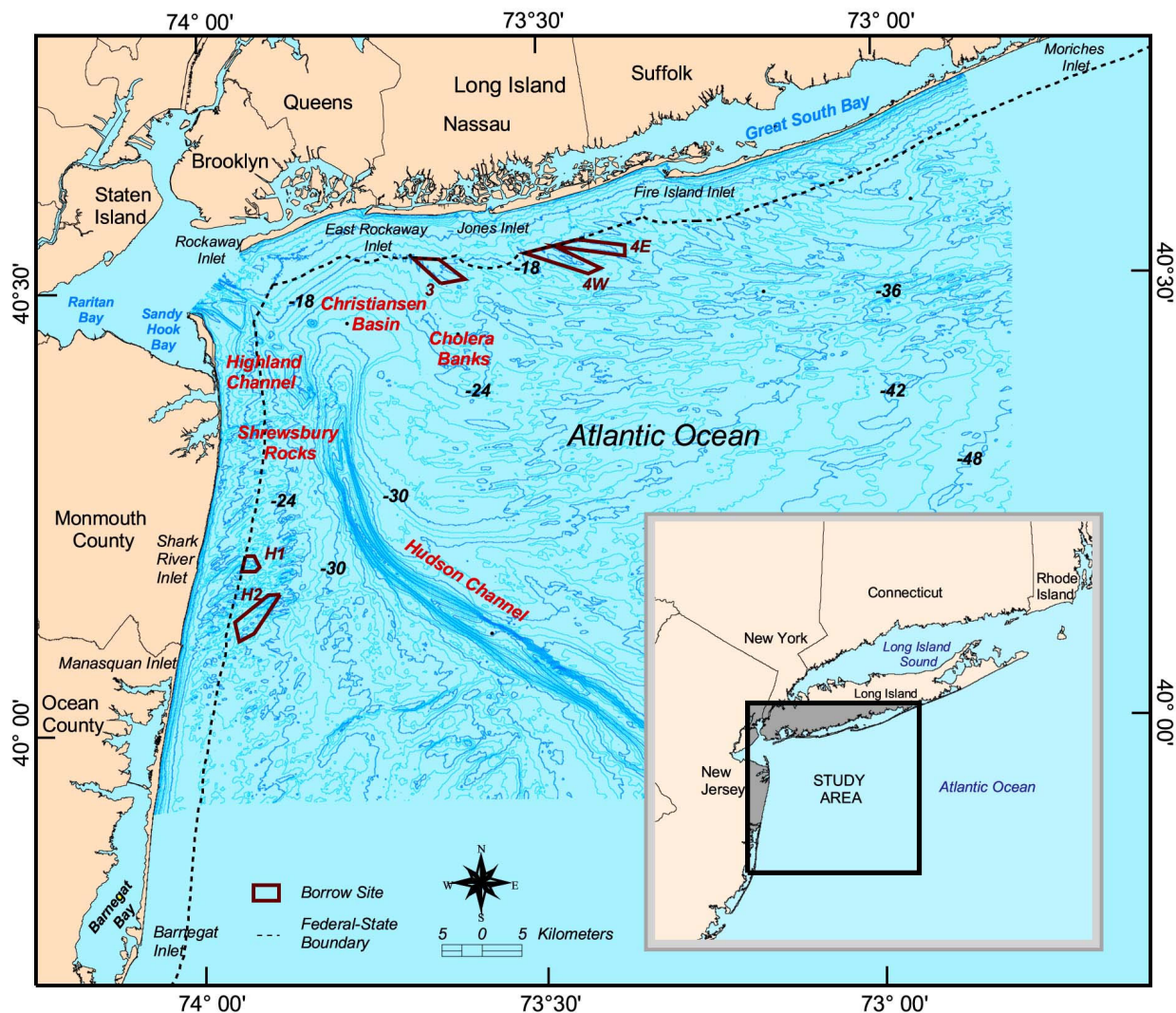


Figure 3-3. Prominent features on the New York Bight continental shelf.

3.1.1.4 Storms

Hurricanes and extratropical storms periodically impact the study area. Some of the most damaging storms include the March 4, 1931 northeaster (re-opened Moriches Inlet), the September 21, 1938 hurricane (the Long Island Express; storm of record for eastern Long Island), the March 6-8, 1962 northeaster (Ash Wednesday Storm), and the December 11, 1992 northeaster (Kana, 1999). Other damaging hurricanes including *Carol* (1954), *Donna* (1960), *Belle* (1976), *Gloria* (1985), and *Bob* (1991), are summarized in Table 3-1.

Date	Name	Type	Comments	Source
March 1888	Blizzard of 1888	Blizzard	http://www2.sunysuffolk.edu/mandias/38/hurricane/	Blizzard Info Index
March 4, 1931	Unnamed	Northeaster	Re-opened Moriches Inlet	Smith et. al., 1999
September 1938	Long Island Express	Hurricane	Storm of record for eastern Long Island. Created Shinnecock Inlet and widened Moriches Inlet	Kana, 1999
September 14, 1944	Unnamed	Hurricane	Category 3 hurricane; caused 390 deaths	Morang et. al., 1999
November 25, 1950	Unnamed	Northeaster	20 foot waves recorded at Jones Beach.	Morang et. al., 1999
1954	Carol	Hurricane		Kana, 1999
1960	Donna	Hurricane		Kana, 1999
March 1962	Ash Wednesday Storm	Northeaster	Northeaster of record for Long Island	Kana, 1999
1976	Belle	Hurricane		Kana, 1999
1984	Unnamed	Northeaster	Inspired creation of New Jersey Beach Profile Network (NJBPN)	NJBPN
1985	Gloria	Hurricane		Kana, 1999
August 1991	Bob	Hurricane		Kana, 1999
October 31, 1991	Halloween Storm	Northeaster		Blizzard Info Index
December 11, 1992	Unnamed	Northeaster		Kana, 1999
January 1998	Unnamed	Northeaster		NJBPN
February 1998	Unnamed	Northeaster	Seventh northeast storm for the season	NJBPN
Winter 1997-98	Winter Storms of 1997-98	Storms/ Northeasters	80% of replenished sand brought into Sandy Hook washed away	Blizzard Info Index

3.1.1.5 Beach Nourishment and Structure Development

Beach nourishment activities have been taking place along parts of the coastline within the study area since the mid-1920s. Historical beach nourishment data documented by Kana (1999), Duke University (<http://www.env.duke.edu/psds/nourishment.htm>) and Valverde et al. (1999), USACE New York District (USACE, 2003), and NJDEP were the primary sources of information regarding beach fill activity in the study area. Data published by Kana (1999) were used to document historical placement events for beaches in southwestern Long Island, and data published by Valverde et al. (1999) and NJDEP were used for historical nourishment events in New Jersey. Information obtained from the New York District was used primarily for documenting recent (late 1990s to present) and projected beach fill activities for beaches along the New York and New Jersey coasts. Within the study area, data for Long Island beaches

document nourishment activity from 1926 to 2001 and data for New Jersey beaches document activity from 1943 to 2003. To summarize these data, seven reaches have been defined within the study area based primarily on natural geomorphic boundaries (Figure 3-4). Information on nourishment volumes, locations, and dates was compiled and summarized by decade for each reach (Tables 3-2 and 3-3). Because placement lengths were not available for each nourishment project, single points have been used to identify approximate fill locations, with placement volumes applied to the entire reach (Figure 3-4). Individual locations have been estimated based on textual descriptions and are considered approximate.

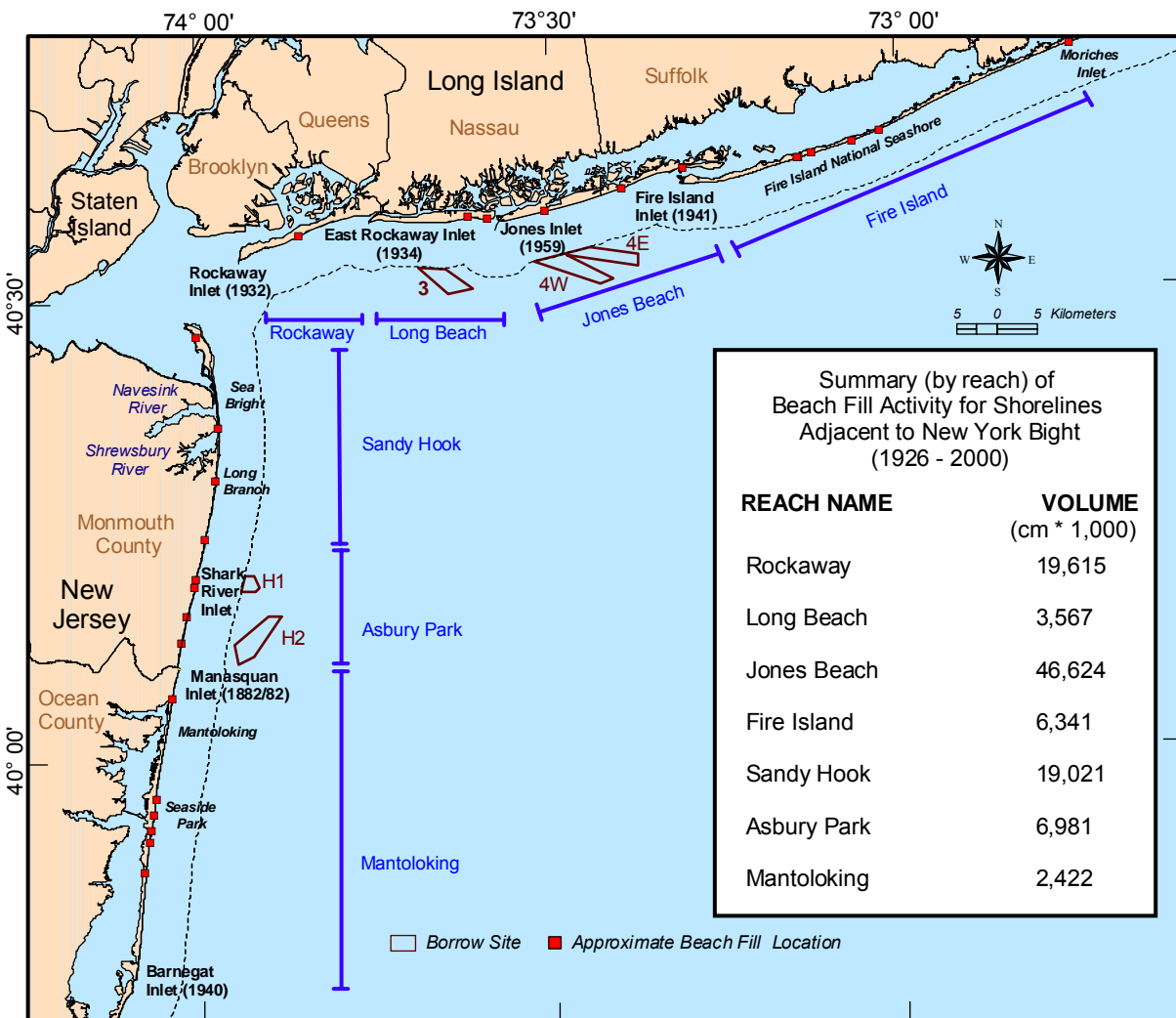


Figure 3-4. Documented beach nourishment activity from Rockaway Point to Moriches Inlet, NY and Sandy Hook to Barnegat Inlet, NJ.

A comparison of data published by Kana (1999) and Valverde et al. (1999) for southern Long Island beaches showed very similar information for Rockaway Beach and Long Beach, but had fairly significant differences along Jones Beach and Fire Island. Because Kana (1999) drew upon information provided in Valverde et al. (1999), in addition to multiple other sources, the information published by Kana (1999) was considered the primary source for Long Island beach nourishment events. Data published by NJDEP were obtained in shapefile format, and included information on volumes, location, and additional notes about each event. Beach fill

volumes obtained from NJDEP for New Jersey beaches were compared with those provided in Valverde et al. (1999). In general, beach nourishment volumes were not in agreement. Numerous additional nourishment events were identified in the NJDEP data than those published by Valverde et al. (1999). In cases where discrepancies existed, published volumes with reliable background information were used. Because some historical beach fill activities have been poorly documented, nourishment events with incomplete data (missing dates and/or volumes) were omitted from the data set, and final volume summaries are considered approximate representations of beach fill activity for each time interval. Locations and quantities were used primarily to qualify observed shoreline change trends with respect to concurrent beach nourishment projects, while noting major placements and associated response. For nourishment events where exact dates were not available (listed by decade rather than by year), a best approximation was used in determining the shoreline change interval to which it applied. A listing of individual volumes and dates for each nourishment event is located in Kana (1999), Valverde et al. (1999), and on the New York District web site.

Reach	1920s	1930s	1940s	1950s	1960s	1970s	1980s	1990s	TOTAL
Rockaway Beach	3,976	4,282	0	956	363	5,222	4,491	326	19,615
Long Beach	0	0	0	421	153	486	873	1,634	3,567
Jones Beach	30,582	0	940	3,731	3,211	3,419	1,682	3,058	46,624
Fire Island	0	0	1,018	651	2,550	144	37	1,940	6,341
TOTAL	34,558	4,282	1,958	5,759	6,277	9,271	7,083	6,958	76,147

Reach	1940s	1950s	1960s	1970s	1980s	1990s	2000s	TOTAL
Sandy Hook	26	3,135	0	3,771	373	10,110	1,606	19,021
Asbury Park		805	485	119	0	3,202	2,370	6,981
Mantoloking		306	1,351	765	0	0		2,422
TOTAL	26	4,426	1,836	4,655	373	13,312	3,976	28,631

Southwestern Long Island Beaches

Reaches for Long Island are defined by the four barrier islands representing the coastline within the study area. These include Rockaway Beach, Long Beach, Jones Beach, and Fire Island (Figure 3-4). The total volume of material placed on beaches between 1926 and 1999 was about 76 mcm. About 26% of this total was placed on Rockaway Beach between 1926 and 1999, about 5% was placed on Long Beach between 1959 and 1999, 61% was placed on Jones Beach between 1927 and 1999, and 8% was placed on Fire Island between the late 1940s and 1999. Historical placement trends for each reach vary, but for most reaches, placement volumes typically have been increasing in recent years (1990s to present). Nourishment activity began in 1926 at Rockaway Beach and Jones Beach, with two very large land reclamation projects that represented about 50% of the total volume placed for all years. Recently, coastal

monitoring and storm damage reduction projects have initiated long-term beach nourishment and protection activities for some reaches.

At Rockaway Beach, placement volumes were considerable in the 1920s and 1930s, decreased between the 1940s and 1960s, and increased again in the 1970s and 1980s with the implementation of the Water Resources Development Act of 1974. Under this agreement, beaches were nourished periodically in 1977, 1980, 1982, 1984, 1986, and 1988. In May, 1994, three additional beach nourishment cycles were authorized for a 6.2-mile section of Rockaway Beach. Beach fills were scheduled to take place at three year intervals, the first of which was completed in 1998, the second in March 2001, and the third is currently scheduled for 2004/05 (USACE, 2003). Because placement volumes for these events were not published, total volumes calculated for Rockaway Beach do not reflect these placements.

Nourishment at Long Beach began in 1959/1960 with an initial placement of about 421,000 m³. Since the 1970s, placement has increased every decade, with volumes nearly doubling at each interval. Long Beach is currently in the process of approving a Storm Damage Reduction Project, which will provide periodic nourishment of a 7-mile segment of beach on a 5-year cycle for the next 50 years (USACE, 2003).

Nourishment at Jones Beach began in 1927 with one of the largest barrier island reclamation projects in the world, placing of a total of about 30.6 mcm of material on the beach. Since the 1940s, nourishment at Jones Beach has remained relatively consistent at about 3 mcm per decade. Most of the sediment comes from disposal of dredged material from Fire Island Inlet (Kana, 1999).

Nourishment at Fire Island did not begin until the late 1940s. Following the initial nourishment, placement was primarily focused at the western or eastern ends of the island, as a disposal area for bay or inlet sediment dredged by Suffolk County. In the 1970s, county dredging virtually stopped, and nourishment for the 1970s and 1980s totaled only about 180,000 m³. In 1992, nourishment resumed, with about 30 fills occurring in the 1990s.

Northeastern New Jersey Beaches

Reaches defined for New Jersey beaches include Sandy Hook (northern tip of Sandy Hook to immediately north of Asbury Park), Asbury Park (town of Asbury Park to Manasquan Inlet), and Mantoloking (Manasquan Inlet to Barnegat Inlet). Historical information regarding nourishment projects along northern New Jersey beaches was more limited than that available for Long Island. Nourishment data for northern New Jersey beaches document significantly less activity than that recorded for beaches in southwestern Long Island (total volume at reaches in New Jersey is about 37.5% of that for reaches in New York; Tables 3-2 and 3-3). While historical beach nourishment records document greatly decreased levels of activity relative to southern Long Island beaches, recent project information indicates that the northern 34 km of northern New Jersey beaches currently are undergoing increased levels of nourishment and several additional nourishment events are planned within the next 30 years (USACE, 2003).

Beach nourishment volumes placed within Sandy Hook reach far exceed those documented for other reaches in northeastern New Jersey. With a total nourishment volume of just over 19 mcm, nourishment levels at Sandy Hook are at least three times as great as totals for other reaches (Table 3-3). According to NJDEP, nourishment commenced in the Sandy Hook reach in the mid-1940s, with two relatively minor fills at Long Branch in 1943 and 1945. Since then, it appears that beach fill activity spiked during the 1950s and 1970s. One of the

largest nourishment projects was completed in this reach in 1958 at beaches in Avon and Belmar, placing over 3 mcm of sand on the beaches. After this fill, there were no events recorded until the 1970s, when five fills produced a total sand volume of about 3.8 mcm. Nourishment essentially ceased in the 1980s, but beach fills have increased greatly since the early 1990s with the inception of the Beach Erosion Control Project designed for Sandy Hook to Barnegat Inlet. This project encompassed a 34-km stretch of shoreline from the Town of Sea Bright to Manasquan Inlet. It is currently the largest beachfill in the world, and the project is divided into two sections: Section I from Sea Bright to Ocean Township and Section II from Asbury Park to Manasquan. Initial placements for Section I began in 1995, with approximately 3.5 mcm, followed by 2.9 mcm in 1996, 3.3 mcm in 1996, and 3.3 mcm in 1999. The project was designed to continue nourishment activities at beaches in the Sandy Hook reach by renourishing areas at about 2.7 mcm of fill every 6 years. Renourishment activities at Sea Bright and Monmouth Beach commenced in May 2002 and were completed in November 2002. A total of 1.6 mcm of sand was pumped to the beach from offshore as part of the initial renourishment effort (USACE, 2003). This level of nourishment greatly exceeds totals for all other decades in the Sandy Hook reach.

Beach nourishment information on the Asbury Park reach indicates that fill activity along this section of shoreline was relatively low until the 1990s. According to documentation, after initial nourishment efforts in the 1950s, beaches were re-nourished at relatively low levels until the mid-1990s. Since then, beach nourishment activity increased, primarily as the result of implementation of the USACE Beach Erosion and Control Project designed for Section II (Asbury Park to Manasquan Inlet). Initial placements of 3.1 mcm and 2.4 mcm were completed in August 1999 and January 2001, respectively. Projected re-nourishment schedules are designed to add material to this section of shoreline at a rate of about 1.7 mcm every six years. This level of nourishment greatly exceeds historical rates documented for this reach.

The Mantoloking reach has the lowest levels of beach nourishment in northeastern New Jersey. Data indicate that nourishment activity commenced in this reach in 1953. A number of small fills occurred within the 1960s, with seven events contributing to a total placement volume of 1.35 mcm. According to available documentation, fill activity was at a peak in the 1960s and 1970s and has subsided in recent years. This section of shoreline, while included as part of the USACE Beach Erosion and Control Project, was not scheduled for nourishment activity as part of the current project design.

Jetty Construction and Rehabilitation

Along the southwestern coast of Long Island, jetties were constructed at all entrances between 1932 and 1959. All entrances have a single jetty constructed on the east bank of the entrance, with additional reinforcements at some locations to prevent or control erosion on the west bank of the inlet. The first jetty constructed was at Rockaway Inlet in 1932 (Table 3-4). Construction took place concurrently with the initial beach nourishment project conducted at Rockaway Beach between 1926 and 1936. Prior to jetty construction, Rockaway Beach was a westward-migrating sand spit. Since jetty construction, barrier beach migration has stopped, and deposition adjacent to the jetty has stabilized the eastern side of the entrance.

The second jetty to be constructed in the study area was on the east side of East Rockaway Inlet in 1934. Numerous subsequent repairs have been made following initial jetty construction, and maintenance dredging of the inlet continues today, with much of the dredged material being placed downdrift at Rockaway Beach. The third inlet to be stabilized was Fire Island. A jetty was constructed on the east side of the inlet in 1941, and subsequent erosion of

Oak Beach to the north and west of the inlet initiated construction of a sand dike extending southeast from Oak Beach in 1959 (Smith et. al., 1999). Records indicate that the jetty was repaired after the Ash Wednesday Storm of 1962. Dredging at Fire Island Inlet has been performed on an almost annual basis since 1954, with most dredged material being placed to the west of the inlet (Smith et. al., 1999).

The fourth inlet stabilized in the study area was Moriches Inlet. Present-day Moriches Inlet was originally formed by a powerful Northeast storm on March 4, 1931. Between 1933 and 1938, Moriches Inlet widened and deepened as tidal currents deposited large sand deltas on the ocean and bay sides of the entrance. The 1938 Hurricane further widened the Inlet to over 4,000 feet (Kassner and Black, 1982). To prevent further westerly migration of the inlet, a rubble-mound revetment was constructed on the western bank of the inlet in 1947/48, 1952, and 1953, and the inlet was reopened during a storm in September 1953. Dredging has been active at the inlet since 1953, with the majority of dredged materials placed west and east of the inlet. The final jetty constructed within the study area was at Jones Inlet in 1959. A 5,200-ft-long jetty was constructed on the east side of the inlet to provide stabilization, and a sand barrier was constructed to prevent shoaling in the inlet.

Initial jetty construction at New Jersey entrances occurred as early as 1882/83 and continued until 1940 (Table 3-4). At each of the entrances, jetties were constructed on the north and south banks. Manasquan Inlet was first armored with timber jetties north and south of the entrance in 1882/83. Two rubble-mound jetties were constructed to replace the timber jetties in 1930/31, and both jetties have been rehabilitated numerous times since then. Documentation for Shark River Inlet is very sparse, but shoreline data provided by the NJDEP illustrate the existence of structures at this entrance by at least the 1930s.

Inlet	Jetty Construction	Modifications
Rockaway	1932	
East Rockaway	1934	1935; 1941; 1946; 1963
Jones	1959	1962
Fire Island	1941	
Moriches	1953/54	
Shark River	1930s?	
Manasquan	1882-1883	1922; 1930/31; 1946; 1955/59; 1979/82

3.1.2 Shoreline Position Data Base

Two sets of high-water shoreline data were compiled to quantify historical shoreline change along portions of the southwestern coast of Long Island, NY and the northeastern coast of New Jersey. Change analyses for each state were completed using digital data obtained from the New York Department of State, the USACE New York District, and the NJDEP. For the New York data set, four outer coast shoreline surveys for the period 1873/88 to 1991/97 were analyzed (Table 3-5). Data extend from Rockaway Point to Moriches Inlet (Figure 3-1). The first two shoreline surveys were conducted by the USC&GS in 1873/88 and 1933/34. The third and fourth surveys were developed from georeferenced aerial photography flown during 1983 and between the years 1991 and 1997. All data were obtained in digital shape file format from the USACE New York District and the New York Department of State. Data sets were

selected from available digital data for years where contiguous shoreline coverage was available. Multiple additional shoreline layers exist for smaller sections of the study area. These additional layers, while not used for change rate calculations, were used as ancillary data to provide visual comparisons of observed trends with those of intervening years.

Date	Data Source	Comments and Map Numbers
1873/88	USC&GS Topographic Maps	T-1449 (1877), 1:5,000; Rockaway Inlet to Rockaway Beach. T-1482a (1878), 1:10,000; Rockaway Beach. T-1482b (1878), 1:10,000; Rockaway Beach to E. Rockaway Inlet. T-1471a (1879/80), 1:10,000; East Rockaway Inlet to Long Beach. T-1538a (1880), 1:10,000; Long Beach to Jones Inlet. T-1538b (1880), 1:10,000; Jones Inlet to Jones Beach. T-1539b (1880), 1:10,000; Jones Beach to Fire Island Inlet. T-1314 (1873), 1:10,000; Fire Island Inlet to Robert Moses State Park. T-1375a (1873/74), 1:10,000; Fire Island. T-1375b (1874), 1:10,000; Fire Island. T-1402 (1875), 1:10,000; Fire Island. T-1842 (1888), 1:10,000; Fire Island to Moriches Inlet.
February to November 1933/34	USC&GS Topographic Maps	T-5334 (1933/34), 1:10,000; Rockaway Inlet to Rockaway Beach. T-5093 (1933/34), 1:10,000; Rockaway Beach to Edgemere. T-5336 (1933/34), 1:10,000; Edgemere to Long Beach. T-5054 (1933/34), 1:10,000; Long Beach to Short Beach. T-5061 (1933/34), 1:10,000; Short Beach to Jones Beach. T-5060 (1933/34), 1:10,000; Jones Beach to Gilgo State Park. T-5059 (1933/34), 1:10,000; Gilgo State Park to Robert Moses State Park. T-5087 (1933/34), 1:10,000; Robert Moses State Park to Ocean Bay Park. T-5086 (1933/34), 1:10,000; Ocean Bay Park to Water Island. T-5085 (1933), 1:10,000; Water Island to Great South Beach. T-5084 (1933), 1:10,000; Great South Beach. T-5083 (1933), 1:10,000; Great South Beach to Moriches Inlet.
April 1983	NY Department of State and USACE New York District	Data developed from georeferenced aerial photography.
1991/97	NY Department of State and USACE New York District	Data developed from georeferenced aerial photography. 1997 - Rockaway Beach; April 1994 - Long Beach 1991 - Jones Beach; April 1994, April 1995 - Fire Island to Montauk Point

Data for northeastern New Jersey include four outer coast high-water shorelines between the years 1836/42 and 1977 (Table 3-6). Data extend along the northeastern Atlantic coastline from Sandy Hook to Barnegat Inlet (Figure 3-1). The first three data sets were developed from USC&GS topographic sheets for the years 1836/39, 1855/75, and 1932/33. The fourth data set was developed from 1977 registered aerial photography. All digital shoreline data were obtained in shapefile format from the NJDEP GIS website.

All high-water shoreline data were projected into a common horizontal coordinate system and datum, in this case Universal Transverse Mercator (UTM) Zone 18N, North American Datum of 1983 (NAD83). Digital shoreline files were edited at Applied Coastal to remove line segments representing structures such as sea walls and jetties.

Date	Data Source	Comments and Map Numbers
1836/39	USC&GS Topographic Maps	T-239 (1836), 1:10,000; Sandy Hook to Highlands. T-114 (1839), 1:10,000; Highlands to Asbury Park. T-115 (1839), 1:10,000; Asbury Park to Manasquan. T-116 (1839), 1:10,000; Manasquan to Mantoloking Shores. T-120 (1839), 1:20,000; Mantoloking Shores to Barnegat Inlet.
1855/75	USC&GS Topographic Maps	T-0486 (1855), 1:10,000; Sandy Hook to Highlands. T-1022 (1866), 1:10,000; Highlands to Asbury Park. T-1083 (1867), 1:10,000; Asbury Park to Manasquan. T-1084 (1868), 1:10,000; Manasquan to Mantoloking Shores. T-1371 (1874), 1:20,000; Mantoloking Shores to Seaside Heights. T-1407 (1875), 1:20,000; Seaside Heights to Barnegat Inlet.
1932/33	USC&GS Topographic Maps	T-5100 (1932/33), 1:10,000; Sandy Hook to Highlands. T-5279 (1932/33), 1:10,000; Highlands to Monmouth Beach. T-5281 (1932/33), 1:10,000; Monmouth Beach to Long Branch. T-5282 (1932/33), 1:10,000; Long Branch to Asbury Park. T-5283 (1932/33), 1:10,000; Asbury Park to Manasquan. T-5284 (1932/33), 1:10,000; Manasquan to Point Pleasant. T-5285 (1932/33), 1:10,000; Point Pleasant to Mantoloking Shores. T-5286 (1932/33), 1:10,000; Mantoloking Shores to Seaside Heights. T-5330 (1932/33), 1:10,000; Seaside Heights to Island Park. T-5097 (1932/33), 1:10,000; Island Park to Barnegat Inlet.
1977	New Jersey Geological Survey	Data developed from registered aerial photography.

When determining shoreline position change, all data contain inherent errors associated with field and laboratory compilation procedures. These errors should be quantified to gauge the significance of measurements used for engineering/research applications and management decisions. Table 3-7 summarizes estimates of potential error for shoreline data sets used in this study. Because individual errors represent standard deviations, root-mean-square error estimates were calculated as a realistic assessment of combined potential error for each data set. All shoreline data were developed at various agencies and institutions. As such, error calculations rely on standard values reported in general mapping guidelines. This can be problematic when assessing error for recent data sets developed from aerial photography. Estimates for data developed from traditional field studies and USC&GS topographic sheets are considered to be standard and can be used for earlier data sets developed from paper maps. However, error can vary widely for data sets developed from aerial photography due to large variation in registration. When registration error is not reported with individual data sets, it is difficult to obtain a suitable value that reflects registration accuracy across data sets. Due to lack of information regarding aerial photo registration for the New York 1983 and 1991/97 data and the New Jersey 1977 data, quality error estimates were not available.

Positional errors for each shoreline can be calculated using the information in Table 3-3; however, change analysis requires comparing two shorelines from the same geographic area but different time periods. Potential error associated with change analysis was computed for data sets where possible. For the New York data set, the magnitude of potential error associated with shoreline change between 1877/88 and 1933/34 was ± 13.1 m, with a corresponding rate of ± 0.3 m/yr. For the New Jersey data, the magnitude of error was calculated at ± 21.5 m between 1836/39 and 1855/75, with a corresponding rate of ± 0.8 m/yr. The magnitude of potential error associated with the 1836/39 to 1932/33 and 1855/75 to 1932/33 comparisons was ± 17.4 m with associated rates of ± 0.2 m/yr and 0.3 m/yr,

respectively. As expected, maximum positional errors are aligned with the oldest shorelines (1877/83, 1928, and 1948) at smallest scale (1:20,000), but most change estimates for the study area document shoreline advance or retreat greater than these values.

Table 3-7. Estimates of potential error associated with Long Island, NY and northeastern New Jersey shoreline position surveys.		
Traditional Engineering Field Surveys (NY 1873/88 shoreline; NJ 1836/39 and 1855/75 shorelines)		
Location of rodded points	±1 m	
Location of plane table	±2 to 3 m	
Interpretation of high-water shoreline position at rodded points	±3 to 4 m	
Error due to sketching between rodded points	up to ±5 m	
Historical Aerial Surveys (NY 1933/34 shoreline; NJ 1932/33 shoreline)	Map Scale	
	1:10,000	1:20,000
Delineating high-water shoreline position	±5 m	±10 m
Cartographic Errors (NY 1873/88 and 1933/34 shorelines; NJ 1836/39, 1855/75, and 1932/33 shorelines)	Map Scale	
	1:10,000	1:20,000
Inaccurate location of control points on map relative to true field location	up to ±3 m	up to ±6 m
Placement of shoreline on map	±5 m	±10 m
Line width for representing shoreline	±3 m	±6 m
Digitizer error	±1 m	±2 m
Operator error	±1 m	±2 m
Digital Aerial Photo Surveys (NY 1983 and 1991/97 shorelines; NJ 1977 shoreline)		
Delineating high-water shoreline	±5 m	
Aerial photo registration error	UNKNOWN	
Sources: Shalowitz, 1964; Ellis 1978; Anders and Byrnes, 1991; Crowell et al., 1991.		

3.1.3 Historical Shoreline Change Trends

Regional change analyses provided an assessment of shoreline response for comparison with predicted changes in wave-energy focusing at the shoreline resulting from potential offshore sand dredging activities. The analysis differs from previous qualitative analyses in that continuous measurements of shoreline change are provided at 30-m along-shore intervals for the periods 1873/88 to 1991/97 (New York) and 1836/39 to 1977 (New Jersey). As such, model results (wave and sediment transport) at discreet intervals along the coast can be compared with historical change trends to develop process/response relationships for evaluating potential impacts. The following discussion focuses on incremental changes in shoreline response for the southwestern shore of Long Island, NY and northeastern New Jersey compared to net, long-term trends in each portion of the study area. Incremental change periods for New York include 1873/88 to 1933/34, 1933/34 to 1983, and 1983 to 1991/97, and those for New Jersey include 1836/39 to 1855/75, 1855/75 to 1932/33, and 1932/33 to 1977. Most shoreline response observed in this region reflects beach nourishment activity and coastal structure development. For each time interval, impacts from inlet construction, beach nourishment, and structure placement (seawalls, jetties, groins) are discussed, along with observed shoreline response within each reach.

3.1.3.1 Southwestern Long Island

Beaches along the south shore of Long Island have experienced enormous change over the past 120 years. West-directed littoral transport, human-induced changes such as beach nourishment and jetty construction, and severe storm events have contributed to significant shoreline position adjustments. Relatively high rates of erosion have affected most of the coast, particularly when considering the volume of material placed on beaches as part of nourishment activities. Coastal erosion impacting the barrier islands has long been identified as a problem for communities in the area. General patterns of erosion and accretion have remained relatively consistent, with highest rates usually located adjacent to inlets, reflecting the direction of net littoral transport. Changes observed for each time period are compared below to document overall trends relative to dominant coastal processes along southwestern Long Island. Calculated rates of change for each time interval are listed in Appendix A. Shoreline reaches and geographic names used in the following discussion are shown in Figure 3-5.

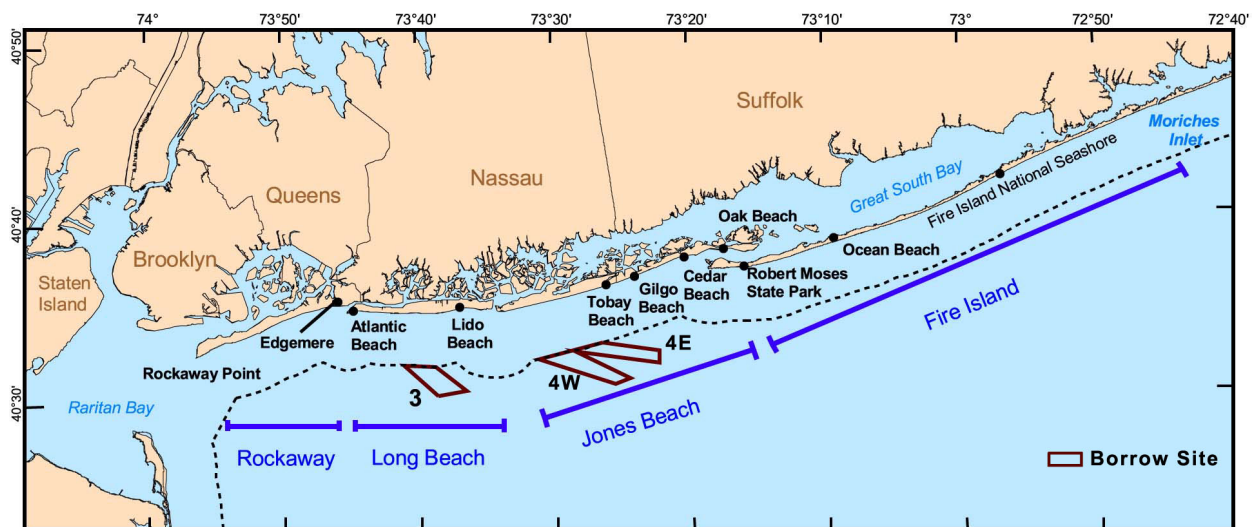


Figure 3-5. Southwestern Long Island reaches between Rockaway Point and Moriches Inlet, NY.

1873/88 to 1933/34

Between 1873/88 to 1933/34, significant changes in shoreline position were recorded as beaches responded to natural coastal processes and human alterations. During this period, the two largest beach nourishment projects on record for the study area were completed at Rockaway Beach (7.95 mcm) and Jones Beach (31.0 mcm). Effects of these nourishment activities are documented as high rates of shoreline advance for much of the western half of the study area (Figure 3-6). Additionally, jetties were constructed at Rockaway Inlet in 1932 and at East Rockaway Inlet in 1934. Prior to 1932, the barrier island system was in a natural state and was unaffected by the numerous jetties, groins, and seawalls that heavily influence shoreline change results for subsequent time intervals. As such, this time period offers a chance to observe primarily natural trends in barrier island migration prior to structure placement. One of the more notable storm events impacting the study area occurred on March 4, 1931, when Moriches Inlet was reopened for the first time since at least the early 1800s (Smith et. al., 1999). Effects from the storm and subsequent inlet reopening are visible along the east side of Fire Island. Shoreline change observed at each of the barrier islands during this period is in the form of west-directed barrier beach migration, reflective of the direction of net longshore transport (Figure 3-6). Some of the west-directed shoreline advance may not be captured by calculated

change rates displayed in Figure 3-6, as the rate of change is calculated normal to shoreline orientation. In those cases, direct measurements have been made to quantify migration rates.

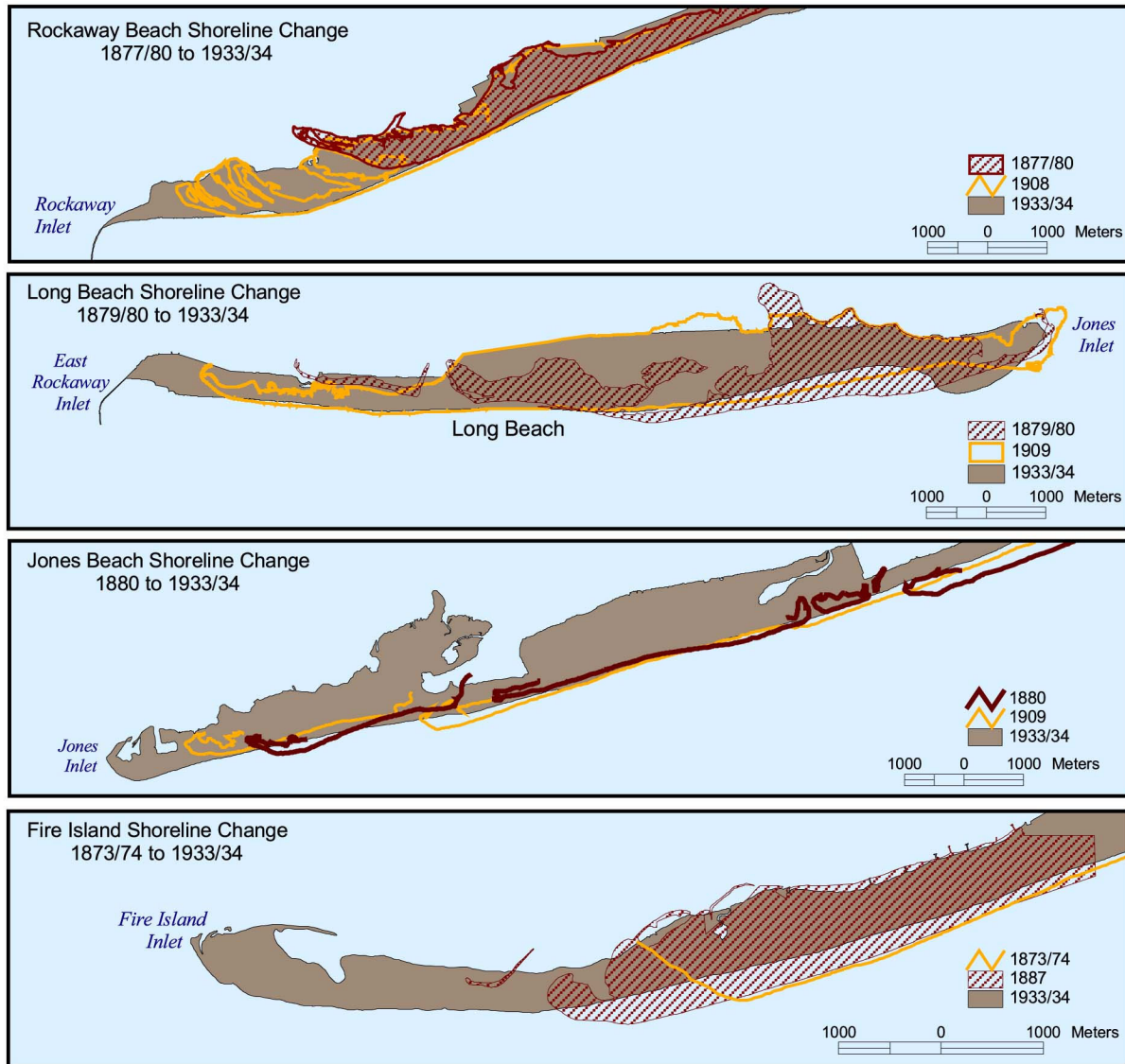


Figure 3-6. Westward island migration along south shore beaches of Long Island, 1873/88 to 1933/34.

Rockaway Beach experienced substantial shoreline advance along the western 75% of the island and west-directed migration of about 50 to 55 m/yr between 1877/78 and 1933/34 (Figure 3-6). Shoreline recession for this period was limited to a small section of coast on the eastern quarter of Rockaway Beach, adjacent to the present location of East Rockaway Inlet. Between 1877/78 and 1933/34, the eastern end of Rockaway Beach shifted west about 2.5 to 3 km. Likewise, East Rockaway Inlet and Long Beach Island were positioned to the east on Long Beach Island, and the western edge of the island was about 3 km east of the 1933/34 position. Two major factors influenced change trends during this period: the 1926 to 1936 beach restoration project and the absence of a jetty at the west end of the island until 1932/33, which allowed Rockaway Point to migrate along-shore for most of this time interval. Prior to construction of the jetty on the west end of Rockaway Beach, Rockaway Beach existed as a

compound recurved spit, migrating west at a rate of about 50 m/yr. Once the jetty was constructed, migration of the spit ceased as sediment was trapped along the western edge of the island adjacent to the structure. Because the jetty was not in place for most of this time period, natural migration patterns for the spit dominated beach evolution. Timing of the 1926 to 1936 beach nourishment at Rockaway Beach also significantly affected shoreline change trends. Because nourishment activities occurred immediately before and during the 1933/34 shoreline survey, shoreline change rates at Rockaway Beach reached about 22.7 m/yr, with greatest change observed adjacent to Rockaway Inlet. As such, recession rates observed for Rockaway Beach during this period were low. Shoreline recession at Rockaway Beach was limited to about a 2.5 km section of shoreline on the east side of the island in the vicinity of the present-day location of the town of Edgemere. Erosion rates in this area ranged from about 0.2 to about 3.4 m/yr, with maximum change located adjacent to East Rockaway Inlet. Overall, calculated change rates for Rockaway Beach ranged from about 22.7 to -3.4 m/yr.

Shoreline position at Long Beach Island also changed dramatically between 1879/80 and 1933/34. The present barrier beach of Long Beach Island was comprised of two smaller barrier islands during the 1879/80 time period. East Rockaway Inlet was located about 3 km east of its 1933/34 location, and an additional inlet (no longer in existence today) was located another 2.5 km to the east. As west-directed littoral drift forced East Rockaway Inlet and the eastern end of Rockaway Beach to the west, the western margin of Long Beach Island migrated similarly at a rate of about 55 m/yr (Figure 3-6). Calculated rates of shoreline change at Long Beach during this interval show a maximum shoreline advance rate of about 10 m/yr in the western half of the island and a maximum recession rate of about 9.5 m/yr on the east half of the island. Shoreline recession along eastern Long Beach Island occurred as sediment was transported west in the littoral drift system, contributing to westward lateral growth of the island. There were no recorded beach fills at Long Beach during this time interval.

Patterns of shoreline change for Jones Beach between 1880 and 1933/34 are similar to those observed for the two western reaches, with an overall decrease in shoreline advance rates and a slight increase in shoreline recession. Shoreline change was influenced substantially by the 1927 beach fill that supplied 31.0 mcm of sand to the beach. Prior to the 1927 fill, the entire shoreline at Jones Beach was composed of barrier hummocks and washovers, characterized on the 1880 shoreline map as an island complex composed of four discrete units (Kana, 1999). The 1927 beach fill transformed the island from a series of disconnected units into a contiguous barrier island. The fill not only advanced the ocean shoreline but also contributed to the littoral transport system feeding west-directed barrier island migration at a rate of about 40 m/yr. Calculated shoreline change rates at Jones Beach document overall patterns similar to those observed for the Rockaway and Long Beach reaches, producing deposition along the western portion of the island and erosion to the east. Maximum shoreline advance at Jones Beach was about 3.6 m/yr adjacent to Jones Inlet, and maximum recession of about 8.9 m/yr was documented near of Cedar Beach.

Shoreline change patterns for Fire Island deviate from those observed along shorelines to the west, documenting significantly lower rates of deposition and a much greater extent (in terms of total area) of shoreline recession (Figure 3-7). Similar to Rockaway Beach, Long Beach, and Jones Beach, the morphology of Fire Island was significantly altered during this time, primarily through natural events. From the early 1800s to 1931, Moriches Inlet was closed to the Atlantic Ocean, and the Fire Island barrier was a single spit from Fire Island Inlet east to Shinnecock Inlet. The northeast storm of March 4, 1931 reopened Moriches Inlet, detaching Fire Island from Westhampton Beach to the east. Moriches Inlet remained open intermittently until it was reopened by a storm in September 1953 when jetties were being constructed on

both banks. West-directed shoreline movement (not captured by calculations normal to the primary orientation of the shoreline) was greater at Fire Island than at other reaches during this period, with the shoreline advancing west at a rate of about 80 m/yr (Figure 3-6). Shoreline change rates observed along the length of Fire Island were more erosional overall than those observed for other reaches in the study area. Beach erosion documented along beaches at Fire Island was transported west as part of the littoral drift system feeding the west side of the migrating sand spit. The absence of beach nourishment during this time resulted in a net deficit in sand volume for most of the reach, as opposed to trends for other reaches where recession was limited primarily to the eastern half. Maximum change values recorded for this reach were about -5.2 m/yr adjacent to Fire Island Inlet and about 0.9 m/yr near the vicinity of the present location of Great South Beach.

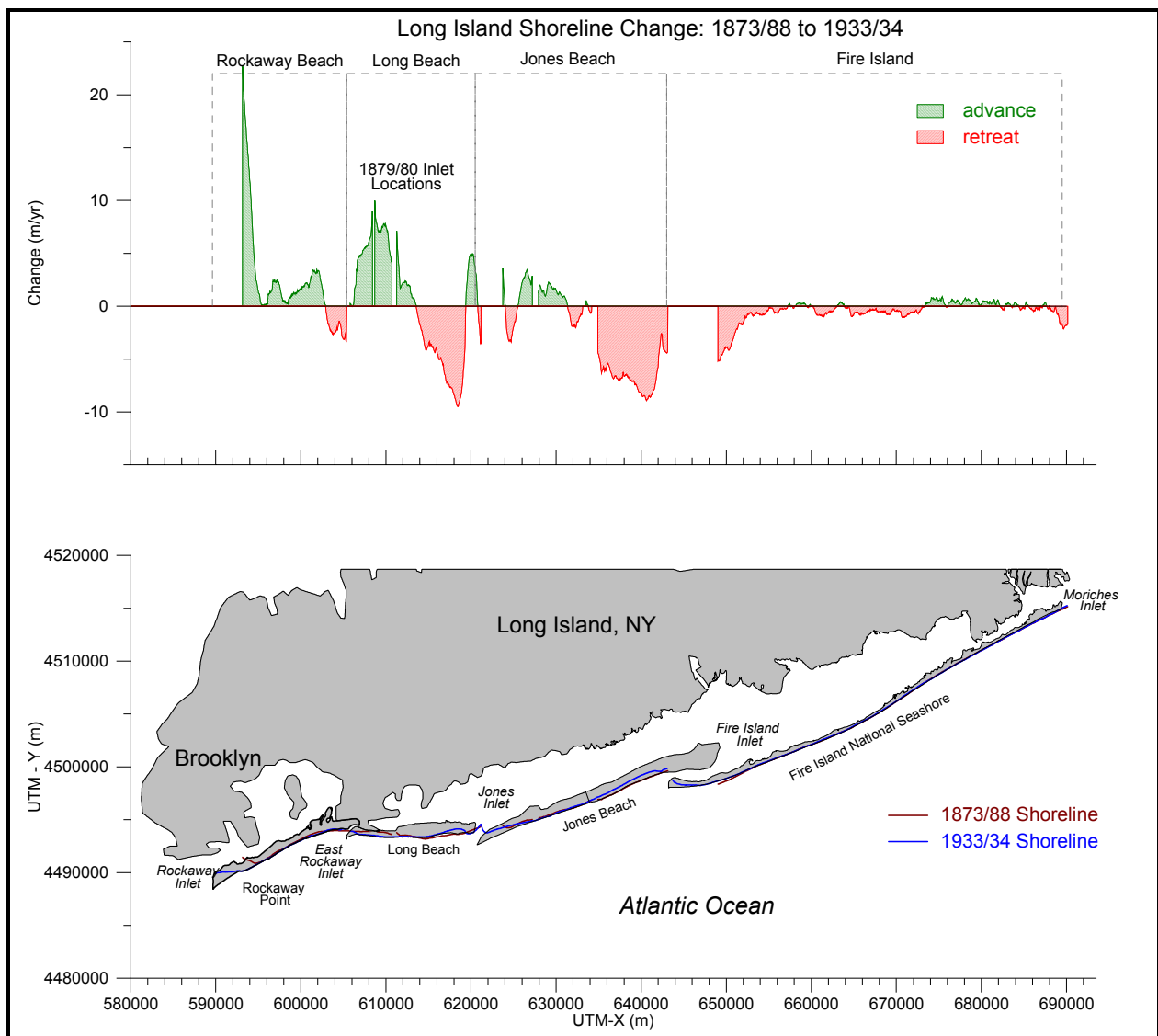


Figure 3-7. Shoreline change along south shore beaches of Long Island, 1873/88 to 1933/34.

1933/34 to 1983

Shoreline change between 1933/34 and 1983 was influenced by engineering alterations in the form of structure placement and beach nourishment. Over 27.5 mcm of sand was documented in placement records for beaches in the study area. Additionally, each of the inlets was armored with an eastern jetty, which transformed west-directed migration visible in the previous time interval into significant shoreline advance adjacent to the new structures. Furthermore, numerous groins and seawalls were constructed primarily along Rockaway Beach and Long Beach, interrupting west-directed littoral drift. In addition to these alterations, there were multiple major storm events recorded, including the Sept 21, 1938 Long Island Express, which created Shinnecock Inlet and widened Moriches Inlet, and the Ash Wednesday Storm of 1962 (Northeaster of record for Long Island). Available records do not document any major storm events between 1976 (Hurricane Belle) and the 1983 shoreline survey. Overall, shoreline change patterns illustrated high rates of deposition along the western margin of most reaches, with smaller zones and lower rates of erosion located primarily along the eastern boundaries of the islands.

Shoreline change along Rockaway Beach was dominated by deposition, with zones of erosion in small areas. A large portion of the shoreline at the eastern side of the island (about 4 km) was not mapped for the 1983 data set (see Figure 3-8). As such, shoreline change could not be calculated for this area. However, visual and calculated change comparisons for other time periods in this area indicate that it has been primarily depositional (about 1 m/yr between 1962 and 1997; about 2 m/yr between 1880 and 1997). The most dramatic change between 1933/34 and 1983 was shoreline response to construction of the jetty at Rockaway Inlet (1932). Initially, the new structure resulted in significant shoreline advance at a rate of about 33 m/yr between 1933/34 and 1962. As sediment accumulated and the zone of deposition expanded farther east, the rate of shoreline advance adjacent to the jetty slowed to about 12 m/yr between 1962 and 1970, and was reduced even further to about 10 m/yr between 1970 and 1983. This adjustment resulted in overall advance at the shoreline immediately adjacent to the jetty of about 20.5 m/yr between 1933/34 and 1983 (Figure 3-9).

East of the deposition zone, shoreline change trends reversed, documenting recession up to about 0.6 m/yr. This section of shoreline historically has been erosional, and numerous groins have existed since 1933/34. As the depositional area continues to expand to the east, it is likely that the influence of the jetty may impact part of this region and some of the erosional area will become depositional, consistent with trends for previous time periods in this region (between 1962 and 1997, the depositional area resulting from the jetty expanded east about 600 m). During this time interval, a total of about 8.1 mcm of sediment was placed on the beach (an increase from rates during the previous time interval at Rockaway Beach), with about 6.5 mcm (approximately 80%) occurring between 1975 and 1982. That equates to an average annual placement of about 928,600 m³ for the 7 years immediately preceding the 1983 shoreline survey. It is likely that beach nourishment activities at Rockaway contributed significantly to the predominance of deposition calculated for this time interval. The second area of erosion is a 900 m section of shoreline located west of East Rockaway Inlet, south of the town of Edgemere. Shoreline recession rates in this area range from about 0.1 to 2.2 m/yr. It is possible that this stretch of coast is being affected by the interruption of littoral drift created by East Rockaway Inlet (located about 500 m east of this area). Overall, maximum recession at Rockaway Beach between 1933/34 and 1983 was about 2.2 m/yr and maximum shoreline advance was about 20.5 m/yr.

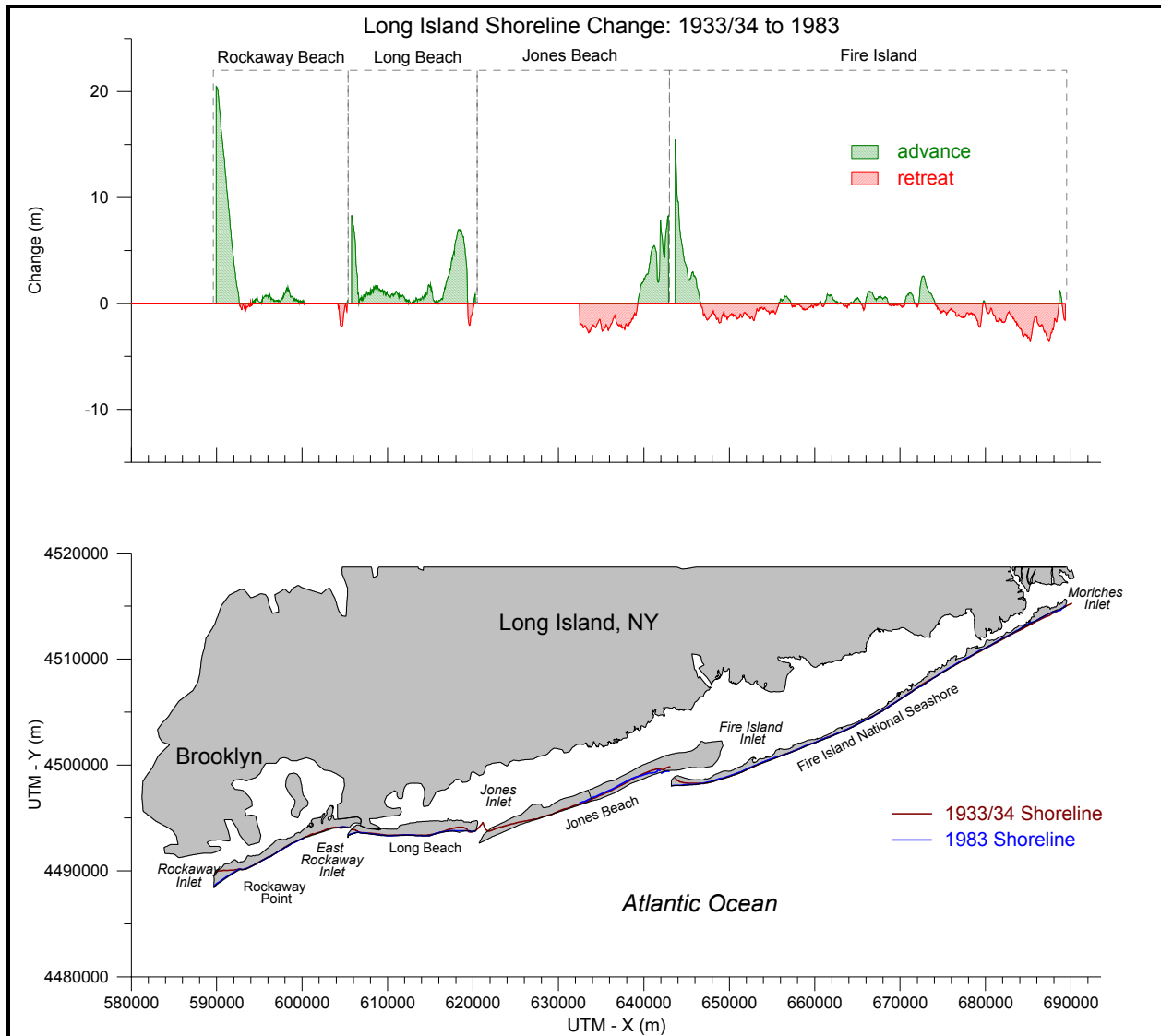


Figure 3-8. Shoreline change along south shore beaches of Long Island, 1933/34 to 1983.

Shoreline change trends documented at Long Beach between 1933/34 and 1983 are similar to those documented for Rockaway Beach. Deposition dominated, with shoreline advance greatest in the vicinity of East Rockaway Inlet (maximum rate of about 8.3 m/yr). Again, deposition was influenced largely by the development of the east jetty at East Rockaway Inlet in 1934 (Table 3-4). From the end of jetty construction in 1934 until 1960, the shoreline advanced at rates ranging from about 4.0 to 15.4 m/yr. In subsequent years, shoreline advance diminished more than that documented at Rockaway Beach. Between 1960 and 1983, shoreline position remained (relatively) stable, retreating somewhat between 1960 and 1970 and advancing somewhat between 1970 and 1983 (Figure 3-10). Reasons for the difference in long-term post-jetty shoreline response may include the fact that Long Beach was not nourished until 1959/60 (Kana, 1999), and thereafter, nourishment rates were much lower than those recorded for Rockaway Beach. Between 1933/34 and 1983, about 1.9 mcm of sediment was placed on Long Beach, with about 70% (1.3 mcm) placed during the 1970s and 1980s (Kana, 1999, Table 3-4). Additionally, according to Kana (1999), nearly 60 groins constructed perpendicular to the shoreline in this region may have caused a reduction in longshore sediment

transport adjacent to the jetty during this time. Overall, the shoreline at Long Beach adjacent to the inlet advanced at rates ranging from about 2.4 to 8.3 m/yr. The shoreline west of this area was primarily depositional as well, with greatest shoreline advance rates in the vicinity of Lido Beach from about 4 to 7 m/yr between 1933/34 and 1983. Shoreline advance was consistent for the 1960 and 1970 shorelines. Increased deposition at this location may be from beach nourishment activities documented at Lido Beach in 1962. Because specific location information is absent for some of the beach nourishment events at Long Beach, it is possible that nourishment activities were located within the vicinity of Lido Beach. Additionally, it is possible that sediment dredged from Jones Inlet may have been placed on down-drift beaches during this period, which would have influenced shoreline position at Lido Beach.

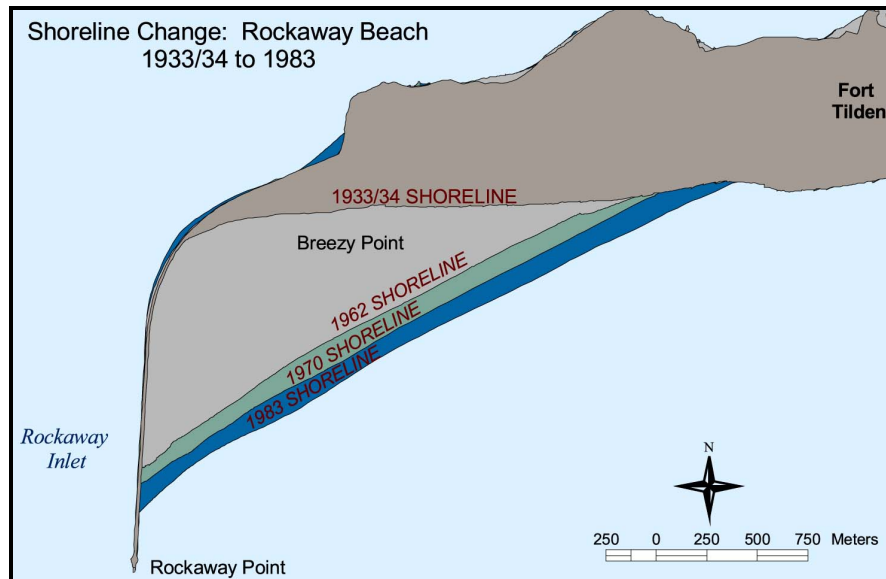


Figure 3-9. Incremental changes in shoreline position adjacent to the jetty at the western end of Rockaway Beach, 1933/34 to 1983.

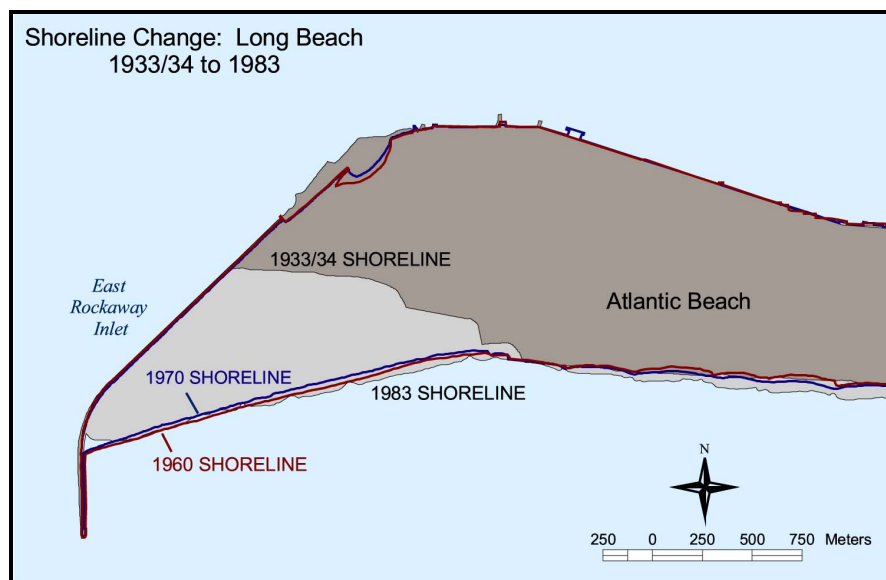


Figure 3-10. Incremental changes in shoreline position adjacent to the jetty at the western end of Long Beach, 1933/34 to 1983.

Shoreline change results at Jones Beach between 1933/34 and 1983 differ from those calculated for the two reaches to the west. Due to a large gap along the western half of Jones Beach for the 1983 shoreline data set, change calculations between 1933/34 and 1983 were limited to the area between Tobay Beach (west) and Cedar Beach (east). The 1947 shoreline survey was used to visually compare long-term trends with intervening years. The 1933/34 to 1983 time interval at Jones Beach was marked initially by shoreline adjustment to the 1927 reclamation project, followed by additional nourishment events throughout each of the following decades, and finally by construction of jetties east of the island at Fire Island Inlet in 1941 and on the west end of the island at Jones Inlet in 1959. Annual dredging has been performed at Fire Island Inlet almost continuously since 1954, with much of the sediment dredged from the inlet placed on the updrift end of Jones Beach (Smith et. al., 1999). Between 1933/34 and 1983, a total of about 12.2 mcm of material was placed on beaches, with much of this beach fill representing disposal of sediments from Fire Island Inlet (Kana, 1999). Beach nourishment volumes for each decade between 1933/34 and 1983 were relatively consistent, with slightly less nourishment activity recorded for the 1980s (Table 3-5). Compared with Rockaway Beach and Long Beach, relatively few structures were constructed along the shoreline at Jones Beach during this time interval. Most of the shoreline at Jones Beach remains undeveloped today (Kana, 1999).

Shoreline position change at Jones Beach documented erosion from the east end of Tobay Beach west to about Gilgo State Park, followed by deposition in the area of Cedar Beach. Shoreline recession in the vicinity of Tobay and Gilgo Beaches is similar to trends observed relative to the 1947 shoreline survey. Deposition in the vicinity of Cedar Beach is most likely related to the combination of increased beach nourishment with sediments dredged from Fire Island Inlet and sand trapped by the sand dike known as the "Thumb" that was constructed at Oak Beach in 1959 (Kana, 1999). The "Thumb" was constructed after initial development of the jetty at Fire Island Inlet to prevent erosion at Oak Beach. It worked as intended, but it also prevented the return of the sand gradually being pushed across the inlet by the tidal currents. Instead, sand was pushed westward by littoral and ebb tidal currents, producing an increase in the width of Cedar Beach (Wolff and Bennington, 2000). Prior to construction of the "Thumb", erosion was dominant in this area, as documented by comparison with the 1947 shoreline. Overall, maximum recession was documented at West Gilgo Beach at a rate of about 2.8 m/yr, and maximum shoreline advance was recorded adjacent to the "Thumb" at a rate of about 8.3 m/yr (Figure 3-8).

Along Fire Island, shoreline change was dominated by recession and, similar to the 1873/88 to 1933/34 interval, was more erosional overall than other reaches in the study area. Jetties were constructed at the east end of Fire Island on both sides of Moriches Inlet in 1953/54 and at the west end of the island at Fire Island Inlet in 1941. Beach fill at Fire Island began in the late 1940s, and since then, it has been concentrated primarily at the eastern and western ends, near Moriches Inlet and at Robert Moses State Park (Kana, 1999). Through the 1980s, about 4.4 mcm of sediment was placed on Fire Island. Records indicate that the majority of sediment was placed during the 1960s, when bay and inlet sediments were being disposed along beaches at Fire Island under the direction of Suffolk County (Kana, 1999). Nourishment activity through the 1970s and 1980s makes up only about 4% of total nourishment activity recorded for this time interval. As with Jones Beach, much of Fire Island remains undeveloped and has experienced less coastal structure development along the outer shoreline than at Rockaway Beach or Long Beach. Fire Island National Seashore was established in 1965, preserving about 42 km of shoreline in this reach.

The most notable change in shoreline position along Fire Island was substantial deposition adjacent to the jetty at the west side of the island (Figure 3-8). Approximately 3 km of shoreline adjacent to the jetty were depositional between 1933/34 and 1983, with maximum rates of about 15.5 m/yr occurring immediately adjacent to the jetty. West of the deposition zone, for approximately 9.4 km, the shoreline was dominated by recession, with rates ranging from about 0.1 to 1.8 m/yr. This area extends from the west side of Robert Moses State Park across much of Great South Beach to about the location of the town of Ocean Beach. For the next 20 km, shoreline change alternates between recession and advance, with relatively low rates of each. The final 16.5 km of shoreline are again primarily erosional, with change rates in this region ranging from about -3.6 to 1.8 m/yr. The overall predominance of shoreline recession along Fire Island as opposed to beaches to the west may be due to the reduction in beach nourishment in this region in the 1970s and 1980s. Additionally, Kana (1999) suggested that sand trapping by the Westhampton groin field (built in the 1960s) had created a net sand deficit compared to the prior two decades.

1983 to 1991/97

Shoreline change for the most recent time interval along southwestern Long Island beaches continued to be affected by beach nourishment activities, structure rehabilitation, and inlet maintenance dredging. The Atlantic Coast of New York Monitoring Program has been conducting monitoring work along beaches in southern Long Island since 1995. Where applicable, results from these efforts are compared with results observed in this data set. Between 1983 and 1991/97, about 15.8 mcm of sediment was placed on beaches. The most significant gains were located at the west end of Jones Beach, with rates of advance reaching about 38 m/yr (Figure 3-11). Additionally, some areas of coastline that previously were consistently erosional were depositional for this time. Most likely, this is due to increased beach nourishment activity that began in the mid-1990s. Storms during 1992 inspired resumption of beach nourishment along parts of the coastline. Furthermore, the smaller time interval between shoreline surveys (7 to 14 years as opposed to 49 and 57 years) may account for increased rates of change. There are eight notable storm events documented for this time period, with three of these documented in 1991/92.

Shoreline change at Rockaway Beach continued to be depositional on the western half of the island but experienced a larger area of shoreline recession along its eastern half (Figure 3-11). Although recession rates on the east side of the island were relatively low, with a maximum of about 2.7 m/yr, the amount of shoreline experiencing erosion increased from only a small section of the entire shoreline between 1933/34 and 1983 to about half of the total shoreline length between 1983 and 1991/97. As with the 1933/34 to 1983 comparison, the large gap in the east side of the 1983 data set prevented change calculations for this portion of the island. Between 1983 and 1991/97, beach nourishment at Rockaway Beach totaled about 3.5 mcm. Recent beach nourishment events for this area completed as part of the Storm Reduction Project, were performed after the 1997 survey (1998 and 2001) and are therefore not included as part of the total. Rates of deposition on the west side of the island are lower than those recorded prior to this time interval. Whereas maximum rates of advance at Rockaway Point from 1878 to 1933/34 and 1933/34 to 1983 were about 22.7 and 20.5 m/yr, respectively, average shoreline advance was about 6.1 m/yr. Although rates of deposition are smaller for this time interval, the extent of deposition extends about 1.5 km east of that for the 1933/34 to 1983 comparison. Shoreline change rates ranged from -2.7 m/yr in the vicinity of Belle Harbor to 6.1 m/yr near Rockaway Point.

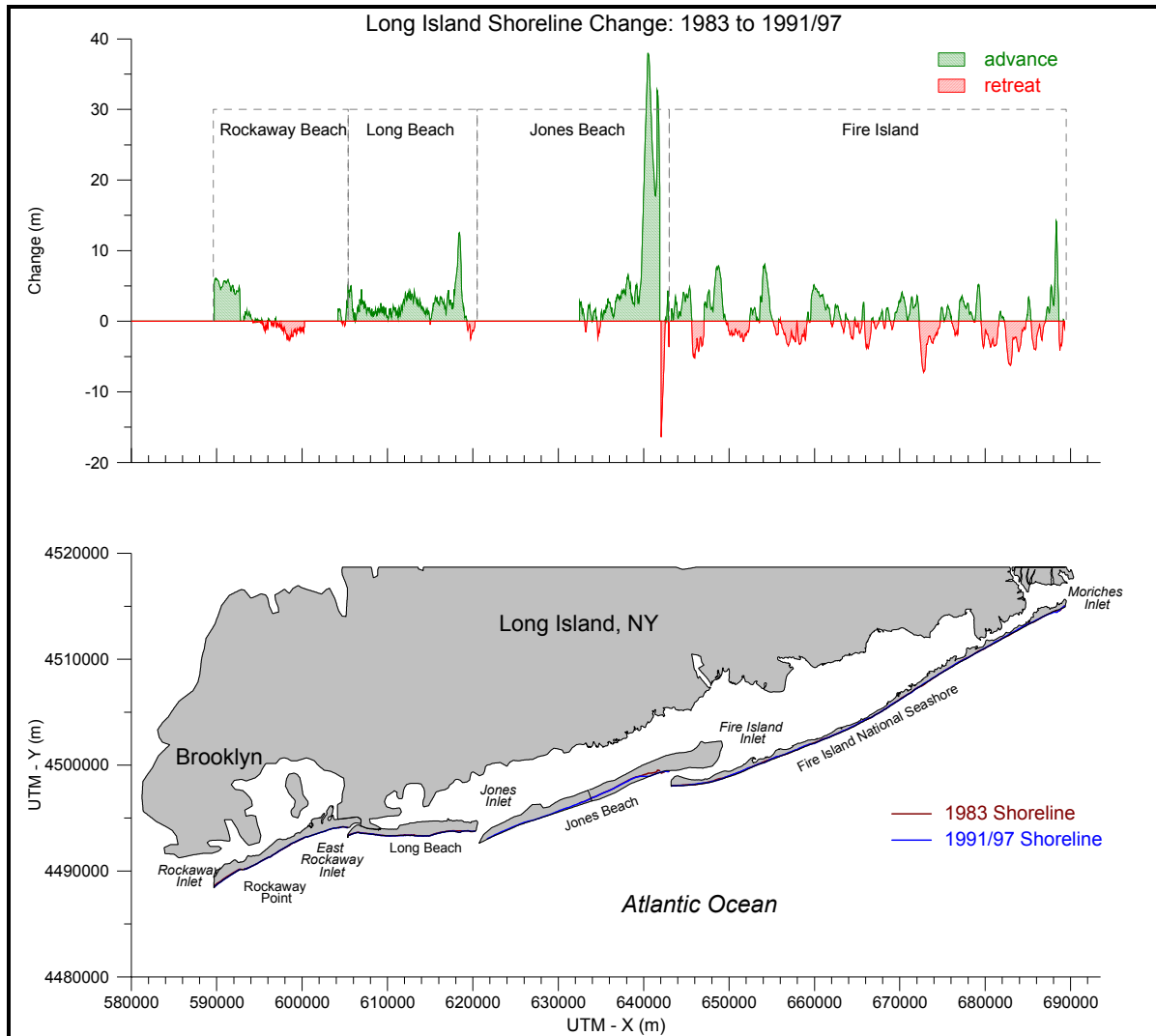


Figure 3-11. Shoreline change along south shore beaches of Long Island, 1983 to 1991/97.

Shoreline change at Long Beach was similar to historical trends, with slightly higher rates of deposition. Between 1983 and 1994, about 1.1 mcm of sediment was placed along beaches at Long Beach, with about 38% of this total deposited in 1994. Deposition was predominant during this time period for a majority of Long Beach, with a minor zone of erosion located at the east end of the island adjacent to Jones Inlet. Future beach nourishment events are scheduled to begin in 2004 at Long Beach as part of the Storm Damage Reduction Act.

Shoreline change at Jones Beach was calculated for the period 1983 and 1991. As with the 1933/34 to 1983 shoreline change observations, the west portion of the island is lacking data for comparison. Shoreline change deviates substantially from that observed for previous time periods in this area. Aside from a few areas of recession along portions of this reach, the entire length of the shoreline is dominated by deposition. Beach nourishment records indicate that at least 3.1 mcm of sediment were placed onto beaches during 1989 and 1991, which likely accounts for the seaward position of the 1991 shoreline. The area of greatest advance is located at Cedar Beach, with deposition rates recorded up to about 38 m/yr (Figure 3-11). Immediately adjacent to Fire Island Inlet, shoreline recession was dominant at rates ranging from about 0.5 to 16.5 m/yr.

Shoreline change at Fire Island also deviated from historical trends, showing an overall increase in deposition (Figure 3-11). Change rates for Fire Island were calculated for the period 1983 and 1995. During this interval, beach fill activity increased dramatically in response to the effects of winter storms in 1991 and 1992. Thirty-one nourishment events were documented in the 1990s, for a total volume of about 1.9 mcm. Because exact dates are missing from the data set, the total number of fills completed prior to the 1995 shoreline survey may be less than the total completed for the 1990s. The increase in beach fill during the 1990s likely has contributed to greater amounts of deposition observed on Fire Island. Overall, shoreline change ranged from -7.2 to about 14.2 m/yr.

1873/88 to 1991/97

Net shoreline change between 1873/88 and 1991/97 was used to document long-term trends for southwestern Long Island beaches within the study area. The 1873/88 data set provides a good baseline for evaluating shoreline change because it represents a time period before the introduction of major engineering activities (i.e., jetty, groin and seawall construction, beach nourishment, and channel dredging). The longer time interval used for this comparison allows for overall trends to be observed within the context of numerous engineering alterations. Overall, deposition along the barrier islands of the south coast of Long Island increased to the west, consistent with the direction of net longshore transport. Maximum deposition was about 10.6 m/yr at Rockaway Point, consistent with trends observed for previous time periods (Figure 3-12). Erosion along the east side of the barrier islands increased to the east, with shoreline response along Fire Island almost entirely recessional. In general, rates of deposition exceed those of erosion within the study area, primarily the result of beach nourishment activities. Trends within each reach generally are similar to those observed from incremental time periods.

Along Rockaway Beach, deposition was dominant for the majority of this reach, with erosion confined to the eastern 2.5 km of the island. The maximum deposition rate of about 10.6 m/yr was located at Rockaway Point. The zone of erosion along the east side of the island is located south of the town of Edgemere, and documents maximum recession of about 1.9 m/yr for this interval.

Shoreline change at Long Beach showed similar trends to those observed at Rockaway Beach. Deposition along the western half of the island ranged from about 0.5 m/yr to 5.4 m/yr and erosion along the eastern side of the island ranged from about 0.1 to 2.1 m/yr (Figure 3-12). Maximum deposition is located near the east side of Atlantic Beach (near the location of the historical inlet in 1879/80) and maximum recession is located at Lido Beach.

Shoreline change trends for Jones Beach documented more erosion over the long term than that observed for the previous two reaches. Maximum shoreline recession of about 4.2 m/yr was located adjacent to the 1880 historical inlet located near the present-day location of Gilgo Beach. Additionally, the area along the east end of Jones Beach that has been predominantly depositional in recent years (due to either beach fills from Fire Island Inlet sediments or sediment accretion from construction of the "Thumb") showed a reduced deposition rate for this time period. The maximum rate of shoreline advance was about 1.5 m/yr immediately adjacent to the "Thumb". Deposition was dominant along the west side of the island for about 7 km of shoreline. The maximum advance rate in this area was about 5.4 m/yr, located at the west end of the island.

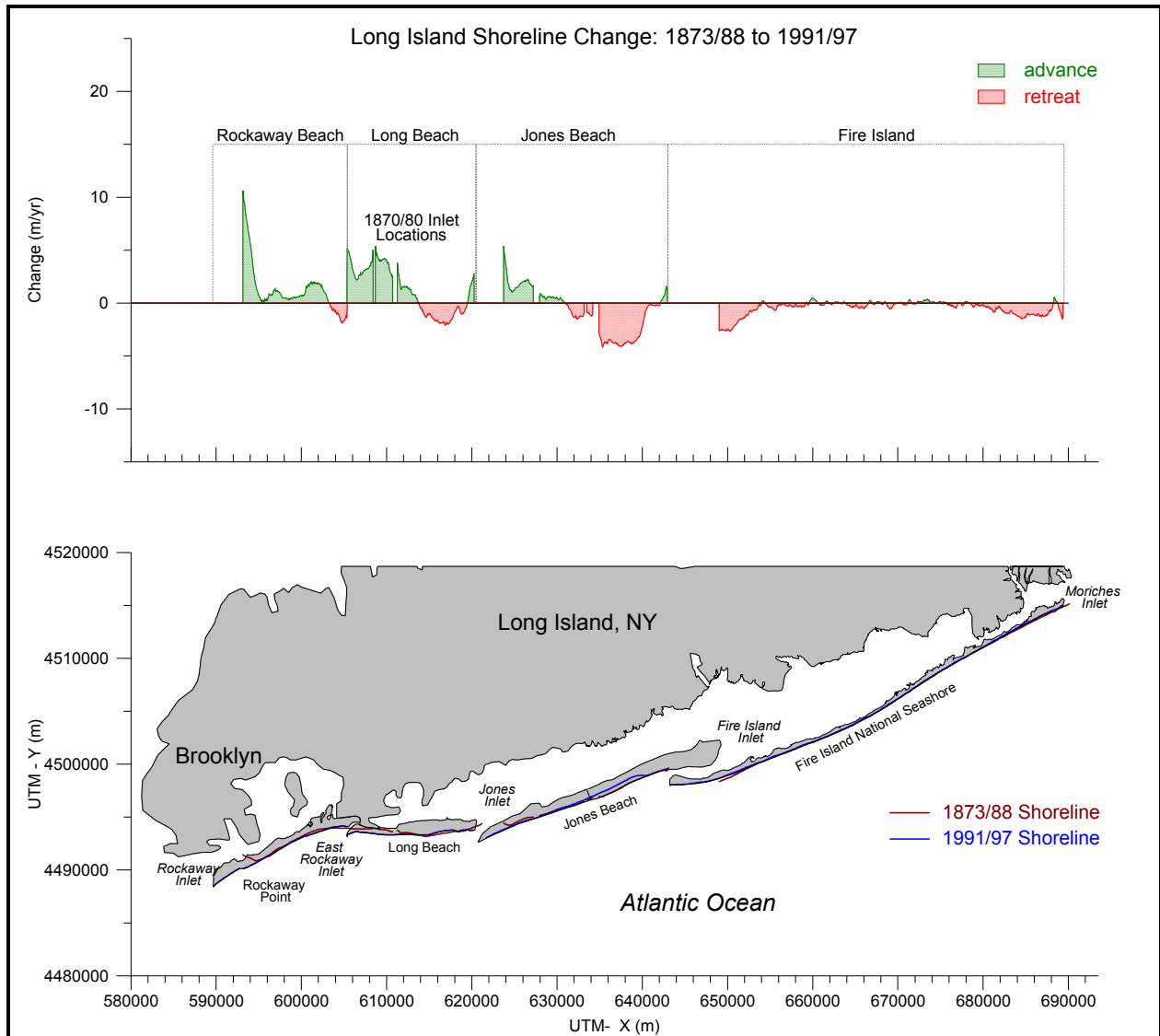


Figure 3-12. Cumulative shoreline change for southern Long Island beaches between Rockaway and Moriches Inlets, 1873/88 to 1991/97.

Shoreline change at Fire Island was dominated by erosion. Small areas of deposition were present along the entire shoreline, but the majority of coast illustrates long-term recession to about 2.6 m/yr. Although the Fire Island shoreline encompasses approximately 40% of the entire study area, the beach received only about 8% of the total beach nourishment for the region. Limited beach nourishment may be the primary cause of dominant long-term recession rates. The exception to this trend was illustrated between 1983 and 1991/97, where shoreline change recorded fairly even amounts of erosion and accretion. Increased deposition was due to increased nourishment activities through the 1990s (approximately 30 independent events). Despite the fact that erosion has been a continuing trend at Fire Island, maximum rates generally have been lower than those documented for other reaches.

3.1.3.2 Northern New Jersey Shoreline Change

Similar to shoreline change patterns observed for Long Island beaches, a majority of the coastline in northeastern New Jersey has experienced persistent erosion problems, which have

affected many of the coastal communities over the past 140 years. General patterns of change in northeastern New Jersey are similar to those found on Long Island, with rapid spit growth in the direction of net littoral transport. Spits located at the northern and southern extents of the study area tend to experience greatest changes, with other rapidly changing areas located in the vicinity of inlets. Shoreline change patterns have also been influenced by beach nourishment and structure development, changing the character of beaches and sometimes altering change trends. Shoreline positions are compared for four time periods to identify long-term change patterns that have occurred historically along the northeastern New Jersey coast. Calculated rates of change for each time interval are listed in Appendix B. Reaches and place names referenced in the following discussion are shown in Figure 3-13.

1836/39 to 1855/75

The period 1836/39 to 1855/75 documents considerable shoreline change as it responded to natural coastal processes. Anthropogenic alterations such as entrance jetty construction, groin and seawall development, and beach nourishment are absent from this interval. This allows observation of natural shoreline response that may be overshadowed or minimized by human-induced changes during subsequent time periods.

Shoreline change in northeastern New Jersey between Sandy Hook and Barnegat Inlet was dominated by recession with small zones of advance located intermittently throughout the area (Figure 3-14). Deposition zones are primarily located adjacent to historical or present-day entrances and tend to reflect the net direction of longshore transport. Change in the direction of net littoral drift in this region centers on a nodal point located in the vicinity of Manasquan Inlet, north of which net transport is to the north and south of which it is to the south. Sediment transported within this system has resulted in substantial shoreline progradation along the terminus of Sandy Hook and the sand spit on the southern boundary of Island Beach State Park at Barnegat Inlet.

Between Sandy Hook and Asbury Park, shoreline change is dominated by erosion. A zone of deposition located at the northern tip of Sandy Hook spit illustrates the direction of net littoral transport. Sandy Hook, a classic recurved spit, developed from northward directed longshore transport. Prior to its development, the Navesink and Shrewsbury Rivers located immediately south of Sandy Hook had direct access to the Atlantic Ocean. Development of a barrier beach over time has blocked these water bodies from entering the sea and they are now diverted to the north into Sandy Hook Bay (Williams and Duane, 1974). The rate of spit progradation to the north and northwest between 1836/39 and 1855/75 was about 5.7 m/yr (Figure 3-14). South of this deposition zone along the spit, erosion was dominant, ranging from about 0.1 to 8.3 m/yr. A second zone of deposition is located on the north side of what appears to be an historical inlet or breach. The existence of this feature was not documented among subsequent shoreline surveys; however, its position along the narrowest portion of the spit separating the Atlantic Ocean from Sandy Hook Bay makes it an ideal location for this type of breach to occur. Additionally, it is centered at the confluence of the Navesink River and Sandy Hook Bay, in the vicinity of the historical discharge point for the river before it was diverted north. As such, the existence of a breach in this location is not surprising. Deposition appears to have filled in the breach, with rates ranging from about 0.2 to 20.9 m/yr. South of this deposition zone, shoreline recession dominates throughout the reach.

Shoreline change trends between Asbury Park and Manasquan Inlet are dominated by recession, with maximum rates of change reaching about -8.4 m/yr near the north side of Manasquan Inlet. A small zone of deposition exists in the vicinity of the present day location of



Figure 3-13. Northern New Jersey shoreline reaches, Sandy Hook to Barnegat Inlet, NJ.

Spring Lake, with maximum change rates of about 0.5 m/yr. Besides this small area, the rest of the reach is dominated by erosion (Figure 3-14). The 1836/39 and the 1855/75 shoreline surveys document the existence of inlets near the present-day locations of Shark River and Manasquan Inlets. The position of Manasquan Inlet for both surveys was about 950 m north of its present location, which was first armored with timber jetties in 1882/83. While shoreline recession is greatest in the vicinity of Manasquan Inlet for this reach, change patterns appear to be affected little by the existence of Shark River Inlet, with retreat rates ranging from about 1.0 to 2.5 m/yr adjacent to the entrance.

From the south side of Manasquan Inlet to the north side of Barnegat Inlet, shoreline change trends remained primarily erosional for this time interval (Figure 3-14). A small section of shoreline (about 4 km) from about the vicinity of Chadwick to Seaside Heights (see Figure 3-13) was depositional (Figure 3-14). The maximum deposition rate observed for this section of shoreline was about 3.4 m/yr. A 3.5 km gap in the 1836/39 shoreline south of this area prevented analysis of this section of coast. Thus, it is possible that the deposition zone may have extended farther to the south, but was cut-off due to lack of data. South of this data gap, the shoreline was dominated by shoreline recession south to Barnegat Inlet. A small zone of deposition on the northern side of Barnegat Inlet was consistent with sand transport trends south of Manasquan Inlet. Sediment transported along-shore by wave-induced currents created significant southward growth of a sand spit at a rate of about 13 m/yr.

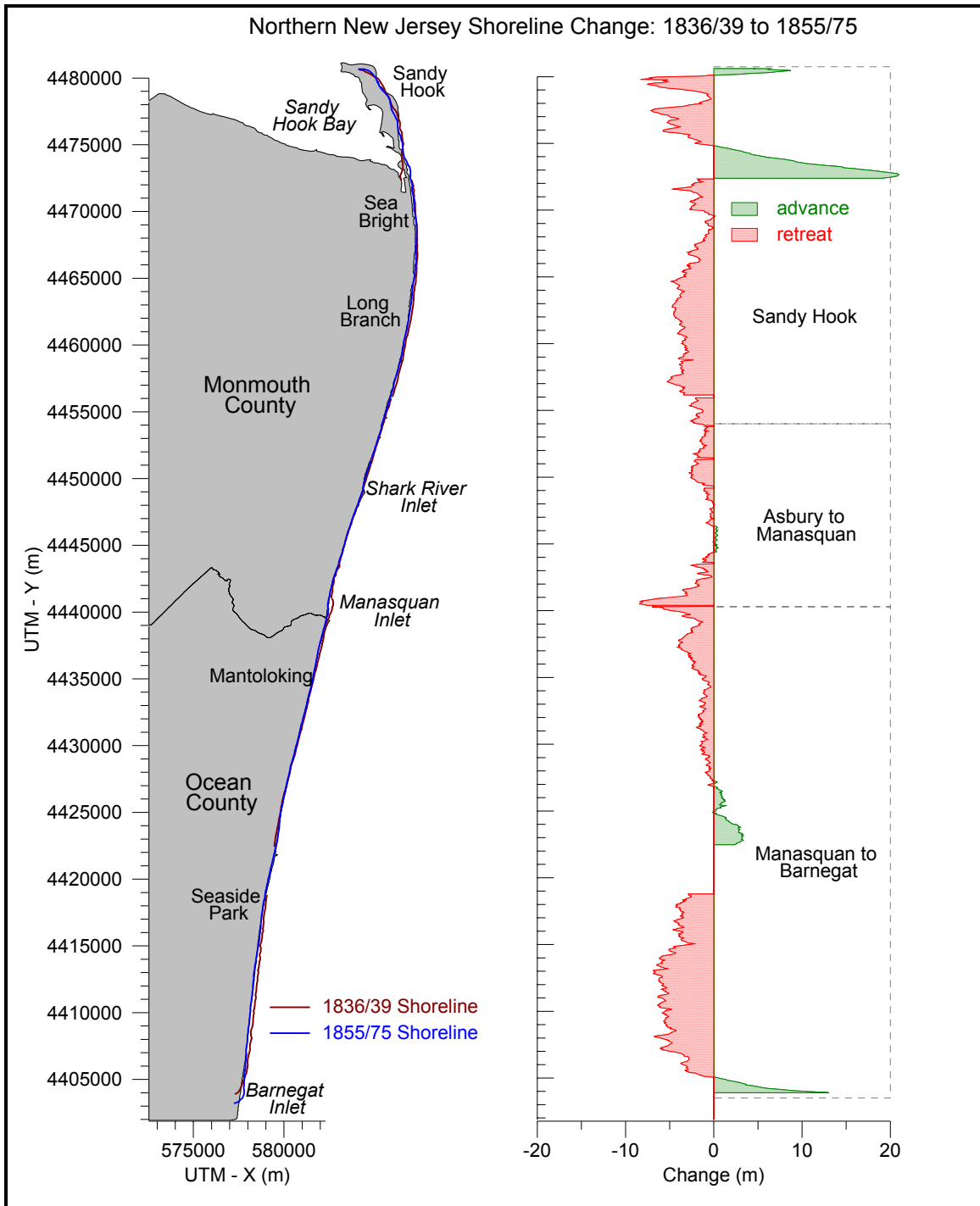


Figure 3-14. Shoreline change along northern beaches of New Jersey, 1836/39 to 1855/75.

1855/75 to 1932/33

Shoreline change between 1855/75 and 1932/33 continued to be dominated by erosion, with small areas of deposition located intermittently throughout the region (Figure 3-15). Jetties were constructed at Manasquan and Shark River Inlets, and various additional shoreline stabilization structures were built. The 1932/33 shoreline documents the existence of various groins, seawalls, and jetties north of Manasquan Inlet, although there is little information

regarding the construction of these features. Two major storms occurred during this period, including the Blizzard of 1888 and the Unnamed Northeaster of March 4, 1931. The 1931 northeaster was powerful enough to re-open Moriches Inlet along southern Long Island, thus it is likely that the position of the 1932/33 shoreline was impacted as well.

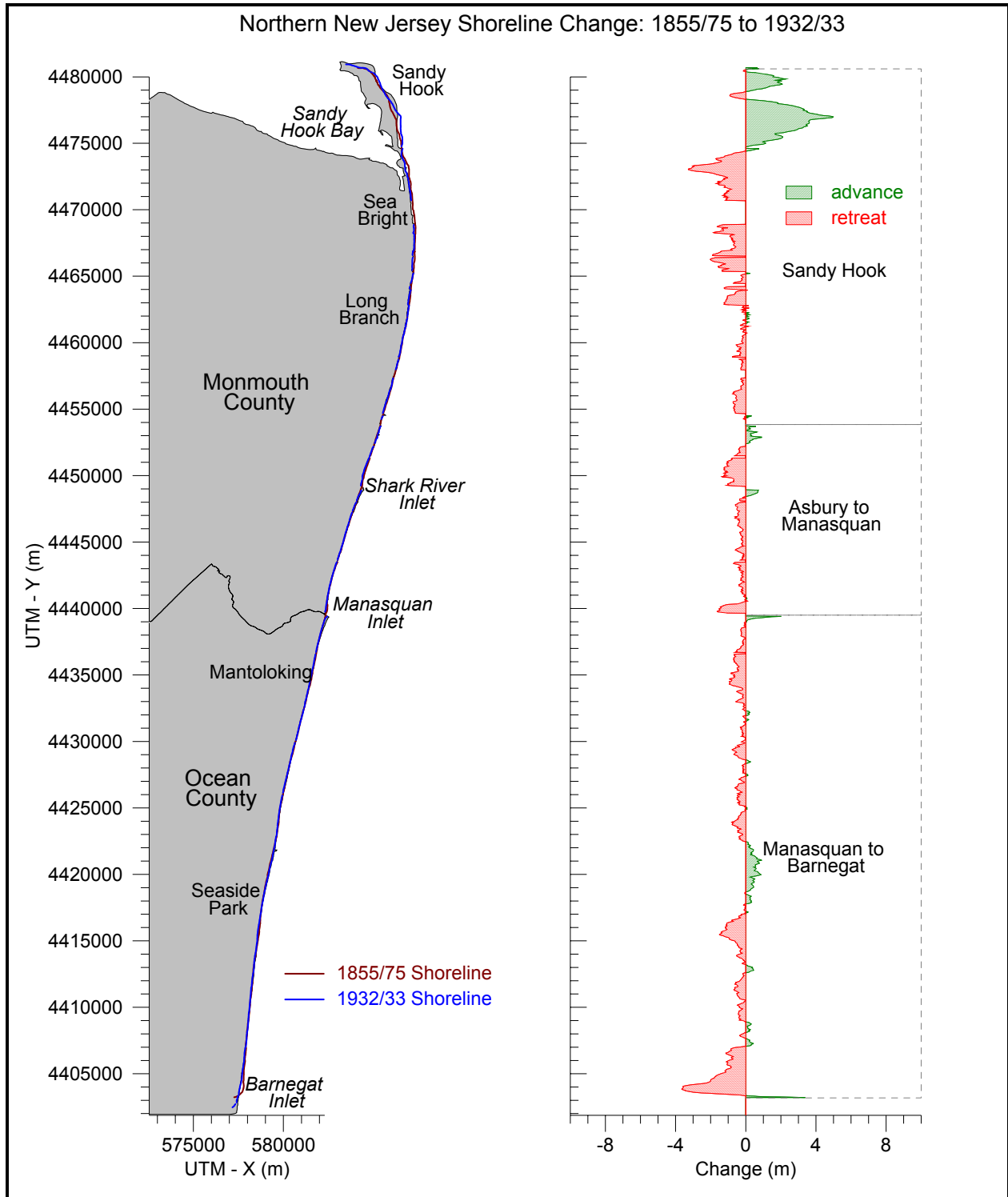


Figure 3-15. Shoreline change along northern beaches of New Jersey, 1855/75 to 1932/33.

Overall, shoreline change rates were lower during this time period than the preceding interval. Reasons for reduced rates may include a longer period of time between surveys, which would potentially minimize some of the larger fluctuations in change; improved mapping procedures that would lead to better surveys than that for the 1836/39 data set; and the introduction of various shoreline stabilization features between 1855/75 and 1932/33, which may have reduced the magnitude of loss. Shoreline advance rates also are reduced, with a maximum rate of about 5 m/yr along the middle of Sandy Hook. General patterns of erosion and deposition are similar to those of the 1836/39 to 1855/75 time period, with the highest rates of deposition located along Sandy Hook and adjacent to the north side of Barnegat Inlet (Figure 3-15).

The northern portion of Sandy Hook experienced significant deposition during this period, with growth occurring along-shore and cross-shore. The terminus of Sandy Hook also began to take on a more northwesterly orientation as sediment deposited on the northwest side of the spit. Along the southern 3 km of the spit, shoreline recession dominated with rates up to about 3.3 m/yr. Greatest recession along the spit was located in the area of historical breaching in 1836/39. Although the area was depositional in 1855/75, by 1932/33, significant shoreline recession was dramatic enough to inspire the development of numerous groins within this area. The 1932/33 shoreline contained numerous structures along this southernmost section of the spit, apparently for protection against erosion that could breach the narrowest portion of the feature. From the southern end of the spit to the north side of the Asbury Park - Manasquan Inlet reach, shoreline change remained erosional, with very small zones of deposition scattered throughout.

Shoreline change between Asbury Park and Manasquan Inlet was dominated by recession, similar to that experienced between 1836/39 and 1855/75. Greatest changes were associated with entrances. The highest rates of recession were located north of each entrance, with a maximum rate of 1.35 m/yr north of Shark River Inlet and 1.63 m/yr north of Manasquan Inlet. Both inlets were armored with jetties during this time, with rubble-mound jetties constructed at Manasquan in 1930/31 (replacing the original timber structures built in 1882/83) and jetties constructed at Shark River some time prior to 1932/33. Additionally, south-directed shoreline migration occurred at each of the inlets, with Shark River migrating south about 160 m and Manasquan migrating south about 760 m. For a small distance south of each entrance, shoreline change was depositional, with rates highest adjacent to the structures.

Shoreline change between Manasquan and Barnegat Inlets remained primarily erosional for this period, with lower rates than those observed during the previous interval (Figure 3-15). Maximum shoreline recession was located immediately north of Barnegat Inlet (3.6 m/yr), which continued to migrate to the south during this time at a rate of about 17.2 m/yr (about 1 km). As the sand spit migrated to the south, much of it also translated landward, resulting in increased rates of recession immediately adjacent to the north side of the entrance. Similar to the previous time period, the shoreline advanced along a small section (about 4.7 km) of the reach (Figure 3-15). The deposition zone extended south from the vicinity of Seaside Heights to immediately north of Island Park. Rates of advance were reduced from those observed for the previous time interval, with maximum advance reaching about 0.9 m/yr. Highest deposition rates are located at Barnegat Inlet and associated with south-directed longshore transport.

1932/33 to 1977

Shoreline evolution between 1932/33 and 1977 responded to the introduction of many coastal engineering alterations, including increased development of shoreline structures,

rehabilitation of existing structures, and the commencement of beach nourishment activities. Change patterns along the northern New Jersey coastline for this 44-year period showed significantly more deposition than that observed for the two previous time periods (Figure 3-16). Numerous structures were placed along the shoreline, with jetties constructed on the north and south sides of Barnegat Inlet in 1940, and several groins and seawalls placed along various sections of coast. This interval also marks the first occurrence of beach fill activities, with about 8.0 mcm placed on northern New Jersey beaches. About 62% of this total was placed on beaches in the Sandy Hook reach, which received about 4.98 mcm of sand between 1943 and 1977. The remaining 38% is relatively evenly split between the two southern reaches, with about 1.36 mcm (about 18%) placed along beaches between Asbury Park and Manasquan Inlet and about 1.65 mcm (about 20%) placed between Manasquan Inlet and Barnegat Inlet. While these totals are significantly smaller than those documented for Long Island beaches, documentation is lacking for some beach fill events that occurred during this time. Eight significant storms impacted the beaches during this period, with two of the more significant events including the Ash Wednesday storm of 1962 and Hurricane Belle in 1976. The Ash Wednesday storm caused over \$56 million in damages (USACE, 2003), and Hurricane Belle was especially damaging to the northern New Jersey coastline because the storm track made direct landfall on Long Island. Overall, the most significant changes observed during this time were located on Sandy Hook where erosion rates along the southern end of the spit more than doubled those found along the remainder of the shoreline (Figure 3-16).

Shoreline change patterns within Sandy Hook reach were similar to those observed for the previous two time periods. The northern portion of the spit continued to grow in a north-northwesterly direction, with rates of deposition along its distal end up to about 6 m/yr (Figure 3-16). South of a small erosional area, the spit continued to advance seaward, depositing sediment along a 2.3 km stretch of shoreline at an average rate of about 3 m/yr. Shoreline recession occurred over a larger portion of the southern half of the spit, with the northern limit of erosion located about 3 km farther north than during the two previous time periods. South of this erosional area, near the present-day location of Highlands, the narrowest portion of the spit experienced deposition, likely as a result of beach fill activity. Most notably among the beach fills in this area were three successive events occurring in 1975, 1976, and 1977, which amounted to about 1.5 mcm of material placed on Sandy Hook prior to the 1977 shoreline survey. Information is lacking regarding the specific locations of these placements, but it is likely that at least a portion of the material would have been placed along the narrowest and historically most erosional areas of the spit, resulting in increased beach widths in this area. South of the deposition zone, the shoreline shows minor variability as it alternates between relatively low rates of erosion and accretion.

Shoreline change between Asbury Park and Manasquan Inlet was quite different than those observed for the prior two time periods. For the previous two time intervals, shoreline change was predominantly erosional; change between 1932/33 and 1977 was almost entirely depositional. Very small zones of shoreline recession existed in the vicinity of Asbury Park and Sea Girt. Aside from these areas, the rest of the shoreline is dominated by deposition, with an average rate of about 0.8 m/yr (Figure 3-16). The most likely cause of this trend reversal is about 1.36 mcm of beach fill. Another possible factor resulting in shoreline advance may be the increased number of structures constructed in this area between 1932/33 and 1977. The 1977 shoreline survey documents the existence of many additional structures than in 1932/33.

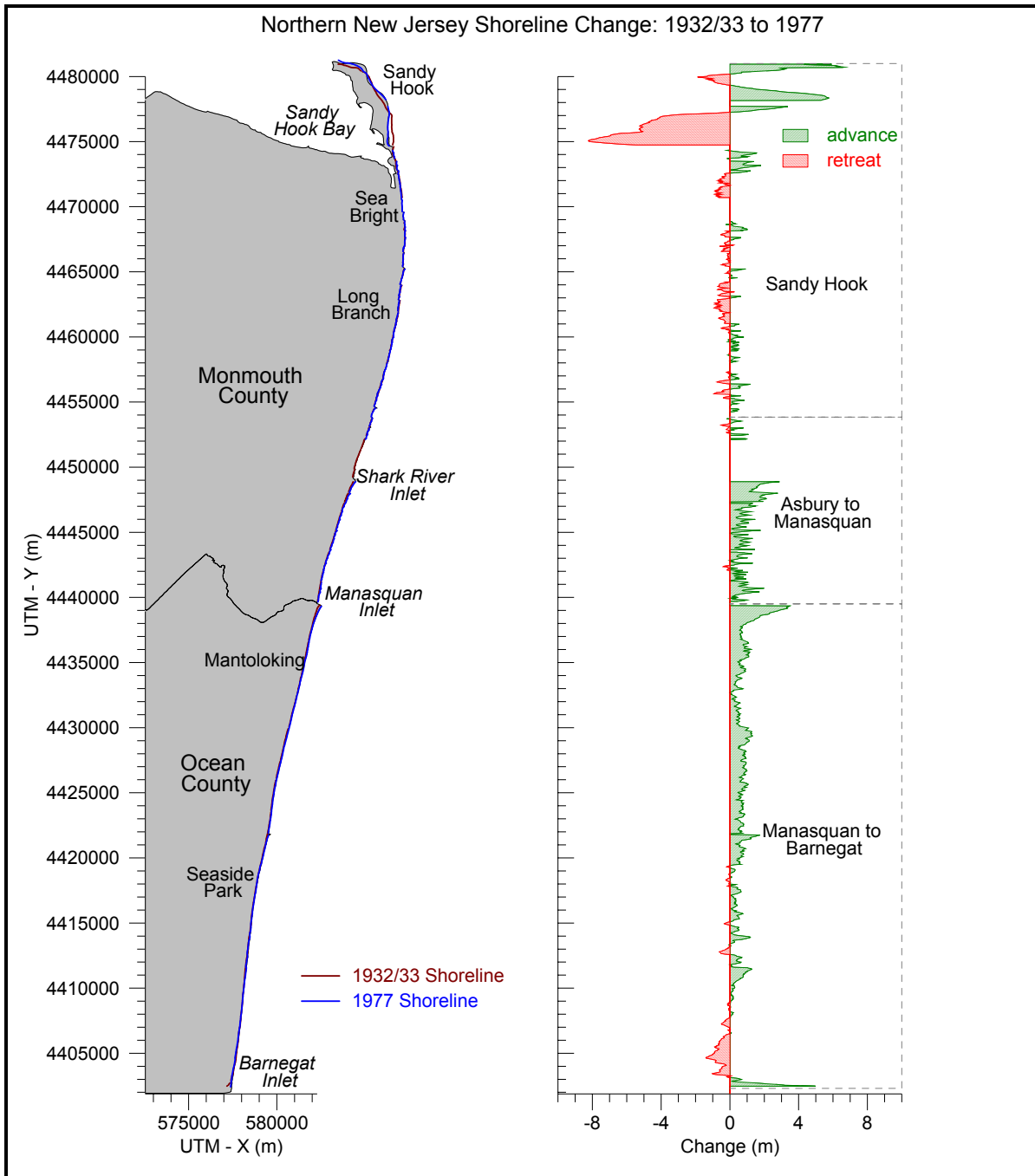


Figure 3-16. Shoreline change along northern beaches of New Jersey, 1932/33 to 1977.

Change results within the Manasquan Inlet – Barnegat Inlet reach also were different than those observed during the two previous two intervals. Shoreline change, particularly adjacent to the south side of Manasquan Inlet, was dominated by deposition for this time period. Apparently, beach nourishment activity has contributed significantly to beach changes. Although net littoral transport south of Manasquan Inlet is documented as southward, it is likely that jetty construction and rehabilitation at Manasquan Inlet contributed to sediment trapping south of the entrance. Beach fill activity in this reach was about 1.66 mcm. There was one nourishment event documented south of Manasquan Inlet in 1963, which contributed about

538,000 m³ to the beach. Immediately north of Barnegat Inlet, deposition is likely the result of shoreline adjustment to the north jetty that was constructed in 1940 impeding south-directed migration of the sand spit. Just north of this accretion zone, a 5-km stretch of shoreline recession was persistent but minor relative to change trends throughout the reach. Overall, this area experienced greatest shoreline advance rates immediately south of Manasquan Inlet and immediately north of Barnegat Inlet, with calculated maximum change of about 3.5 and 5.0 m/yr, respectively.

1836/39 to 1977

Cumulative shoreline change documented long-term trends for northern New Jersey beaches. The 1836/39 shoreline provides a good baseline for evaluating change because it represents a time period before the introduction of major engineering activities (i.e., jetty, groin, and seawall construction; beach nourishment; and channel dredging). Comparing this shoreline with the most recent survey provided a good assessment of net long-term change. Although major engineering and nourishment events have affected overall change results, the longer time interval allows for overall trends to be observed within the context of numerous engineering alterations to the beaches.

In evaluating shoreline change trends between 1836/39 and 1977, a general pattern emerged that highlighted the extent of erosion experienced along beaches in this region (Figure 3-17). The dominance of shoreline recession along a majority of the beaches in northeastern New Jersey is a problem that has been addressed by numerous Federal, State, and local agencies, with several studies recently undertaken to analyze and mitigate these issues. Most notable are the on-going beach nourishment projects by the USACE New York District along the Sandy Hook and Asbury Park-Manasquan Inlet reaches. Overall, cumulative change trends illustrated patterns of advance and retreat that were consistent with those documented between 1836/39 and 1932/33. Shoreline recession was dominant for most of the area, and small zones of deposition were situated in similar locations throughout. Calculated rates of shoreline change were generally lower for this time period than during previous intervals, with a maximum recession rate of 2.5 m/yr and a maximum advance rate of 3.5 m/yr. Both of these maxima are located adjacent to each other along the southern end of Sandy Hook spit. This is particularly significant because Sandy Hook received about 85% of beach nourishment documented for the study area between the 1950s and the 1970s, without which even larger rates of loss may have occurred in the region. Additionally, direct measurements along the north side of the spit indicate a high rate of deposition for this area, with northwest-directed shoreline advance occurring at a rate of about 7.5 m/yr. The area associated with subaerial deposition along the terminal end of Sandy Hook was approximately 1.02 million m². Along the shoreline south of this area, smaller zones of deposition are primarily located along the lateral sides or distal ends of prograding spits or adjacent to the updrift sides of jetty structures.

Cumulative shoreline change within the Asbury Park-Manasquan Inlet reach was the least erosional region within the study area. Immediately south of Shark River Inlet for a distance of about 5 km, beach change was predominantly depositional, with an average of about 0.3 m/yr. Greatest advance rates in this zone (about 1.1 m/yr) were located adjacent to the south side of Shark River Inlet, which is consistent with north-directed longshore transport. South of the inlet, deposition was reduced, and trends reversed in the vicinity of the town of Sea Girt. From Sea Girt south to Manasquan Inlet, shoreline change is dominated by relatively high rates of recession, with rates generally increasing near the entrance. The average recession rate in this area was about 0.8 m/yr, and maximum loss was about 1.9 m/yr. Erosion along this section of shoreline is consistent with patterns observed for this area during incremental time periods.

Between 1836/39 and 1977, the character of Manasquan Inlet changed dramatically, evolving from a small, bifurcated inlet into a larger federally-maintained entrance armored on both sides with rock jetties. Prior to construction of jetties, the entrance migrated south about 900 m. After jetty construction, the adjacent shoreline north of the entrance receded. The existence of the inlet and associated structures at Manasquan may have contributed to erosion documented along the shoreline north of this area.

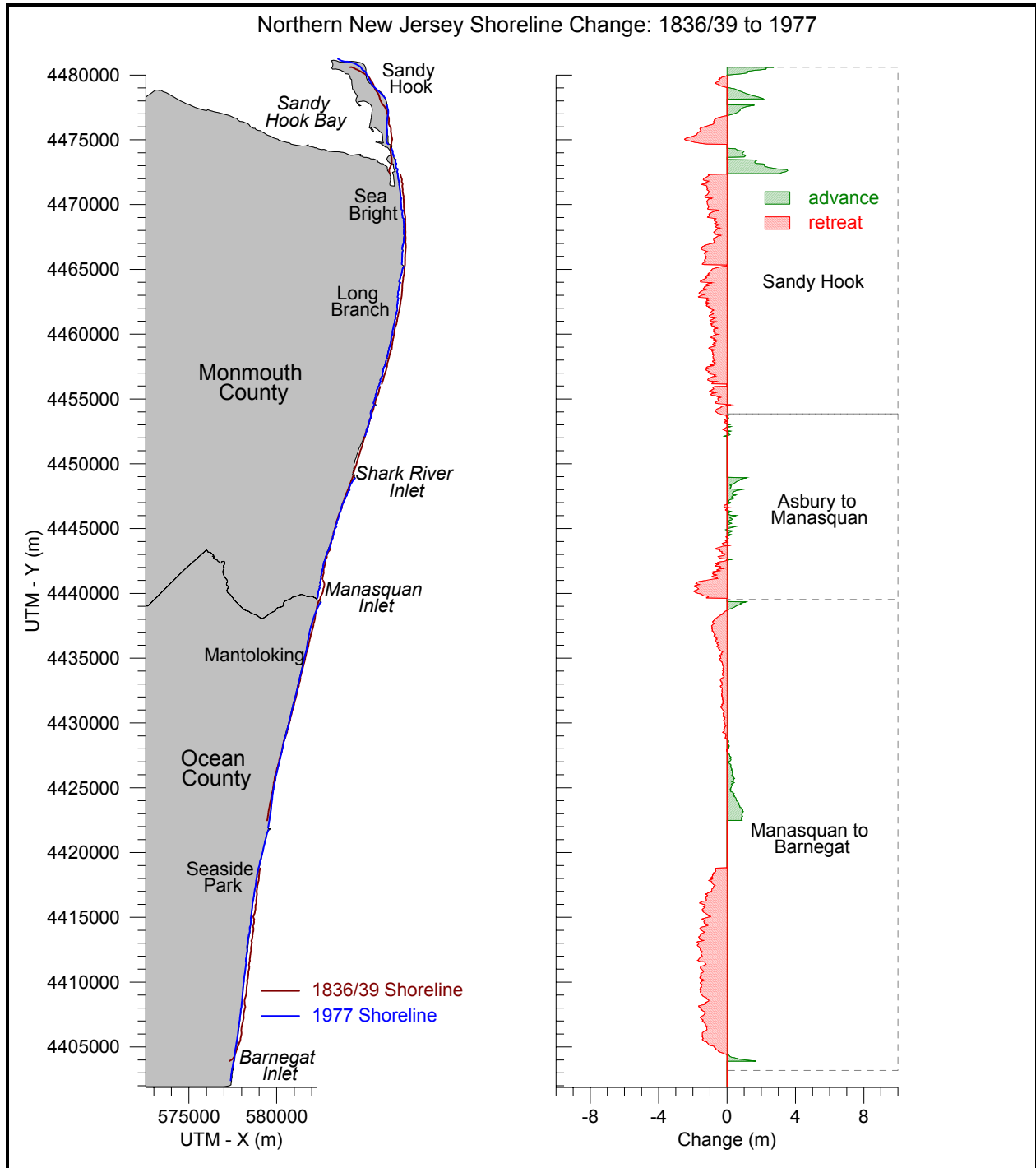


Figure 3-17. Shoreline change along northern New Jersey beaches, 1836/39 to 1977.

The Manasquan Inlet-Barnegat Inlet reach also was dominated by erosion for this time interval. Three small zones of shoreline advance are illustrated on Figure 3-17, two of which are associated with changes at entrances. The small zone of deposition immediately south of Manasquan Inlet is common for all time intervals. Shoreline advance rates south of the entrance averaged about 0.5 m/yr, with a maximum rate of about 1.1 m/yr immediately adjacent to the entrance. The deposition zone extends about 750 m south of the entrance, with rates generally decreasing to the south. South of Manasquan Inlet for a distance of about 10 km, the shoreline experienced continuous erosion. Recession rates were generally low, with a maximum overall rate of about 0.9 m/yr. South of this area, between the towns of Chadwick and Seaside Heights, shoreline change has been depositional for most time intervals. Although cumulative rates of advance do not exceed 1 m/yr for the entire zone, this region has been characterized by deposition for all incremental time intervals except 1855/75 to 1932/33. South of this region for about the next 14 km, shoreline change is again dominated by beach erosion until Barnegat Inlet, where the southern margin of the shoreline was advancing to the south in response to south-directed littoral transport. At the north side of Barnegat Inlet, the maximum rate of shoreline advance was 1.5 m/yr, although southward-directed spit growth for this interval was on the order of 13 m/yr.

3.2 NEARSHORE BATHYMETRY CHANGE

3.2.1 Bathymetry Data Base and Potential Errors

Seafloor elevation measurements collected during historical hydrographic surveys are used to identify changes in nearshore bathymetry for quantifying sediment transport trends relative to natural processes and engineering activities. For the present study, digital bathymetric data were available from surveys completed by the USC&GS between 1927 and 1997. Within this time period, three major intervals (1927-1937, 1942-1951, and 1975-1997) were isolated to document shelf morphology and characterize temporal bathymetric change. Change was evaluated qualitatively for the entire study area and quantitatively at each resource site between the specified intervals. Due to survey coverage, comprehensive bathymetric surfaces were generated for the periods 1927/37 and 1927/97. Individual hydrographic surveys used for each time period are summarized in Table 3-8.

Data coverage and survey line spacing for the 1927/37 data set was very well represented for surface characterization and temporal change analysis. Cross-line spacing was generally better than 500 m, and points along survey lines were typically collected every 100 to 200 m. Additionally, nearshore data collection generally extended to about 3 m water depth, providing reasonable data coverage on the shoreface. As such, the 1927/37 surface provided a good basis for characterizing shelf features and comparing against the modern time period. Recent bathymetric surveys (1975 to 1997) contained high quality data for surface characterization as well. Cross-line spacing was generally closer than 250 m for all surveys, with the most recent surveys containing data collected at intervals of about 100 m. Although data available were considered very good quality, the area of coverage left gaps across portions of the shelf. As such, the recent bathymetric surface contains data from 1975 to 1997 for most of the study area, but areas lacking coverage were populated with data from the 1927/37 era. Duplicate surveys can be identified in Table 3-8 and corresponding areas of overlap are displayed in Figure 3-18. All data sets were developed from digital USC&GS hydrographic surveys compiled by the National Geophysical Data Center (NGDC) and were registered to a common horizontal coordinate system and datum, in this case UTM Zone 18 North, NAD83.

Date	Data Source	Comments and Map Numbers
1927/37	USC&GS Hydrographic Sheets	1927 - H-04797 (1) 1932 - H-05234 (1) 1933 - H-05300 (1), H-05367 (2), H-05369 (2), H-05370 (1), H-05371 (2), H-05377 (1) 1934 - H-05615 (1), H-05732 (1), H-05734 (1), H-05735 (2), H-05616 (1), H-05638 (1), H-05639 (2) 1936 - H-06188 (3), H-06189 (3), H-06190 (3), H-06136 (2), H-06026 (3) 1937 - H-06223 (3)
1927/97	USC&GS Hydrographic Sheets	1927 - H-04797 (1) 1933 - H-05300 (1), H-05367 (2), H-05369 (2), H-05370 (1), H-05371 (2), H-05377 (1) 1934 - H-05615 (1), H-05732 (1), H-05735 (2), H-05616 (1), H-05638 (1) 1936 - H-06188 (3), H-06189 (3), H-06190 (3), H-06136 (2) 1950 - H-07870 (2) 1951 - H-07947 (2) 1975 - H-09546 (3), H-09531 (3), H-09532 (4), H-09550 (3), H-09567 (3), H-09568 (2), H-09577 (3) 1979 - H-09820 (1) 1982 - H-10035 (1), H-10031 (1) 1986 - H-10224 (2) 1988 - H-10284 (1), H-10287 (1), H-10290 (1), H-10291 (1), FE0312 (2), H-10286 (1) 1996 - H-10683 (1), H-10668 (1), H-10675 (1), H-10686 (1) 1997 - H-10750 (1)
(1) = 1:10,000, (2) = 1:20,000, (3) = 1:40,000, (4) = 1:80,000		

Because seafloor elevations were temporally and spatially inconsistent for the entire data set, adjustments to depth measurements were made to bring all data to a common plane of reference. These corrections include changes in relative sea level and differences in reference vertical datums. Vertical adjustments were made to each data set based on the time of data collection and the original vertical reference datum. All vertical adjustments for this study were made based on vertical reference information reported at Sandy Hook, NJ tidal benchmark number 8531680 (Figure 3-19). Tidal benchmark data were obtained from the NOS Center for Operational Oceanographic Products and Services (CO-OPS) website <http://www.co-ops.nos.noaa.gov/> in addition to historical information published by NOAA for the years 1932 to 1986 (Lyles et. al., 1988). Yearly mean sea level variations were plotted between 1932 and 2002 to obtain an average rate of sea level change (m/yr) for the study area (Figure 3-20). Depths for all surveys were adjusted to NAVD and were projected to average sea level for 2000 (most recent survey date). The unit of measure for all surfaces is meters, and final values were rounded to decimeters before cut and fill computations were completed.

In order to produce continuous data sets extending seaward from the high water line, all bathymetry data were combined with temporally consistent shoreline data. A value of 2.6 m (NAVD) was assigned to the shoreline elevation, which was based on recent beach profile data obtained from the NJBPN website <http://gannet.stockton.edu/njbpn/index.asp> and the USACE New York District Coastalview application CD. Six monuments were selected from the NJBPN database to estimate the elevation of the berm crest from Sandy Hook Bay to Barnegat Inlet. Four monuments were selected from the Coastalview database to evaluate the New York coastline between Rockaway Point and Moriches Inlet (Figure 3-21). Profiles were selected to

provide a good representation of average elevation of the berm crest across the entire region. A plot illustrating beach profile examples for New York portrays the typical beach shape observed in this region with an identifiable berm crest at elevations ranging from 2.6 to 3.2 m NAVD (Figure 3-21).

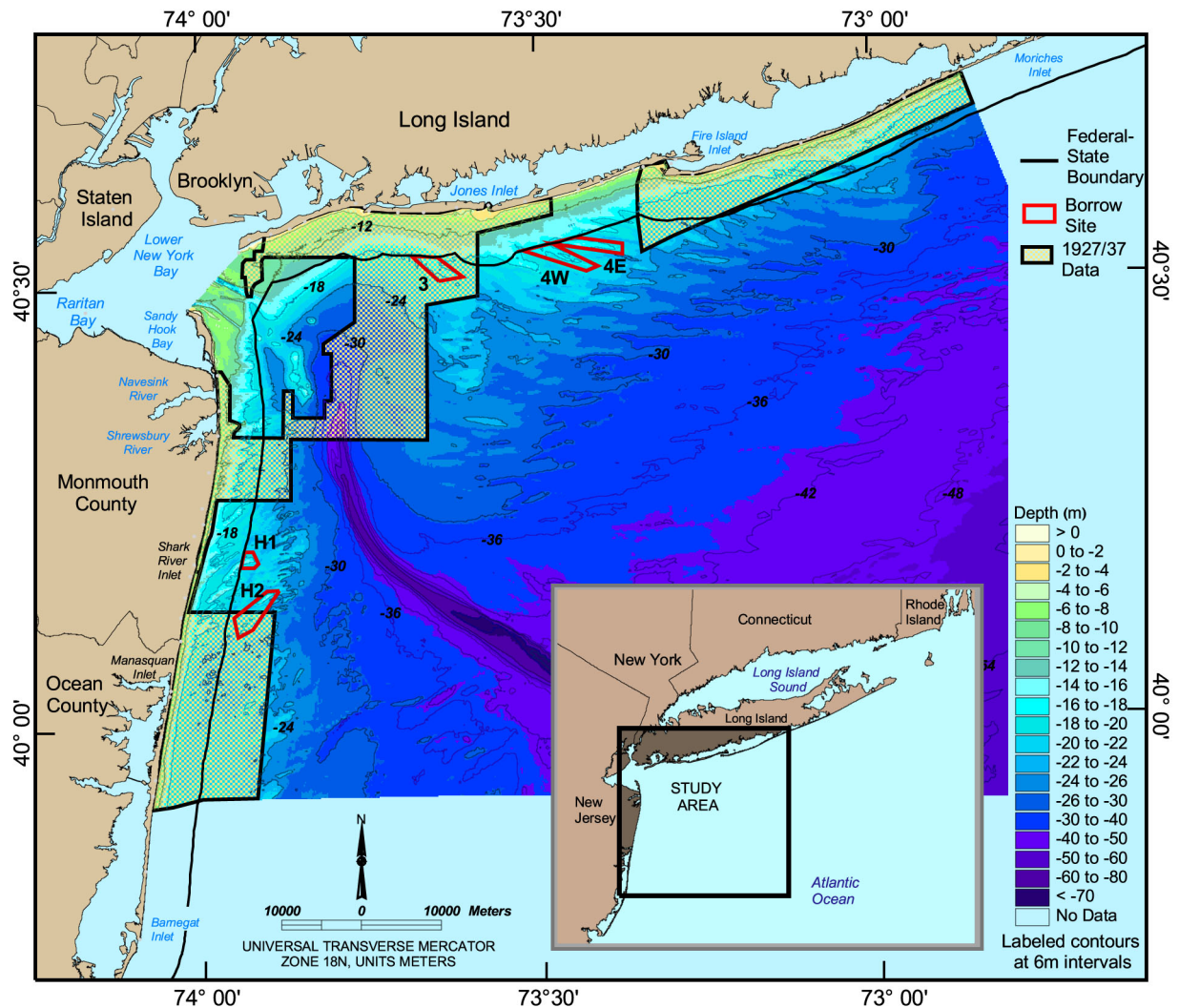


Figure 3-18. Locations of 1927/37 bathymetric data used to fill gaps in the most recent surface.

As with shoreline data, measurements of seafloor elevation contain inherent errors associated with data acquisition and compilation. It is important to quantify limitations in survey measurements and document potential systematic errors that can be eliminated during quality control procedures. However, most measurement errors associated with present and past surveys are considered random over large areas. As such, random errors cancel relative to change calculations derived from two surfaces. A better means of gauging limits of reliability associated with erosion and accretion areas is to quantify uncertainty associated with interpolating across bathymetric surfaces. Interpolation between measured points always includes a degree of uncertainty associated with terrain irregularity and data density. The density of bathymetry data, survey line orientation, and the magnitude and frequency of terrain irregularities are the most important factors influencing uncertainties in volume change calculations between two

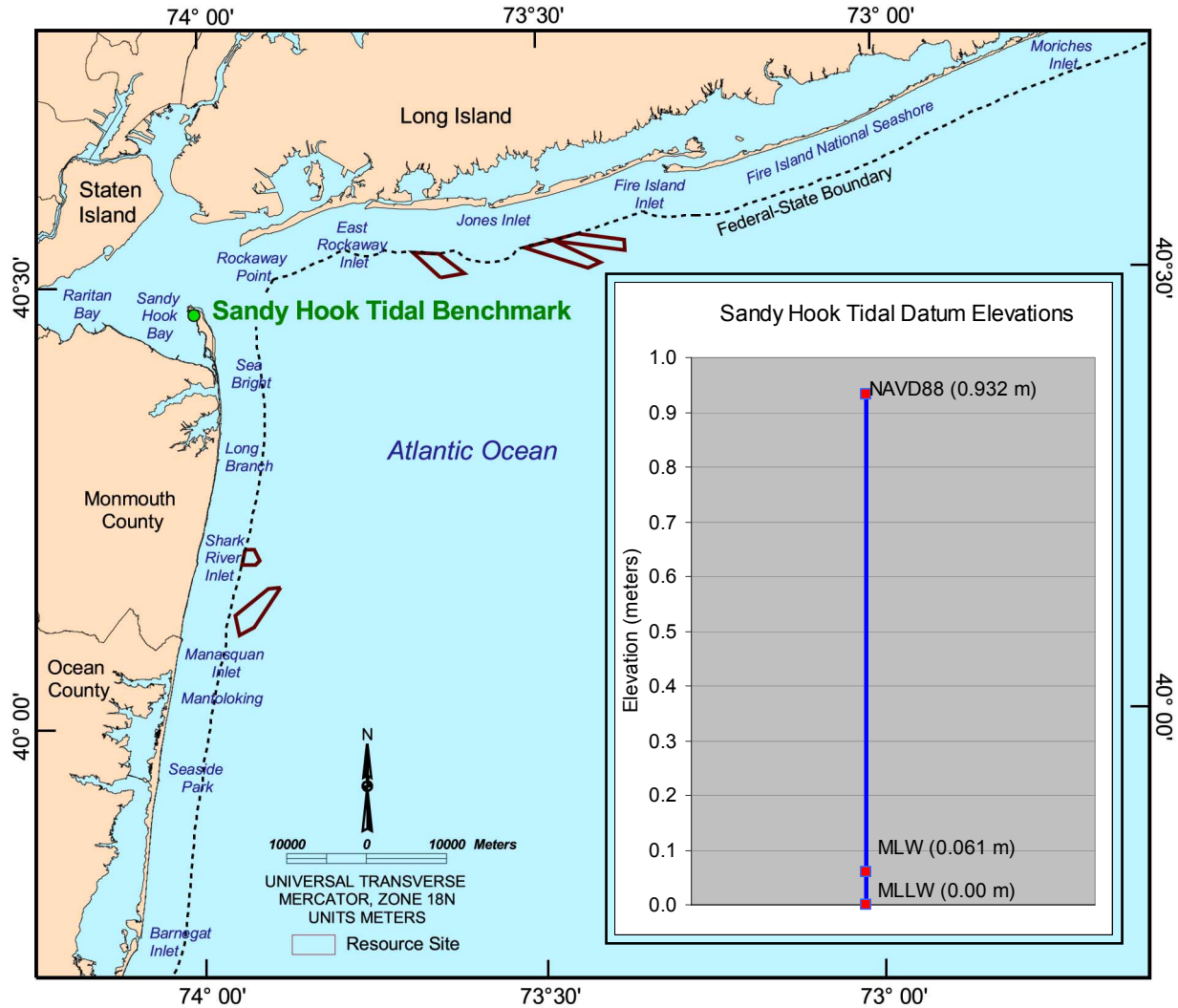


Figure 3-19. Sandy Hook, NJ tidal benchmark elevation information.

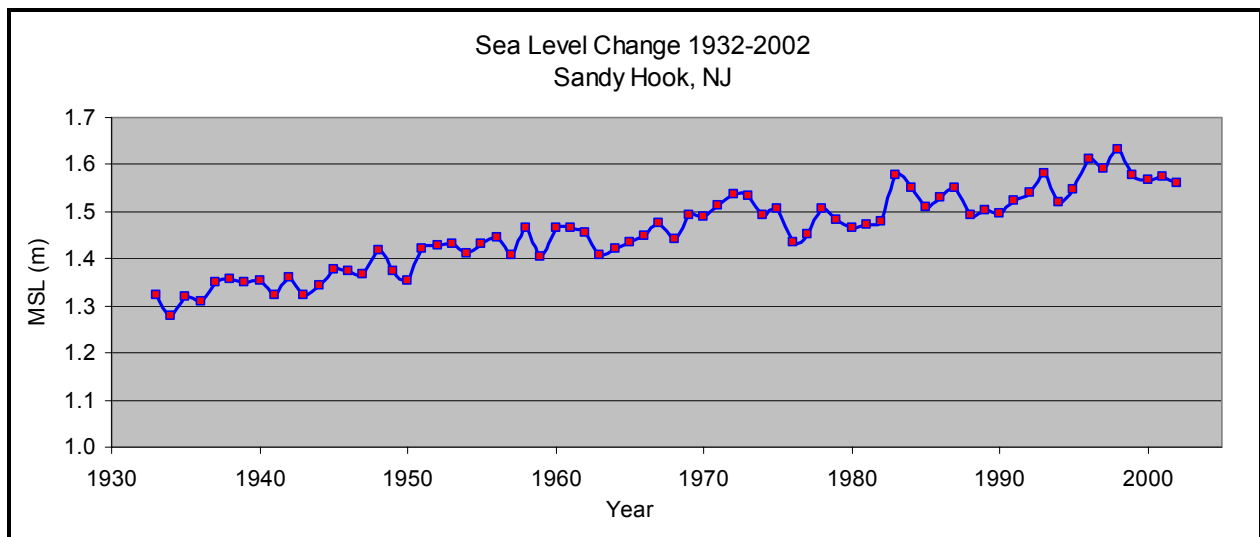


Figure 3-20. Sandy Hook, NJ sea level change, 1932 to 2002.

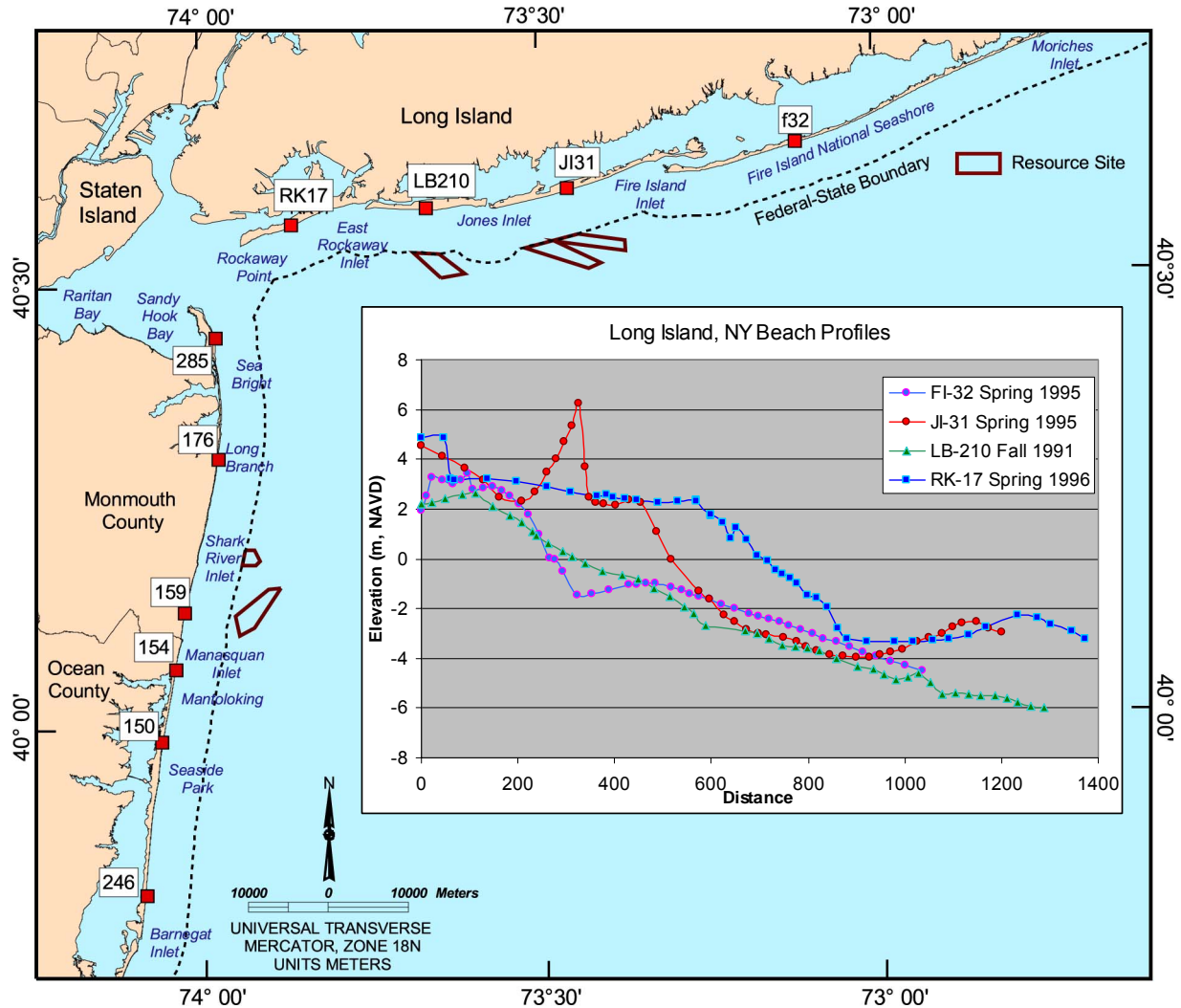


Figure 3-21. Beach profile location for coastal New York and New Jersey.

bathymetric surfaces. Volume uncertainty relative to terrain irregularities and data density can be determined by comparing surface characteristics at adjacent survey lines. Large variations in depth between survey lines (i.e., few data points describing variable bathymetry) will result in large uncertainty calculations between lines. This computation provides the best estimate of uncertainty for gauging the significance of volume change estimates between two surfaces.

Uncertainty estimates were calculated for the 1927/37, and 1927/97 bathymetric surfaces using the methods outlined in Byrnes et al. (2002). Multiple sets of line pairs were compared for each time period to represent terrain variability across the surveyed area. Line pairs were chosen that would accurately reflect track line spacing for each survey and the irregularity of prominent geomorphic features in the region. A total of six line pairs were used to estimate uncertainty for each surface. Uncertainty estimates were determined for major sea floor features in this region, including the shoreface, across the Hudson Shelf Valley, and along nearshore ridges and depressions that dominate the sea floor of the inner shelf. An example of line pairs used for the 1927/37 surface is displayed in Figure 3-22. Line pairs were adjusted for each time period to overlay survey lines for that year. Bathymetry data were extracted along

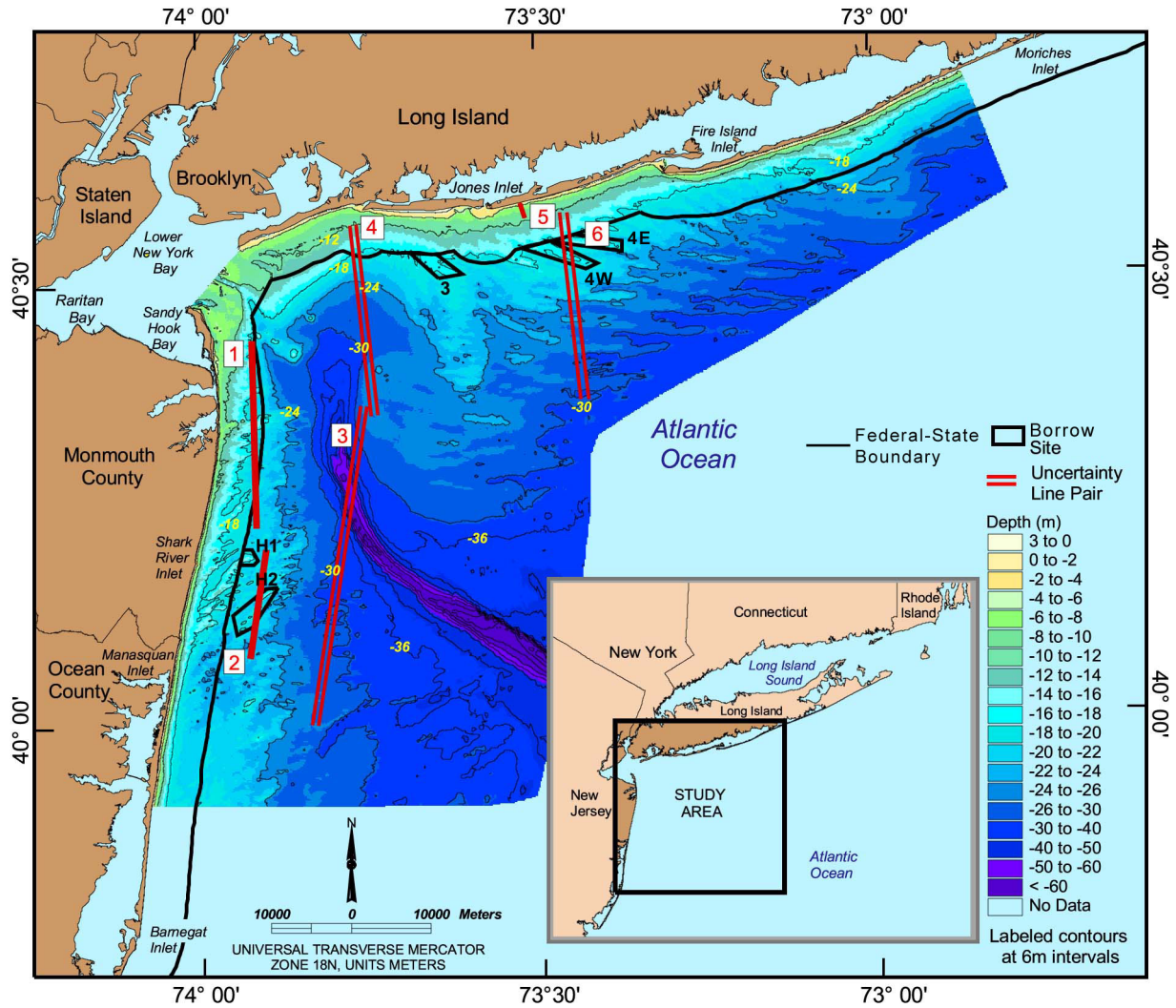


Figure 3-22. Line pairs used to estimate potential uncertainty for the 1927/37 surface.

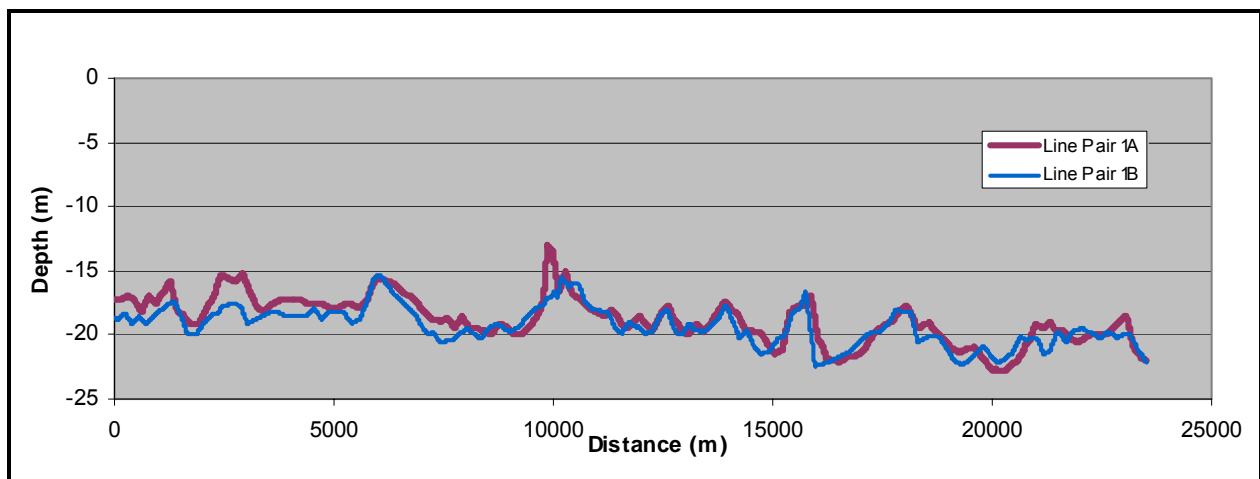


Figure 3-23. Depths extracted along Line Pair 1 for determining potential surface uncertainty.

each line to calculate the variation in elevation between line pairs (Figure 3-23). Depths were extracted at five meter intervals along each line and the absolute values of the differences were averaged to calculate the potential uncertainty for each pair. Line pair uncertainty values were then averaged for each surface to estimate potential uncertainty associated with each data set.

Potential uncertainty for the 1927/37 surface was larger than that for the 1927/97 data set (± 0.8 to 0.2 m, respectively). This was expected due to better survey coverage and track-line orientation for more recent data sets. Combining this information to gauge the impact of potential uncertainties associated with volume change calculations derived from these surfaces resulted in a root-mean-square variation of ± 0.8 m. For all bathymetric change calculations for this study, a range of -0.8 to 0.8 m was used to delineate areas of no determinable change.

3.2.2 Digital Surface Models

Historical bathymetry data within the study area provided geomorphic information on characteristic surface features that form in response to dominant coastal processes (waves and currents) and relative sea level change. Comparing two or more surfaces documents net sediment transport patterns relative to incident processes and sediment supply. The purpose of conducting this analysis throughout the study area was to document net sediment transport trends on the shelf and to quantify the magnitude of change to calibrate the significance of short-term wave and sediment transport numerical modeling results. Net sediment transport rates on the shelf were determined using historical bathymetry data sets to address potential infilling rates for sand resource sites.

3.2.2.1 1927/37 Bathymetric Surface

Bathymetry data for the period 1927/37 were combined with the 1932/33 and 1933/34 shoreline data sets to create a continuous surface from the shoreline seaward to about the -30 to -40 m (NAVD) contour. Data for the 1927/37 surface extend east from Rockaway Point to about 10 km west of Moriches Inlet and south from Sandy Hook to about Seaside Park. The most prominent sea floor feature visible in the 1927/37 bathymetric surface is the submarine Hudson River Channel, which extends southeast across the continental shelf from its head in the Christiansen Basin toward the shelf break, bisecting the New York Bight (Figures 3-24 and 3-25). On either side of the valley, the shelf surface is dominated by numerous isolated and shore-attached linear sand shoals and ridges that illustrate opposing orientations along their crests. South of Long Island, contours outlining linear shoals document a northwest-southeast orientation, whereas contours along shoal features west of the Hudson Channel document a northeast-southwest orientation. Changes in this general character of the linear shoal network are attributed to localized outcrops of Cretaceous strata and smaller topographic highs associated with anthropogenic dumping, which has been occurring in the region since the early 1800s (Williams and Duane, 1974; Butman et al., 1998; Schwab et al., 2000b). Morphologic characteristics of the 1927/37 shelf surface south of Long Island are discussed first, followed by an examination of morphologic features on the shelf east of New Jersey. In general, the discussion of sea floor features follows from west to east along the shelf south of Long Island, and from north to south along the shelf east of New Jersey.

The western section of the shelf south of Long Island adjacent to Rockaway Beach exhibits moderately smooth contour spacing from the shoreface seaward to the head of the Hudson Channel. Linear sand shoals dominating the shelf east and south of this area are noticeably absent in this region. Minor surface irregularities are primarily the result of anthropogenic disposal activities, which are visible as cone-shaped mounds seaward of the -24 m contour. Bathymetry contours east of this area document northwest-southeast alternating

sand ridges characteristic of the shelf in this area. Sand ridges offshore Long Beach illustrate a more dominant north-south orientation than those on the remaining portion of the shelf south of Long Island, varying from shore-perpendicular to slightly shore-oblique. Sand ridges in this region have been interpreted by Schwab et al. (2000b) as rippled scour depressions. These lineations are located to the north and west of Borrow Site 3, which is positioned along a northwest-southeast trending shoal delineated by the -18 m contour. South of Borrow Site 3, a north-south trending topographic high known as Cholera Banks is documented on the 1927/37 surface within the -24 m contour. This feature has been characterized by numerous studies as an eastward extension of one or more Coastal Plain strata (Williams and Duane, 1974; Schwab et al., 2002).

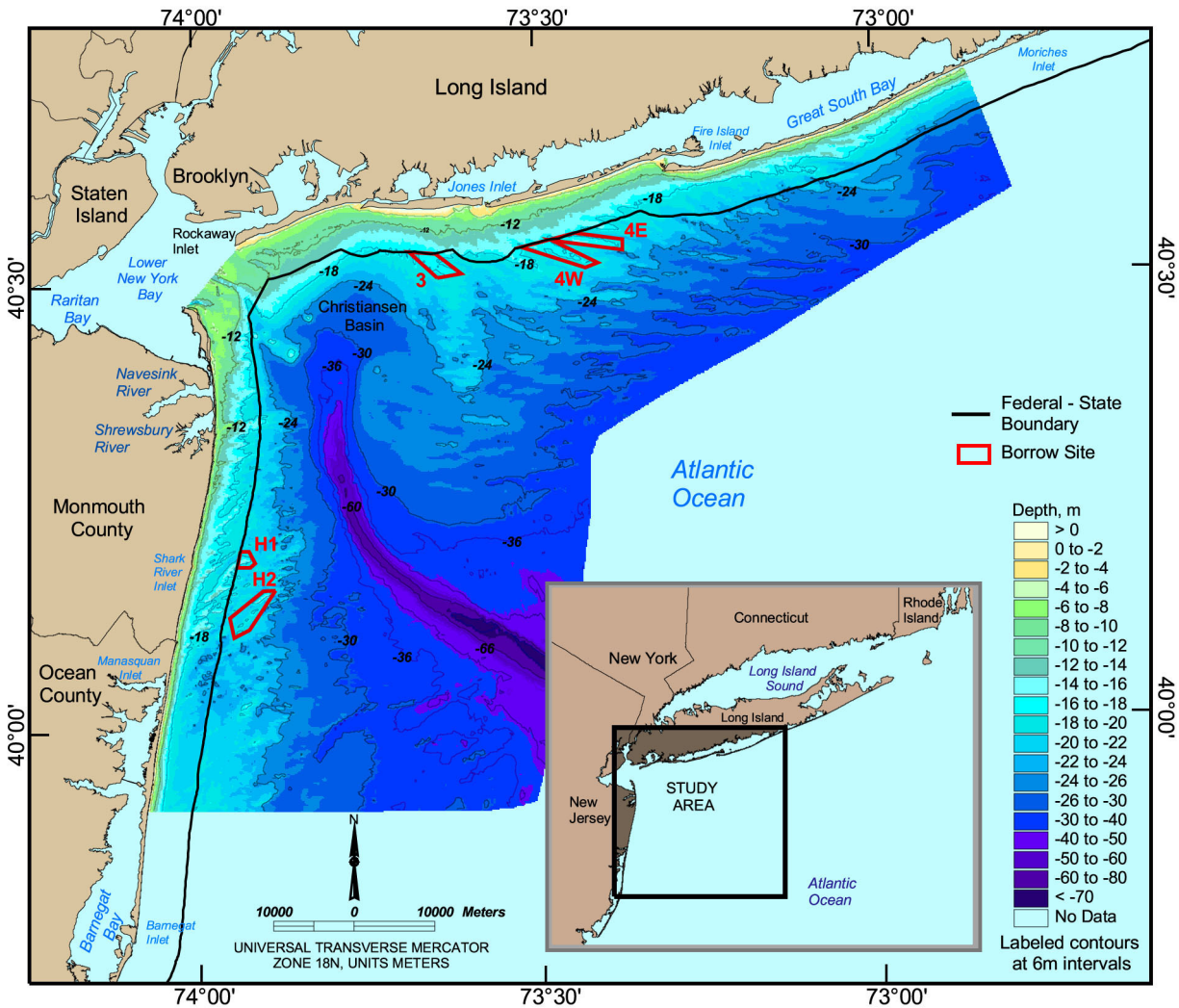


Figure 3-24. 1927/37 bathymetric surface within the New York Bight.

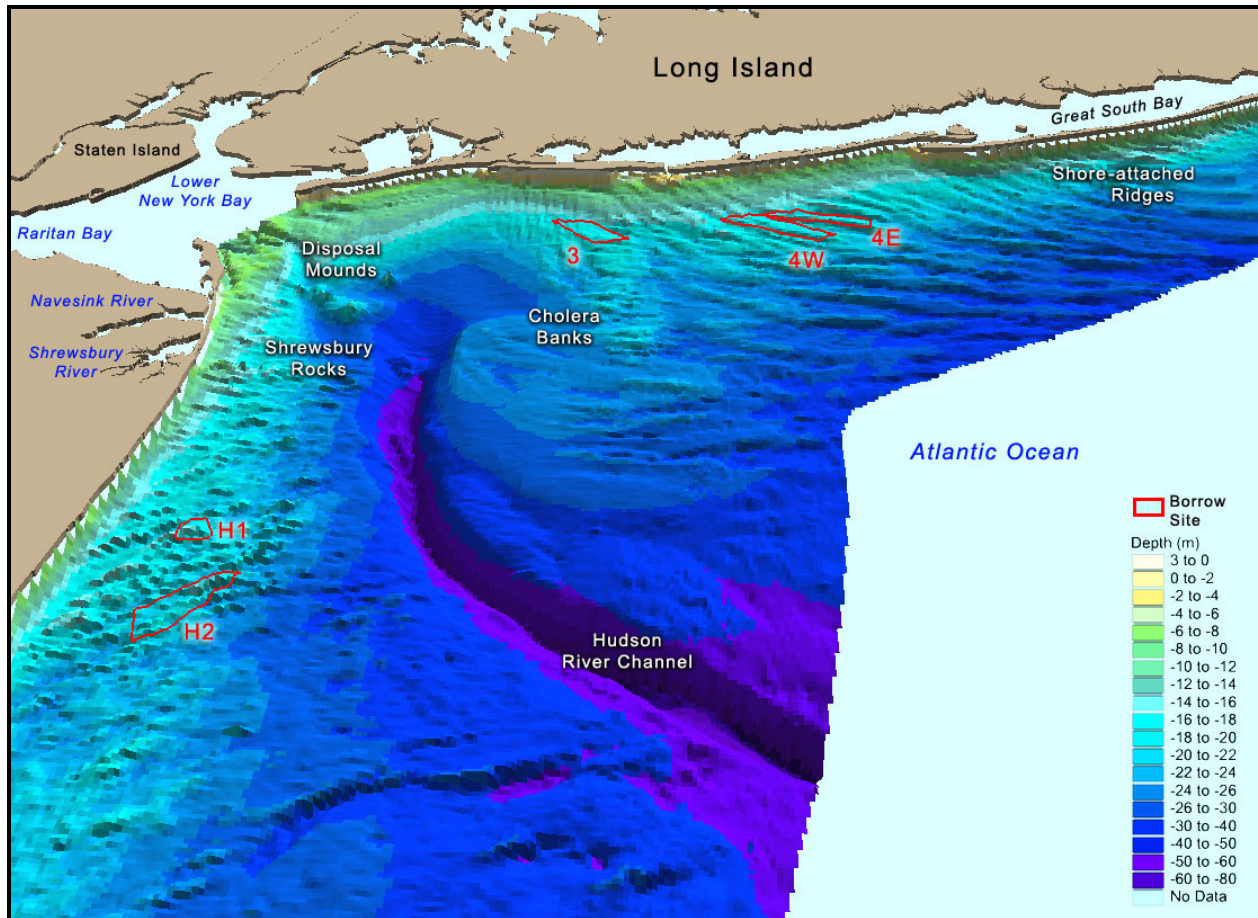


Figure 3-25. Three-dimensional view of the 1927/37 bathymetric surface in the New York Bight region.

East of Borrow Site 3, seafloor morphology is dominated by isolated and shore-attached sand ridges. Ridge features are visible offshore Jones Beach along the -18 m contour and are more oblique to the shoreline than those found off Long Beach. Borrow Sites 4W and 4E are located along two shoreface-attached shoals, located immediately seaward of the Federal-State boundary. Isolated sand ridges in this area formed as shoreface-attached sand ridges that were subsequently stranded during Holocene transgression (Schwab et al., 2000b). Southward asymmetry exhibited by these shoals is attributed to the action of coast-parallel, southeasterly, storm-generated currents (Duane et al., 1972). Shoreface-attached shoals are found to the east of this area offshore Fire Island. Schwab et al. (1999) attribute the formation of these shoals to erosion during the early Holocene of a broad outcrop of Cretaceous coastal plain strata offshore Watch Hill. According to Schwab et al (1999), sediment furnished downdrift during marine transgression was reworked by oceanographic processes into a series of shoreface-attached linear sand ridges.

The continental shelf east of New Jersey is similarly dominated by linear sand shoals. The bathymetry defining the offshore area has been divided into northern and southern components by Williams and Duane (1974), separated by an outcrop of Coastal Plain strata known as Shrewsbury Rocks. The sea floor adjacent to Sandy Hook is generally irregular and varied, unlike the more uniform northeast-southwest trending ridge and swale topography found to the south. Shrewsbury Rocks is visible in the 1927/37 surface along the -18- and -24-m contours extending offshore northeastern New Jersey adjacent to the Shrewsbury River. North

of Shrewsbury Rocks, the shoreface is relatively wide and gentle. South of Shrewsbury Rocks, the shoreface is noticeably steeper, much more so than that observed to the north and along the shelf south of Long Island.

South of Shrewsbury Rocks, isolated linear shoals dominate the nearshore between Long Branch and Manasquan Inlet, particularly along the shelf landward of the -24 m contour. Linear shoal characteristics illustrated on the 1927/37 surface are consistent with those documented by Duane et al. (1972). According to Duane et al. (1972), linear shoals in this area are separated from the coast by about 4 km, vary in length from 1 to 3 nm, and have a mean width of about 450 m. All shoals have their long axis oriented east northeast and have an average angle of about 30° to 85° with the shoreline. Borrow Sites H1 and H2 are located along two of these shoals seaward of Shark River Inlet, in depths ranging from about 18 to 20 m (NAVD). South of Manasquan, the density of shoals decreases in the nearshore zone and the shelf becomes gentler as it slopes toward the Hudson Valley.

3.2.2.2 1927/97 Bathymetric Surface

Bathymetry data for the period 1927/97 were combined with temporally consistent shoreline data and 1997 beach profile data to create a continuous surface from the shoreline seaward to about 55 m water depth (NAVD) (Figures 3-26 and 3-27). Data from the 1927/37 surface were used to fill gaps in the most recent data set. General characteristics of the 1927/97 bathymetric surface are similar to those of 1927/37 with a couple of exceptions. First, there was a large increase in size of the anthropogenic disposal mound located to the west of the Hudson River Channel. This is especially evident in the 1927/97 surface at the -24 m contour interval, which extends about 4 km further to the southwest than that of the 1927/37 surface near the Historic Area Remediation Site and the Dredged Material Disposal Site (see Chapter 2). Second, geomorphic features are better defined on the 1927/97 surface because the number of data points describing the surface is larger. The shape and position of shoals is very consistent for both surfaces, but additional detail associated with the shoals and linear sand ridges on the shoreface provides a better understanding of the geomorphic characteristics of potential sand borrow sites.

Characteristics of surface and sub-surface sediments at shoals south of Long Island were examined as part of the 1976 ICONS investigation which rated their suitability for beach nourishment and developed estimates of minimum sand thicknesses. Borrow Sites 3, 4W, and 4E are adjacent to areas that were identified as having a minimum thickness potential of about 3 to 5 m (see Chapter 2). Additionally, study of surface and subsurface shoal sediments from cores taken on the northern New Jersey shelf indicates that shoals are composed of medium-grained, polished, well-sorted quartzose sand (Duane et al., 1972). Borrow Sites H1 and H2 are located on two of the prominent shoals found in this region.

3.2.3 Shelf Sediment Transport Dynamics

Although the general characteristics of the 1927/37 and 1927/97 bathymetric surfaces appear similar, a digital comparison yields a difference plot that isolates areas of erosion and accretion for documenting sediment transport patterns and quantifying trends. The most significant changes occurring during this 60-yr interval were associated with deposition at anthropogenic disposal mounds, erosion and deposition along the margins of the Hudson River Valley, and deposition along the seaward extension of prograding spits (Figure 3-28). Bathymetric change along the shoreface and within the nearshore zone was not calculated for most of the region due to a lack of data for the most recent time interval. As such, bathymetry change in the nearshore was evaluated only along Sandy Hook spit and adjacent to the eastern

two-thirds of Jones Island. Based on the consistency observed in overall shoreline change patterns throughout the study area, it was inferred that bathymetric change trends calculated for these areas also would retain a consistent pattern. Overall, erosion and accretion patterns tend to reflect net littoral transport trends and follow shoal and ridge contour shapes. Often, updrift zones of erosion are associated with downdrift linear deposits, illustrating the magnitude and direction of sediment transport associated with shoals on the shelf surface. Polygons of erosion and accretion indicated shoal migration in response to dominant transport processes.

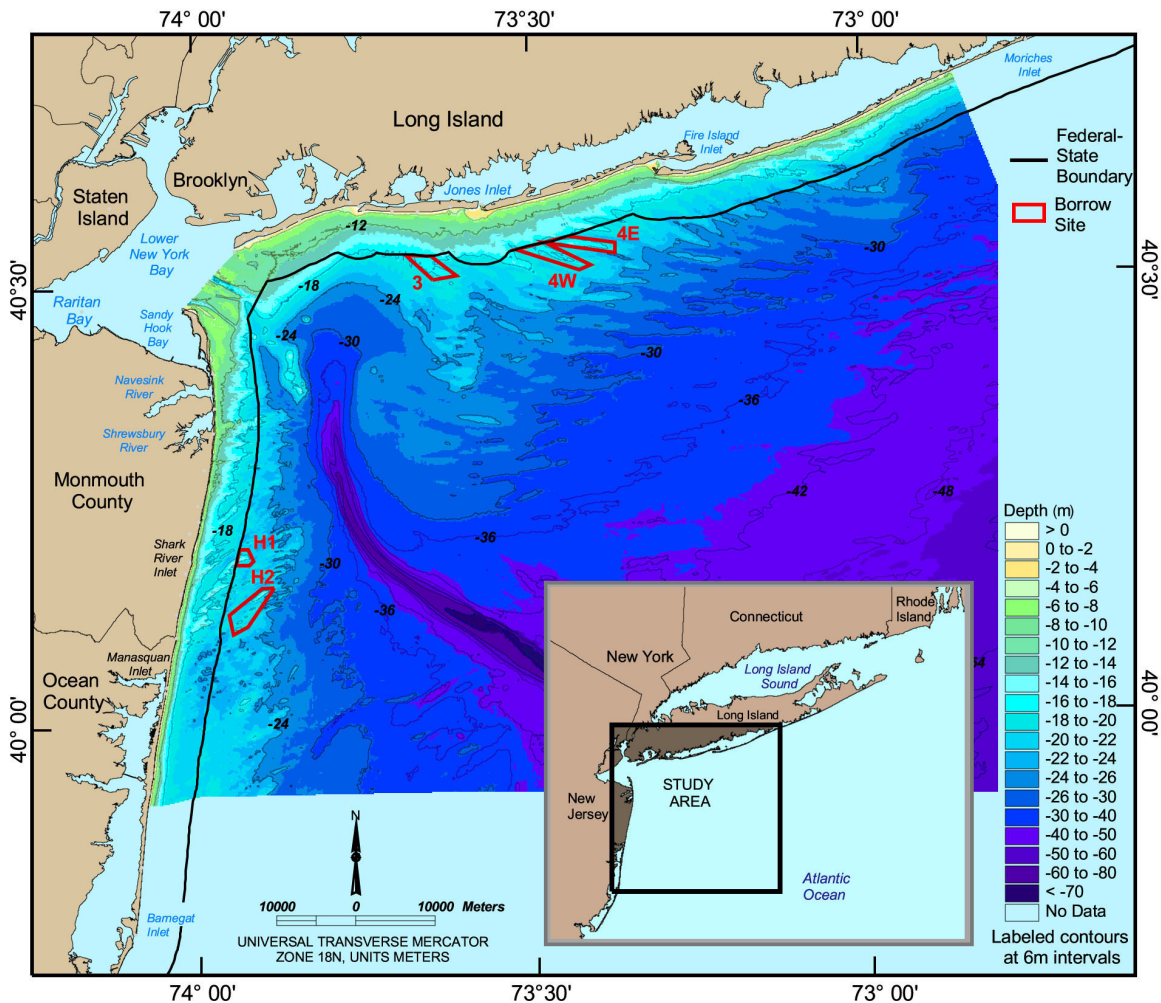


Figure 3-26. 1927/97 bathymetric surface.

Fluid flow and sediment transport adjacent to shorelines in southwestern Long Island and northeastern New Jersey produce pronounced geomorphic changes. Littoral currents mobilize substantial quantities of sediment near the coastline and on the upper shoreface, resulting in spit growth along the downdrift margins of islands and shoal migration at and adjacent to entrances. This is particularly evident at Sandy Hook spit, which illustrated substantial deposition along its northern edge for the period of record. Spit growth represented a terminal point for alternating zones of erosion and accretion adjacent to the shoreline, reflecting sediment transport on the upper shoreface in response to a changing shoreline orientation. Depositional zones are found along northwest-southeast alignments, whereas erosional zones are found in areas of north-south orientation. Deposition along the down-drift side of spit features has been observed in shoreline change results for all time periods.

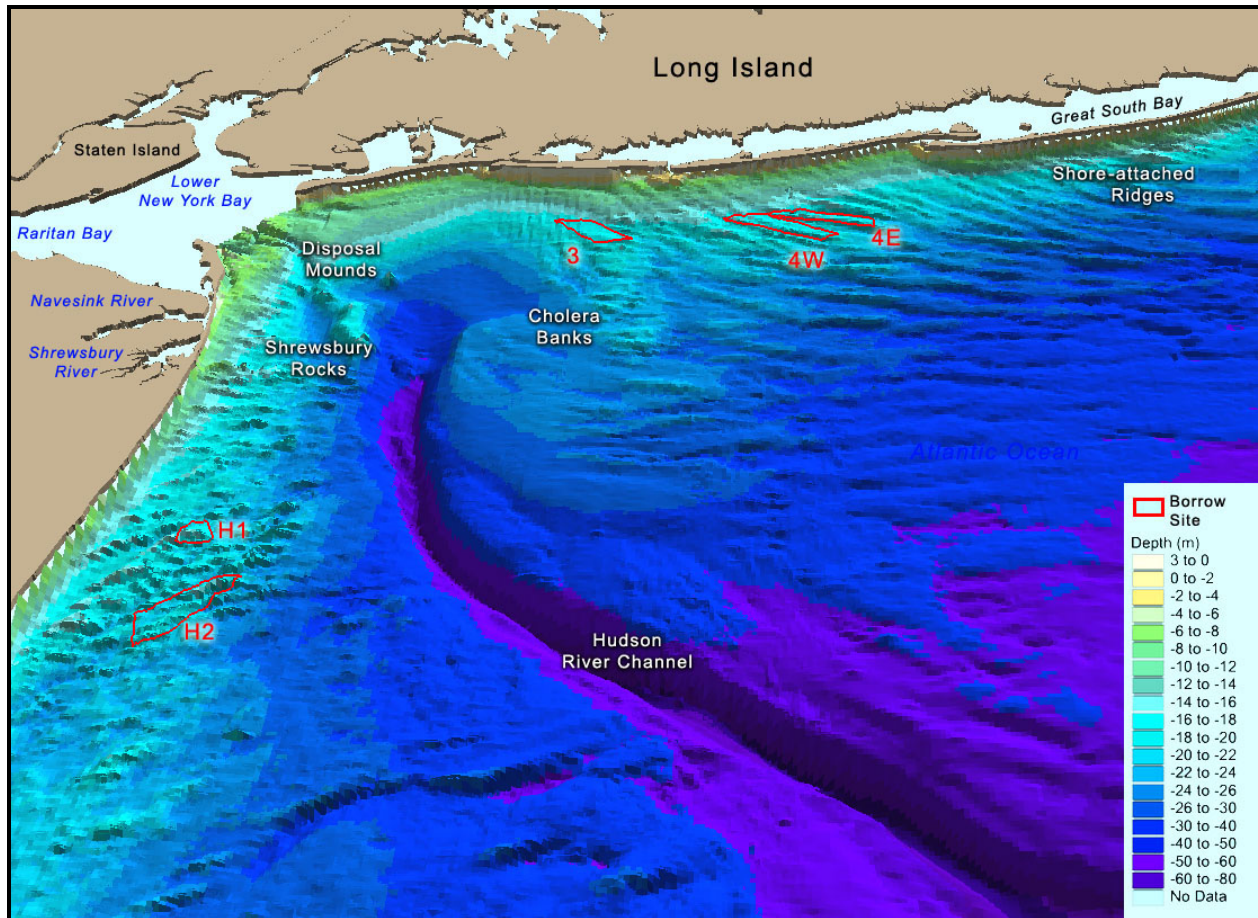


Figure 3-27. Three-dimensional representation of the 1927/97 bathymetric surface.

Alternating zones of erosion and accretion were identified in smaller magnitudes along the eastern two-thirds of Jones Beach. Shoreward of the -6 m contour, the eastern portion of the island displayed a moderately long stretch of erosion with total elevation change of up to 4 m, followed by a similar zone of deposition along the down-drift side of the island. This pattern of updrift erosion and downdrift deposition along Jones Beach was reflective of shoreline change patterns observed for the barrier-island system in southwestern Long Island as a whole. As such, this trend could be expected to occur in the nearshore along the other three barrier islands as well.

Additional areas of erosion and accretion also are present in smaller magnitudes along isolated and shore-connected shoals. Polygons of erosion and deposition generally follow contour shapes defining shoals and troughs on the continental shelf. As expected, regions with lowest relief and slightest irregularities (in the offshore area south of Rockaway out to the head of the Hudson Channel) display the least amount of bathymetric change, whereas zones with increasing shore-attached and offshore sand ridges (such as offshore Shark River Inlet) tend to display a more actively evolving surface. The character of bathymetric change is closely aligned with shoal orientation off Shark River Inlet. As the density of sand shoals in the vicinity of the inlet begins to decrease to the east toward the Hudson River Channel, a corresponding reduction in bathymetric change was apparent.

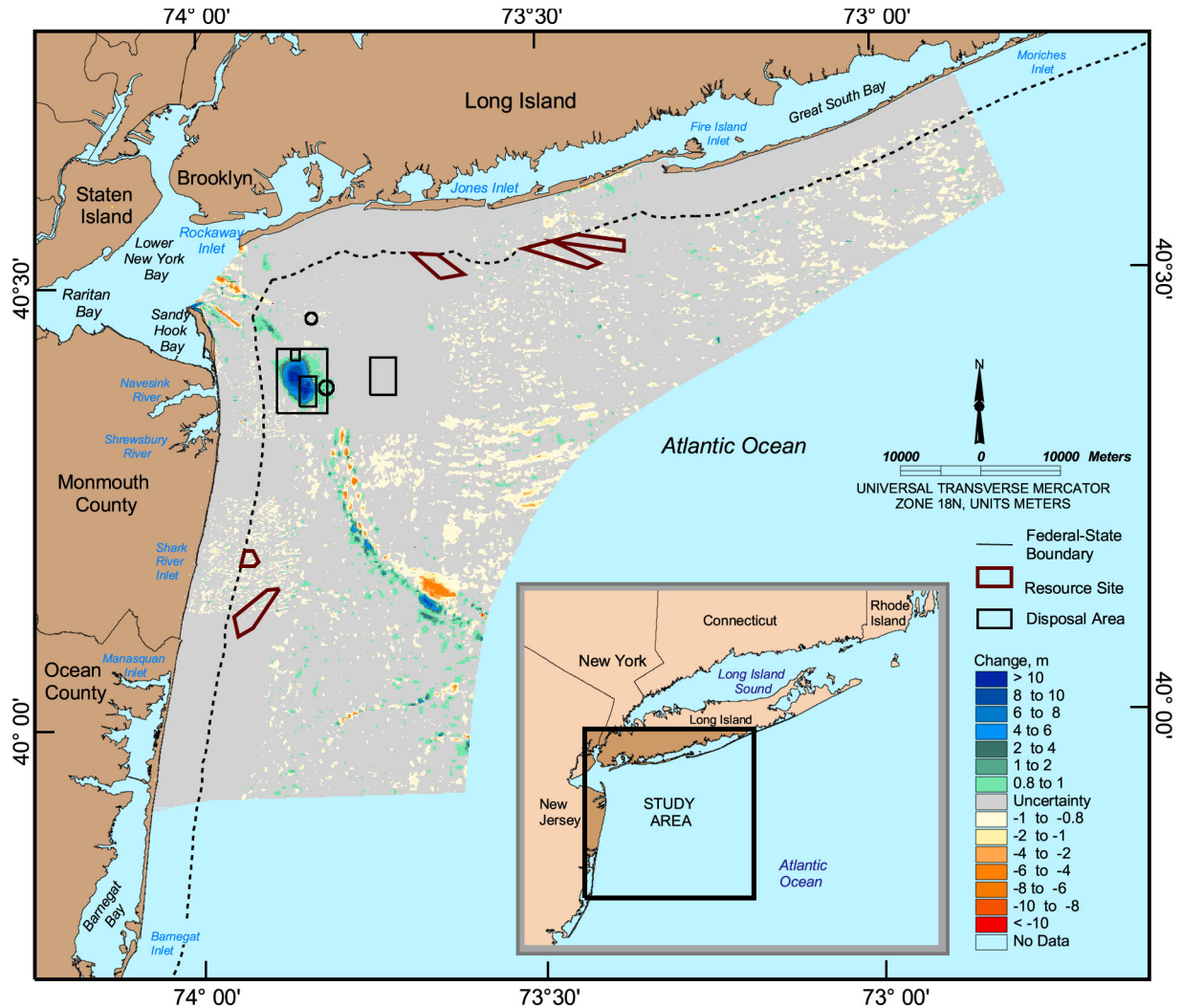


Figure 3-28. Bathymetric change in the New York Bight between 1927/37 and 1927/97.

Bathymetric change along the Hudson Shelf Valley follows the shape of the channel and reflects an overall trend of sediment loss along its eastern side and into the trough, and sediment gain along its western bank. Sediment erosion and accretion thicknesses associated with this area are relatively high, ranging from about 8.5 m of deposition to about 5 m of erosion. Areas with significant levels of change associated with the Hudson Shelf Valley are confined primarily to the extent of the channel and its lateral walls. Erosion and deposition zones tend to complement each other and tend to alternate across the width of the channel. Offshore disposal mounds located at the head of the channel contain the areas of greatest change. Polygons delineating historical and current disposal sites were displayed on the change surface for reference (Figure 3-8).

Sand volume change calculations for zones of accretion and erosion along the shore and on the shelf surface are used to estimate net sand transport rates (see Sections 3.2.4 and 3.2.5). Historical sand transport rates were used to calibrate simulations of borrow site infilling and nearshore sand transport (Section 5.2).

3.2.4 Magnitude and Direction of Change

Patterns of seafloor erosion and accretion on the continental shelf seaward of southwestern New York and northeastern New Jersey document the net direction of sediment transport throughout the study area (Figure 3-28). Although overall trends are helpful for assessing potential impacts of sand extraction from the OCS, the specific purpose of the historical bathymetry change assessment is to quantify sediment erosion and accretion and to derive transport rates specifically related to potential sand extraction sites. Of the five (5) borrow sites defined for this study, two (2) were evaluated for potential infilling rates under proposed sand extraction scenarios. These two borrow sites (H1 and 4E) were used as proxies for evaluating conditions at the remaining three sites within the study area. These sites were chosen based on data coverage and sampling density. It was assumed that conditions along adjacent shoals were similar for other borrow sites defined within the study area.

Overall, calculated infilling rates were remarkably consistent across the shelf surface. For Borrow Sites H1 and 4E, sediment erosion zones parallel to shoreface ridges indicated that the potential transport rate available for infilling any proposed sand borrow site in the area was about 98,000 m³/yr (over a period of 39 years). This calculation assumed that sediment eroded from areas nearby potential borrow sites reflected the rate at which material was available for infilling at the borrow sites. The dredging geometry for each potential borrow site (depth to width to length), as well as the type of sediment available for infilling, are controlling factors for determining sediment infilling (see Section 5.2). This rate was used as a potential infilling estimate for the remaining three borrow sites.

3.2.5 Net Longshore Sand Transport Rates

Net longshore transport rates have been well documented on beaches in southwestern Long Island and northeastern New Jersey. In general, the direction of net littoral transport along beaches south of Long Island is east to west, ranging from 122,000 to 344,000 m³/yr (Taney, 1961; Figure 2-5). Along beaches in northern New Jersey, littoral transport rates were documented at about 382,000 m³/yr to the north between Manasquan and Sandy Hook and about 38,000 m³/yr to the south between Manasquan and Barnegat Inlet (Caldwell, 1966). Shoreline deposition patterns observed along the western ends of barrier islands in New York and at the northern and southern extents of Sandy Hook and Barnegat Inlets reflect these trends. For the present study, bathymetry and shoreline data were combined to calculate nearshore bathymetric change and determine sediment transport rates. These data were used along with rate information published by Taney (1961) and Caldwell (1966) to calculate rates of sediment transport along the outer coast within the study area.

Along the northeastern coast of New Jersey, alternating zones of erosion and accretion, as determined from historical bathymetry comparisons, were evaluated with respect to the net sediment budget to estimate longshore sand transport rates. Sediment deposition at the northern tip of Sandy Hook represents a terminal point for an alternating sequence of erosion and accretion zones located immediately adjacent to the shoreline (Figure 3-28). As such, volume change calculated within these zones provides a good means for evaluating the rate of sediment transport along this portion of the coast. Bathymetric change calculated between 1927/37 and 1927/97 was evaluated for each zone, and a sediment budget was created using these data and the rate published by Caldwell (1966) for northern New Jersey (~382,000 m³/yr to the north). Assuming the validity of this rate, net longshore transport rates ranged from 223,000 to 382,000 m³/yr along the northernmost 6 km of Sandy Hook spit. Due to a lack of bathymetry data for a large portion of the remaining nearshore region in the study area, valid estimates of net longshore transport rates were unable to be developed. However, there is

general agreement between observed shoreline change trends and those published by previous investigators. Additionally, net longshore transport rates for Sandy Hook were generally in agreement with those published previously. As such, values published by previous investigations for sections of the coast lacking data for this study are interpreted as reliable rates of net longshore transport, and observed change trends are used as validation of trends reported by others.

3.3 SUMMARY

Shoreline position and nearshore bathymetry change document four important trends relative to study objectives. First, there are three dominant directions of longshore sand transport within the study area. Between Rockaway Point and Moriches Inlet, the dominant direction of transport is east to west. In northeastern New Jersey, between Sandy Hook and Manasquan, longshore transport from south to north dominates, while south of Manasquan Inlet, the dominant direction is to the south. Along both coasts, the dominant direction of transport is illustrated by barrier island migration and shoreline advance adjacent to inlet jetties. Barrier islands along the south coast of Long Island have historically migrated from east to west, and seaward shoreline advance subsequent to jetty construction has occurred along the east sides of entrances. In northeastern New Jersey, Sandy Hook spit historically has migrated rapidly to the north and, prior to structural development at Barnegat Inlet, the spit north of the entrance was rapidly migrating to the south. The greatest amount of shoreline change observed for this study was associated with beaches adjacent to inlets, most notably along the leading edge of prograding barrier spits.

Second, the most dynamic features within the study area, in terms of nearshore sediment transport, are migrating barrier island/spit complexes along the northeastern New Jersey and southwestern Long Island coasts, in addition to natural and anthropogenic change along the Hudson River Channel. Areas of significant erosion and accretion are documented between 1927/37 and 1927/97 at Sandy Hook spit, reflecting wave and current dynamics that carry sediment northward and deposit it along the terminal edge of the spit. High rates of deposition also are prominent at entrances south of Sandy Hook and along the southwestern coast of Long Island. Shoreline and bathymetric changes associated with these features reflects morphologic response to wave and current dynamics and shoreline adjustment to the construction of engineering structures. Pronounced bathymetric change observed along the head and sides of the Hudson River Channel reflects natural and anthropogenic processes. Large areas showing significant deposition at the head of the Hudson River Channel reflect high levels of offshore disposal activity, and patches of erosion and accretion paralleling each other along the length of the channel reflect natural bathymetric changes.

Third, alternating bands of erosion and accretion paralleling ridge features illustrated the steady reworking of the shelf surface as sand ridges migrated in the direction of net sediment transport. The process by which this was occurring was relatively consistent across the shelf. At Borrow Site H1, bathymetric comparisons suggested that the borrow site in this region would fill with sand transported from the adjacent seafloor at rates of about 98,000 m³/yr. Areas of erosion and accretion documented between 1927/37 and 1927/97 at Borrow Site 4E illustrated the amount of sediment available for infilling at sites south of Long Island was also about 98,000 m³/yr. Calculations for these two borrow sites were used as indicators of potential infilling rates for all borrow sites within the study area.

Finally, net longshore transport rates determined from seafloor changes in the littoral zone along Sandy Hook spit indicated maximum transport rates near the distal end of the spit, with

lower rates to the south. These calculations, along with data published by Caldwell (1966) indicate a range in net longshore transport along Sandy Hook from about 223,000 m³/yr to 382,000 m³/yr.

4.0 ASSESSMENT OF WAVE CLIMATE IMPACT BY OFFSHORE BORROW SITES

Excavation of an offshore borrow site can affect wave heights and the direction of wave propagation. The existence of an excavated hole or trench on the OCS can cause waves to refract toward the shallow edges of a borrow site. This alteration to a wave field by a borrow site may change local sediment transport rates, resulting in some areas experiencing a reduction in longshore transport and other areas showing an increase. To determine potential physical impacts associated with dredging borrow sites offshore the northeastern coast of New Jersey and the southwestern coast of Long Island, New York, wave transformation modeling and sediment transport potential calculations were performed for existing and post-dredging bathymetric conditions. Comparison of computations between existing and post-dredging conditions illustrated the relative impact of borrow site excavation on wave-induced coastal processes.

The most effective means of quantifying physical environmental effects of sand dredging from shoals on the continental shelf is through use of wave transformation numerical modeling tools that recognize the random nature of incident waves as they propagate onshore. Spectral wave models, such as STWAVE (STeady-state spectral WAVE model), REF/DIF-S (REFraction/DIFfraction model for Spectral wave conditions), SWAN (Simulation of Waves Nearshore), and others, typically provide more realistic results than monochromatic wave models relative to field measurements. As such, spectral wave transformation modeling was applied in this study to evaluate potential impacts to coastal and nearshore sites from long-term dredging and significant removal of sand from offshore sand borrow sites. Although interpretation of wave modeling results is relatively straightforward, evaluating the significance of predicted changes for accepting or rejecting a borrow site is more complicated.

As part of any offshore sand mining effort, the MMS requires an evaluation of potential environmental impacts associated with alterations to nearshore wave patterns. To determine potential physical impacts associated with borrow site excavation, the influence of borrow site geometry on local wave refraction patterns was evaluated. Because large natural spatial and temporal variability exists within the wave climate at a particular site, determination of physical impacts associated with sand mining must consider the influence of process variability. A method based on historical wave climate variability, as well as local wave climate changes directly attributable to borrow site excavation, has been applied to determine appropriate criteria for assessing impact significance.

To directly assess impacts to coastal processes associated with sand mining, an approach was utilized that considers spatial (longshore) and temporal aspects of the local wave climate, as described by Kelley et al. (2004). This method was applied by performing wave model runs using mean conditions developed from the entire 20-year Wave Information Study (WIS) record, and then 20 year-long blocks of the WIS record to determine annual variability of the wave climate along this shoreline. In this manner, temporal variations in wave climate are

considered relative to average annual conditions. From these wave model runs, sediment transport potential curves are derived for average annual conditions (based on the full 20-year WIS record) and each 1-year period (based on the 20 1-year wave records parsed from the full record). Applying this information, the average and standard deviation in calculated longshore sediment transport potential are determined every 200 m along the shoreline.

Assuming the temporal component of sediment transport potential is normally distributed, the suggested criterion for accepting or rejecting a potential borrow site is based on a range of one standard deviation about the mean. As proposed, the criterion would require that if any portion of the sediment transport potential curve associated with a sand mining project exceeds one-half the standard deviation of natural temporal variability in sediment transport potential, the site would be rejected. Conversely, a borrow site design would be accepted as long as the transport potential change determined for post-dredging conditions at a site occurs within the range of one-half the standard deviation.

The natural variability envelope provides a basis for judging the impacts of a borrow site relative to sediment transport processes along a coastline. Because there is a greater than 50% chance that the transport computed for a particular year will occur outside the $\pm 0.5\sigma$ envelope about the mean, impacts determined for a particular borrow site that occur within this range will be indistinguishable from observed natural variations. For this reason, sites with large natural variation in wave climate and associated sediment transport potential would be allowed to have larger impacts associated with an offshore sand mining project.

An application of this method is illustrated in Figure 4-1 (from Kelley et al., 2004), where alterations in wave climate caused by numerically excavating a proposed borrow site offshore St. Lucie Inlet, Florida were determined relative to natural variability in wave climate. In this example, dredged quantities of 12 and $24 \times 10^6 \text{ m}^3$ were evaluated. The computed significance envelope varied between $\pm 50,000 \text{ m}^3/\text{yr}$ at the southern extent of the modeled domain, to approximately $\pm 100,000 \text{ m}^3/\text{y}$ at the northern limit of the study area. Impacts associated with the $24 \times 10^6 \text{ m}^3$ plan exceeded the significance envelope, resulting in rejection of this excavation scenario. Alternately, the $12 \times 10^6 \text{ m}^3$ plan was deemed acceptable because predicted changes to sediment transport potential did not exceed the limits defined by the $\pm 0.5\sigma$ envelope about the mean sediment transport potential.

As a management tool for the MMS, this methodology provides several advantages over methods previously employed to assess the significance of borrow site impacts. The primary advantages include:

1. Observed long-term shoreline change is compared with computed longshore change in sediment transport potential. Close comparison between these two curves indicates that longshore sediment transport potential calculations are appropriate for assessing long-term natural change. Therefore, this methodology has a model-independent component (observed shoreline change) used to ground truth model results.
2. The method is directly related to sediment transport potential and associated shoreline change. Therefore, impacts associated with borrow site excavation can be directly related to their potential influence on observed coastal processes (annualized variability in shoreline position).
3. Site-specific temporal variability in wave climate and sediment transport potential is calculated as part of the methodology. For sites that show little natural variability in inter-annual wave climate, coastal processes impacts associated with borrow site

dredging similarly would be limited, and *vice versa*. In this manner, the inter-annual temporal component of the natural wave climate is a major component in determining impact significance.

4. Similar to methodologies incorporated in previous MMS studies, the longshore spatial distribution of borrow site impacts was considered. However, an acceptable limit of longshore sediment transport variability was computed from the temporal component of the analysis. Therefore, the final results of this analysis provided a spatially-varying envelope of natural variability in addition to the modeled impacts directly associated with borrow site excavation. The methodology accounts for spatial and temporal variability in wave climate, as well as providing a defensible means of assessing significance of impacts relative to site-specific conditions.

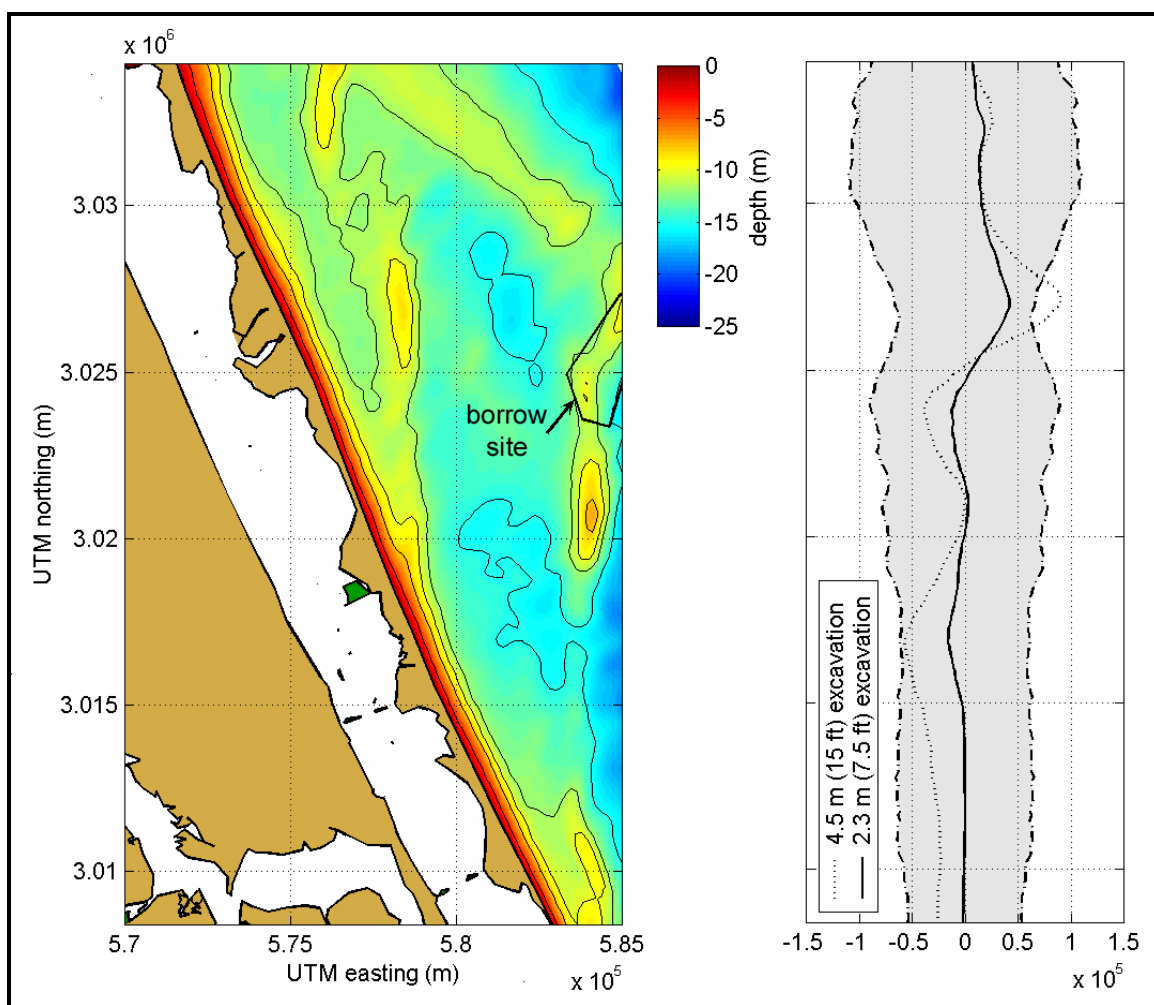


Figure 4-1. Example of spatial/temporal variability method for determining significance of borrow site dredging impacts (Kelley et al., 2004). The difference plot illustrates modeled change in net transport potential (solid black and dotted lines) resulting from two different dredging scenarios at the proposed borrow site. The plot also illustrates the dredging significance envelope ($\pm 0.5\sigma$) determined for this shoreline (gray-shaded area). The 4.5 m excavation (dotted line, $24 \times 10^6 \text{ m}^3$) exceeds the significance envelope boundary and would be rejected. However, the 2.3 m excavation (solid line, $12 \times 10^6 \text{ m}^3$) does not exceed the natural variability envelope, and would be acceptable.

4.1 ANALYSIS APPROACH

Sediment transport rates along a coastline are dependent on local wave climate. For this study, nearshore wave heights and directions along the shoreline landward of proposed borrow sites were estimated using the USACE spectral wave model STWAVE, which was used to simulate the propagation of offshore waves to the shoreline. Offshore wave data, from hindcast model runs performed specifically for this study by Offshore & Coastal Technologies, Inc. (OCTI), were used to derive input wave conditions for STWAVE.

4.1.1 Wave Modeling

Developed by the USACE Waterways Experiment Station (WES), STWAVE v2.0 is a steady state, spectral wave transformation model (Smith et al., 1999). Two-dimensional (frequency and direction versus energy) spectra were used as input to the model. STWAVE is able to simulate wave refraction and shoaling induced by changes in bathymetry and by wave interactions with currents. The model includes a wave breaking model based on water depth and wave steepness. Model output includes significant wave height (H_s), peak wave period (T_p), and mean wave direction ($\bar{\theta}$).

STWAVE is an efficient program that requires minimal computing resources to run well. The model is implemented using a finite-difference scheme on a regular Cartesian grid (grid increments in the x and y directions are equal). During a model run, the solution is computed starting from the offshore open boundary and is propagated onshore in a single pass of the model domain. As such, STWAVE can propagate waves only in directions within the $\pm 87.5^\circ$ half plane. A benefit of using this single pass approach is that it uses minimal computer memory because the only memory-resident spectral data are for two grid columns. Accordingly, changing wave spectra across each grid column are computed using information solely from the previous grid column.

STWAVE is based on a form of the wave action balance equation. The wave action density spectrum, which includes the effects of currents, is conserved along wave rays. In the absence of currents, wave rays correspond to wave orthogonals, and the action density spectrum is equivalent to the wave energy density spectrum. A diagram showing the relationship of wave orthogonal, wave ray, and current directions is shown in Figure 4-2. The governing equation of wave transformation, using the action balance spectrum, in tensor notation is written as (Smith et al., 1999)

$$(C_{ga})_i \frac{\partial}{\partial x_i} \frac{C_a C_{ga} \cos(\mu - \alpha) E}{\omega_r} = \sum \frac{S}{\omega_r} \quad (4.1)$$

where

$E = E(f, \theta)$ wave energy density spectrum,

S = energy source and sink terms (e.g., white capping, breaking, wind input),

α = wave orthogonal direction,

μ = wave ray direction (direction of energy propagation),

ω_r = relative angular frequency ($2\pi f_r$),

C_a, C_{ga} = absolute wave celerity and group celerity, respectively.

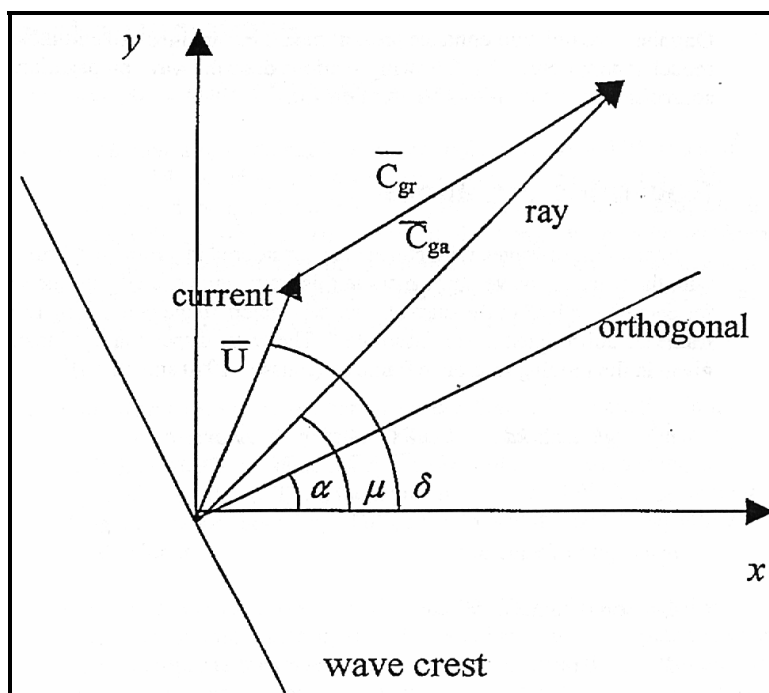


Figure 4-2. Wave and current vectors used in STWAVE. Subscript *a* denotes values in the *absolute* frame of reference, and subscript *r* denotes values in the *relative* frame of reference (with currents).

The breaking model in STWAVE is based on a form of the Miche criterion as discussed by Battjes and Janssen (1978). It sets a maximum limit on the zero-moment wave height (H_{mo}), the wave height based on the distribution of energy in the wave spectrum. The formulation of this model is

$$H_{mo(max)} = 0.1L \tanh(kd) \quad (4.2)$$

where L is the wavelength, k is the wave number ($k = 2\pi/L$), and d is the depth at the point where the breaking limit is being evaluated. This equation is used together with a simpler breaking model, which was used alone in earlier versions of STWAVE, where the maximum H_{mo} wave height is always expressed as a constant ratio of water depth

$$H_{mo(max)} = 0.64 d \quad (4.3)$$

An advantage of using Equation 4.2 over Equation 4.3 is that it accounts for increased wave breaking resulting from wave steepening caused by wave-current interactions. Once model wave heights exceed $H_{mo(max)}$, STWAVE uses a simple method to reduce the energy spectrum to set the value of $H_{mo} = H_{mo(max)}$. Energy at each frequency and direction is reduced by the same percentage. As a result, non-linear transfers of energy to high frequencies during breaking are not included in STWAVE.

4.1.1.1 Input Spectra Development

Offshore wave conditions used as input for wave modeling can be derived from two main sources: measured spectral wave data from offshore buoys or hindcast simulation time series data. In general, buoy data are the preferred source of wave information for modeling because they represent actual offshore measurements rather than hindcast information derived from

large-scale models. However, very few sites along the U.S. east coast have directional wave records of sufficient length to justify their use as a source of long-term information. As an alternative to measured data, one publicly available hindcast data source is WIS (Hubertz et al., 1993). WIS data recently have been updated and now cover the 20-year period from 1980 to 1999.

For this study, wave input conditions for simulations offshore northeastern New Jersey and southwestern Long Island were developed using wave hindcast data specifically modeled by OCTI for this project. This site-specific wave hindcast data set has two main advantages over the standard WIS data source: 1) wave conditions were developed for points at the open boundaries of each model grid, which eliminates the need to numerically refract waves inshore from WIS stations farther offshore; and 2) in addition to bulk wave parameters (e.g., wave height, period, and direction), the complete 2-dimensional wave spectra for each individual time step in the wave hindcast (6-hour interval) were provided. This approach allows for a more detailed analysis of parameters governing the shape of various wave spectra.

Wave input conditions for simulations offshore northeastern New Jersey and southwestern Long Island were developed using the spectral OCTI hindcast data. Station locations are shown in Figure 4-3 with the limits of coarse computational grids. Hindcast records include the 20-year period from January 1980 to December 1999. Wave hindcast station OCTI-NJ is located approximately 13.7 km east of Shark River Inlet in approximately 26.7 m water depth. The station offshore southwestern Long Island (OCTI-NY) is located approximately 12.8 km south of Jones Inlet in 24.7 m of water. Both stations are located at the along-shore mid-point of the open boundary for their respective grid.

Two wave roses showing percent occurrence of waves for the hindcast stations are shown in Figures 4-4 and 4-5. Plots for Station OCTI-NY, offshore southwestern Long Island, are shown in Figure 4-4. The left wave rose shows wave height distribution relative to direction. The majority of waves (63%) propagate between 78.75° and 191.25° (east through south sectors). The dominant wave direction is from the southern sector, from which 17% of waves in the record propagate. Mean height for all waves in the record is 0.99 m, with a standard deviation of 0.6 m. Mean height for waves from the dominant wave sector is 0.93 m, also with a standard deviation of 0.6 m. The right wave rose in Figure 4-4 illustrates the distribution of peak wave periods in the record. A significant number of wave events (19.5%) have peak periods greater than 6 sec, and the mean peak period for the entire record is 4.3 sec (compared with 5.0 sec for WIS Station 123).

Plots for Station OCTI-NJ, offshore northeastern New Jersey, are shown in Figure 4-5. Similar to offshore Long Island, the majority of waves (64%) propagate onshore between 78.75° and 191.25° . The dominant wave direction is from the South, from which 18% of waves in the record propagate. Mean height for all waves in the record is 0.96 m, with a standard deviation of 0.6 m. Mean height for waves from the dominant wave sector is 0.91 m, with a standard deviation of 0.5 m. From this record, 7.6% of the wave events have peak periods greater than 6 sec, and the mean peak period for the entire record is 4.2 sec (compared to 4.9 sec for WIS Station 128).

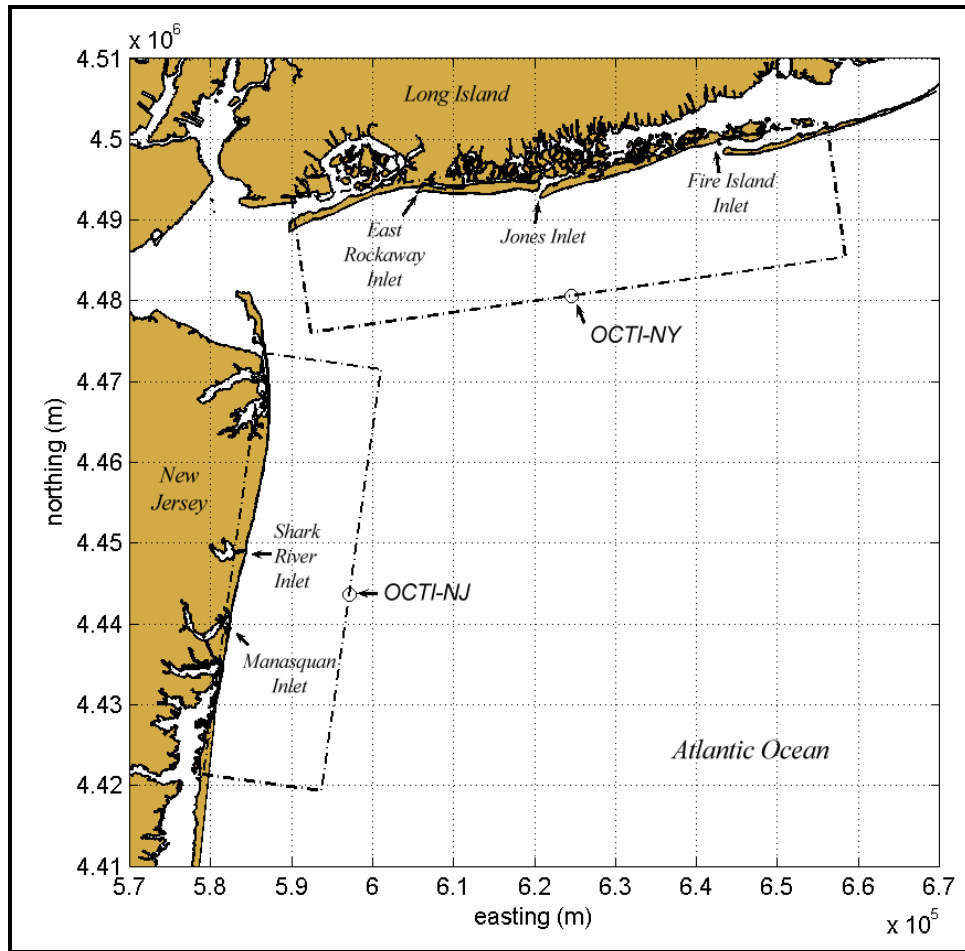


Figure 4-3. Shoreline of northeastern New Jersey and southwestern Long Island with coarse grid limits and OCTI wave input data station locations.

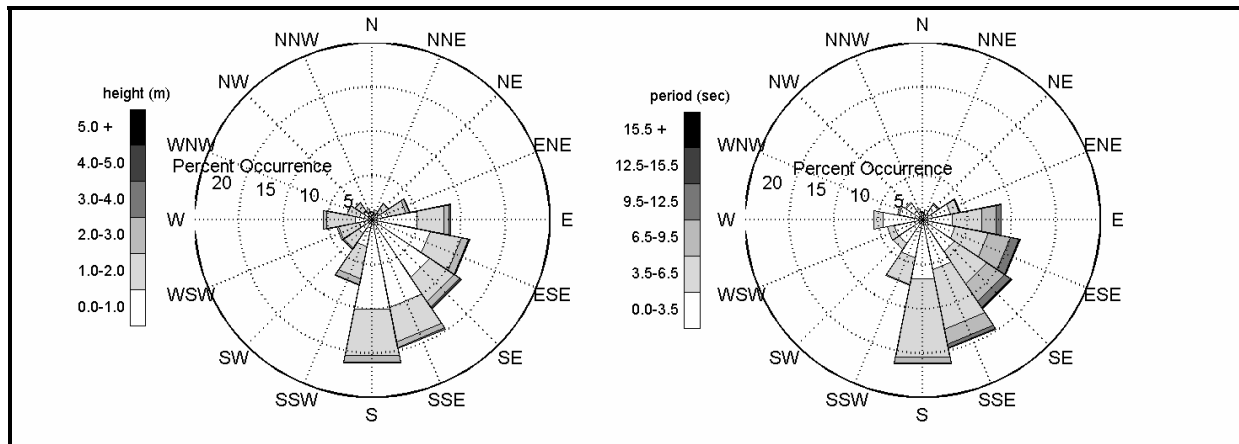


Figure 4-4. Wave height and period roses for OCTI hindcast data offshore southwestern Long Island (Station OCTI-NY) for the 20-year period January 1980 to December 1999. Direction indicates from where waves were traveling relative to true north. Length of gray tone segments indicates percent occurrence for each wave height and period range. Combined length of segments in each sector indicates percent occurrence of waves from that direction.

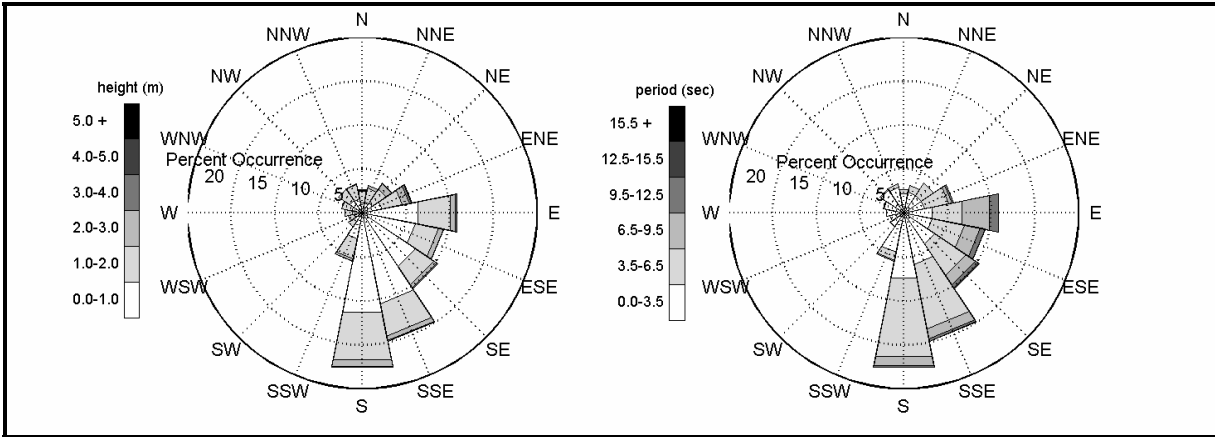


Figure 4-5. Wave height and period roses for OCTI hindcast data offshore northeastern New Jersey (OCTI-NJ) for the 20-year period between January 1980 and December 1999. Direction indicates from where waves were traveling relative to true north. Length of gray tone segments indicates percent occurrence for each wave height and period range. Combined length of segments in each sector indicates percent occurrence of waves from that direction.

STWAVE input spectra were developed using the spectral data provided in the OCTI wave hindcasts. An example of an input spectrum is presented in Figure 4-6. Wave conditions were binned based on wave angle and peak frequency. Ten direction bins (each an 18 degree sector) and two period bins (greater or less than 6.5 sec) were used to sort the 29,215 six-hourly wave conditions in each hindcast data file. Wave spectra corresponding to wave parameters that fall within the limits of individual direction and period bins are summed, and a mean spectrum for all waves in each bin is computed based on the total number of wave events in the bin. From the 20 total bins, STWAVE model run conditions were selected based on the percent occurrence and percent energy for conditions in each bin.

Selected conditions have a percent occurrence greater than 1%, and also contain more than 1% of the energy of the entire wave record. Conditions selected for model runs are shown in Tables 4-1 and 4-2, with the significant parameters of each input spectrum.

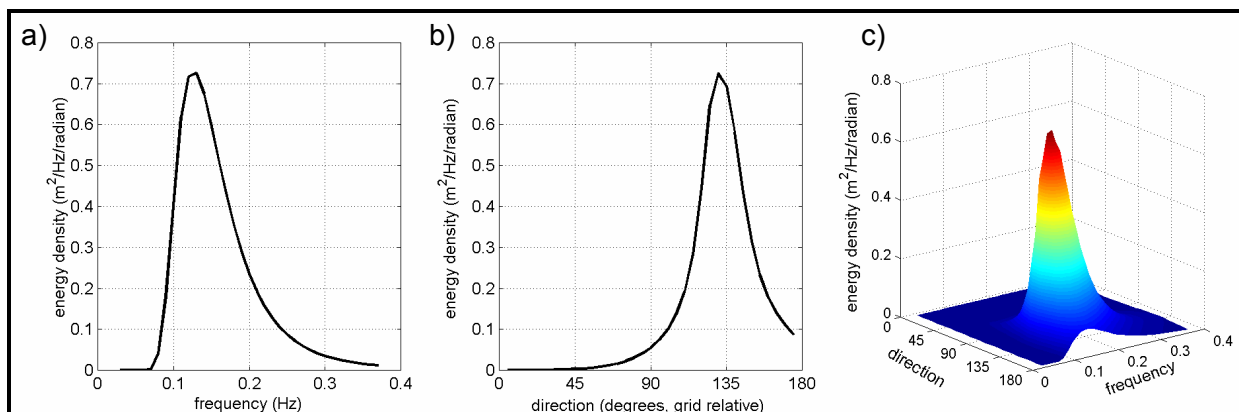


Figure 4-6. STWAVE input spectrum developed using 20-year OCTI hindcast spectral data. Plots show a) frequency distribution of energy at peak direction, b) directional distribution of energy at peak frequency, and c) surface plot of two-dimensional energy spectrum ($H_{mo} = 0.9$ m, $\theta_{mean} = 130^\circ$ grid relative).

	STWAVE Model Input Condition	Percent Occurrence	H _{mo} Wave Height (m)	Peak Wave Period, T _p (sec)	Peak Wave Direction, θ _p (° true north)	Direction Bin (grid relative)
Period Band 1	1A	4.8	0.7	4.0	92	0 to 18
	2A	6.1	0.8	4.0	112	18 to 36
	3A	6.8	0.8	4.0	112	36 to 54
	4A	7.3	0.7	4.0	137	54 to 72
	5A	9.9	0.8	4.0	157	72 to 90
	6A	13.5	0.8	4.0	162	90 to 108
	7A	9.7	1.0	4.0	182	108 to 126
	8A	4.9	1.0	4.0	202	126 to 144
	9A	3.0	0.7	4.0	227	144 to 162
	10A	3.1	0.7	4.0	247	162 to 180
Period Band 2	11A	2.1	1.3	9.1	112	18 to 36
	12A	2.7	1.4	9.1	117	36 to 54
	13A	2.2	1.4	9.1	137	54 to 72
	14A	1.6	1.6	9.1	137	72 to 90

	STWAVE Model Input Condition	Percent Occurrence	H _{mo} Wave Height (m)	Peak Wave Period, T _p (sec)	Peak Wave Direction, θ _p (° true north)	Direction Bin (grid relative)
Period Band 1	1B	3.6	0.6	4.0	13	0 to 18
	2B	2.5	0.8	4.0	23	18 to 36
	3B	3.3	1.1	4.0	43	36 to 54
	4B	3.9	1.3	4.0	68	54 to 72
	5B	5.2	1.1	4.0	88	72 to 90
	6B	6.2	0.9	4.0	93	90 to 108
	7B	6.3	0.8	4.0	113	108 to 126
	8B	6.8	0.8	4.0	133	126 to 144
	9B	9.6	0.7	4.0	158	144 to 162
	10B	15.6	0.7	4.0	158	162 to 180
Period Band 2	11B	2.1	1.3	9.1	88	72 to 90
	12B	2.6	1.2	7.7	93	90 to 108
	13B	1.5	1.1	7.7	113	108 to 126
	14B	1.1	1.2	7.7	133	126 to 144
	15B	1.0	1.4	9.1	138	144 to 162
	16B	1.0	1.3	7.7	158	162 to 180

4.1.1.2 Grid Development

Input spectra and two coarse bathymetry grids were developed for each modeled area for simulating wave propagation over existing and post-dredging bathymetry. A fine grid, nested within coarse grids, was developed to obtain greater resolution of wave characteristics in the nearshore, landward of borrow sites. One coarse grid encompasses existing bathymetry over which representative wave conditions are propagated. The second coarse grid includes excavated depths at identified sand borrow sites over which the same representative wave conditions are propagated. Most recent surveys (see Section 3.0) were the primary source of bathymetric data for creating grids. However, these data were supplemented by more recent local bathymetric data and beach profiles where available. Contour plots of existing conditions grids for each modeled area are shown in Figures 4-7 (offshore southwestern Long Island) and 4-8 (offshore northeastern New Jersey).

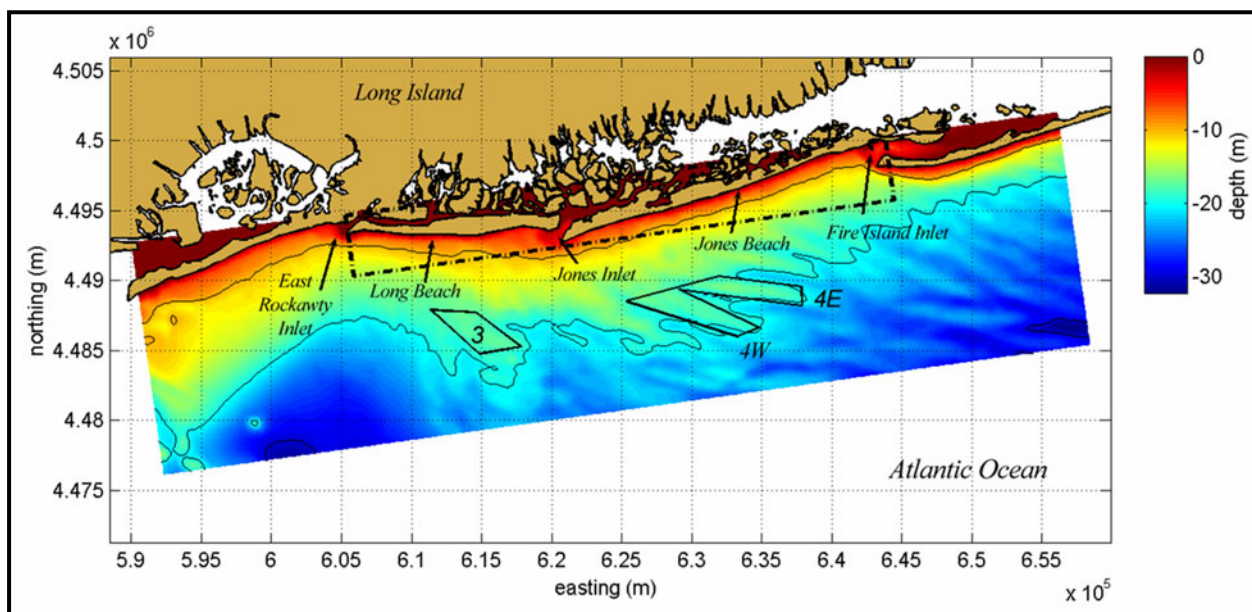


Figure 4-7. Coarse model grid (200 x 200 m spacing) used for STWAVE simulations offshore southwestern Long Island. Depths are relative to NAVD. Borrow site locations are indicated by solid black lines, and fine grid limits are indicated by a dashed line.

Dimensional characteristics of each area grid are presented in Table 4-3. Geographical limits for each grid were chosen based on the wave conditions selected for model simulations. Wave conditions with relatively small angles to the shoreline require a wide grid so the area of potential impact does not occur within the shadow of the lateral grid boundaries. The coarse grid developed for offshore southwestern Long Island encompasses an area that extends approximately 14 km offshore and 65 km along-shore. Depths at the offshore boundary ranged between 19 and 32 m (NAVD) with a mean depth of approximately 26 m. The coarse grid developed for offshore northeastern New Jersey covers a region that extends approximately 17 km offshore of Shark River Inlet and 53 km along-shore. Depths at the offshore boundary ranged between 21 and 38 m (NAVD), with a mean depth of approximately 27 m.

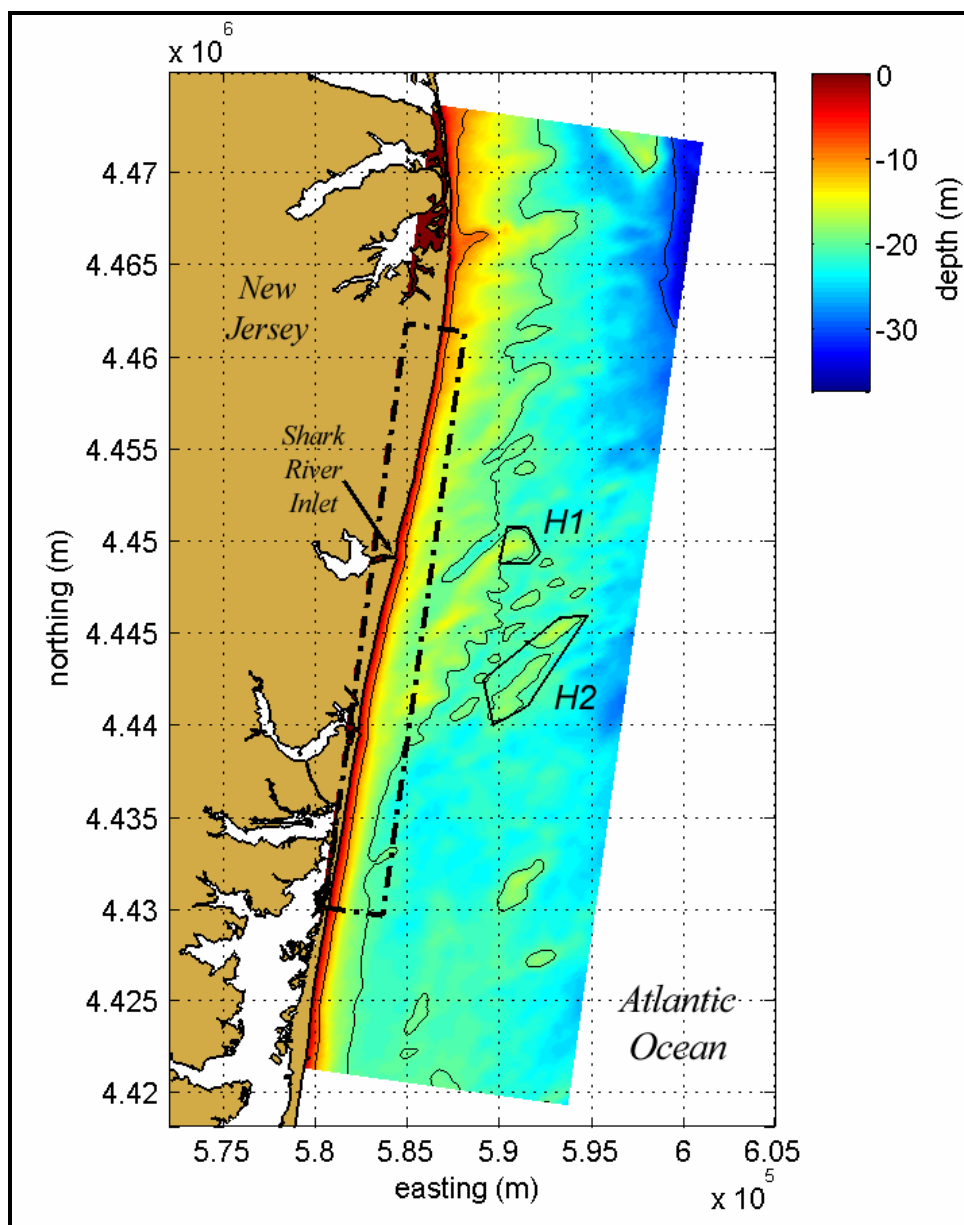


Figure 4-8. Color contour plot of coarse model grid (200 m x 200 m grid spacing) used for STWAVE model simulations of waves offshore Shark River Inlet, New Jersey. Depths are relative to NAVD. Borrow site locations are indicated by solid black lines, and fine grid limits are indicated by a dashed line.

Post-dredging coarse grids were developed by imposing modifications to the existing conditions bathymetry; Table 4-4 presents the resource characteristics of modeled borrow sites. For each site, bathymetry was excavated to the indicated depth. Bathymetry deeper than the excavated depth was not modified. In addition to the coarse grids, a single fine grid was developed for each area to obtain greater resolution of waves in the nearshore landward of borrow sites. For each modeled area, the same fine grid was used for existing conditions and post-dredging simulations. Spatially varying boundary conditions (wave spectra) for fine grids were extracted from coarse grid simulations. As such, the fine grid solution was nested within the coarse grid solution.

Table 4-3. Numerical grid dimensions for offshore (coarse) and nearshore (fine) grids. Dimensions are given as cross-shore x along-shore.					
Region	Coarse Grid (200-m spacing)		Fine Grid (20-m spacing)		Grid Angle (° true north)
	Nodes	Distance (km)	Nodes	Distance (km)	
Offshore Southwestern Long Island	85x335	17x67	221x1951	4.4x39.0	88
Offshore Northeastern New Jersey	75x265	15x53	161x1601	3.2x32.0	8

Table 4-4. Sand resource characteristics at potential borrow sites offshore northeastern New Jersey and southwestern Long Island, NY.								
Borrow Site	Borrow Site Surface Area (x 10 ⁶ m ²)	Maximum Excavation Depth (m)	Borrow Site Sand Volume (x 10 ⁶ m ³)	Average Sediment Thickness (m)	Shoal Relief (m)	D10 (mm)	D50 (mm)	D90 (mm)
H1	3.28	20	4.8	1.5	5	0.95	0.52	0.26
H2	13.13	20	9.5	0.7	5	0.67	0.35	0.19
3	9.40	19	11.2	1.2	2	1.92	1.13	0.36
4W	12.23	20	19.8	1.6	4	0.65	0.36	0.22
4E	9.39	20	16.6	1.8	4	1.05	0.45	0.27

D10 = grain diameter above which 10% of the distribution is retained; D50 = median grain diameter; D90 = grain diameter above which 90% of the distribution is retained

4.1.2 Sediment Transport Potential

As a first step in evaluating sediment transport along the coastline of southwestern Long Island and northeastern New Jersey, calculations of sediment transport potential were performed to indicate the maximum quantity of sand transport possible based on a sediment-rich environment. Results from spectral wave modeling formed the basis for quantifying changes in sediment transport rates along the beach because wave-induced transport is a function of wave breaker height, wave period, and wave direction. Longshore transport depends on long-term fluctuations in incident wave energy and the resulting longshore current; therefore, annual transport rates were calculated from long-term wave statistics.

The sediment transport equation used for longshore analyses is based on the work of Rosati et al. (2002). In general, the longshore sediment transport rate is assumed to be proportional to the longshore wave energy flux at the breaker line, which is dependent on wave height and direction. Because the transport equation was calibrated in sediment-rich environments, it typically over predicts sediment transport rates. However, it provides a useful technique for comparing erosion/accretion trends along a shoreline of interest.

Sediment transport computations were based on wave information at breaking for each grid cell along the modeled coastline. This shoreline segment incorporates the influence of all changes to the nearshore wave climate associated with proposed dredging activities. Computations of sediment transport rates for each wave condition was performed and then weighted by the annual percentage occurrence. Sediment transport potential was computed for existing and post-dredging conditions.

The volumetric longshore sand-transport rate, Q_ℓ , past a point on a shoreline is computed using the relationship:

$$Q_\ell = \frac{I_\ell}{(s-1)\rho g a'} \quad (4.4)$$

where I_ℓ is the immersed-weight longshore sand-transport rate, s is the specific gravity of the sediment, a' is the void ratio of the sediment, g is the acceleration of gravity, and ρ is the density of seawater.

For this study, I_ℓ was computed using two methods. The first method is commonly referred to as the CERC (Coastal Engineering Research Center) formula,

$$I_\ell = K P_{\ell s} \quad (4.5)$$

where K is a dimensionless coefficient and $P_{\ell s}$ is the longshore-directed wave energy flux computed using the following relationship:

$$P_{\ell s} = \frac{\rho g^{3/2}}{16\sqrt{\gamma}} H_{sb}^{5/2} \sin 2\alpha_b \quad (4.6)$$

where H_{sb} is the significant wave height at breaking, γ is the coefficient for the inception of wave breaking ($\gamma = H_b/h_b$), and α_b is the breaking wave angle. A value of $K = 0.4$ was used for this study, appropriate for significant wave heights (computed by STWAVE), rather than the more familiar value $K = 0.77$, which is used with RMS wave height.

The second method used to compute the immersed-weight longshore sand-transport rate was described by Kamphuis (1990). This method is a modification to the original CERC formula that adds a dependency on median grain diameter of beach sand and the surf similarity parameter (Irrabarren number), ξ_b , which is expressed as

$$\xi_b = \frac{m}{(H_b/L_0)^{0.5}} \quad (4.7)$$

where m is the bottom slope, H_b is the wave-breaker height, and L_0 is the incident deep-water wave length. The complete expression of Kamphuis is given by

$$I_\ell = K^* \rho g \left(\frac{g}{2\pi} \right)^{0.75} \xi_b T^{0.5} (md_{50})^{-0.25} H_s^{2.5} \sin^{0.6}(2\theta_b) \quad (4.8)$$

where the coefficient $K^* = 0.0013$.

4.2 MODEL RESULTS

Redistribution of wave energy and alteration of wave directions resulting from offshore sand excavation are expected to change longshore sediment transport patterns landward of

potential sand borrow sites offshore southwestern Long Island and northeastern New Jersey. Depending on the net direction of local sediment transport, the influence of borrow site conditions can either increase or decrease net littoral drift. Example model cases for each potential sand borrow site are discussed in the following subsections. Complete wave model output for the four modeled regions, showing wave heights and wave height difference plots between existing and post-dredging conditions for all modeled wave cases, is provided in Appendix C.

4.2.1 Wave Modeling

From existing conditions model results, bottom features offshore northeastern New Jersey modified the wave field as it propagated shoreward. As an example, the shoal in the vicinity of Monmouth Beach, NJ (an area of approximately 10 m water depth 1.7 km offshore) refracts and focuses wave energy, resulting in an area of increased wave heights shoreward of the shoal (Figure 4-9). Wave heights landward of the shoal were about 0.2 m greater than wave heights seaward of the shoal. As the shoal focused wave energy and caused an increase in wave height in one area, there was a corresponding decrease in wave energy in adjacent areas. Because energy was conserved, wave focusing behind the shoal caused a reduction of energy at the southern edge of the shoal, which is illustrated by reduced wave heights.

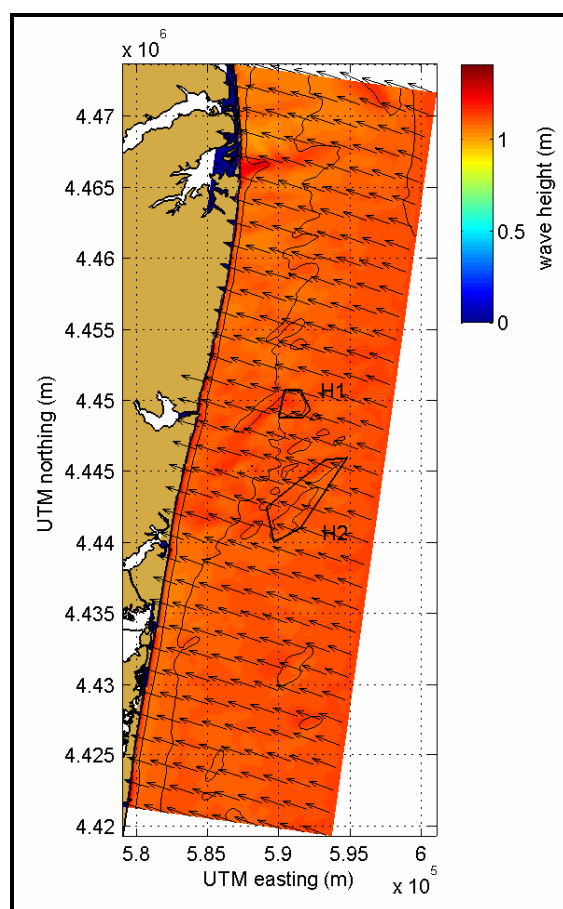


Figure 4-9. STWAVE output for the coarse grid (200 x 200 m grid cells) offshore Shark River Inlet in northeastern New Jersey (model case 13B; $H_{m0} = 1.1$ m, $T_p = 7.7$ sec, $\theta_{peak} = 113^\circ$). Color contours indicate H_{m0} wave height. Vectors indicate mean wave direction. Seafloor contours are shown as black lines at a 10 m interval.

In addition to the effects of bottom features far offshore, waves were refracted by straight and parallel bottom contours in the nearshore. In Figure 4-10, fine grid model results illustrate how wave directions changed as the wave field propagates shoreward. For the same east-southeast wave condition as in Figure 4-9, waves refracted and the mean direction of wave propagation near the shoreline became shore-normal (perpendicular to the shoreline). In addition to the change in wave direction, wave heights also were modified by nearshore bathymetry. Waves began to shoal (increase in height) about 200 m offshore and increased in height by 0.2 m before breaking began. Wave heights were reduced as energy was dissipated in the surf zone, which was about 60 m wide in this example.

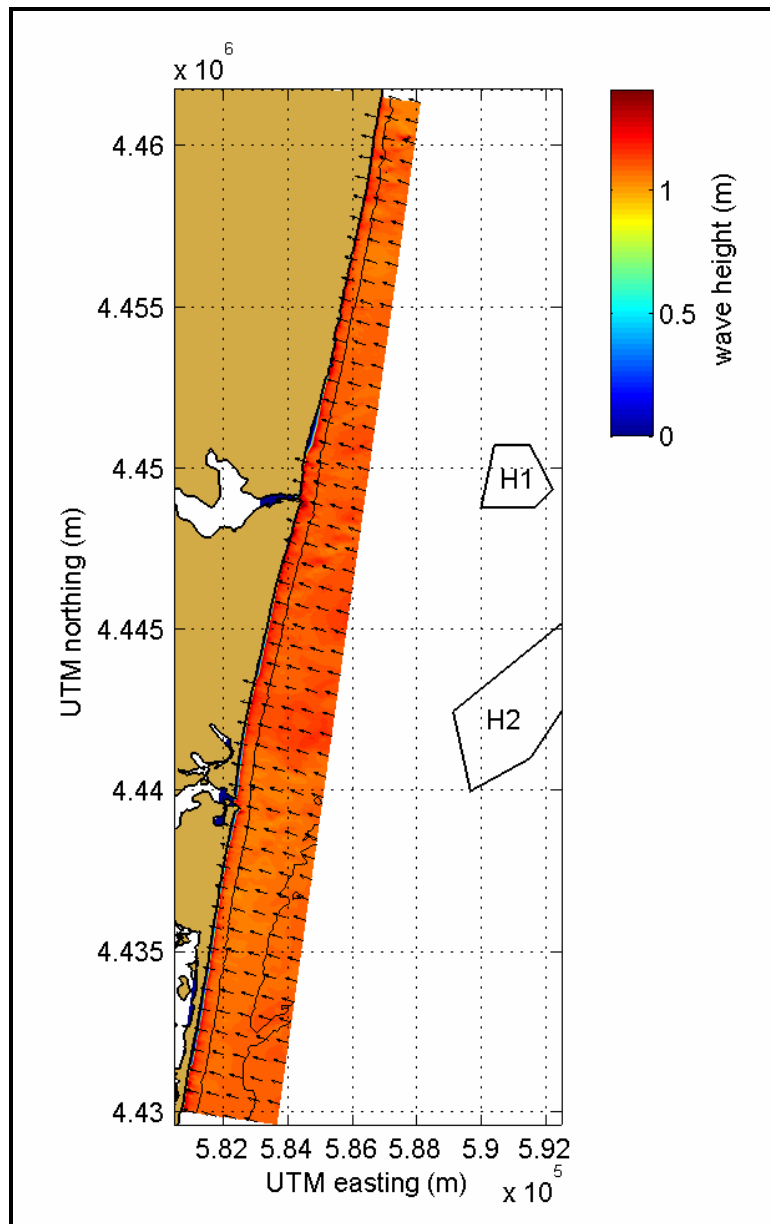


Figure 4-10. STWAVE output for the fine grid (20 x 20 m grid cells) offshore Shark River Inlet in northeastern New Jersey (model case 13B; $H_{m0} = 1.1$ m, $T_p = 7.7$ sec, $\theta_{peak} = 113^\circ$). Color contours indicate H_{m0} wave height. Vectors indicate mean wave direction. Seafloor contours are shown as black lines at a 10-m interval.

Overall, post-dredging wave model output illustrated reduced wave heights landward of borrow sites and increased wave heights at the longshore limits of each borrow site. This effect was enhanced in cases with larger wave heights. As waves propagated across a borrow site (deeper water than the surrounding area), waves refracted away from the center of the borrow site and toward the shallower edges. The net effect was to create a shadow zone of reduced wave energy immediately landward of a borrow site and a zone of increased wave energy updrift and downdrift of a borrow site.

This shadowing effect was apparent in the wave height difference plot presented in Figure 4-11. Color contours represent wave height differences between model results computed for existing and post-dredging conditions. For this particular wave case, maximum wave height reduction occurred landward of Site H1, where wave heights were reduced by 0.06 m. Areas of greatest wave height increase were identified along the northeastern edge of Site H1, where wave heights increased 0.02 m over existing conditions. Wave height changes at Site H2 were smaller, with a maximum wave height reduction of 0.03 m at the northeast extent of the site and a proximate area with a maximum increase of 0.01 m over existing conditions.

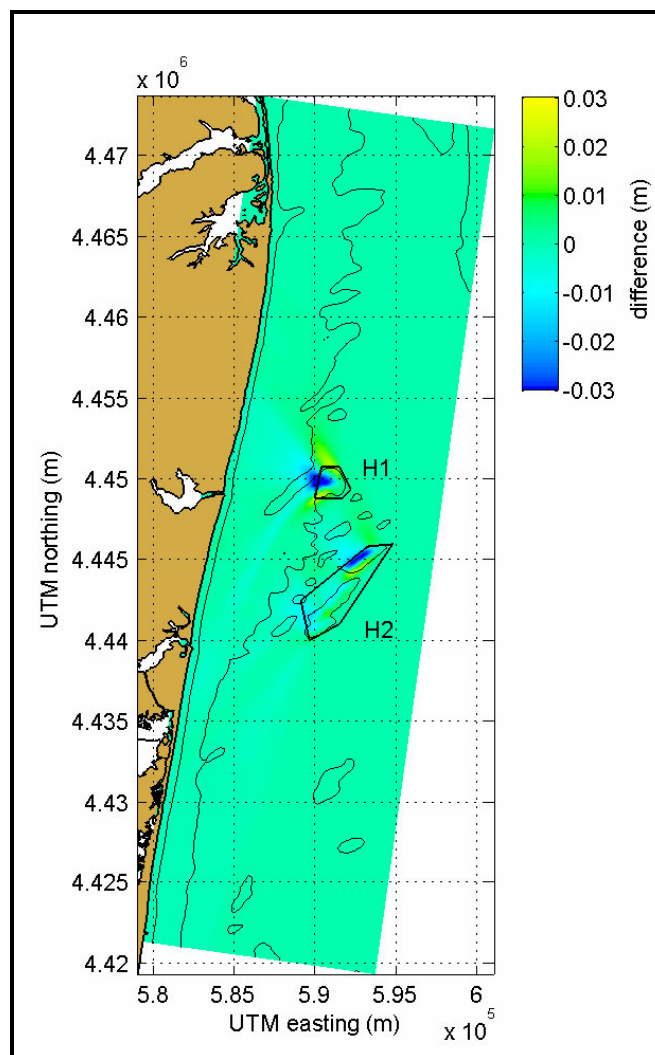


Figure 4-11. Wave height difference plot ($H_{\text{difference}} = H_{\text{post}} - H_{\text{existing}}$) for coarse grid model of offshore Shark River Inlet. Seafloor contours are shown at a 10-m interval.

Because these are spectral wave model results, and because different frequencies in the spectrum are refracted by varying degrees at the borrow sites, areas of increased and reduced wave height gradually diffuse as the wave field approaches shore. This resulted in smaller changes in wave heights close to the shoreline relative to those identified near the borrow sites (Figure 4-12). Another result of the energy diffusion process was that the length of shoreline affected by a borrow site (or combination of borrow sites) can be considerably longer than the borrow site. In Figure 4-12, the length of affected shoreline was approximately three times longer than the along-shore limits of the two borrow sites (i.e., the northern boundary corner of Site H1 and the south corner of Site H2).

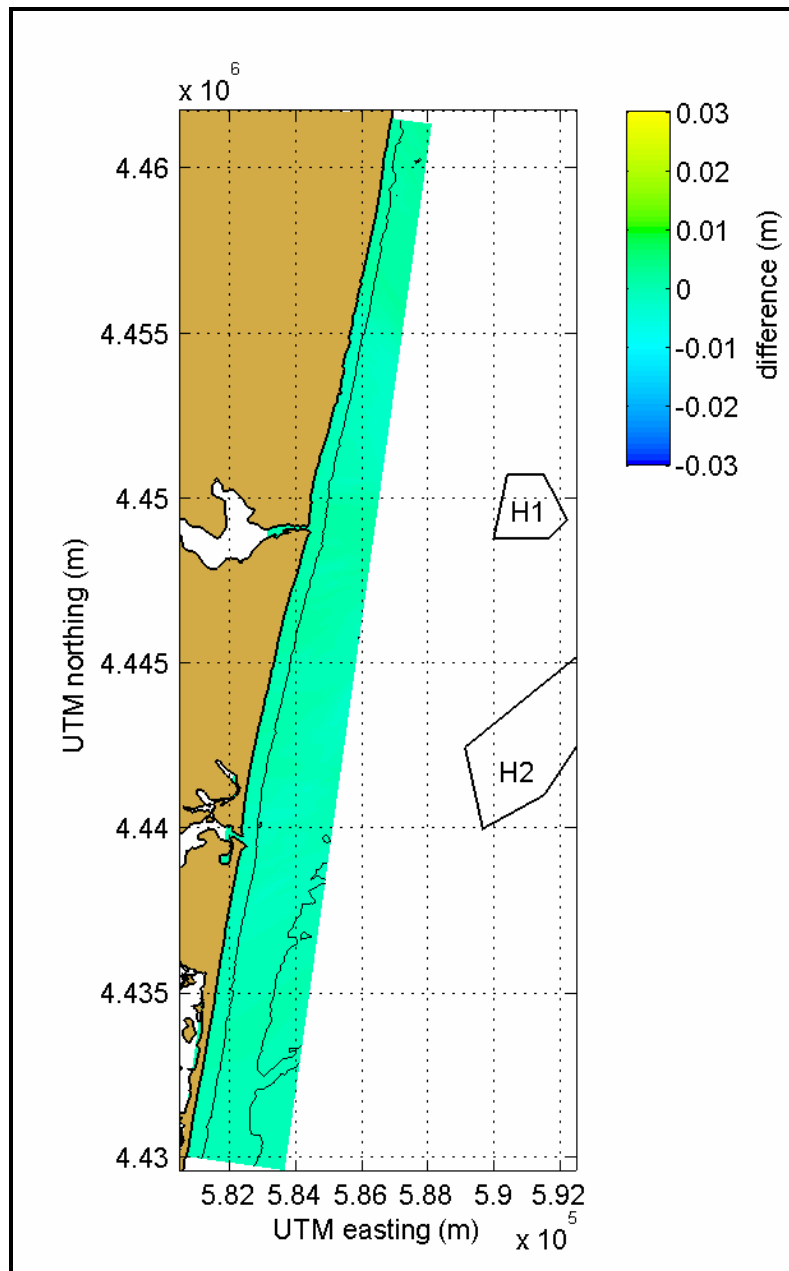


Figure 4-12. Wave height difference plot for fine grid model simulations offshore Shark River Inlet. Seafloor contours are shown at a 10-m interval.

4.2.1.1 Offshore Southwestern Long Island

Examples of wave model output for existing conditions simulations offshore southwestern Long Island (seaward of Jones Inlet) for wave Cases 11A and 14A (Table 4-1) are presented in Figure 4-13 through 4-16. Figure 4-13 illustrates coarse grid results for wave Case 11A ($H_s = 1.3$ m, $T_{peak} = 9.1$ sec, $\theta_{peak} = 112^\circ$). According to the hindcast record, waves from this direction occur 8.2 percent of the time. The shoals encompassed by Borrow Sites 4W and 4E had the greatest influence on waves in the modeled area; however, effects to waves were relatively small because these shoals are located in approximately 17 m water depth. Wave modeling results from wave Case 14A ($H_s = 1.6$ m, $T_{peak} = 9.1$ sec, $\theta_{peak} = 137^\circ$) are illustrated in Figure 4-14. This case has a similar peak wave period, but a slightly greater wave height than Case 11A. Because the wave period is the same for both wave cases, waves refract over offshore shoals similarly. The primary difference between the wave cases is the offshore incident wave angle, which is more shore-normal in Case 14A. As a result, there is less change in wave direction as waves approach the shoreline.

Post-dredging wave height changes at Sites 3, 4W (4 west), and 4E (4 east) are documented in Figures 4-15 and 4-16 for Cases 11A and 14A, respectively. To simulate dredging at borrow sites, seafloor topography within each site was lowered to an isobathic level (-19 m for Site 3, and -20 m for Sites 4W and 4E). By lowering the shoal crest to a constant level, most material is removed near the center of the site. The difference plot in Figure 4-15 is computed by subtracting waves heights for existing conditions from those derived for post-dredging conditions. Therefore, negative difference values indicate areas where wave heights decrease after dredging occurs, and positive differences indicate areas where heights increase after dredging.

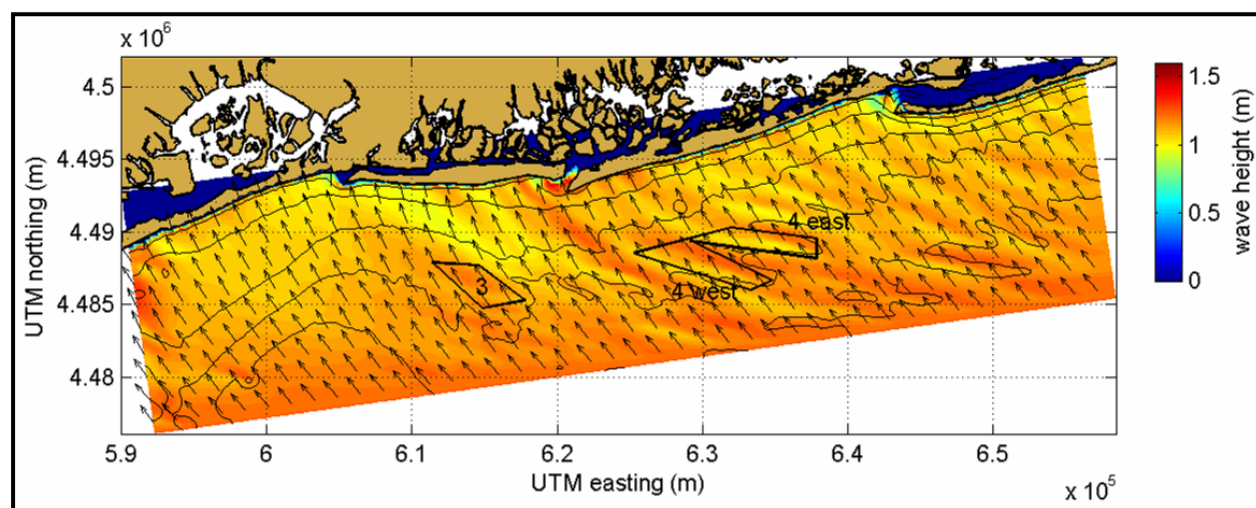


Figure 4-13. STWAVE model output for offshore southwestern Long Island, wave Case 11A ($H_s = 1.3$ m, $T_{peak} = 9.1$ sec, $\theta_{peak} = 112^\circ$). Color contours indicate wave height, and vectors show mean direction of wave propagation. Seafloor contours are shown at 10-m intervals.

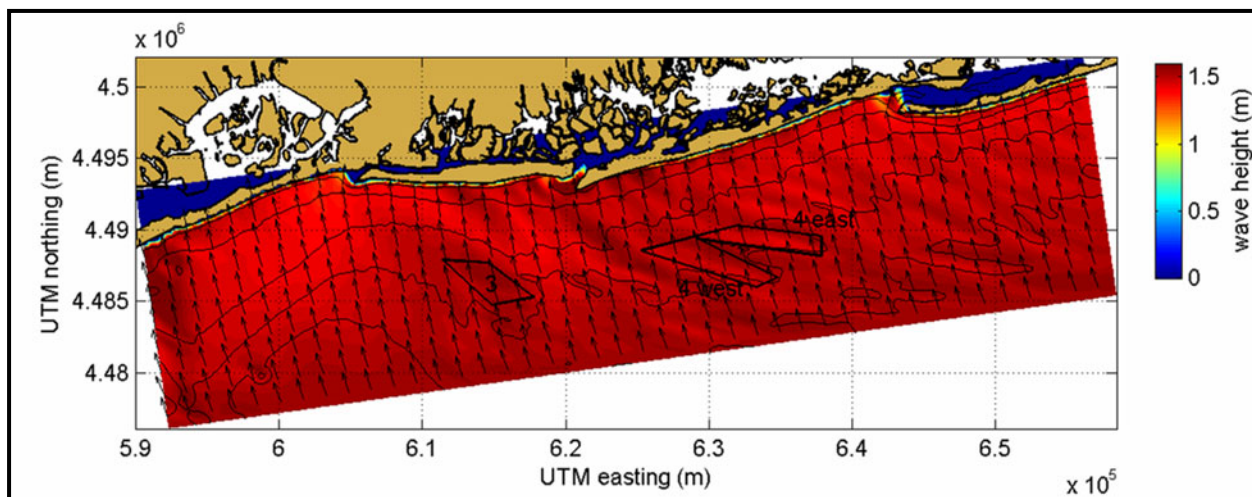


Figure 4-14. STWAVE model output for offshore southwestern Long Island, wave Case 14A ($H_s = 1.6$ m, $T_{peak} = 9.1$ sec, $\theta_{peak} = 137^\circ$). Color contours indicate wave height, and vectors show mean direction of wave propagation. Seafloor contours are shown at 10-m intervals.

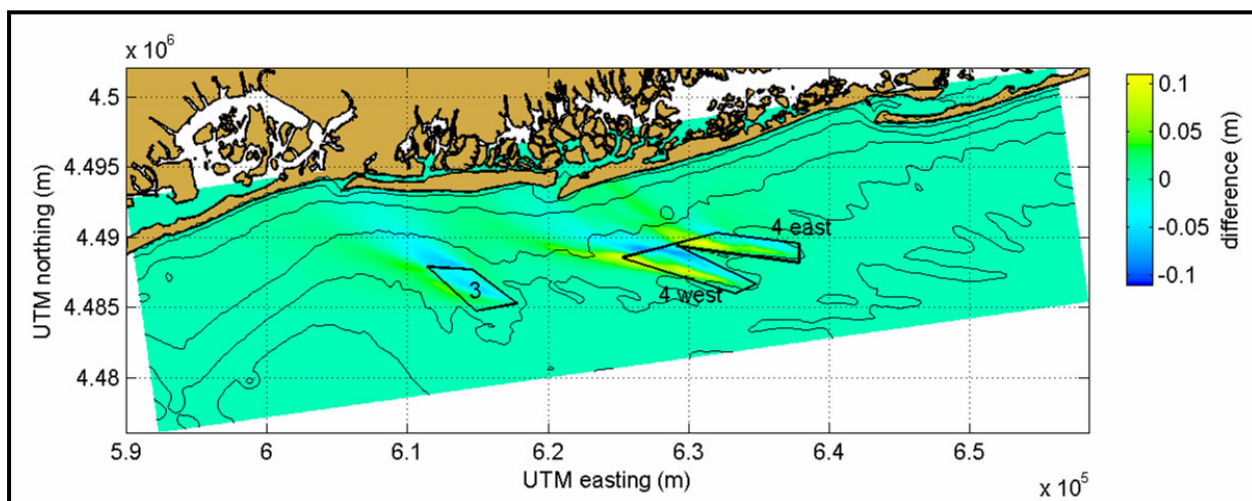


Figure 4-15. Wave height change between existing and post-dredging conditions for offshore southwestern Long Island, wave Case 11A ($H_s = 1.3$ m, $T_{peak} = 9.1$ sec, $\theta_{peak} = 112^\circ$). Seafloor contours are shown at 10-m intervals.

For wave Case 11A, borrow sites have no measurable influence on waves over a long section of coastline (>44 km), but changes on the order of 0.01 m do occur along 20 km of coast in the combined shadow of the three borrow sites (Figure 4-15). At Site 4E, maximum wave height decrease was approximately 0.05 m, and the maximum increase was 0.10 m at the landward boundary of the site. At Site 4W, maximum wave height increase was 0.10 m, and maximum wave height decrease was 0.09 m. Seafloor excavation at Site 3 produced smallest wave height changes for borrow sites offshore southwestern Long Island, with a maximum decrease of 0.06 m and a maximum increase of 0.04 m. Minimal computed changes at Site 3 may be due to the relatively small volume of sand excavated from this site, and because changes in seafloor elevation for post-dredging conditions are less (approximately 2 m change for Site 3, versus 4 m for Sites 4W and 4E).

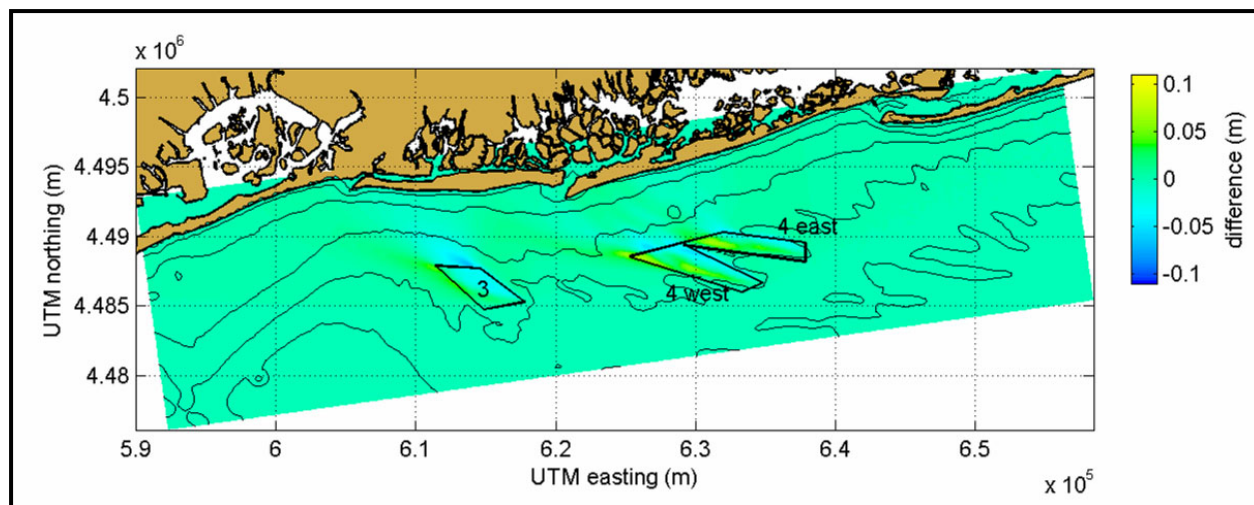


Figure 4-16. Wave height change between existing and post-dredging conditions for offshore southwestern Long Island, wave Case 14A ($H_s = 1.6$ m, $T_{peak} = 9.1$ sec, $\theta_{peak} = 137^\circ$). Seafloor contours are shown at 10-m intervals.

For Case 14A, changes in wave field propagation resulting from dredging at the three offshore borrow sites were smaller than those computed for Case 11A, even though the wave height for this case is larger. This effect may be due to a combination of incident wave angle and directional orientation of shoals upon which borrow sites are located. For Case 11A, the wave approach angle is oriented closer to the centerline axis of the shoal ridge, which causes slightly more wave energy focusing than in Case 14A. The wave shadow zone from these three sites affects approximately 45 km of shoreline, but greatest changes are on the order of 0.01 m and occurs within a 4 km stretch of shoreline at the western extent of Jones Beach (Figure 4-16). At Site 4E, maximum wave height changes range between +0.07 and -0.04 m. At Site 4W, wave height changes are similar in magnitude (+0.07 and -0.05 m). For Borrow Site 3, wave height changes are equivalent to those for Case 11A, with a maximum wave height increase of 0.04 m and a corresponding decrease of 0.06 m.

4.2.1.2 Offshore Northeastern New Jersey

Wave model output for offshore northeastern New Jersey (Borrow Sites H1 and H2) are shown in Figures 4-17 through 4-20. Figure 4-17 shows coarse grid results for wave case 11B, a 1.3 m, 9.1 sec wave propagating from the E; waves from this direction occurred about 2.1 percent of the time. For this wave case, minimal wave focusing was illustrated landward of the shoal field encompassing the designated borrow site boundaries. The approximate minimum water depths at Sites H1 and H2 are 16 and 17 m, respectively. For the shoal at Site H1, maximum wave height increase was 0.13 m due to the focusing effect of the sand ridge. As illustrated in other areas (see Figure 4-9), bathymetric features adjacent to designated borrow sites may affect propagating waves. For the modeled area offshore northeastern New Jersey, a nearshore ridge centered offshore Monmouth Beach has a smaller impact on wave heights compared with the impact from ridges farther offshore. However, shoreline impacts from this nearshore feature are potentially more significant than the impact from offshore shoals at the borrow sites because it is closer to shore and its area of influence is not as diffuse along the shoreline.

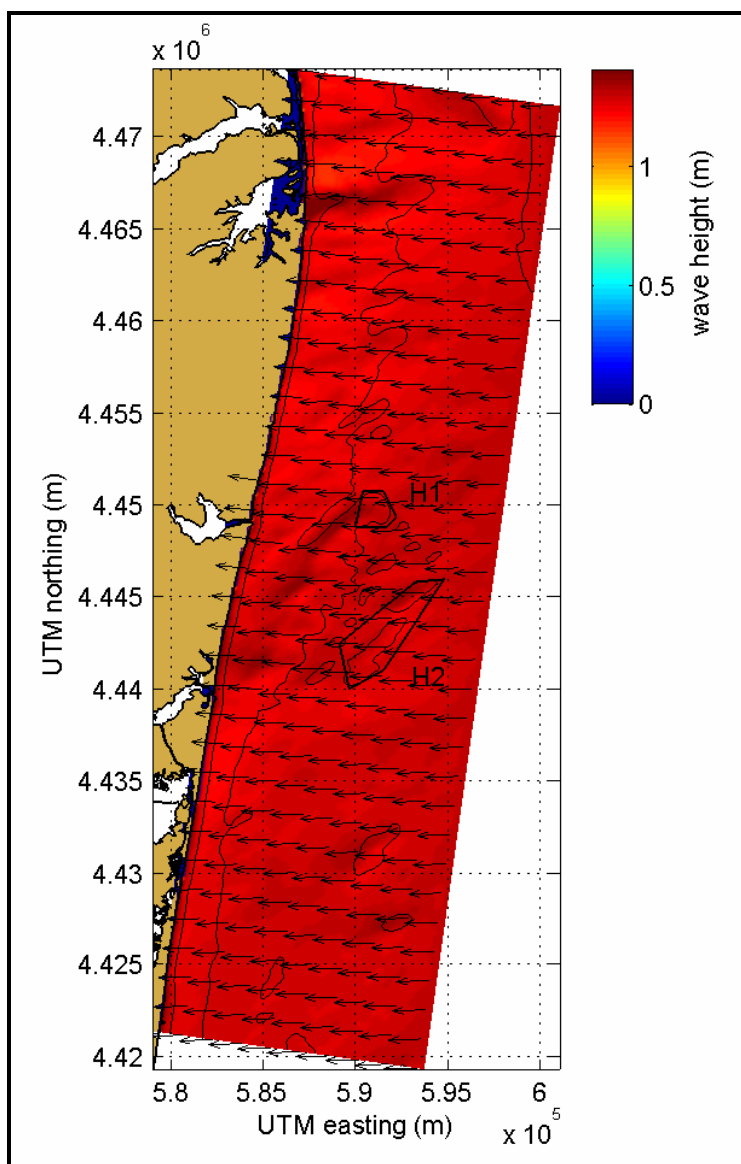


Figure 4-17. STWAVE output for offshore northeastern New Jersey, wave Case 11B ($H_s = 1.3$ m, $T_{peak} = 9.1$ sec, $\theta_{peak} = 88^\circ$). Color contours indicate wave height, and vectors show mean direction of wave propagation. Bottom contours are also shown at 10-m intervals.

For wave Case 16B (a 1.3 m, 7.7 sec wave propagating from the SSE), wave height changes at Sites H1 and H2 are not as pronounced as those for Case 11B (Figure 4-18). The primary reason for this difference is that offshore bathymetry has less effect on wave focusing for shorter peak period incident waves. Closer to shore in shallower water, approaching waves eventually are influenced by the seafloor as they refract to a more shore normal angle.

Wave height differences resulting from numerically excavating Sites H1 and H2 are illustrated in Figure 4-19 for wave Case 11B. Wave height changes along the shoreline are relatively small and diffuse, and wave height changes at the modeled shoreline are less than 0.01 m. At Site H1, maximum changes in wave height ranged from -0.06 to +0.04 m. At Site H2, maximum wave heights changes decreased by 0.05 m and increased by 0.03 m. Overall, wave height changes were quite small relative to natural wave height variability.

Wave height changes for Case 16B (Figure 4-20) indicate that borrow sites have an overlapping influence at the shoreline for waves propagating from the SSE. Similar to the results of Case 11B, wave height changes at the shoreline relative to potential offshore sand dredging are never greater than 0.01 m. Wave height changes at borrow sites are smaller than those for Case 11B, primarily due to a shorter wave period for Case 16B. Site H1 resides within the wave shadow zone for Site H2, but wave height changes remain relatively small. At Site H1, maximum wave height changes range from +0.04 to -0.04 m; at Site H2, maximum changes were half this magnitude (+0.02 to -0.02 m).

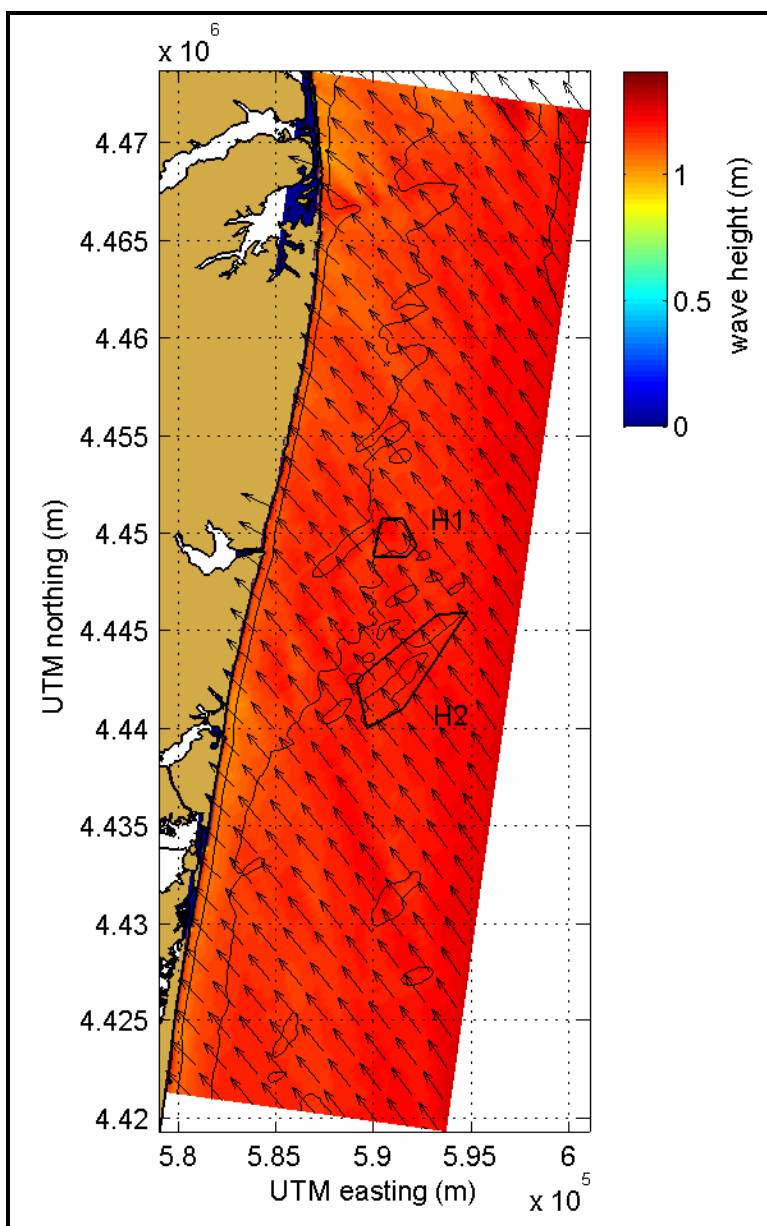


Figure 4-18. STWAVE output for offshore northeastern New Jersey, wave Case 16B ($H_s = 1.3$ m, $T_{peak} = 7.7$ sec, $\theta_{peak} = 158^\circ$). Color contours indicate wave height, and vectors show mean direction of wave propagation. Bottom contours are also shown at 10-m intervals.

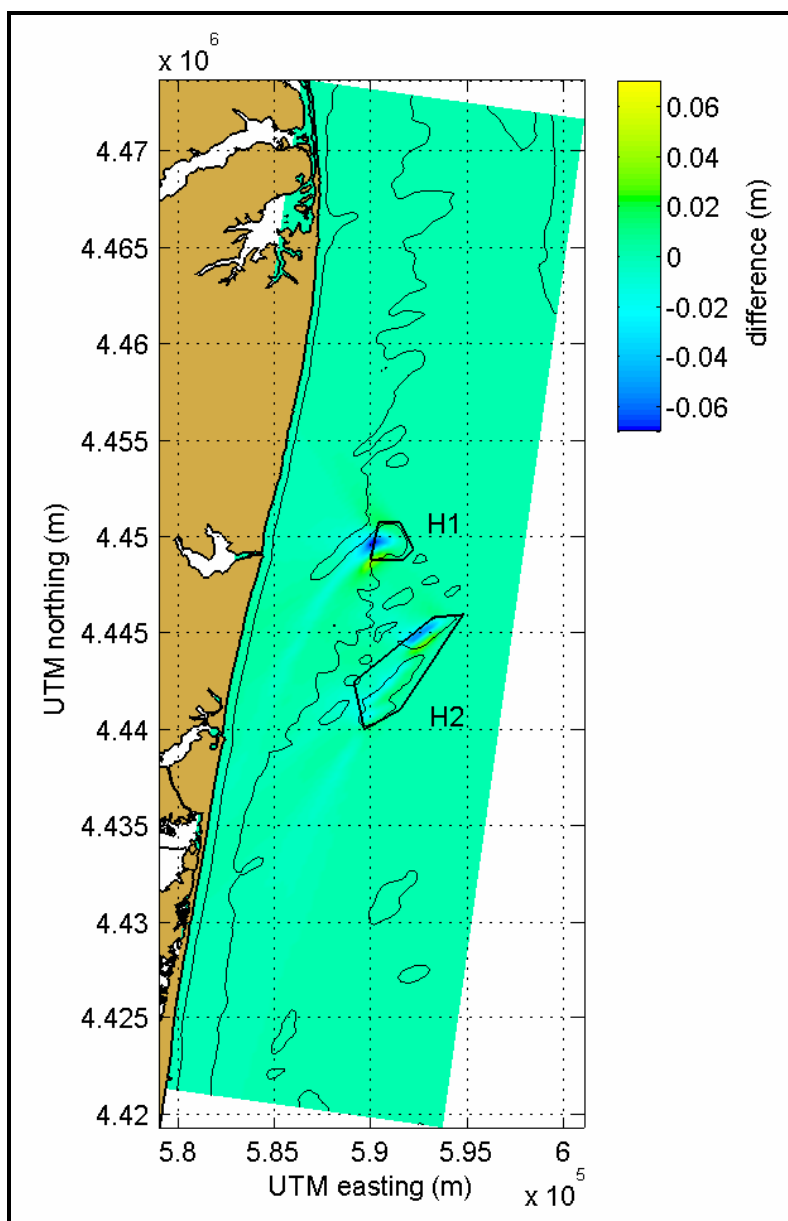


Figure 4-19. Wave height change between existing and post-dredging conditions for offshore northeastern New Jersey, wave Case 11B ($H_s = 1.3$ m, $T_{peak} = 9.1$ sec, $\theta_{peak} = 88^\circ$). Seafloor contours are shown at 10-m intervals.

4.2.2 Sediment Transport Potential

Comparisons of average annual sediment transport potential were performed for existing and post-dredging conditions to document the relative impact of dredging at borrow sites on longshore sediment transport processes. Sediment transport potential is a useful indicator of shoreline impacts caused by offshore borrow sites because the computations include the borrow site influence on wave height and direction. Though largest changes to the wave field occur at a borrow site, impacts cannot be adequately assessed without determining the resulting impact to coastal processes at the shoreline. As an example, a large borrow site that causes a large change in wave height at the site, but is far offshore, could have less shoreline impact than a much smaller site located closer to shore.

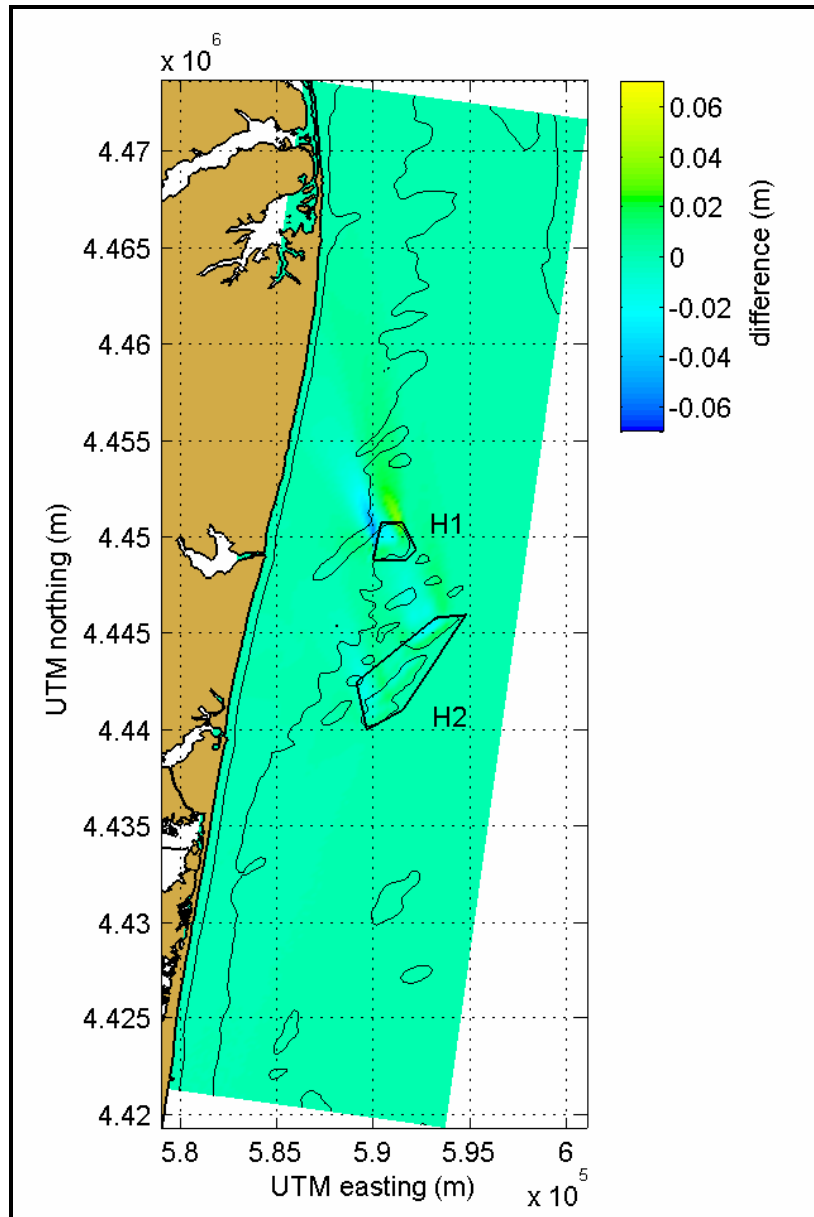


Figure 4-20. Wave height change between existing and post-dredging conditions for offshore northeastern New Jersey, wave Case 16B ($H_s = 1.3$ m, $T_{peak} = 7.7$ sec, $\theta_{peak} = 158^\circ$). Seafloor contours are shown at 10-m intervals.

Net sediment transport potential associated with average annual conditions (Tables 4-1 and 4-2) was computed for shorelines landward of proposed sand borrow sites. Transport potential was computed using fine grid model results. In addition to the average annual results, wave model simulations and sediment transport potential calculations were performed for 20 individual years of the OCTI wave hindcast data to provide information necessary to develop a $\pm 0.5\sigma$ significance envelope. Wave modeling for 20 individual years proceeded in a similar fashion to the modeling effort for average annual conditions (i.e., wave data for each separate year was binned according to direction and period to develop several wave cases for each year). For this study, more than 1200 individual wave model runs were completed to determine average annual conditions and associated transport significance envelopes.

Mean sediment transport potential calculated for offshore southwestern Long Island for the modeled 20-year period is shown with computed transport curves for the 20 individual years used to determine the $\pm 0.5\sigma$ significance envelope (Figures 4-21). The beaches east of Jones Inlet indicated net westerly transport ranging from about 54,000 m³/yr at Fire Island Inlet to 170,000 m³/yr at Jones Inlet. Along Long Beach, net westerly transport increased from about 50,000 m³/yr west of Jones Inlet to a maximum of about 150,000 m³/yr at the approximate mid-point of the barrier beach, before decreasing to about 88,000 m³/yr at East Rockaway Inlet. Net transport was always west directed for the modeled shoreline reach, and the transport significance envelope for 20 individual years of wave data ranged from a maximum of about 290,000 m³/yr along the western end of Jones Beach and central Long Beach to about 125,000 m³/yr along eastern Jones Beach. For the length of the modeled shoreline, the single year with the least modeled net westerly transport was 1988, and the year with the greatest westerly transport potential was 1995.

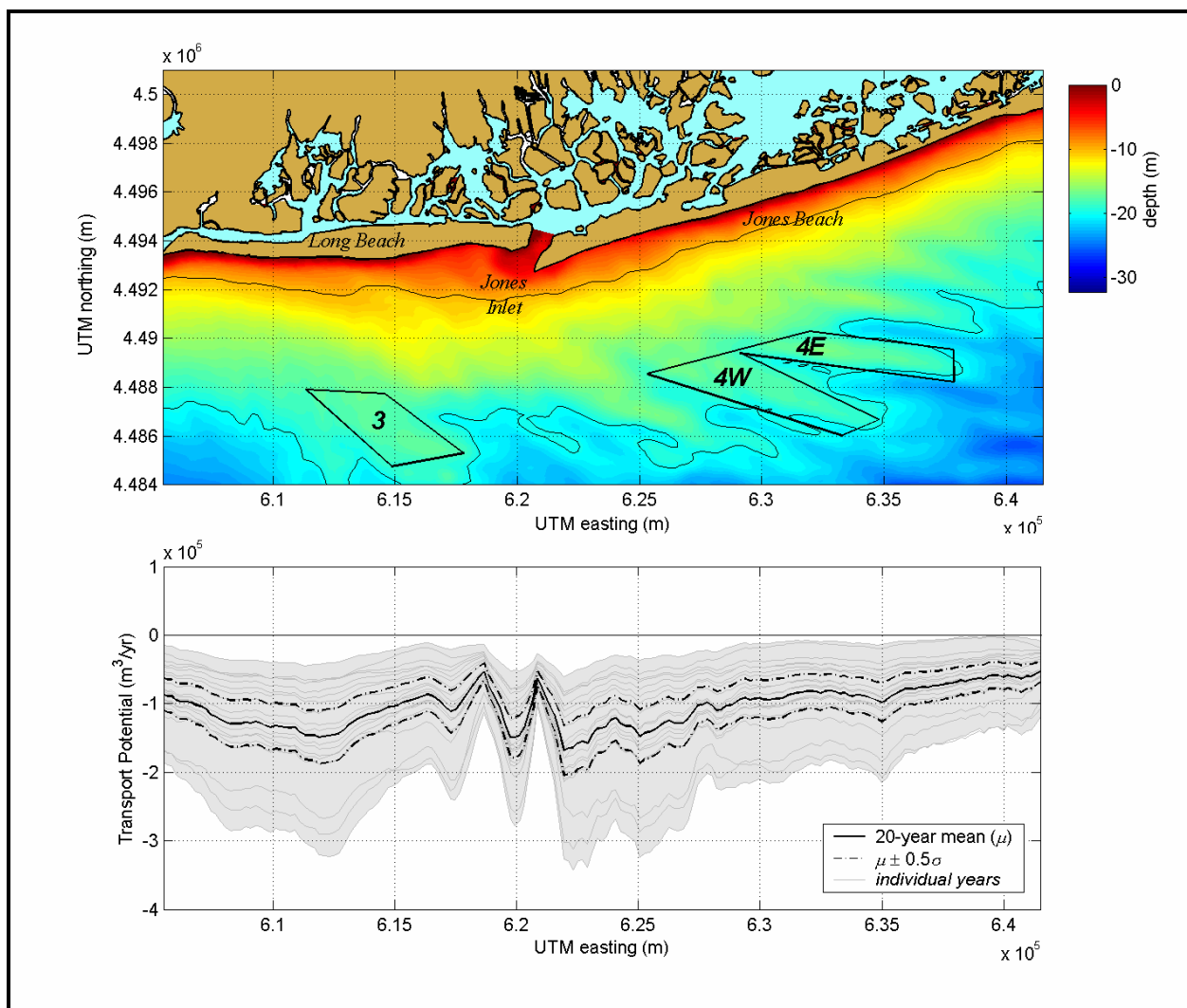


Figure 4-21. Average annual sediment transport potential (solid black line) computed for the shoreline landward of Borrow Sites 3, 4W, and 4E. Net transport potential curves determined for 20 individual years of wave hindcast data are indicated by the gray shaded area. The $\pm 0.5\sigma$ significance envelope (black dot-dash lines) about the mean net transport was determined using the 20 net potential curves.

Average annual transport results along the shoreline landward of Borrow Sites 3, 4W, and 4E documented gross westerly- and easterly-directed transport potential, with average net transport, for the 20-year modeled period (Figure 4-22). The modeled shoreline had an overwhelming gross westerly transport, with a maximum gross easterly transport potential of 20,000 m³/yr. Maximum gross easterly transport occurred about 3 km west of Jones and Fire Island Inlets.

Mean sediment transport potential along the northeast coast of New Jersey for the modeled 20-year period is shown with computed transport curves for the 20 individual years used to determine the $\pm 0.5\sigma$ significance envelope (Figure 4-23). Results indicated that the dominant transport direction was determined to be net northerly but more bi-directional for shorter term annual results. There was an approximate $\pm 55,000$ m³/yr range in annual net transport rates. Long-term potential transport rates reached a maximum of approximately 30,000 m³/yr within the modeled study area, and a minimum occurred just north of Shark River Inlet. Results of transport potential calculations indicated that the year with the greatest net southerly transport was 1987, and the year with the greatest northerly directed transport was 1995.

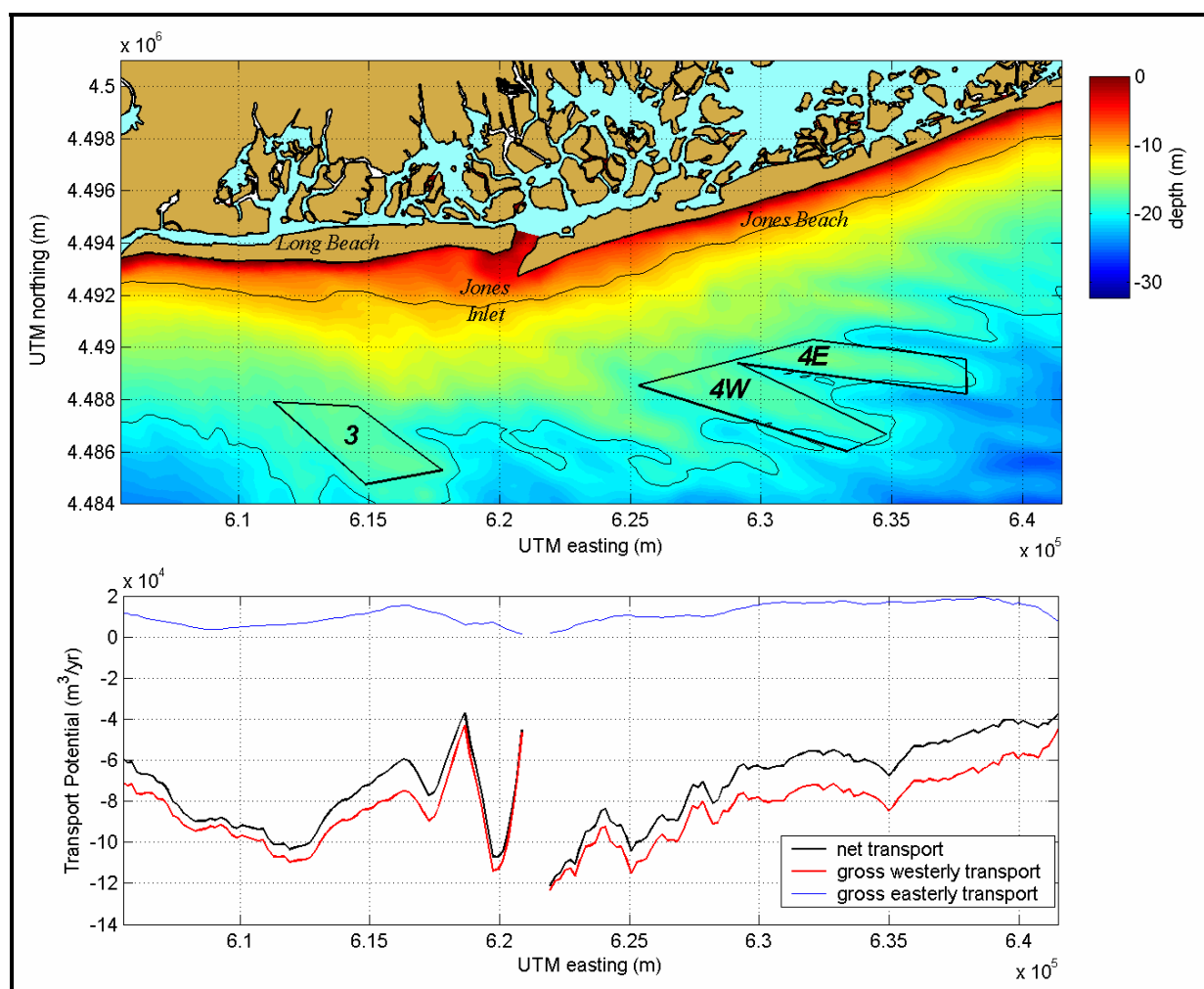


Figure 4-22. Average net transport potential (black line) with gross westerly- and easterly-directed transport potential (red and blue lines, respectively) for the shoreline landward of Borrow Sites 3, 4W, and 4E.

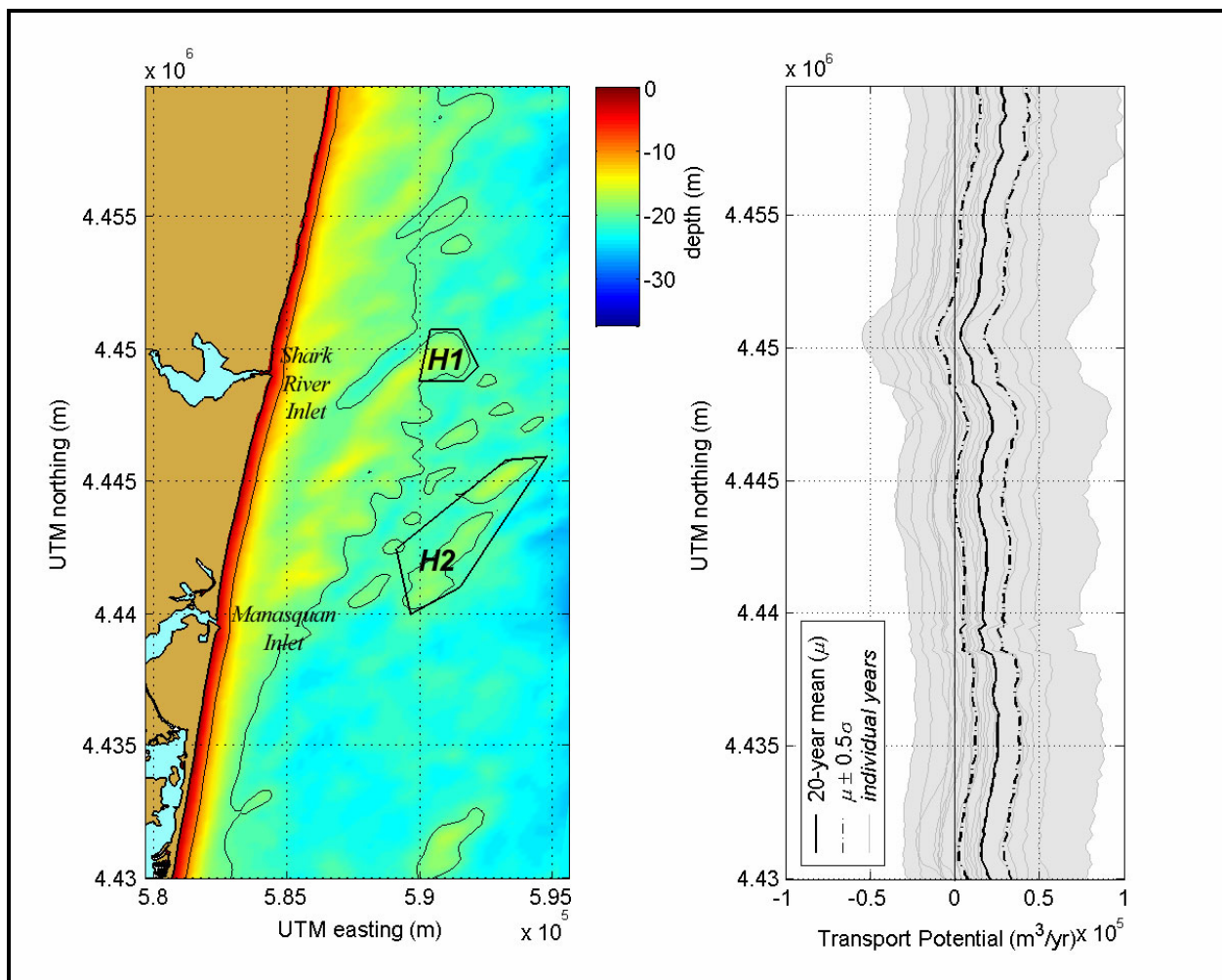


Figure 4-23. Average annual sediment transport potential (solid black line) computed for the shoreline landward of Borrow Sites H1 and H2. Net transport potential curves determined for 20 individual years of wave hindcast data are indicated by the gray shaded area. The $\pm 0.5\sigma$ significance envelope (black dot-dash lines) about the mean net transport was determined using the 20 net potential curves.

Average annual results for the northeast New Jersey coast show the breakdown of gross northerly- and southerly-directed transport potential, with average net transport, for the total 20-year modeled period (Figure 4-24). The transport potential along this stretch of coast is more bi-directional than the modeled southwestern Long Island shoreline. Total gross transport potential along the modeled northeast New Jersey shoreline is approximately 100,000 m^3/yr , though average transport potential is nearly an order of magnitude smaller.

Results presented in Figures 4-23 and 4-24 indicate that this region falls within the *nodal zone* that exists along the northeastern New Jersey shoreline. Within this section of coast, sediment transport ranges from southerly in the south to northerly along most of the coast north of Manasquan Inlet. Location of the nodal zone has been described by Ashley et al. (1986) and others (see Section 3.0). A range of positional estimates for the nodal zone exists along the 96 km stretch of shoreline between Beach Haven Inlet (south) and Monmouth Beach (north).

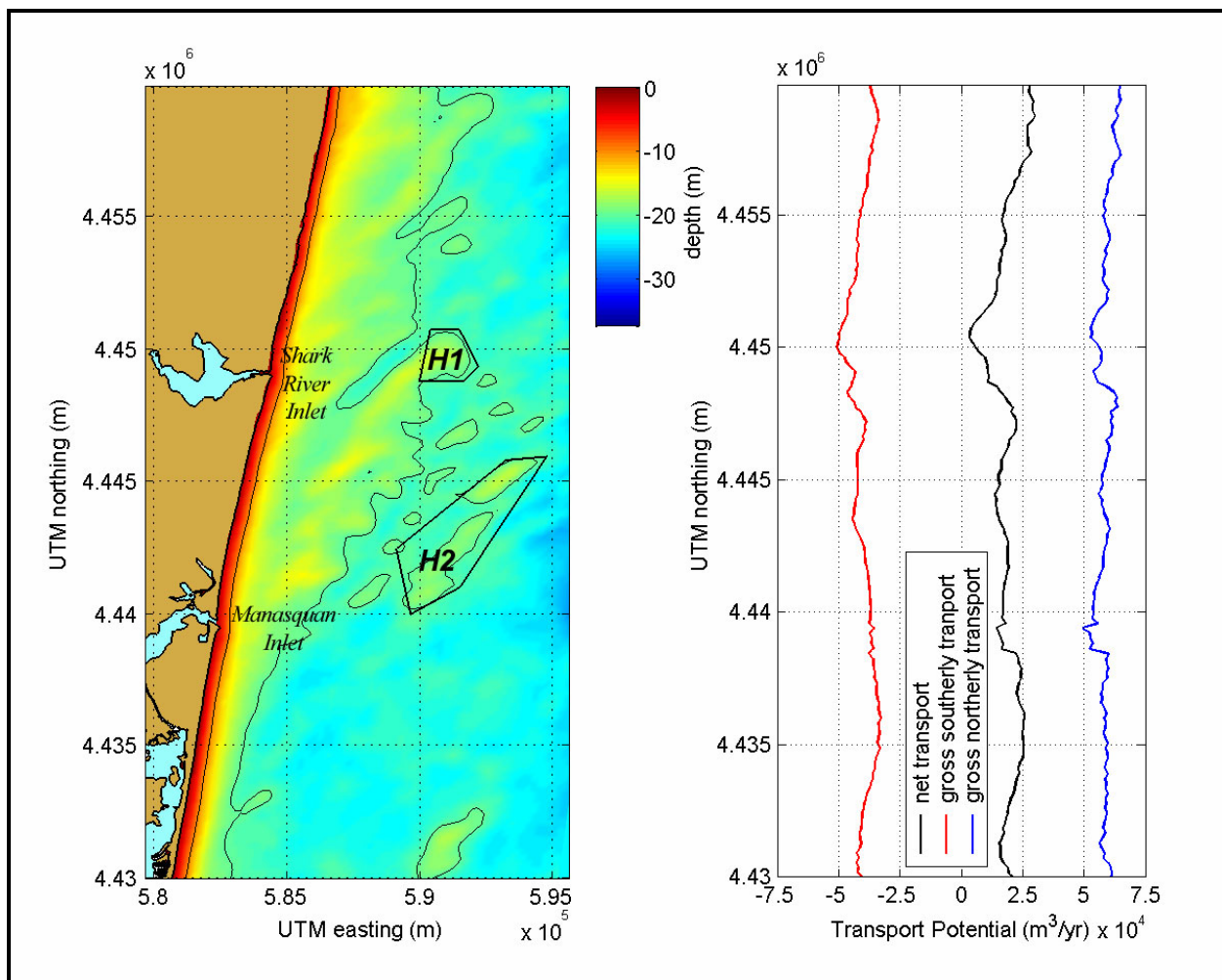


Figure 4-24. Average net transport potential (black line) with gross southerly- and northerly-directed transport potential (red and blue lines, respectively) for the shoreline landward of Borrow Sites H1 and H2.

4.2.2.1 Model Comparison with Historical Shoreline Change

To ensure that spectral wave modeling and associated longshore sediment transport potential could be used effectively to evaluate long-term alterations to the littoral system, a comparison of model predictions with observed shoreline change was performed. This analysis provided a semi-quantitative method for determining whether a) wave-induced longshore transport was responsible for observed shoreline change, and b) long-term shoreline change trends were consistent with shorter time-period (20-year) sediment transport potential analyses. An evaluation of model output was performed using a comparison of computed gradients in sediment transport to historical shoreline change data. The basis for this comparison is the relationship between shoreline movement and the longshore gradient in sediment transport. Simply expressed, this relationship is

$$\frac{\partial Q}{\partial y} \propto \frac{\partial x}{\partial t} \quad (4.9)$$

where Q is sediment transport, y is along-shore distance, x is cross-shore position of the shoreline, and t is time. A comparison of results should illustrate similar trends in long-term shoreline change and transport potential computed using wave conditions that represent long-term average conditions. The gradient in sediment transport potential was not expected to perfectly simulate this process, but good general agreement between these two quantities would suggest that the transport potential model reasonably represented long-term coastal processes for a given area, and thus, the model's ability to predict likely impacts that may result from offshore dredging.

The time variation in shoreline position was determined from an analysis of historical shoreline data for each of the study areas. Regional change analysis provided a without-project assessment of shoreline response for comparison with predicted changes in wave-energy focused at the shoreline resulting from potential offshore sand dredging activities. Because continuous measurements of historical shoreline change are available at 30-m along-shore intervals (see Section 3.0), model results (wave and sediment transport) at discrete intervals along the coast can be compared with historical data to develop process/response relationships for evaluating potential impacts.

For southwestern Long Island beaches, long-term shoreline change data covering the period 1878 to 1997 were used to quantify trends (see Section 3.0). Along-shore variations in sediment transport were determined using computed sediment transport potential for each shoreline for modeled and existing conditions. Difficulties with comparisons arise with modeled shorelines due to long histories of extensive beach nourishments and shoreline development, particularly for the Jones Beach shoreline (Kana, 1999 and USACE, 2003).

A comparison between measured shoreline change and the modeled sand transport gradient for the southwestern Long Island shoreline is shown in Figure 4-25. Trends in historical shoreline change on Long Beach generally agree with modeled transport gradients. Long-term shoreline change rates indicate that the beach landward of Borrow Site 3 ranges from erosional (approximately 2 m/yr) near Jones Inlet to accreting (approximately 5 m/yr) along the western end of Long Beach. The computed gradient in sediment transport potential illustrated greater erosion near Jones Inlet, and a gradual increase in accretion along western Long Beach. Along Jones Beach (i.e., the shoreline from Jones Inlet to Fire Island Inlet), a comparison between shoreline change data and model output of the transport gradient is more complicated. Difficulties arise due to large nourishment projects along this shoreline, including a $31 \times 10^6 \text{ m}^3$ nourishment in 1927 (Kana, 1999) and a series of four relic inlets that have existed on Jones Beach in the past 120 years (Smith and Leatherman, 2000).

For offshore northeastern New Jersey, shoreline change data for the period 1855/75 to 1933 were compared with the computed gradient in sediment transport potential. Long-term and short-term shoreline change rates indicate that the modeled area is stable-to-erosional, with change rates generally less than 1 m/yr (Figure 4-26). The computed gradient in sediment transport potential indicates a relatively stable shoreline, with few areas of significantly different change rates than background. A couple of exceptions include a small erosional peak at Manasquan Inlet and an erosional area downdrift (north) of Shark River Inlet, which roughly correspond to areas of increased erosion in the shoreline change data set.

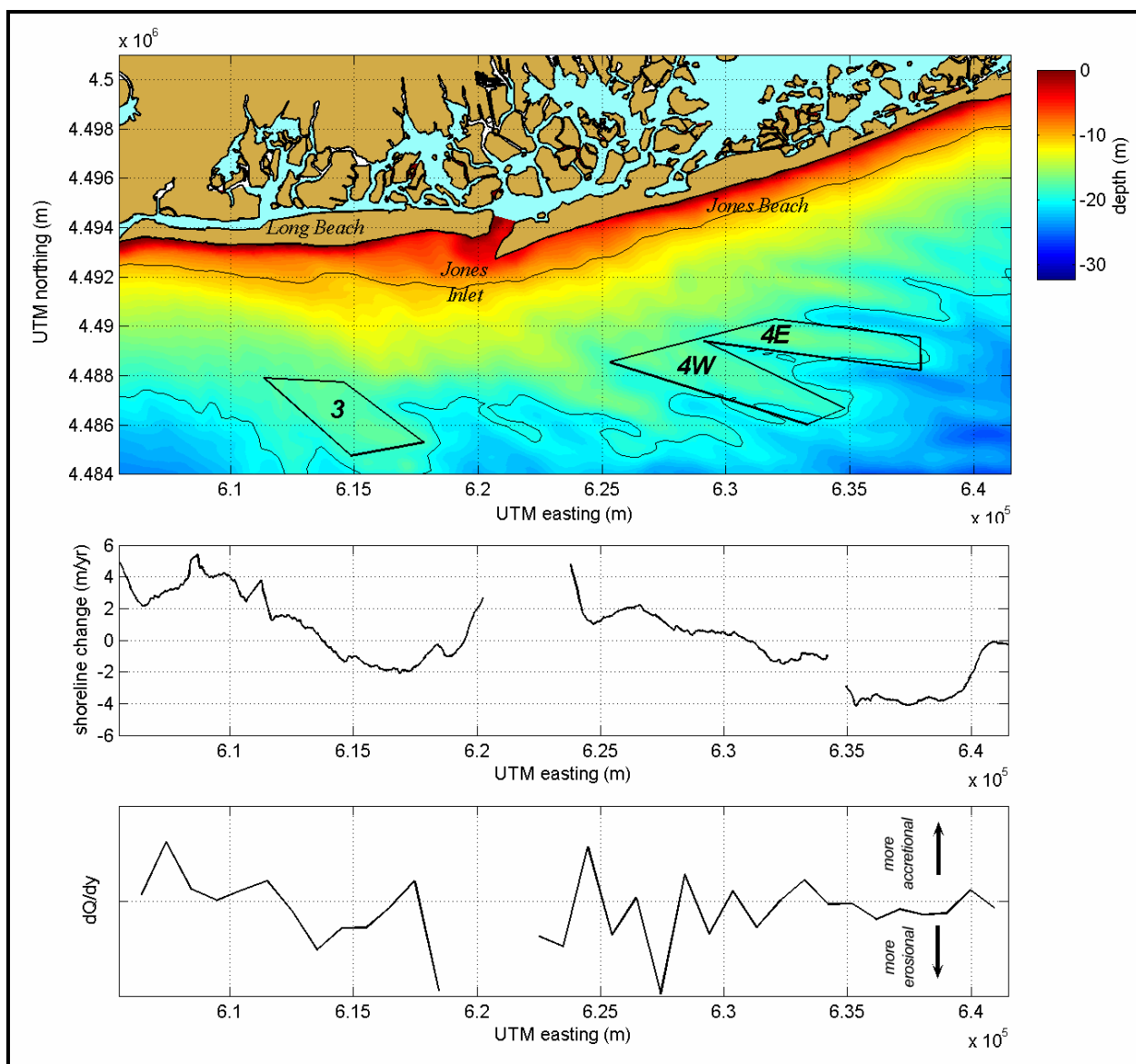


Figure 4-25. Historical shoreline change and gradient of modeled transport potential (dQ/dy) for the modeled shoreline landward of Sites 3, 4W, and 4E offshore southwestern Long Island. The middle plot illustrates measured shoreline change for the period 1878 to 1997. The gradient in transport potential was determined using the total net transport computed using 20 years of wave hindcast data.

4.2.2.2 Significance of proposed dredging

The significance of changes to longshore transport along the modeled shoreline resulting from dredging proposed borrow sites to their maximum design depths was determined using the method described in Kelley et al. (2004). For each modeled area, dredging impact significance was determined using several wave model runs in addition to the runs executed to determine the magnitude of borrow site impacts from existing to post-dredging conditions. Twenty 1-year periods were run for each area using the same directional binning as existing and post-dredging runs. Sediment transport potential was computed for each 1-year period. The standard deviation of transport potential then was computed at each grid node, providing an estimate of annual variability in sediment transport potential along the shoreline. As such, this method

incorporated the temporal and spatial variability of transport potential along the modeled shoreline. The criterion for determining dredging significance was one-half of a standard deviation ($\pm 0.5\sigma$). For modeled borrow site impacts that exceed this limit, the borrow site would be rejected as designed.

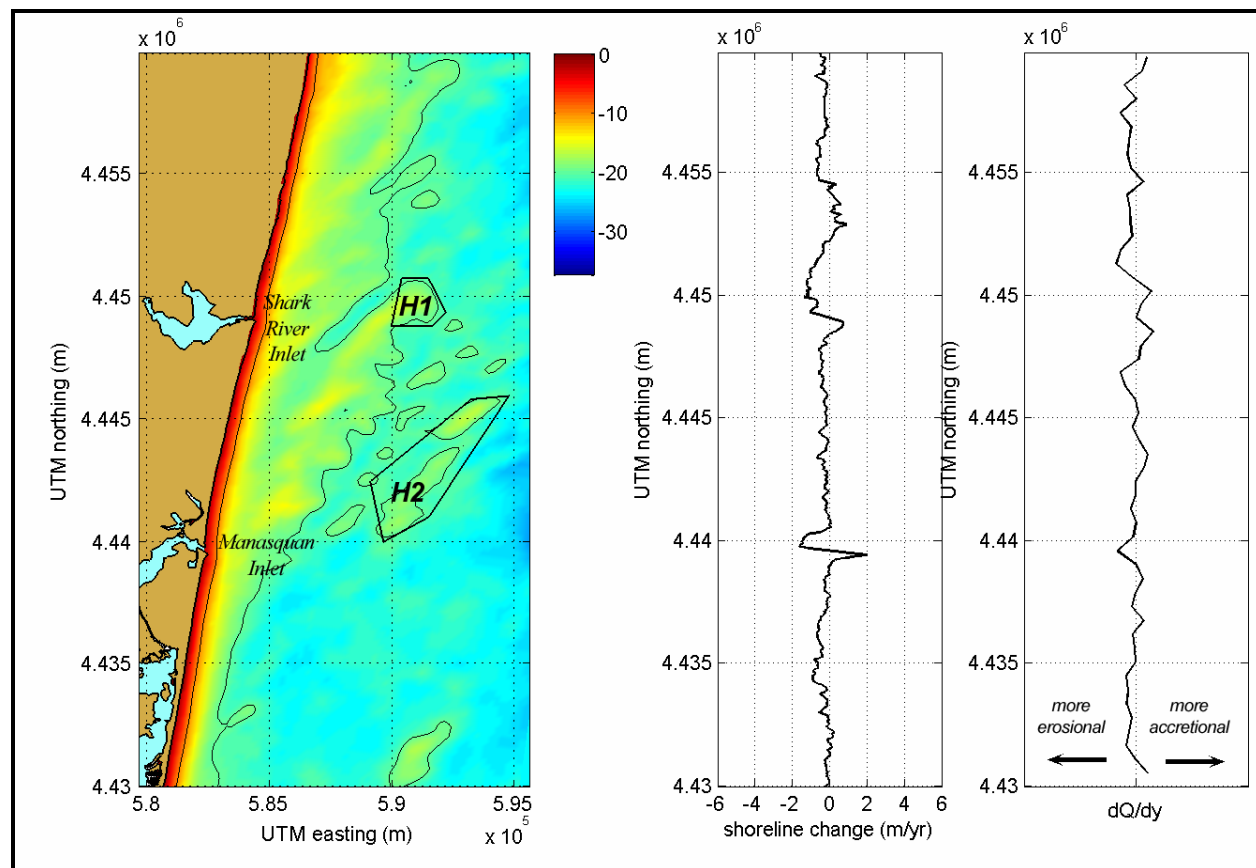


Figure 4-26. Historical shoreline change and gradient of modeled transport potential (dQ/dy) for the modeled shoreline landward of Sites H1 and H2 offshore northeastern New Jersey. The middle plot illustrates measured shoreline change for the period 1855/75 to 1933. The gradient in transport potential was determined using the total net transport computed using 20 years of wave hindcast data.

Results of the significance analysis for borrow sites offshore southwestern Long Island indicated that the $\pm 0.5\sigma$ significance envelope increased along Jones Beach from $\pm 20,000 \text{ m}^3/\text{yr}$ at Fire Island Inlet to $\pm 40,000 \text{ m}^3/\text{yr}$ at Jones Inlet (Figure 4-27). The significance envelope for Long Beach had a similar range, with a maximum value midway between Jones Inlet and East Rockaway Inlet. Potential dredging impacts to longshore transport rates from excavation at Sites 3, 4W, and 4E are well within the transport significance envelope. As such, proposed dredging at these sites would not result in significant modifications to coastal processes along this shoreline. Potential dredging impacts are computed by subtracting the transport potential curve computed for existing seafloor conditions from the potential computed for post-dredging conditions. Largest calculated differences between existing and post-dredging transport potential occur east of Jones Inlet, where the transport rate becomes more westerly by $3,000 \text{ m}^3/\text{yr}$. The resulting change is negligible, even though offshore sand extractions are large

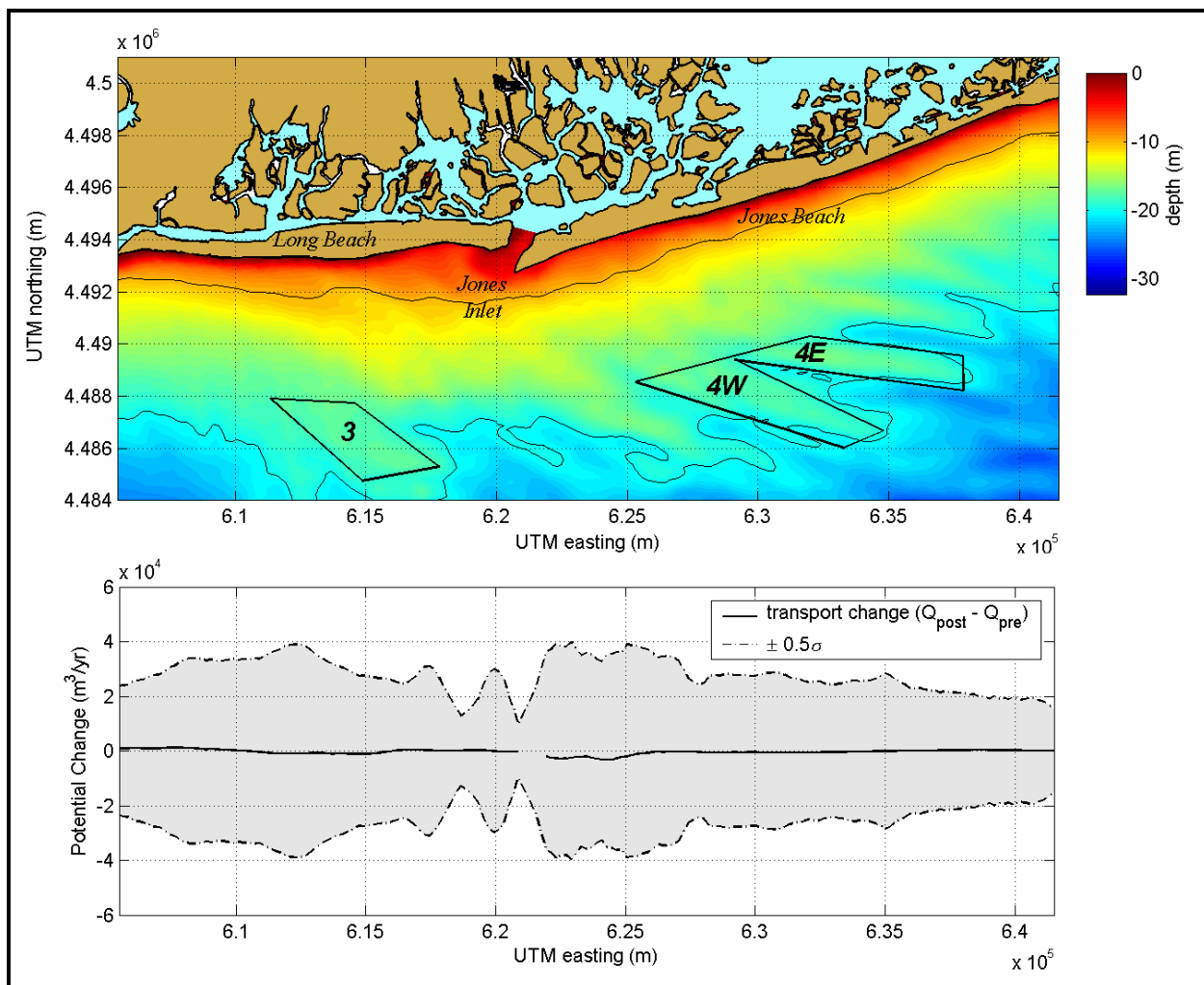


Figure 4-27. Transport potential difference between existing and post-dredging conditions, with transport significance envelope for the shoreline landward of Borrow Sites 3, 4W, and 4E. Negative change indicates that the post-dredging transport potential is more southerly than the computed existing transport potential.

(i.e., a total dredged volume of $48 \times 10^6 \text{ m}^3$ for all three sites). Shoreline impacts are negligible due to the relatively deep water at potential borrow sites (19 m for Site 3 and 20 m for Sites 4W and 4E), their distance offshore, and wave climate (dominated by relatively short-period waves).

Results of the impact significance analysis for sites offshore northeastern New Jersey indicated that the $\pm 0.5\sigma$ significance envelope computed for this area was generally constant at $\pm 15,000 \text{ m}^3/\text{yr}$ (Figure 4-28). Impacts from dredging Sites H1 and H2 are well within the significance envelope, and proposed sites would be acceptable under the simulated conditions. Similar to sites offshore Long Island, potential shoreline impacts were negligible due to the relatively deep water at potential borrow sites (20 m for Sites H1 and H2), their distance offshore, and wave climate (dominated by relatively short-period waves).

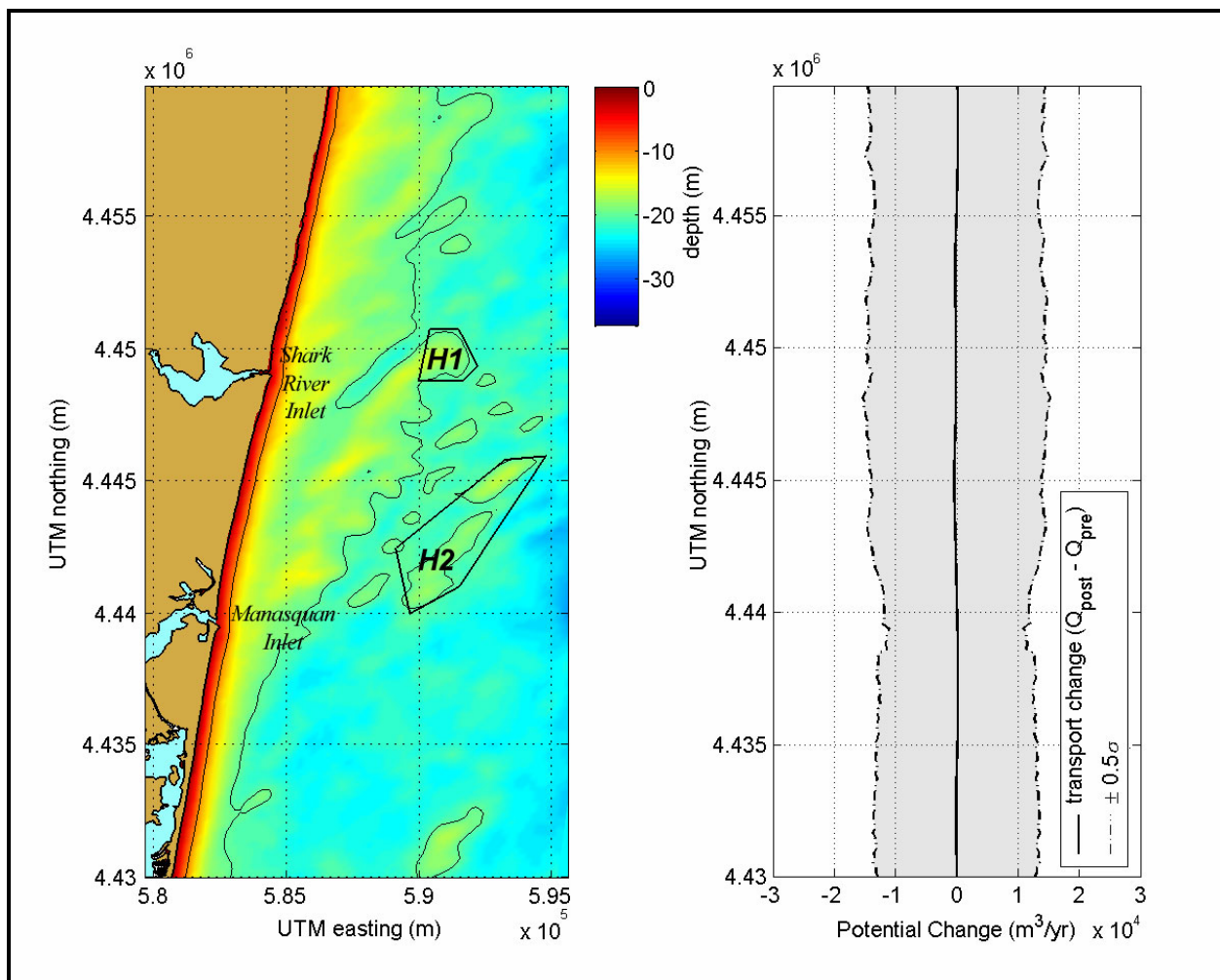


Figure 4-28. Transport potential difference between existing and post-dredging conditions, with transport significance envelope for the shoreline landward of Borrow Sites H1 and H2. Negative change indicates that the post-dredging transport potential is more southerly than the computed existing transport potential.

4.3 SUMMARY

This section documented results of wave modeling and sediment transport potential computations performed to assess the significance of impacts that may result from dredging sand at five proposed borrow sites offshore northeastern New Jersey and southwestern Long Island. STWAVE simulated how wave fields were modified by bathymetry. Dominant wave conditions were developed using a 20-year wave hindcast performed specifically for this study at stations offshore investigated borrow sites. The same wave conditions were run for existing and post-dredging conditions. Wave model output was then used to determine sediment transport potential along the entire shoreline. Along-shore variations in the computed gradient of sand transport were compared to measured shoreline change to ensure that spectral wave modeling and associated longshore sediment transport potential could be used effectively to evaluate long-term alterations to the littoral system.

Once the change in sediment transport potential was determined for existing and post-dredging conditions, the significance of these changes was evaluated by applying a criterion

developed by Kelley et al. (2004) based on the natural temporal and spatial variability of sediment transport along a modeled coastline. Each of the 20 years in the wave hindcast record were modeled individually to determine the significance criterion envelope. The standard deviation of sediment transport potential then was computed for each modeled area. A determination of dredging significance was made by comparing predicted change in transport potential between existing and post-dredging conditions to a significance envelope of $\pm 0.5\sigma$ in natural transport variability along the shoreline. It was determined that no significant changes in longshore sediment transport potential would result from modeled borrow site configurations for any of the proposed borrow sites.

5.0 CIRCULATION AND SEDIMENT TRANSPORT DYNAMICS

This section analyzes the dominant physical processes on the inner continental shelf offshore southwestern Long Island and northeastern New Jersey (New York Bight) and discusses circulation, wave, and sediment transport processes to evaluate potential environmental impacts of offshore sand mining. Current and wave processes provide physical mechanisms for moving sediment throughout the coastal zone. The following discussion documents the physical mechanisms potentially impacted by sand mining within specific offshore locations.

5.1 CURRENTS AND CIRCULATION

Circulation patterns observed at specific locations within the study area were evaluated relative to potential offshore sand mining operations. The following discussion uses current measurements obtained during previous studies in the New York Bight to provide an understanding of temporal variations of inner shelf circulation (time scales ranging from hours to months). Analyses presented in this section describe circulation characteristics within the study area, including major forcing influences, time scales of variability, and the magnitude of resulting currents. The results from this section are used to provide estimates of sediment transport potential at offshore borrow sites.

5.1.1 Historical Data

Available data documenting circulation patterns in the New York Bight include Acoustic Doppler Current Profiler (ADCP) observations recorded at inlets located along the southwestern Long Island and northeastern New Jersey shorelines; ADCP data collected offshore Little Egg Inlet, NJ at the Long-term Ecosystem Observatory (LEO-15); ADCP and current meter measurements collected at the Hudson Shelf Valley (Butman et al., 2003); and hydrodynamic modeling results for the New York Bight (Scheffner et al., 1994). Data were evaluated with respect to borrow site proximity and appropriate geomorphic representation. Of the available data sets, ADCP and current meter observations by Butman et al. (2003) along the Hudson Shelf Valley were determined to be best suited for representing borrow site conditions. Data collected at inlets along the New York and New Jersey coastlines were excluded due to differences in flow characteristics associated with channels relative to shelf environments, and data from the LEO-15 site were excluded due to the distance between these stations and the borrow sites. Of the available Hudson Shelf Valley data, measurements recorded at Stations D and E (Figure 5-1) were chosen based on relative bathymetric similarities and borrow site proximity. Current flows at Stations A, B, C, and F were influenced by the geomorphology of the Hudson Shelf Valley and do not reflect bathymetric characteristics of the borrow sites. Data selected for this analysis were obtained over a 5-month period from early December to mid-April and represent a high-energy environment due to the increased frequency of storm events typical for the winter season. Hydrodynamic modeling data were used to compare trends observed for the winter months with variations during summer months.

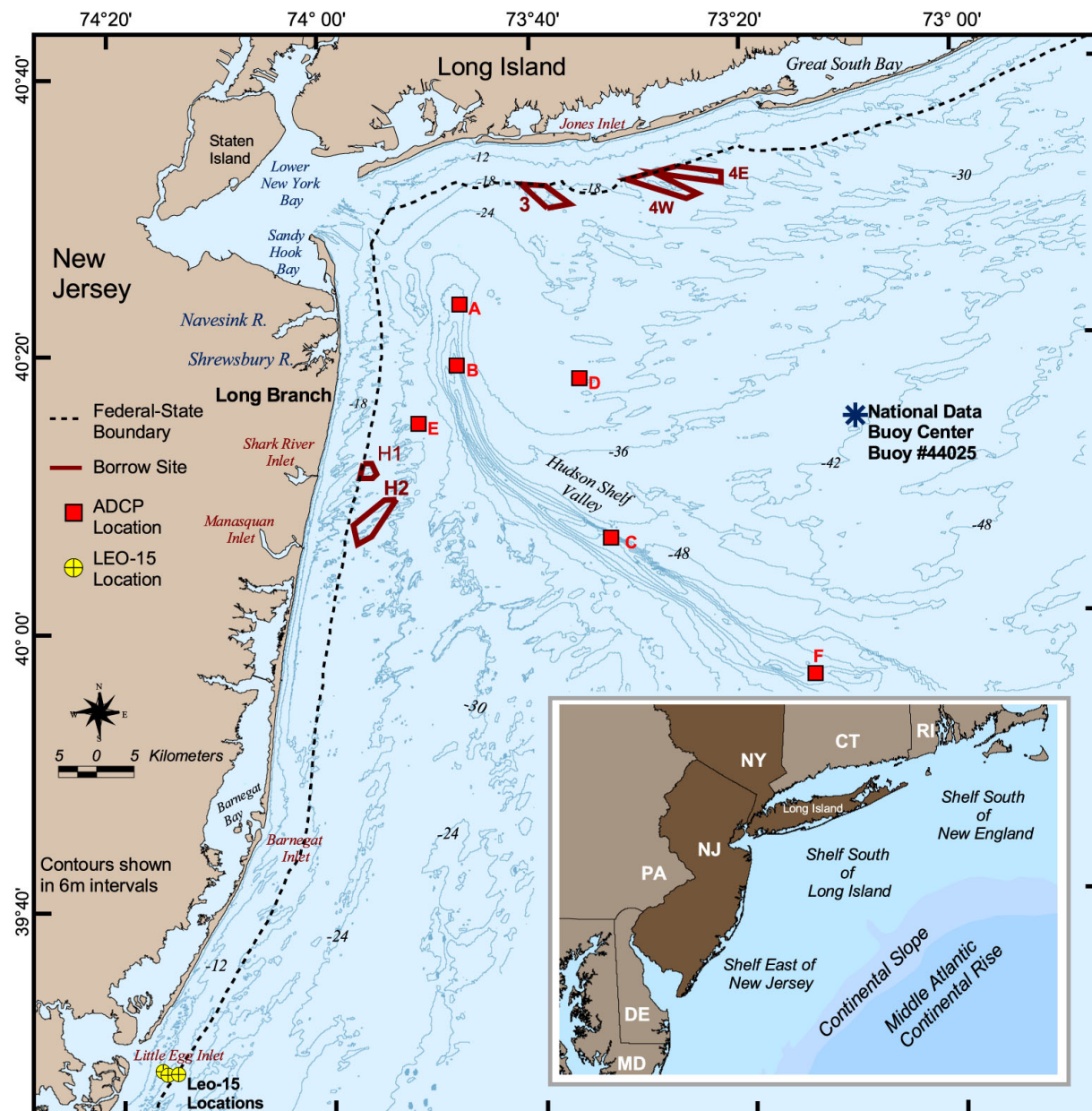


Figure 5-1. Current meter and borrow site locations in the New York Bight.

Station D is located in approximately 26 m water depth on the continental shelf south of Long Island, approximately 16.5 km east of the Hudson Shelf Valley ($40^{\circ}18.01' \text{ N}$, $73^{\circ}35.99' \text{ W}$; Butman et al., 2003). Current profiles at Station D were recorded with an RD Instruments ADCP (300 kHz Workhorse) mounted on a tripod approximately 3 m above the sea floor. Data from the ADCP were compiled in 1-m bins, with a blanking distance of 1.8 m. Bottom currents were recorded with two Benthic Acoustic Stress Sensors (BASS) mounted on the tripod 0.4 and 1.0 m above the sea floor (Butman et al., 2003). Figure 5-2 illustrates the location of the tripod mooring, bottom photographs, and sediment grab samples. The background image represents backscatter intensity from multibeam surveys, where backscatter intensity is shown as a suite of eight colors ranging from blue (fine-grained sediment) to red (rock outcrops and coarse-grained

sediment) with bathymetric contours in white. Contours illustrate shallower bathymetry west of the Station D and deeper bathymetry to the southeast. Surface sediment texture is documented with a photograph below the map. All sediment samples associated with Station D contained at least 99% sand, and median grain size ranged from 0.13 to 0.15 mm (fine sand).

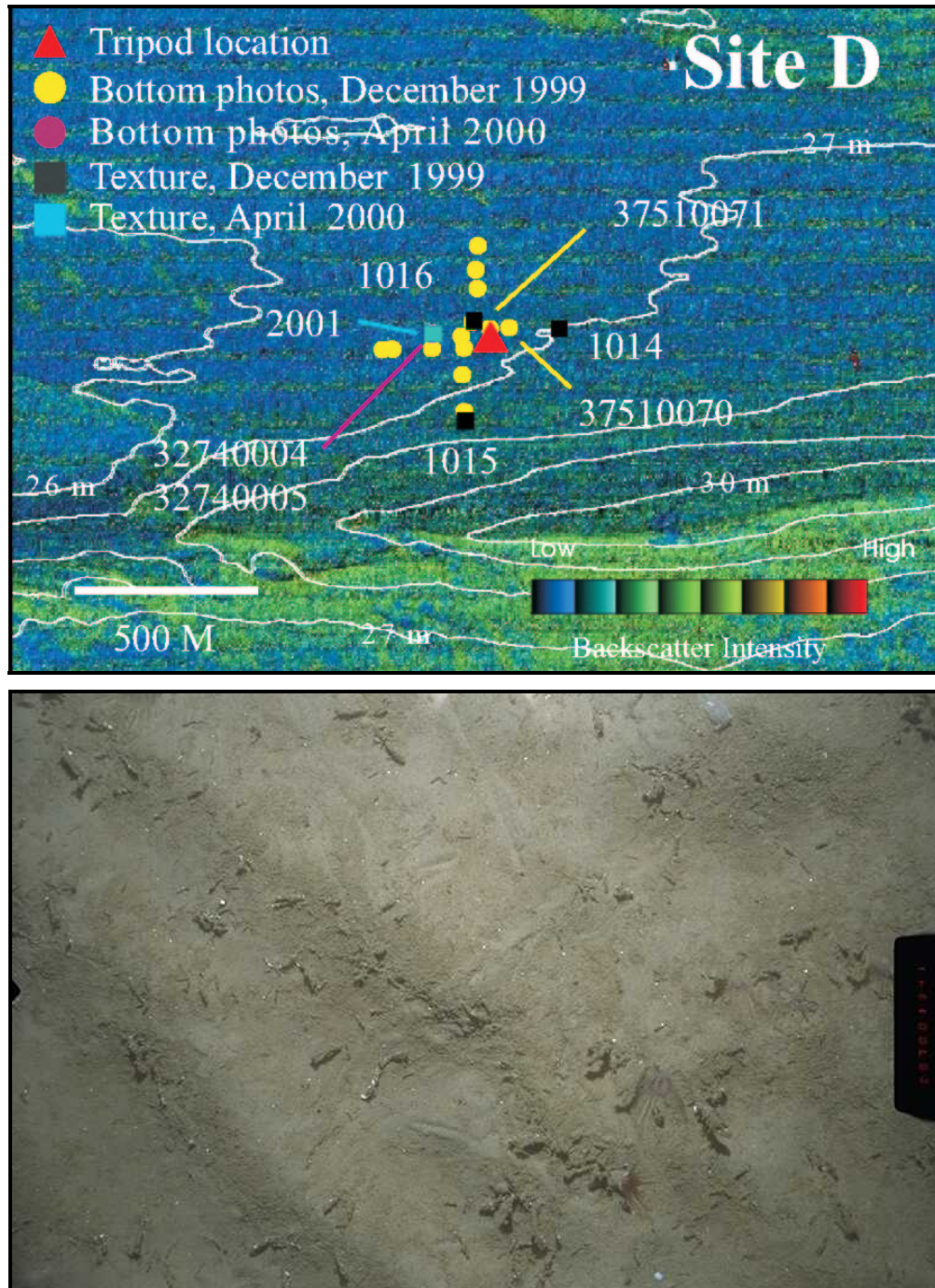


Figure 5-2. Location of current meter mooring Station D on the Long Island shelf to the east of the Hudson Shelf Valley (~26 m water depth; see Figure 5-1) showing the location of the tripod mooring, bottom photographs, and sediment grab samples. The photograph below the map illustrates bottom topography and sediment texture representative of the area surrounding the mooring tripod (from Butman et al., 2003).

Station E was located in approximately 25 m water depth offshore Long Branch, NJ, approximately 6.3 km west of the Hudson Shelf Valley (40°14.87' N, 73°51.06' W). Current profiles at Station E were recorded with an RD Instruments ADCP (300 kHz Workhorse) mounted on a tripod approximately 2 m above the sea floor. Data from the ADCP were compiled in 1-m bins, with a blanking distance of about 1.8 m. Bottom currents were recorded with a Modular Acoustic Velocity Sensor (MAVS) mounted on the tripod 0.4 m above the sea floor (Butman et al., 2003). Figure 5-3 illustrates the location of the tripod mooring, bottom photographs, and sediment grab samples. The background image represents backscatter intensity from multibeam surveys, where backscatter intensity is shown as a suite of eight colors ranging from blue (finer-grained sediments) to red (rock outcrops and coarse-grained sediments) with bathymetric contours in white. Contours illustrate a north-south elongated bathymetric high located to the west of Station E. Variations in surface sediment texture are documented with photographs below the map. All sediment samples associated with the low backscatter area west of Station E contained at least 99% sand, and median grain size ranged from 0.20 to 0.27 mm (fine to medium sand). One sediment sample, located east of Station E in the high backscatter area in Figure 5-3, contained 44% gravel and 54% sand (bottom right image), resulting in a median grain size of 0.81 mm (coarse sand).

Hudson Shelf Valley current observations were obtained from the USGS, Woods Hole, as hourly averaged and low-pass filtered data. Low-pass filtered data were processed at the USGS to remove tidal constituents and were sub-sampled every 6 hours. Data were received with velocity separated into north and east components and oriented with respect to true north (Figure 5-4). At Applied Coastal, data were converted into degrees and separated into 22.5 degree bins centered on the 16 inter-cardinal points (N, NNE, NE, ENE, E, etc). Data also were filtered to remove anomalous recordings and all velocity values were rounded to the nearest 1 cm/s. Percent occurrence by velocity and direction was evaluated, with maximum velocity, corresponding direction, mean velocity, mean direction, and standard deviation calculated from the data. Values were plotted in rose plots (Figure 5-5), with velocity represented as grayscale in the inter-cardinal bars and percent occurrence represented by the length of the bar. In some cases, low-pass data were unreliable due to a low percentage of valid data points. The lower left corner of each graph displays the percentage of reliable data points used in generating the rose plot.

Scheffner et al. (1994) conducted hydrodynamic modeling of currents in the New York Bight based on water surface height and vertical temperature and salinity gradients for summer months. Hydrodynamic model results, when run with zero wind and inflows of fresh water, illustrated a tendency for currents to flow from northeast to southwest along the continental shelf. Two general exceptions to this trend included a northerly flow along the coast of New Jersey and a flow reversal along the Hudson Shelf Valley, where currents at the northern extent tend to bend northward toward the shore of Long Island and currents in the south tend to flow offshore down the valley (Figure 5-6). A second modeling scenario was generated with summer inflow from the Hudson River and included a southwesterly wind force of 28 dynes/cm² (~3.9 m/s). The primary location impacted by this simulation was nearshore regions, enhancing northerly flow along the Long Island continental shelf.

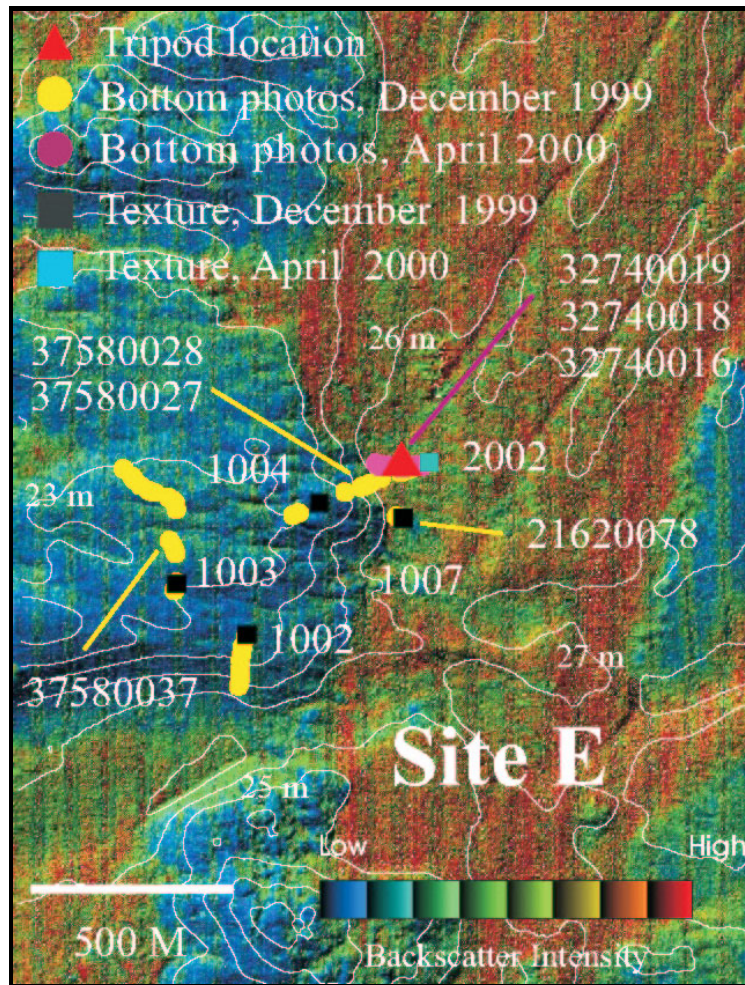


Figure 5-3. Location of current meter mooring Station E on the northern New Jersey shelf to the west of the Hudson Shelf Valley (~25 m water depth; see Figure 5-1) showing the location of the tripod mooring, bottom photographs, and sediment grab samples. The photographs below the map illustrate bottom topography and sediment texture representative of the low backscatter intensity area west of the tripod (blue) and the high backscatter intensity area east of the tripod (green to red) (from Butman et al., 2003).

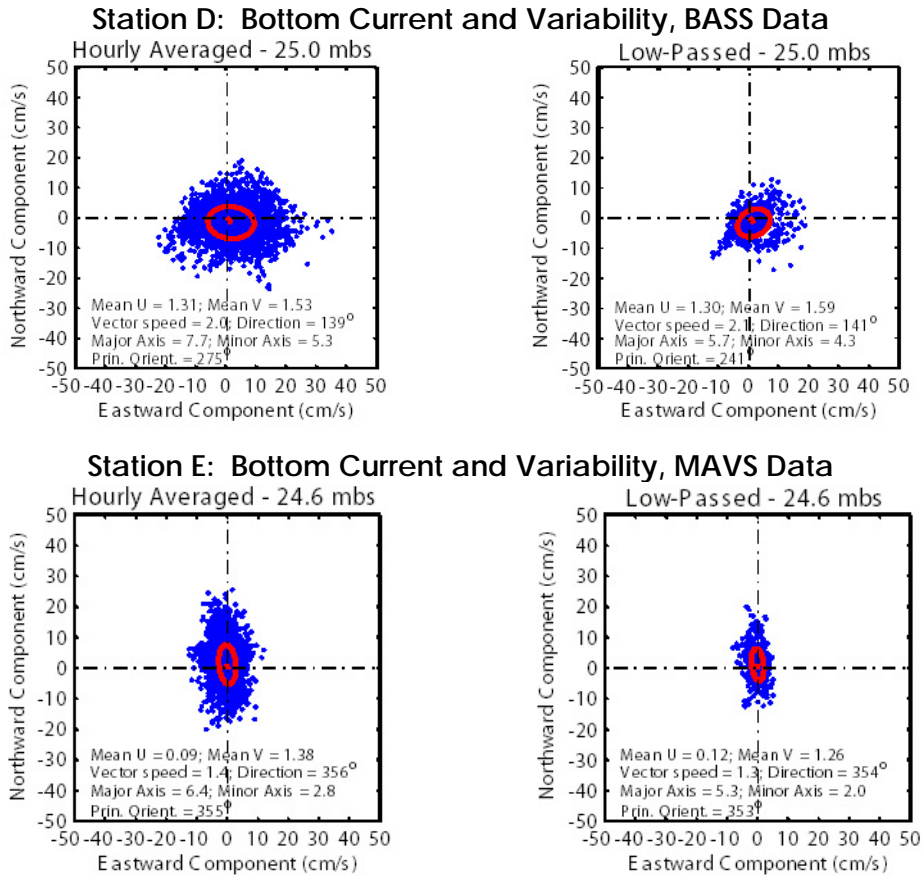


Figure 5-4. Hourly averaged bottom current speed and variability at Station D (December 5, 1999 to April 15, 2000 at 25 meters below the surface [mbs]) and Station E (December 4, 1999 to April 15, 2000 at 24.6 mbs). Low-passed plots exclude tidal currents (from Butman et al., 2003).

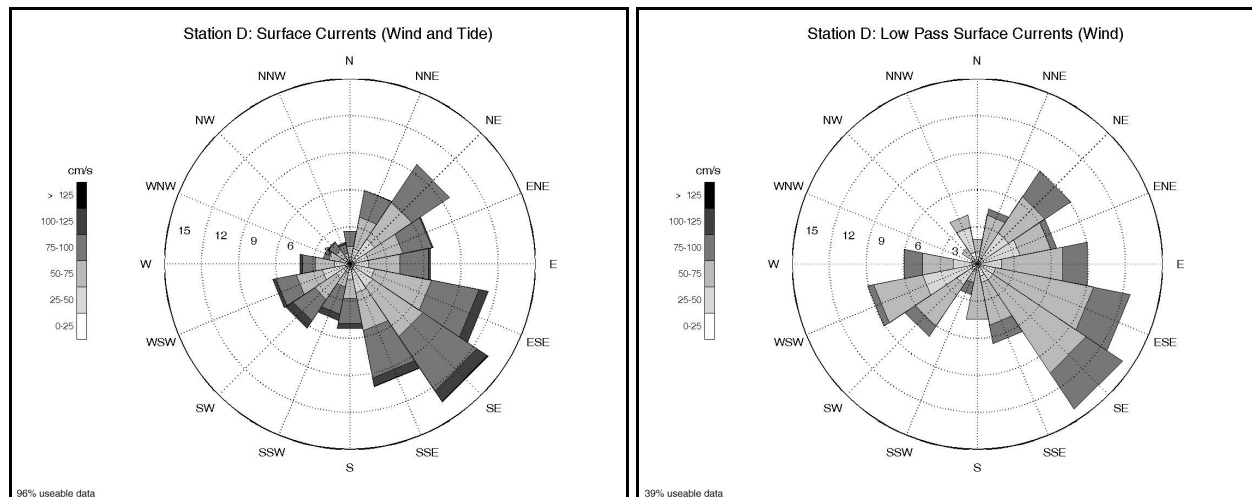


Figure 5-5. Speed and direction for surface currents at Station D, December 5, 1999 to April 15, 2000. The percentage of reliable data points is provided in the lower left corner of each plot. Current speeds are represented by percent occurrence and shading in the inter-cardinal bars. The length of each bar represents total percent occurrence by direction (data from Butman et al., 2003).

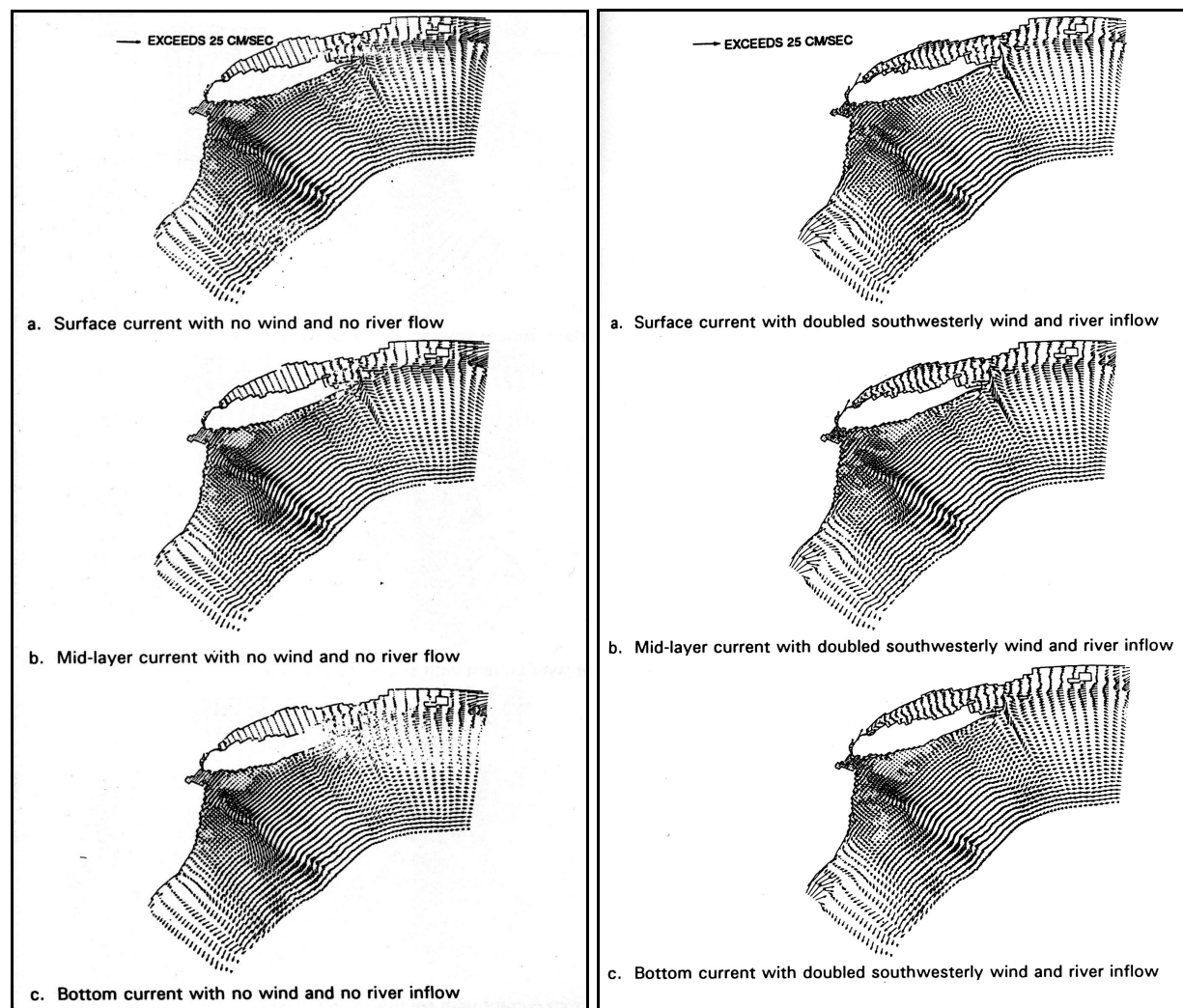


Figure 5-6. Summer current flows in the New York Bight. Left panel: modeled currents with no wind and no river inflow. Right panel: modeled current flows with southwesterly wind of 28 dynes/cm² (~3.9 m/s) and Hudson River summer inflow rates (from Scheffner et al., 1994).

5.1.1.1 Description and Analysis of Observed Currents

Butman et al. (2003) measured currents at Stations D and E for the period from December 4, 1999 to April, 15 2000. Data analysis revealed considerable variability in current direction and velocity. Overall, the predominant direction of surface flow at Stations D and E was similar, varying from southeast (Station D; Figure 5-7) to south-southeast (Station E; Figure 5-8). Surface current magnitudes also were consistent, showing similar maximums, means, and standard deviations. Bottom current measurements illustrated greater variability in direction and magnitude. Station D showed predominant bottom current flow varying from east-southeast to west, while the predominant bottom current flow at Station E varied from north to south-southeast (Figures 5-9 and 5-10). Differences in bottom flow between stations may be explained by the presence of the Hudson Shelf Valley, which bisects the continental shelf in this region causing currents to veer to the north as they flow cross contour into the bathometric low from northeast to southwest. Strong northerly flow within the valley prevents currents south and west of this area from flowing to the east-northeast.

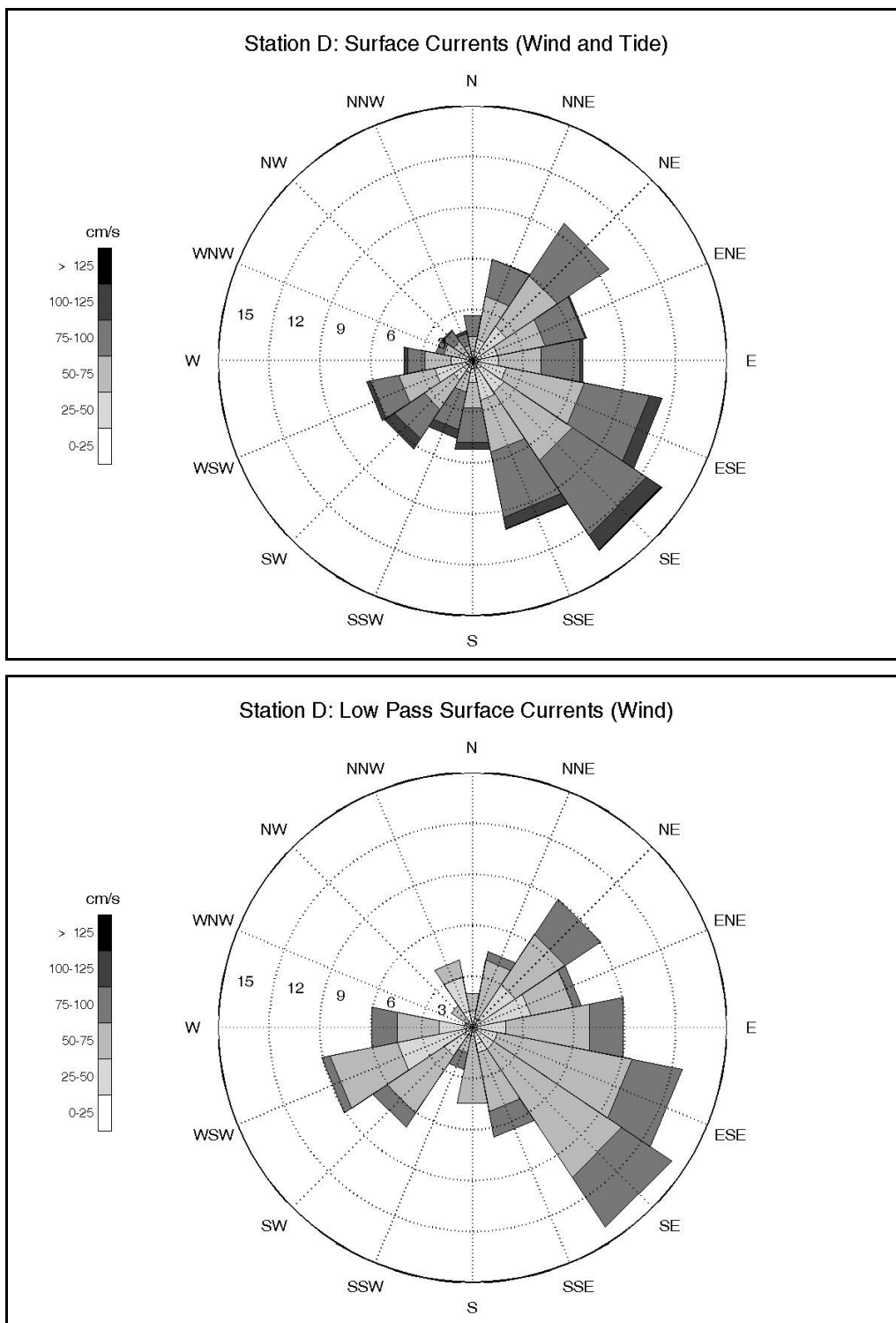


Figure 5-7. Surface current speed and direction east of the Hudson Shelf Valley for Station D, December 5, 1999 to April 15, 2000. Current speeds are represented by percent occurrence and shading in the inter-cardinal bars. The length of each bar represents total percent occurrence by direction (data from Butman et al., 2003).

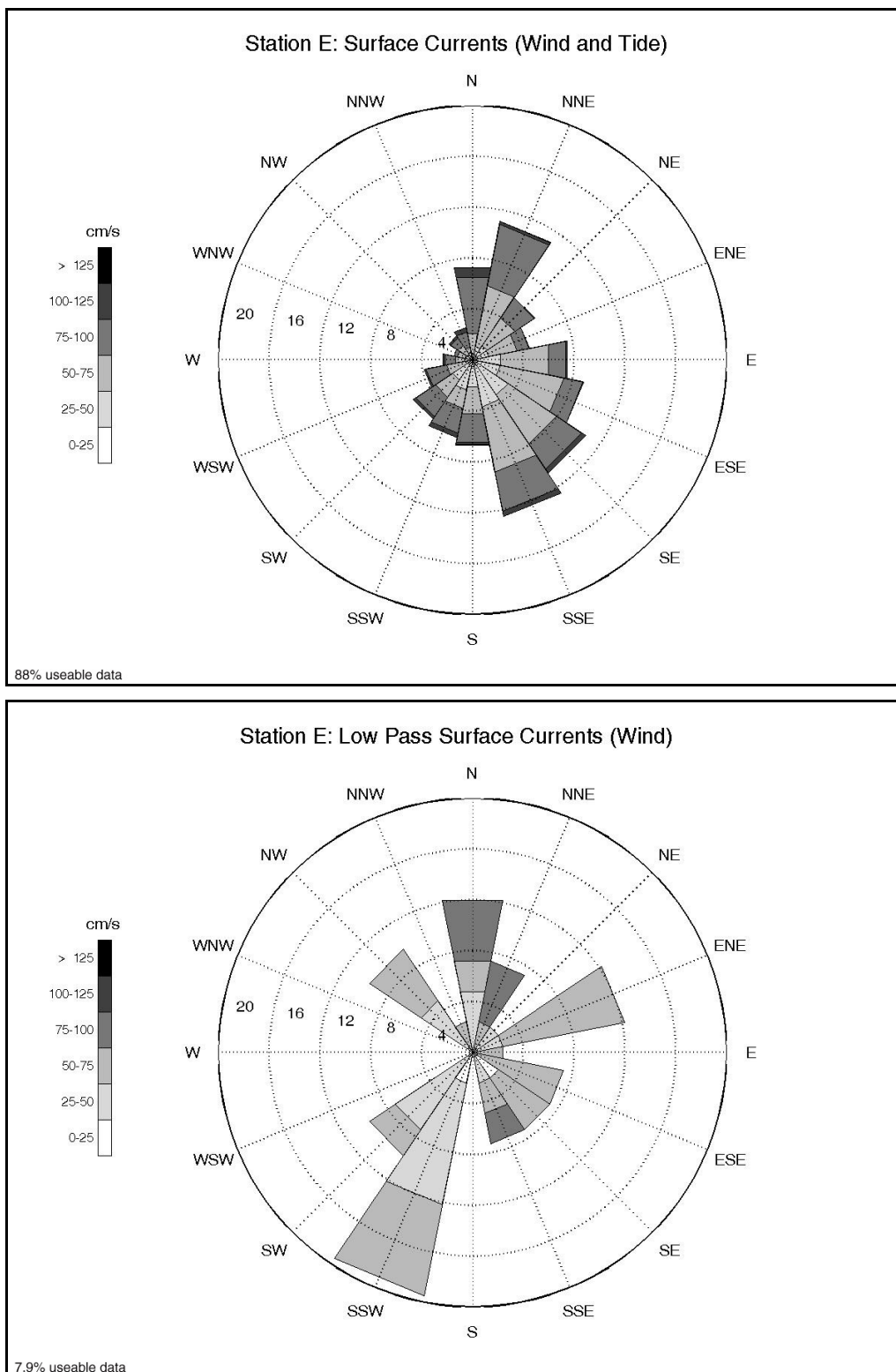


Figure 5-8. Surface current speed and direction west of the Hudson Shelf Valley for Station E, December 4, 1999 to April 15, 2000. Current speeds are represented by percent occurrence and shading in the inter-cardinal bars. The length of each bar represents total percent occurrence by direction (data from Butman et al., 2003).

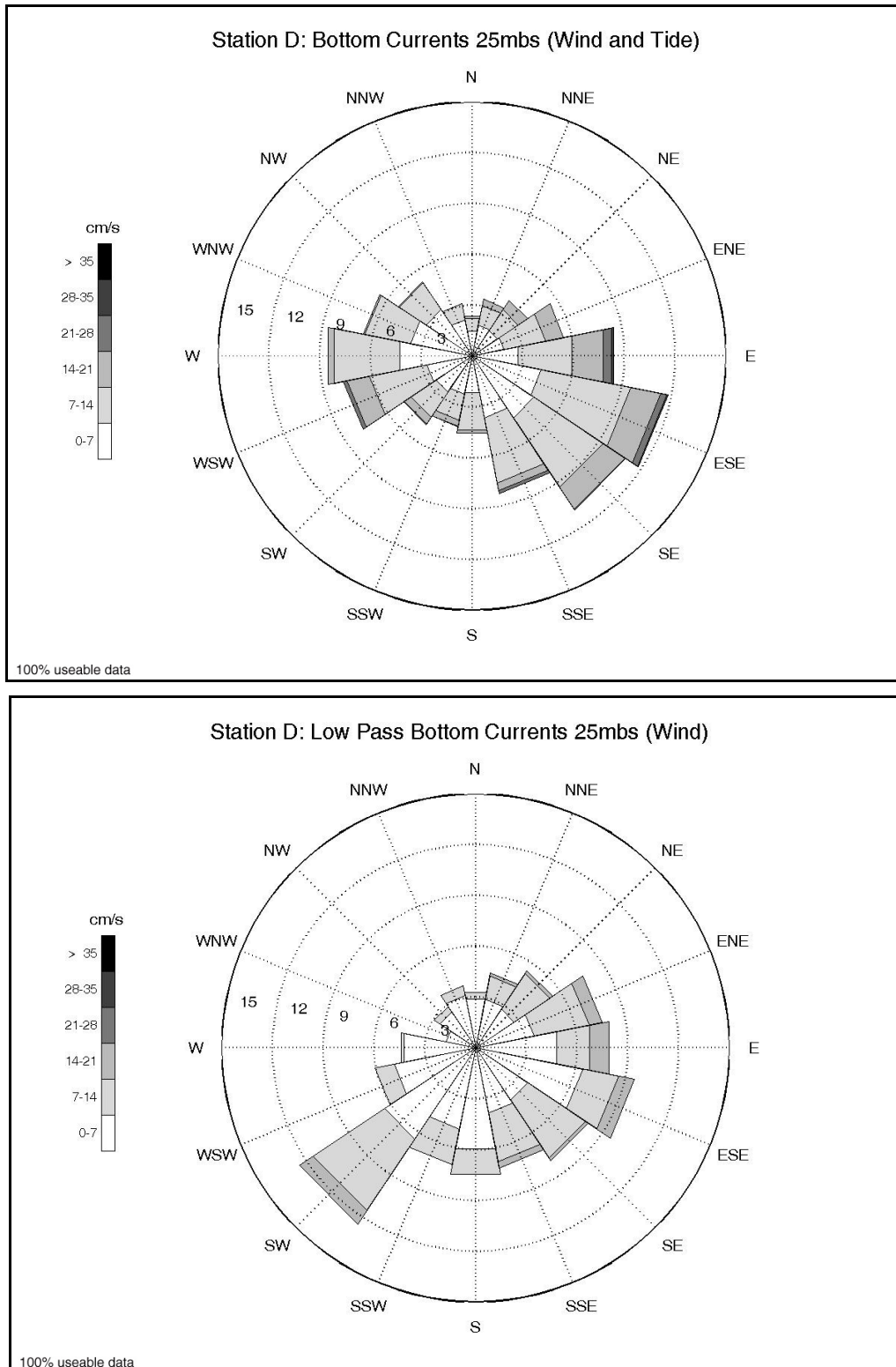


Figure 5-9. Bottom current speed (25 mbs) and direction east of the Hudson Shelf Valley for Station D, December 5, 1999 to April 15, 2000. Current speeds are represented by percent occurrence and shading in the inter-cardinal bars. The length of each bar represents total percent occurrence by direction (data from Butman et al., 2003).

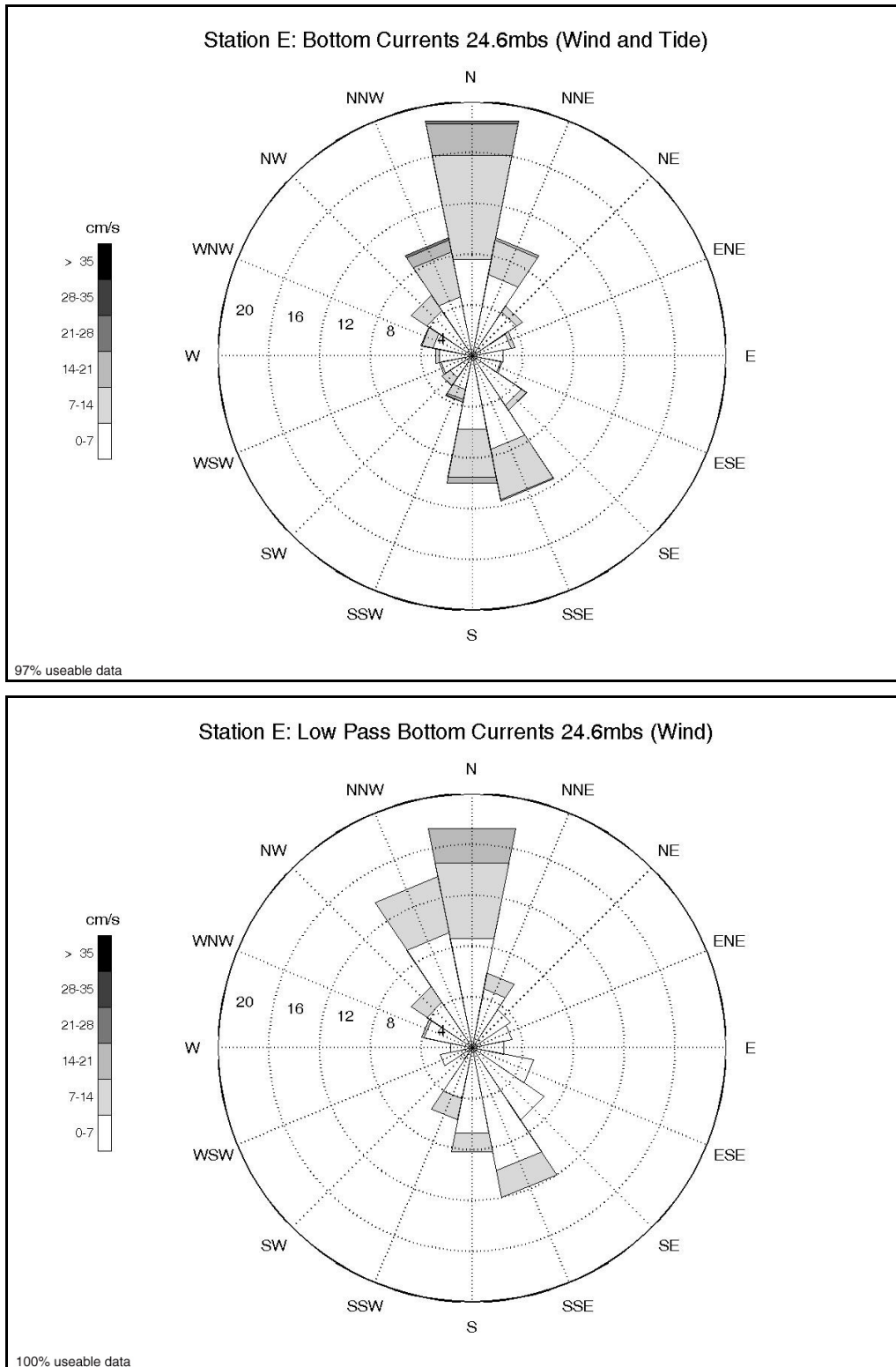


Figure 5-10. Bottom current speed (24.6 mbs) and direction west of the Hudson Shelf Valley for Station E, December 4, 1999 to April 15, 2000. Current speeds are represented by percent occurrence and shading in the inter-cardinal bars. The length of each bar represents total percent occurrence by direction (data from Butman et al., 2003).

Predominant surface flows recorded between December 5 and April 15 at Station D were to the southeast (13% of total), while bottom currents measured 25 mbs predominately flowed east-southeast (11% of total). Surface flow recorded at Station E between December 4 and April 15 was predominantly south-southeast (12% of total) and bottom currents (24.6 mbs) were dominated by north-northwest flow (19% of total). Wind data collected by the National Data Buoy Center (NDBC) at Buoy #40255 recorded predominant wind direction for same time interval to the east-southeast (12% of total) (Figure 5-11).

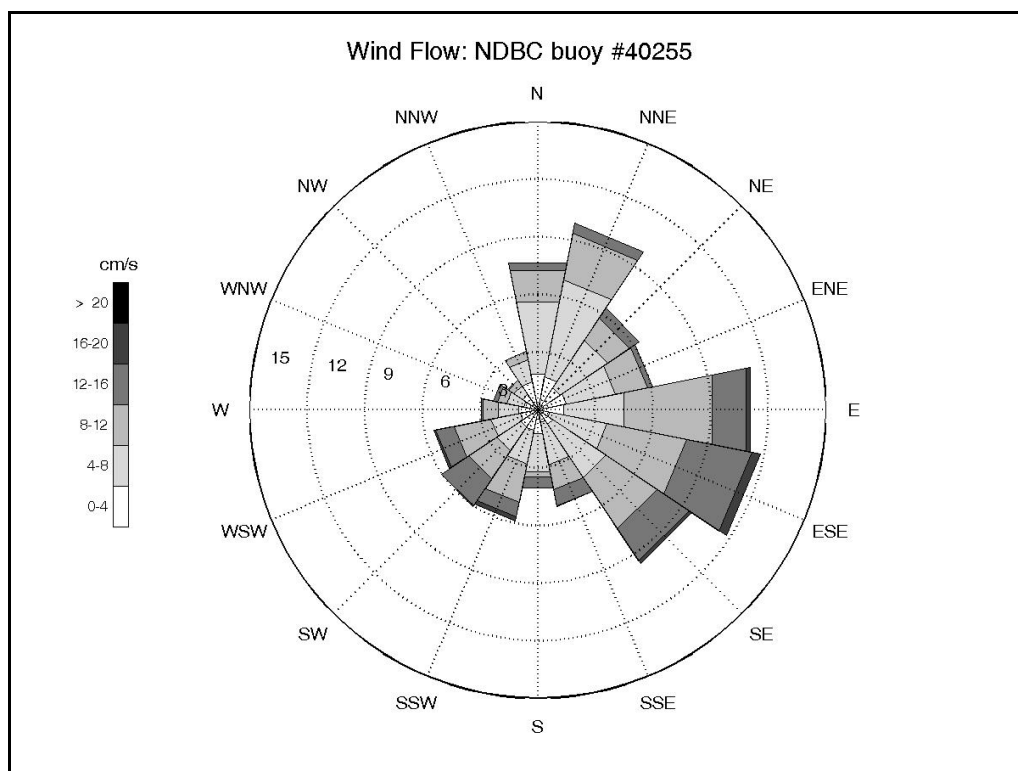


Figure 5-11. Wind speed and direction from NDBC Buoy #40255; December 1, 1999 to April 30, 2000. Wind speeds are represented by percent occurrence and shading in the inter-cardinal bars. The length of each bar represents total percent occurrence by direction (data from Butman et al., 2003).

Maximum surface current velocity at Station D was 135 cm/s to the southeast, with a mean speed of 67 cm/s (± 23 cm/s) in the same direction. After filtering tidal currents (low-pass filtered), maximum current speed was reduced to 95 cm/s to the southwest, with a mean speed of 59 cm/s (± 17 cm/s) to the southeast. Maximum bottom current speed at 25 m below the surface at Station D was 35 cm/s flowing east, with a mean speed of 8 cm/s (± 5 cm/s) flowing southeast (see Figure 5-4). Low-pass filtering of these data produced a minimal reduction in maximum current speed to 21 cm/s to the southeast; the mean current was 6 cm/s (± 4 cm/s) to the south-southeast. Furthermore, monthly variations in mean flow indicate only minor changes in current direction when tidal currents are filtered from the record (Figure 5-12). These observations suggest that wind-driven currents dominate the total current signal at Station D.

Maximum surface current velocity at Station E was 138 cm/s flowing south, with a mean velocity of 65 cm/s (± 22 cm/s) flowing southeast. Low-pass filtering of tide-induced currents resulted in a reduction in maximum surface current speed to 84 cm/s to the north, with a mean speed of 55 cm/s (± 16 cm/s) to the southeast. The maximum bottom current velocity at 24.6 m

below the surface at Station E was 26 cm/s flowing north, with a mean velocity of 6 cm/sec (± 4 cm/s) flowing north (see Figure 5-4). After applying a low-pass filter, maximum bottom current speed was reduced to 20 cm/s to the north, and mean current speed was 5 cm/s (± 4 cm/s) to the south-southeast. In addition, monthly variations in mean flow illustrated insignificant changes in current direction when tidal currents were filtered from the record (Figure 5-13). These observations again suggest that wind-driven currents dominate the total current signal at Station E.

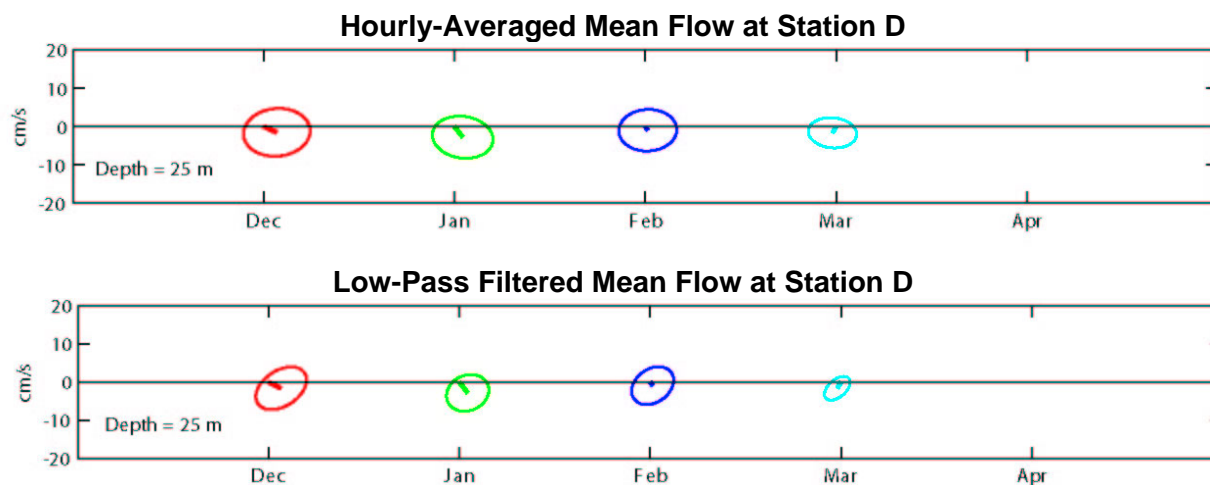


Figure 5-12. Monthly observed mean current flow and the variability (shown as an ellipse centered around the tip of the mean flow arrow) for near-bottom current for Station D. Up is to the north and right is to the east. The current ellipse calculated from hour-averaged data is typically dominated by tidal currents, whereas low-pass filtered mean flow has tidal currents removed (from Butman et al., 2003).

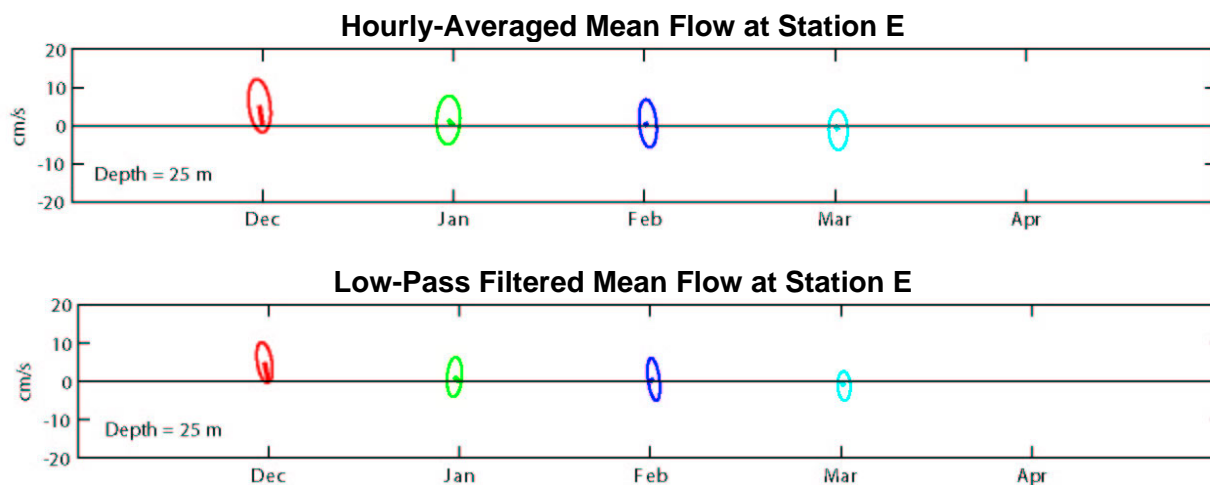


Figure 5-13. Monthly observed mean current flow and the variability (shown as an ellipse centered around the tip of the mean flow arrow) for near-bottom current for Station E. Up is to the north and right is to the east. The current ellipse calculated from hour-averaged data is typically dominated by tidal currents, whereas low-pass filtered mean flow has tidal currents removed (from Butman et al., 2003).

Strongest surface currents at Station D were observed flowing toward the bathymetric low to the southeast of the station. Within 4 hours, the current shifted position over 160 degrees to the north-northwest. This was accompanied by a reduction of maximum current speed (135 cm/s) by 80 cm/s. The strongest surface current flow recorded at Station E was in the along-shelf direction followed by a current shift of over 158 degrees to the north-northwest, accompanied by a reduction in the maximum current (138 cm/s) of 94 cm/s. Other flow reversals were frequently noted. When compared to the wind record, a link between current velocities and wind shifts is apparent. Sharp changes in current speed and direction occurred shortly after a rapid changes in wind speed and direction.

Further observation of currents revealed a relationship between sustained wind direction and current speeds (Figure 5-14). Because much of the low-pass filtered data contained large gaps, a full comparison of complete data sets was not possible. However, plotting small sections of low-passed current data (on the order of 7 days) with wind data from NDBC Buoy #40255 illustrated a relationship between sustained wind direction and current speed, fluctuating with wind speed.

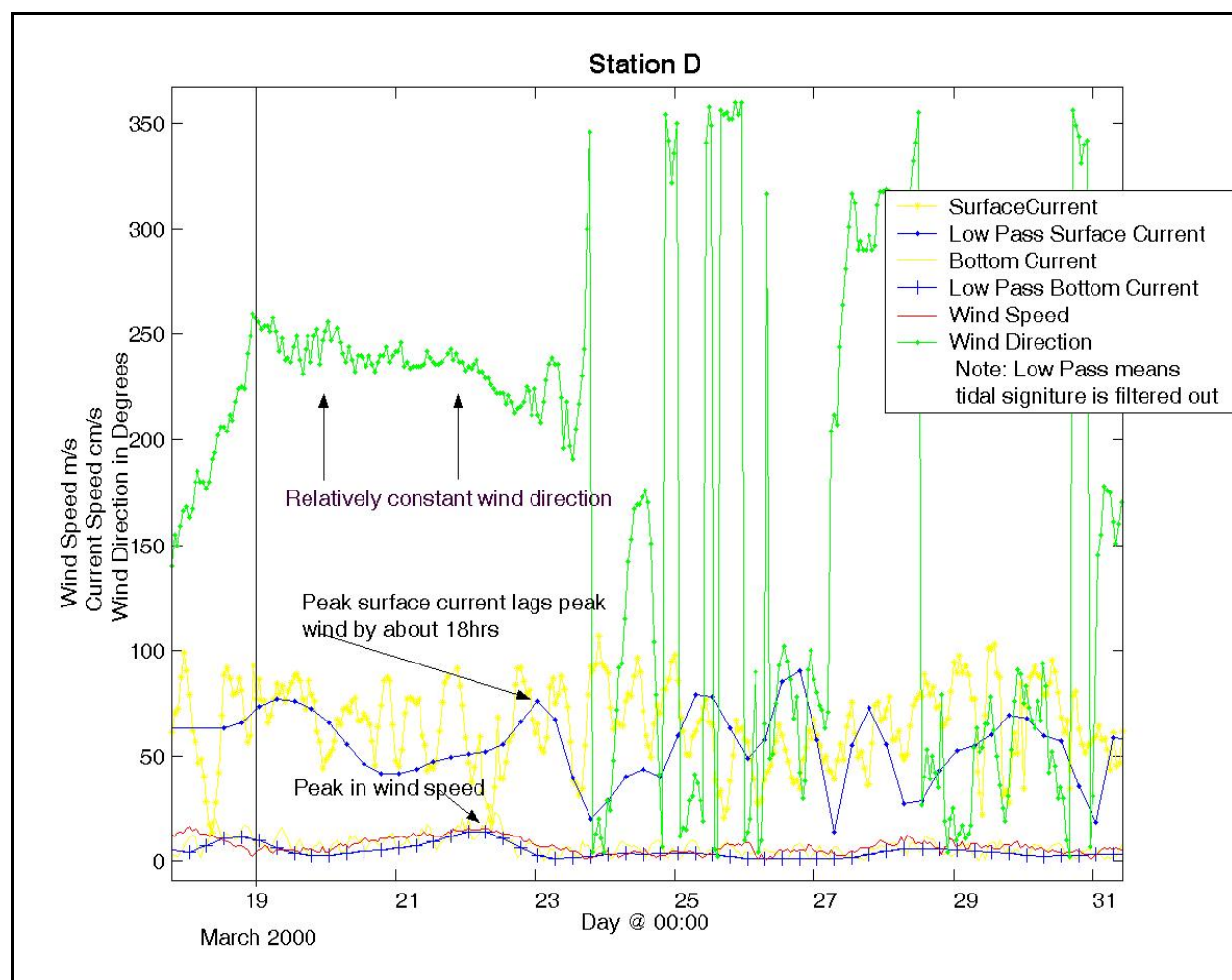


Figure 5-14. Wind speed and direction versus surface and bottom currents, March 19 to 31, 2000 (data from Butman et al., 2003).

5.1.1.2 Tidal Currents

Butman et al. (2003) computed the amplitude and phase of tidal constituents using the tidal analysis program T_TIDE (Pawlowicz et al., 2002). Because tides in the New York Bight are semi-diurnal, the principal tidal constituents are K1, O1, M2, N2, and S2. Butman et al. (2003) analyzed tidal constituents for a depth of 15 m below the surface for each station. Tidal ellipses were plotted and the results showed M2 to be the most significant tidal constituent. The M2 tidal constituent is oriented northwest to southeast. This elongated ellipse explains frequently noted changes in current direction and magnitude with the variance from a full reciprocal vector caused by wind driven velocities and lesser tidal constituents. N2 and S1 are oriented in the same relative direction as M2. Deviations from this trend include K1, oriented north-northwest to south-southeast at Stations D and E, and O2 oriented north-northeast to south-southwest at Station D. This alteration in trend causes a more radial tidal signature, most notably at Station D (Figure 5-15). In Figure 5-15, the size of the current ellipse is proportional to current magnitude. The M2 tidal ellipse is scaled to 10 times the distance a water molecule would travel in one tidal cycle at map scale. The tidal ellipse for the remaining tidal constituents is 40 times the distance a water molecule would travel in one tidal cycle at map scale (Butman et al., 2003).

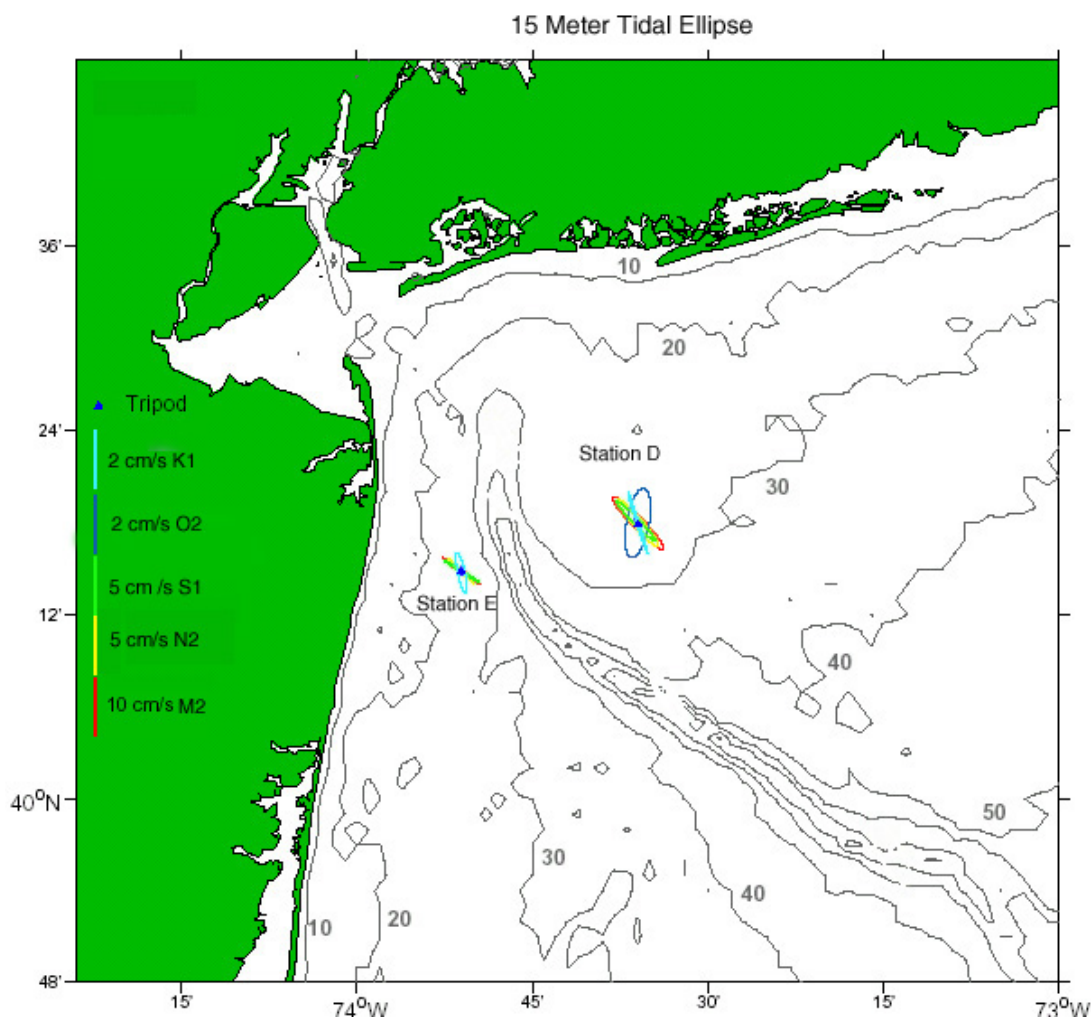


Figure 5-15. Tidal ellipses for major tidal constituents at 15 m below the surface (adapted from Butman et al., 2003).

5.1.1.3 Summary of Flow Regimes at Offshore Borrow Sites

The analysis presented above documents speed and direction related to current and wind patterns recorded between December 4, 1999 and April 15, 2000. Data evaluated are considered to be a good representation for borrow site conditions because of proximity to the borrow sites and similarities in bathymetric characteristics. The high-energy environment associated with winter storm events is capable of suspending and transporting sediment and is well suited for determining maximum sediment transport rates for the region. Data analyzed by Butman et al. (2003) agrees with the overall trend Scheffner et al. (1994) modeled; bottom currents in the vicinity of offshore borrow sites are driven primarily by winds and influenced by tidal flows.

The controlling factor for current velocities on the New York Bight is wind direction and intensity, and local bathymetric features control current direction. Currents tend to flow parallel to contours causing currents to diverge around localized bathymetric highs and converge near bathymetric lows. A localized bathymetric high is located west of the Station D and a bathymetric trough is located to the southeast running east west (Figure 5-2). This geomorphic configuration causes currents to flow from west to east around the bathymetric high and toward the bathymetric low. Figure 5-3 documents an elongated (north to south) bathymetric high to the west of the Station E. This shoal causes current flows to be channeled north and south at Station E between bathymetric contours and the north-northwest and south-southeast flow associated with the Hudson Shelf Valley. Bathymetric relief to the east is consistent moving offshore the New Jersey coastline. Current analyses conducted at points south of the study area along the New Jersey shoreline showed similar directional flow (Byrnes et al., 2004).

In general, bottom flows at the borrow sites offshore New York and New Jersey are driven primarily by wind speed and direction. At Station D, bottom currents generally flow east-southeast or east and west with deviations caused by wind direction. At Station E, bottom currents generally flow north and south along bathymetric contours. Bottom current speeds at both sites primarily are controlled by wind speeds, and the direction of flow is controlled by local bathymetry.

The above information infers some general trends about the borrow sites located offshore New York and New Jersey. At borrow sites south of Long Island, along-contour flow can be expected, flowing predominantly east-northeast or west-southwest with little variation to the north (onshore flow). At borrow sites offshore northeastern New Jersey, flow was predominantly north-northeast or south-southwest with little variation to the west (onshore flow) due to localized bathymetric control and the channeling affect of the Hudson Shelf Valley.

5.2 OFFSHORE SEDIMENT TRANSPORT

Infilling rates for potential offshore borrow sites were computed based on a method outlined in Madsen (1987), which relies on earlier work described by Grant and Madsen (1986) for wave-current interaction in the bottom boundary layer outside the surf zone.

On the continental shelf, currents are driven by a combination of forces resulting from winds, tides, and atmospheric pressure gradients. Surface waves also create currents on the sea bottom. These wave-induced currents are oscillatory and fluctuate with the passing of each wave. In Grant and Madsen (1986), the interaction of wave-induced currents (high-frequency) and background currents with longer time scales (low frequency) was modeled. This analysis provided a method for estimating the combined wave-current friction factor (f_{cw}), which is necessary for computing sediment transport at a borrow site.

5.2.1 Determining Bottom Transport and Infilling Rates

As outlined in Madsen (1987), the net transport q_{net} at the sea bottom in the presence of waves is computed as the averaged instantaneous transport $q(t)$ over the cycle of a wave period T ,

$$q_{net} = \frac{1}{T} \int_0^T q_s(t) dt \quad (5.1)$$

The instantaneous value of sediment transport is computed using a formula given by Madsen (1987) which is based on an earlier empirical relationship known as the Einstein-Brown formula (Brown, 1950) for bottom sediment transport in steady unidirectional flow. The Einstein-Brown relationship gives the dimensionless transport rate ϕ as a function of the Shields parameter Ψ ,

$$\phi = 40\Psi^3 \quad (5.2)$$

The Shields parameter is used as an indicator of incipient sediment motion, and is the ratio of the shear force τ acting on bottom sediment to the submerged weight of grains. The Shields parameter is expressed as

$$\Psi = \frac{\tau}{(s-1)\rho g d} \quad (5.3)$$

where s is the sediment specific gravity, ρ is the density of water, g is the acceleration of gravity, and d is the sediment grain diameter. The shear stress is a function of the bottom friction factor, f , and the magnitude of the fluid velocity U at the sediment bed. It is expressed as

$$\tau = \frac{1}{2} f \rho U^2 \quad (5.4)$$

A critical value for the Shields parameter is determined using the Shields diagram, which defines the point of incipient sediment motion based on the boundary Reynolds number. For instantaneous values of the Shields parameter that are less than the critical value, no sediment motion will occur.

Therefore, during portions of the wave period that sediment motion does occur, the instantaneous dimensional sediment transport rate, expressed in a similar form as equation (5.2) is

$$q(t) = c_q w d \left\{ \frac{0.5 \rho f_{cw} [u^2(t) + v^2(t)]}{(s-1)\rho g d} \right\}^3 \quad (5.5)$$

where w is the fall velocity of sediment, c_q is a constant, f_{cw} is the combined wave-current friction factor, and u and v are the velocity components that result from the combination of high-frequency (wave driven) and low-frequency (atmospheric and tide driven) currents.

A method for computing f_{cw} is given by Madsen (1987), which is essentially an iterative method that modifies the bottom boundary layer based on interaction with waves. Initially, the wave friction factor, f_{wc} , for waves in the presence of currents is determined by using the equation

$$\frac{1}{4\sqrt{f_{wc}/C_\mu}} + \log \frac{1}{4\sqrt{f_{wc}/C_\mu}} = \log \frac{C_\mu u_b}{k_s \omega} - 0.17 \quad (5.6)$$

where k_s is a characteristic bottom roughness, ω is the wave radian frequency ($2\pi/T$), u_b is the magnitude of the velocity under the wave (in linear wave theory $u_b(t) = \sin[kx - \sigma t]$), and the coefficient C_μ is described as

$$C_\mu = (1 + 2\mu \cos \theta_c + \mu^2)^{1/2} \quad (5.7)$$

where

$$\mu = \left(\frac{u_{*c}}{u_{*wm}} \right)^2 \quad (5.8)$$

and θ_c is the angle between the wave approach and the current direction, u_{*c} is the current shear velocity, and u_{*wm} is the magnitude of the maximum wave shear velocity in the presence of currents. In this procedure, an initial guess for the value of μ must be made, because u_{*wm} is initially not known.

The final value of f_{cw} is computed using the equation

$$f_{cw} = 2 \left(\frac{u_{*c}}{u_r} \right)^2 \quad (5.9)$$

where u_{*c} is the current shear velocity, and u_r is the magnitude of the measured current, measured at a particular height above bottom, z_r . The current shear velocity is determined by the equation

$$u_r = \frac{u_{*c}}{\kappa} \left(\ln \frac{z_r}{\delta_{cw}} + \frac{u_{*c}}{u_{*m}} \ln \frac{\delta_{cw}}{z_0} \right); \text{ for } z_r > \delta_{cw} \quad (5.10)$$

which is quadratic in u_{*c} , and

$$u_{*wm}^2 = \frac{1}{2} f_{wc} u_b^2, \quad (5.11)$$

$$u_{*m}^2 = C_\mu u_{*wm}^2, \quad (5.12)$$

$$\delta_{cw} = \frac{\kappa u_{*m}}{\omega}, \quad (5.13)$$

where,

- u_{wm}^* = magnitude of the maximum wave shear velocity in the presence of currents,
 f_{wc} = wave friction factor, for waves in the presence of currents,
 u_m^* = combined wave-current shear velocity,
 δ_{cw} = wave bottom boundary layer thickness,
 u_m^* = combined wave-current shear velocity, and
 κ = von Karman's constant (=0.4).

A computer program was developed using the relationships of Grant and Madsen (1986) for the purpose of computing infilling rates at a borrow site. This program uses wave model output (Section 4.0) with current data to determine bottom sediment transport potential at the perimeter of the borrow site and a resulting annualized volume rate of sediment that will enter the borrow site.

5.2.2 Model Input Data

Wave data from STWAVE model runs provided input conditions for determining borrow site infilling rates. Wave data were extracted from the existing condition model runs at the perimeter nodes of each proposed borrow site. These are the same STWAVE model runs used to determine sediment transport potential at the coastline (see Section 4.0). Wave model input conditions used for each resource area are listed in Tables 5-1 and 5-2. Surface current speeds used to determine infilling rates are given in Tables 5-3 and 5-4. These currents are based on analyses presented in Section 5.1. Currents were applied in the model based on their percent occurrence. Ambient current directions were set as alongshore and based on the direction of wave propagation for each modeled wave case.

Table 5-1. Wave model input conditions used to compute offshore sediment transport potential for borrow sites offshore northeastern New Jersey. STWAVE model output from each modeled condition, and at each borrow site perimeter grid node, was used as input to the wave-current interaction model used to determine bottom sediment transport potential.				
Wave Period Band	Peak Wave Direction, θ_p deg true north	H_{m0} Wave Height m	Mean Wave Period, T_p sec	% Occurrence
Band 1	13	0.6	4.0	3.6
	23	0.8	4.0	2.5
	43	1.1	4.0	3.3
	68	1.3	4.0	3.9
	88	1.1	4.0	5.2
	93	0.9	4.0	6.2
	113	0.8	4.0	6.3
	133	0.8	4.0	6.8
	158	0.7	4.0	9.6
	158	0.7	4.0	15.6
Band 2	88	1.3	9.1	2.1
	93	1.2	7.7	2.6
	113	1.1	7.7	1.5
	133	1.2	7.7	1.1
	138	1.4	9.1	1.0
	158	1.3	7.7	1.0

In addition to wave and current inputs, other data and parameters were specified for each bottom transport potential model run performed for each borrow site. Depths at each perimeter node were taken from the wave model grid. Bottom sediment characteristic grain sizes (d_{90} and d_{50}) also were specified individually for each site. Parameters used for the model runs at each borrow site are listed in Table 5-5.

Table 5-2. Wave model input conditions used to compute offshore sediment transport potential for borrow sites offshore southwestern Long Island. STWAVE model output from each modeled condition, and at each borrow site perimeter grid node, was used as input to the wave-current interaction model used to determine bottom sediment transport potential.				
Wave Period Band	Peak Wave Direction, θ_p deg true north	H_{m0} Wave Height m	Mean Wave Period, T_p sec	%Occurrence
Band 1	92	0.7	4.0	4.8
	112	0.8	4.0	6.1
	112	0.8	4.0	6.8
	137	0.7	4.0	7.3
	157	0.8	4.0	9.9
	162	0.8	4.0	13.5
	182	1.0	4.0	9.7
	202	1.0	4.0	4.9
	227	0.7	4.0	3.0
	247	0.7	4.0	3.1
Band 2	112	1.3	9.1	2.1
	117	1.4	9.1	2.7
	137	1.4	9.1	2.2
	137	1.6	9.1	1.6

Table 5-3. Surface currents used to compute offshore sediment transport potential for sites offshore northeastern New Jersey based on the analysis in Section 5.1. Currents were binned by four compass sectors (N, E, S and W) and magnitude (<10, 10 to 20, 20 to 30, and >30 cm/sec).			
Sector	Current Direction (deg)	Current Magnitude (cm/sec)	Occurrence (%)
N sector	359	7	31.5
	356	17	10.2
	354	29	0.6
	4	41	<0.1
E sector	88	4	12.1
	66	15	0.1
S sector	171	7	25.8
	178	16	3.8
	187	28	<0.1
W sector	279	6	12.3
	290	15	0.8

Table 5-4. Surface currents used to compute offshore sediment transport potential for sites offshore southwestern Long Island based on the analysis in Section 5.1. Currents were binned by four compass sectors (N, E, S and W) and magnitude (<10, 10 to 20, 20 to 30, and >30 cm/sec).			
Sector	Current Direction (deg)	Current Magnitude (cm/sec)	Occurrence (%)
N sector	354	7	11.8
	13	18	2.4
	29	27	0.1
E sector	101	8	19.9
	97	18	12.6
	100	30	1.3
S sector	100	43	0.1
	171	8	17.9
	167	17	6.2
W sector	158	31	0.3
	273	8	21.0
	259	17	7.0
	243	29	0.4
	241	42	<0.1

Table 5-5. Sand resource and bottom characteristics at potential borrow sites offshore northeastern New Jersey and southwestern Long Island, NY.			
Borrow Site	Average Bottom Depth (m)	Sediment Size, d_{10} (mm)	Sediment Size, d_{50} (mm)
H1	20.1	0.95	0.52
H2	21.0	0.67	0.35
3	18.2	1.92	1.13
4W	18.8	0.65	0.36
4E	19.9	1.05	0.45

D10 = grain diameter above which 10% of the distribution is retained; D50 = median grain diameter

5.2.3 Infilling Model Results

Infilling rates computed for each of the five borrow sites offshore northeastern New Jersey and southwestern Long Island represented the total potential sediment transport into each of the sites from the combined influence of wave-induced and ambient bottom currents (Table 5-6). These results likely represent average, non-storm conditions for sediment transport at each site. For the five modeled borrow sites, computed transport rates were extremely low, with infilling rates ranging from 0.13 m³/yr to approximately 580 m³/yr. A number of factors contributed to the low transport rates, including water depth (typically 20 m, which reduced the impact of wave-induced currents), relatively short period waves dominating the regional wave climate, absence of storm events in the wave and current data sets that drive sediment transport in this area, coarse grain size of *in situ* materials, and relatively weak ambient shelf currents. Furthermore, potential borrow site excavations consisted of dredging an existing shoal to the same elevation as the surrounding seafloor. Therefore, potential borrow site excavation would primarily flatten the shoal and not create a seafloor depression. Based on extremely low potential transport

rates of *in situ* sediment and the geomorphic character of dredged deposits, it is unlikely that any of these borrow sites will reform as shoal deposits in the near future.

Borrow Site	Borrow Site Surface Area (x 10 ⁶ m ²)	Borrow Site Sand Volume (x 10 ⁶ m ³)	Average Bottom Depth (m)	Computed Transport Rate (m ³ /yr)
H1	3.28	4.8	20.1	0.13
H2	13.13	9.5	21.0	0.14
3	9.40	11.2	18.2	551
4W	12.23	19.8	18.8	575
4E	9.39	16.6	19.9	583

6.0 BIOLOGICAL FIELD SURVEYS

6.1 BACKGROUND

Two field surveys for biological characterization provided environmental data in and near the four sand borrow sites offshore northern New Jersey (Borrow Sites H1 and H2) and southern New York (Borrow Sites 3 and 4). The surveys were conducted in September 2001 (Survey 1) and June 2002 (Survey 2). Data were collected concerning water column parameters, sediment grain size, infauna, epifauna, and demersal fishes. The following sections provide the methods, results, and discussion for the biological field surveys.

6.2 METHODS

6.2.1 Survey Design

The primary objective of the biological field surveys was to characterize benthic ecological conditions (i.e., sediment, infauna, epifauna, and demersal fishes) in the four sand borrow sites off New Jersey and New York (Figure 6-1). Supporting data collected in the borrow sites consisted of water column profiles. A secondary objective was to obtain descriptive data on sediment and infauna in adjacent areas. The following discussion describes the design of the surveys to meet these objectives.

The total numbers of samples by type that originally were proposed for Surveys 1 and 2 were as follows:

SAMPLE TYPE	SURVEY 1 (Sept 2001)	SURVEY 2 (June 2002)
Water Column Sea-Bird Conductivity, Temperature, Depth (CTD) Sensor	6 Stations	6 Stations
Sediment and Infauna Smith-McIntyre Grab	30 Stations 1 grab/station	30 Stations 1 grab/station
Sediment Profile Imaging Camera	12 Stations 2 images/station	
Epifauna/Demersal Fishes Mongoose Trawl	6 Transects	6 Transects

The sampling plan for Surveys 1 and 2 is summarized in Table 6-1. This table lists the sand borrow sites and adjacent stations along with corresponding water depths and sample types. Sampling locations are illustrated in Figures 6-2 through 6-5 and provided in Appendix D, Table D-1.

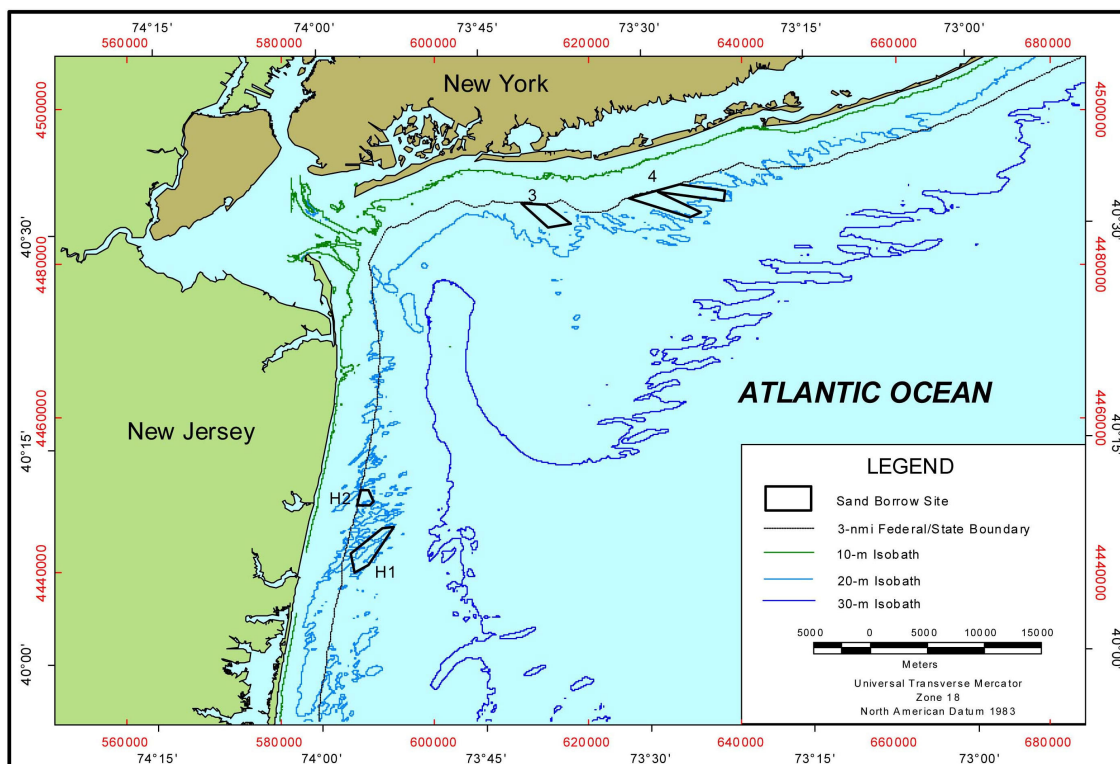


Figure 6-1. Sand Borrow Sites H1, H2, 3, and 4 offshore New Jersey and New York.

Table 6-1. Sampling plan summary for the September 2001 Survey 1 and June 2002 Survey 2 offshore New Jersey and New York.

Sand Borrow Site (H1,H2,3,4) or Adjacent Station (NJ-1, NY-1, etc.)	Water Depth (m)	Sample Type						
		Sea-Bird Water Column Profile Stations		Sediment Profile Imaging Stations	Smith-McIntyre Sediment Grain Size and Infaunal Stations		Epifaunal and Fish Trawl Transects	
		Survey 1	Survey 2	Survey 1	Survey 1	Survey 2	Survey 1	Survey 2
H1	16-24	2	2	3	6	6	2	2
H2	14-20	1	1	1	4	4	1	1
3	16-18	1	1	2	4	4	1	1
4	16-20	2	2	6	10	10	2	2
NJ-1					1	1		
NJ-2					1	1		
NJ-3					1	1		
NY-1					1	1		
NY-2					1	1		
NY-3					1	1		
Total Number of Stations		6	6	12	24 + 6 = 30	24 + 6 = 30	6	6

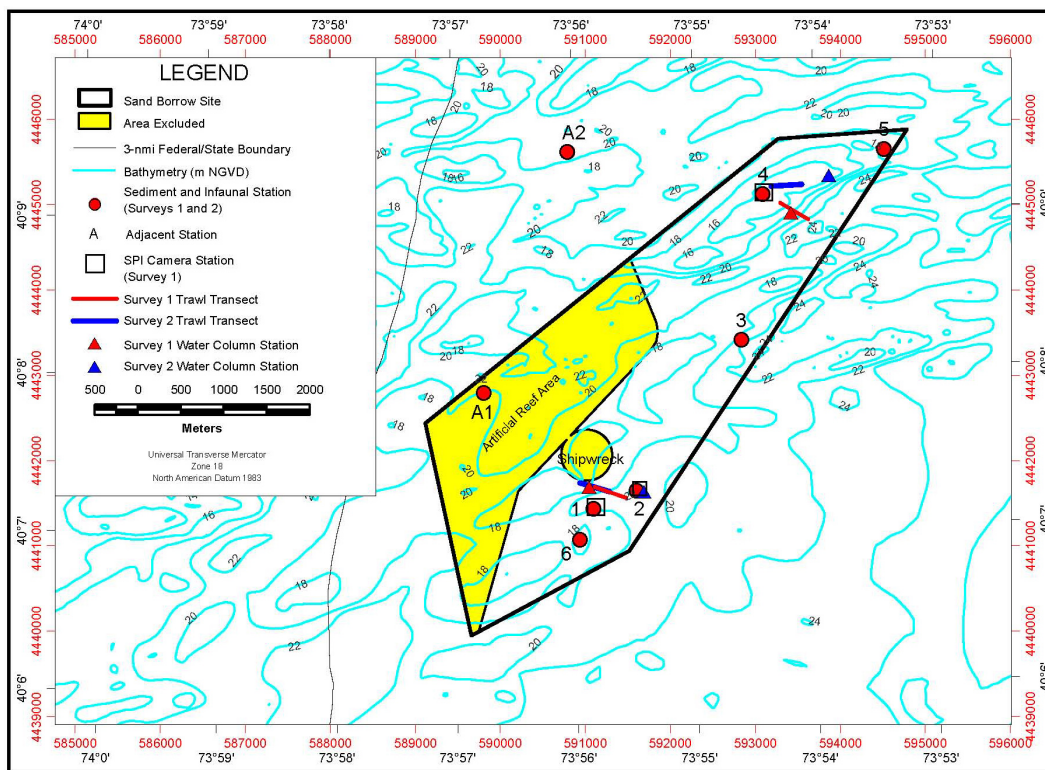


Figure 6-2. Environmental features, area excluded, and sampling stations relative to Sand Borrow Site H1 offshore New Jersey.

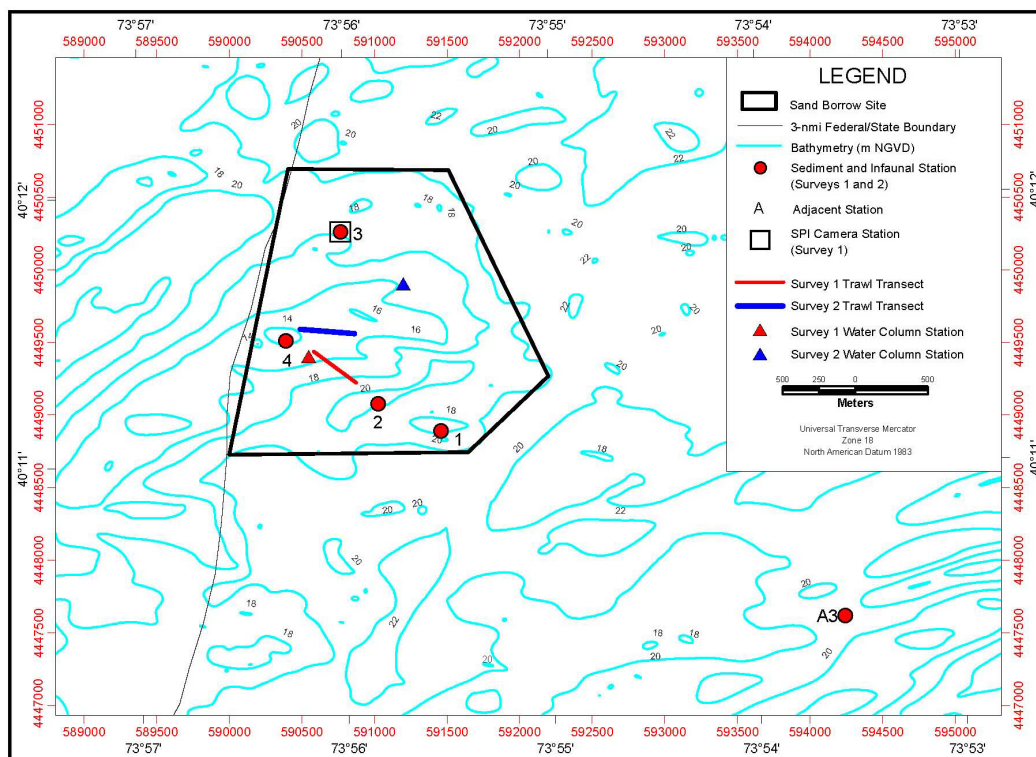


Figure 6-3. Environmental features and sampling stations relative to Sand Borrow Site H2 offshore New Jersey.

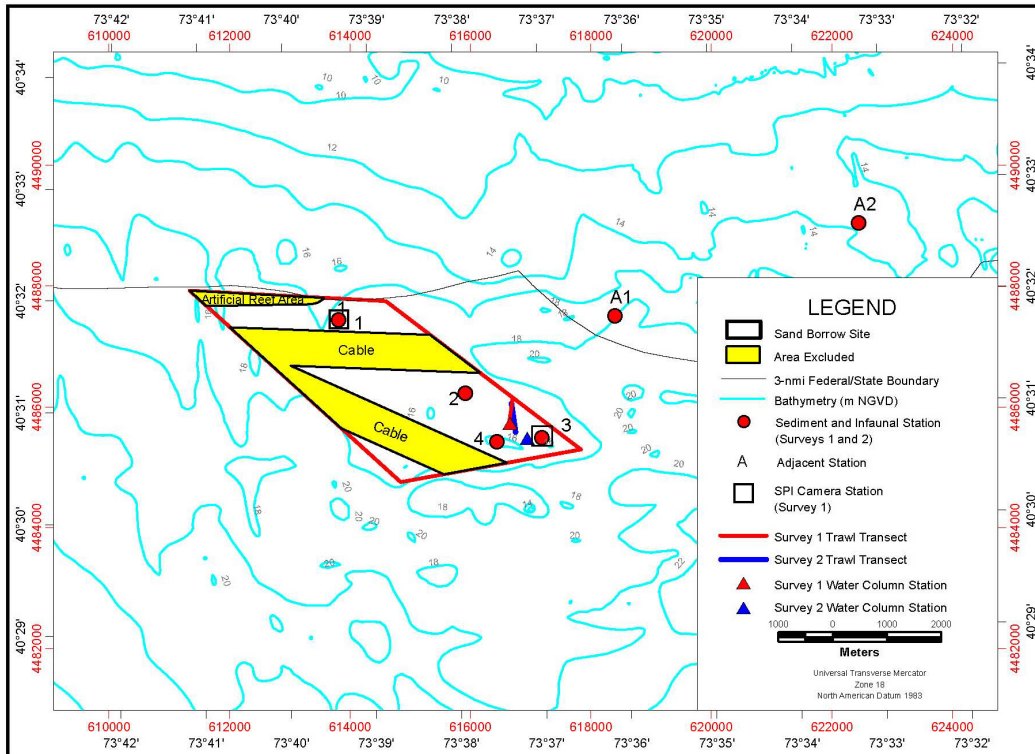


Figure 6-4. Environmental features, area excluded, and sampling stations relative to Sand Borrow Site 3 offshore New York.

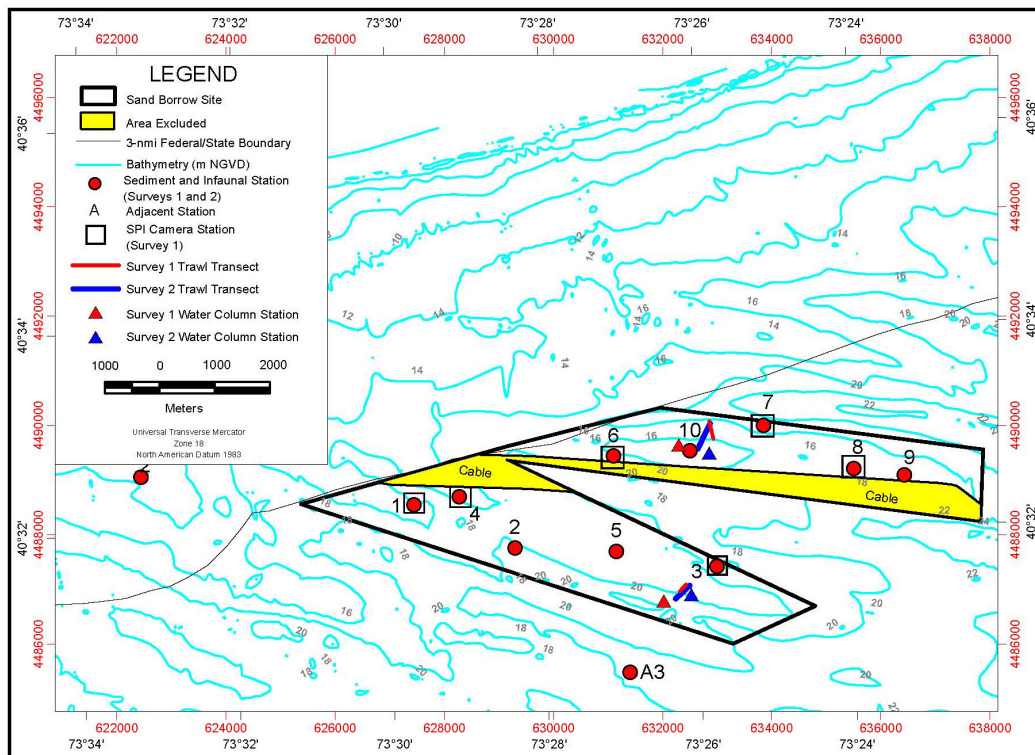


Figure 6-5. Environmental features, area excluded, and sampling stations relative to Sand Borrow Site 4 offshore New York.

6.2.1.1 Spatial Data Files and Exclusionary Mapping

Spatial data files of environmental features (e.g., sand borrow sites, artificial reefs, shipwrecks, submarine cables, etc.) and exclusionary mapping were used to design the field surveys as discussed in detail in Appendix E. The purpose of exclusionary mapping was to ensure that sampling would include areas in Federal waters shallower than 21 m and exclude areas that were unlikely to be dredged due to the presence of environmental features. Spatial data and exclusionary mapping files were analyzed in ArcView to determine locations for sampling (see Appendix E).

6.2.1.2 Water Column

Six water column profiles were made during each survey at locations illustrated in Figures 6-2 through 6-5. A water column profile was made at the beginning point of each trawl transect prior to actual trawling (see Section 6.2.1.5 for the rationale used for selecting trawl locations).

6.2.1.3 Sediment and Infauna

Of the 30 stations originally proposed for samples that would be analyzed for both sediment and infauna for each survey, 6 stations were positioned adjacent to but outside of the sand borrow sites, leaving 24 stations to be located within the four borrow sites. Four of the 24 stations to be sampled within the four borrow sites were allocated for discretionary sample locations, so that areas of interest such as topographic highs that were not included in the random sampling would be sampled.

The six adjacent stations were randomly located near the sand borrow sites as illustrated in Figures 6-2 to 6-5. For Sand Borrow Sites H1 and H2 off northern New Jersey (NJ), a rectangular area encompassing the two borrow sites was created as a polygon within ArcView, and the borrow sites within were excluded from selection. The remaining area was divided into three approximately equal cells, and a station then was randomly selected within each cell. These three adjacent (A) stations were labeled NJ-1, NJ-2, and NJ-3. This same process was repeated for Sites 3 and 4 off southern New York (NY), and the adjacent (A) stations were labeled NY-1, NY-2, and NY-3.

To determine the number of samples to collect in each sand borrow site during each survey for sediment and infaunal analyses, the surface area and percent of the total surface area for each of the sand borrow sites were calculated after exclusionary mapping was completed (see Appendix E). The percent of the total surface area remaining after exclusionary mapping for each of the sand borrow sites then was multiplied by 20 stations. This yielded 5 stations for Site H1, 2 stations for Site H2, 3 stations for Site 3, and 10 stations for Site 4 (see Appendix E). To allow for a minimum of three samples per borrow site, one sample was deducted from Site 4 and added to Site H2 so that there would be nine and three stations in each of these sand borrow sites, respectively.

Attention then was directed to selecting locations for the sediment and infaunal samples. The goal in placement of the stations was to provide broad spatial and depth coverage within the sand borrow sites and, at the same time, ensure that the samples would be independent of one another to satisfy statistical assumptions. To accomplish this goal, a sampling approach was used to provide broad spatial and depth coverage of the target populations. Each sand borrow site was divided into smaller cells of approximately equal areas. The number of cells depended on the number of samples allocated for the sand borrow site. One sampling station then was randomly placed within each cell of each sand borrow site. Randomizing within grid

cells eliminated biases that could be introduced by unknown spatial periodicities in a sampling area. This sampling approach resulted in designation of 20 sediment and infaunal sample locations within the four borrow sites.

The 20 locations for collecting samples that would be analyzed for sediment and infauna then were examined to determine where best to place the 4 discretionary stations. Because the 20 locations were randomly located, there were cases where isobaths indicated that high points of shoals would not be sampled. Therefore, the remaining four discretionary stations were located on the tops of shoals in Sand Borrow Sites H1, H2, 3, and 4 (Figures 6-2 to 6-5).

6.2.1.4 Sediment Profile Imaging

Twelve sediment profile imaging (SPI) stations were available for data collection during Survey 1. Two photographs were planned for each station. Based on percent of the total surface area of each sand borrow site remaining after exclusionary mapping, the SPI camera stations were assigned to the sand borrow sites as follows: three stations in Site H1, one station in Site H2, two stations in Site 3, and six stations in Site 4 (see Appendix E). For comparative purposes, the SPI camera stations were located at the same positions as some of the sediment/infaunal stations (there were no SPI camera stations that were not associated with sediment/infaunal stations). The allocated SPI stations were selected randomly from the previously located sediment/infaunal stations using a random number generator within a spreadsheet (Figures 6-2 to 6-5).

6.2.1.5 Epifauna and Demersal Fishes

Six trawl transects for epifauna and demersal fishes were originally proposed for each survey. Two trawl transects were assigned to both Sand Borrow Sites H1 and 4, and one trawl transect was allotted to both Sand Borrow Sites H2 and 3, for a total of six trawls per survey. Transect locations were manually assigned to attempt to cross isobaths and maximize characterization of existing assemblages with respect to water depth (Figures 6-2 to 6-5).

6.2.2 Field Methods

6.2.2.1 Vessel

Both field surveys were conducted aboard the M/V SAMANTHA MILLER. Survey 1 was mobilized on 5 September 2001, conducted from 6 to 8 September, and demobilized on 9 September. Survey 2 was mobilized on 24 June 2002 conducted from 25 to 27 June, and demobilized on 27 June.

6.2.2.2 Navigation

A differential global positioning system (DGPS) was used to navigate the survey vessel to all sampling stations. The DGPS was connected to an on-board computer equipped with Hypack Navigation Software Version 6.4 (Coastal Oceanographics, 1996). With this system, the ship's position was displayed in real-time on a monitor affixed to a countertop in the wheelhouse. All sampling stations were pre-plotted and stored in the Hypack program. While in the field, the actual positions of all samples collected were recorded and stored by the program.

6.2.2.3 Water Column

Conductivity, temperature, and dissolved oxygen were measured throughout the water column with a Sea-Bird electronic conductivity, temperature, depth (CTD) unit.

6.2.2.4 Sediment and Infauna

Sediment and infaunal samples were taken with a Smith-McIntyre grab. Once a sample was deemed acceptable (i.e., adequate sample quantity), a subsample of sediment was removed with a 5-cm diameter acrylic core tube and placed in a labeled plastic bag for grain size analyses. This sediment sample was stored at 4°C (i.e., on ice). The remainder of the grab sample was sieved through 0.5-mm sieve for infaunal analyses. The infaunal sample was placed in a container and preserved in 10% formalin with rose bengal stain.

6.2.2.5 Sediment Profile Imaging

Five replicate images were taken at each pre-plotted station to ensure acquisition of at least two suitable images for analysis; each SPI replicate is identified by the time recorded on the film and on disk along with vessel position. Even though multiple images were taken at each location, each image was assigned a unique frame number by the data logger and cross-checked with the time stamp in the navigational system's computer data file. Redundant sample logs were kept by the field crew. At the beginning of each survey day, the time on the camera's data logger was calibrated with the internal clock on the computerized navigation system being used to conduct the survey.

Test exposures were fired on deck at the beginning and end of each roll of film to verify that all internal electronic systems were working to design specifications and to provide a color standard against which final film emulsion could be checked for proper color balance. After deployment of the camera at each station, the frame counter was checked to make sure that the requisite number of replicates had been taken. In addition, a prism penetration depth indicator on the camera frame was checked to verify that the optical prism had actually penetrated the bottom to a sufficient depth to acquire an image. If images were missed (frame counter indicator), additional replicates were taken. Because of the paucity of fine-grained sediments in the study area, all available prism weights (total of 114 kg) were kept in the camera for the entire survey to maximize the camera's prism penetration.

6.2.2.6 Epifauna and Demersal Fishes

A 7.6-m mongoose trawl was towed for 10 minutes (bottom time) along transect lines. The tow path of each trawl tow was logged into the Hypack navigation system. Once the trawl was on deck, the contents of the catch bag were sorted and identified to the lowest practical identification level (LPIL), then returned to the sea.

6.2.3 Laboratory Methods

6.2.3.1 Sediment

Sediment analyses were conducted using combined sieve and hydrometer analyses according to recommended American Society for Testing and Materials (ASTM) procedures. Grain size samples were washed in demineralized water, dried, and weighed. Coarse and fine fractions (sand/silt) were separated by sieving through a U.S. Standard Sieve Mesh No. 230 (62.5 μm). Sediment texture of the coarse fraction was determined at half-phi intervals by passing the sediment through nested sieves. The weight of the materials collected in each particle size class was recorded. Boyocouse hydrometer analyses were used to analyze the fine fraction (<62.5 μm).

6.2.3.2 Sediment Profile Imaging

After the color slides were developed, the images were digitized using a Nikon Coolscan[®] film scanner and stored electronically in .jpg format. All digital images were analyzed using Sigma-scan Pro[®] (Aspire Software International) image analysis software. Calibration information was determined by measuring 1-cm graduations from the Kodak Color Separation Guide. This calibration information was applied to all images analyzed. Linear and area measurements were recorded as number of pixels and converted to scientific units using the calibration information. Measured parameters were recorded on an electronic spreadsheet. All data were subsequently checked as an independent quality assurance/quality control review of the measurements before final interpretation was performed.

Parameters measured from SPI images included the following:

- Sediment type (grain size major mode and range);
- Camera prism penetration depth;
- Small-scale surface boundary roughness;
- Thickness of depositional layers;
- Mud clasts (presence and diameter);
- Apparent redox potential discontinuity (RPD) depth; and
- Infaunal successional stage.

A detailed explanation of how these measurements were performed and their interpretation is provided below.

Sediment Type

Sediment grain size major mode and range were estimated visually from the photographs by overlaying a grain size comparator that was at the same scale. This comparator was prepared by photographing a series of Udden-Wentworth size classes (equal to or less than coarse silt up to granule and larger sizes) with the SPI camera. Seven grain size classes were on this comparator: 4 phi, 4 to 3 phi, 3 to 2 phi, 2 to 1 phi, 1 to 0 phi, 0 to -1 phi, and < -1 phi. The lower limit of optical resolution of the photographic system was about 62 μm , allowing recognition of grain sizes equal to or greater than coarse silt (≥ 4 phi). The accuracy of this method has been documented by comparing SPI estimates with grain size statistics determined from laboratory sieve analyses.

The comparison of the images with Udden-Wentworth sediment standards photographed through the SPI optical system also was used to map near-surface stratigraphy such as sand-over-mud and mud-over-sand. When mapped on a local scale near facies boundaries, this stratigraphy can provide information on transport directions.

Camera Prism Penetration Depth

The SPI camera prism penetration depth was measured from the bottom of the image to the sediment-water interface. Average penetration depth was determined by digitizing the entire cross-sectional area of sediment and dividing this result by the calibrated image width. Linear maximum and minimum depths of penetration also were measured. Maximum, minimum, and average penetration depths were recorded in the data file.

Prism penetration is potentially a noteworthy parameter; because the number of weights used in the camera was held constant throughout this survey, the camera functioned as a static-

load penetrometer. Comparative penetration values from stations with similar grain size give an indication of the relative water content of the sediment. Highly bioturbated sediments and rapidly accumulating sediments tend to have the highest water contents and greatest prism penetration depths.

The depth of the camera's penetration into the bottom also reflects the bearing capacity and shear strength of local sediments. Over-consolidated or relic sediments and shell-bearing sands resist camera penetration. Highly bioturbated, sulfidic, or methanogenic muds are the least consolidated, and deep penetration is typical. Seasonal changes in camera prism penetration are typically observed at the same station and are related to the control of sediment geotechnical properties by bioturbation (Rhoads and Boyer, 1982). The effect of water temperature on bioturbation rates appears to be important in controlling both biogenic surface relief and prism penetration depth (Rhoads and Germano, 1982).

Small-Scale Surface Boundary Roughness

Surface boundary roughness was determined by measuring the vertical distance (parallel to the film border) between the highest and lowest points of the sediment-water interface. Surface boundary roughness (sediment surface relief) measured over a horizontal distance of 15 cm typically ranges from 0.02 to 3.8 cm and may be related to either physical structures (ripples, rip-up structures, mud clasts) or biogenic features (burrow openings, fecal mounds, foraging depressions). Biogenic roughness typically changes seasonally and is related to the interaction of bottom turbulence and bioturbational activities.

The camera must be level in order to take accurate boundary roughness measurements. In sandy sediments, boundary roughness can be a measure of sand wave height. On silt/clay bottoms, boundary roughness values often reflect biogenic features such as fecal mounds or surface burrows.

Mud Clasts

When fine-grained, cohesive sediments are disturbed, either by physical bottom scour or faunal activity (e.g., decapod foraging), intact clumps of sediment often are scattered about the seafloor. These mud clasts can be seen at the sediment-water interface in the images. During analyses, the numbers of clasts were counted, the diameters of typical clasts were measured, and their oxidation states were assessed. The abundance, distribution, oxidation state, and angularity of mud clasts can be used to make inferences about the recent pattern of seafloor disturbance in an area.

Depending on their place of origin and the depth of disturbance of the sediment column, mud clasts can be reduced or oxidized (in the images, the oxidation state is apparent from the reflectance value; see the following subsection titled Apparent Redox Potential Discontinuity Depth). Also, once at the sediment-water interface, these mud clasts are subject to bottom-water oxygen levels and currents. Based on laboratory microcosm observations of reduced sediments placed within an aerobic environment, oxidation of reduced surface layers by diffusion alone is quite rapid, occurring within 6 to 12 hours (Germano, 1983). Consequently, the detection of reduced mud clasts in an obviously aerobic setting suggests a recent origin. The size and shape of the mud clasts also are revealing. Mud clasts may be moved and broken by bottom currents and animals (macro- or meiofauna; Germano, 1983). Over time, large angular clasts become small and rounded.

Apparent Redox Potential Discontinuity Depth

Aerobic near-surface marine sediments typically have higher reflectance values relative to underlying hypoxic or anoxic sediments. Surface sands washed free of mud also have higher optical reflectance than underlying muddy sands. These differences in optical reflectance are readily apparent in the images; oxidized surface sediment contains particles coated with ferric hydroxide (an olive or tan color when associated with particles), while reduced and muddy sediments below this oxygenated layer are darker, generally grey to black. The boundary between the colored ferric hydroxide surface sediment and underlying grey to black sediment is called the apparent RPD.

The depth of the apparent RPD in the sediment column is an important time-integrator of dissolved oxygen conditions within sediment porewaters. In the absence of bioturbating organisms, this high reflectance layer (in muds) typically will reach a thickness of 2 mm (Rhoads, 1974). This depth is related to the supply rate of molecular oxygen by diffusion into the bottom and the consumption of that oxygen by the sediment and associated microbiota. In sediments that have very high sediment oxygen demand (SOD), the sediment may lack a high reflectance layer even when the overlying water column is aerobic.

In the presence of bioturbating macrofauna, the thickness of the high reflectance layer may be several centimeters. The relationship between the thickness of this high reflectance layer and the presence or absence of free molecular oxygen in the associated porewaters must be assumed with caution. The actual RPD is the boundary (or horizon) that separates the positive Eh region of the sediment column from the underlying negative Eh region. The exact location of this Eh = 0 potential can be determined accurately only with microelectrodes; hence, the relationship between the change in optical reflectance, as imaged with the SPI camera, and the actual RPD can be determined only by making the appropriate *in situ* Eh measurements. For this reason, the optical reflectance boundary, as imaged, was described in this study as the "apparent" RPD and it was recorded as a mean value. In general, the depth of the actual Eh = 0 horizon will be either equal to or slightly shallower than the depth of the optical reflectance boundary. This is because bioturbating organisms can mix ferric hydroxide-coated particles downward into the bottom below the Eh = 0 horizon. As a result, the apparent mean RPD depth can be used as an estimate of the depth of porewater exchange, usually through porewater irrigation (bioturbation). Biogenic particle mixing depths can be estimated by measuring the maximum and minimum depths of imaged feeding voids in the sediment column. This parameter represents the particle mixing depths of head-down feeders (mainly polychaetes).

Apparent mean RPD depth also can be affected by local erosion. Peaks of disposal mounds commonly are scoured by divergent flow over mounds. This scouring can wash away fines and shell or gravel lag deposits and can result in a very thin apparent RPD depth. During storm periods, erosion may completely remove any evidence of the apparent RPD (Fredette et al., 1988).

Another important characteristic of the apparent RPD is the contrast in reflectance values at this boundary. This contrast is related to the interactions among the degree of organic loading, the bioturbational activity in the sediment, and the levels of bottom-water dissolved oxygen in an area. High inputs of labile organic material increase SOD and, subsequently, sulfate reduction rates (and the abundance of sulfide end products). This results in more highly reduced (lower-reflectance) sediments at depth and higher RPD contrasts. In a region of generally low RPD contrasts, images with high RPD contrasts indicate localized sites of

relatively high past inputs of organic-rich material such as organic or phytoplankton detritus, dredged material, and sewage sludge.

Infaunal Successional Stage

Information concerning infaunal successional stages in fine-grained sediments may be collected with SPI technology. These stages are recognized in the images by the presence of dense assemblages of near-surface polychaetes and/or subsurface feeding voids; both may be present in the same image. The concept of successional stages is based on the theory that organism-sediment interactions follow a predictable sequence after a major seafloor perturbation. This theory states that primary succession results in "the predictable appearance of macrobenthic invertebrates belonging to specific functional types following a benthic disturbance. These invertebrates interact with sediment in specific ways. Because functional types are the biological units of interest ... our definition does not demand a sequential appearance of particular invertebrate species or genera" (Rhoads and Boyer, 1982). This theory is formally developed in Rhoads and Germano (1982) and Rhoads and Boyer (1982).

This continuum of change in animal communities after a disturbance (primary succession) has been divided arbitrarily into three stages: Stage I is the initial community of tiny, densely populated polychaete assemblages; Stage II is the start of the transition to head-down deposit feeders; and Stage III is the mature community of deep-dwelling, head-down deposit feeders (Figure 6-6).

After an area of bottom is disturbed (whether from natural or anthropogenic events), the first invertebrate assemblage (Stage I) appears within days after the disturbance. Stage I consists of dense assemblages of tiny tube-dwelling marine polychaetes that reach population densities of 10^4 to 10^6 individuals per m^2 . These animals feed at or near the sediment-water interface and physically stabilize or bind the sediment surface by producing a mucous "glue" that they use to build their tubes. Sometimes deposited dredged material layers contain Stage I tubes still attached to mud clasts from their location of origin; these transported individuals are considered as part of the *in situ* fauna in the assignment of successional stages.

If there are no repeated disturbances to the newly colonized area, then these initial tube-dwelling suspension or surface-deposit feeding taxa are followed by burrowing, head-down deposit-feeders that rework the sediment deeper over time and mix oxygen from the overlying water into the sediment. Animals in these later-appearing communities (Stage II or III) are larger, have lower overall population densities (10 to 10^2 individuals per m^2), and can rework sediments to depths of 3 to 20 cm or more. These animals "loosen" the sedimentary fabric, increase the water content in the sediment (thereby lowering the sediment shear strength), and actively recycle nutrients because of the high exchange rate with the overlying waters resulting from their burrowing and feeding activities.

While the successional dynamics of invertebrate communities in fine-grained sediments have been well-documented, the successional dynamics of invertebrate communities in sand and coarser sediments are not well-known. Subsequently, the insights gained from SPI technology regarding biological community structure and dynamics in sandy and coarse-grained bottoms are fairly limited.

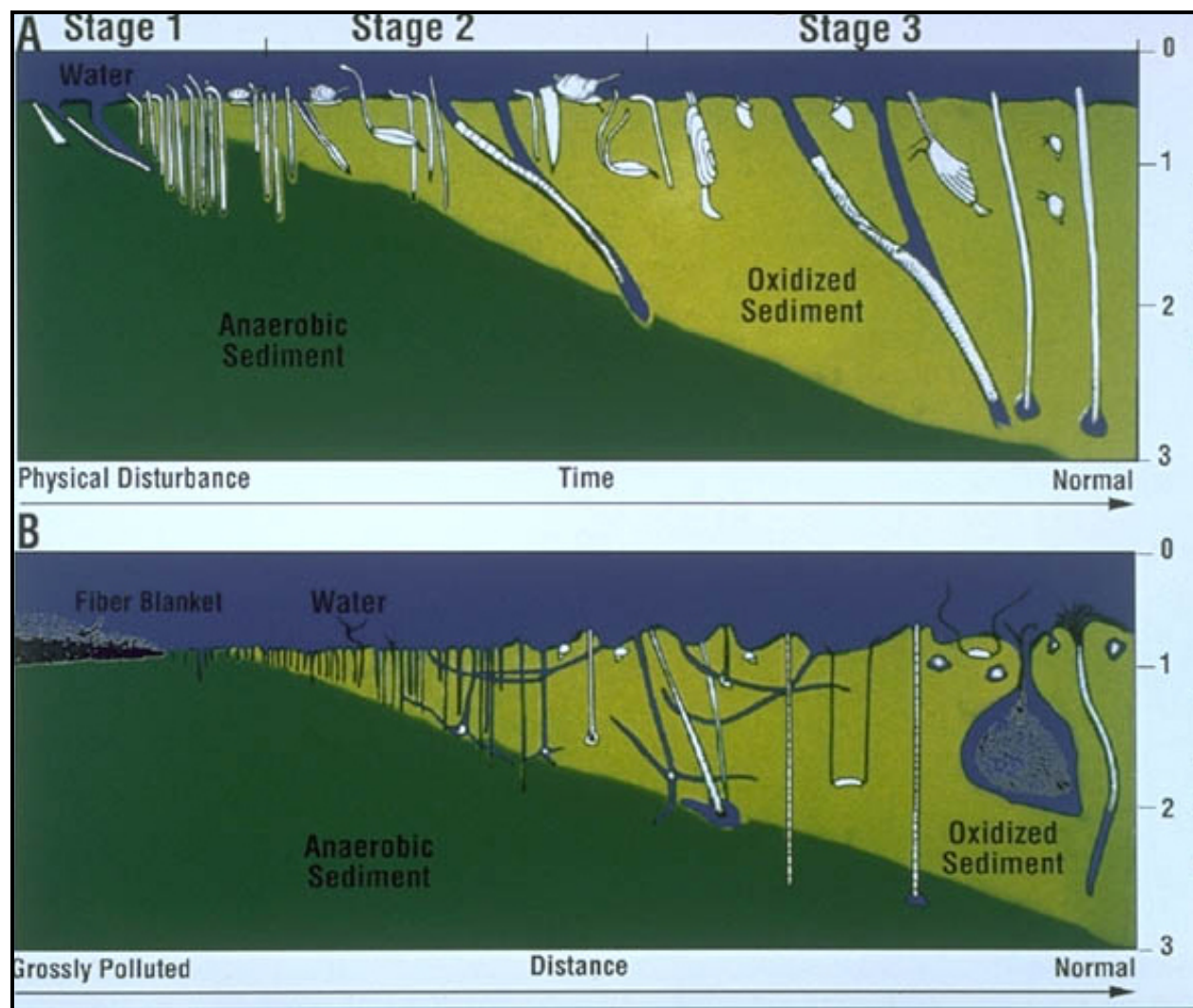


Figure 6-6. The successional change in benthic community following a disturbance over time (top) or over distance from a source of pollution (bottom) is illustrated (from Rhoads and Germano, 1982, 1986).

6.2.3.3 Infauna

Formalin-preserved infaunal samples were rinsed on a U.S. Standard No. 30 (0.59-mm) sieve and transferred to 70% isopropanol. Before sorting, samples were passed through a series of sieves (0.3, 0.5, 0.6, 1, and 2 mm) to separate the organisms into size classes. Samples were sorted by hand under dissecting microscopes. All sediment in each sample was examined by a technician who removed all infauna observed. Organisms were identified to the LPIL and counted. A minimum of 10% of all samples were resorted by different technicians as a quality control measure. Voucher specimens of each taxon were archived at the Barry A. Vittor & Associates, Inc. laboratory.

6.2.4 Data Analysis

6.2.4.1 Water Column

Conductivity, temperature, dissolved oxygen, and depth values were entered into an electronic spreadsheet and tabulated. Depth profiles were plotted for salinity, temperature, and dissolved oxygen.

6.2.4.2 Sediment

A computer algorithm was used to determine size distribution and provide summary statistics for each sediment sample using Folk inclusive graphic measures and Method of Moment calculations. For each sample, the following parameters were recorded: sample weight; percentages of gravel, sand, silt, and clay; Folk's classification; median size; moment measures (mean, standard deviation, skewness, and kurtosis); and Folk inclusive graphic measures (mean, standard deviation, skewness, and kurtosis).

6.2.4.3 Infauna

Summary statistics including number of taxa, number of individuals, density, diversity (H'), evenness (J'), and species richness (D) were calculated for each sampling station. Diversity (H'), also known as Shannon's index (Pielou, 1966), was calculated as follows:

$$H' = - \sum_{i=1}^S p_i \ln(p_i)$$

where S is the number of taxa in the sample, i is the i th taxa in the sample, and P_i is the number of individuals of the i th taxa divided by (N) the total number of individuals in the sample.

Evenness (J') was calculated with Pielou's (1966) index of evenness:

$$J' = \frac{H'}{\ln(S)}$$

where H' is Shannon's index as calculated above and S is the total number of taxa in a sample.

Species richness (D) was calculated by Margalef's index:

$$D = \frac{(S - 1)}{\ln(N)}$$

where S is the total number of sample taxa and N is the number of individuals in the sample.

Spatial and temporal patterns in infaunal assemblages were examined with cluster analysis. Cluster analyses were performed on similarity matrices constructed from raw data matrices consisting of taxa and samples (station – survey). Only species-level taxa, with the exception of two species complexes that can be reliably identified only to genus, were included in the analyses. Of these taxa, only those contributing at least 0.1% of the total abundance of species level taxa were included. Raw counts of each individual infaunal taxon in a sample (n)

were transformed with the $\log_{10}(n+1)$ transformation prior to similarity analysis. Both normal (stations) and inverse (taxa) similarity matrices were generated using the Bray-Curtis index that was calculated using the following formula:

$$B_{jk} = \frac{2 \sum_i \min(x_{ij}, x_{ik})}{\sum_i (x_{ij} + x_{ik})}$$

where B_{jk} (for normal analysis) is the similarity between samples j and k ; x_{ij} and x_{ik} are the abundances of species i in samples j and k . B ranges from 0.0 when two samples have no species in common to 1.0 when the distribution of individuals among species is identical between samples. For inverse analysis, the B_{jk} is the similarity between species j and k ; x_{ij} and x_{ik} are the abundances of species j and k in sample i . Normal and inverse similarity matrices were clustered using the group averaging method of clustering (Boesch, 1973).

The extent to which sample groups formed by normal cluster analysis of the entire data set could be explained by environmental variables such as sedimentary parameters was examined by canonical discriminant analysis (SAS Institute Inc., 1989). Canonical discriminant analysis identifies the degree of separation among predefined groups of variables in multivariate space. This analysis examined the relationships among the environmental variables and the station groups as indicated by the normal cluster analysis. Environmental variables used in the analysis were water depth (meters), survey (1 or 2), northing (x), easting (y), % gravel, % sand, and % fines.

6.2.4.4 Epifauna and Demersal Fishes

Raw counts of individual epifaunal and demersal fish taxa were tabulated by sand borrow site for both field surveys.

6.3 RESULTS

6.3.1 Water Column

Depth profiles of temperature, salinity, and dissolved oxygen for the September 2001 Survey 1 are depicted in Figures 6-7 and 6-8. Two profiles were made in Sand Borrow Sites H1 and 4 and one profile each in Sites H2 and 3. These profiles indicated, with the exception of the near bottom portion, that the water column was well mixed in the sand borrow sites during the September survey. Temperature recorded at the surface ranged from 21.3°C at Station 4-2 to 22.9°C at Stations H1-1 and H2. Bottom temperatures ranged from 17.0°C at Station H1-1 to 21.1°C at Station H1-2. Salinity profiles were fairly uniform from surface to bottom at all sites (Figure 6-7). Surface and bottom salinity varied little during the September survey; overall values ranged from 31.8 ppt at the bottom at Station H1-1 to 30.9 ppt at the surface at Station H2. Dissolved oxygen profiles in Sites 3 and 4 were uniform in the upper 10 m of the water column, decreased within the 10 to 15 m depth interval, then stabilized and were uniform to the bottom (Figure 6-8). Surface values for dissolved oxygen ranged from 7.3 mg/l at Station 3 to 6.6 mg/l at Station H1-1, and bottom dissolved oxygen values ranged from 4.1 mg/l at Station H2 to 7.0 at Station H1-2.

Depth profiles of temperature, salinity, and dissolved oxygen for the June 2002 Survey 2 are shown in Figures 6-9 to 6-10. Profiles recorded during this survey indicated that temperature and dissolved oxygen decreased continuously with depth across all sand borrow

sites. Surface temperatures ranged from 21.9°C in Site 4 to 19.7°C at Station H1-1. Bottom temperatures ranged from 14.8°C in Site 4 (Station 4-1) to 12.2°C at Station H1-1. Salinity profiles were generally uniform from surface to bottom during June. Surface salinity measurements varied from 30.9 ppt at Station H1-1 to 29.2 ppt at Station 4, and bottom values ranged from 32.2 ppt at Station H1 to 31.6 ppt at Station 4. Dissolved oxygen in surface waters ranged from 11.4 mg/l at Station 4 to 8.1 mg/l at Station 3. Bottom values ranged from 6.7 mg/l at Station H1-1 to 5.8 mg/l at Station H2-1.

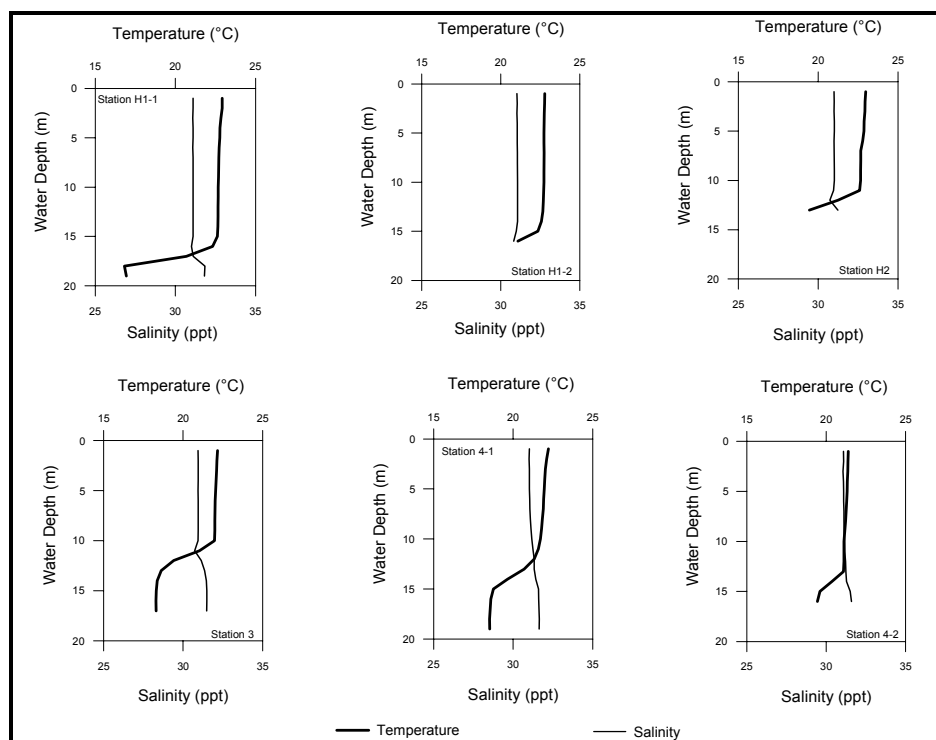


Figure 6-7. Temperature and salinity profiles recorded during the September 2001 Survey 1 in Sand Borrow Sites H1, H2, 3, and 4 offshore New Jersey and New York.

6.3.2 Sediment

Results of the sediment analyses of grab samples from borrow sites and adjacent stations are provided in Appendix D, Table D-2. Sedimentary characteristics of grab samples consisted of various proportions of gravel, sand, silt, and clay. These proportions were used to assign Folk's classification (Folk, 1974) to individual samples that provide a general qualitative description of sediments found in each sand borrow site. Table 6-2 shows that most samples (30 samples; 50%) were sand, followed by slightly gravelly sand (19 samples; 32%), gravelly sand (9 samples, 15%), and sandy gravel (2 samples; 3%).

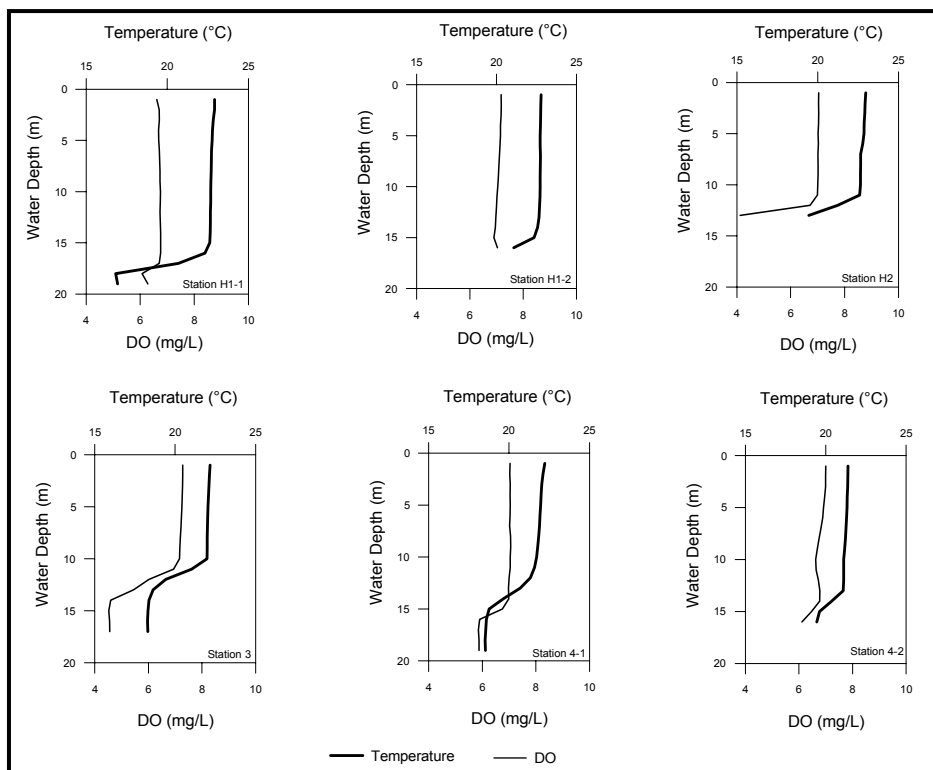


Figure 6-8. Temperature and dissolved oxygen (DO) profiles recorded during the September 2001 Survey 1 in Sand Borrow Sites H1, H2, 3, and 4 offshore New Jersey and New York.

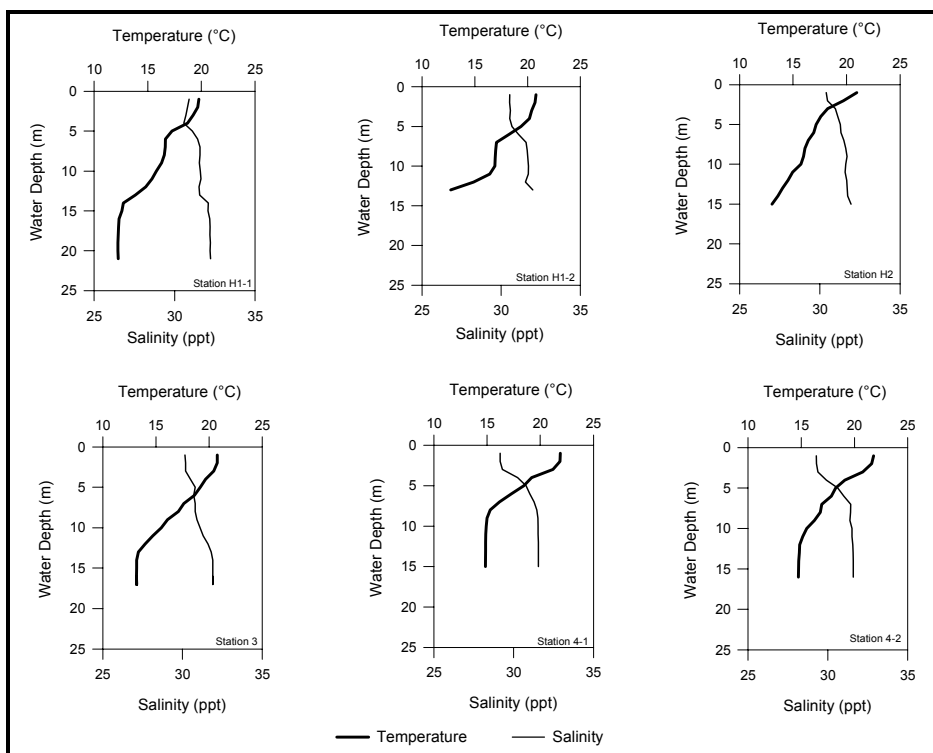


Figure 6-9. Temperature and salinity profiles recorded during the June 2002 Survey 2 in Sand Borrow Sites H1, H2, 3, and 4 offshore New Jersey and New York.

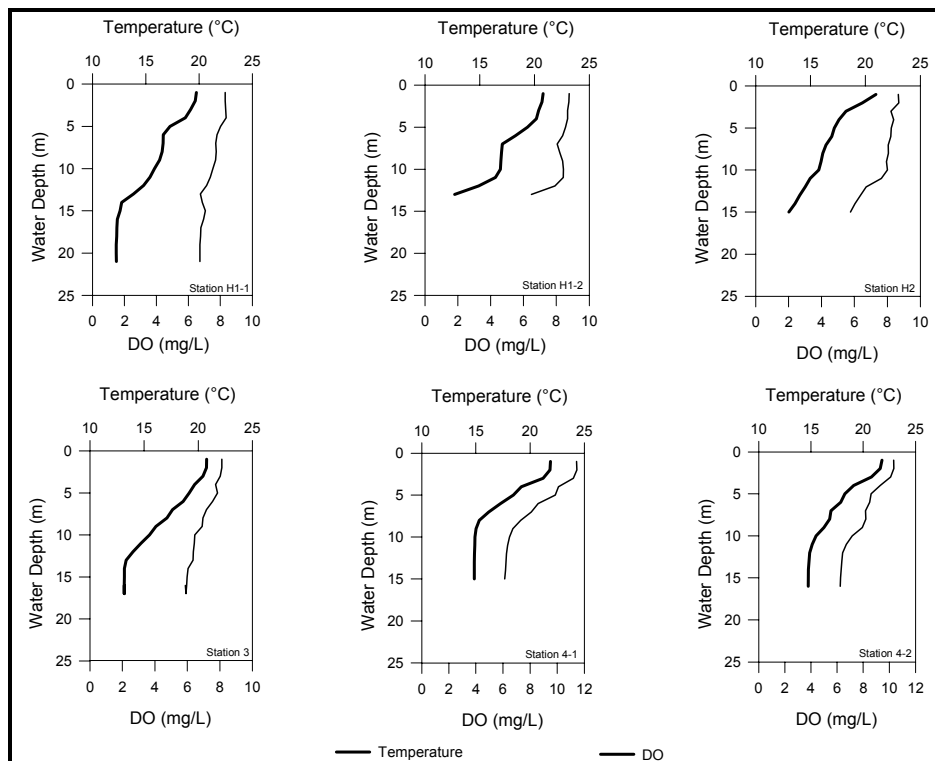


Figure 6-10. Temperature and dissolved oxygen (DO) profiles recorded during the June 2002 Survey 2 in Sand Borrow Sites H1, H2, 3, and 4 offshore New Jersey and New York.

Grab samples from offshore New Jersey (Borrow Sites H1 and H2, Adjacent Stations NJ-A1, NJ-A2, and NJ-A3) were generally similar in sedimentary composition to those from offshore southern New York (Borrow Sites 3 and 4, Adjacent Stations NY-A1, NY-A2, and NY-A3). Most samples (4 of 6) collected during September in Site H1 were classified as sand with the remainder slightly gravelly sand and gravelly sand. In Site H2, most samples collected in September (3 of 4) were slightly gravelly sand with only one classified as sand. Samples collected in Site 3 during the September survey yielded only gravelly sand (2 of 4), slightly gravelly sand (1 of 4), and sandy gravel (1 of 4). Samples collected in September from Site 4 were half (5 of 10) sand and half (5 of 10) slightly gravelly sand.

During June, most grab samples (3 of 6) from Site H1 were slightly gravelly sand followed by sand (2 of 6 samples) and gravelly sand (1 of 6 samples). In Site H2, all four samples collected in June were sand. Samples collected from Site 3 consisted of gravelly sand (3 of 4) and sandy gravel (1 of 4), and all 10 samples taken from Site 4 were classified as sand.

6.3.3 Sediment Profile Imaging

A minimal number of sediment profile stations (12) were sampled during the September survey only. While the small data set does not allow for a thorough discussion of individual sedimentary characteristics or biological community trends by site, the images do provide some detailed context for interpretation of the grab sampling results. The complete image analysis results from all 24 images are presented in Appendix D, Table D-3.

Table 6-2. Sediment type summary from grab samples for the September 2001 Survey 1 and June 2002 Survey 2 in the sand borrow sites and adjacent stations offshore New Jersey and New York.						
Sand Borrow Site (H1, H2, 3, 4) or Adjacent Station (NJ-1, NY-1, etc.)	Survey	Total No. of Samples Collected	No. of Samples with Particular Sediment Types Based on Folk's Classifications			
			Sandy Gravel	Gravelly Sand	Slightly Gravelly Sand	Sand
H1	1	6		1	1	4
	2	6		1	3	2
H2	1	4			3	1
	2	4				4
3	1	4	1	2	1	
	2	4	1	3		
4	1	10			5	5
	2	10				10
NJ-1	1	1			1	
	2	1				1
NJ-2	1	1			1	
	2	1			1	
NJ-3	1	1		1		
	2	1		1		
NY-1	1	1			1	
	2	1				1
NY-2	1	1			1	
	2	1				1
NY-3	1	1			1	
	2	1				1
Total No. of Samples		60	2	9	19	30

Similar to previous investigations of sand resource areas performed in 1998 off the New Jersey coast (Byrnes et al., 2000), the areas surveyed with SPI technology in September 2001 were dominated at the decimeter scale by wave-generated bedforms. Sediments primarily were very fine to medium sands, with some stations coarsening toward the gravel end of the scale. Despite having all the lead weights on the camera system, prism penetration was limited, ranging from approximately 3.5 cm to a little over 7 cm (less than 1/3 of the vertical distance of the camera's faceplate; see Appendix D, Table D-3) because of the sandy sediments found at all stations sampled. While minor fractions of silt/clay size particles were present at all stations, the sediment grain size major mode was in the very fine or fine sand categories at most stations sampled (Appendix D, Table D-3); the one notable exception was Station 1 at Site 3 (Figure 6-11), where the sediment grain size major mode was in the granule to pebble range in the Wentworth size classification (Folk, 1974).

6.3.3.1 Site H1

Three stations (Stations 1, 2, and 4) were surveyed with the profile camera at Site H-1 (Figure 6-2). Sediment grain sizes from the grab samples (Appendix D, Table D-2) for these three stations were gravelly sand (Station 1) or sand (Stations 2 and 4), with over 90% of the

sediments in the sand size fraction. While SPI results for sediment grain size major mode agreed with the conventional grab results, the images showed a somewhat finer discrimination of the sediment major mode in this broad “sand” category from Appendix D, Table D-2, with the sediment grain size major mode in the medium sand interval for Station 1 (2-3 phi), very fine sand for Station 2 (4-3 phi), and fine sand for Station 3 (3-2 phi). The slight shift in sediment grain size major mode most likely reflects the difference in near-bed energy regime at these three stations within the site. Stronger bottom currents are more likely prevalent at Station 1, where finer grains have been winnowed away and small-scale ripples can be seen on the sediment surface (Figure 6-12).

The one major discrepancy between the sediment grain size data from the grab and the profile images among all samples collected occurs at Station 2 in Site H1 (Appendix D, Tables D-2 and D-3). Grab results showed no detectable sediment in the silt/clay size fraction (100% of the sediment was in the sand size interval; Appendix D, Table D-2), while sediment profile images from this station clearly show fine-grained muds mixed in with the fine sand (Figure 6-13). In fact, it was precisely because of the presence of fine-grained muds at this station that sufficient organic material was present to actually be able to measure the thickness of the apparent RPD; this was the only station of the 12 sampled (Appendix D, Table D-3) where an RPD depth could be measured during image analysis of the digital files. These differences between co-located grab/SPI results are an excellent illustration of the small-scale heterogeneity of ridge and swale topography (Schaffner and Boesch, 1982) that can exist in such a dynamic kinetic regime.



Figure 6-11. Sediment profile image from Site 3, Station 1 showing the pebble to granule-sized layer of gravel on top of poorly sorted medium to coarse sands. Scale: width of image = 16.8 cm.



Figure 6-12. Sediment profile image from Site H1, Station 1 showing small-scale ripples on the sediment surface. Scale: width of image = 16.7 cm.

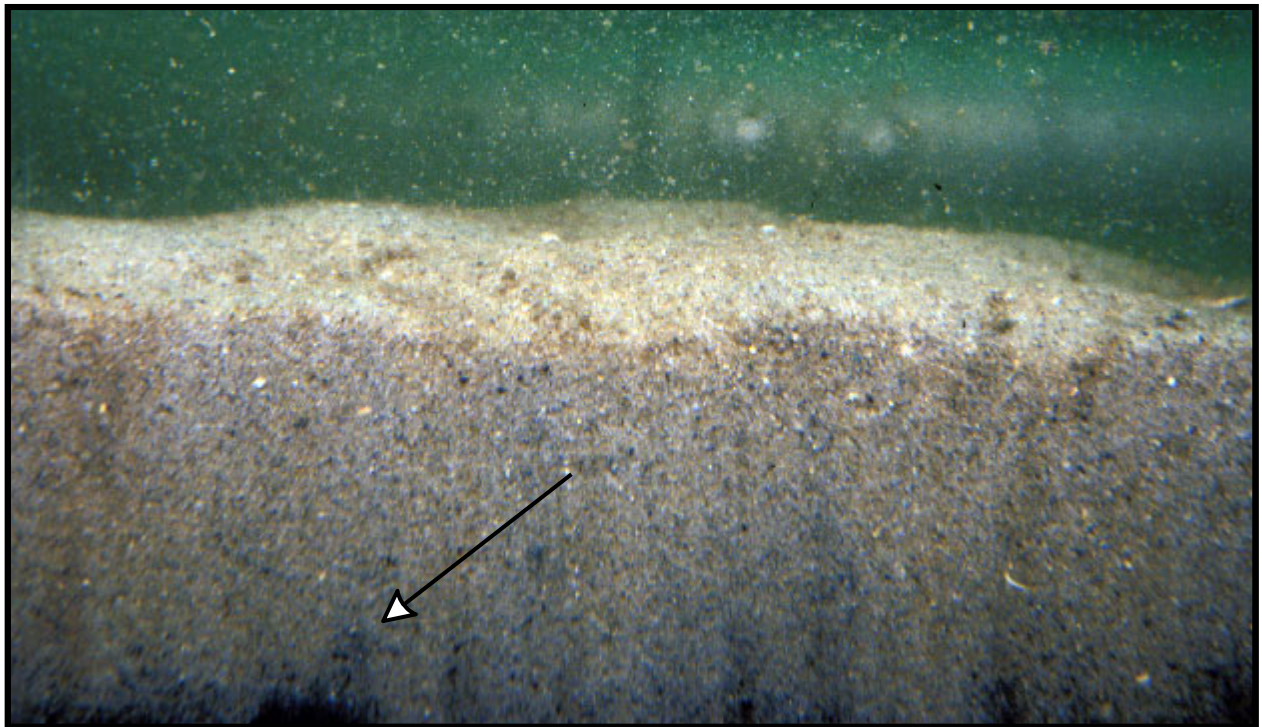


Figure 6-13. Sediment profile image from Site H1, Station 2 showing a clear gradation from fine sand to finer silt/clay particles at the bottom of the image (arrow). Scale: width of image = 16.8 cm.

Biological information from sediment profile images in sandy bottoms is typically very restricted due to the shallow prism penetration, and images from the September 2001 survey were no exception. However, evidence of two of the numerically dominant taxa (*Polygordius* and *Echinarachnius*) noted in the grab results (Table 6-3) was seen in images from Station 1 (Figure 6-14) and Station 4 (Figure 6-15).

6.3.3.2 Site H2

One station (Station 3; Figure 6-3) was sampled in Site H2. Both images had shallow penetration and showed poorly-sorted, silty sand with a layer of fine detritus on the sediment surface (Figure 6-16). *E. parma* (Figure 6-16) and *Diopatra* (Figure 6-17) were evident at this location.

6.3.3.3 Site 3

The two stations (Stations 1 and 3, Figure 6-4) surveyed in Site 3 had substantially different sediment types. Station 1 (Appendix D, Table D-2, Figure 6-11) was located in a high kinetic regime and had almost equal proportions of sand and gravel. Station 3 was located in an area with a rippled bottom and primarily fine sand (Figure 6-18). The numerically dominant organism at this site based on grab results (Table 6-3) was a gammarid amphipod. These crustaceans are free-swimming and forage at the sediment surface, and they would not usually be expected to be seen in sediment profile images. However, densities were sufficiently high that two of the animals were photographed in one of the replicates from this station (Figure 6-19).

6.3.3.4 Site 4

Six stations were surveyed at Site 4 (Stations 1, 3, 4, 6, 7, and 8; Figure 6-5). The sediment grain size major modes at these six stations were very similar, alternating between very fine sand (4-3 phi) and fine sand (3-2 phi; Appendix D, Table D-3). All six stations showed evidence of rippled bottoms, indicating relatively high kinetic energy on the bottom. Some stations showed recent evidence of bedform mobility (Figure 6-20). While no evidence of the numerically dominant polychaete *Polygordius* (based on grab results; Table 6-3) could be seen in any of the images, evidence of another one of the numerically dominant taxa, *E. parma*, could be seen in images from four of the six stations surveyed (Figure 6-21).

6.3.4 Infauna

A taxonomic listing of infauna collected in bottom grabs during the September and June surveys is presented in Appendix D, Table D-4. Over both surveys, a total of 19,334 individuals was collected, representing 150 taxa in 9 separate phyla. Most taxa collected were polychaetes (77 taxa), followed by crustaceans (38), and bivalve (14) and gastropod (8) mollusks. Overall abundance was similar across surveys. Grab samples yielded 10,107 individuals in September and 9,227 in June. Seventy-four taxa (51% of total) were common to both surveys. There were 39 taxa restricted to the June survey, and the September survey included 33 taxa not found in June samples.

The archiannelid *Polygordius* was numerically dominant in the grabs, representing 31% of all infauna censused over both surveys. Other than *Polygordius*, taxa that were among the top 10 numerical dominants during both the September and June surveys included the echinoid *Echinarachnius parma*, polychaetes of the genus *Aricidea*, the tanaid *Tanaissus psammophilus*, and non-identified tubificid oligochaetes.

Table 6-3. Ten most abundant taxa in grab samples from Sand Borrow Sites H1, H2, 3, and 4 and Adjacent Areas NJA and NYA for the September 2001 Survey 1 offshore New Jersey and New York.					
Site	Taxonomic Name	Count	Site	Taxonomic Name	Count
H1	<i>Polygordius</i> (LPIL)	710	NJA	<i>Polygordius</i> (LPIL)	1,208
	<i>Tanaissus psammophilus</i>	198		<i>Echinarachnius parma</i>	144
	<i>Pseudunciola obliquua</i>	180		<i>Cirrophorus ilvana</i>	97
	<i>Echinarachnius parma</i>	135		<i>Pellucistoma</i> (LPIL)	57
	<i>Pellucistoma</i> (LPIL)	79		<i>Hemipodus roseus</i>	56
	<i>Spisula solidissima</i>	75		<i>Lumbrinerides dayi</i>	46
	<i>Cirrophorus ilvana</i>	58		<i>Nephtys picta</i>	35
	<i>Aricidea catherinae</i>	51		<i>Pseudunciola obliquua</i>	32
	<i>Glycera capitata</i>	36		<i>Enchytraeidae</i> (LPIL)	31
	<i>Unciola irrorata</i>	32		<i>Aricidea cerrutii</i>	31
H2	<i>Polygordius</i> (LPIL)	225	NYA	Tubificidae (LPIL)	138
	<i>Tanaissus psammophilus</i>	74		<i>Echinarachnius parma</i>	121
	<i>Echinarachnius parma</i>	61		<i>Spisula solidissima</i>	100
	<i>Pseudunciola obliquua</i>	51		<i>Exogone hebes</i>	71
	<i>Rhynchocoela</i> (LPIL)	14		<i>Aricidea catherinae</i>	64
	<i>Parahaustorius attenuatus</i>	10		<i>Polygordius</i> (LPIL)	49
	<i>Spisula solidissima</i>	10		<i>Pseudunciola obliquua</i>	48
	<i>Nephtys picta</i>	9		<i>Tellina agilis</i>	46
	<i>Pellucistoma</i> (LPIL)	9		<i>Rhepoxynius hudsoni</i>	27
	<i>Caulleriella</i> sp. J	8		<i>Nucula proxima</i>	25
3	<i>Gammarus annulatus</i>	560	ALL	<i>Polygordius</i> (LPIL)	3,521
	<i>Polygordius</i> (LPIL)	349		<i>Gammarus annulatus</i>	851
	<i>Aricidea</i> (LPIL)	74		<i>Echinarachnius parma</i>	708
	<i>Lumbrinerides dayi</i>	67		<i>Pseudunciola obliquua</i>	656
	<i>Tanaissus psammophilus</i>	66		<i>Tanaissus psammophilus</i>	465
	Oligochaeta (LPIL)	54		<i>Spisula solidissima</i>	316
	<i>Aricidea catherinae</i>	52		<i>Cirrophorus ilvana</i>	258
	<i>Aricidea cerrutii</i>	44		<i>Aricidea catherinae</i>	194
	<i>Crenella glandula</i>	34		Tubificidae (LPIL)	180
	<i>Astarte castanea</i>	33		<i>Pellucistoma</i> (LPIL)	180
4	<i>Polygordius</i> (LPIL)	980	LPIL = Lowest practical identification level.		
	<i>Pseudunciola obliquua</i>	345			
	<i>Gammarus annulatus</i>	291			
	<i>Echinarachnius parma</i>	237			
	<i>Protohaustorius wigleyi</i>	124			
	<i>Spisula solidissima</i>	108			
	<i>Tanaissus psammophilus</i>	96			
	<i>Cirrophorus ilvana</i>	79			
	<i>Acanthohaustorius millsii</i>	61			
	<i>Rhepoxynius hudsoni</i>	45			



Figure 6-14. Sediment profile image from Site H1, Station 1 showing one of the numerically dominant polychaetes (*Polygordius*) found in grab samples from this location. Scale: width of image = 16.7 cm.

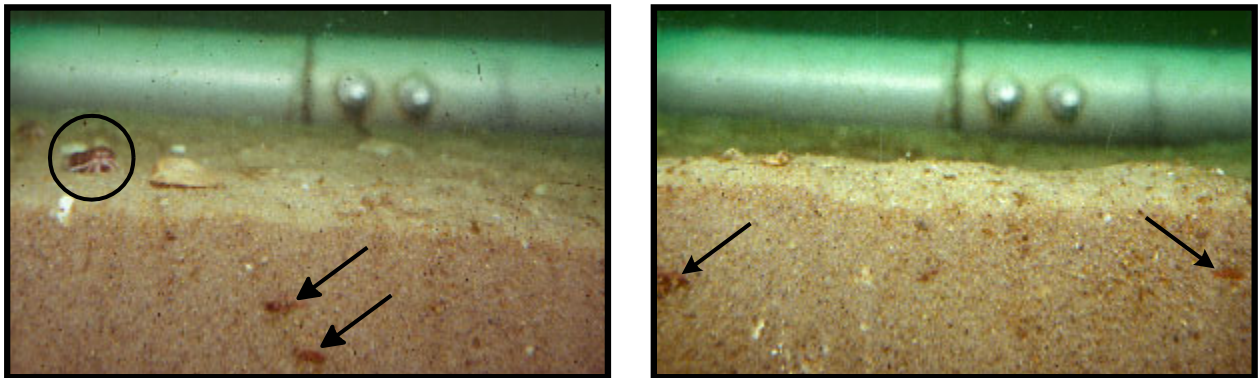


Figure 6-15. Replicate sediment profile images from site H1, Station 4 showing buried sand dollars (*Echinarachnius parma*) (arrows). Note the hermit crab (circle) on the sediment surface in the image on the left. Scale: width of image = 16.7 cm.



Figure 6-16. Both replicate sediment profile images from Site H2, Station 3 showed a layer of fine detritus (arrow) on the sediment surface. Note the bisected edge of a partially buried sand dollar (*Echinarachnius parma*) on the right side of image (circle). Scale: width of image = 16.7 cm.



Figure 6-17. Sediment profile image from Site H2, Station 3 showing a prominent tube of the polychaete *Diopatra* projecting above the sediment-water interface. Scale: width of image = 16.7 cm.



Figure 6-18. Sediment profile image from Site 3, Station 3 showing well-sorted, rippled, granitic fine sands. Scale: width of image = 16.7 cm.



Figure 6-19. Sediment profile image from Site 3, Station 3 showing two gammarid amphipods in the upper right corner swimming above the rippled fine sandy bottom. Scale: width of image = 16.7 cm.



Figure 6-20. Sediment profile image from Site 4, Station 7 showing a sharply defined arcuate bedform with an active mobile surface layer (arrow). Scale: width of image = 16.7 cm.

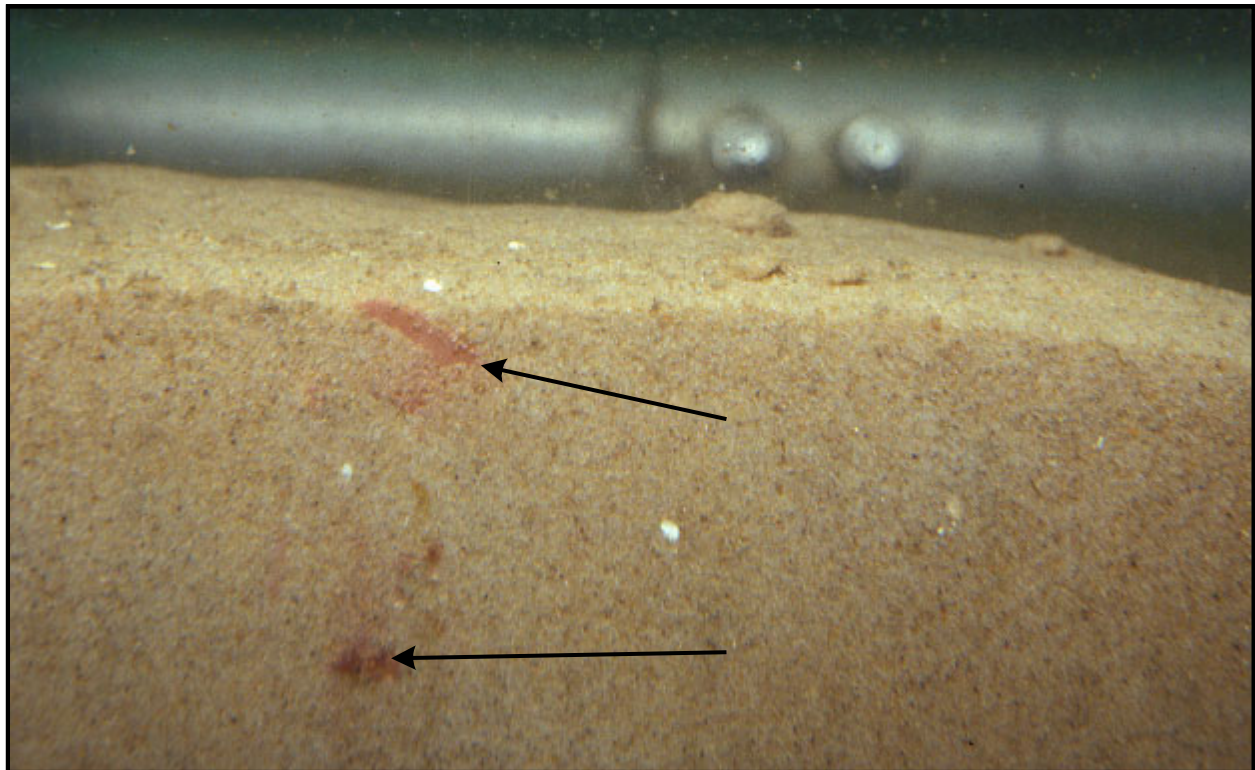


Figure 6-21. Sediment profile image from Site 4, Station 6 showing partially buried sand dollars (*Echinarachnius parma*) found at many station in this site. Scale: width of image = 16.7 cm.

Table 6-3 lists the numerically dominant infaunal taxa sampled from each of the sand borrow sites and overall for the September survey. The numerically dominant taxa collected during the September survey were *Polygordius* (35% of all individuals collected), the amphipod *Gammarus annulatus* (8.4%), the echinoid *E. parma* (7%), the amphipod *Pseudunciola obliquua* (6.5%), and the tanaid *T. psammophilus* (4.6%). Together, these taxa comprised 61% of infaunal individuals collected in September. Surfclam *Spisula solidissima* was among the top 10 numerically dominant taxa in Sand Borrow Sites H1, H2, and 4 and NY adjacent stations (NYA) during September (Table 6-3).

The numerically dominant taxa sampled during the June survey included *Polygordius* (27% of all individuals collected), echinoid *E. parma* (9.3%), polychaetes *Aricidea catherinae* and *A. cerrutii* (8%), tanaid *T. psammophilus* (4.1%), and tubificid oligochaetes (3.3%) (Table 6-4). Together, these taxa comprised 52% of infaunal individuals collected in June. During the June survey, surfclam *S. solidissima* was not among the top 10 numerically dominant taxa in any sand borrow site.

Table 6-5 presents summary statistics for each of the sand borrow sites for the September and June surveys. Values are provided for number of taxa, number of individuals, density, species diversity, evenness, and richness.

The highest mean number of infaunal taxa per station occurred in Site 3 (35 taxa) and NJ adjacent stations (NJA) (34) during September and in Site 3 (37) in June. Site H2 yielded the lowest mean number of taxa per station during both September and June (20 and 26, respectively). Highest infaunal densities were from NJA (station average = 6,980 individuals/m²) in September and Site 3 (5,620/m²) during June. Lowest mean densities were from Site H2 in both September (1,390/m²) and June (1,005/m²).

Mean values of species diversity ($F = 17.1$, $p < 0.0001$), evenness ($X^2 = 3.98$, $p < 0.046$), and richness ($F = 15.78$, $p < 0.0002$) were greater in June than September. During September, highest mean values of species diversity (H') were in Sites H1 and 3 (station mean = 2.13) and in Site H2 during June (2.62). Highest mean values of species richness (D) were found in Site 3 during September (5.76) and June (5.92). NJA had the lowest mean values of species diversity during September (1.80) and June (2.27). Lowest mean values of species richness were recorded during September from Site H2 (3.97) and NYA (3.98). Site H2 and NJA yielded the lowest mean values of richness (5.31 and 5.34, respectively) during June. Site H2 had the highest mean evenness (J') during June (0.82), and NJA had the lowest evenness during September (0.51) and June (0.65). Otherwise, evenness values between sand borrow sites and adjacent stations were similar within surveys.

6.3.4.1 Juvenile Surfclam

All sand borrow sites yielded surfclam (*S. solidissima*) during both surveys. Table 6-6 presents mean values of surfclam abundance from each of the sand borrow sites and adjacent stations. Surfclam abundance was greater during September than June. Mean surfclam densities in September ranged from 333 clams/m² at NYA stations to 8 clams/m² in Site 3. Mean surfclam densities in June ranged from 8 clams/m² at Site H1 stations to 0 clams/m² in NJA and NYA. Over both surveys, NYA stations yielded the highest average abundance of surfclams (167 clams/m²), and Site 3 yielded the lowest mean density (5 clams/m²) over both surveys. Surfclams were collected from stations with sand, slightly gravelly sand, and gravelly sand but were not predominantly associated with any particular sedimentary habitat.

Table 6-4. Ten most abundant taxa in grab samples from Sand Borrow Sites H1, H2, 3, and 4 and Adjacent Areas NJA and NYA for the June 2002 Survey 2 offshore New Jersey and New York.					
Site	Taxonomic Name	Count	Site	Taxonomic Name	Count
H1	<i>Polygordius</i> (LPIL)	464	NJA	<i>Polygordius</i> (LPIL)	388
	<i>Echinarachnius parma</i>	179		<i>Echinarachnius parma</i>	80
	<i>Tanaissus psammophilus</i>	93		<i>Cirrophorus ilvana</i>	50
	<i>Pseudoleptocuma minor</i>	70		<i>Aricidea cerrutii</i>	38
	<i>Cirrophorus ilvana</i>	61		Tubificidae (LPIL)	35
	<i>Hemipodus roseus</i>	57		Cirratulidae (LPIL)	31
	<i>Nephtys picta</i>	55		<i>Nephtys picta</i>	31
	<i>Caulleriella sp. J</i>	46		<i>Tanaissus psammophilus</i>	30
	<i>Sigalion arenicola</i>	32		<i>Hemipodus roseus</i>	29
	<i>Podocopida</i> (LPIL)	32		<i>Pseudoleptocuma minor</i>	25
H2	<i>Echinarachnius parma</i>	78	NYA	<i>Echinarachnius parma</i>	215
	<i>Pseudoleptocuma minor</i>	55		<i>Polygordius</i> (LPIL)	198
	<i>Protohaustorius wigleyi</i>	27		Tubificidae (LPIL)	67
	Tubificidae (LPIL)	21		<i>Spiophanes bombyx</i>	60
	<i>Nephtys picta</i>	21		<i>Nucula proxima</i>	60
	<i>Politolana polita</i>	15		<i>Nephtys picta</i>	54
	<i>Pseudunciola obliquua</i>	14		Tellinidae (LPIL)	37
	<i>Tanaissus psammophilus</i>	13		<i>Podocopida</i> (LPIL)	35
	<i>Caulleriella sp. J</i>	12		<i>Aricidea catherinae</i>	34
	<i>Acanthohaustorius millsi</i>	12		<i>Aricidea</i> (LPIL)	31
3	<i>Polygordius</i> (LPIL)	589	ALL	<i>Polygordius</i> (LPIL)	2,536
	<i>Aricidea catherinae</i>	303		<i>Echinarachnius parma</i>	854
	<i>Aricidea cerrutii</i>	290		<i>Aricidea catherinae</i>	399
	<i>Lumbrinerides dayi</i>	134		<i>Tanaissus psammophilus</i>	374
	Tubificidae (LPIL)	88		<i>Aricidea cerrutii</i>	337
	<i>Rhynchocoela</i> (LPIL)	85		Tubificidae (LPIL)	300
	<i>Cirrophorus ilvana</i>	83		<i>Pseudoleptocuma minor</i>	287
	Cirratulidae (LPIL)	71		<i>Cirrophorus ilvana</i>	242
	<i>Brania wellfleetensis</i>	50		<i>Nephtys picta</i>	229
	<i>Parapionosyllis longicirrata</i>	46		Cirratulidae (LPIL)	215
4	<i>Polygordius</i> (LPIL)	894	LPIL = Lowest practical identification level.		
	<i>Echinarachnius parma</i>	301			
	<i>Tanaissus psammophilus</i>	196			
	<i>Pseudunciola obliquua</i>	163			
	<i>Protohaustorius wigleyi</i>	141			
	<i>Pseudoleptocuma minor</i>	113			
	<i>Rhepoxynius hudsoni</i>	85			
	<i>Exogone hebes</i>	76			
	<i>Spiophanes bombyx</i>	74			
	<i>Goniadella gracilis</i>	71			

Table 6-5. Summary of infaunal statistics for the September 2001 Survey 1 and June 2002 Survey 2 in Sand Borrow Sites H1, H2, 3, and 4 and Adjacent Areas NJA and NYA offshore New Jersey and New York.

Site or Area	No. of Stations (n)	No. of Taxa		No. of Individuals		Density (Individuals/m ²)		<i>H'</i> Diversity		<i>J'</i> Evenness		<i>D</i> Richness	
		Mean Per Station	Standard Deviation	Mean Per Station	Standard Deviation	Mean Per Station	Standard Deviation	Mean Per Station	Standard Deviation	Mean Per Station	Standard Deviation	Mean Per Station	Standard Deviation
September 2001 Survey 1													
H1	6	27	7.99	328	315.30	3,275	3,153.00	2.13	0.33	0.66	0.12	4.60	0.98
H2	4	20	9.95	139	140.59	1,390	1,405.94	1.84	0.51	0.67	0.19	3.97	1.35
NJA	3	34	8.62	698	394.58	6,980	3,945.77	1.80	0.71	0.51	0.20	5.08	1.12
3	4	35	5.06	422	225.59	4,215	2,255.87	2.13	0.23	0.60	0.08	5.76	0.63
4	10	24	8.86	295	368.44	2,949	3,684.42	2.07	0.34	0.67	0.12	4.17	1.03
NYA	3	24	10.60	286	71.45	2,857	714.52	2.04	0.47	0.65	0.06	3.98	1.72
June 2002 Survey 2													
H1	6	31	8.80	260	148.09	2,598	1,480.94	2.43	0.45	0.72	0.12	5.50	1.38
H2	4	26	6.19	101	26.50	1,005	265.02	2.62	0.32	0.82	0.05	5.31	1.12
NJA	3	32	5.29	330	42.22	3,303	422.18	2.27	0.47	0.65	0.10	5.34	0.82
3	4	37	7.55	562	491.81	5,620	4,918.11	2.44	0.35	0.69	0.12	5.92	0.42
4	10	33	2.21	302	91.83	3,016	918.31	2.45	0.32	0.70	0.08	5.73	0.60
NYA	3	32	6.11	337	125.69	3,370	1,256.94	2.40	0.76	0.69	0.19	5.36	1.24

September 2001			
Site or Area	Number of Samples	Mean Density (clams/m ²)	Standard Deviation
H1	6	125	84.56
H2	4	25	36.97
NJA	3	67	38.59
3	4	8	11.73
4	10	108	336.04
NYA	3	333	568.71
June 2002			
Site or Area	Number of Samples	Mean Density (clams/m ²)	Standard Deviation
H1	6	8	20.41
H2	4	5	10.00
NJA	3	0	0.00
3	4	3	6.12
4	10	4	16.73
NYA	3	0	0.00

6.3.4.2 Cluster Analysis

Patterns of infaunal similarity among stations were examined with cluster analysis. Cluster analysis excluded those taxa that were redundant (*i.e.*, had an LPIL designation), except for *Polygordius* (LPIL). When examined over both surveys, normal cluster analysis produced three groups (Groups A through C) of stations (samples) that were similar with respect to species composition and relative abundance. Two depauperate September samples from Site H2 were placed in an outlier Group X. Normal cluster analysis of samples is shown in Figure 6-22. Figure 6-23 shows the geographic distribution of infaunal stations grouped by normal analysis.

Station Group A was represented by just two stations sampled during September. The two stations comprising Group A were distinguished from other stations primarily by yielding low numbers and few of the ubiquitous taxa from the surveys. Group A was characterized by the polychaete *Nephtys picta* and bivalves *Nucula proxima*, *S. solidissima*, and *Tellina agilis*. Sediments at Group A stations were sand or slightly gravelly sand.

Groups B (14 stations) and C (42 stations) included samples collected during both surveys, and together these included most of the project samples. Group B mostly included stations with relatively high gravel content. Ten stations had gravelly sand and two stations had sandy gravel. Stations in Group B were characterized most prominently by the amphipod *Unciola irrorata* and polychaetes *Aricidea catherinae*, *A. cerrutii*, *Cirrophorus ilvana*, *Goniadella gracilis*, *Hemipodus roseus*, *Lumbrinerides dayi*, *Pisione remota*, and *Scoletoma acicularum*. The 14 stations in Group B were composed of the same 7 stations during both surveys, primarily from Site 3 (4 stations), 1 station each in Sites 4 and H1, and a single NJA station.

Group C stations, which yielded fewer of those taxa that were abundant in Group B stations, had sand (26 stations) or slightly gravelly sand (16 stations) bottoms. Site 3 was not represented, but otherwise Group C stations were distributed across all other borrow sites and both surveys. All but one Site 4 station was included in Group C. Stations in Group C were characterized most prominently by relatively high numbers of the amphipods *Protohaustorius wigleyi* and *Pseudunciola obliquua*, the decapod *Crangon septemspinosa*, the echinoid *Echinarachnius parma*, the polychaetes *Exogone hebes*, *Caulleriella* sp. J, and *Sigalion arenicola*, and the tanaid *Tanaissus psammophilus*. Group B stations were largely depauperate with respect to some of these taxa, particularly *E. hebes*, *E. parma*, and *P. wigleyi*.

The inverse cluster analysis examining both the September and June surveys resulted in three groups of taxa (Groups 1 through 3) that reflected their co-occurrence in the samples (Table 6-7; Figure 6-24). Many infauna included in the cluster analysis were relatively rare and heterogeneously distributed; these taxa were not included in the three groups defined by the inverse analysis. Species Group 1 included the most homogeneously distributed and many of the most abundant taxa collected during the study, both among the various sand borrow sites and among surveys. Ubiquitous taxa from Group 1 included *Polygordius*, polychaetes *Nephtys picta* and *Sigalion arenicola*, and tanaid *T. psammophilus*. Species Group 1 taxa were particularly associated with Station Group D, which tended to have sediments with sand or relatively low gravel content, and in addition to the ubiquitous taxa included the amphipods *P. obliquua* and *P. wigleyi*, decapods *Cancer irroratus* and *C. septemspinosa*, the echinoid *E. parma*, and polychaetes *Aricidea wassi*, *Caulleriella* sp. J, *E. hebes*, and *Spiophanes bombyx*. Taxa in Group 2 generally were distributed across surveys and borrow sites but at lower densities than ubiquitous taxa in Group 1. Members of Group 2 generally were associated with sandy and gravelly sediments and included the bivalves *Nucula proxima*, *Spisula solidissima*, and *Tellina agilis*, gastropod *Ilyanassa trivittata*, and polychaetes *Aricidea catherinae* and *Scoletoma acicularum*. Group 3 taxa were associated primarily with Station Group C, which had sediments with measurable gravel. Most members of Group 3 were polychaetes, including *Aricidea cerrutii*, *Cirrophorus ilvana*, *Goniadella gracilis*, *Hemipodus roseus*, *Lumbrinerides dayi*, *Monticellina dorsobranchialis*, *Parapionosyllis* sp. D, and *Pisione remota*, in addition to the amphipod *Unciola irrorata* and bivalve *Astarte castanea*.

6.3.4.3 Canonical Discriminant Analysis

Data collected during the two surveys were analyzed using canonical discriminant analysis to determine which environmental factors most affected the distribution of infaunal assemblages. The first two canonical discriminant variates were used to analyze variability among those station groups identified by normal cluster analysis as being similar with respect to species composition and relative abundance. The first canonical variate (CAN1) correlated best with percent gravel (0.792167) and percent sand (-0.792538). The second canonical variate (CAN2) best correlated with survey (0.541434), albeit weakly.

6.3.5 Epifauna

Trawlable epifauna (invertebrates) of the area included crustaceans, mollusks and echinoderms common to the New York Bight region. Crustaceans were represented by Atlantic rock crab (*Cancer irroratus*), longnose spider crab (*Libinia dubia*), swimming crab *Ovalipes ocellatus*, and hermit crabs *Pagurus longicarpus* and *P. pollicaris*. Mollusks included gastropods *Euspira heros* and *Nassarius trivittatus* and squid *Loligo* sp. Echinoderms such as the sand dollar *Echinarachnius parma* and the Forbes sea star (*Asterias forbesi*) were abundant in the trawl collections.

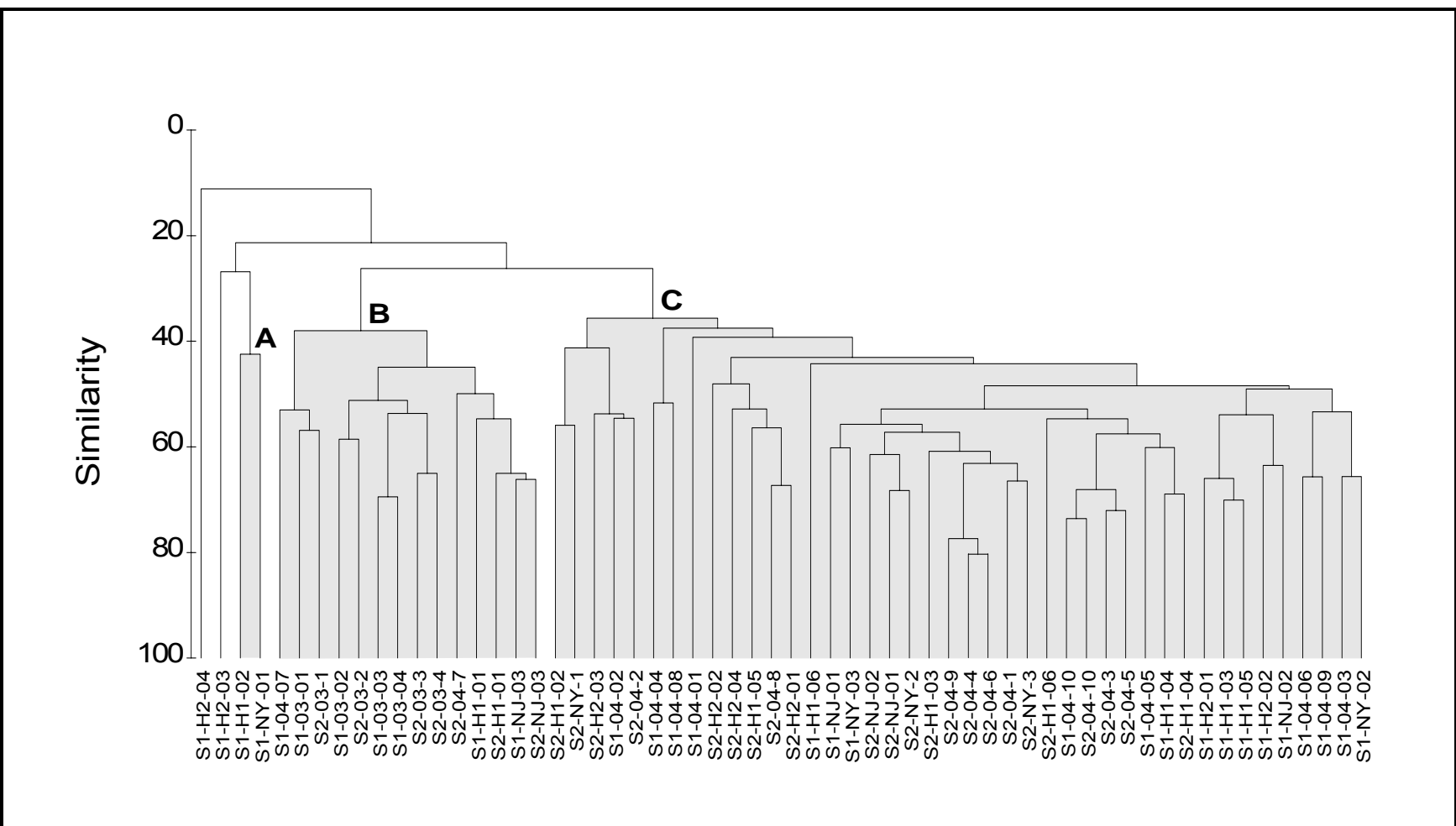


Figure 6-22. Normal cluster analysis of infaunal samples collected during the September 2001 Survey 1 and June 2002 Survey 2 in Sand Borrow Sites H1, H2, 3, and 4 offshore New Jersey and New York.

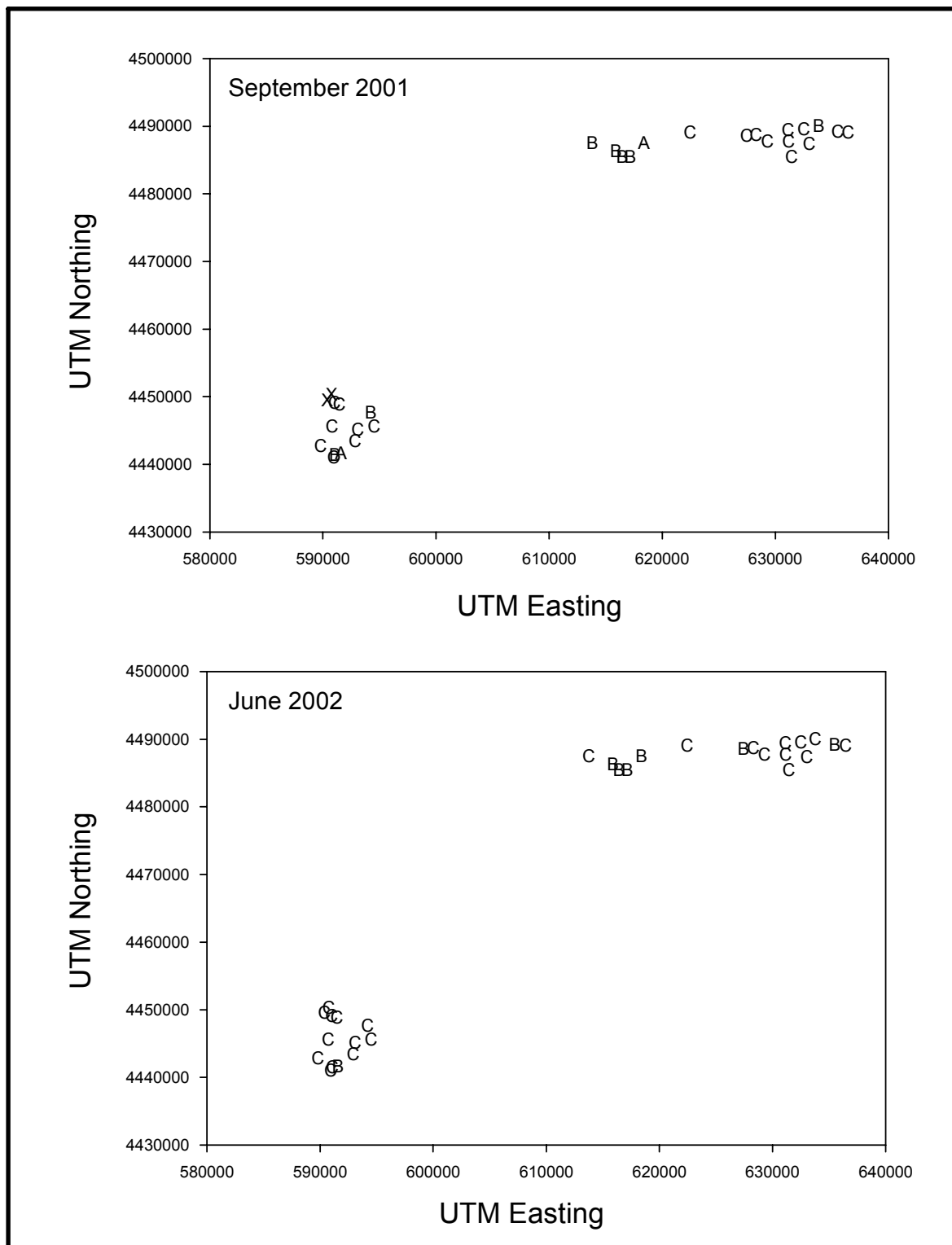


Figure 6-23. Station Groups A through C formed by normal cluster analysis of infaunal samples collected during the September 2001 Survey 1 and June 2002 Survey 2 in Sand Borrow Sites H1, H2, 3, and 4 offshore New Jersey and New York. Two outlying samples are represented by an X.

Table 6-7. Infaunal species groups resolved from inverse cluster analysis of all samples collected during the September 2001 Survey 1 and June 2002 Survey 2 in the four sand borrow sites and adjacent stations offshore New Jersey and New York.	
<p>GROUP 1</p> <p><i>Protohaustorius wigleyi</i> – A</p> <p><i>Pseudunciola obliquua</i> – A</p> <p><i>Polygordius</i> (LPIL) – Ar</p> <p><i>Pseudoleptocuma minor</i> – Cu</p> <p><i>Cancer irroratus</i> – D</p> <p><i>Crangon septemspinosa</i> – D</p> <p><i>Echinarachnius parma</i> – E</p> <p><i>Chiridotea tuftsi</i> – I</p> <p><i>Aricidea wassi</i> – P</p> <p><i>Cauleriella</i> sp. J – P</p> <p><i>Exogone hebes</i> – P</p> <p><i>Magelona papillicornis</i> – P</p> <p><i>Nephtys picta</i> – P</p> <p><i>Sigalion arenicola</i> – P</p> <p><i>Spiophanes bombyx</i> – P</p> <p><i>Tanaissus psammophilus</i> – Ta</p>	<p>GROUP 2</p> <p><i>Nucula proxima</i> – B</p> <p><i>Spisula solidissima</i> – B</p> <p><i>Tellina agilis</i> – B</p> <p><i>Ilyanassa trivittata</i> – G</p> <p><i>Aricidea catherinae</i> – P</p> <p><i>Scoletoma acicularum</i> – P</p> <p>GROUP 3</p> <p><i>Unciola irrorata</i> – A</p> <p><i>Aricidea cerrutii</i> – P</p> <p><i>Astarte castanea</i> – P</p> <p><i>Cirrophorus ilvana</i> – P</p> <p><i>Goniadella gracilis</i> – P</p> <p><i>Hemipodus roseus</i> – P</p> <p><i>Lumbrinerides dayi</i> – P</p> <p><i>Monticellina dorsobranchialis</i> – P</p> <p><i>Parapionosyllis</i> sp. D – P</p> <p><i>Pisione remota</i> – P</p>
<p>Key: A = amphipod; Ar = archiannelid; B = bivalve; Cu = cumacean; D = decapod; E = echinoderm; G = gastropod; I = isopod; P = polychaete; Ta = tanaid.</p> <p>LPIL = Lowest practical identification level.</p>	

During September, a total of 3,103 individuals in 8 invertebrate taxa was collected in 6 trawls at the borrow sites (Table 6-8). An extremely large catch of the sand dollar *E. parma* from Trawl Transect H1-B contributed 2,475 individuals to this total. Epifauna excluding the sand dollar contributed 7 taxa and 127 specimens to the trawl catches. The squid *Loligo* sp., Forbes sea star (*A. forbesi*), longnose spider crab (*Libinia dubia*), and Atlantic rock crab (*C. irroratus*) were the top ranking species in terms of abundance. Total catches during September varied among sand borrow sites, ranging from 23 individuals in Sand Borrow Site 3 (Trawl Transect 3-A) to 2,511 individuals in Site H1 (Trawl Transect H1-B). The average catch per haul was 517.2 individuals.

During June, trawl samples produced 11 invertebrate taxa represented by 1,806 individuals (Table 6-9). As with the September survey, the most abundant species was sand dollar *E. parma* represented by 1,492 individuals. Other abundant invertebrates included sea star (*A. forbesi*), flatclaw hermit crab (*Pagurus pollicaris*) and Atlantic rock crab (*C. irroratus*). Epifaunal catches during June ranged from 35 individuals in Site H1 (Trawl Transect H1-A) to 590 individuals in Site 4 (Trawl Transect 4-A). Trawl catches averaged 301.0 epifaunal individuals per haul. The highest number of total taxa collected during June (8) came from Site 3 (Trawl Transect 3-A) (Table 6-9). Site H1 (Trawl Transect H1-B) yielded the fewest total taxa (3) in a single trawl. On average, the total number of taxa per haul was 5.7.

Table 6-8. Epifauna and demersal fishes collected by mongoose trawl during the September 2001 Survey 1 of the four sand borrow sites offshore New Jersey and New York.							
Taxa	Trawl Transect						
	H1-A	H1-B	H2-A	3-A	4-A	4-B	Total
INVERTEBRATES							
<i>Echinarachnius parma</i>	314	2,475	151		25	11	2,976
<i>Loligo sp.</i>	11	26	16	11		5	69
<i>Asterias forbesi</i>	1		1	1	9	7	19
<i>Libinia dubia</i>	1	6	3	3	1	1	15
<i>Cancer irroratus</i>		1		6		2	9
<i>Pagurus pollicaris</i>		3	1	2	1		7
<i>Euspira heros</i>					1	5	6
<i>Ovalipes ocellatus</i>						2	2
FISHES							
<i>Stenotomus chrysops</i>	10	11	25			32	78
<i>Prionotus carolinus</i>	4	4	1	2	2	2	15
<i>Paralichthys oblongus</i>		6	3			1	10
<i>Paralichthys dentatus</i>			8	1			9
<i>Peprilus triacanthus</i>			2	7			9
<i>Raja eglanteria</i>		1		2	2	1	6
<i>Citharichthys sp.</i>		3					3
<i>Urophycis regia</i>	1						1
<i>Hippocampus erectus</i>				1			1
<i>Centropristis striatus</i>						1	1
<i>Tautoga onitis</i>				1			1
INVERTEBRATE TOTALS							
Total Individuals	327	2,511	172	23	37	33	3,103
Total Taxa	4	5	5	5	5	7	8
FISH TOTALS							
Total Individuals	15	25	39	14	4	37	134
Total Taxa	3	5	5	6	2	5	11
FISH AND INVERTEBRATE TOTALS							
Grand Total Individuals	342	2,536	211	37	41	70	3,237
Grand Total Taxa	7	10	10	11	7	12	19

6.3.6 Demersal Fishes

Demersal fishes collected by trawl included common representatives of the regional fauna such as clearnose skate (*Raja eglanteria*), searobins *Prionotus carolinus* and *P. evolans*, porgy (*Stenotomus chrysops*), and lefteye flounders *Paralichthys dentatus*, *P. oblongus*, and *Scophthalmus aquosus*.

Numbers of individuals in hauls from the September survey totaled 134 (Table 6-8). The most abundant species caught in September was scup (*S. chrysops*), which were present as small juveniles during that survey. The total number of fish species collected in September was 11. Numbers of fish species collected during September ranged from 4 at Site H1 (Trawl Transect H1-A) to 7 species from Site 4 (Trawl Transect 4-B).

The total number of individuals collected in June was 51 (Table 6-9). The most abundant species collected in June were summer flounder (*P. dentatus*) and clearnose skate (*Raja eglanteria*). June trawl hauls yielded nine species over all sampling stations. Numbers of species collected during June ranged from none in Trawl Transect H1-A to 5 in Trawl Transects H2-A and 4-A.

6.4 DISCUSSION

Benthic assemblages surveyed from the New Jersey and New York sand borrow sites consisted of members of the major invertebrate and vertebrate groups commonly found in the region of the New York Bight. Numerically dominant infaunal groups included numerous crustaceans, echinoderms, mollusks, and polychaetes, while epifaunal taxa consisted primarily of decapods, sand dollars, gastropods, and squids, all typical components of benthic assemblages in the study area. Similarly, the numerically dominant demersal fishes collected in trawls within the borrow sites revealed consistency with previous surveys. Fishes such as clearnose skate (*Raja eglanteria*), northern searobin (*Prionotus carolinus*), scup (*Stenotomus chrysops*), and summer flounder (*Paralichthys dentatus*) were numerical dominants during the surveys, and these species consistently are among the most ubiquitous and abundant demersal taxa in the Bight region (Able and Hagen, 1995; Barry A. Vittor & Associates, Inc., 1999b).

Results of this investigation support the findings of other studies that found strong associations of infaunal taxa with particular sedimentary habitats (Steimle and Stone, 1973; Pearce et al., 1981; Chang et al., 1992; Theroux and Wigley, 1998). Discriminant analysis indicated that the composition of benthic assemblages was affected primarily by relative percentages of gravel and sand at survey stations. Infaunal assemblage distributions therefore reflected sediment type distributions to a large degree. In the Bight, differences in water depth, presence of bathymetric features, and proximity to the Hudson/Raritan estuary plume are important in structuring infaunal assemblages, along with sediment characteristics (Barry A. Vittor & Associates, 2002).

Most resource stations in this study had sand or slightly gravelly sand bottoms. These stations were characterized most prominently by relatively high numbers of the amphipods *Protohaustorius wigleyi* and *Pseudunciola obliquua*, the decapod *Crangon septemspinosa*, echinoid *Echinarachnius parma*, and polychaetes *Exogone hebes* and *Caulleriella* sp. J, agreeing with numerous prior surveys in the study area that detected these taxa as components of a sand habitat community (e.g., Pearce et al., 1981; Reid et al., 1991; Chang et al., 1992). Gravel stations were largely depauperate with respect to sand taxa, particularly the polychaete *E. hebes*, sand dollar *E. parma*, and amphipod *P. wigleyi*. Likewise, sand stations tended to yield relatively few taxa that were abundant at stations with sandy gravel or gravelly sand stations. Ubiquitous taxa collected from both sand and gravel areas included the archiannelid *Polygordius*, polychaetes *Aricidea catherinae*, *Nephtys picta*, and *Sigalion arenicola*, and tanaid *Tanaissus psammophilus*. *Polygordius* is usually found in its highest abundance associated with low organic, coarse sand sediments (Caracciolo and Steimle, 1983; Battelle Ocean Sciences, 1996) and was by far the numerically dominant taxon in this study.

Juvenile surfclams (*Spisula solidissima*) were collected from stations with sand, slightly gravelly sand, and gravelly sand but were not predominantly associated with any particular sedimentary habitat in the borrow sites. Prior investigations of Middle Atlantic shelf waters (Parker, 1967; Parker and Fahlen, 1968) found that offshore areas with gravel bottoms tended to yield greater abundance than sites with high percentages of sand. Juvenile surfclams in this

study also were common in sand habitats, as has been observed by other investigations in the Bight (Pearce et al., 1981; Caracciolo and Steimle, 1983).

Table 6-9. Epifauna and demersal fishes collected by mongoose trawl during the June 2002 Survey 2 of the four sand borrow sites offshore New Jersey and New York.							
Taxa	Trawl Transect						Total
	H1-A	H1-B	H2-A	3-A	4-A	4-B	
INVERTEBRATES							
<i>Echinarachnius parma</i>	33	500	23	17	569	350	1,492
<i>Asterias forbesi</i>		3	179	32	2	5	221
<i>Pagurus pollicaris</i>				14	5	4	23
<i>Cancer irroratus</i>			1	17		1	19
<i>Euspira heros</i>		2		1	7	5	15
<i>Loligo sp.</i>		8		2	2		12
<i>Pagurus longicarpus</i>			2	6			8
<i>Nassarius trivittatus</i>	1				4	2	7
Nudibranch				4			4
<i>Ovalipes ocellatus</i>					1	2	3
<i>Libinia dubia</i>	1	1					2
FISHES							
<i>Raja eglanteria</i>		3	8			2	13
<i>Paralichthys dentatus</i>		3	7		2		12
<i>Prionotus carolinus</i>		5	1			1	7
<i>Stenotomus chrysops</i>					5		5
<i>Urophycis regia</i>				2	1	1	4
<i>Scophthalmus aquosus</i>			4				4
<i>Prionotus evolans</i>			3				3
<i>Paralichthys oblongus</i>					1	1	2
<i>Peprilus triacanthus</i>					1		1
INVERTEBRATE TOTALS							
Total Individuals	35	514	205	93	590	369	1,806
Total Taxa	3	5	4	8	7	7	11
FISH TOTALS							
Total Individuals		11	23	2	10	5	51
Total Taxa		3	5	1	5	4	9
FISH AND INVERTEBRATE TOTALS							
Total Individuals	35	525	228	95	600	374	1,857
Total Taxa	3	8	9	9	12	11	24

Station depth did not account for any differences in assemblage composition during the study because depths were similar across the study area. Reid et al. (1991) and Steimle and Stone (1973) both found that the number of species increased from inshore to offshore stations in relation to Bight water depth, and Wigley and Theroux (1981) reported that highest infaunal densities in the Bight occurred at relatively shallow depths. In addition to absolute depth, bathymetric features such as inter-shoal troughs have been found to support distinct

assemblages in the region (Byrnes et al., 2000), however no stations were located in a trough, and this likely also contributed to a lack of depth-related variability.

In addition to sediment-based spatial variability, there were significant temporal differences in the composition of infaunal assemblages. Just half of all collected taxa were common to both surveys. There were 39 taxa restricted to the June survey, and the September survey included 33 taxa not included in June samples. Whereas overall abundance was similar across surveys, with grab samples containing 337 individuals per sample in September and 308 per sample in June, mean values of species diversity, evenness, and richness all were significantly greater in June compared to the September survey.

A recent open shelf survey offshore the southern portion of New Jersey (Byrnes et al., 2000) found the opposite pattern from this survey, when greater taxa richness was found in September 1998 compared to May 1998. In general, it is expected that species richness would increase after spring and toward fall months because reproduction of benthic invertebrates is largely tied to increased temperatures (Sastry, 1978). However, there are data indicating that climatic conditions during the surveys was abnormal compared to historic trends. According to the National Climatic Data Center (National Oceanic and Atmospheric Administration, 2002), preliminary data indicate that the northeastern U.S. had its warmest winter on record during 2001-2002, during which the Bight region had "much above normal" temperatures for most of the first 6 months of 2002. The apparently anomalous climatic environment potentially may have affected normal reproductive periodicity in the Bight region.

Temporal variation occurring on multiple scales has long been noted in shallow marine benthic communities. Many of the numerically dominant infauna inhabiting the study area are known to exhibit either year-round or late winter-early spring periods of recruitment, however, there often is highly variable recruitment from year to year due to the harshness of larval life in the plankton (Thorson, 1966), together with frequently intense predation soon after settlement. These processes can result in wide and unpredictable fluctuations in infaunal numbers (Warwick, 1980).

The four faunal indices examined (density, diversity, evenness, and richness) are interrelated. Species diversity is dependent on both the number of taxa present (species richness) and the distribution of all individuals among those species (evenness). Diversity and evenness indices reflect the equitability of the total number of organisms among species. The diversity, evenness, and richness indices employed in this study all are determined by the number of taxa and individuals in the samples. Greater species evenness during June, as compared to September, indicated more equitable distribution of individuals among the various taxa during the second survey. The 10 most abundant taxa during September comprised 79% of all collected infauna, whereas the 10 numerically dominant taxa collected in June comprised 57% of all individuals. Much of this difference was due to the most abundant taxon, *Polygordius*, which comprised 38% of all individuals collected during September and 25% of all individuals yielded by grab samples in June. The less even distribution of abundance across taxa in the September survey was partly responsible for lower measures of diversity and species richness compared to June. Numbers of taxa per grab (including adjacent stations) averaged 27 taxa in September and 32 taxa in June, and this also contributed to the significant increase in community indices during the second survey.

Juvenile surfclam (*Spisula solidissima*) abundance was greater during September than June. This temporal distribution pattern would be expected given this species' reproductive

characteristics. Surfclam spawning has been described both as a single event and as multiple events from July to early November (Weinberg, 1998).

In a previous open shelf study offshore New Jersey, abundance of most epifaunal taxa was low in winter, then increased to peak densities in summer and declined in fall (Hales et al., 1995). While this was true overall for the project, with 3,103 individuals in September and 1,806 individuals in June trawls, most of this difference was due to abundance of the sand dollar *Echinarachnius parma*. During both surveys, trawls were numerically dominated by *E. parma*, a common invertebrate in the Bight (Steimle and Stone, 1973; Pearce et al., 1981; Chang et al., 1992), which contributed 96% and 83% of total invertebrate abundance in September and June, respectively. In September, invertebrates excluding *E. parma* contributed 127 individuals to the trawls, whereas invertebrates other than *E. parma* numbered 314 individuals in June. Most of the non-sand dollar collection in June was composed of the sea star *Asterias forbesi*, particularly in Site H2. Individual abundance therefore was similar across surveys when considering taxa other than sand dollars and sea stars.

There were few apparent differences in epifaunal species composition between surveys. Invertebrates contributed 8 taxa to the trawl catches in September and 11 taxa during June. Threeline mud snails (*Nassarius trivittatus*), longwrist hermit crab (*Pagurus longicarpus*), and nudibranchs were present in June trawls but not September trawls; otherwise, all other collected invertebrate taxa were present during both surveys.

There were some apparent between-survey differences in abundance for certain epifauna. Sea stars were more abundant during June. There usually is only one sea star breeding season per year, which occurs in spring in temperate waters (Barnes, 1980), although it is unknown whether project trawls contained relatively recent recruits or mature breeding adults. Longfin squid (*Loligo* sp.) were collected in greater numbers during September. Squids were collected in 5 of 6 trawl hauls and averaged 12 individuals per haul in September, whereas in June they were collected in just 3 of 6 trawl hauls and averaged 2 individuals per haul. There is a general seasonal migratory pattern for the Middle Atlantic Bight *Loligo* population, in which adults move offshore in fall and remain there until April, when adults and young migrate back into shelf waters for summer (Lange and Sissenwine, 1980). Relative paucity of squids in June samples compared to September therefore may have reflected densities prior to completion of summer migration into shelf waters.

Within surveys, overall taxa composition in the trawls was similar, except for one of the June trawls in Site H1 (Trawl Transect H1-A), in which just three invertebrates were collected in relatively low numbers and no fishes were taken. On average, the total number of combined taxa per haul during the June survey was 8.67. The second trawl haul in Site H1 (Trawl Transect H1-B) yielded abundance and numbers of individuals similar to June trawls in the other sand borrow sites. Reasons for the paucity of taxa and individuals in Trawl Transect H1-A are not apparent and may simply be due to natural variability. Hydrologic parameters, including dissolved oxygen levels, were similar across sand borrow sites during the June survey.

Offshore New Jersey, there is considerable variation in the abundance and distribution of demersal taxa, both spatially and seasonally (Able and Hagen, 1995; Barry A. Vittor & Associates, Inc., 1999b). September trawls yielded 134 individuals in 11 fish taxa and were numerically dominated by scup (*Stenotomus chrysops*), which comprised 58% of collected individuals. The most abundant fish species during the June survey were clearnose skate (*Raja eglanteria*) and southern flounder (*Paralichthys dentatus*). All demersal taxa collected during

the surveys are typical components of benthic assemblages in the study area (Able and Hagen, 1995; Barry A. Vittor & Associates, Inc., 1999b).

Compared to September, fishes were less abundant overall in June, when trawl samples yielded 51 individuals in nine taxa. This abundance pattern agrees with the results of previous long-term sampling efforts that found peak fish abundance occurs in shelf waters offshore New Jersey during the months September through November (Able and Hagen, 1995). Scup was much less abundant in the June survey compared to September. This species tends to aggregate along the shelf break during winter and occurs at all depths on the shelf during summer months (Grosslein, 1976).

Some variability among sites was apparent in the composition of trawls. In particular, during the June survey, in Trawl Transect H1-A, no fishes were collected. Reasons for this distributional variability are not apparent, and the depauperate contents of this trawl may be due to natural spatial variability, which is often prominent. Epifaunal abundance also was very low in Trawl Transect H1-A in June, possibly causing fishes to forage in other areas with greater prey abundance. Fish abundance and species richness was more comparable among borrow sites during the September survey.

The results of the sand borrow site surveys agree well with previous descriptions of benthic assemblages residing in shallow shelf waters offshore New Jersey and New York. Overall, discriminant analysis indicated that sedimentary regime most affected the composition of infaunal assemblages. Other physical environmental characteristics that normally affect infaunal population distributions, such as water depth, were similar across the study area and therefore did not differentially affect abundance and distribution patterns. Temporal patterns of infaunal community indices did not meet expected patterns, potentially due to abnormally high temperatures in the region during the first half of 2002. Despite inherent spatial and temporal heterogeneity in the distribution and abundance of demersal taxa, results of the 2001-2002 surveys of the New Jersey and New York sand borrow sites generally are consistent with historical demersal survey results in the region.

7.0 POTENTIAL EFFECTS

One of the primary purposes of this project was to provide site-specific information for decisions on requests for non-competitive sand leases from local, State, and Federal agencies. The information may be used to determine whether or not stipulations need to be applied to a lease. The information also may be incorporated into an Environmental Assessment (EA) or Environmental Impact Statement (EIS), if so required.

Environmental impact analyses of mining operations should be based on commodity-specific, technology-specific, and site-specific information, whenever possible (Hammer et al., 1993). First, the specific mineral of interest and the technological operations for a specific mining operation need to be defined because these two parameters determine the impact producing factors that need to be considered. Once the impact producing factors are known, this information can be translated into statements concerning the impacts that might occur to the full suite of potentially affected environmental resources that may need to be addressed, including geology, chemical and physical oceanography, air quality, biology, and socioeconomics. Then, decisions can be made regarding the type of mitigation necessary to determine the preferred alternative for a specific marine mining operation to acquire project approval.

This section focuses on providing information on potential impacts related to physical processes and biological considerations of sand mining for beach nourishment from five sand borrow sites offshore northeastern New Jersey and southwestern Long Island. Two primary dredging technologies are available for offshore sand mining operations, depending on distance from source to project site, the quantity of sand being dredged, and the depth to which sand is extracted at a site (Herbich, 1992). They are: 1) cutterhead suction dredge, where excavated sand is transported through a direct pipeline to shore, and 2) hopper dredge, where sand is pumped to the hopper, transported close to the replenishment site, and pumped to the site through a pipeline from the hopper or from a temporary offshore disposal area close to the beach fill site. As a general rule, cutterhead suction dredging is most effective for projects where the sand resource is close to shore (within 8 km), the dredging volumes are large ($>8 \times 10^6 \text{ m}^3$), and the excavation depth is on the order of 2.5 to 4 m (A. Taylor, 1999, personal communication). Hopper dredging becomes a more efficient procedure when the sand resource areas are greater than 8 km from shore, dredging volumes are relatively small ($<2 \times 10^6 \text{ m}^3$), and the excavation depth at the sand resource area is less than 2 m (A. Taylor, 1999, personal communication). Ultimately, a combination of these factors will be evaluated by dredgers to determine the most cost effective method of sand extraction and beach replenishment for a given project. Availability of dredging equipment also may be a factor for determining the technique to be used; however, the number of cutterhead suction and hopper dredges in operation is about equal in the industry today (A. Taylor, 1999, personal communication). As such, both technologies will be evaluated for potential biological effects.

7.1 OFFSHORE SAND BORROW SITES

Five potential sand borrow sites were defined for this study based on practical water depth extraction, environmental impact minimization, and suitable geologic characteristics. Most sand borrow sites are geologically similar (coarse-to-medium sand with maximum relief of about 3 to 5 m and resource volumes of at least $5 \times 10^6 \text{ m}^3$) and exist on either shoreface-attached or offshore linear sand shoals immediately seaward of the Federal-State boundary. The lone exception to this trend is the westernmost borrow site offshore Long Island (Site 3) that contains very coarse sand and has relatively low relief ($\sim 2 \text{ m}$). Three primary criteria were used to isolate potential borrow sites. First, water depths greater than 20 m were excluded as a practical limitation for sand extraction. This eliminated any potential site east of Fire Island Inlet because the 20 m depth contour exists at or landward of the Federal-State boundary. Second, we were most interested in sand ridges as potential borrow sites to minimize the extent of excavation below the ambient continental shelf surface adjacent to these sites. It is expected that this procedure will limit potential physical environmental impacts to waves and currents resulting from dredging. Third, the geologic characteristics of offshore sand deposits had to be compatible with beach environments where fill is to be placed. Although these five potential sand borrow sites were designated as ones with greatest potential, it is possible that sand could be dredged from intervening offshore areas because consistency of shoal deposits is widespread seaward of the northern New Jersey and southern Long Island coast.

The amount of dredging that occurs at any site is a function of Federal, State, and local requirements for beach replenishment. It is nearly impossible to predict the exact sand quantities needed in the foreseeable future, so a representative value for any given project was estimated based on discussions with MMS, USACE, and State personnel. Preliminary analysis of short-term impacts (storm and normal conditions) at specific locations along the coast landward of sand borrow sites indicates that at least $1 \times 10^6 \text{ m}^3$ of sand would be needed for a given beach replenishment event. Long-term shoreline change data sets indicate that a replenishment interval of about 5 to 10 years would be expected to maintain beaches. This does not consider the potential for multiple storm events impacting the coast over a short time interval, nor does it consider longer time intervals without destructive storm events. Instead, the estimate represents average change over decades that is a reasonable measure for coastal management applications.

Given the quantity of at least $1 \times 10^6 \text{ m}^3$ of sand per beach replenishment event, the surface area covered for evaluating potential environmental impacts is a function of average dredging depth. Two factors should be considered when establishing dredging practice and depth limits for proposed extraction scenarios. First, regional shelf sediment transport patterns should be evaluated to determine net transport directions and rates. It is good sand resource management practice to dredge the leading edge of a migrating shoal because infilling of dredged sites occurs more rapidly at these locations (Byrnes and Groat, 1991; Van Dolah et al., 1998). Second, shoal relief above the ambient shelf surface should be a determining factor controlling depth of dredging. Geologically, shoals form and migrate on top of the ambient shelf surface, indicating a link between fluid dynamics, sedimentology, and environmental evolution (Swift et al., 1976). As such, average shoal relief is a reasonable threshold for maintaining environmentally-sound sand extraction procedures.

A primary question addressed by modeling efforts relates to sediment transport and infilling estimates at potential borrow sites and the impact of dredging operations on these estimates. Combined wave-current interaction (waves mobilize the seabed and currents transport the sediment) at offshore borrow sites results in a net direction of transport into and

out of potential sand resource sites. Historical sediment transport dynamics suggest that the net direction of sediment movement is from east to west along the Long Island shelf and north to south along the New Jersey shelf, and the rate at which sand moves on the shelf varies.

7.2 WAVE TRANSFORMATION MODELING

Excavation of borrow sites in the nearshore can affect offshore wave heights and the direction of wave propagation. The existence of offshore topographic relief can cause waves to refract toward the shallow edges of borrow sites. This alteration to the wave field by a borrow site may change local sediment transport rates, where some areas may experience a reduction in transport, while other areas may show an increase. To determine the potential physical impacts associated with dredging borrow sites offshore southwestern Long Island and northeastern New Jersey, wave transformation modeling and sediment transport potential calculations were performed for existing and post-dredging bathymetric conditions. Comparison of results for existing and post-dredging conditions illustrated the relative impact of borrow site excavation on wave-induced coastal processes. Although the interpretation of wave modeling results was relatively straightforward, evaluating the significance of predicted changes for accepting or rejecting a borrow site was more complex (see Section 4.0 for details).

7.2.1 Offshore Southwestern Long Island

Linear offshore sand shoals, oriented obliquely to the shoreline in a northwest-southeast direction, are the primary geomorphic features influencing wave propagation offshore southwestern Long Island beaches. Two relatively long-period wave cases were selected to simulate the impact of dredging on wave transformation across borrow sites. For 1.3 m, 9.1 sec waves propagating from the east-southeast (Case 11A), shoals encompassed by Borrow Sites 3, 4W, and 4E had the greatest influence on waves in the modeled area; however, effects to waves were relatively small because these shoals are located in approximately 17 to 20 m water depth. For 1.6 m, 9.1 sec waves propagating from the southeast (Case 14A), propagation over offshore shoals is similar to Case 11A. The primary difference between wave cases is the offshore incident wave angle, which is more shore-normal for Case 14A. As a result, there is less change in wave direction as waves approach the shoreline.

Post-dredging wave height changes at Sites 3, 4W, and 4E illustrate the impact of sand extraction at borrow sites, where seafloor topography within each site was lowered to a level not exceeding water depths at the base of the shoals (approximately -20 m). For wave Case 11A, borrow site dredging had no measurable influence on waves over a long section of coastline (>44 km), but changes on the order of 0.01 m do occur along 20 km of coast in the combined shadow of the three borrow sites. At Site 4E, maximum wave height decrease was approximately 0.05 m, and the maximum increase was 0.10 m at the landward boundary of the site. At Site 4W, maximum wave height increase was 0.10 m, and maximum wave height decrease was 0.09 m. Seafloor excavation at Site 3 produced smallest wave height changes for borrow sites offshore southwestern Long Island, with a maximum decrease of 0.06 m and a maximum increase of 0.04 m. Minimal computed changes at Site 3 may be due to the relatively small volume of sand excavated from this site, and because changes in seafloor elevation for post-dredging conditions were less (approximately 2 m change for Site 3, versus 4 m for Sites 4W and 4E).

For wave Case 14A, changes in wave field propagation resulting from dredging at the three offshore borrow sites were smaller than those computed for Case 11A, even though the wave height for this case is larger. This effect may be due to a combination of incident wave angle and directional orientation of shoals upon which borrow sites are located. For Case 11A,

the wave approach angle is oriented closer to the centerline axis of the shoal ridge, which causes slightly more wave energy focusing than in Case 14A. The wave shadow zone from these three sites affects approximately 45 km of shoreline, but greatest changes are on the order of 0.01 m and occur within a 4 km stretch of shoreline at the western end of Jones Beach. At Site 4E, maximum wave height changes range between +0.07 and -0.04 m. At Site 4W, wave height changes are similar in magnitude (+0.07 and -0.05 m). For Borrow Site 3, wave height changes are equivalent to those for Case 11A, with a maximum wave height increase of 0.04 m and a corresponding decrease of 0.06 m.

7.2.2 Offshore Northeastern New Jersey

Potential sand borrow sites offshore northeastern New Jersey are oriented obliquely to the shoreline in a northeast-southwest direction and have minimal influence on wave propagation to the shoreline. Two relatively long-period wave cases were selected to simulate the impact of dredging on wave transformation across borrow sites. For 1.3 m, 9.1 sec waves propagating from the east (Case 11B), shoals encompassed by Borrow Sites H1 and H2 exhibited minimal wave focusing. The approximate minimum water depths at Sites H1 and H2 are 16 and 17 m, respectively. For the shoal at Site H1, maximum wave height increase was 0.13 m due to the focusing effect of the sand ridge. For 1.3 m, 7.7 sec waves propagating from the south-southeast (Case 16B), wave height changes at Sites H1 and H2 are not as pronounced as those for Case 11B. The primary reason for this difference is that offshore bathymetry has less effect on wave focusing for shorter peak period incident waves. Closer to shore in shallower water, approaching waves eventually are influenced by the seafloor as they refract to a more shore normal angle.

Post-dredging wave height changes at Sites H1 and H2 simulate the impact of sand extraction at borrow sites, where seafloor topography within each site was lowered to a level not exceeding water depths at the base of the shoals (approximately -20 m). Wave height differences for wave Case 11B resulting from numerically excavating Sites H1 and H2 are relatively small and diffuse, and wave height changes at the modeled shoreline are less than 0.01 m. At Site H1, maximum changes in wave height ranged from -0.06 to +0.04 m. At Site H2, maximum wave height changes decreased by 0.05 m and increased is 0.03 m.

For Case 16B, wave height changes indicated that borrow sites have an overlapping influence at the shoreline for waves propagating from the SSE. Similar to the results of Case 11B, wave height changes at the shoreline relative to potential offshore sand dredging were never greater than 0.01 m. Wave height changes at borrow sites are smaller than those for Case 11B, primarily due to a shorter wave period for Case 16B. Site H1 exists within the wave shadow zone for Site H2, but wave height changes remain relatively small. At Site H1, maximum wave height changes ranged from +0.04 to -0.04 m; at Site H2, maximum changes were half this magnitude (+0.02 to -0.02 m). Overall, wave height differences between existing and post-dredging conditions were quite small relative to natural wave height variability.

7.3 CURRENTS AND CIRCULATION

Circulation patterns on either side of the Hudson Shelf Valley near potential offshore sand borrow sites documented speed and direction related to current and wind patterns recorded between December 4, 1999 and April 15, 2000. The high-energy environment associated with winter storm events is capable of suspending and transporting sediment and is well suited for determining maximum sediment transport rates for the region. Current meter data analyzed by Butman et al. (2003) agrees with the overall trend Scheffner et al. (1994) modeled; bottom currents in the vicinity of offshore borrow sites are driven primarily by winds and influenced by

tidal flows. Overall, the predominant direction of surface flow within the study area varied from southeast (west of Hudson Shelf Valley) to south-southeast (east of the Hudson Shelf Valley). Surface current magnitudes also were consistent, showing similar maximums, means, and standard deviations. Bottom current measurements illustrated greater variability in direction and magnitude. Offshore northeastern New Jersey, predominant bottom current flow varied from east-southeast to west, while the predominant bottom current flow east of the Hudson Shelf Valley varied from north to south-southeast. Differences in bottom flow may be explained by the presence of the Hudson Shelf Valley, which bisects the continental shelf in this region causing currents to veer to the north as they flow cross contour into the bathymetric low from northeast to southwest. Strong northerly flow within the valley prevents currents south and west of this area from flowing to the east-northeast.

The controlling factor for bottom current velocities in the vicinity of proposed sand borrow sites was wind direction and intensity, and local bathymetric features controlled current direction. Bottom currents tended to flow parallel to contours causing currents to diverge around localized bathymetric highs and converge near bathymetric lows. In general, bottom flows at the borrow sites offshore southwestern Long Island flowed east-southeast or east and west with deviations caused by wind direction. Maximum bottom current speed was about 35 cm/s flowing east, with a mean speed of 8 cm/s (± 5 cm/s) flowing southeast. Offshore northeastern New Jersey, bottom currents generally flow north and south along bathymetric contours. Maximum bottom current speed for this area was about 26 cm/s flowing north, with a mean velocity of 6 cm/sec (± 4 cm/s) flowing north. Bottom current speeds at both sites primarily were controlled by wind speeds, and the direction of flow was controlled by local bathymetry.

The above information infers some general trends about the borrow sites located offshore southwestern Long Island and northeastern New Jersey. At borrow sites offshore Long Island, along-contour flow can be expected, flowing predominantly east-northeast or west-southwest with little variation to the north (onshore flow). At borrow sites offshore northeastern New Jersey, flow was predominantly north-northeast or south-southwest with little variation to the west (onshore flow) due to localized bathymetric control and the channeling affect of the Hudson Shelf Valley.

7.4 SEDIMENT TRANSPORT

Current measurements and analyses, and wave transformation modeling, provided baseline information on incident processes impacting coastal environments under existing conditions and with respect to proposed sand mining activities for beach replenishment. Ultimately, the most important information for understanding physical processes impacts from offshore sand extraction is changes in sediment transport dynamics resulting from potential sand extraction scenarios relative to existing conditions.

Three independent sediment transport analyses were completed to evaluate physical environmental impacts due to sand mining. First, historical sediment transport trends were quantified to document regional, long-term sediment movement throughout the study area using historical bathymetric data sets. Erosion and accretion patterns were documented, and sediment transport rates in the littoral zone and at offshore borrow sites were evaluated to assess potential changes due to offshore sand dredging activities. Second, sediment transport patterns at proposed offshore borrow sites were evaluated using wave modeling results and current measurements. Post-dredging wave model results were integrated with regional current measurements to estimate sediment transport trends for predicting borrow site infilling rates. Third, potential longshore sediment transport was computed using wave modeling output to estimate potential impacts along the coast (beach erosion and accretion). All three methods

were compared for documenting consistency of measurements relative to predictions, and potential physical environmental impacts were identified.

7.4.1 Historical Sediment Transport Patterns

Regional geomorphic changes between 1873/88 and 1991/97 (southwestern Long Island) and 1836/39 and 1977 (northeastern New Jersey) were analyzed for assessing long-term, net coastal sediment transport dynamics. Although these data did not provide information on potential impacts of sand dredging from proposed borrow sites, they did provide a means of verifying predictive sediment transport models relative to infilling rates at borrow sites and longshore sand transport.

Shoreline position and nearshore bathymetry change documented four important trends relative to study objectives. First, there were three dominant directions of longshore sand transport within the study area. Between Rockaway Point and Moriches Inlet, the dominant direction of transport was east to west. In northern New Jersey, between Sandy Hook and Manasquan, longshore transport from south to north dominated, while south of Manasquan Inlet, the dominant direction was to the south. Along both coasts, the dominant direction of transport was illustrated by barrier island migration and shoreline advance adjacent to inlet jetties. Barrier islands along the south coast of Long Island have historically migrated from east to west, and seaward shoreline advance subsequent to jetty construction has occurred along the east sides of entrances. In northern New Jersey, Sandy Hook spit historically has migrated rapidly to the north, and prior to structural development at Barnegat Inlet, the spit north of the entrance was rapidly migrating to the south. The greatest amount of shoreline change observed for this study was associated with beaches adjacent to entrances, most notably along the leading edge of prograding barrier spits.

Second, the most dynamic features within the study area, in terms of nearshore sediment transport, are migrating barrier island/spit complexes along the northeastern New Jersey and southwestern Long Island coasts, in addition to natural and anthropogenic change along the Hudson River Channel. Areas of significant erosion and accretion are documented between 1927/37 and 1927/97 at Sandy Hook spit, reflecting wave and current dynamics that carry sediment northward and deposit it along the terminal edge of the spit. High rates of deposition also were prominent at entrances south of Sandy Hook and along the southwestern coast of Long Island. Shoreline and bathymetric changes associated with these features reflect morphologic response to wave and current dynamics and shoreline adjustment to placement of engineering structures. Pronounced bathymetric change observed along the head and sides of the Hudson River Channel reflects natural and anthropogenic processes. Large areas showing significant deposition at the head of the Hudson River Channel reflect high levels of offshore disposal activity, and patches of erosion and accretion paralleling each other along the length of the channel reflect natural bathymetric changes.

Third, alternating bands of erosion and accretion paralleling ridge features illustrated the steady reworking of the shelf surface as sand ridges migrated in the direction of net sediment transport. The process by which this was occurring was relatively consistent across the shelf. At Borrow Site H1, bathymetric comparisons suggested that the borrow site in this region would fill with sand transported from the adjacent seafloor at rates of about 98,000 m³/yr. Areas of erosion and accretion documented between 1927/37 and 1927/97 at Borrow Site 4E illustrated the amount of sediment available for infilling at sites south of Long Island was also about 98,000 m³/yr. Calculations for these two borrow sites were used as indicators of potential infilling rates for all borrow sites within the study area.

Finally, net longshore transport rates determined from seafloor changes in the littoral zone along Sandy Hook spit indicated maximum transport rates near the distal end of the spit, with lower rates to the south. These calculations, along with data published by Caldwell (1966) indicate a range in net longshore transport along Sandy Hook from about 223,000 m³/yr to 382,000 m³/yr. According to Taney (1961), the direction of net littoral drift along southwestern Long Island beaches is east to west, ranging from 122,000 to 344,000 m³/yr.

7.4.2 Sediment Transport Modeling at Potential Borrow Sites

In addition to predicted modifications to the wave field, potential sand mining at offshore borrow sites resulted in minor changes in sediment transport pathways in and around potential dredging sites. Modifications to bathymetry caused by sand mining only influenced local hydrodynamic and sediment transport processes in the offshore area. Wave height changes at and adjacent to dredged borrow sites experienced minor changes in wave or sediment transport characteristics.

For water depths at the proposed borrow sites, minimal impacts to waves, currents, and regional sediment transport are expected during infilling. Infilling rates computed for each of the five borrow sites offshore northeastern New Jersey and southwestern Long Island represented the total potential sediment transport at each of the sites from the combined influence of wave-induced and ambient bottom currents. These results likely represent average, non-storm conditions for sediment transport at each site. For the five modeled borrow sites, computed transport rates were extremely low, with infilling rates ranging from 0.13 m³/yr to approximately 580 m³/yr. A number of factors contributed to the low transport rates, including water depth (typically 20 m, which reduced the impact of wave-induced currents), relatively short period waves dominating the regional wave climate, absence of storm events in the wave and current data sets that drive sediment transport in this area, coarse grain size of *in situ* materials, and relatively weak ambient shelf currents. Furthermore, potential borrow site excavations consisted of dredging an existing shoal to the same elevation as the surrounding seafloor. Therefore, potential borrow site excavation would primarily flatten the shoal and not create a seafloor depression. Based on extremely low potential transport rates of *in situ* sediment and the geomorphic character of dredged deposits, it is unlikely that any of these borrow sites will reform as shoal deposits in the near future.

7.4.3 Nearshore Sediment Transport Potential

Comparisons of average annual sediment transport potential were performed for existing and post-dredging conditions to indicate the relative impact of dredging to longshore sediment transport processes. Mean sediment transport potential calculated for beaches east of Jones Inlet indicated net westerly transport ranging from about 54,000 m³/yr at Fire Island Inlet to 170,000 m³/yr at Jones Inlet. Along Long Beach, net westerly transport increased from about 50,000 m³/yr west of Jones Inlet to a maximum of about 150,000 m³/yr at the approximate mid-point of the barrier beach, before decreasing to about 88,000 m³/yr at East Rockaway Inlet.

Mean sediment transport potential along the northeast coast of New Jersey for the modeled 20-year period indicated that dominant transport was net northerly but more bi-directional for shorter term annual results. There was an approximate $\pm 55,000$ m³/yr range in annual net transport rates. Long-term potential transport rates reached a maximum of approximately 30,000 m³/yr within the modeled study area, and a minimum occurred just north of Shark River Inlet. Results of transport potential calculations indicated that the year with the greatest net southerly transport was 1987, and the year with the greatest northerly directed transport was 1995.

The significance of changes to longshore transport along the modeled shoreline resulting from dredging proposed borrow sites to their maximum design depths was determined using the method described in Kelley et al. (2004). Results of the significance analysis for borrow sites offshore southwestern Long Island indicated that the $\pm 0.5\sigma$ significance envelope increased along Jones Beach from $\pm 20,000 \text{ m}^3/\text{yr}$ at Fire Island Inlet to $\pm 40,000 \text{ m}^3/\text{yr}$ at Jones Inlet. The significance envelope for Long Beach had a similar range, with a maximum value midway between Jones Inlet and East Rockaway Inlet. Potential dredging impacts to longshore transport rates from excavation at Sites 3, 4W, and 4E are well within the transport significance envelope. As such, proposed dredging at these sites would not result in significant modifications to coastal processes along this shoreline. Largest calculated differences between existing and post-dredging transport potential occur east of Jones Inlet, where the transport rate becomes more westerly by $3,000 \text{ m}^3/\text{yr}$. The resulting change is negligible, even though offshore sand extractions are large (i.e., a total dredged volume of $48 \times 10^6 \text{ m}^3$ for all three sites). Shoreline impacts are negligible due to the relatively deep water at potential borrow sites (19 m for Site 3 and 20 m for Sites 4W and 4E), their distance offshore, and wave climate (dominated by relatively short-period waves).

Results of the impact significance analysis for sites offshore northeastern New Jersey indicated that the $\pm 0.5\sigma$ significance envelope computed for this area was generally constant at $\pm 15,000 \text{ m}^3/\text{yr}$. Impacts from dredging Sites H1 and H2 are well within the significance envelope, and proposed sites would be acceptable under the simulated conditions. Similar to sites offshore Long Island, potential shoreline impacts were negligible due to the relatively deep water at potential borrow sites (20 m for Sites H1 and H2), their distance offshore, and wave climate (dominated by relatively short-period waves).

7.5 BENTHIC ENVIRONMENT

The purpose of this section is to address potential effects of offshore sand dredging on benthic organisms, including analyses of recolonization periods and success following cessation of dredging activities. This section is divided into three parts. The first two parts provide reviews of information from existing literature on effects and recolonization. The first part (Section 7.5.1) summarizes potential impacts to benthic organisms from physical disturbance of dredging, which causes removal, suspension/dispersion, and deposition of sediments. The second part (Section 7.5.2) is a synthesis of information concerning recolonization periods and success. The third part (Section 7.5.3) provides predictions of impacts and recolonization relative to the four sand borrow sites off New Jersey and New York.

Ecological effects of marine mining and beach nourishment operations have been reviewed by numerous authors (Thompson, 1973; Naqvi and Pullen, 1982; Nelson, 1985; Cruickshank et al., 1987; Goldberg, 1989; Grober, 1992; Hammer et al., 1993; National Research Council, 1995). Effects vary from detrimental to beneficial, short to long term, and direct to indirect (National Research Council, 1995).

Most reviews on the effects of beach nourishment operations have focused on potential impacts at the beach. Comprehensive assessments of effects on biological resources at open ocean sand borrow sites have been limited (National Research Council, 1995). Alterations to biological resources in offshore sand borrow sites are generally of longer duration, and the consequences of those changes have not been well-defined (National Research Council, 1995). The remainder of this section focuses on potential impacts of dredging operations at offshore sand resource areas.

7.5.1 Effects of Offshore Dredging on Benthic Biota

The primary impact producing factor relative to dredging offshore sand borrow sites is mechanical disturbance of the seabed. This physical disruption includes removal, suspension/dispersion, and deposition of dredged material, which may make the benthic environment less suitable for some species and better for other biota. The following subsections focus on potential effects of these physical processes on benthic biota.

7.5.1.1 Sediment Removal

Physical removal of sediments from a borrow site removes benthic habitat along with infauna and epibiota that are incapable of avoiding the dredge, resulting in drastic reductions in number of individuals, number of species, and biomass. Extraction of habitat and biological resources may in turn disrupt the functioning of existing communities. Removal of benthic resources is of concern because the resources are important in the food web for commercially and recreationally important fishes and invertebrates, and contribute to the biodiversity of the pelagic environment through benthic-pelagic coupling mechanisms. These mechanisms include larval transport and diurnal migrations of organisms, which may have substantial impact on food availability, feeding strategies, and behavioral patterns of other members of the assemblage (Hammer and Zimmerman, 1979; Hammer, 1981).

The influence of sediment composition on benthic community composition has been recognized since the pioneer studies of Peterson (1913), Jones (1950), Thorson (1957), and Sanders (1958). However, more recent reviews suggest that precise relationships between benthic assemblages and specific sediment characteristics are poorly understood (Gray, 1974; Snelgrove and Butman, 1994; Newell et al., 1998). Sediment grain size, chemistry, and organic content may influence recolonization of benthic organisms (McNulty et al., 1962; Thorson, 1966; Snelgrove and Butman, 1994), although the effects of sediment composition on recolonization patterns of various species are not always significant (Zajac and Whitlatch, 1982). Because the complexity of soft sediment communities may defy any simple paradigm relating to any single factor, Hall (1994) and Snelgrove and Butman (1994) proposed a shift in focus towards understanding relationships between organism distributions and the dynamic sedimentary and hydrodynamic environments. It is likely that the composition of benthic assemblages is controlled by a wide array of physical, chemical, and biological factors that interact in complex ways and are variable with time.

Removal of sand resources can expose underlying sediments and change the sediment structure and composition of a borrow site, consequently altering its suitability for burrowing, feeding, or larval settlement of some benthic organisms. Many studies show decreases in mean grain size, and in some cases, increases in silt and clay in borrow sites following dredging (National Research Council, 1995). Changes in sediment composition could potentially prevent recovery to an assemblage similar to that which occurred in the borrow site prior to dredging and could by implication affect the nature and abundance of food organisms for commercial and recreational fishery stocks (Coastline Surveys Limited, 1998; Newell et al., 1998). In some cases, dredging borrow sites may create new and different habitats from surrounding substrates, which could result in beneficial impacts in terms of increased habitat complexity, biomass, and biodiversity of an area.

Removal of sediments from borrow sites can alter seabed topography, creating pits that may refill rapidly or cause detrimental impacts for extended periods of time. The term "borrow site" can be misleading because often material is returned only by natural sediment transport processes. Nearly 12 years may be required for some offshore borrow sites to refill to pre-

dredge profiles (Wright, 1977), and other borrow sites have been known to remain well-defined 8 years after dredging (Marsh and Turbeville, 1981; Turbeville and Marsh, 1982). Intentionally locating borrow sites in highly depositional areas may dramatically reduce the time for refilling (Van Dolah et al., 1998). In general, shallow dredging over large areas causes less harm than small but deep pits, particularly pits opening into a different substrate surface (Thompson, 1973; Applied Biology, Inc., 1979). Deep pits also can hamper commercial trawling activities and harm level-bottom communities (Thompson, 1973). If borrow pits are deep, current velocity is reduced at the bottom, which can lead to deposition of fine particulate matter and in turn a biological assemblage much different in composition than the original. Increasing water depths and turbidity from dredging may reduce the photic zone for benthic primary producers. Recovery of the physical environment and benthic assemblages to pre-dredging conditions will probably take decades for a deep pit dredged 3.6 km offshore Coney Island (Barry A Vittor & Associates, Inc., 1999a). Deep holes may decrease dissolved oxygen to hypoxic or anoxic levels and increase hydrogen sulfide levels (Murawski, 1969; Saloman, 1974; National Research Council, 1995). Not all impacts from dredge pits are detrimental. Borrow pits are known to attract numerous fishes (Gustafson, 1972; Michals, 1997; Weakley, 2001), even to the extent that some dredge holes have been referred to as "reefs in reverse" (Weakley, 2001). Borrow pits also provide resting places for loggerhead sea turtles (Michals, 1997).

Seabed topography and benthic communities can be altered when sediment is removed by dredging bathymetric peaks such as ridges or shoals rather than level sea bottoms or depressions. Little information exists regarding the relationship between biological assemblages and removal of shoals by dredging. Numerous benthic organisms and fishes inhabit offshore shoal areas, but specifics regarding species, assemblages, and ecological interrelationships between the topographic features and associated biota are not well known. Potential long-term physical and biological impacts could occur if dredging significantly changes the physiography of shoals. The MMS has funded several studies to address environmental questions concerning use of shoals by fishes and mobile invertebrates, potential impacts to these species from offshore sand dredging, and ways to preclude or minimize long-term impacts. Burlas et al. (2001) monitored borrow sites with bathymetric high points off northern New Jersey and found that essentially all infaunal assemblage patterns recovered within 1 year after dredging disturbance except recovery of average sand dollar weight and biomass composition, which required 2.5 years.

7.5.1.2 Sediment Suspension/Dispersion

Dredging causes suspension of sediments, which increases turbidity over the bottom. This turbidity undergoes dispersion in a plume that drifts with the water currents. The extent of suspension/dispersion depends on a multitude of factors, including the type of dredging equipment, techniques for operating the equipment, amount of dredging, thickness of the dredged layer, sediment composition, and sediment transport processes. Although turbidity plumes associated with dredging often are short lived and affect relatively small areas (Cronin et al., 1970; Nichols et al., 1990), resuspension and redispersion of dredged sediments by subsequent currents and waves can propagate dredge-related turbidity for extended periods after dredging ends (Onuf, 1994). Biological responses to turbidity depend on all of these physical factors coupled with the type of organism, geographic location, and time of year.

Herbich and Brahme (1991) and Herbich (1992) reviewed sediment suspension caused by existing dredging equipment and discussed potential technologies and techniques to reduce suspension and the associated environmental impacts. In general, cutterhead suction dredges produce less turbidity than hopper dredges. A cutterhead suction dredge consists of a rotating

cutterhead, positioned at the end of a ladder, that excavates the bottom sediment. The cutterhead is swung in a wide arc from side to side as the dredge is stepped forward on pivoting spuds, and excavated material is lifted from the bottom by a suction pipe and transferred by pipeline as a slurry (Hrabovsky, 1990; LaSalle et al., 1991). Sediment suspension is caused by the rotating action of the cutterhead and the swinging action of the ladder (Herbich, 1992). Well designed and properly operated cutterhead dredges can limit sediment suspension to the lower portion of the water column (Herbich and Brahme, 1991; Herbich, 1992). Turbidity can be reduced by selecting an appropriate cutterhead for a given sediment, determining the best relationship between cutterhead rotational speed and hydraulic suction magnitude, establishing a suitable swing rate for the cutterhead, and using hooded intakes, although these conditions are rarely achieved (Herbich, 1992). Measurements around properly operated cutterhead dredges show that suspended sediments can be confined to the immediate vicinity of the cutterhead and dissipate rapidly with little turbidity reaching surface waters (Herbich and Brahme, 1991; LaSalle et al., 1991; Herbich, 1992). Maximum suspended sediment concentrations typically occur within 3 m above the cutterhead and decline exponentially to the sea surface (LaSalle et al., 1991). Suspended sediments in near-bottom waters may occur several hundred meters laterally from the cutterhead location (LaSalle et al., 1991).

A hopper dredge consists of one, two, or more dragarms and attached dragheads mounted on a ship-type hull or barge with hoppers to hold the material dredged from the bottom (Herbich and Brahme, 1991). As the hopper dredge moves forward, sediments are hydraulically lifted through the dragarm and stored in hopper bins on the dredge (Taylor, 1990; LaSalle et al., 1991). Hopper dredging operations produce turbidity as the dragheads are pulled through bottom sediments. However, the main source of turbidity during hopper dredging operations is sediment release during hopper overflow (Herbich and Brahme, 1991; LaSalle et al., 1991; Herbich, 1992). A plume may occasionally be visible at distances of 1,200 m or more (LaSalle et al., 1991).

Much attention has been given to turbidity effects from dredging, although most reviews have concerned estuaries, embayments, and enclosed waters (e.g., Sherk and Cronin, 1970; Sherk, 1971; Sherk et al., 1975; Moore, 1977; Peddicord and McFarland, 1978; Stern and Stickle, 1978; Herbich and Brahme, 1991; LaSalle et al., 1991; Kerr, 1995; Newcombe and Jensen, 1996; Wilber and Clarke, 2001). Turbidity effects may be less important in unprotected offshore areas for several reasons. Offshore sands tend to be coarser with less clay and silt than inshore areas. The open ocean environment also provides more dynamic physical oceanographic conditions, which minimize settling effects. In addition, offshore organisms are adapted to sediment transport processes, which create scouring, natural turbidity, and sedimentation effects under normal conditions. Impacts should be evaluated in light of natural variability as well as high level disturbances associated with such events as storms, trawling, floods, hypoxia/anoxia, etc. (Sosnowski, 1984; Herbich, 1992). Physical disturbance of the bottom and resulting biological impacts from dredging are similar to those of storms and trawling but at a much smaller spatial scale. The following suggestions from Hughes and Connell (1999) also are instructive regarding the complexities of analyzing effects of multiple stressors (broadly defined as natural or man-made disturbances). Long-term approaches are necessary to understand biological responses to multiple stressors because studying single events in isolation can be misleading. The effects of a particular disturbance often depend critically on impacts from previous perturbations. Consequently, even the same type of recurrent stressor can have different effects at different times, depending on history. Accordingly, when the added dimension of time is considered, the distinction between single and multiple stressors becomes blurred (Hughes and Connell, 1999).

Turbidity from dredging can elicit a variety of benthic responses primarily because attributes of the physical environment are affected (Wilber and Clarke, 2001). Large quantities of bottom material placed in suspension decrease light penetration and change the proportion of wavelengths of light reaching the bottom, leading to decreases in photosynthesis and primary productivity of benthic organisms (Phinney, 1959; Courtenay et al., 1972; Owen, 1977; Onuf, 1994). Light has long been known as an ecological factor affecting dispersal and settlement of marine invertebrate larvae (Thorson, 1964). Suspended materials can prevent growth of benthic organisms that provide habitat complexity and biological structures used by many other species for shelter and egg attachment (Phinney, 1959; Cronin et al., 1969; Owen, 1977; Nelson, 1989; Connell, 1997).

Turbidity can affect food availability for benthic organisms. Changes in light penetration and wavelengths due to turbidity can affect visibility and may be detrimental or beneficial, depending on whether an organism is predator or prey. Suspension and dispersion processes uncover and displace benthic organisms, temporarily providing extra food for bottom feeding species (Centre for Cold Ocean Resources Engineering, 1995). Turbidity can interfere with food gathering processes of filter feeders and organisms that feed by sight by inundation with nonnutritive particles. In addition to altered feeding rates, other biological responses to turbidity include reduced hatching success, slowed growth, abnormal development, tissue abrasion, and increased mortality (Wilber and Clarke, 2001). In general, egg and larval stages are more sensitive to turbidity effects than older life history stages. Although a considerable amount of information is available on the effects of sediment suspension and dispersion to some benthic organisms, little or no information exists for many other species, particularly those associated with hard bottom (Dodge and Vaisnys, 1977; Bak, 1978; Nelson, 1989; Rogers, 1990; Kerr, 1995; Renaud et al., 1996, 1997).

Suspension and dispersion of sediments may cause changes in sediment and water chemistry as nutrients and other substances are released from the substratum and dissolved during dredging. For aggregate mining operations using hopper dredges, the far-field visible plume contains an organic mixture of fats, lipids, and carbohydrates from organisms entrained and fragmented during the dredging process and discharged with the overflow (Coastline Surveys Limited, 1998; Newell et al., 1999). Dredging may produce localized hypoxia or anoxia in the water column due to oxygen consumption of suspended sediments (LaSalle et al., 1991). Flocculation of suspended sediments can mechanically trap inorganic and organic particles and plankton and carry them to the bottom (Bartsch, 1960 as cited in Levin, 1970).

7.5.1.3 Sediment Deposition

Suspended sediments settle and are deposited nearby or some distance from dredged sites. The extent of deposition and the boundaries of biological impact are dependent on type and amount of suspended sediments and physical oceanographic characteristics of the area.

Dredging effects are not necessarily limited to the borrow site alone. Far-field impacts from suspension, dispersion, and deposition of sediments during dredging can be detrimental or beneficial. Deposition of sediments can suffocate and bury benthic fauna, although some organisms are able to migrate vertically to the new surface (Maurer et al., 1986; Nelson, 1988). Johnson and Nelson (1985) found decreases in infaunal abundances and numbers of taxa at nondredged stations, although these decreases were not as extreme as those observed in the borrow site. McCaully et al. (1977; as cited by Johnson and Nelson, 1985) also observed that dredging effects can extend to other nearby areas, and noted decreases in infaunal abundances ranging from 34% to 70% at undredged stations within 100 m of a dredged area. Conversely,

benthos may show increased biodiversity downstream from dredged sites (Centre for Cold Ocean Resources Engineering, 1995). In some areas, population density and species composition of benthic invertebrates increased rapidly outside dredged sites, with the level of enhancement decreasing with increasing distance from the dredged site up to a distance of 2 km (Stephenson et al., 1978; Jones and Candy, 1981; Poiner and Kennedy, 1984). The enhancement was ascribed to release of organic nutrients from the dredge plume, a process known from other studies (Ingle, 1952; Biggs, 1968; Sherk, 1972; Oviatt et al., 1982; Coastline Surveys Limited, 1998; Newell et al., 1998, 1999). This suggestion was supported by records of nutrient releases from benthic areas during intermittent, wind-driven bottom resuspension events (Walker and O'Donnell, 1981), significant increases in water column nutrients from simulated storm events in the laboratory (Oviatt et al., 1982), and review of the literature indicating a major restructuring force in infaunal communities is the response of species to resources released from the sediments by periodic disturbance (Thistle, 1981). Fishing may improve temporarily down current of the dredging area and continue for some months (Centre for Cold Ocean Resources Engineering, 1995). Additional far-field impacts can occur by resuspension, redispersion, and redeposition of fine dredged materials by wave and current actions long after dredging has been completed.

7.5.2 Recolonization Periods and Success

7.5.2.1 Adaptations for Recolonization and Succession

In dynamic areas that undergo frequent perturbations, benthic invertebrates tend to be small bodied, short lived, and adapted for maximum rate of population increase with high fecundity, efficient dispersal mechanisms, dense settlement, and rapid growth rates. In contrast, organisms in stable areas tend to be relatively larger and longer lived with low fecundity, poor dispersal mechanisms, slow growth rates, and adaptations for non-reproductive processes such as competition and predator avoidance. Recolonization of a disturbed area often is initiated by organisms that have adaptive characteristics for rapid invasion and colonization of habitats where space is available due to some natural or man-induced disturbance. These early colonizers frequently are replaced during the course of succession through competition by other organisms, unless the habitat is unstable or frequently perturbed (MacArthur, 1960; MacArthur and Wilson, 1967; Odum, 1969; Pianka, 1970; Grassle and Grassle, 1974).

Although the distinction between the adaptive strategies is somewhat arbitrary and is blurred in habitats that are subject to only mild disturbance, the lifestyle differences are fundamentally important because they help explain variations in succession and recolonization rate and success following disturbance (Coastline Surveys Limited, 1998; Newell et al., 1998). Knowledge of faunal component lifestyles allows some predictions of dredging impacts and subsequent recolonization and recovery of community composition (Coastline Surveys Limited, 1998; Newell et al., 1998).

7.5.2.2 Successional Stages

When discussing succession in soft bottom habitats, it is important to point out that most past studies have concerned silt-clay bottoms rather than sand habitats. Little is known about succession in sand bottoms of offshore borrow areas.

Successional theory states that organism-sediment interactions result in a predictable sequence of benthic invertebrates belonging to specific functional types following a major seafloor disturbance (Rhoads and Germano, 1982, 1986). Because functional types are the

biological units of interest, the succession definition does not rely on the sequential appearance of particular species or genera (Rhoads and Boyer, 1982). This continuum of change in benthic communities has been divided arbitrarily into three stages (Rhoads et al., 1978; Rhoads and Boyer, 1982; Rhoads and Germano, 1982):

- Stage I is the initial pioneering community of tiny, densely populated organisms that appears within days of a natural or anthropogenic disturbance. Stage I communities are composed of opportunistic species that have high tolerance for and can indicate disturbance by physical disruption, organic enrichment, and chemical contamination of sediments. The organisms have high rates of recruitment and ontogenetic growth. Stage I communities tend to physically bind sediments, making them less susceptible to resuspension and transport. For example, Stage I communities often include tube-dwelling polychaetes or oligochaetes that produce mucous to build their tubes, which stabilizes the sediment surface. Stage I communities include suspension or surface deposit-feeding animals that feed at or near the sediment-water interface. The Stage I initial community may reach population densities of 10^4 to 10^6 individuals per m^2 ;
- Stage II is the beginning of the transition to burrowing, head-down deposit feeders that rework the sediment deeper with time and mix oxygen from the overlying water into the sediment. Stage II animals may include tubicolous amphipods, polychaetes, and mollusks. These animals are larger and have very low population densities compared to Stage I animals; and
- Stage III is the mature and stable community of deep-dwelling, head-down deposit feeders. In contrast to Stage I organisms, these animals rework the sediments to depths of 3 to 20 cm or more, loosening the sedimentary fabric and increasing the water content of the sediment. They also actively recycle nutrients because of the high exchange rate with the overlying water resulting from their burrowing and feeding activities. The presence of Stage III taxa can be a good indication that the sediment surrounding these organisms has not been severely disturbed recently, resulting in high benthic stability and health. Loss of Stage III species results in the loss of sediment stirring and aeration and may be followed by a build-up of organic matter (eutrophication) of the sediment. Because Stage III species tend to have relatively low rates of recruitment and ontogenetic growth, they may not reappear for several years once they are excluded from an area. These inferences are based on past work, primarily in temperate latitudes, showing that Stage III species are relatively intolerant to physical disturbance, organic enrichment, and chemical contamination of sediments. Population densities are low (10 to 10^2 individuals per m^2) compared to Stage I.

The general pattern of succession of benthic species in a marine sediment following cessation of dredging or other environmental disturbance begins with initial recolonization. Initial recolonization occurs relatively rapidly by small opportunistic species that may reach peak population densities within months of a new habitat becoming available after catastrophic mortality of the previous assemblage. As the disturbed area is invaded by additional larger species, the population density of initial colonizers declines. This transitional period and assemblage with higher species diversity and a wide range of functional types may last for

years, depending on numerous environmental factors. Provided environmental conditions remain stable, some members of the transitional assemblage are eliminated by competition, and the species assemblage forms a recovered community composed of larger, long-lived, and slow growing species with complex biological interactions with one another.

7.5.2.3 Recolonization Periods

The rate of recolonization is dependent on numerous physical and biological factors and their interactions. Physical factors include time of year, dredging technologies and techniques, borrow site dimensions, water currents, water quality, sediment composition, bedload transport, temperature, salinity, natural energy levels in the area, frequency of disturbance, latitude, etc. Recovery times may be shorter in warmer waters at lower latitudes as compared to colder waters at higher latitudes (Coastline Surveys Limited, 1998; Newell et al., 1998). Spatial and temporal variability in physical conditions may in some cases exert more influence on initial stages of recolonization than biological responses of species considered to be opportunists (Zajac and Whitlatch, 1982).

Biological factors influencing the rate of recolonization include the size of the pool of available colonists (Bonsdorff, 1983; Hall, 1994) and life history characteristics of colonizing species (Whitlatch et al., 1998). Recolonization of borrow sites may occur by transport of eggs, larvae, juveniles, and adults from neighboring populations by currents, immigration of motile species from adjacent areas, organisms contained in sediment slumping from the sides of pits, or return of undamaged organisms from the dredge plume. Other biological factors such as competition and predation also determine the rate of recolonization and the composition of resulting benthic communities. Timing of dredging is important because many benthic species have distinct peak periods of reproduction and recruitment. Because larval recruitment and adult migration are the primary recolonization mechanisms, biological recovery from physical impacts generally should be most rapid if dredging is completed before seasonal increases in larval abundance and adult activity (Herbich, 1992). Recovery of a community disturbed after peak recruitment, therefore, will be slower than one disturbed prior to peak recruitment (LaSalle et al., 1991).

Benthic recolonization and succession have been reviewed to varying extents for a wide variety of habitats throughout the world (e.g., Thistle, 1981; Thayer, 1983; Hall, 1994; Coastline Surveys Limited, 1998; Newell et al., 1998). Recolonization is highly variable, depending on the habitat type and other physical and biological factors. Focusing on dredging, Coastline Surveys Limited (1998) and Newell et al. (1998) suggested that, in general, recovery times of 6 to 8 months are characteristic for many estuarine muds, 2 to 3 years for sand and gravel, and 5 to 10 years as the deposits become coarser.

The Centre for Cold Ocean Resources Engineering (1995) estimated times for recovery of a reasonable biodiversity (number of species and number of individuals) based on sediment type. In this study, recovery was defined as attaining a successional community of opportunistic species providing evidence of progression towards a community equivalent to that previously present or at non-impacted sites. Fine-grained sediments may need only 1 year before achieving a recovery level biodiversity, medium-grained deposits 1 to 3 years, and coarse-grained deposits 5 or more years. For a hypothetical borrow site dredging scenario off Ocean City, Maryland, the Centre for Cold Ocean Resources Engineering (1995) stated that virtually all benthic species would be lost, but there may be temporary improvement of fishing due to release of nutrients. Recolonization would start within weeks of closure, and moderate biodiversity would occur within 1 year. The borrow site would be colonized initially by a very

different species complex than originally present. An estimate of 2 to 3 years was given for the community to begin to show succession to pre-impact sand habitat species.

Recolonization of a borrow site was studied 3 km offshore of Great Egg Harbor Inlet near Ocean City, New Jersey (Scott and Kelley, 1998). Macrobenthic organisms were able to colonize the borrow site rapidly. Approximately 2 years after the last dredging, the number of taxa, diversity, and abundance in the borrow site recovered to conditions that existed in other borrow sites and undisturbed areas before dredging. The community composition within the borrow site may have changed, although the community change was described as not significant and not a result of dredging because the community composition of the borrow site was similar to the composition observed at the adjacent stations. Good juvenile surfclam recruitment occurred in the borrow site, but the population may not have reached size levels in nearby undisturbed sites 2 years after the last dredging. Although biomass and size of surfclams appeared diminished, there was no indication that the population would not stabilize given additional time. As dredging events were conducted in all seasons and no apparent effect was detected, no changes in the timing of dredging appeared to be necessary (Scott and Kelley, 1998).

Recolonization also was studied by Burlas et al. (2001) at borrow areas near Sites H1 and H2. Similar to the present study, their borrow areas were bathymetric high points on the seascape with strong currents and sand movement. Burlas et al. (2001) summarized their results by stating that abundance, biomass, richness, and the average size of the biomass dominant, which was the sand dollar *Echinarachnius parma*, declined immediately after dredging. Abundance, biomass, and richness recovered quickly after the first dredging operation with no detectable difference between dredged and undisturbed areas by the following spring. Abundance also recovered quickly after a second dredging operation, but biomass and richness were still reduced the next spring. Species and biomass composition were altered in similar manners by each operation. Immediately after dredging, the relative contribution of echinoderm biomass declined and the abundance of the spionid polychaete *Spiophanes bombyx* increased. Changes in biomass composition were longer lasting with the assemblage taking 1.5 to 2.5 years to return to undredged conditions.

Studies of recolonization listed and discussed by Grober (1992) and the National Research Council (1995) indicate that recolonization of offshore borrow sites is highly variable. This variability is not surprising considering differences among studies in geographic locations, oceanographic conditions, sampling methods and times, etc. Part of the problem in determining recolonization patterns is seasonal and year to year fluctuations in benthic community characteristics and composition. Without adequate seasonal and yearly data prior to dredging, it is difficult to determine whether differences in community characteristics and composition are due to temporal changes or dredging disturbance.

Results and conclusions from these offshore borrow site studies indicate that recolonization usually begins soon after dredging ends. Recolonization periods range in duration from a few months (Saloman et al., 1982; Jutte et al., 2002) for shallow dredging to possibly decades for deep pits (Barry A. Vittor & Associates, Inc., 1999a). Although abundance and diversity of benthic infauna within borrow sites often returned to levels comparable to pre-dredging or reference conditions within less than 1 year, several studies documented changes in benthic species composition that lasted much longer, particularly where sediment composition was altered (e.g., Saloman, 1974; Wright, 1977; Johnson and Nelson, 1985; Bowen and Marsh, 1988; Van Dolah et al., 1992, 1993; Wilber and Stern, 1992; Barry A. Vittor & Associates, Inc., 1999a).

Most recolonization studies of borrow sites concentrated on three main features of infaunal communities, namely the number of individuals (population density), number of species (diversity), and weight (biomass as an index of growth). Dredging is usually accompanied by an immediate and significant decrease in the number of individuals, species, and biomass of benthic infauna. Using biological community parameters (e.g., total taxa, total number of individuals, species diversity, evenness, richness, etc.), previous studies tend to indicate that recovery of borrow sites occurs in approximately 1 year after dredging. However, these parameters do not necessarily reflect the complex changes in community structure and composition that occur during the recovery process. Major changes in species assemblages and community composition usually occur shortly after dredging such that a different type of community exists. Although the number of individuals, species, and biomass of benthic infauna may approach pre-dredging levels within a relatively short time after dredging, recovery of community composition may take longer.

7.5.2.4 Recolonization Success and Recovery

Assessing impacts of dredging and recolonization and recovery of borrow sites is difficult because most biological communities are complex associations of species that often undergo major changes in population densities and community composition, even in areas that are far removed and unaffected by dredging and other disturbances. Recolonization success and recovery do not necessarily mean that communities should be expected to return to the pre-dredged species composition. To gauge recovery, it is important to compare the community composition of dredged areas with control areas during the same seasons because community composition changes with time.

When long-term alterations in sediment structure and composition occur as a result of dredging, long-term differences in the composition of benthic assemblages inhabiting those sites may occur as well. The recovery time of benthic assemblages after dredging can depend in large measure on the degree and duration of sediment alteration from sand borrowing (Van Dolah, 1996). Recolonization success and recovery also are controlled by compaction and stabilization processes involving complex interactions between particle size, water currents, waves, and biological activities of the benthos following sediment deposition (Oakwood Environmental Ltd., 1999). While the abundance and diversity of infaunal assemblages may recover relatively rapidly in dredged areas, it may take years to recover in terms of sediment and species composition.

One conclusion commonly held is that perturbations to infaunal communities in borrow sites are negligible because organisms recolonize rapidly (Wilber and Stern, 1992). This conclusion often is based on measures including densities, species diversity/evenness indices, relative distribution of classes or phyla, and species-level dendrograms. For example, many researchers have recognized that borrow and reference area infaunal communities can differ considerably at the species level, although these differences usually are considered insignificant because species diversity is high. According to Wilber and Stern (1992), reliance on these studies may lead to a premature conclusion that impacts to borrow site infauna are minimal because these measures are relatively superficial and ambiguous characteristics of infaunal communities. Wilber and Stern (1992) reexamined infaunal data from four borrow site projects by grouping species into functional groups called ecological guilds based on similarities in feeding mode, locomotory ability, and sediment depth occurrence. Their analyses showed that infaunal communities in borrow and control areas can differ in several ways and that these differences can last several years. Polychaetes and amphipods that recolonize borrow sites are

small-bodied and confine their movement and feeding to the surface sediment or the interface between the sediment and water column. In contrast, control areas have well-developed infaunal communities commonly consisting of large-bodied organisms that move and feed deep in the sediment (Wilber and Stern, 1992). They concluded that the infaunal communities recolonizing borrow sites may remain in an early successional stage for 2 to 3 years or longer as opposed to being completely recovered in shorter time frames.

The conclusions of Wilber and Stern (1992) coincide with the model of succession discussed previously. The model states pioneering or opportunistic species are the first to colonize an area after a physical disturbance to the bottom (e.g., dredging borrow sites). Pioneering species tend to share several ecological traits, including a tendency to confine activities to the sediment-water interface, possibly because subsurface conditions cannot support a significant number of organisms. The subsurface environment changes with time after the disturbance, possibly by actions of early colonizers, and becomes suitable for deposit feeders and mid-depth burrowers. The relative absence of deposit feeders and mid-depth burrowers is interpreted to mean an area is still in the state of recovery.

Although most of the literature on recolonization rate and success in borrow sites concerns infauna, some information exists for soft bottom epifauna. The numbers of taxa and individuals collected by trawls in a borrow site off Duval County, Florida greatly exceeded the control area numbers 4 months after dredging and were generally higher 7 and 13 months after dredging (Applied Biology, Inc., 1979). There were no detectable differences between pre-dredging and post-dredging (8 and 16 months) epifaunal communities in a borrow site surveyed by otter trawl and video camera off Egmont Key, Florida (Blake et al., 1995).

7.5.3 Predictions Relative to the Borrow Sites

Based on the commodity-specific, technology-specific, and site-specific information provided previously, the following predictions can be made regarding the potential effects of offshore dredging on benthic organisms (Section 7.5.3.1) and the recolonization rate and success (Section 7.5.3.2) relative to the four sand borrow sites off New Jersey and New York.

7.5.3.1 Potential Benthic Effects

Sediment Removal

The immediate impact of excavating upper sediments of a sand borrow site would be removal of portions of the benthic invertebrate populations that inhabit surficial shelf sediments. Lost individuals would be those with slow-moving or sessile lifestyles, primarily those comprising infaunal populations. Surveys within and adjacent to each of the candidate borrow sites, as well as benthic investigations of nearby waters, reveal that infaunal assemblages of inner shelf waters of the study area predominantly are invertebrates, including crustaceans, echinoderms, mollusks, and polychaetous annelids.

The expected loss of benthic fauna due to sediment excavation from the sand borrow sites could be considered to represent a negligible impact on the ecosystem when evaluating the impact on a broad spatial scale. Use of any of the sand borrow sites does not entail complete excavation of those areas. Impacts most likely would be localized and short-term. Specific locations within borrow sites that are to be dredged will be selected based on particular sedimentary and bathymetric characteristics, leaving a significant extent of non-dredged areas surrounding and interspersed throughout the impacted areas. These undisturbed areas would be a primary source of colonizing fauna for the excavated sites (Van Dolah et al., 1984) and

would complement colonization of altered substrata via larval recruitment. Preservation of non-dredged areas throughout an offshore borrow site, through avoidance by the dredge, has been cited as a factor contributing to more rapid community recovery after dredging (Jutte et al., 2002). The great densities and fecundity of invertebrate populations, along with the relatively small areas of impact proposed, likely would preclude significant long-term negative effects on benthic populations.

Correlation between sediment composition and the composition of infaunal assemblages has been demonstrated in numerous environmental surveys, including the 2001-2002 surveys of the New Jersey and New York sand borrow sites. Invertebrate populations inhabiting marine soft bottoms of the Bight exhibit heterogeneous distributions that largely are the result of local sedimentary regime. Modification of surficial sediments and local bathymetry could result in an alteration of the areal extent and relative distribution of assemblage types, by altering the distribution of sediment types capable of supporting those assemblages.

It is possible that a change in the composition of surficial sediments within excavated areas could become a long-term result of dredging. Several factors could contribute to such an outcome, primarily the type of sediments exposed by dredging and the degree of fine sediment deposition into dredged areas. These factors would depend primarily on the depth of excavation, which would be determined by the vertical relief of the sand shoal to be excavated, the vertical extent of those sediments suitable for coastal nourishment projects, and the volume of sand required.

Because the inner shelf ecosystem of the Bight exhibits some heterogeneity in sediment types and their associated assemblages, those transitional infaunal assemblages that initially colonize dredged areas likely would be similar to some naturally occurring assemblages that inhabit nearby non-dredged areas, especially fine sediment areas within inter-ridge troughs. When viewed within a context of scale, removal of sediments from portions of the inner continental shelf would at most minimally alter the existing spatial balance of habitat (sediment) types. Moreover, those habitats that have relatively high levels of finer sediments are not uninhabitable or necessarily less functional in an ecological sense when compared to sand or gravel substrata. Various sediment habitat types merely differ in their level of suitability for certain types of infaunal taxa. Localized changes in habitat suitability that result from sand removal likely will be ephemeral and inconsequential in the shelf ecosystem, a system where both infaunal assemblage types and sedimentary parameters are dynamic and spatially variable.

Motile populations, including non-migratory foragers, would be less stressed by sediment removal than infauna or sessile epifauna. Most macroepifaunal and demersal fish populations would have a low probability of being adversely impacted directly by the dredging of surficial sediments. Slow-moving or burrowing sessile epifauna inhabiting the project area include echinoderm and decapod taxa, and local populations of these types of benthic organisms would most likely experience a reduction in density due to sediment removal. Motile epifauna generally are migratory and are not endemic to the sand borrow sites. Most demersal populations exhibit naturally dynamic distributions, moving between areas within the Middle Atlantic Bight on a seasonal basis (Able and Hagen, 1995).

Any impacts of sediment removal on epifaunal and demersal taxa likely would be indirect in nature, through habitat alteration. A reduction of infaunal biomass resulting from sediment removal could have an indirect effect on the distribution of certain demersal fishes and other epibenthic predators by interrupting established energy pathways to the higher trophic levels

represented by these foraging taxa. Reductions in densities of the preferred prey of bottom-feeding taxa could induce migration of foragers to unimpacted areas. However, a relatively small percentage of infaunal prey items that typically are consumed by demersal taxa would be rendered unavailable for consumption as a result of prey removal along with surficial sediments. Benthic predators simply would select alternative areas in which to forage. The loss of infaunal biomass due to sediment excavation, therefore, is unlikely to adversely affect normal energy flow through New Jersey and New York inner shelf sand bottoms.

In addition to widely documented spatial variation, the location and extent of inner shelf-inhabiting infaunal and demersal populations vary seasonally in the study area. Seasonal variability should be considered when evaluating potential impacts due to sand removal. The timing of sand removal would seem to be less critical for minimizing the impact on infauna than for other faunal categories of concern (e.g., key pelagic species), due to the great abundance and reproductive potential of infaunal populations. Many numerically dominant infaunal taxa inhabiting the study area are known to exhibit either year-round or late winter-early spring periods of recruitment. Because of these patterns of recruitment and lower winter densities, removal of sand between late fall and early spring might result in less stress on benthic populations.

Sediment Suspension/Dispersion

Whether cutterhead suction dredging or hopper dredging ultimately is utilized for sand mining, the amount of sediment suspension that results from these excavation methods is not anticipated to be of a scale that would cause significant negative impacts to the benthic community. New Jersey and New York sand borrow sites are characterized by a relatively limited volume of fine sediments, indicating that the shelf encompassing the areas currently is not a depositional environment but is hydrologically dynamic. In general, benthic assemblages of the Bight inner shelf probably are adapted to periodic reworking of surficial sediments caused by storm events. Impacts of dredging-induced elevations in turbidity (associated mainly with hopper dredging) would be short-term and localized. Demersal fishes and other motile taxa could avoid turbid areas.

Sediment Deposition

Of the various faunal categories, infaunal and burrowing epifaunal populations would be most negatively affected by significant deposition of sediments; however, efficient methods of sediment excavation would preclude all but a relatively minor amount of sediment deposition. Suspension and transport of sediments away from dredged sites should be minimal, and any subsequent deposition would be insignificant in degree. In the unlikely event that significant dredging-related deposition of fine-grained sediments were to occur, the deposited sediments likely would not persist on the seafloor because of the high-energy inner shelf environment. However, some low or depressional areas of the seafloor could exhibit a substantial deposition of fine sediments under this scenario. Given the relatively small amount of sediment suspension anticipated to occur during dredging, the degree of burial should be substantially less than would be required to impact negatively on the infaunal community. Consequently, indirect impacts to bottom feeding fishes would be minimal.

7.5.3.2 Potential Recolonization Periods and Success

The rate of post-dredging recovery of benthic assemblages within an excavated borrow site will depend primarily on the depth of sand excavation. While surface area of impact could be minimized by excavating a shoal to a greater depth, deep excavation likely would extend the

time for complete recovery of infaunal assemblages within the impacted area. The creation of a bathymetrically abrupt pit has potential to inhibit water current flow through such a feature, possibly resulting in a "dead zone" characterized by deposition of fine particles and hypoxia or anoxia. This scenario would extend the duration of ecological impact beyond that which would occur with a more shallow cut over a much larger area.

Recent results of long-term environmental monitoring of a borrow site located 3.6 km offshore Coney Island have demonstrated potential consequences of dredging an abrupt pit feature (Barry A. Vittor & Associates, Inc., 1999a). A nearby reference area also was sampled before (1992) and after dredging (1995 through 1998). Prior to dredging, average water depths were approximately 3 to 4 m at the Coney Island borrow site and in the reference area. After the last dredging in 1995 and until the last monitoring event (1998), depths of borrow site stations varied from 6 to 15 m, while the average depth of reference area stations did not change during the study period. Prior to dredging, sediments at the borrow site were 55% medium to coarse sands but by 1995 were fine to medium sands (<20% medium to coarse sand). By 1998, the silt/clay fraction (>20%) of borrow site sediments was significantly higher than in reference area sediments (4%). During each year following the last dredging event, infaunal assemblage composition at the borrow site was numerically dominated by deposit-feeding polychaetes (*Spio setosa* and *Streblospio benedicti*) and mollusks (primarily *Tellina agilis*); none of these species were ever sampled from the reference area. Although hypoxic conditions were never detected at the Coney Island borrow site, bathymetric alteration and subsequent deposition of fine sediments resulted in persistent alteration of the natural assemblage composition.

While the initial impact to benthic assemblages would increase with increasing surface area of sand removal, the persistence of ecological impact that would occur with a relatively shallow excavation would be less than that of a deep pit because a more smoothly-graded, trough-like feature would allow greater bottom current flow than would an abrupt pit. The inner continental shelf in the study area has natural inter-ridge trough features. These bathymetric depressions can be depositional areas for finer sediments, and they often support benthic assemblages that are different from nearby assemblages inhabiting gravel and sand (Byrnes et al., 2000).

The length of time required for reestablishment of infaunal assemblages within excavated areas partly depends on the length of time required for refilling of those mined areas. The relatively shallow water benthic habitats of the New Jersey and New York inner shelf are strongly influenced by factors such as tidal currents and circulation, and storms (Stubblefield et al., 1975). These same forces would tend to modify impacted areas in the direction of pre-dredging conditions. The rate of reestablishment of the natural benthic conditions at dredged sites may depend especially on the extent of storm-induced sediment transport, which can be substantial at relatively shallow depths such as those in the region of the sand borrow sites.

The process of sediment refilling and reworking at excavated sites would be accomplished mainly by storm-induced sorting and, to a lesser degree, longshore sediment drift. Parker (1996) indicated that movement of shelf sediments in offshore New Jersey waters occurs primarily as a result of the high winds and waves that characterize intense storms, while transport of New Jersey shelf sediments due to sand shoal migration appears to be relatively minimal. Tropical and extra-tropical storms impact the offshore Bight region on an annual basis, and these events would tend to modify seafloor depressions formed by dredging. The rate of the sand shoal reformation process will depend on the frequency and intensity of storms.

Assuming that the depth of sand excavation will not be so great as to substantially alter local hydrological characteristics, removal of benthic organisms along with sediments would quickly be followed by initial recolonization of the dredged areas by opportunistic infaunal taxa. Early-stage succession will begin within days of sediment removal, through settlement of larval recruits, primarily annelids and bivalves. Initial larval recruits likely would be dominated by populations of deposit feeding, opportunistic taxa (e.g., the polychaete *Asabellides oculata* and bivalves *Nucula proxima* and *Tellina agilis*). These species are well adapted to environmental stress and exploit suitable habitat when it becomes available. Later successional stages of benthic recolonization will be more gradual, and involve taxa that generally are less opportunistic and longer lived. Immigration of motile annelids, crustaceans, and echinoderms into impacted areas also would begin soon after excavation.

The length of time required for reestablishment of infaunal assemblages depends in large measure on sediment composition after dredging. Shoal sediments consist of well-sorted sands and gravel and also appear to be vertically uniform in sedimentary regime. In addition, New Jersey and New York sand borrow sites are characterized by a limited amount of fine sediments, indicating that they are not depositional in nature. It may be predicted that recolonization of dredged areas in sand borrow sites by later colonizing taxa likely will occur in a timely manner and without persistent inhabitation by initial transitional assemblages, not unlike the process that has been documented in comparable regional habitats (Kropp, 1995; Scott and Kelley, 1998).

Because the sedimentary regime of shoals is vertically uniform within the New Jersey and New York sand borrow sites, recolonization of surficial sediments by later successional stages likely will proceed even if dredged shoals are not completely reestablished. Furthermore, dredging of only a small portion of the area within each of the borrow sites will ensure that a supply of non-transitional, motile taxa will be available for rapid migration into dredged areas. While community composition may differ for a period of time after the last dredging, the infaunal assemblage type that exists in mined areas will be similar to naturally occurring assemblages in the study area, particularly those assemblages inhabiting inter-ridge troughs. Based on previous observations of infaunal reestablishment in dredged areas, the infaunal community in dredged sites within sand borrow sites most likely will become reestablished within 2 years, exhibiting levels of infaunal abundance, diversity, and composition comparable to nearby non-dredged areas.

7.6 PELAGIC ENVIRONMENT

7.6.1 Squids

7.6.1.1 Physical Injury

No information exists regarding impacts of hydraulic dredging on squids. Nevertheless, squids could be entrained if they encountered the suction field of a hydraulic dredge. Some general aspects of squid behavior increase the chance of encountering the bottom-oriented dredge suction field. Adult squids are generally demersal by day and enter the water column at night to feed on zooplankton (Fischer, 1978). In addition, squids lay their eggs in large clusters on the seafloor (Vecchione, 1981).

7.6.1.2 Attraction

Because some squid species are attracted to lights at night (Fischer, 1978), it is likely that squids could be attracted to lights of a working dredge. This could draw them into the suction field and increase the chance of entrainment.

7.6.1.3 Project Scheduling

With no information on local squid populations available, reasonable predictions of demographic effects are difficult to make. As with the other pelagic organisms, dredging is unlikely to significantly impact squid populations in the vicinity of the sand borrow sites. This precludes the need for an environmental window or specific project scheduling to protect squid resources.

7.6.2 Fishes

Potential impact producing factors from dredging operations in the sand borrow sites that may affect pelagic fishes offshore New Jersey and New York include physical injury, attraction, turbidity, and noise. These factors along with potential impacts are described in following subsections. Project scheduling considerations and essential fish habitat (EFH) also are discussed in separate subsections.

7.6.2.1 Physical Injury

Physical injury through entrainment of adult fishes by hydraulic dredging has been reported for several projects (Larson and Moehl, 1988; McGraw and Armstrong, 1988; Reine et al., 1998). The most comprehensive study of fish entrainment took place in Grays Harbor, Washington during a 10-year period when 27 fish taxa were entrained (McGraw and Armstrong, 1988). Most entrained fishes were demersal species such as flatfishes, sand lance, and sculpin; however, three pelagic species (anchovy, herring, and smelt) were recorded. Entrainment rates for the pelagic species were very low, ranging from 1 to 18 fishes/1,000 cy (McGraw and Armstrong, 1988). Comparisons between relative numbers of entrained fishes with numbers captured by trawling showed that some pelagic species were avoiding the dredge. Another entrainment study conducted near the mouth of the Columbia River, Washington reported 14 fish taxa entrained at an average rate of 0.008 to 0.341 fishes/cy (Larson and Moehl, 1988). Few of the pelagic fishes occurring offshore of New Jersey and New York should become entrained because the dredge's suction field exists near the bottom and many pelagic species have sufficient mobility to avoid the suction field.

7.6.2.2 Attraction

Even though dredges are temporary structures, they can still attract roving pelagic fishes. This attraction would be similar to an artificial reef effect, where both small and large coastal pelagic fishes become associated with fixed structures. This may temporarily disrupt migratory routes for some members of the stock, but it is unlikely that there would be an appreciable negative effect.

7.6.2.3 Turbidity

Turbidity can cause feeding impairment, avoidance and attraction movements, and physiological changes in adult pelagic fishes. As discussed for larval fishes, pelagic species are primarily visual feeders, and when turbidity reduces light penetration, the fishes reactive distance decreases (Vinyard and O' Brien, 1976). Light scattering caused by suspended sediment also can affect a visual predator's ability to perceive and capture prey (Benfield and

Minello, 1996). Some fishes have demonstrated the ability to capture prey at various turbidity levels, but the density of prey and light penetration are important factors (Grecay and Targett, 1996).

Some species will actively avoid or be attracted to turbid water. Experiments with pelagic kawakawa (*Euthynnus affinis*) and yellowfin tuna (*Thunnus albacares*) demonstrated that these species would actively avoid experimental turbidity clouds but also would swim directly through them during some trials (Barry, 1978). Turbidity plumes emanating from coastal rivers may retard or affect movements of some pelagic species.

Gill cavities can be abraded and clogged by suspended sediment, preventing normal respiration and mechanically affecting food gathering in planktivorous species (Bruton, 1985). High suspended sediment levels generated by storms have contributed to the death of nearshore and offshore fishes by clogging gill cavities and eroding gill lamellae (Robins, 1957). High concentrations of fine sediments can coat respiratory surfaces of the gills, preventing gas exchange (Wilber and Clarke, 2001).

Understanding and predicting effects of suspended sediments on fishes requires some information on the range and variation of turbidity levels found at a project site prior to dredging (Wilber and Clarke, 2001). The spatial and temporal extents of turbidity plumes from either cutterhead or hopper dredges are expected to be limited. Therefore, there should be negligible impact on adult pelagic fishes. However, removal of coarse sediment from borrow sites could promote chronic turbidity if finer underlying sedimentary layers are exposed and resuspended.

7.6.2.4 Noise

Noise associated with all aspects of the dredging process may affect organisms in several ways. Some reef fish larvae have been shown to respond to sound stimuli as a sensory cue to settlement sites (Stobutzki and Bellwood, 1998; Tolimieri et al., 2000). Alterations of background noise could impair the ability of newly settled fishes to locate preferred substrate. Changes in noise levels also may affect feeding or reproductive activities of reef fishes that depend on sound for these activities (Myrberg and Fuiman, 2002). Continental Shelf Associates, Inc. (2004) reviewed effects of noise on fishes. This report stated that all fish species investigated can hear, with varying degrees of sensitivity, within the frequency range of sound produced by cutterhead dredges, hopper dredges, and clamshell excavators. These sounds can mask the sounds normally used by fishes in their normal acoustic behaviors at levels as low as 60 to 80 dB (just above detection thresholds for many species). Levels as high as 160 dB may cause receiving fish to change their behaviors and movements that may temporarily affect the usual distribution of animals and commercial fishing. Continuous, long-term exposure to levels above 180 dB has been shown to cause damage to the hair cells of the ears of some fishes under some circumstances. These effects may not be permanent because damaged hair cells are repaired and/or regenerated in fishes. None of the dredge types proposed for this project produce continuous sounds above 120 dB (Richardson et al., 1995). Due to the short duration of most dredging projects, the effects of underwater noise on fish populations should be minimal.

7.6.2.5 Project Scheduling

When data are inadequate to accurately predict the magnitude of dredging effects, environmental windows have been required to provide a conservative approach and lessen potential effects on key species. However, LaSalle et al. (1991) and Reine et al. (1998) have stressed the need to base future environmental windows on sound evidence and have argued

against subjectively selected environmental windows. Environmental windows delay projects and greatly increase costs (Dickerson et al., 1998), and their use should not be driven by subjective or overly conservative approaches. There is not enough evidence from which to base an environmental window for the sand borrow sites. Excluding summer and fall months could be considered to avoid dredging when fish juveniles and larvae are most prevalent, but only if additional data become available to determine the extent of impacts and justify the restriction. These months may be more sensitive to disruption of benthic-pelagic coupling. Dredging-related turbidity could preclude phytoplankton production, thereby affecting organic input to the sediments. Additional information on the strength of benthic-pelagic coupling over the shelf would be needed to further evaluate these statements. Progress toward understanding the real need for environmental windows can only be achieved by reducing the degree of uncertainty surrounding impacts and the means to avoid them (Dickerson et al., 1998).

7.6.3 Marine Turtles

Major impact producing factors to marine turtles resulting from activities associated with the proposed action are entrainment by suction and/or the cutting action of the dredge head, modification of feeding habitat(s) within borrow sites, water column turbidity within the dredge plume, and noise produced by dredge vessels and dredge support vessels. Each impact producing factor and its effect on marine turtles within the study area is discussed below.

7.6.3.1 Physical Injury

The main potential effect of dredging on marine turtles is physical injury or death caused by the suction and/or cutting action of the dredge head and subsequent entrainment of turtles that may be resting on the bottom within the path of the dredge head or those venturing too close to the head during operation. Numerous marine turtle injuries and mortalities have been documented during dredging projects, particularly along Florida's east coast (Studt, 1987; Dickerson et al., 1992; Slay, 1995). Impacts typically have been minimized by some combination of project scheduling (see Section 7.6.3.5) and equipment selection, accompanied if necessary by turtle removal and/or monitoring. Several turtles have been taken during dredging operations in New Jersey and Delaware (NMFS, 1996). However, dredging has not been implicated as a major cause of death or injury to marine turtles in the region (NMFS, 1996).

Of the four turtle species that typically occur off New Jersey and New York, three (loggerhead, green, and Kemp's ridley) are considered to be at risk from dredging activities because of their benthic feeding habits (Dickerson et al., 1992). Loggerheads are the most abundant turtles in the study area and historically have been the species most frequently entrained during hopper dredging, possibly accounting for up to 86% of the total (Reine and Clarke, 1998). Green and Kemp's ridley turtles historically have accounted for much smaller portions of the total number of entrained turtles. Leatherbacks, which also occur in New Jersey and New York waters, are unlikely to be affected by dredging because they feed in the water column rather than on the bottom (NMFS, 1996).

Physical impact can occur when a turtle feeding or resting on the seafloor is contacted by the dredge head. Two types of dredges may be used on the proposed project. Cutterhead suction dredges are considered unlikely to kill or injure turtles, perhaps because the cutterhead encounters a smaller area of seafloor per unit time, allowing more opportunity for turtles to escape (Palermo, 1990). Hopper dredges are believed to pose the greatest risk to sea turtles (Dickerson, 1990; NMFS, 1997). There has been considerable research into designing modified

hopper dredges with turtle deflectors that reduce the likelihood of entraining sea turtles (Studd, 1987; Berry, 1990; Dickerson et al., 1992; Banks and Alexander, 1994; USACE, 1999). If a hopper dredge is used during the turtle season of June through November, the NMFS may require visual surveys for turtles or removal of turtles prior to dredge activities via trawling, and the use of a turtle-deflecting draghead (NMFS, 1996).

Previous bathymetric surveys indicate that water depths approximately range from 14 to 24 m in the sand borrow sites. Studies in New York waters have shown that chelonid sea turtles (i.e., those other than leatherbacks) feed primarily in depths of 15 m or less (NMFS, 1996). The risk of physical impacts to turtles would appear to be greatest in these shallow water depths. However, there also is risk in deeper water because when turtles feed there, they tend to stay on the bottom longer (NMFS, 1996).

7.6.3.2 Habitat Modification

Juvenile and subadult loggerhead, green, and Kemp's ridley turtles use northeastern U.S. coastal waters as developmental habit, foraging primarily on benthic invertebrates and plants (see Section 2.3.2.3). When borrow sites have significant concentrations of benthic resources, dredging can reduce food availability to these turtles by removing potential food items and altering the benthic habitats (NMFS, 1996). These effects would be temporary, as benthic populations would be expected to recover over a period of months to years, depending on the resource and the alteration of the habitats (see Section 7.5.3). In addition, borrow sites represent only a small portion of shallow benthic habitats available off northern New Jersey and southern New York. Trawl sampling in support of this document showed that potential turtle food items such as various benthic crustaceans, mollusks, and echinoderms were present in the borrow sites (see Section 6.3.5).

7.6.3.3 Turbidity

Marine turtles in and near the study area may encounter turbid water within the suspended sediment plume generated during dredging operations. This turbid water could temporarily interfere with feeding. However, due to the limited areal extent and transient occurrence of the dredge plume, turbidity is considered unlikely to significantly affect turtle behavior or survival.

7.6.3.4 Noise

Dredging is one of many human activities in the marine environment that produce underwater noise. Marine turtles seem to have limited hearing ability (Ridgway et al., 1969; Lenhardt, 1994; Bartol et al., 1999), and the role of hearing in their life cycle and behavior is poorly known. It is believed that marine turtles do not rely on sound to any significant degree for communication or food location, although it has been suggested that reception of low frequency sounds may be involved in natal beach homing behavior (Dodd, 1988). The latter would not be a consideration in this case because the study area is not near any significant nesting beach.

There are indications that underwater noise is unlikely to significantly affect turtles. First, studies in the Gulf of Mexico have shown some evidence for positive association of sea turtles with offshore oil and gas platforms (Rosman et al., 1987; Lohofener et al., 1990), despite the industrial noise associated with these structures. Second, experiments testing the use of seismic airguns to repel turtles from dredging activities have found that even loud noises cause turtle avoidance only at very close range (i.e., 100 m or less) (Zawila, 1994). Furthermore, turtles observed during these experiments became habituated to the airgun noise after repeated

exposure (Moein et al., 1994). Therefore, if noise does have any impact on turtles, it would most likely be positive by encouraging avoidance of the dredge head.

7.6.3.5 Project Scheduling

Project scheduling is one way to avoid or minimize impacts to turtles during dredging (Studt, 1987; Arnold, 1992). If a cutterhead suction dredge is used, seasonal or other restrictions are considered unnecessary because there is little likelihood of killing or injuring marine turtles. If a hopper dredge is used, then it would be best to avoid the June through November turtle season. However, the NMFS (1996) has recognized that the vagaries of winter weather off northern New Jersey and southern New York make it infeasible to prohibit dredging during these months. If use of a hopper dredge during this season cannot be avoided, then other mitigation and monitoring requirements are likely to be imposed, such as turtle monitoring and use of a turtle-deflecting draghead (NMFS, 1996).

7.6.4 Marine Mammals

Major impact producing factors to marine mammals resulting from activities associated with the proposed action are physical injury to endangered cetaceans resulting from collisions with dredge and dredge support vessels, water column turbidity within the dredge plume, and noise produced by dredge vessels. Each impact producing factor and how it may affect marine mammals within the study area is discussed below.

7.6.4.1 Physical Injury

Unlike marine turtles, most marine mammals are unlikely to be physically injured by dredging *per se* because they generally do not rest on the bottom and they can easily avoid contact with dredging vessels and equipment. Odontocete (toothed) marine mammals most likely to be found on the continental shelf off northern New Jersey and New York, such as bottlenose dolphin and common dolphin, are agile swimmers that are presumed capable of avoiding physical injury during dredging operations.

However, physical injury from vessel strikes is a serious concern for three endangered species of mysticetes (baleen whales): North Atlantic right whale, fin whale, and humpback whale. Recovery plans for these three species identify vessel strikes as a contributing factor impeding their recovery (NMFS, 1991a,b; Reeves et al., 1998). Vessel strikes are an especially serious concern for right whales. NMFS published regulations in February 1997 restricting vessel approaches of right whales. These regulations prohibit all approaches within 460 m of any right whale, whether by vessel, aircraft, or other means (NMFS, 1998). It is likely that measures to minimize the potential for vessel strikes of endangered whales would be part of any Biological Opinion issued by the NMFS for dredging off New Jersey and New York (e.g., NMFS, 1996).

The harbor porpoise, an odontocete marine mammal that has been proposed for listing as a threatened species, is, as a result of its agility, unlikely to be injured by dredging vessels or equipment. The major threat to the recovery of this species is gillnetting (NMFS, 1998). The NMFS has indicated that interactions of this species with dredging are unlikely (U.S. Environmental Protection Agency, 1997).

7.6.4.2 Turbidity

Marine mammals in and near the study area may encounter turbid water within the suspended sediment plume generated during dredging operations. This turbidity could

temporarily interfere with feeding or other activities; however, these animals could easily swim out of the turbid sediment plume area. Due to the limited extent and transient occurrence of the sediment plume, turbidity is considered unlikely to significantly affect marine mammal behavior or survival.

7.6.4.3 Noise

Dredging can be a significant source of continuous underwater noise in nearshore areas, particularly in low frequencies (<1,000 Hz) (Richardson et al., 1995). This noise typically diminishes to background levels within about 20 to 25 km of the source (Richardson et al., 1995). Noise levels are not sufficient to cause hearing loss or other auditory damage to marine mammals (Richardson et al., 1995). However, some observations of marine mammals in the vicinity of dredging operations and other industrial activities have documented avoidance behavior, while in other cases, animals seem to develop a tolerance for the industrial noise (Malme et al., 1983; Richardson et al., 1995). Due to the frequency range of their hearing, mysticetes (baleen whales) are more likely to be affected by low frequency noise associated with dredging operations than are odontocetes (toothed whales and dolphins). Consequently, it is possible that dredging noise could cause avoidance by humpback whales and North Atlantic right whales during their seasonal migrations.

7.6.4.4 Project Scheduling

Common marine mammal species of the continental shelf, such as bottlenose dolphin, may be present year-round and, as noted above, are unlikely to be adversely affected by dredging. Harbor porpoise occurrence is more seasonal, but the likelihood of impact is so low that it does not warrant seasonal restrictions on dredging.

Fin and humpback whales would be most likely to occur during winter or spring, and right whales as transients during spring and fall. There is no "resident" population of endangered whales in the study area; rather, they would be temporary inhabitants, or would be transiting the area during seasonal migrations. Generally, the probability of encountering these species in the project area would be lowest during summer. However, due to the low likelihood of impact, seasonal restrictions on dredging probably are not warranted. Instead, measures to minimize possible vessel interactions with these endangered species during dredging operations are likely to be required by the NMFS.

7.7 ESSENTIAL FISH HABITAT

The Magnuson-Stevens Fishery Conservation and Management Act (16 United States Code [U.S.C.] §1801-1882) established regional Fishery Management Councils and mandated that Fishery Management Plans (FMPs) be developed to responsibly manage exploited fish and invertebrate species in U.S. Federal waters. When Congress reauthorized this act in 1996 as the Sustainable Fisheries Act, several reforms were made. One change was to charge the NMFS with designating and conserving EFH for species managed under existing FMPs. This is intended to minimize, to the extent practicable, any adverse effects on habitat caused by fishing or non-fishing activities and to identify other actions to encourage the conservation and enhancement of such habitat.

EFH is defined as "those waters and substrate necessary to fish for spawning, breeding, feeding or growth to maturity" (16 U.S.C. §1801[10]). The EFH interim final rule summarizing EFH regulations (62 FR 66531-66559) outlines additional interpretation of the EFH definition. Waters, as defined previously, include "aquatic areas and their associated physical, chemical,

and biological properties that are used by fish, and may include aquatic areas historically used by fish where appropriate." Substrate includes "sediment, hard bottom, structures underlying the waters, and associated biological communities." Necessary is defined as "the habitat required to support a sustainable fishery and the managed species' contribution to a healthy ecosystem." "Fish" includes "finfish, mollusks, crustaceans, and all other forms of marine animal and plant life other than marine mammals and birds," whereas "spawning, breeding, feeding or growth to maturity" cover the complete life cycle of those species of interest.

The Mid-Atlantic Fishery Management Council (MAFMC) has produced several FMPs for single and mixed groups of species including those for Atlantic surfclam and ocean quahog; Atlantic mackerel, squid, and butterfish; summer flounder, scup, and black seabass; bluefish; and spiny dogfish. Each of these FMPs was amended to include EFH designations (MAFMC, 1998a, b, c, d, 1999). Because of the transitory nature of the fish fauna of the region, some migratory species managed by other entities were included in the table. Other management entities include the Atlantic States Marine Fisheries Commission and New England Fisheries Management Council.

Broadly defined EFH for managed species (including specific life stages) of the area encompassed by the sand borrow sites are given in Tables 7-1 to 7-5. These tables cover invertebrates, sharks, coastal pelagic fishes, and highly migratory fishes. The species include fishes and invertebrates managed by various regional councils and highly migratory species (sharks, tunas, and swordfish) managed by the NMFS. Table 7-6 presents a summary matrix of EFH species groups by impact producing factors. The nature of effects on EFH for these species would be similar to those discussed generally for squids (Section 7.6.1) and fishes (Section 7.6.2). In addition, impacts to infaunal assemblages during dredging projects would certainly affect the prey base for benthic foraging fishes. Projected recolonization and recovery of infauna impacted by dredging in the sand borrow sites was discussed above in Section 7.5.2.4. Although many aspects of offshore marine mining in the sand borrow sites can impact EFH, the limited spatial and temporal extent of these dredging activities suggests that impacts will not adversely affect EFH on a broad scale.

Table 7-1. Invertebrate species and life stages with Essential Fish Habitat identified in the project area (source Mid-Atlantic Fishery Management Council, 1998a ¹ , b ²).				
Species	Eggs	Larvae	Juveniles	Adults
Ocean quahog <i>Arctica islandica</i> ¹	Insufficient information	Insufficient information	Throughout the sedimentary substrate to a depth of 1 m in Federal waters from the eastern edge of Georges Bank and the Gulf of Maine throughout the Atlantic Exclusive Economic Zone (EEZ) to Cape Hatteras, NC. Water depths from 8 to 244 m.	Throughout the sedimentary substrate to a depth of 1 m in Federal waters from the eastern edge of Georges Bank and the Gulf of Maine throughout the Atlantic EEZ to Cape Hatteras, NC. Water depths from 8 to 244 m.
Surfclam <i>Spisula solidissima</i> ¹	Insufficient information	Pelagic shelf waters from the Gulf of Maine to Cape Hatteras, NC. Water temperatures from 14 to 30°C.	Throughout the sedimentary substrate to a depth of 1 m in Federal waters from the eastern edge of Georges Bank and the Gulf of Maine throughout the Atlantic EEZ. From the beach zone out to about 65 m water depths.	Throughout the sedimentary substrate to a depth of 1 m in Federal waters from the eastern edge of Georges Bank and the Gulf of Maine throughout the Atlantic EEZ. From the beach zone out to about 65 m water depths.
Longfin squid <i>Loligo pealei</i> ²	Attached to rocks, boulders, or submerged vegetation in continental shelf waters less than 50 m deep.	Pelagic waters of the continental shelf from the Gulf of Maine through Cape Hatteras, NC from shore to 213 m water depths. Water temperatures between 3.8 to 27°C.	Pelagic waters of the continental shelf from the Gulf of Maine through Cape Hatteras, NC from shore to 305 m water depths in temperatures ranging between 3.8 to 27°C.	Pelagic waters of the continental shelf from the Gulf of Maine through Cape Hatteras, NC from shore to 305 m water depths in temperatures ranging between 3.8 to 27°C.
Shortfin squid <i>Illex illecebrosus</i> ²	Insufficient information	Insufficient information	Pelagic waters of the continental shelf from the Gulf of Maine through Cape Hatteras, NC from shore to 183 m water depths. Water in temperatures between 2.2 to 22.8°C.	Pelagic waters of the continental shelf from the Gulf of Maine through Cape Hatteras, NC from shore to 183 m water depths in temperatures between 3.8 to 19°C.

Species	Neonate/Early Juveniles	Late juveniles/subadults	Adults
Spiny dogfish <i>Squalus acanthias</i> ¹	Continental shelf waters from the Gulf of Maine to Cape Hatteras, NC. Generally in water depths from 10 to 390 m and temperatures from 2.8 to 27.8°C.	Continental shelf waters from the Gulf of Maine to Cape Hatteras, NC. Generally in water depths from 10 to 390 m and temperatures from 2.8 to 27.8°C.	Continental shelf waters from the Gulf of Maine to Cape Hatteras, NC. Generally in water depths from 10 to 450 m and temperatures from 2.8 to 27.8°C.
Sand tiger shark <i>Carcharias taurus</i> ²	Shallow coastal waters less than 25 m deep from Barnegat Inlet, NJ to Cape Canaveral, FL (27.5°N).	Insufficient information.	Shallow coastal waters less than 25 m from Barnegat Inlet, NJ to Cape Canaveral, FL (27.5°N).
Thresher shark <i>Alopias vulpinus</i> ²	Offshore Long Island, NY and southern New England in the northeastern United States, in pelagic waters deeper than 50 m, between 70°W and 73.5°W, south to 40°N.	Offshore Long Island, NY and southern New England in the northeastern United States, in pelagic waters deeper than 50 m, between 70°W and 73.5°W, south to 40°N.	Offshore Long Island, NY and southern New England in the northeastern United States, in pelagic waters deeper than 50 m, between 70°W and 73.5°W, south to 40°N.
Basking shark <i>Cetorhinus maximus</i> ²	Insufficient information.	Offshore the Mid-Atlantic United States south of Nantucket Shoals at 70°W to the northern edge of Cape Hatteras, NC at 35.5°N in waters from 50 to 200 m deep.	Offshore southern New England, west of Nantucket Shoals at 70°W to Montauk, Long Island, NY (72°W) in waters from 50 to 200 deep.
White shark <i>Carcharodon carcharias</i> ²	Insufficient information.	Offshore southern New Jersey and Long Island, NY in pelagic waters from the 25 to the 100 m isobaths in the New York Bight Area, bounded to the east at 71.5°W and to the south at 39.5°N.	Insufficient information.
Shortfin mako <i>Isurus oxyrinchus</i> ²	Between the 50 and 2,000 m isobaths from Cape Lookout, NC (35°N) north to just east of Georges Bank (42°N and 66°W) to the Exclusive Economic Zone (EEZ) boundary, and between the 25 and 50 m isobaths from the V/NC border to southwest of Georges Bank.	Between the 25 and 2,000 m isobaths from offshore Onslow Bay, NC north to Cape Cod, MA and extending west between 38°N and 41.5°N to the EEZ boundary.	Between the 25 and 2,000 m isobaths from offshore Cape Lookout, NC north to Long Island, NY, and extending west between 38.5°N and 41.5°N to the EEZ boundary.
Dusky shark <i>Carcharhinus obscurus</i> ²	Shallow coastal waters, inlets, and estuaries in waters less than 25 m deep.	Shallow coastal waters, inlets, and estuaries in waters less than 25 m deep.	Not in project area.
Sandbar shark <i>Carcharhinus plumbeus</i> ²	Shallow coastal waters, inlets, and estuaries in waters less than 25 m deep from Montauk, NY to Cape Canaveral, FL (27.5°N).	Shallow coastal waters, inlets, and estuaries in waters less than 25 m deep from Montauk, NY to Cape Canaveral, FL (27.5°N).	Shallow coastal areas from the shore to the 50 m isobath from Nantucket, MA south to Miami, FL.
Tiger shark <i>Gaelocerdo cuvier</i> ²	Shallow coastal waters to the 200 m isobath from Cape Canaveral, FL (27.5°N) to Montauk, NY.	North of the mouth of Chesapeake Bay to offshore Montauk, NY between the 25 and 100 m isobaths.	Not in project area.

Table 7-3. Coastal pelagic fish species and life stages with Essential Fish Habitat identified in the project area (source Reid et al., 1999 ¹ ; Fahay et al., 1999 ² ; Mid-Atlantic Fishery Management Council, 1999 ³).			
Species	Eggs and Larvae	Juveniles	Adults
Atlantic herring <i>Clupea harengus</i> ¹	Not in project area.	Pelagic continental shelf waters from the Gulf of Maine through the Mid-Atlantic Bight (Cape Hatteras, NC).	Pelagic continental shelf waters from the Gulf of Maine through the Mid-Atlantic Bight (Cape Hatteras, NC).
Bluefish <i>Pomatomus saltatrix</i> ²	Pelagic waters of the continental shelf from southern New England to Cape Hatteras in water temperatures 18 to 24°C.	Estuaries, bays, and coastal ocean from Long Island Sound to south of North Carolina.	Open ocean, large embayments, and estuaries throughout their range in water temperatures exceeding 14°C.
Atlantic mackerel <i>Scomber scomber</i> ³	Pelagic continental shelf waters from the Gulf of Maine through Cape Hatteras, NC. Inshore areas include high salinity portions of estuaries on the Atlantic Coast from Passamoquaddy Bay, ME to James River, VA. Water depths from shore to 1,828 m.	Pelagic continental shelf waters from the Gulf of Maine through Cape Hatteras, NC. Inshore areas include high salinity portions of estuaries on the Atlantic Coast from Passamoquaddy Bay, ME to James River, VA. Water depths from shore to 1,828 m.	Pelagic continental shelf waters from the Gulf of Maine through Cape Hatteras, NC. Inshore areas include high salinity portions of estuaries on the Atlantic Coast from Passamoquaddy Bay, ME to James River, VA. Water depths from shore to 1,828 m.
Butterfish <i>Peprilus triacanthus</i> ³	Pelagic continental shelf waters from the Gulf of Maine through Cape Hatteras, NC. Inshore areas include high salinity portions of estuaries on the Atlantic Coast from Passamoquaddy Bay, ME to James River, VA. Water depths from shore to 1,828 m.	Pelagic continental shelf waters from the Gulf of Maine through Cape Hatteras, NC. Inshore areas include high salinity portions of estuaries on the Atlantic Coast from Passamoquaddy Bay, ME to James River, VA. Water depths from 10 to 366 m.	Pelagic continental shelf waters from the Gulf of Maine through Cape Hatteras, NC. Inshore areas include high salinity portions of estuaries on the Atlantic Coast from Passamoquaddy Bay, ME to James River, VA. Water depths from 10 to 366 m.

Table 7-4. Demersal fish species and life stages with Essential Fish Habitat identified in the project area (source Steimle et al., 1999 ¹ ; New England Fishery Management Council, 2004 ² ; Mid-Atlantic Fishery Management Council, 1998c ³ ; Chang et al., 1999 ⁴).			
Species	Eggs and Larvae	Juveniles	Adults
Red hake <i>Urophycis chuss</i> ¹	Pelagic continental shelf waters from the Gulf of Maine through the Mid-Atlantic Bight (to Cape Hatteras, NC) in temperatures from 8 to 23°C and water depths of 10 to 200 m.	Demersal continental shelf waters from the Gulf of Maine through the Mid-Atlantic Bight in water temperatures from 2 to 20°C and depths of 5 to 200 m.	Demersal continental shelf waters from the Gulf of Maine through the Mid-Atlantic Bight in water temperatures from 2 to 22°C and depths of 5 to 300 m.
Monkfish <i>Lophius americanus</i> ²	Pelagic continental shelf waters from the Gulf of Maine through the Mid-Atlantic Bight in temperatures below 15°C and water depths of 15 to 1,000 m.	Demersal continental shelf waters from Gulf of Maine through the Mid-Atlantic Bight in water temperatures below 13°C and depths of 25 to 200 m.	Demersal continental shelf waters from Gulf of Maine through the Mid-Atlantic Bight in water temperatures below 13°C and depths of 25 to 200 m.
Black seabass <i>Centropristis striata</i> ³	Pelagic waters over continental shelf from Cape Hatteras, NC to the Gulf of Maine. High salinity segments of regional estuaries from Virginia to New York.	Demersal waters over the continental shelf from Cape Hatteras, NC to the Gulf of Maine. Estuaries from Virginia to Massachusetts where salinity exceeds 18 ppt and temperature exceeds 6.0°C. Structured habitat (artificial or natural) preferred.	Demersal waters over the continental shelf from Cape Hatteras, NC to the Gulf of Maine. Structured habitat (artificial or natural) preferred.
Scup <i>Stenotomus chrysops</i> ³	Estuaries of the region where salinity exceeds 15 ppt and water temperature ranges from 13 to 23°C.	Demersal waters over the continental shelf from Cape Hatteras, NC to the Gulf of Maine. Estuaries from Virginia to Massachusetts where salinity exceeds 15 ppt and temperature exceeds 7.2°C.	Demersal waters over the continental shelf from Cape Hatteras, NC to the Gulf of Maine. Estuaries from Virginia to Massachusetts where salinity exceeds 15 ppt and temperature exceeds 7.2°C.
Summer flounder <i>Paralichthys dentatus</i> ³	Pelagic waters over the continental shelf from Cape Hatteras, NC to the Gulf of Maine. Eggs in water depths of 10 to 120 m; larvae in 10 to 80 m.	Demersal waters over the continental shelf from Cape Hatteras, NC to the Gulf of Maine. Estuaries where salinity ranges from 10 to 30 ppt.	Demersal waters over the continental shelf from Cape Hatteras, NC to the Gulf of Maine to water depths of 152 m. Estuaries where salinity ranges from 10 to 30 ppt.
Windowpane <i>Scophthalmus aquosus</i> ⁴	Pelagic waters over the continental shelf from Cape Hatteras, NC to the Gulf of Maine in water depths less than 70 m.	Demersal waters over the continental shelf from Cape Hatteras, NC to the Gulf of Maine. Estuaries where salinity ranges from 15 to 33 ppt.	Demersal waters over the continental shelf from Cape Hatteras, NC to the Gulf of Maine.

Table 7-5. Highly migratory fish species and life stages with Essential Fish Habitat identified in the project area (source National Marine Fisheries Service, 1999).			
Species	Spawning, Eggs, and Larvae	Juveniles/Subadults	Adults
Yellowfin tuna <i>Thunnus albacares</i>	Not in project area.	Pelagic waters from the surface to 100 m deep between 18 and 31°C from offshore Cape Cod, MA (70°W) southward to Jekyll Island, GA (31°N) between 200 and 2,000 m.	Pelagic waters from the surface to 100 m deep between 18 and 31°C from offshore Cape Cod, MA (70°W) southward to Jekyll Island, GA (31°N) between 200 and 2,000 m.
Albacore <i>Thunnus alalunga</i>	Not in project area.	In offshore surface waters with temperatures between 15.6 and 19.4°C in the Mid-Atlantic Bight from the 50 to 2,000 m isobaths with 71°W as the northeast boundary and 38°N as the southwest boundary.	Not in project area.
Bluefin tuna <i>Thunnus thynnus</i>	Not in project area.	All inshore and surface waters warmer than 12°C from Cape Ann, MA (42.75°N) east to 69.75°W, continuing south to and including Nantucket Shoals at 70.5°W to off Cape Hatteras, NC (35.5°N).	All inshore and surface waters warmer than 12°C from Cape Ann, MA (42.75°N) east to 69.75°W, continuing south to and including Nantucket Shoals at 70.5°W to off Cape Hatteras, NC (35.5°N).
Skipjack tuna <i>Katsowonus pelamis</i>	Not in project area.	Not in project area.	Pelagic surface waters from 20 to 31°C in the Mid-Atlantic Bight from the 25 to 200 m isobaths.
Swordfish <i>Xiphias gladius</i>	Not in project area.	Pelagic waters warmer than 18°C from the surface to a depth of 500 m, from Manasquan Inlet, NJ at 40°N, east to 73°W, south to Georgia at 31.5°N.	Not in project area.

Table 7-6. Summary matrix of impact producing factors and potential effects on members of managed species groups and their Essential Fish Habitat expected from dredging the sand borrow sites offshore of northern New Jersey and southern New York.				
Species Group	Seafloor Disturbance	Entrainment	Turbidity	Noise
Invertebrates (Atlantic surf clam and Quahog)	Direct habitat loss; burial or direct damage to organisms.	All stages.	Mortality/feeding impairment of early life stages.	None expected.
Invertebrates (Squid)	Removal and burial of demersal eggs.	All stages.	Mortality/feeding impairment of all life stages.	None expected.
Sharks	Loss of feeding areas for benthic feeding life stages.	Entrainment of neonate/early juveniles.	None expected.	Temporary alteration of acoustic environment.
Coastal pelagic fishes	None expected.	None expected.	Mortality/feeding impairment of early life stages.	Temporary alteration of acoustic environment.
Demersal fishes	Adult and juvenile habitat loss. Displacement of feeding areas.	Entrainment of adults and juveniles.	Mortality/feeding impairment of early life stages.	Temporary alteration of acoustic environment.
Highly migratory fishes	None expected.	None expected.	Mortality/feeding impairment of juveniles and adults.	Temporary alteration of acoustic environment.

7.8 POTENTIAL CUMULATIVE EFFECTS

Cumulative physical environmental impacts from multiple sand extraction scenarios at one or all sand borrow sites within the study area were evaluated to assess long-term effects at potential borrow sites and along the coastline. Results presented above for wave and sediment transport processes reflect the impact of large extraction scenarios from one or multiple offshore sites that are expected to be within the cumulative sand resource needs for the next 10 years. It was determined that no significant changes to longshore sediment transport will result from the modeled borrow site configurations offshore northeastern New Jersey (H1 and H2) and southwestern Long Island (3, 4W, and 4E).

Given that the expected beach replenishment interval is on the order of 5 to 10 years, and that the expected recovery time of the affected benthic community after sand removal is anticipated to be much less than that (within 2 years), the potential for significant cumulative benthic impacts is remote. No cumulative impacts to the pelagic environment, including squids, fishes, sea turtles, and marine mammals, are expected from multiple sand mining operations within a sand borrow site.

8.0 CONCLUSIONS

The primary purpose of this study was to address environmental concerns raised by the potential for dredging sand from the OCS offshore northeastern New Jersey and southwestern Long Island for beach replenishment. Primary concerns focused on physical and biological components of the environment at five proposed sand resource areas. Physical processes and biological characterization data were analyzed to assess the potential impacts of offshore dredging activities within the study area to minimize or preclude long-term adverse environmental impacts at potential borrow sites and along the coastline landward of resource sites. The following summary documents conclusions regarding the potential environmental effects of sand mining on the OCS for replenishing sand to eroding beaches. Because benthic and pelagic biological characteristics are in part determined by spatially varying physical processes throughout the study area, physical processes analyses are summarized first.

8.1 WAVE TRANSFORMATION MODELING

Excavation of an offshore borrow site can alter incoming wave heights and the direction of wave propagation. Offshore topographic relief causes waves to refract toward the shallow edges of borrow sites. Changes in the wave field caused by borrow site geometry may change local sediment transport rates, where some areas may experience a reduction in longshore transport and other areas may show an increase. The most effective means of quantifying physical environmental effects of sand dredging from shoals on the continental shelf is by applying wave transformation numerical modeling tools that recognize the random nature of incident waves as they propagate onshore. To determine the potential physical impacts associated with dredging at borrow sites offshore northeastern New Jersey and southwestern Long Island, spectral wave transformation modeling (STWAVE) was performed for existing and post-dredging bathymetric conditions. Comparison of computations for existing and post-dredging conditions illustrated the relative impact of borrow site excavation on wave-induced coastal processes.

As part of any offshore sand mining effort, the MMS requires an evaluation of potential environmental impacts associated with alterations to nearshore wave patterns. To determine potential physical impacts associated with borrow site excavation, the influence of borrow site geometry on local wave refraction patterns was evaluated. Because large natural spatial and temporal variability exists within the wave climate at a particular site, determination of physical impacts associated with sand mining must consider the influence of process variability. A method based on historical wave climate variability, as well as local wave climate changes directly attributable to borrow site excavation, has been applied to determine appropriate criteria for assessing impact significance.

To directly assess impacts to coastal processes associated with sand mining, an approach was utilized that considers spatial (longshore) and temporal aspects of the local wave climate, as described by Kelley et al. (2004). This method was applied by performing wave model runs using mean conditions developed from the entire 20-year WIS record, and then

20 year-long blocks of the WIS record to determine annual variability of the wave climate along this shoreline. In this manner, temporal variations in wave climate are considered relative to average annual conditions. From these wave model runs, sediment transport potential curves are derived for average annual conditions (based on the full 20-year WIS record) and each 1-year period (based on the 20 1-year wave records parsed from the full record). Applying this information, the average and standard deviation in calculated longshore sediment transport potential are determined every 200 m along the shoreline.

Linear offshore sand ridges, oriented obliquely to the shoreline in a northwest-southeast direction, are the primary geomorphic features influencing wave propagation offshore southwestern Long Island beaches. For 1.3 m, 9.1 sec waves propagating from the east-southeast, shoals encompassed by Borrow Sites 3, 4W, and 4E had the greatest influence on waves in the modeled area; however, effects to waves were relatively small because these shoals are located in approximately 17 to 20 m water depth. Post-dredging wave height changes at the borrow sites illustrated the impact of sand extraction at borrow sites, where seafloor topography within each site was lowered to a level not exceeding water depths at the base of the shoals (approximately -20 m). For the 1.3 m, 9.1 sec wave condition, borrow site dredging had no measurable influence on waves over a long section of coastline (>44 km), but changes on the order of 0.01 m did occur along 20 km of coast in the combined shadow of the three borrow sites. At Site 4E, maximum wave height decrease was approximately 0.05 m, and the maximum increase was 0.10 m at the landward boundary of the site. At Site 4W, maximum wave height increase was 0.10 m, and maximum wave height decrease was 0.09 m. Seafloor excavation at Site 3 produced smallest wave height changes for borrow sites offshore southwestern Long Island, with a maximum decrease of 0.06 m and a maximum increase of 0.04 m. Minimal computed changes at Site 3 may be due to the relatively small volume of sand excavated from this site, and because changes in seafloor elevation for post-dredging conditions were less (approximately 2 m change for Site 3, versus 4 m for Sites 4W and 4E).

For a 1.6 m, 9.1 sec wave from the southeast, changes in wave field propagation resulting from dredging at the three offshore borrow sites were smaller than those computed for the wave condition above, even though the wave height for this case is larger. This effect may be due to a combination of incident wave angle and directional orientation of shoals upon which borrow sites are located. The wave shadow zone from these three sites affected approximately 45 km of shoreline, but greatest changes were on the order of 0.01 m and occurred within a 4 km stretch of shoreline at the western end of Jones Beach.

Potential sand borrow sites offshore northeastern New Jersey are oriented obliquely to the shoreline in a northeast-southwest direction and have minimal influence on wave propagation to the shoreline. For 1.3 m, 9.1 sec waves propagating from the east, shoals encompassed by Borrow Sites H1 and H2 exhibited minimal wave focusing. The approximate minimum water depths at Sites H1 and H2 are 16 and 17 m, respectively. For the shoal at Site H1, maximum wave height increase was 0.13 m due to the focusing effect of the sand ridge. Post-dredging wave height changes at Sites H1 and H2 simulated the impact of sand extraction at borrow sites, where seafloor topography within each site was lowered to a level not exceeding water depths at the base of the shoals (approximately -20 m). Wave height differences resulting from numerically excavating Sites H1 and H2 are relatively small and diffuse, and wave height changes at the modeled shoreline are less than 0.01 m. At Site H1, maximum changes in wave height ranged from -0.06 to +0.04 m. At Site H2, maximum wave height changes decreased by 0.05 m and increased by 0.03 m.

For 1.3 m, 7.7 sec waves propagating from the south-southeast, wave height changes were not as pronounced as those for the previous wave case. The primary reason for this difference is that offshore bathymetry has less effect on wave focusing for shorter peak period incident waves. Wave height changes indicated that borrow sites had an overlapping influence at the shoreline for waves propagating from the SSE. Similar to the previous wave case, wave height changes at the shoreline relative to potential offshore sand dredging were never greater than 0.01 m. Site H1 exists within the wave shadow zone for Site H2, but wave height changes remain relatively small. At Site H1, maximum wave height changes ranged from +0.04 to -0.04 m; at Site H2, maximum changes were half this magnitude (+0.02 to -0.02 m). Overall, wave height differences between existing and post-dredging conditions were quite small relative to natural wave height variability.

8.2 CIRCULATION AND SEDIMENT TRANSPORT DYNAMICS

Circulation patterns on either side of the Hudson Shelf Valley near potential offshore sand borrow sites documented speed and direction related to current and wind patterns recorded between December 4, 1999 and April 15, 2000. Overall, the predominant direction of surface flow within the study area varied from southeast (west of Hudson Shelf Valley) to south-southeast (east of the Hudson Shelf Valley). Surface current magnitudes also were consistent, showing similar maximums, means, and standard deviations. Bottom current measurements illustrated greater variability in direction and magnitude. Offshore northeastern New Jersey predominant bottom current flow varied from east-southeast to west, while the predominant bottom current flow east of the Hudson Shelf Valley varied from north to south-southeast. Differences in bottom flow may be explained by the presence of the Hudson Shelf Valley, which bisects the continental shelf in this region causing currents to veer to the north as they flow cross contour into the bathymetric low from northeast to southwest. Strong northerly flow within the valley prevents currents south and west of this area from flowing to the east-northeast.

The controlling factor for bottom current velocities in the vicinity of proposed sand borrow sites was wind direction and intensity, and local bathymetric features controlled current direction. Bottom currents tended to flow parallel to contours causing currents to diverge around localized bathymetric highs and converge near bathymetric lows. In general, bottom flows at the borrow sites offshore southwestern Long Island flowed east-southeast or east and west with deviations caused by wind direction. Maximum bottom current speed was about 35 cm/s flowing east, with a mean speed of 8 cm/s (± 5 cm/s) flowing southeast. Offshore northeastern New Jersey, bottom currents generally flow north and south along bathymetric contours. Maximum bottom current speed for this area was about 26 cm/s flowing north, with a mean velocity of 6 cm/sec (± 4 cm/s) flowing north. Bottom current speeds at both sites primarily were controlled by wind speeds, and the direction of flow was controlled by local bathymetry.

Three independent sediment transport analyses were completed to evaluate physical environmental impacts due to sand mining. First, historical sediment transport trends were quantified to document regional, long-term sediment movement throughout the study area using historical bathymetric data sets. Erosion and accretion patterns were documented, and sediment transport rates in the littoral zone and at offshore borrow sites were evaluated to assess potential changes due to offshore sand dredging activities. Second, sediment transport patterns at proposed offshore borrow sites were evaluated using wave modeling results and current measurements. Post-dredging wave model results were integrated with regional current measurements to estimate sediment transport trends for predicting borrow site infilling rates. Third, potential longshore sediment transport was computed using wave modeling output to estimate potential impacts along the coast (beach erosion and accretion). All three methods

were compared for documenting consistency of measurements relative to predictions, and potential physical environmental impacts were identified.

8.2.1 Historical Sediment Transport Patterns

Regional geomorphic changes between 1873/88 and 1991/97 (southwestern Long Island) and 1836/39 and 1977 (northeastern New Jersey) were analyzed for assessing long-term, net coastal sediment transport dynamics. Although these data did not provide information on potential impacts of sand dredging from proposed borrow sites, they did provide a means of verifying predictive sediment transport models relative to infilling rates at borrow sites and longshore sand transport.

Shoreline position and nearshore bathymetry change documented four important trends relative to study objectives. First, there were three dominant directions of longshore sand transport within the study area. Between Rockaway Point and Moriches Inlet, the dominant direction of transport was east to west. In northern New Jersey, between Sandy Hook and Manasquan, longshore transport from south to north dominated, while south of Manasquan Inlet, the dominant direction was to the south. Along both coasts, the dominant direction of transport was illustrated by barrier island migration and shoreline advance adjacent to inlet jetties. Barrier islands along the south coast of Long Island have historically migrated from east to west, and seaward shoreline advance subsequent to jetty construction has occurred along the east sides of entrances. In northern New Jersey, Sandy Hook spit historically has migrated rapidly to the north, and prior to structural development at Barnegat Inlet, the spit north of the entrance was rapidly migrating to the south. The greatest amount of shoreline change observed for this study was associated with beaches adjacent to entrances, most notably along the leading edge of prograding barrier spits.

Second, the most dynamic features within the study area, in terms of nearshore sediment transport, are migrating barrier island/spit complexes along the northeastern New Jersey and southwestern Long Island coasts, in addition to natural and anthropogenic change along the Hudson River Channel. Areas of significant erosion and accretion are documented between 1927/37 and 1927/97 at Sandy Hook spit, reflecting wave and current dynamics that carry sediment northward and deposit it along the terminal edge of the spit. High rates of deposition also were prominent at entrances south of Sandy Hook and along the southwestern coast of Long Island. Shoreline and bathymetric changes associated with these features reflect morphologic response to wave and current dynamics and shoreline adjustment to placement of engineering structures. Pronounced bathymetric change observed along the head and sides of the Hudson River Channel reflects natural and anthropogenic processes. Large areas showing significant deposition at the head of the Hudson River Channel reflect high levels of offshore disposal activity, and patches of erosion and accretion paralleling each other along the length of the channel reflect natural bathymetric changes.

Third, alternating bands of erosion and accretion paralleling ridge features illustrated the steady reworking of the shelf surface as sand ridges migrated in the direction of net sediment transport. The process by which this was occurring was relatively consistent across the shelf. At Borrow Site H1, bathymetric comparisons suggested that the borrow site in this region would fill with sand transported from the adjacent seafloor at rates of about 98,000 m³/yr. Areas of erosion and accretion documented between 1927/37 and 1927/97 at Borrow Site 4E illustrated the amount of sediment available for infilling at sites south of Long Island was also about 98,000 m³/yr. Calculations for these two borrow sites were used as indicators of potential infilling rates for all borrow sites within the study area.

Finally, net longshore transport rates determined from seafloor changes in the littoral zone along Sandy Hook spit indicated maximum transport rates near the distal end of the spit, with lower rates to the south. These calculations, along with data published by Caldwell (1966) indicate a range in net longshore transport along Sandy Hook from about 223,000 m³/yr to 382,000 m³/yr. According to Taney (1961), the direction of net littoral drift along southwestern Long Island beaches is east to west, ranging from 122,000 to 344,000 m³/yr.

8.2.2 Sediment Transport Modeling at Potential Borrow Sites

In addition to predicted modifications to the wave field, potential sand mining at offshore borrow sites resulted in minor changes in sediment transport pathways in and around potential dredging sites. For water depths at the proposed borrow sites, minimal impacts to waves, currents, and regional sediment transport are expected during infilling. Infilling rates computed for each of the five borrow sites offshore northeastern New Jersey and southwestern Long Island represented the total potential sediment transport at each of the sites from the combined influence of wave-induced and ambient bottom currents. These results likely represent average, non-storm conditions for sediment transport at each site. For the five modeled borrow sites, computed transport rates were extremely low, with potential transport rates ranging from 0.13 m³/yr to approximately 580 m³/yr. A number of factors contributed to the low transport rates, including water depth (typically 20 m, which reduced the impact of wave-induced currents), relatively short period waves dominating the regional wave climate, absence of significant storm events in the wave and current data sets that drive sediment transport in this area, coarse grain size of *in situ* materials, and relatively weak ambient shelf currents. Furthermore, potential borrow site excavations consisted of dredging an existing shoal to the same elevation as the surrounding seafloor. Therefore, potential borrow site excavation would primarily flatten the shoal and not create a seafloor depression. Based on extremely low potential transport rates of *in situ* sediment and the geomorphic character of dredged deposits, it is unlikely that any of these borrow sites will reform as shoal deposits in the near future.

8.2.3 Nearshore Sediment Transport Potential

Comparisons of average annual sediment transport potential were performed for existing and post-dredging conditions to indicate the relative impact of dredging to longshore sediment transport processes. Mean sediment transport potential calculated for beaches east of Jones Inlet indicated net westerly transport ranging from about 54,000 m³/yr at Fire Island Inlet to 170,000 m³/yr at Jones Inlet. Along Long Beach, net westerly transport increased from about 50,000 m³/yr west of Jones Inlet to a maximum of about 150,000 m³/yr at the approximate mid-point of the barrier beach, before decreasing to about 88,000 m³/yr at East Rockaway Inlet. The impact significance envelope for longshore transport, relative to offshore borrow site dredging, increased along Jones Beach from ±20,000 m³/yr at Fire Island Inlet to ±40,000 m³/yr at Jones Inlet. The significance envelope for Long Beach had a similar range, with a maximum value midway between Jones Inlet and East Rockaway Inlet. Potential dredging impacts to longshore transport rates from excavation at Sites 3, 4W, and 4E are well within the transport significance envelope. As such, proposed dredging at these sites are not expected to result in significant modifications to coastal processes along this shoreline. Shoreline impacts are negligible due to the relatively deep water at potential borrow sites (19 m for Site 3 and 20 m for Sites 4W and 4E), their distance offshore, and wave climate (dominated by relatively short-period waves).

Mean sediment transport potential along the northeast coast of New Jersey for the modeled 20-year period indicated that dominant transport was net northerly but more bi-directional for shorter term annual results. There was an approximate ±55,000 m³/yr range in annual net transport rates. Long-term potential transport rates reached a maximum of

approximately 30,000 m³/yr within the modeled study area, and a minimum occurred just north of Shark River Inlet. Results of transport potential calculations indicated that the year with the greatest net southerly transport was 1987, and the year with the greatest northerly directed transport was 1995. The dredging impact significance envelope computed for this area was generally constant at $\pm 15,000$ m³/yr. Impacts from dredging Sites H1 and H2 are well within the significance envelope, and proposed sites would be acceptable under the simulated conditions. Similar to sites offshore Long Island, potential shoreline impacts were negligible due to the relatively deep water at potential borrow sites (20 m for Sites H1 and H2), their distance offshore, and wave climate (dominated by relatively short-period waves).

8.3 BENTHIC ENVIRONMENT

Benthic assemblages surveyed from the New Jersey and New York sand borrow sites consisted of members of the major invertebrate and vertebrate groups commonly found in the region of the New York Bight. Numerically dominant infaunal groups included crustaceans, echinoderms, mollusks, and polychaetes, while epifaunal taxa consisted primarily of decapods, sand dollars, gastropods, and squids, all typical components of benthic assemblages in the study area. Similarly, the numerically dominant demersal fishes collected in trawls within the borrow sites revealed consistency with previous surveys. Fishes such as clearnose skate (*Raja eglanteria*), northern searobin (*Prionotus carolinus*), scup (*Stenotomus chrysops*), and summer flounder (*Paralichthys dentatus*) were numerical dominants during the surveys, and these species consistently are among the most ubiquitous and abundant demersal taxa in the Bight region.

Field surveys indicated that infaunal distribution and abundance was correlated broadly with sediment grain size. Groups of organisms characterized samples from different sediment types (e.g., sand and gravel). Juvenile surfclams (*Spisula solidissima*) were collected from stations with sand, slightly gravelly sand, and gravelly sand but were not predominantly associated with any particular sedimentary habitat in the borrow sites. Other physical environmental characteristics that normally affect infaunal population distributions, such as water depth, were similar across the study area and therefore did not differentially affect abundance and distribution patterns. In addition to sediment-based spatial variability, there were significant temporal differences in the composition of infaunal assemblages. Just half of all collected taxa were common to both surveys. Temporal patterns of infaunal community indices did not meet expected patterns, possibly due to abnormally high temperatures in the region during the first half of 2002. Despite inherent spatial and temporal heterogeneity in the distribution and abundance of demersal taxa, results of the 2001-2002 surveys of the New Jersey and New York sand borrow sites generally are consistent with historical demersal survey results in the region.

Infaunal assemblages in the sand borrow sites will be completely destroyed within areas excavated by dredges; however, these assemblages are expected to recover. The rate of post-dredging recovery of benthic assemblages within an excavated borrow site will depend primarily on the depth of sand excavation. Although an excavation with a large surface area would initially impact a greater number of infaunal organisms, the recovery process within such an excavation would be quicker than it would be for a smaller, deeper pit. Creation of a steep-sided pit may inhibit water flow through such a feature, possibly resulting in a "dead zone" characterized by deposition of fine particles and hypoxia or anoxia. This scenario would extend the duration of ecological impact beyond that which would occur with a more shallow cut over a much larger area.

Impacts to infauna are expected to be limited in spatial extent relative to the broad shelf area of the New York Bight. Recovery time for any impacts to the benthic environment will vary depending on the organisms affected, seasonal timing of dredging, and type of excavation. Impacts to infauna will affect benthic feeding fishes and epifauna. Based on previous observations of infaunal reestablishment in dredged areas, the infaunal community in dredged sites within sand borrow sites most likely will become reestablished within 2 years, exhibiting levels of infaunal abundance, diversity, and composition comparable to nearby non-dredged areas.

8.4 PELAGIC ENVIRONMENT

Pelagic invertebrates and fishes were not sampled during the biological field surveys, but their consideration was based on a concern of water column effects related to dredging. The most important pelagic invertebrates in the study area are squids, represented by two species, shortfin and longfin squids. These species occur in the area and were collected in bottom trawls taken during the biological field surveys. Squids could be entrained if they encountered the suction field of a hydraulic dredge. In addition, squid eggs are laid in large clusters on the seafloor and could be removed with sediments. Dredging is unlikely to significantly impact squid populations in the vicinity of the sand borrow sites. This precludes the need for an environmental window or specific project scheduling to protect squid resources.

Pelagic fishes in the area include highly migratory species, coastal pelagic species, and anadromous species. Members of all of these groups are managed by Federal or State agencies. Dredging should not present a significant problem for pelagic fishes offshore of New Jersey and New York. Factors related to offshore sand dredging that could be detrimental to pelagic fishes are physical injury (entrainment), attraction, turbidity, and noise. If an environmental window is sought to protect pelagic fishes from dredging impacts, the spring to fall period would encompass the peak seasons for the economically important species. Quantitative data are lacking to support the use of an environmental window to lessen effects on pelagic fishes.

EFH for several fish species (and life stages) overlap the sand borrow sites, but the area encompassed by the sites is very small relative to the known EFH. For this reason, the effect of dredging on EFH for the managed species is expected to be minimal.

The main potential effect of dredging on sea turtles is physical injury or death caused by the suction and/or cutting action of the dredge head. No significant effects on turtles are expected from turbidity or noise. Three sea turtle species that typically occur off New Jersey (loggerhead, green, and Kemp's ridley) are considered to be at risk because of their benthic feeding habits. Loggerheads are the most abundant turtles in the project area, and historically, they have been the species most frequently entrained during hopper dredging. If a hopper dredge is used, then it would be best to avoid the June through November turtle season. However, the vagaries of winter weather off New Jersey make it infeasible to prohibit dredging during these months. If use of a hopper dredge during this season cannot be avoided, then other mitigation and monitoring requirements may be appropriate, such as turtle monitoring and use of a turtle-deflecting draghead. If a cutterhead suction dredge is used, seasonal or other restrictions are considered unnecessary because there is little likelihood of killing or injuring sea turtles.

Marine mammal species occurring commonly on the shelf, such as bottlenose dolphin and common dolphin, may be present year-round but are unlikely to be adversely affected by

dredging due to their agility. Harbor porpoise occurrence is more seasonal, but the likelihood of impact is so low that it does not warrant seasonal restrictions on dredging. Fin and humpback whales would be most likely to occur during winter or spring, and right whales as transients during spring and fall. There is no "resident" population of any of these whales in the study area; rather, they would be temporary inhabitants, or would be transiting the area during seasonal migrations. Generally, the probability of encountering these species in the project area would be lowest during summer. However, due to the low likelihood of impact, seasonal restrictions on dredging probably are not warranted. Instead, measures to minimize possible vessel interactions with these endangered species may be appropriate.

8.5 SYNTHESIS

The data collected, analyses performed, and simulations conducted for this study indicate that proposed sand dredging at sites evaluated on the OCS offshore northeastern New Jersey and southwestern Long Island are expected to have minimal environmental impact on fluid and sediment dynamics and biological communities. Short-term impacts to benthic communities are expected due to the physical removal of borrow material, but the potential for significant cumulative benthic impacts is remote. Additionally, no cumulative effects to any of the pelagic groups are expected from potential sand mining operations.

Minimal physical environmental impacts due to potential sand dredging operations have been identified through wave and sediment transport simulations. The significance of changes to longshore transport along the modeled shoreline, resulting from dredging proposed borrow sites to their maximum design depths, was determined by comparing predicted change in transport potential between existing and post-dredging conditions to a transport significance envelope of one-half the standard deviation ($\pm 0.5\sigma$) of the variability in annual transport along the shoreline. Under representative wave conditions for each of the model grids, it was determined that no significant changes in longshore sediment transport potential would result from modeled borrow site configurations due to the relatively deep water at potential borrow sites (approximately -17 to -20 m), their distance offshore, and wave climate (dominated by relatively short-period waves). However, because minor impacts to wave and sediment transport dynamics and biology at borrow sites may occur under conditions similar to those imposed in the present study, additional data collection and analysis may be required for a specific sand extraction scenario to determine the extent of impacts.

9.0 LITERATURE CITED

- Able, K.W. and M.P. Fahay, 1998. *The First Year in the Life of Estuarine Fishes in the Middle Atlantic Bight*. Rutgers University Press, New Brunswick, NJ, 343 pp.
- Able, K.W. and S.M. Hagen, 1995. *Fishes in the Vicinity of Beach Haven Ridge: Annual and Seasonal Patterns of Abundance During the Early 1970s*. Institute of Marine and Coastal Sciences, Rutgers University, NJ, Technical Report #95-24, 36 pp.
- Alpine Ocean Seismic Survey, 1988. *Identification and Delineation of Potential Borrow Areas for the Atlantic Coast of New Jersey, Asbury Park to Manasquan: Detailed Investigation of the Sea Bright Sand Borrow Areas*. Final Report to the U.S. Army Corps of Engineers, Contract #DACW51-87-C-0011, New York District, NY.
- Amato, R.V., 1994. *Sand and Gravel Maps of the Atlantic Continental Shelf with Explanatory Text*. U.S. Minerals Management Service, OCS Monograph, MMS 93-0037, 35 pp. + 4 maps.
- Anders, F.J. and M.R. Byrnes, 1991. Accuracy of shoreline change rates as determined from maps and aerial photographs. *Shore and Beach*, 59(1): 17-26.
- Applied Biology, Inc., 1979. *Biological Studies Concerning Dredging and Beach Nourishment at Duval County, Florida with a Review of Pertinent Literature*. U.S. Army Corps of Engineers, Jacksonville District, Jacksonville, FL.
- Arnold, D.W., 1992. The scientific rationale for restricting coastal construction activities during the marine turtle nesting season. In: L.S. Tait (compiler), *New Directions in Beach Management*. Proceedings of the 5th Annual National Conference on Beach Preservation Technology, St. Petersburg, FL, pp. 374-380.
- Ashley, G.M., S.D. Halsey, and C.B. Buteux, 1986. New Jersey's longshore current pattern. *Journal of Coastal Research*, 2(4): 453-463.
- ASMFC, 1998. *Amendment 1 to the Interstate Fishery Management Plan for Atlantic Sturgeon*. Atlantic States Marine Fisheries Commission (ASMFC) Atlantic Sturgeon Plan Development Team, Fishery Management Report No. 31, 60 pp.
- Bak, R.P.M., 1978. Lethal and sublethal effects of dredging on reef coral. *Marine Pollution Bulletin*, 9(1): 14-16.
- Banks, G.E. and M.P. Alexander, 1994. *Development and Evaluation of a Sea Turtle-Deflecting Hopper Dredge Draghead*. Miscellaneous Paper HL-94-5, U.S. Army Engineer Waterways Experiment Station, Vicksburg, MS.
- Barnes, R.D., 1980. *Invertebrate Zoology, Fourth Edition*. Saunders College, Philadelphia, PA.
- Barry A. Vittor & Associates, Inc., 1999a. *Pre- and Post-Dredging Monitoring of Macroinvertebrate Assemblages at a Borrow Area Located Offshore of Coney Island, New York: 1992-1998 Data Synthesis*. Prepared for the U.S. Army Corps of Engineers, New York District, 10 pp. + app.
- Barry A. Vittor & Associates, Inc., 1999b. *Post-Construction Monitoring, Borrow Area Finfish Sampling (BAFS) Summary Report, Section II, Asbury Park to Manasquan, New Jersey*. Beach Erosion Control Project Biological Monitoring Program. Prepared for the U.S. Corps of Engineers, New York District.
- Barry A. Vittor & Associates, Inc., 2002. *Characterization of Benthic Assemblages in the Vicinity of the New York Bight Apex*. Prepared for the U.S. Corps of Engineers, New York District.
- Barry, M., 1978. *Behavioral Response of Yellowfin Tuna, Thunnus albacares, and Kawakawa, Euthynnus affinis, to Turbidity*. U.S. Department of Commerce, National Oceanic and Atmospheric Administration, Environmental Research Laboratories, Pacific Marine Environmental Laboratory, Seattle, WA. Deep Ocean Mining Environmental Study (DOMES), Unpublished Manuscript Number 31. National Technical Information Service No. PB-297, 106 pp.

- Bartol, S.M., J. Musick, and M.L. Lenhardt, 1999. Auditory evoked potentials of the loggerhead sea turtle (*Caretta caretta*). *Copeia*, 1999(3): 836-840.
- Bartsch, A.F., 1960. Settleable solids, turbidity, and light penetration as factors affecting water quality. In: C. Tarzwell (ed.), *Biological Problems in Water Pollution*. U.S. Public Health Service Publication Number W60-3, pp. 118-127.
- Battelle Ocean Sciences, 1996. Sediment Survey at the Mud Dump Site and Environs. U.S. Environmental Protection Agency Report, Region II, New York, NY.
- Battjes, J.A. and J.P. Janssen, 1978. Energy loss and set-up due to breaking of random waves. Proc. 23rd International Conference on Coastal Engineering, ASCE, pp. 569-587.
- Beardsley, R.C. and W.C. Boicourt, 1981. On estuarine and continental shelf circulation in the Middle Atlantic Bight. In: B.A. Warren and C. Wunsch (editors), *Evolution of Physical Oceanography*, MIT Press, pp.198-233.
- Benfield, M.C. and T.J. Minello, 1996. Relative effects of turbidity and light intensity on reactive distance and feeding of an estuarine fish. *Environmental Biology of Fishes*, 46: 211-216.
- Berry, S.A., 1990. Canaveral Harbor entrance channel operational measures to protect sea turtles. In: D.D. Dickerson and D.A. Nelson (compilers), *Proceedings of the National Workshop on Methods to Minimize Dredging Impacts on Sea Turtles*, Jacksonville, Florida. U.S. Army Engineer Waterways Experiment Station, Environmental Effects Laboratory, Vicksburg, MS, Miscellaneous Paper EL-90-5, pp. 49-52.
- Biggs, R.B., 1968. Environmental effects of overboard spoil disposal. *Journal of Sanitary Engineering Division*, Proceeding Paper 5979, 94(SA3): 477-478.
- Bishop, J.M., 1975. An Analytical Sea Current Model for Coastal Regions With Application to the New York Bight. Oceanographic Unit Technical Report 75-2, U.S. Coast Guard, 27 pp.
- Blake, N.J., L.J. Doyle, and J.J. Culter, 1995. Impacts and Direct Effects of Sand Dredging for Beach Renourishment on the Benthic Organisms and Geology of the West Florida Shelf. U.S. Department of the Interior, Minerals Management Service, Office of International Activities and Marine Minerals, Herndon, VA. Executive Summary, OCS Report MMS 95-0004, 23 pp. Final Report, OCS Report MMS 95-0005, 109 pp. Appendices, OCS Report MMS 95-0005.
- Blaylock, R.A., J.W. Hain, L.J. Hansen, D.L. Palka, and G.T. Waring, 1995. U.S. Atlantic and Gulf of Mexico Marine Mammal Stock Assessments. NOAA Technical Memorandum NMFS-SEFSC-363, 211 pp.
- Boesch, D.F., 1972. Species diversity of marine macrobenthos in the Virginia area. *Chesapeake Science*, 13(3): 206-211.
- Boesch, D.F., 1973. Classification and community structure of macrobenthos in the Hampton Roads area, Virginia. *Marine Biology*, 21: 226-244.
- Boesch, D.F., 1977. A new look at the zonation of benthos along the estuarine gradient. In: B.C. Coull (editor), *Ecology of Marine Benthos*. University of South Carolina Press, Columbia, SC, pp. 245-266.
- Bonsdorff, E., 1983. Recovery potential of macrozoobenthos from dredging in shallow brackish waters. In: L. Cabioch et al. (editors), *Fluctuations and Succession in Marine Ecosystems*, Proceedings of the 17th European Symposium on Marine Biology, *Oceanologica Acta*, pp. 27-32.
- Bowen, P.R. and G.A. Marsh, 1988. Benthic Faunal Colonization of an Offshore Borrow Pit in Southeastern Florida. U.S. Army Engineer Waterways Experiment Station, Vicksburg, MS, Miscellaneous Paper D-88-5.
- Brodziak, J. and L. Hendrickson, 1999. An analysis of environmental effects on survey catches of squids *Loligo pealei* and *Illex illecebrosus* in the northwest Atlantic. *Fishery Bulletin*, 97: 9-24.
- Brodziak, J.K.T. and W.K. Macy III, 1996. Growth of longfinned squid, *Loligo pealei*, in the northwest Atlantic. *Fishery Bulletin*, 94: 212-236.
- Brown, C.B., 1950. Sediment Transportation. In: H. Rouse (editor), *Engineering Hydraulics*, John Wiley and Sons, NY, 1,039 pp.
- Bruton, M.N., 1985. The effects of suspensoids on fish. *Hydrobiologia*, 125: 221-241.
- Bumpus, D.F., 1973. A description of the circulation on the continental shelf of the east coast of the United States. *Progress in Oceanography*, 6: 111-157.
- Burke, V.J., S.J. Morreale, P. Logan, and E.A. Standora, 1992. Diet of Green Turtles (*Chelonia mydas*) in the waters of Long Island, New York. In: M. Salmon and J. Wyneken (editors), *Proceedings of the Eleventh Annual*

- Workshop on Sea Turtle Biology and Conservation, NOAA Technical Memorandum NMFS-SEFC-302, pp. 140-142.
- Burke, V.J., E.A. Standora, and S.J. Morreale, 1993. Diet of juvenile Kemp's Ridley and Loggerhead sea turtles from Long Island, New York. *Copeia*, 1993: 1,176-1,180.
- Burlas, M., G.L. Ray, and D. Clarke, 2001. The New York District's Biological Monitoring Program for the Atlantic Coast of New Jersey, Asbury Park to Manasquan Section Beach Erosion Control Project. U.S. Army Corps of Engineers, New York District, and Engineer Research and Development Center, Waterways Experiment Station, Vicksburg, MS. (<http://www.nan.usace.army.mil/business/prilinks/coastal/asbury/index.htm>)
- Butman, B., W. Danforth, W. Schwab, and M. Buchholtz ten Brink, 1998. Multibeam Bathymetric and Backscatter Maps of the Upper Hudson Shelf Valley and Adjacent Shelf, Offshore of New York. USGS Open File Report 98-616, U.D. Department of the Interior.
- Butman, B., P.S. Alexander, C.K. Harris, P.A. Traykovski, M.B. ten Brink, F.S. Lightsom, and M.A. Martini, 2003. Oceanographic Observations in the Hudson Shelf Valley, December 1999 – April 2000: Data Report. U.S. Geological Survey Open File Report 02-217 (DVD-ROM), U.S. Department of the Interior.
- Byles, R.A., 1988. Satellite Telemetry of Kemp's Ridley Sea Turtle, *Lepidochelys kempii*, in the Gulf of Mexico. Report to the National Fish and Wildlife Foundation, 40 pp.
- Byrnes, M.R. and C.G. Groat, 1991. Characterization of the Development Potential of Ship Shoal Sand for Beach Replenishment of Isles Dernieres. Final Report, U.S. Department of the Interior, Minerals Management Service, Office of International Activities and Marine Minerals, Herndon, VA, 164 pp.
- Byrnes, M.R., R.M. Hammer, B.A. Vittor, J.S. Ramsey, D.B. Snyder, J.D. Wood, K.F. Bosma, T.D. Thibaut, and N.W. Phillips, 2000. Environmental Survey of Potential Sand Resource Sites: Offshore New Jersey. U.S. Department of the Interior, Minerals Management Service, International Activities and Marine Minerals Division (INTERMAR), Herndon, VA. OCS Report MMS 2000-052, Volume I: Main Text, 380 pp. + Volume II: Appendices, 291 pp.
- Byrnes, M.R., J.L. Baker, and F. Li, 2002. Quantifying Potential Measurement Errors and Uncertainties Associated with Bathymetric Change Analysis. Coastal and Hydraulics Engineering Technical Note IV-50, U.S. Army Engineer Waterways Experiment Station, Coastal and Hydraulics Laboratory, Vicksburg, MS.
- Byrnes, M.R., R.M. Hammer, and T.D. Thibaut, 2004. Effects of sand mining on physical processes and biological communities offshore New Jersey. *Journal of Coastal Research*, 20(1): 25-43.
- Cadrin, S.X., 1998. Longfin inshore squid. In: S.H. Clark (editor), Status of Fishery Resources off the Northeastern United States for 1998. U.S. Department of Commerce, NOAA Technical Memorandum NMFS-NE-115, pp. 118-119.
- Caldwell, J.M., 1966. Coastal Processes and Beach Erosion. *Journal of the Society of Civil Engineers*, 53(2): 142-157.
- Caracciolo, J. and F.W. Steimle, Jr., 1983. An Atlas of the Distribution and Abundance of Dominate Benthic Invertebrates in the New York Bight Apex, with Reviews of Their Life Histories. NOAA Technical Report NMFS SSRF-776.
- Carr, A., 1987. New perspectives on the pelagic stage of sea turtle development. *Conservation Biology*, 1: 103-121.
- Centre for Cold Ocean Resources Engineering (C-CORE), 1995. Proposed Marine Mining Technologies and Mitigation Techniques: A Detailed Analysis With Respect to the Mining of Specific Offshore Mineral Commodities. Contract report for U.S. Department of the Interior, Minerals Management Service, OCS Report MMS 95-0003, C-CORE Publication 96-C15, 280 pp. + appendices.
- Cerame-Vivas, M.J. and I.E. Gray, 1966. The distribution pattern of benthic invertebrates of the continental shelf off North Carolina. *Ecology*, 47: 260-270.
- Chang, S., F.W. Steimle, Jr., R.N. Reid, S.A. Fromm, V.S. Zdanowicz, and R.A. Pikanowski, 1992. Association of benthic macrofauna with habitat types and quality in the New York Bight. *Marine Ecology Progress Series*, 89: 237-251.
- Chang, S., P.L. Berrien, D.L. Johnson, and W.W. Morse, 1999. Essential Fish Habitat Source Document: Windowpane, *Scophthalmus aquosus*, Life History and Habitat Characteristics. U.S. Department of Commerce, National Marine Fisheries Service, National Oceanic and Atmospheric Administration (NOAA), NOAA Technical Memorandum NMFS-NE-137.

- Chuang, W.S., D.P. Wang, and W.C. Boicourt, 1979. Low-frequency current variability on the southern Mid-Atlantic Bight. *Journal of Physical Oceanography*, 9: 1,144-1,154.
- Coastal Oceanographics, 1996. Hypack Navigation Software Version 6.4.
- Coastline Surveys Limited, 1998. Marine Aggregate Mining Benthic and Surface Plume Study. Final report to the U.S. Department of the Interior, Minerals Management Service and Plume Research Group, Report 98/555/03, 168 pp.
- Colvocoresses, J.A. and J.A. Musick, 1984. Species associations and community composition of the Middle Atlantic Bight continental shelf demersal fishes. *Fishery Bulletin*, 82(4): 295-314.
- Connell, J.H., 1997. Disturbance and Recovery of Coral Assemblages. In: H.A. Lessios, I.G. Macintyre, and M. McGee (eds.), *Proceedings of the 8th International Coral Reef Symposium Panama*, 1: 9-22.
- Continental Shelf Associates, Inc., 2004. Geological and Geophysical Exploration for Mineral Resources on the Gulf of Mexico Outer Continental Shelf – Final Programmatic Environmental Assessment. OCS EIS/EA MMS 2004-054, Prepared for the U.S. Department of the Interior, Minerals Management Service Gulf of Mexico OCS Region, New Orleans, LA.
- Courtenay, W.R., Jr., D.J. Herrema, M.J. Thompson, W.P. Azzinaro, and J. van Montfrans, 1972. Ecological monitoring of two beach nourishment projects in Broward County, Florida. *Shore and Beach*, 40(2): 8-13.
- Cowen, R.K., J.A. Hare, and M.P. Fahay, 1993. Beyond hydrography: can physical processes explain larval fish assemblages within the Middle Atlantic Bight? *Bulletin of Marine Science*, 53(2): 567-587.
- Cronin, E.L., G. Gunter, and S.H. Hopkins, 1969. Effects of Engineering Activities on Coastal Ecology. U.S. Army Corps of Engineers, Office of Chief of Engineers, Interim Report.
- Cronin, E.L., R.B. Biggs, D.A. Flemer, G.T. Pfitzmeier, F. Goodwin, Jr., W.L. Dovel, and D.E. Richie, Jr., 1970. Gross Physical and Biological Effects of Overboard Spoil Disposal in Upper Chesapeake Bay. University of Maryland, Chesapeake Biological Laboratory, Natural Resources Institute Special Report Number 3, 66 pp.
- Crowell, M., S.P. Leatherman, and M.K. Buckley, 1991. Historical shoreline change: Error analysis and mapping accuracy. *Journal of Coastal Research*, 7(3): 839-852.
- Cruickshank, M.J., J.P. Flanagan, B. Holt, and J.W. Padan, 1987. Marine Mining on the Outer Continental Shelf: Environmental Effects Overview. U.S. Department of the Interior, Minerals Management Service, OCS Report 87-0035, 66 pp.
- Csanady, G.T., 1982. *Circulation in the Coastal Ocean*. D. Reidel Publishing Company, Dordrecht, Holland, 279 pp.
- Day, J.H., J.G. Field, and M.P. Montgomery, 1971. The use of numerical methods to determine the distribution of the benthic fauna across the continental shelf of North Carolina. *Journal of Animal Ecology*, 40: 93-125.
- Diaz, R.J., G.R. Cutter, Jr., and K. W. Able, 2003. The importance of physical and biogenic structure to juvenile fishes on the shallow inner continental shelf. *Estuaries*, 26(1): 12-20.
- Dickerson, D.D., 1990. Workgroup 1 Summary. In: D.D. Dickerson and D.A. Nelson (compilers), *Proceedings of the National Workshop on Methods to Minimize Dredging Impacts on Sea Turtles*. U.S. Army Engineer Waterways Experiment Station, Vicksburg, MS, Miscellaneous Paper EL-90-5, 89 pp.
- Dickerson, D.D., D.A. Nelson, M. Wolff, and L. Manners, 1992. Summary of dredging impacts on sea turtles: Kings Bay, Georgia and Cape Canaveral, Florida. In: M. Salmon and J. Wyneken (compilers), *Proceedings of the Eleventh Annual Workshop on Sea Turtle Biology and Conservation*, Jekyll Island, GA. NOAA Technical Memorandum NMFS-SEFSC-302, pp. 148-151.
- Dickerson, D.D., K.J. Reine, and D.G. Clarke, 1998. Economic Impacts of Environmental Windows Associated with Dredging Operations. U.S. Army Engineer Research and Development Center, Vicksburg, MS, DOER Technical Note TN DOER-E3.
- Dodd, C.K., Jr., 1988. Synopsis of the Biological Data on the Loggerhead Sea Turtle *Caretta caretta* (Linnaeus 1758). U.S. Fish and Wildlife Service Biological Report 88(4), 110 pp.
- Dodge, R.E. and J.R. Vaisnys, 1977. Coral populations and growth patterns: responses to sedimentation and turbidity associated with dredging. *Journal of Marine Research*, 35(4): 715-730.
- Dornhelm, R., 2004. Beach master. *Invention and Technology*, 20(1): 42-48.

- Duane, D.B. and W.L. Stubblefield, 1988. Sand and gravel resources: U.S. Atlantic Continental Shelf. In: R.E. Sheridan and J.A. Grow (editors), *The Atlantic Continental Margin: U.S., Volume I-2, The Geology of North America*, Geological Society of America, Boulder, CO, pp. 481-500.
- Duane, D.B., M.E. Field, E.P. Meisburger, D.J.P. Swift, and S.J. Williams, 1972. Linear shoals on the Atlantic inner continental shelf, Florida to Long Island. In: D.J.P. Swift, D.B. Duane, and O.H. Pilkey (editors), *Shelf Sediment Transport: Process and Pattern*. Dowden Hutchinson, and Ross. Stroudsburg, PA, pp. 447-498.
- Eckert, K.L., 1995. Leatherback Sea Turtle, *Dermochelys coriacea*. In: P.T. Plotkin (editor), *National Marine Fisheries Service and U. S. Fish and Wildlife Service Status Reviews for Sea Turtles Listed Under the Endangered Species Act of 1973*, Silver Spring, MD.
- Eckert, S.A., D.W. Nellis, K.L. Eckert, and G.L. Kooyman, 1986. Diving patterns of two leatherback sea turtles (*Dermochelys coriacea*) during internesting intervals at Sandy Point, St. Croix, U.S. Virgin Islands. *Herpetologica*, 42(3): 381-388.
- Ellis, M.Y., 1978. *Coastal Mapping Handbook*. U.S. Department of the Interior, Geological Survey, U.S. Department of Commerce, National Ocean Service, U.S. Government Printing Office, Washington, D.C., 199 pp.
- Emery, K.O. and E. Uchupi, 1965. Structure of Georges Bank. *Marine Geology*, 3: 349-358.
- Emery, K.O., R.L. Wigley, A.S. Barlett, M. Rubin, and E.S. Barghoorn, 1967. Freshwater peat on the continental shelf. *Science*, 158: 1301-1307.
- Fahay, M.P., P.L. Berrien, D.L. Johnson, and W.W. Morse, 1999. *Essential Fish Habitat Source Document: Bluefish, *Pomatomus saltatrix*, Life History and Habitat Characteristics*. U.S. Department of Commerce, National Marine Fisheries Service, National Oceanic and Atmospheric Administration (NOAA), NOAA Technical Memorandum NMFS-NE-144.
- Fauchald, K. and P. Jumars, 1979. The diet of worms: a study of polychaete feeding guilds. *Oceanography and Marine Biology Annual Review*, 17: 193-284.
- Field, M.E. and D.B. Duane, 1976. Post-Pleistocene history of the United States inner continental shelf: significance to the origin of barrier islands. *Geological Society of America Bulletin*, 87: 691-702.
- Fischer, W. (editor), 1978. *FAO Species Identification Sheets for Fishery Purposes, Western Central Atlantic (Fishing Area 31), Volume VI*.
- Fisher, J., 1967. Origin of barrier chain shorelines, Middle Atlantic States. *Geological Society of America Special Paper* 115, pp. 66-67.
- Fisher, J., 1968. Barrier island formation – discussion. *Geological Society of America Bulletin*, 79: 1421-1426.
- Flagg, C.N., 1977. *The Kinematics and Dynamics of the New England Continental Shelf and Shelf/Slope Front*. Ph.D. Dissertation, Massachusetts Institute of Technology/Woods Hole Oceanographic Institution, WHOI Ref. 77-67, 207 pp.
- Flint, R.W. and J.S. Holland, 1980. *Benthic Infaunal Variability on a Transect in the Gulf of Mexico*. University of Texas Marine Science Institute, Contribution No. 328, Academic Press, London.
- Folk, R.L., 1974. *Petrology of Sedimentary Rocks*. Hemphill Publishing Company, Austin, TX.
- Foster D.S., B.A. Swift, and W.C. Schwab 1999. *Stratigraphic Framework Maps of the Nearshore Area of Southern Long Island from Fire Island to Montauk Point, New York*: U.S. Geological Survey Open File Report 99-559.
- Frankenberg, D. and A.S. Leiper, 1977. Seasonal cycles in benthic communities of the Georgia continental shelf. In: B.C. Coull (ed.), *Ecology of Marine Benthos*. University of South Carolina Press, Columbia, SC, pp. 383-397.
- Fray, C.T. and J. Ewing, 1961. *Project 555 – Monmouth County Offshore Borings*. Report No. 1, New Jersey Department of Conservation and Economic Development.
- Frazier, N.B., 1995. Loggerhead sea turtle, *Caretta caretta*. In: P.T. Plotkin (editor), *National Marine Fisheries Service and U. S. Fish and Wildlife Service Status Reviews for Sea Turtles Listed under the Endangered Species Act of 1973*. Silver Spring, MD.
- Fredette, T.J., W.F. Bohlen, D.C. Rhoads, and R.W. Morton, 1988. Erosion and resuspension effects of Hurricane Gloria at Long Island Sound dredged material disposal sites. In: *Proceedings of the Water Quality '88 Seminar*, Charleston, South Carolina. U.S. Army Corps of Engineers, Hydraulic Engineering Center, Davis, CA.

- Garrison, L.E. and R.L. McMaster, 1966. Sediments and geomorphology of the continental shelf off southern New England. *Marine Geology*, 4: 273-289.
- Garrison, L.P. and J.S. Link, 2000. Dietary structure of the fish community in the northeast United States continental shelf ecosystem. *Marine Ecology Progress Series*, 202: 231-240.
- Gaskin, D.E., 1992. The status of the harbour porpoise. *Canadian Field-Naturalist*, 106: 36-54.
- Germano, J.D., 1983. Infaunal Succession in Long Island Sound: Animal-Sediment Interactions and the Effects of Predation. Ph.D. Dissertation, Yale University, New Haven, CT, 206 pp.
- Goldberg, W.M., 1989. Biological effects of beach nourishment in South Florida: the good, the bad, and the ugly. *Proceedings of Beach Preservation Technology Conference*, Shore and Beach Preservation Association, Tallahassee, FL.
- Grant, W.D. and O.S. Madsen, 1986. The continental shelf bottom boundary layer. *Annual Review Fluid Mechanics*, 18: 265-305.
- Grassle, J.F. and J.P. Grassle, 1974. Opportunistic life histories and genetic systems in marine benthic polychaetes. *Journal of Marine Research*, 32: 253-284.
- Gray, J.S., 1974. Animal-sediment relationships. *Oceanography and Marine Biology Annual Review*, 12: 223-261.
- Grecay, P.A. and T.E. Targett, 1996. Spatial patterns in conditions and feeding of juvenile weakfish in Delaware Bay. *Transactions of the American Fisheries Society*, 125(5): 803-805.
- Griscom, C.A., 1968. An Analysis of Subsurface Currents and Temperatures at a Site on the Continental Shelf of the Northeast United States. Office of Naval Research Technical Report U413-68-109, 60 pp.
- Grober, L.E., 1992. The Ecological Effects of Beach Replenishment. M.S. Thesis, Duke University, School of the Environment, NC, 109 pp.
- Grosslein, M.D., 1976. Some results of fish surveys in the mid-Atlantic: important for assessing environmental impacts. In: G. Gross (editor), *Middle Atlantic Continental Shelf and the New York Bight*, Proceedings of the Symposium, American Museum of Natural History, New York City, 1975, American Society of Limnology and Oceanography, Inc., Allen Press, Inc., Lawrence, KS, pp. 312-328.
- Grosslein, M.D. and T.R. Azarovitz, 1982. Fish distribution, MESA New York Bight Atlas Monograph 15. New York Sea Grant Institute, 182 pp.
- Gustafson, J.F., 1972. Ecological effects of dredged borrow pits. *World Dredging and Marine Construction*, 8(10): 44-48.
- Hales, L.S., Jr., R.S. McBride, E.A. Bender, R.L. Hoden, and K.W. Able, 1995. Characterization of Non-Target Invertebrates and Substrates from Trawl Collections During 1991-92 at Beach Haven Ridge (LEO-15) and Adjacent Sites in Great Bay and on the Inner Continental Shelf Off New Jersey. Institute of Marine and Coastal Sciences, Rutgers University, Contribution No. 95-09, 34 pp.
- Hall, S.J., 1994. Physical disturbance and marine benthic communities: life in unconsolidated sediments. *Oceanography and Marine Biology Annual Review*, 32: 179-239.
- Hammer, R.M., 1981. Day-night differences in the emergence of demersal zooplankton from a sand substrate in a kelp forest. *Marine Biology*, 62: 275-280.
- Hammer, R.M. and R.C. Zimmerman, 1979. Species of demersal zooplankton inhabiting a kelp forest ecosystem off Santa Catalina Island, California. *Bulletin of Southern California Academy of Sciences*, 78(3): 199-206.
- Hammer, R.M., B.J. Balcom, M.J. Cruickshank, and C.L. Morgan, 1993. Synthesis and Analysis of Existing Information Regarding Environmental Effects of Marine Mining. Final report by Continental Shelf Associates, Inc. for the U.S. Department of the Interior, Minerals Management Service, Office of International Activities and Marine Minerals, Herndon, VA, OCS Study MMS 93-0006, 392 pp.
- Harper, D.E., Jr., 1991. Macroinfauna and macroepifauna. In: J.M. Brooks and C.P. Giamonna (eds.), *Mississippi-Alabama Continental Shelf Ecosystem Study Data Summary and Synthesis, Volume II: Technical Narrative*. U.S. Department of the Interior, Minerals Management Service, 14-12-0001-30346, OCS Study MMS 91-0063.
- Hendrickson, L., 1998. Northern Shortfin Squid. In: S.H. Clark (editor), *Status of Fishery Resources Off the Northeastern United States for 1998*. U.S. Department of Commerce, NOAA Technical Memorandum NMFS-NE-115, pp. 116-117.

- Herbich, J.B., 1992. Handbook of Dredging Engineering. McGraw-Hill, Inc., New York, NY, 740 pp.
- Herbich, J.B. and S.B. Brahme, 1991. Literature Review and Technical Evaluation of Sediment Resuspension During Dredging. U.S. Army Engineer Waterways Experiment Station, Vicksburg, MS., Contract Report HL-91-1.
- Houston, J.R., 1995. Beach nourishment. *Shore and Beach*, 63(1): 21-24.
- Houston, J.R., 2002. The economic value of beaches – a 2002 update. *Shore and Beach*, 70(1): 9-12.
- Hrabovsky, L., 1990. Hydraulic cutterhead pipeline dredging. In: D.D. Dickerson and D.A. Nelson (compilers), Proceedings of the National Workshop on Methods to Minimize Dredging Impacts on Sea Turtles, Jacksonville, FL. U.S. Army Engineer Waterways Experiment Station, Vicksburg, MS, Miscellaneous Paper EL-90-5, pp. 56-58.
- Hubertz, J.M., R.M. Brooks, W.A. Brandon, and B.A. Tracy, 1993. Hindcast Wave Information for the U.S. Atlantic Coast. WIS Report 30, U.S. Army Engineer Waterways Experiment Station, Coastal Engineering Research Center, Wave Information Study, Vicksburg, MS.
- Hughes, T.P. and J.H. Connell, 1999. Multiple stressors on coral reefs: a long-term perspective. *Limnology and Oceanography*, 44(3, Part 2): 932-940.
- Ingle, R.M., 1952. Studies on the Effect of Dredging Operations Upon Fish and Shellfish. Florida State Board of Conservation, Technical Series 5, 26 pp.
- Jefferson, T.A., S. Leatherwood, and M.A. Webber, 1993. FAO Species Identification Guide. Marine Mammals of the World. Rome, FAO, 320 pp.
- Johnson, R.G., 1970. Variations in diversity within benthic marine communities. *The American Naturalist*, 104: 285-300.
- Johnson, R.O. and W.G. Nelson, 1985. Biological effects of dredging in an offshore borrow area. *Florida Scientist*, 48: 166-188.
- Jones, G. and S. Candy, 1981. Effects of dredging on the macrobenthic infauna of Botany Bay. *Australian Journal of Marine and Freshwater Research*, 32: 379-399.
- Jones, N.S., 1950. Marine bottom communities. *Biological Review*, 25: 283-313.
- Jutte, P.C., R.F. Van Dolah, and P.T. Gayes, 2002. Recovery of benthic communities following offshore dredging, Myrtle Beach, South Carolina. *Shore & Beach*, 70: 25-30.
- Kamphuis, J.W., 1990. Alongshore sediment transport rate. Proc. 22nd Coastal Engineering Conference, Delft, Netherlands.
- Kana, T.W., 1999. Long Island's south shore beaches, a century of dynamic sediment management. In: N.C. Kraus and W.G. McDougal (editors), Coastal Sediments '99, American Society of Civil Engineers, New York, NY, pp. 1584-1596.
- Kassner, J. and J.A. Black, 1982. Efforts to stabilize a coastal inlet: a case study of Moriches Inlet, NY. *Shore and Beach*, 51(2): 22-26.
- Kelley, S.W., J.S. Ramsey, and M.R. Byrnes, 2004. Evaluating the physical effects of offshore sand dredging for beach nourishment. *Journal of Coastal Research*, 20(1): 89-100.
- Kenney, R.D., 1990. Bottlenose dolphins off the northeastern United States. In: S. Leatherwood and R.R. Reeves (editors), *The Bottlenose Dolphin*. Academic Press, San Diego, CA, pp. 369-386.
- Kerr, S.J., 1995. Silt, Turbidity, and Suspended Sediments in the Aquatic Environment: An Annotated Bibliography and Literature Review. Ontario Ministry of Natural Resources, Southern Region Science and Technology Transfer Unit, Technical Report TR-008, 277 pp.
- Klitgord, K.D., D.R. Hutchinson, and H. Schouten, 1988. U.S. Atlantic continental margin: structural and tectonic framework. In: R.E. Sheridan and J.A. Grow (editors), *The Atlantic Continental Margin: U.S.*, Volume I-2, The Geology of North America, Geological Society of America, Boulder, CO, pp. 19-55.
- Knebel, H.J., 1981. Processes controlling the characteristics of the surficial sand sheet, U.S. Atlantic outer continental shelf. *Marine Geology*, 42: 349-368.
- Knebel, H.J. and E.C. Spiker, 1977. Thickness and age of surficial sand sheet, Baltimore Canyon Trough area. *American Association of Petroleum Geologists Bulletin*, 61: 861-871.

- Knott, S.T., and H. Hoskins, 1968. Evidence of Pleistocene events in the structure of the continental shelf off the northeastern US. *Marine Geology*, 6: 5-43.
- Kocik, J., 1998a. River Herring. In: S.H. Clark (editor), Status of Fishery Resources off the Northeastern United States for 1998. U.S. Department of Commerce, NOAA Technical Memorandum NMFS-NE-115, pp. 134-135.
- Kocik, J., 1998b. American Shad. In: S.H. Clark (editor), Status of Fishery Resources off the Northeastern United States for 1998. U.S. Department of Commerce, NOAA Technical Memorandum NMFS-NE-115, pp. 136-137.
- Kraus, S.D., A.R. Knowlton, and J.H. Prescott, 1988. Surveys for Wintering Right Whales (*Eubalaena glacialis*) Along the Southeastern United States, 1984-1988. Final Report to the Department of the Interior, Minerals Management Service, Branch of Environmental Studies, Washington, DC, 19 pp. + app.
- Kraus, S.D., R.D. Kenney, A.R. Knowlton, and J.N. Ciano, 1993. Endangered Right Whales of the Southwestern North Atlantic. Final report to the Department of the Interior, Minerals Management Service, Atlantic OCS Region, Herndon, VA, 69 pp.
- Kropp, R.K., 1995. Environmental Post-Dredge Monitoring, Great Egg Harbor Inlet and Peck Beach, Ocean City, New Jersey. Final Report to the Corps of Engineers, Philadelphia District, Philadelphia, PA, 44 pp. + app.
- Lange, A.M.T. and M.P. Sissenwine, 1980. Biological considerations relevant to the management of squid (*Loligo pealei* and *Illex illecebrosus*) of the northwest Atlantic. *Marine Fishery Review*, 42(7-8): 23-38.
- Larson, K.W. and C.E. Moehl, 1988. Entrainment of anadromous fish by hopper dredge at the mouth of the Columbia River. In: C.A. Simenstad (editor), Effects of Dredging on Anadromous Pacific Coast Fishes, Workshop Proceedings, University of Washington Sea Grant, pp. 102-112.
- Larson, M. and N.C. Kraus, 1995. Prediction of cross-shore sediment transport at different spatial and temporal scales. In: J.H. List and J.H.J. Terwindt (editors), Large-Scale Coastal Behavior, *Marine Geology Special Issue*, 126(1/4): 111-128.
- LaSalle, M.W., D.G. Clarke, J. Homziak, J.D. Lunz, and T.J. Fredette, 1991. A Framework for Assessing the Need for Seasonal Restrictions on Dredging and Disposal Operations. U.S. Army Engineer Waterways Experiment Station, Vicksburg, MS, Technical Report D-91-1, 74 pp.
- Lenhardt, M.L., 1994. Seismic and very low frequency sound induced behaviors in captive Loggerhead marine turtles (*Caretta caretta*). In: K.A. Bjorndal, A.B. Bolten, D.A. Johnson, and P.J. Eliazar (compilers), Proceedings of the Fourteenth Annual Symposium on Sea Turtle Biology and Conservation, Hilton Head, SC, U.S. Department of Commerce, National Oceanic and Atmospheric Administration, National Marine Fisheries Service, Southeast Fisheries Science Center, Miami, FL.
- Levin, J., 1970. A Literature Review of the Effects of Sand Removal on a Coral Reef Community. University of Hawaii Sea Grant Program, UNIH-SEA GRANT-TR-71-01, 78 pp.
- Lohofener, R., W. Hoggard, K. Mullin, C. Roden, and C. Rogers, 1990. Association of Sea Turtles with Petroleum Platforms in the North-central Gulf of Mexico. U.S. Department of the Interior, Minerals Management Service, Gulf of Mexico OCS Region, New Orleans, LA, OCS Study MMS 90-0025, 90 pp.
- Louis Berger Group, 1999. Use of Federal Offshore Sand Resources for Beach and Coastal Restoration in New Jersey, Maryland, Delaware, and Virginia. U.S. Department of the Interior, Minerals Management, OCS Study MMS 99-0036, 355 pp.
- Lutcavage, M. and J.A. Musick, 1985. Aspects of the biology of sea turtles in Virginia. *Copeia*, 1985(2): 449-456.
- Lyles, S.D., L.E. Hickman, H.A. Debaugh, 1988. Sea Level Variations for the United States, 1855-1986. U.S. Department of Commerce, National Oceanic and Atmospheric Administration, National Ocean Service, Rockville, MD, 182 pp.
- Lyons, W.G., 1989. Nearshore marine ecology at Hutchinson Island, Florida: 1971-1974. XI. Mollusks. Florida Marine Research Publication 47.
- MacArthur, R.H., 1960. On the relative abundance of species. *American Naturalist*, 94: 25-36.
- MacArthur, R.H. and E.O. Wilson, 1967. *Theory of Island Biogeography*. Princeton University Press, Princeton, NJ, 203 pp.
- Madsen, O.S., 1987. *Mechanics of Sediment Transport in the Wave-Dominated Environment*. ASCE Short Course Notes, Coastal Sediments '87, New Orleans, LA, 94 p.

- Mahon, R., S.K. Brown, K.C.T. Zwanenburg, D.B. Atkinson, K.R. Buja, L. Clafin, G.D. Howell, M.E. Monaco, R.N. O'Boyle, and M. Sinclair, 1998. Assemblages and biogeography of demersal fishes of the east coast of North America. *Canadian Journal of Fisheries and Aquatic Sciences*, 55: 1,704-1,738.
- Malme, C.I., P.R. Miles, C.W. Clark, P. Tyack, and J.E. Bird, 1983. Investigations of the Potential Effects of Underwater Noise from Petroleum Industry Activities on Migrating Gray Whale Behavior. Report by Bolt, Beranek and Newman, Inc., Cambridge, MA, for the U.S. Department of the Interior, Minerals Management Service, Anchorage, AK, BBN Rep. 5366.
- Marine Turtle Expert Working Group, 1996a. Status of the Loggerhead Turtle Population (*Caretta caretta*) in the Western North Atlantic. 50 pp.
- Marine Turtle Expert Working Group, 1996b. Kemp's Ridley Sea Turtle (*Lepidochelys kempii*) Status Report. 49 pp.
- Marquez, R.M., 1990. Sea Turtles of the World. FAO Species Catalogue, Volume 11. FAO, Rome, 81 pp.
- Marsh, G.A. and D.B. Turbeville, 1981. The environmental impact of beach nourishment: two studies in southeastern Florida. *Shore and Beach*, 49(3): 40-44.
- Maurer, D., R.T. Keck, J.C. Tinsman, W.A. Leathem, C. Wethe, C. Lord, and T.M. Church, 1986. Vertical migration and mortality of marine benthos in dredged material: a synthesis. *Internationale Revue der Gesamten Hydrobiologie*, 71: 49-63.
- Mayer, D.A., 1982. The structure of circulation: MESA physical oceanographic studies in New York Bight. *Journal Geophysical Research*, 87: 9579-9588.
- Mayer, D.A., D.V. Hansen, and D.A. Ortman, 1979. Long-term current and temperature observations on the Middle Atlantic shelf. *Journal Geophysical Research*, 84: 1776-1792.
- McBride, R.A. and Moslow, T.F., 1991. Origin, evolution, and distribution of shoreface sand ridges, Atlantic inner shelf, U.S.A. *Marine Geology*, 97: 57-85.
- McBride, R.S. and K.W. Able, 1998. Ecology and fate of butterflyfishes, *Chaetodon* spp., in the temperate, western North Atlantic. *Bulletin of Marine Science*, 63(2): 401-416.
- McCaully, J.E., R.A. Parr, and D.R. Hancock, 1977. Benthic infauna and maintenance dredging: a case study. *Water Research*, 11: 233-242.
- McClennen, C.E., 1973. New Jersey continental shelf near bottom current meter records and recent sediment activity. *Journal of Sedimentary Petrology*, 43(2): 371-380.
- McClennen, C.E., 1983. Middle Atlantic Nearshore Seismic Survey and Sidescan Sonar Survey: Potential Geologic Hazards off the New Jersey Coastline. U.S. Geological Survey Open File Report 83-824, Reston, VA, 30 p.
- McClennen, C.E. and R.L. McMaster, 1971. Probable Holocene transgressive effects on the geomorphic features of the continental shelf off New Jersey, United States. *Maritime Sediment*, 7: 69-72.
- McGraw, K.A. and D.A. Armstrong, 1988. Fish entrainment by dredges in Grays Harbor, Washington. In: C.A. Simenstad (editor), *Effects of Dredging on Anadromous Pacific Coast Fishes*, Workshop Proceedings, University of Washington Sea Grant, pp. 113-131.
- McKinney, T.F. and G.M. Friedman, 1970. Continental shelf sediments of Long Island, New York. *Journal of Sedimentary Petrology*, 40: 213-248.
- McNulty, J.K., R.C. Work, and H.B. Moore, 1962. Some relationships between the infauna of the level bottom and the sediment in South Florida. *Bulletin of Marine Science in the Gulf and Caribbean*, 12: 322-332.
- Michals, R., 1997. There's a hole in the bottom of the sea. *Florida Sportsman*, 29(1): 21-28.
- Mid-Atlantic Fishery Management Council, 1998a. Amendment 12 to the Atlantic Surfclam and Ocean Quahog Fishery Management Plan. Mid-Atlantic Fishery Management Council, Dover, DE, 249 pp.
- Mid-Atlantic Fishery Management Council, 1998b. Amendment 8 to the Atlantic Mackerel, Squid, and Butterfish Fishery Management Plan. Mid-Atlantic Fishery Management Council, Dover, DE, 351 pp. + apps.
- Mid-Atlantic Fishery Management Council, 1998c. Amendment 12 to the Summer Flounder, Scup, and Black Sea Bass Fishery Management Plan. Mid-Atlantic Fishery Management Council, Dover, DE, 398 pp. + apps.
- Mid-Atlantic Fishery Management Council, 1998d. Amendment 1 to the Bluefish Fishery Management Plan. Mid-Atlantic Fishery Management Council, 2 Vols., Dover, DE, 341 pp. + apps.

- Mid-Atlantic Fishery Management Council, 1999. The Spiny Dogfish Fishery Management Plan. Mid-Atlantic Fishery Management Council, 292 pp. + apps.
- Miller, A.R., 1952. Pattern of Surface Coastal Circulation Inferred from Surface-Temperature Data and Drift Bottle Recoveries. Woods Hole Oceanographic Institution Ref. No. 52-28.
- Miller, M.L., 1993. The rise of coastal marine tourism. *Ocean and Coastal Management*, 20: 181-199.
- Moein, S.E., J.A. Musick, J.A. Keinath, D.E. Barnard, M.L. Lenhardt, and R. George, 1994. Evaluation of Seismic Sources for Repelling Sea Turtles from Hopper Dredges. Virginia Institute of Marine Science, College of William and Mary, Gloucester Point, VA, final contract report to U.S. Army Engineer Waterways Experiment Station. As excerpted in: Sea Turtle Research Program Summary Report. Prepared by U.S. Army Engineer Waterways Experiment Station, Vicksburg, MS for U.S. Army Engineer Division, South Atlantic, Atlanta, GA and U.S. Naval Submarine Base, Kings Bay, GA, Technical Report CHL-97-31, NTIS ADA332588, 147 pp.
- Moody, J.A., B. Butman, R.C. Beardsley, W.S. Brown, P. Daifuku, J.D. Irish, D.A. Mayer, H.O. Mofjeld, B. Petrie, S. Ramp, P. Smith, and W.R. Wright, 1983. Atlas of Tidal Elevation and Current Observations on the Northeast American Continental Shelf and Slope. U.S. Geological Survey Bulletin Survey Bulletin 1611, 122 pp.
- Moore, P.G., 1977. Inorganic particulate suspensions in the sea and their effects on marine animals. *Oceanography and Marine Biology Annual Review*, 15: 225-363.
- Morang, A., D.S. Rahoy, and W.G. Grosskopf, 1999. Regional geologic characteristics along the south shore of Long Island, New York. In: N.C. Kraus and W.G. McDougal (editors), *Coastal Sediments '99*, American Society of Civil Engineers, New York, NY, pp. 1568 – 1583.
- Morreale, S., A. Meylan, S. Sadove, and E. Standora, 1992. Annual occurrence and winter mortality of marine turtles in New York waters. *Journal of Herpetology*, 26(3): 301-308.
- Mortimer, J.A., 1982. Feeding ecology of sea turtles. In: K.A. Bjorndal (editor), *Biology and Conservation of Sea Turtles*. Smithsonian Institution Press, Washington, DC, pp. 103-109.
- Murawski, W.S., 1969. A Study of Submerged Dredge Holes in New Jersey Estuaries with Respect to their Fitness as Finfish Habitat. New Jersey Department of Conservation and Economic Development, Division of Fish and Game, Miscellaneous Report No. 2M, 32 pp.
- Myrberg, A.A., Jr. and L.A. Fuiman, 2002. The sensory world of coral reef fishes. In: P.F. Sale (ed.), *Coral Reef Fishes: Dynamics and Diversity in a Complex Ecosystem*. Academic Press, San Diego, CA, pp.123-148.
- Naqvi, S. and E. Pullen, 1982. Effects of Beach Nourishment and Borrowing on Marine Organisms. U.S. Army Corps of Engineers, Coastal Engineering Research Center, Fort Belvoir, VA, Miscellaneous Report No. 82-14.
- National Audubon Society, 2002. National Audubon Society Guide to the Marine Mammals of the World. A. Knopf, NY, 527 pp.
- National Marine Fisheries Service, 1991a. Recovery Plan for the Humpback Whale (*Megaptera novaeangliae*). Prepared by the Humpback Whale Recovery Team for the National Marine Fisheries Service, Silver Spring, MD, 105 pp.
- National Marine Fisheries Service, 1991b. Recovery Plan for the Northern Right Whale (*Eubalaena glacialis*). Prepared by the Right Whale Recovery Team for the National Marine Fisheries Service, Silver Spring, MD, 86 pp.
- National Marine Fisheries Service, 1996. Endangered Species Act, Section 7 Consultation, Biological Opinion Concerning Dredging Activities Within the Philadelphia District of the U.S. Department of the Army. Prepared by the National Marine Fisheries Service, Northeast Regional Office, 43 pp.
- National Marine Fisheries Service, 1997. Regional Biological Opinion for Hopper Dredging of Channels and Beach Nourishment Activities in the Southeastern United States from North Carolina through Florida East Coast. October 1997.
- National Marine Fisheries Service, 1998. Marine Mammal Protection Act of 1972 Annual Report, January 1, 1997 to December 31, 1997. Office of Protected Resources, National Marine Fisheries Service, Silver Spring, MD.
- National Marine Fisheries Service, 1999. Fishery Management Plan for Atlantic Tunas, Swordfish, and Sharks, Volume II. National Marine Fisheries Service Division of Highly Migratory Species, Office of Sustainable Fisheries, Silver Spring, MD, 302 pp.
- National Marine Fisheries Service and U.S. Fish and Wildlife Service, 1991. Recovery Plan for U.S. Population of Atlantic Green Turtle. National Marine Fisheries Service, Washington, DC, 52 pp.

- National Marine Fisheries Service and U.S. Fish and Wildlife Service, 1992. Recovery Plan for the Kemp's Ridley Sea Turtle (*Lepidochelys kempii*). National Marine Fisheries Service, St. Petersburg, FL, 40 pp.
- National Oceanic and Atmospheric Administration, National Climatic Data Center, 2002. Climate of 2002 - Preliminary Annual Review, U.S. Summary.
<http://lwf.ncdc.noaa.gov/oa/climate/research/2002/ann/ann02.html>.
- National Research Council, 1995. Beach Nourishment and Protection. National Academy Press, 334 pp.
- Nelson, W.G., 1985. Physical and Biological Guidelines for Beach Restoration Projects. Part 1. Biological Guidelines. Florida Sea Grant College Program, Report No. 76.
- Nelson, W.G., 1988. An overview of the effects of beach nourishment on the sand beach fauna. In: Proceedings of the 1988 National Conference on Beach Preservation Technology, Florida Shore and Beach Preservation Association, Tallahassee, FL, pp. 295-310.
- Nelson, W.G., 1989. Beach nourishment and hard bottom habitats: the case for caution. In: Proceedings of the 1989 National Conference on Beach Preservation Technology, Florida Shore and Beach Preservation Association, Tallahassee, FL, pp. 109-116.
- New England Aquarium, 2004. Right Whale Research. <http://www.neaq.org/scilearn/research/rtwhale.html>.
- New England Fishery Management Council, 1998. Amendment 11 to the Northeast Multispecies Fishery Management Plan, Amendment 9 to the Atlantic Sea Scallop Fishery Management Plan, Amendment 1 to the Monkfish Fishery Management Plan, Amendment 1 to the Atlantic Salmon Fishery Management Plan, Components of the Proposed Atlantic Herring Fishery Management Plan for Essential Fish Habitat, Volume 1. Prepared by the New England Fishery Management Council, Newburyport, MA.
- New England Fishery Management Council, 2004. Draft Amendment 2 to the Monkfish Fishery Management Plan Including a Draft Supplemental Environmental Impact Statement (DSEIS), Preliminary Regulatory Economic Evaluation, and Stock Assessment and Fishery Evaluation (SAFE) Report for the 2002 Fishing Year. Prepared by the New England Fishery Management Council, Mid-Atlantic Fishery Management Council, and National Marine Fisheries Service.
- Newcombe, C.P. and J.O.T. Jensen, 1996. Channel suspended sediment and fisheries: a synthesis for quantitative assessment of risk and impact. *North American Journal of Fisheries Management*, 16(4): 693-727.
- Newell, R.C., L.J. Seiderer, and D.R. Hitchcock, 1998. The impact of dredging works in coastal waters: A review of the sensitivity to disturbance and subsequent recovery of biological resources on the seabed. *Oceanography and Marine Biology Annual Review*, 36: 127-178.
- Newell, R.C., D.R. Hitchcock, and L.J. Seiderer, 1999. Organic enrichment associated with outwash from marine aggregates dredging: A probable explanation for surface sheens and enhanced benthic production in the vicinity of dredging operations. *Marine Pollution Bulletin*, 38(9): 809-818.
- Nichols, M., R.J. Diaz, and L.C. Shaffner, 1990. Effects of hopper dredging and sediment dispersion, Chesapeake Bay. *Environmental Geology and Water Science*, 15: 31-43.
- Noble, M., B. Butman, and E. Williams, 1983. On the longshelf structure and dynamics of subtidal currents on the eastern United States Continental Shelf. *Journal Physical Oceanography*, 13(12): 2125-2147.
- Nordstrom, K.F., S.F. Fisher, M.A. Burr, E.L. Frankel, T.C. Buckalew, and G.A. Kucma, 1977. The Coastal Geomorphology of New Jersey. Center for Coastal and Environmental Studies Technical Report NJ/RU-OCZM-TR 1-200-12/77, 129 pp.
- Nyman, R.M. and D.O. Conover, 1988. The relation between spawning season and the recruitment of young-of-the-year bluefish, *Pomatomus saltatrix*, to New York. *Fishery Bulletin*, 86(2): 237-250.
- Oakwood Environmental Ltd., 1999. Strategic Cumulative Effects of Marine Aggregates Dredging (SCEMAD). Prepared for the U.S. Department of the Interior, Minerals Management Service, 175 pp.
- Odum, E.P., 1969. The strategies of ecosystem development. *Science*, 16: 262-270.
- Onuf, C.P., 1994. Seagrasses, dredging, and light in Laguna Madre, Texas, U.S.A. *Estuarine, Coastal and Shelf Science*, 39: 75-91.
- Overholtz, W., 1998a. Atlantic Mackerel. In: S.H. Clark (editor), Status of Fishery Resources off the Northeastern United States for 1998. U.S. Department of Commerce, NOAA Technical Memorandum NMFS-NE-115, pp. 106-107.

- Overholtz, W., 1998b. Butterfish. In: S.H. Clark (editor), Status of Fishery Resources off the Northeastern United States for 1998. U.S. Department of Commerce, NOAA Technical Memorandum NMFS-NE-115, pp. 108-109.
- Oviatt, C.A., C.D. Hunt, G.A. Vargo, and K.W. Kopchynski, 1982. Simulation of a storm event in a marine microcosm. *Journal of Marine Research*, 39: 605-618.
- Owen, R.M., 1977. An assessment of the environmental impact of mining on the continental shelf. *Marine Mining*, 1(1/2): 85-102.
- Palermo, M.R., 1990. Workgroup 2 Summary. In: D.D. Dickerson and D.A. Nelson (compilers), Proceedings of the National Workshop on Methods to Minimize Dredging Impacts on Sea Turtles, Jacksonville, FL. U.S. Army Engineer Waterways Experiment Station, Vicksburg, MS, Miscellaneous Paper EL-90-5, pp. 76-80.
- Parker, P., 1967. Clam survey, Ocean City, Maryland to Cape Charles, Virginia. *Commercial Fisheries Review*, 29(5): 53-77.
- Parker, P. and L. Fahlen, 1968. Clam survey off Virginia (Cape Charles to False Cape). *Commercial Fisheries Review*, 30(1): 25-36.
- Parker, P.C., 1996. Nearshore Ridges and Underlying Upper Pleistocene Sediments on the Inner Continental Shelf of New Jersey. Masters Thesis, Rutgers University, NJ, 157 pp.
- Pawlowicz, R., Beardsley, B., and Lentz, S., 2002. Classical tidal harmonic analysis including error estimates in MATLAB using T_TIDE. *Computers and Geosciences*, 28(8): 929-937.
- Pearce, J.B., J.V. Caracciolo, M.B. Halsey, and L.H. Rogers, 1976. Temporal and spatial distributions of benthic macroinvertebrates in the New York Bight. In: G. Gross (ed.), Middle Atlantic Continental Shelf and the New York Bight, Proceedings of the Symposium, American Museum of Natural History, New York City, 1975. American Society of Limnology and Oceanography, Inc., Allen Press, Inc., Lawrence, KS, pp. 394-403.
- Pearce, J.B., D.J. Radosh, J.V. Caracciolo, and F.W. Steimle, Jr., 1981. Benthic Fauna: Marine EcoSystems Analysis (MESA) Program, MESA New York Bight Project. MESA New York Bight Atlas Monograph 14, New York Sea Grant Institute, Albany, NY, 79 pp.
- Peddicord, R.K. and V.A. McFarland, 1978. Effects of Suspended Dredged Material on Aquatic Animals. U.S. Army Engineer Waterways Experiment Station, Vicksburg, MS, Technical Report D-78-29, 102 pp. + app.
- Peterson, C.G.J., 1913. Valuation of the Sea. II. The Animal Communities of the Sea-Bottom and Their Importance for Marine Zoogeography. Report of the Danish Biological Station to the Board of Agriculture, 21: 1-44.
- Phinney, H.K., 1959. Turbidity, Sedimentation, and Photosynthesis. Proceedings of the Symposium on Siltation, Its Effects on the Aquatic Environment (Portland). U.S. Public Health Service, pp. 4-12.
- Pianka, E.R., 1970. On R- and K-selection. *American Naturalist*, 104: 592-597.
- Pielou, E.C., 1966. Species-diversity and pattern-diversity in the study of ecological succession. *Journal of Theoretical Biology*, 10: 370-383.
- Poiner, I.R. and R. Kennedy, 1984. Complex pattern of change in the macrobenthos of a large sandbank following dredging. I. community analysis. *Marine Biology*, 78: 335-352.
- Polloni C., L.J. Poppe, M.E. Hastings, and K. Joy, 2000. Chapter 3: Visualizing Sediment Data Layers Using Geographic Mapping Tools USGS East-Coast Sediment Analysis: Procedures, Database, and Georeferenced Displays, USGS Open-File Report 00-358. <http://pubs.usgs.gov/of/of00-358/text/chapter3.htm#DATA%20LAYERS>
- Poppe, L.J., J.S. Schlee, and H.J. Knebel, 1994. Map Showing Distribution of Surficial Sediment on the Mid-Atlantic Continental Margin, Cape Cod to Ablemarle Sound. U.S. Geological Survey, Miscellaneous Investigations Series, Map I-1987-D.
- Quinn, M.L., 1977. The History of the Beach Erosion Board. U.S. Army Corps of Engineers, Coastal Engineering Research Center, Miscellaneous Report 77-9, Vicksburg, MS, 181 pp.
- Reeves, R., B. Stewart, and S. Leatherwood, 1992. The Sierra Club Handbook of Seals and Sirenians. Sierra Club Books, San Francisco, 359 pp.
- Reeves, R.R., G.K. Silber, and P.M. Payne, 1998. Draft Recovery Plan for the Fin Whale, *Balaenoptera physalus* and Sei whale, *Balaenoptera borealis*. Prepared for the Office of Protected Resources, National Marine Fisheries Service, Silver Spring, MD, 65 pp.

- Reid, R.N., D.J. Radosh, A.B. Frame, and S.A. Fromm, 1991. Benthic Macrofauna of the New York Bight. U.S. Department of Commerce, National Marine Fisheries Service, NOAA Tech. Rep. NMFS 103, 50 pp.
- Reid, R.N., L.M. Cargnelli, S.J. Griesbach, D.B. Packer, D.L. Johnson, C.A. Zetlin, W.W. Morse, and P.L. Berrien, 1999. Essential Fish Habitat Source Document: Atlantic Herring, *Clupea harengus*, Life History and Habitat Characteristics. U.S. Department of Commerce, National Marine Fisheries Service, National Oceanic and Atmospheric Administration (NOAA), NOAA Technical Memorandum NMFS-NE-126.
- Reine, K.J. and D.G. Clarke, 1998. Entrainment by Hydraulic Dredges - A Review of Potential Impacts. U.S. Army Engineer Research and Development Center, Vicksburg, MS, Dredging Operations and Environmental Research Technical Notes Collection, TN DOER-E1.
- Reine, K.J., D.D. Dickerson, and D.G. Clarke, 1998. Environmental Windows Associated with Dredging Operations. U.S. Army Engineer Research and Development Center, Vicksburg, MS, DOER Technical Note TN DOER-E2.
- Renaud, P.E., W.G. Ambrose, S.R. Riggs, and D.A. Syster, 1996. Multi-level effects of severe storms on an offshore temperate hard-bottom system: benthic sediments, macroalgae, and implications for fisheries. *Marine Ecology*, 17: 383-398.
- Renaud, P.E., S.R. Riggs, W.G. Ambrose, Jr., K.A. Schmid, and S.W. Snyder, 1997. Biological-geological interactions: storm effects on microalgal communities mediated by sediment characteristics and distribution. *Continental Shelf Research*, 17(1): 37-56.
- Revsbech, N.P., J. Sørensen, and T.H. Blackburn, 1980. Distribution of oxygen in marine sediments measured with microelectrodes. *Limnology and Oceanography*, 25: 403-411.
- Rhoads, D.C., 1974. Organism-sediment relations on the muddy seafloor. *Oceanography and Marine Biological Annual Review*, 12: 263-300.
- Rhoads, D.C. and L.F. Boyer, 1982. The effects of marine benthos on physical properties of sediments: a successional perspective. In: P.L. McCall and M.J.S. Tevesz (editors), *Animal-Sediment Relations, The Biogenic Alteration of Sediments*. Plenum Press, New York, NY, pp. 3-52.
- Rhoads, D.C. and J.D. Germano, 1982. Characterization of organism-sediment relations using sediment profile imaging: An efficient method of remote ecological monitoring of the seafloor (REMOTS™ System). *Marine Ecology Progress Series*, 8: 115-128.
- Rhoads, D.C. and J.D. Germano, 1986. Interpreting long-term changes in benthic community structure: a new protocol. *Hydrobiologia*, 142: 291-308.
- Rhoads, D.C., P.L. McCall, and J.Y. Yingst, 1978. Disturbance and production on the estuarine seafloor. *American Science*, 66: 577-586.
- Richardson, W.J., C.R. Greene, Jr., C.I. Malme, and D.H. Thomson, 1995. *Marine Mammals and Noise*. Academic Press, San Diego, 576 pp.
- Ridgway, S.H., E.G. Wever, J.G. McCormick, J. Palin, and J.H. Anderson, 1969. Hearing in the giant sea turtle, *Chelonia mydas*. *Proceedings of the National Academy of Sciences*, 64(3): 884-890.
- Robins, C.R., 1957. Effects of storms on the shallow-water fish fauna of southern Florida with records of fishes from Florida. *Bulletin of Marine Science in the Gulf and Caribbean*, 7(3): 266-275.
- Roden, C., 1998. Cruise Results: Summer Atlantic Marine Mammal Survey, NOAA Ship Relentless Cruise RS 98-01(3). National Marine Fisheries Service, Southeast Fisheries Science Center, Mississippi Laboratories, Pascagoula Facility, Pascagoula, MS.
- Rogers, C.S., 1990. Responses of coral reefs and reef organisms to sedimentation. *Marine Ecology Progress Series*, 62: 185-202.
- Rosati, J.D., M.B. Gravens, W.G. Smith, 1999. Regional sediment budget for Fire Island to Montauk Point, New York, USA. In: N.C. Kraus and W.G. McDougal (editors), *Coastal Sediments '99*, American Society of Civil Engineers, New York, NY, pp. 802-817.
- Rosati, J.D., T.L. Walton, and K. Bodge, 2002. Longshore Sediment Transport. In: Walton, T.L. (editor), *Coastal Engineering Manual, Part III, Coastal Sediment Processes, Chapter III-2, Engineer Manual 1110-2-1100*, U.S. Army Corps of Engineers, Washington, DC.
- Rosman, I., G.S. Boland, L. Martin, and C. Chandler, 1987. Underwater Sightings of Sea Turtles in the Northern Gulf of Mexico. U.S. Department of the Interior, Minerals Management Service, Gulf of Mexico OCS Region, New Orleans, LA, OCS Study MMS 87-0107, 37 pp.

- Rotunno, T. and R.K. Cowen, 1997. Temporal and spatial spawning patterns of the Atlantic butterfish, *Peprilus triacanthus*, in the South and Middle Atlantic Bights. *Fishery Bulletin*, 95(4): 785-799.
- Saloman, C.H., 1974. Physical, Chemical, and Biological Characteristics of Nearshore Zone of Sand Key, Florida, Prior to Beach Restoration. National Marine Fisheries Service, Gulf Coastal Fisheries Center, Panama City Laboratory, Panama City, FL.
- Saloman, C.H., S.P. Naughton, and J.L. Taylor, 1982. Benthic Community Response to Dredging Borrow Pits, Panama City Beach, Florida. U.S. Army Corps of Engineers, Coastal Engineering Research Center, Fort Belvoir, VA, Miscellaneous Report No. 82-3, 138 pp.
- Sanders, H.L., 1958. Benthic studies in Buzzards Bay: animal-sediment relationships. *Limnology and Oceanography*, 3: 245-258.
- Sanders, J.E. and N. Kumar, 1975. Holocene shoestring sand on the inner continental shelf off Long Island, New York. *American Association of Petroleum Geologists Bulletin*, 59: 997-1,009.
- SAS Institute Inc., 1989. SAS/STAT Users Guide, Version 6, Fourth Edition, Volume 1. SAS Institute Inc., Cary, NC, 943 pp.
- Sastry, A.N., 1978. Physiology and ecology of reproduction in marine invertebrates. In: F.J. Vernberg (ed.), *Physiological Ecology of Estuarine Organisms*. University of South Carolina Press, Columbia, SC, pp. 279-299.
- Schaeff, C.M., S.D. Kraus, M.W. Brown, and B.N. White, 1993. Assessment of the population structure of western North Atlantic right whales (*Eubalaena glacialis*) based on sighting and mtDNA data. *Canadian Journal of Zoology*, 71(2): 339-345.
- Schaffner L.C. and D.F. Boesch, 1982. Spatial and temporal resource use by dominant benthic Amphipoda (*Ampeliscidae* and *Corophiidae*) on the Middle Atlantic Bight outer continental shelf. *Marine Ecology Progress Series*, 9: 231-243.
- Scheffner, N.W., S.R. Vemulakonda, D.J. Mark, H.L. Butler, and K.W. Kim, 1994. New York Bight Study Report 1: Hydrodynamic Modeling. Technical Report CERC-94-4, U.S. Army Corps of Engineers, Waterways Experiment Station, Vicksburg, MS, 150 pp. + Appendices.
- Schlee, J.S., 1964. New Jersey offshore gravel deposit. *Pit and Quarry*, 57: 80-81.
- Schwab, W.C., M.A. Allison, W. Corso, L.L. Lotto, B. Butman, M. Buchholtz ten Brink, J.F. Denny, W.W. Danforth, and D.S. Foster, 1997. Initial results of high-resolution sea-floor mapping offshore of the New York-New Jersey metropolitan area using sidescan sonar. *Northeastern Geology and Environmental Sciences*, 19(4): 243-267.
- Schwab, W.C., R.T. Thielier, J.S. Allen, D.S. Foster, A.S. Swift, J.F. Denny, and W.W. Danforth, 1999. Geologic mapping of the nearshore area offshore Fire Island, NY. In: N.C. Kraus and W.G. McDougal (editors), *Coastal Sediments '99*, American Society of Civil Engineers, New York, NY, pp. 1552-1567.
- Schwab, W.C., E.R. Thielier, J.F. Denny, W.W. Danforth, and J.C. Hill, 2000a. Seafloor Sediment Distribution Off Southern Long Island, New York. U.S. Geological Survey, Open File Report 00-243.
- Schwab, W.C., J.F. Denny, B. Butman, W.W. Danforth, D.S. Foster, B.A. Swift, L.L. Lotto, M.A. Allison, E.R. Thielier, and J.C. Hill, 2000b. Seafloor Characterization Offshore of the New York-New Jersey Metropolitan Area Using Sidescan-Sonar. U.S. Geological Survey, Open File Report 00-295.
- Schwab, W.C., E.R. Thielier, J.R. Allen, D.S. Foster, B.A. Swift, J.F. Denny, 2000c. Influence of inner-continental shelf framework on the evolution and behavior of the barrier-island system between Fire Island Inlet and Shinnecock Inlet, Long Island, New York. *Journal of Coastal Research*, 16(2): 408-422.
- Schwab, W.C., J.F. Denny, D.S. Foster, L.L. Lotto, M.A. Allison, E. Uchupi, W.W. Danforth, B.A. Swift, E.R. Thielier, and B. Butman, 2002. High-Resolution Quaternary Seismic Stratigraphy of the New York Bight Continental Shelf. USGS Open-File Report 02-152.
- Scott, L.C. and F.S. Kelley, 1998. An Evaluation and Comparison of Benthic Community Assemblages and Surf Clam Populations Within the Offshore Sand Borrow Site for the Great Egg Harbor Inlet and Peck Beach, Ocean City, New Jersey Project. Prepared for the U.S. Army Corps of Engineers, Philadelphia District, Philadelphia, PA by Versar, Inc., Columbia, MD, 36 pp. + app.
- Shalowitz, A.L., 1964. Shoreline and Sea Boundaries, Volume 2. U.S. Department of Commerce Publication 10-1, U.S. Coast and Geodetic Survey, U.S. Government Printing Office, Washington, DC, 420 pp.

- Shaver, D.J., 1991. Feeding ecology of wild and headstarted Kemp's Ridley sea turtles in south Texas waters. *Journal of Herpetology*, 25(3): 327-334.
- Sherk, J.A., Jr., 1971. The Effects of Suspended and Deposited Sediment on Estuarine Organisms: Literature Summary and Research Needs. University of Maryland, Natural Resources Institute, Chesapeake Biological Laboratory Contribution No. 43, 73 pp.
- Sherk, J.A., Jr., 1972. Current status of the knowledge of the biological effects of suspended and deposited sediments in Chesapeake Bay. *Chesapeake Science*, 13 (Supplement): S137-S144.
- Sherk, J.A., Jr. and L.E. Cronin, 1970. The Effects of Suspended and Deposited Sediments on Estuarine Organisms, an Annotated Bibliography of Selected References. University of Maryland, Chesapeake Biological Laboratory, Natural Resources Institute, Reference No. 70-19, 62 pp.
- Sherk, J.A., J.M. O'Connor, and D.A. Newman, 1975. Effects of suspended and deposited sediments on estuarine environments. In: L.F. Cronin (editor), *Estuarine Research Volume 2*. Academic Press, New York, NY, pp. 541-558.
- Shoop, C.R. and R.D. Kenney, 1992. Seasonal distributions and abundances of loggerhead and leatherback sea turtles in waters of the northeastern United States. *Herpetological Monographs*, 6: 43-67.
- Slay, C.K., 1995. Sea turtle mortality related to dredging activities in the southeastern U.S.: 1991. In: J.I. Richardson and T.H. Richardson (compilers), *Proceedings of the Twelfth Annual Workshop on Sea Turtle Biology and Conservation*, Jekyll Island, GA, NOAA Technical Memorandum NMFS-SEFSC-361, pp. 132-133.
- Smith, P.C., 1996. Nearshore Ridges and Underlying Upper Pleistocene Sediments on the Inner Continental Shelf of New Jersey. Masters Thesis, Rutgers University, Geological Sciences, New Brunswick, NJ, 157pp.
- Smith, J.J. and S.P. Leatherman, 2000. Erosion anomaly on eastern Jones Beach Island, New York: genesis and management implications. *Shore and Beach*, 68(3): 29-32.
- Smith, W., P. Berrien, and T. Potthoff, 1994. Spawning patterns of bluefish, *Pomatomus saltatrix*, in the northeast continental shelf ecosystem. *Bulletin of Marine Science*, 54(1): 8-15.
- Smith, W.G., K. Watson, D. Rahoy, C. Rasmussen, and J.R. Headland, 1999. Historic geomorphology and dynamics of Fire Island, Moriches, and Shinnecock Inlets, New York. In: N.C. Kraus and W.G. McDougal (editors), *Coastal Sediments '99*, American Society of Civil Engineers, New York, NY, pp. 1597-1612.
- Snedden, J.W., R.W. Tillman, R.D. Kreisa, W.J. Schweller, S.J. Culver, and R.D. Winn, 1994. Stratigraphy and genesis of a modern shoreface-attached sand ridge, Peahala Ridge, New Jersey. *Journal of Sedimentary Research, Section B: Stratigraphy and Global Studies*, B64(4): 560-581.
- Snelgrove, P.V.R. and C.A. Butman, 1994. Animal-sediment relationships revisited: cause versus effect. *Oceanography and Marine Biology Annual Review*, 32: 111-177.
- Sosnowski, R.A., 1984. Sediment resuspension due to dredging and storms: an analogous pair. In: R.L. Montgomery and J.W. Leach (eds.), *Conference Proceedings, Dredging '84, Dredging and Dredged Material Disposal*, 14-16 November 1984, Clearwater Beach, FL, American Society of Civil Engineers, pp. 609-618.
- Steimle, F.W., Jr. and R.B. Stone, 1973. Abundance and Distribution of Inshore Benthic Fauna off Southwestern Long Island, N.Y. NOAA Technical Report SSRF-673, U.S. Department of Commerce, National Oceanic and Atmospheric Administration, National Marine Fisheries Service, Seattle, WA.
- Steimle, F.W., W.W. Morse, P.L. Berrien, and D.L. Johnson, 1999. Essential Fish Habitat Source Document: Red Hake, *Urophycis chuss*, Life History and Habitat Characteristics. U.S. Department of Commerce, National Marine Fisheries Service, National Oceanic and Atmospheric Administration (NOAA), NOAA Technical Memorandum NMFS-NE-133.
- Stephenson, W.W.T., S.D. Cook, and S.J. Newland, 1978. The macrobenthos of the Middle Banks of Moreton Bay. *Memoirs of the Queensland Museum*, 18: 95-118.
- Stern, E.M. and W.B. Stickle, 1978. Effects of Turbidity and Suspended Material in Aquatic Environments: Literature Review. U.S. Army Engineer Waterways Experiment Station, Vicksburg, MS, Technical Report D-78-21, 117 pp.
- Steves, B.P., R.K. Cowen, and M.H. Malchoff. 1999. Settlement and nursery habitats for demersal fishes on the continental shelf of the New York Bight. *Fishery Bulletin*, 98: 167-188.
- Stobutzki, I.C. and D.R. Bellwood, 1998. Nocturnal orientation to reefs by late pelagic stage coral reef fishes. *Coral Reefs*, 17: 103-110.

- Stoffer, P. and P. Messina, 1996. Geology and Geography of New York Bight Beaches. <http://www.geo.hunter.cuny.edu/bight/index.html>
- Stubblefield, W.L., J.W. Lavelle, D.J.P. Swift, and T.F. McKinney, 1975. Sediment response to the present hydraulic regime on the central New Jersey shelf. *Journal of Sediment Petrology*, 45: 337-358.
- Stubblefield, W.L., D.W. McGrail, and D.G. Kersey, 1984. Recognition of transgressive and post-transgressive sand ridges on the New Jersey continental shelf. In: R.W. Tillman and C.T. Siemers (editors), *Siliclastic Shelf Sediments*, Society of Economic Paleontologists and Mineralogists, Special Publication 34: 1-23.
- Studt, J.F., 1987. Amelioration of maintenance dredging impacts on sea turtles, Canaveral Harbor, Florida. In: W. Witzell (editor), *Ecology of East Florida Sea Turtles*. Proceedings of the Cape Canaveral, Florida Sea Turtle Workshop, Miami, FL, NOAA Technical Report NMFS 53, pp. 55-58.
- Sullivan, M.C., R.K. Cowen, K.W. Able, and M.P. Fahay, 2000. Spatial scaling of recruitment in four continental shelf fishes. *Marine Ecology Progress Series*, 207: 141-154.
- Swift, D.J.P., 1976. Continental shelf sedimentation. In: D.J. Stanley and D.J.P. Swift (editors), *Marine Sediment Transport and Environmental Management*. Wiley and Sons, New York, NY, pp. 311-350.
- Swift, D.J.P., J.W. Kofoed, F.P. Salsbury, and P. Sears, 1972. Holocene evolution of the shelf surface, central and southern Atlantic shelf of North America. In: D.J.P. Swift, D.B. Duane, and O.H. Pilkey (editors), *Shelf Sediment Transport: Process and Pattern*. Dowden Hutchinson, and Ross. Stroudsburg, PA, pp. 499-575.
- Swingle, W.M., S.G. Barco, T.D. Pitchford, W.A. McLellan, and D.A. Pabst, 1993. Appearance of juvenile humpback whales feeding in the nearshore waters of Virginia. *Marine Mammal Science*, 9(3): 309-315.
- Taney, N.E., 1961. Geomorphology of the South Shore of Long Island, New York. U.S. Army Corps of Engineers, Beach Erosion Board, Washington DC, TM No. 128.
- Taylor, A.S., 1990. The Hopper Dredge. In: D.D. Dickerson and D.A. Nelson (compilers), *Proceedings of the National Workshop on Methods to Minimize Dredging Impacts on Sea Turtles*, Jacksonville, FL, U.S. Army Engineer Waterways Experiment Station, Vicksburg, MS, Miscellaneous Paper EL-90-5, pp. 59-63.
- Tenore, K.R., 1985. Seasonal changes in soft bottom macrofauna of the U.S. South Atlantic Bight. In: L.P. Atkinson, D.W. Menzel, and K.A. Bush (eds.), *Oceanography of the Southeastern U.S. Continental Shelf*. American Geophysical Union, Washington, DC, pp. 130-140.
- Terciero, M., 1998. Bluefish. In: S.H. Clark (editor), *Status of Fishery Resources off the Northeastern United States for 1998*. U.S. Department of Commerce, NOAA Technical Memorandum NMFS-NE-115, pp. 110-111.
- Thayer, C.W., 1983. Sediment-mediated biological disturbance and the evolution of marine benthos. In: M.J.S. Tevesz and P.L. McCall (editors), *Biotic Interactions in Recent and Fossil Benthic Communities*. Plenum Press, NY, pp. 479-625.
- Theroux, R.B. and R.L. Wigley, 1998. Quantitative Composition and Distribution of the Macrobenthic Invertebrate Fauna of the Continental Shelf Ecosystems of the Northeastern United States. U.S. Department of Commerce, NOAA Technical Report NMFS 140, 240 pp.
- Thistle, D., 1981. Natural physical disturbances and communities of marine soft bottoms. *Marine Ecology Progress Series*, 6: 223-228.
- Thompson, J.R., 1973. Ecological Effects of Offshore Dredging and Beach Nourishment: A Review. U.S. Army Engineer Waterways Experiment Station MP 1-73, U.S. Army Corps of Engineers, Coastal Engineering Research Center, Fort Belvoir, VA, Report 1-73.
- Thorson, G., 1957. Bottom communities (sublittoral or shallow shelf). *Geological Society of America Memoir*, 67: 461-534.
- Thorson, G., 1964. Light as an ecological factor in the dispersal and settlement of larvae of marine bottom invertebrates. *Ophelia*, 1(1): 167-208.
- Thorson, G., 1966. Some factors influencing the recruitment and establishment of marine benthic communities. *Netherlands Journal of Sea Research*, 3(2): 267-293.
- Tolimieri, N., A. Jeffs, and J. Montgomery, 2000. Ambient sound as a cue for navigation by the pelagic larvae of reef fishes. *Marine Ecology Progress Series*, 207: 219-224.
- Turbeville, D.B. and G.A. Marsh, 1982. Benthic Fauna of an Offshore Borrow Area in Broward County, Florida. U.S. Army Corps of Engineers, Coastal Engineering Research Center, Miscellaneous Report 82-1, 43 pp.

- Uchupi, E., 1968. Atlantic Continental Shelf and Slope of the United States – Physiography. U.S. Geological Survey Professional Paper 529-C, 30 p.
- Uchupi, E., 1970. Atlantic Continental Shelf and Slope of the United States – Shallow Structure. Professional Paper 529-1, U.S. Geological Survey, Washington DC, 1970.
- Uptegrove, J., L.G. Mullikin, J.S. Waldner, G. Ashley, R.E. Sheridan, D.W. Hall, J.T. Gilroy, and S.C. Farrell, 1995. Characterization of Offshore Sediments in Federal Waters as Potential Sources of Beach Replenishment Sand – Phase I. New Jersey Geological Survey Open File Report 95-1, New Jersey Department of Environmental Protection Division of Science and Research Geological Survey, Trenton, NJ.
- Uptegrove, J., J.S. Waldner, D.W. Hall, P.C. Smith, G.M. Ashley, R.E. Sheridan, Z. Allen-Lafayette, M.C. Goss, F.L. Muller, and E. Keller, 1997. Characterization of Offshore Sediments in Federal Waters as Potential Sources of Beach Replenishment Sand – Phase II. Final Report to U.S. Minerals Management Service, Cooperative #14-35-0001-30751, New Jersey Geological Survey, Trenton, NJ, 28 p.
- USACE, 1971. National Shoreline Study Report. Washington, DC.
- USACE, 1990. Sea Bright to Ocean Township General Design Memorandum; Appendix C: Borrow Area Investigations. U.S. Army Corps of Engineers, New York District, New York.
- USACE, 1995. Asbury Park to Manasquan General Design Memorandum; Appendix C: Borrow Area. U.S. Army Corps of Engineers, New York District, New York.
- USACE, 1999. Hopper Dredge Sea Turtle Deflector Draghead and Operational Requirements. Online at <http://www.saj.usace.army.mil/pd/turtle.htm>.
- USACE, 2003. Project Fact Sheets, U.S. Army Corps of Engineers, New York District.
<http://www.nan.usace.army.mil/business/prjlinks/coastal/eastrock/index.htm>
<http://www.nan.usace.army.mil/business/prjlinks/coastal/longbeac/index.htm>
<http://www.nan.usace.army.mil/business/prjlinks/coastal/sandyhok/index.htm>
- USDOI, MMS, 1989. In: S.A. Abernathy (ed.), Description of the Mid-Atlantic Environment. Atlantic OCS Region, MMS 89-0064.
- U.S. Environmental Protection Agency, 1997. Supplement to the Environmental Impact Statement on the New York Dredged Material Disposal Site Designation for the Designation of the Historic Area Remediation Site (HARS) in the New York Bight Apex. Prepared by U.S. Environmental Protection Agency, Region 2, New York, NY with the assistance of Battelle, Duxbury, MA.
- USFWS, 1997. Significant Habitats and Habitat Complexes of the New York Bight Watershed. U.S. Fish and Wildlife Service, Southern New England - New York Bight Coastal Ecosystems Program Charlestown, Rhode Island.
<http://training.fws.gov/library/pubs5/begin.htm>
- Valverde, H.R., A.C. Trembanis, and O.H. Pilkey, 1999. Summary of beach nourishment episodes on the U.S. east coast barrier islands. *Journal of Coastal Research*, 15(4): 1100-1118.
- Van Dolah, R.F., 1996. Impacts of beach nourishment on the benthos: what have we learned? *Proceedings of the Twenty-fourth Annual Benthic Ecology Meeting*, Columbia, SC, p. 82.
- Van Dolah, R.F., D.R. Calder, and D.M. Knott, 1984. Effects of dredging and open-water disposal on benthic macroinvertebrates in a South Carolina estuary. *Estuaries*, 7: 28-37.
- Van Dolah, R.F., P.H. Wendt, R.M. Martore, M.V. Levisen, and W.A. Roumillat, 1992. A Physical and Biological Monitoring Study of the Hilton Head Beach Nourishment Project. Final Report submitted to the Town of Hilton Head Island and South Carolina Coastal Council by the South Carolina Wildlife and Marine Resources Department, Marine Resource Research Institute, 159 pp.
- Van Dolah, R.F., R.M. Martore, and M.V. Levisen, 1993. Supplemental Report for the Physical and Biological Monitoring Study of the Hilton Head Beach Nourishment Project. Prepared by the South Carolina Marine Resources Division, Marine Resources Research Institute for the for the Town of Hilton Head Island, SC.
- Van Dolah, R.F., B.J. Digre, P.T. Gayes, P. Donovan-Ealy, and M.W. Dowd, 1998. An Evaluation of Physical Recovery Rates in Sand Borrow Sites Used for Beach Nourishment Projects in South Carolina. Final report to the U.S. Department of the Interior, Minerals Management Service, Office of International Activities and Marine Minerals by the South Carolina Department of Natural Resources, Marine Resources Research Institute, 76 pp. + app.
- Veatch, A.C. and P.A. Smith, 1939. Atlantic Submarine Valleys of the United States and the Congo Submarine Valley. *Geological Society of America Special Paper No. 7*, 101 p., 17 plates.

- Vecchione, M., 1981. Aspects of the early life history of *Loligo pealei* (Cephalopoda; Myopsida). *Journal of Shellfish Research*, 1: 171-180.
- Vinyard, G.L. and J.W. O'Brien, 1976. Effects of light and turbidity on the reactive distance of bluegill (*Lepomis macrochirus*). *Journal of the Fisheries Research Board of Canada*, 33: 2,845-2,849.
- Viscido, S.V., D.E. Stearns, and K.W. Able, 1997. Seasonal and spatial patterns of an epibenthic crustacean assemblage in northwest Atlantic continental shelf waters. *Estuarine, Coastal, and Shelf Science*, 45: 377-392.
- Walker, T.A. and G. O'Donnell, 1981. Observations on nitrate, phosphate, and silicate in Cleveland Bay, Northern Queensland. *Australian Journal of Marine and Freshwater Research*, 32: 877-887.
- Warwick, R.M., 1980. Population dynamics and secondary production of benthos. In: K.R. Tenore and B.C. Coull (eds.), *Marine Benthic Dynamics*. University of South Carolina Press, Columbia, SC, pp. 1-24.
- Weakley, J., 2001. Reefs in reverse. *Florida Sportsman*, 33(6): 75-80.
- Weber, M., 1995. Kemp's Ridley Sea Turtle, *Lepidochelys kempii*. In: P.T. Plotkin (editor), *National Marine Fisheries Service and U. S. Fish and Wildlife Service Status Reviews for Sea Turtles Listed under the Endangered Species Act of 1973*. Silver Spring, MD.
- Weinberg, J.R., 1998. Atlantic Surfclam. In: S.H. Clark (ed.), *Status of Fishery Resources off the Northeastern United States for 1998*. U.S. Department of Commerce, NOAA Technical Memorandum NMFS-NE-115, pp. 125-127.
- Wenner, E.L. and T.H. Read, 1982. Seasonal composition and abundance of decapod crustacean assemblages from the South Atlantic Bight, USA. *Bulletin of Marine Science*, 32(1): 181-206.
- Werner, S.A. and A.M. Landry, Jr., 1994. Feeding ecology of wild and head started Kemp's Ridley sea turtles (*Lepidochelys kempii*). In: K.A. Bjorndal, A.B. Bolten, D.A. Johnson, and P.J. Eliazar (compilers), *Proceedings of the Fourteenth Annual Symposium on Sea Turtle Biology and Conservation*, NOAA Tech. Memo. NMFS-SEFSC-351, U.S. Department of Commerce, Miami, FL, pp. 163.
- Weston, D.P., 1988. Macrobenthos-sediment relationships on the continental shelf off Cape Hatteras, North Carolina. *Continental Shelf Research*, 8(3): 267-286.
- Whitlatch, R.B., A.M. Lohrer, S.F. Thrush, R.D. Pridmore, J.E. Hewitt, V.J. Cummings, and R.N. Zajac, 1998. Scale-dependent benthic recolonization dynamics: life stage-based dispersal and demographic consequences. *Hydrobiologia*, 375/376: 217-226.
- Wiegel, R.L. and T. Saville, 1996. History of coastal engineering in the USA. In: N.C. Kraus (editor), *History and Heritage of Coastal Engineering*, American Society of Civil Engineers, New York, NY, p. 513-600.
- Wigley, R.L. and R.B. Theroux, 1981. Atlantic Continental Shelf and Slope of the United States-Macrobenthic Invertebrate Fauna of the Middle Atlantic Bight Region-Faunal Composition and Quantitative Distribution. U.S. Geological Survey Professional Paper 529-N, 198 pp.
- Wilber, D.H. and D.G. Clarke, 2001. Biological effects of suspended sediments: a review of suspended sediment impacts on fish and shellfish with relation to dredging activities in estuaries. *North American Journal of Fisheries Management*, 21: 855-875.
- Wilber, P. and M. Stern, 1992. A re-examination of infaunal studies that accompany beach nourishment projects. In: *New Directions in Beach Management: Proceedings of the 5th Annual National Conference on Beach Preservation Technology*, Florida Shore and Beach Preservation Association, Tallahassee, FL, pp. 242-257.
- Wiley, D.N., R.A. Asmutis, T.D. Pitchford, and D.P. Gannon, 1995. Stranding and mortality of humpback whales, *Megaptera novaeangliae*, in the mid-Atlantic and southeast United States, 1985-1992. *Fishery Bulletin*, 93: 196-205.
- Williams, R.G., and F.A. Godshall, 1977. Summarization and interpretation of historical physical oceanographic and meteorological information for the mid-Atlantic region. Interagency Agreement AA550-IA6-12. Prepared by NOAA for the Bureau of Land Management. 295 pp.
- Williams, S.J., 1976. Geomorphology, Shallow Sub-bottom Structure, and Sediments of the Atlantic Inner Continental Shelf Off long Island, New York. U.S. Army Engineer Coastal Engineering Research Center, Technical Paper No. 76-2, Fort Belvoir, VA.
- Williams, S.J., 1992. *Coasts in Crisis*. U.S. Geological Survey Circular 1075, 32 pp.

- Williams, S.J. and D.B. Duane, 1974. Geomorphology and Sediments of the Inner New York Bight Continental Shelf. U.S. Army Engineer Coastal Engineering Research Center, Technical Memorandum No. 76-2, Fort Belvoir, VA.
- Williams, S.J. and E.P. Meisburger, 1987. Sand sources for the transgressive barrier coast of Long Island, New York: evidence for landward transport of sediments. In: N.C. Kraus (editor), Coastal Sediments '87, American Society of Civil Engineers, New York, NY, pp. 1517 – 1532.
- Winn, H.E. (editor), 1982. A Characterization of Marine Mammals and Turtles in the Mid- and North Atlantic Areas of the U.S. Outer Continental Shelf. Final report of the Cetacean and Turtle Assessment Program. University of Rhode Island, Kingston, RI, Prepared for U.S. Department of the Interior, Bureau of Land Management, Washington, DC, Available through National Technical Information Service, Springfield, VA, PB83-215855.
- Wolff, M.P., 1982. Evidence of onshore sand transfer along the south shore of Long Island, New York and its implications against the Bruun Rule. *Northeast Geology*, 4:10-16.
- Wolff, M. and J.B. Bennington, 2000. A Comparison of Changes Between Natural and Re-Nourished Beaches - The 1997-2000 Interval Between Sand Replenishment at Eastern Jones Beach Island and Western Fire Island, New York. Geology Department, Hofstra University, Hempstead, New York.
http://pbisotopes.ess.sunysb.edu/liq/Conferences/abstracts_00/wolff/wolffabstract.html
- Woodworth-Lynas, C. and L. Davis, 1996. Proposed Marine Mining Technologies and Mitigation Techniques: A Detailed Analysis with Respect to the Mining of Specific Offshore Mineral Commodities. Final Report. Prepared by the Centre for Cold Ocean Resources Engineering for the U.S. Department of the Interior, Minerals Management Service. Contract No. 14-35-0001-30723, OCS Report MMS 95-0003, 279 pp. + 6 Appendices.
- Wright, D.G., 1977. Artificial Islands in the Beaufort Sea: A Review of Potential Impacts. Department of Fisheries and Environment, Winnipeg, Manitoba, 38 pp.
- Young, D.K. and D.C. Rhoads, 1971. Animal-sediment relations in Cape Cod Bay, Massachusetts: a transect study. *Marine Biology*, 11: 242-254.
- Zajac, R.N. and R.B. Whitlatch, 1982. Responses of estuarine infauna to disturbance. I. Spatial and temporal variation of initial recolonization. *Marine Ecology Progress Series*, 10: 1-14.
- Zawila, J.S., 1994. Analysis of a Seismic Air Gun Acoustic Dispersal Technique at the Fort Pierce Sea Turtle Trial Site. Contract report to U.S. Army Engineer Waterways Experiment Station, as excerpted in: Sea Turtle Research Program Summary Report. Prepared by U.S. Army Engineer Waterways Experiment Station, Vicksburg, MS for U.S. Army Engineer Division, South Atlantic, Atlanta, GA and U.S. Naval Submarine Base, Kings Bay, GA, Technical Report CHL-97-31, NTIS ADA332588, 147 pp.